AUSTRALIAN GEOMECHANICS SOCIETY

NEW ZEALAND GEOTECHNICAL SOCIETY INC

15th Young Geotechnical Professionals Conference

6-9 November 2024
Adelaide, South Australia

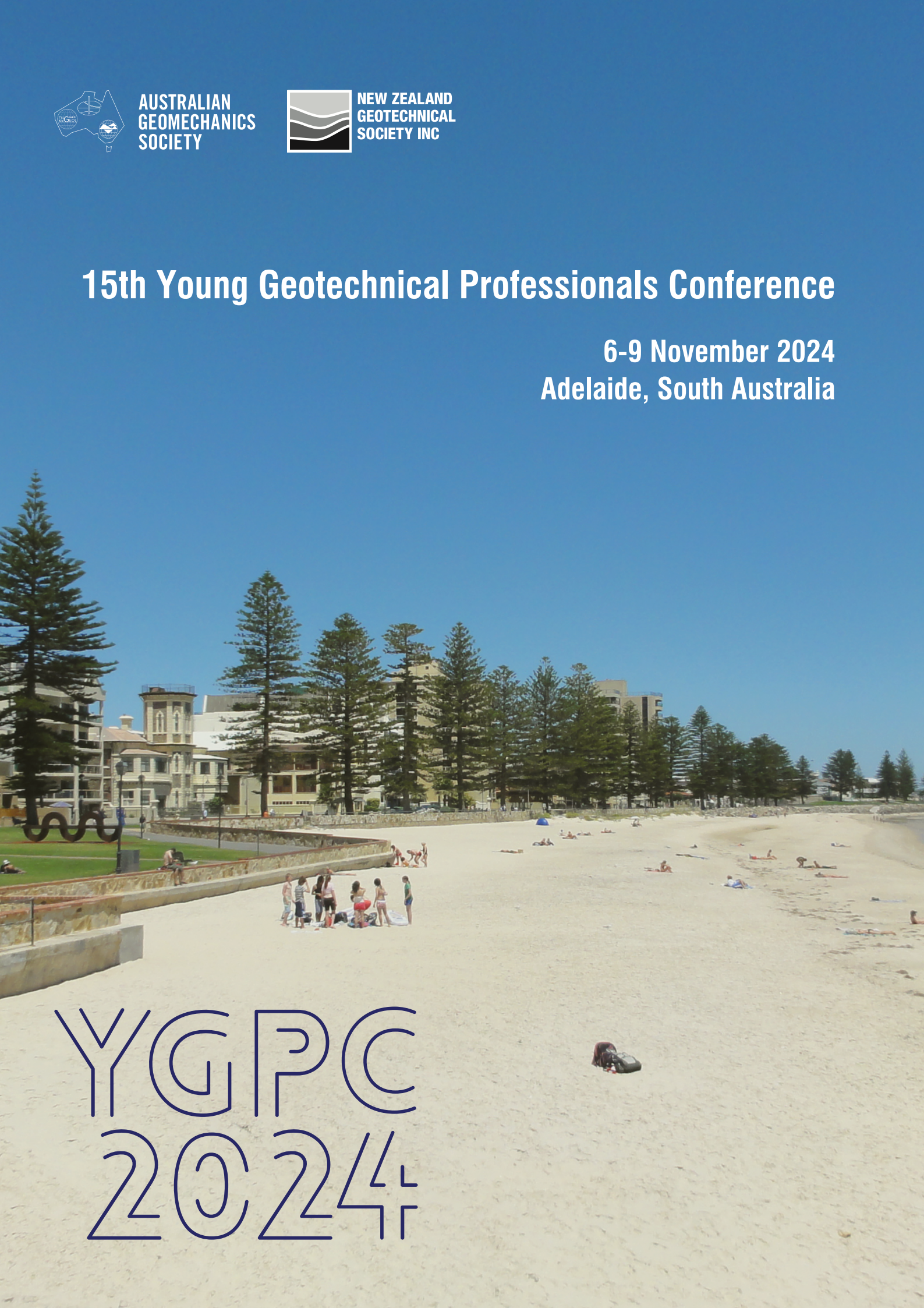

YGPC 2024

THANKS TO OUR SPONSORS

GOLD SPONSORS

SILVER SPONSORS

BRONZE SPONSOR

ACKNOWLEDGEMENT OF COUNTRY

The 15YGPC organising committee acknowledges that we are meeting on the traditional Country of the Kaurna people of the Adelaide Plain and pays respect to Elders past and present. We recognise and respect their cultural heritage, beliefs and relationship with the land. We acknowledge that they are of continuing importance to the Kaurna people living today.

Reconciliation Artwork by Paul Herzich, commissioned by Adelaide City Council

CONFERENCE PARTNERS

15TH AUSTRALIA AND NEW ZEALAND YOUNG GEOTECHNICAL PROFESSIONALS CONFERENCE

15YGPC —Adelaide, Australia, November 2024

ORGANISING COMMITTEE

Nikki Manche	WSP	Australia
Christoph Kraus	NZGS YGP Representative / Beca	New Zealand
Sean Goodall	Douglas Partners	Australia
Michael Crisp	Mott MacDonald	Australia
Lauren Amato	Arup	Australia
Jon Gibbs	AGS National Secretary	Australia
Mark Jaksa (mentor)	University of Adelaide	Australia

MENTORS

Darren Paul	AGS Past Chair / WSP	Australia
Mark Jaksa	AGS Past Chair / University of Adelaide	Australia
Emilia Stocks	NZGS Treasurer / Tonkin + Taylor	New Zealand
Romy Ridl	KiwiRail	New Zealand

FIELD TRIP TOUR GUIDE

Mark Drechsler	SMEC	Australia

TECHNICAL REVIEWERS

The 15YGPC Organising Committee would like to thank the following reviewers for the arduous task of undertaking reviews of papers presented at this Conference.

Jeffrey Lee	**Vipman Tandjiria**	**Chaminda Gallage**	**David Airey**
Jun Z Sugawara	**Jinsong Huang**	**Babak Shahbodaghkhan**	**Derek Arnott**
Adrian Smith	**George Kouretzis**	**Vivek Vinkitesh**	**Garry Mostyn**
Richard Merifield	**Bari Thomas**	**Prisantha Dissanayake**	**Mark Orr**
Ian Shipway	**Marc Woodward**	**Jason Fong**	**Jianfeng Xue**
David Williams	**Rick Piovesan**	**Colin Mazengarb**	**Burt Look**
Klaus Thoeni	**Gia Dat Phan**	**Michael Broise**	**Anthony Bowden**
Richard Justice	**Rolando Orense**	**Fred Verheyde**	**Robert Kamuhangire**
Paul Horrey	**Nick Peters**	**Nima Taghipouran**	**Ioannis Antonopoulos**
Eleni Gkeli	**Sally Hargreaves**	**Liam Wotherspoon**	**Ross Roberts**
Ayoub Riman	**Philip Robins**	**Martin Brook**	**Pathmanathan Brabhaharan (Brabha)**
Camilla Gibbons	**Geoffrey Farquhar**	**Rori Green**	

PUBLISHED BY

Australian Geomechanics Society

WELCOME FROM THE 15YGPC ORGANISING COMMITTEE

Nikki Manche
15YGPC Organising Committee Chair

The organising committee are delighted to welcome you to the 15th Australia and New Zealand (ANZ) Young Geotechnical Professionals Conference (15YGPC) which is being held at the Stamford Grand, Adelaide from 6th to 9th November 2024. Held every 2 years, this YGPC event is a unique 3-day conference facilitated by a joint initiative of Australian Geomechanics Society (AGS) and New Zealand Geotechnical Society (NZGS) and led by a volunteer committee of fellow young geo-professionals.

The aim of the 15YGPC is to provide younger professionals, both in industry and academia, experience in technical paper preparation and conference presentation. We hope that delegates not only gain technical knowledge, but confidence in presenting, form new connections and enjoy the process. Presenting at this conference is the culmination of many months of paper preparation and peer review by senior professionals in the industry. Conference attendance is limited to only presenting authors with what is likely to be their first technical paper to their peers and supported by a panel of senior industry professionals. The YGPC is historically a popular event, and this year is no exception, with 80 high quality abstract nominations received. We would like to congratulate the invited delegates on their acceptance, and we look forward to their participation in the conference.

We are thrilled to have Darren Paul (WSP & former AGS National Chair), Mark Jaksa (University of Adelaide & former AGS National Chair), Emilia Stocks (Tonkin + Taylor & NZGS Treasurer) and Romy Ridl (KiwiRail) as our senior industry mentoring panel. This panel not only has vast technical knowledge but also provides a direct link between the YGPs and both societies.

In addition to the conference presentations, we are excited for the various events of the 15YGPC including a social dinner at the Glenelg Surf Club, the conference dinner at the Stamford Grand, and a field trip to Hallett Cove, one of Australia's best known geological sites, and Wirra Wirra Vineyards in the iconic McLaren Vale winery region. We would like to extend our sincere gratitude to Mark Drechsler (SMEC) who will guide us through the various areas of geological significance at Hallett Cove.

We wish to acknowledge the financial support provided by the sponsors of this conference to ensure its success. We also thank the peer reviewers who gave their time and technical expertise to provide thorough and supportive reviews of the papers.

Finally, I wish to acknowledge the hard work and dedication of the organising committee and guidance of both AGS and NZGS national steering committees. Without their efforts and the support of their respective home organisations, this conference would not be possible. We would also like to extend our sincere gratitude to Mark Jaksa for his guidance as a mentor for the organising committee and Jon Gibbs for his support as Secretary of the AGS.

Welcome to Adelaide, relax and most importantly enjoy the events and happenings planned in the next few days. We hope that the 15YGPC provides an enjoyable and informative event aimed at the development of future leaders in the geotechnical profession.

WELCOME FROM THE AGS NATIONAL CHAIR

Tim Thompson
National Chair, Australian Geomechanics Society

I want to welcome you to the 15th Young Geotechnical Professionals Conference (YGPC), co-organised by the Australian Geomechanics Society (AGS) and New Zealand Geotechnical Society (NZGS). I also want to thank you for the time you are taking to attend, and for the time you have already taken to prepare a technical paper. Our two technical societies depend upon membership participation and the YGPC aims in part to embed an awareness of that dependence into the younger side of us. Some of you will inevitably become leaders of the AGS and NZGS in the future, so I expect the experience you have at this year's YGPC will be of lasting benefit not just to your career, but to the sustainability of our respective societies.

The YGPC is unique among the conferences and symposia that we organise. At some point everyone presents to everyone else, a feat that obviously requires the numbers to be limited if all the talking is to fit in the space of two days. From the list of papers, I can see that among other topics, you will be talking and hearing about landslides, seismic hazards, expansive soils, finite elements, artificial intelligence, climate change, ground improvements, and pile design. It appears that one among you will be leading a journey through digital transformation in modern geotechnics, and another has taken on the necessary task of reminding us all why understanding geology matters for engineering design. The topics you have chosen for your papers would fit well at any of our quarterly ANZ conferences and I encourage you to stay engaged with our societies in the future through your chapters or branches and our regional events.

Finally, I want to thank Nikki, Lauren, Michael, Sean, and Christoph for their time and efforts on the organising committee, and Mark, Darren, Romy and Emilia for helping as mentors.

My counterpart of the NZGS Phil Robins and I both look forward to meeting you.

WELCOME FROM THE NZGS CHAIR

Philip Robins
Chair, New Zealand Geotechnical Society

Kia ora kotau,

Welcome to the 15th Australia – New Zealand Young Geotechnical Professionals Conference (15YGPC) for 2024. Hosted in the vibrant city of Adelaide, South Australia. This YGP Conference, from its origins dating back to the inaugural event in Sydney in 1994, symbolises the professional unity between our two Societies. The success of this biennial gathering is underscored by the enthusiasm and support from up-and-coming geo-professionals in both countries.

Special thanks are due to the organising committee, chaired by Nicola Manche, with members Mark Jaksa, Michael Crisp, Sean Goodall, Lauren Amato, Jon Gibbs (AGS secretary), and Christoph Kraus (NZGS). Both the Australian Geomechanics Society (AGS) and the New Zealand Geotechnical Society (NZGS) take immense pride in their Young Geotechnical Groups.

Again, this year, we received many high-calibre abstracts, making the selection process particularly challenging for the committee. The conference proceedings feature an excellent collection of papers, from project case studies in Australia, New Zealand, and abroad, to innovative research.

This event offers a platform for our younger members to engage in a conference of international calibre and network with colleagues across the regions. Reflecting on my experience as a mentor at the previous ANZ YGP Conference in Rotorua, New Zealand, I was impressed by the exceptional talent on display, and it left me with a renewed confidence in the future of our craft.

I extend my thanks and appreciation to our mentors, including Romy Ridl and Emilia Stocks from New Zealand, and Mark Jaksa and Darren Paul from Australia. Their guidance and support are what truly distinguish this Conference. Additionally, my sincere thanks go to our sponsors for their generous contributions. I look forward to an inspiring and rewarding ANZ YGP Conference 2024.

Ngā mihi

MENTORS

Emilia Stocks
NZGS Treasurer / Tonkin + Taylor

Emilia is the Principal Geotechnical Engineer at Tonkin and Taylor Ltd in Wellington. She holds a Master of Civil Engineering from Sheffield University and is a Chartered Engineer in NZ. Emilia is the Treasurer for the New Zealand Geotechnical Society and is the convener for the planned 2025 NZGS Symposium in Auckland.

Emilia's expertise encompasses a strong foundation in geotechnical engineering, proficient project and risk management skills, and a comprehensive understanding of design and construction processes and standards.

Emilia has worked in the UK, Hong Kong, and NZ on several complex projects, including the Finningley and Rossington Route Regeneration Scheme in the UK, the West Island Line in Hong Kong, Dilmunia Health Island in Bahrain. In NZ, she worked on the PwC building and the Tākina Convention & Exhibition Centre foundations in Wellington. She was also involved in the gravel liquefaction mapping and assessment at Wellington Port after the Kaikōura earthquake in 2016.

Outside of engineering, Emilia volunteers with NZ Emergency Response Teams and Wellington Free Ambulance. She loves the outdoors, gardening, crafting, and playing board games.

Professor Mark Jaksa
AGS Past Chair / University of Adelaide

Mark Jaksa is Professor Emeritus of Geotechnical Engineering in the School of Architecture and Civil Engineering at the University of Adelaide, Australia, where he has been for 36 years. Before becoming an academic, he spent 4 years practicing as a consulting geotechnical and civil engineer in Adelaide and Canberra in Australia. He has a Bachelor of Engineering (Honours) degree in Civil Engineering and a PhD, both from the University of Adelaide.

He has published more than 240 journal and conference papers, chapters and reports on various aspects of geotechnical engineering research and teaching. His primary areas of expertise are in the characterisation of the spatial variability of soils, probabilistic analyses, artificial intelligence, ground improvement, unsaturated soils, lunar geotechnics, and enhancing learning in geotechnical engineering. He has received several awards recognising his contributions to research, and learning and teaching in geotechnical engineering.

Mark is a former Vice-President for Australasia and Treasurer of the International Society for Soil Mechanics and Geotechnical Engineering and Chair of the Australian Geomechanics Society. He is also a past Chair of the ISSMGE's Technical Committee, TC306, on Geo-engineering Education and a member of TC304, on Risk Assessment and Management.

MENTORS

Dr. Romy Ridl
KiwiRail

Romy is the Technical Manager – Civil at KiwiRail in New Zealand. She is an Engineering Geologist with BSc and BSc (Honours) obtained from the University of KwaZulu-Natal in Durban, South Africa and a PhD obtained from the University of Canterbury in Christchurch, New Zealand.

Romy's professional interests lie in site characterization and development of ground models, rock mechanics and rock engineering, risk-based solutions and more recently has been focused on strategic asset management. Romy has had a varied career ranging from Engineering Geologist to Senior Engineering Geologist, QA/QC Manager for large-scale projects, Team Leader, Technical Manager and Lecturer. She has worked on numerous large-scale projects in countries such as: Australia, Madagascar, Malawi, Mozambique, New Zealand, South Africa, Zambia covering greenfield-brownfield transport infrastructure projects, Earthquake and Cyclone Recovery projects, pipelines and Industrial developments.

Outside of work, you will likely find Romy playing outdoors (skiing, surfing, tramping) typically not far from a landslide or DIY renovations on a house.

Darren Paul
AGS Past Chair / WSP

Darren is an Engineering Geologist and Lead Technical Director for Geotechnics and Tunnels at WSP Australia. He holds a Bachelor of Civil Engineering and Bachelor of Science in Geology, a combination which took him into the fields of geotechnical engineering and engineering geology. He also has an MSc in Engineering Geology from Imperial College London.

Darren's professional interests are in ground model development, the identification, assessment and management of geological uncertainty, landslide risk assessment and terrain evaluation. He has worked on many notable projects in Melbourne including the Burnley Tunnel, Eureka Tower, the Melbourne Metro Project and currently North East Link. He has also worked on large projects in Africa, the Middle East and PNG. In 2008 Darren was awarded the Young Professional Engineer Award for Victoria and in 2010 was awarded The Richard Wolters Prize from the IAEG. He was chair of the 2022 International Young Geotechnical Engineers Conference held in Sydney and currently chair of the committee revising the Australian Geomechanics Society Guidelines for Landslide Risk Management.

Outside of engineering geology, Darren was in the army reserve for 12 years and is currently an officer of army cadets. He enjoys travelling and getting outdoors with his wife and three young boys.

FIELD TRIP

Mark Drechsler
SMEC

Mark is a Technical Principal Engineering Geologist at SMEC in Adelaide. He holds a Bachelor of Science with Honours in Geology and a Master of Business Administration and is currently undertaking a PhD in Minerals Science and Resources at the University of South Australia.

Mark has over 40 years' experience as an engineering geologist involved in investigation, design and construction of mining, civil and transport infrastructure projects throughout Australia and Papua New Guinea. Mark has had some involvement in most mining and infrastructure projects in South Australia over the last 25 years through his technical expertise in quarrying, earthworks and construction materials for mining haul roads and road pavements and that expertise extends into track formation design for rail projects across Australia.

Mark has a passion for innovative 'green' technologies such as geopolymer concrete using waste materials. Mark is undertaking a full time PhD on the energy and mineral processing benefits of his innovative crushing technology being developed in South Australia for the mining and cement industry. Mark has a casual role with SMEC providing his technical expertise to selected projects across Australia and continues his mentoring of junior professionals and supporting STEM studies at high schools.

CONFERENCE PROGRAM

Wednesday 6 November 2024: Welcome Function and Registration	
14:00	**Check-in opens – Stamford Grand Adelaide Hotel, Glenelg** Registration desk opens Delegates to bring presentation on USB to upload
17:00	Registration desk closes **Welcome Reception at Stamford Grand Horizon's Cocktail Lounge (hosted by Beca)** Welcome on behalf of the Organising Committee Introductions of Organising Committee and Mentors Welcome from the AGS / NZGS Acknowledgement of Sponsors
19:00	Welcome function concludes

Thursday 7 November 2024: First Day Presentations	
08:15	Last chance for presentations to be uploaded
08:30	**Session 1** Opening Announcements Presentation of papers 1-6 Mentor Summary
10:30	Morning break and refreshments (coffee cart hosted by ConeTec)
11:00	**Session 2** Gold Sponsor acknowledgement (WSP) Presentation of papers 7-12 Mentor Summary
12:30	Lunch
13:30	**Session 3** Presentation of papers 13-18 Mentor Summary
15:00	Afternoon break and refreshments
15:30	**Session 4** Gold Sponsor acknowledgement (Hully) Presentation of papers 19-24 Mentor Summary Closing announcements
17:00	First Day Presentations conclude
18:45	Meet at reception to walk as a group to dinner
19:00	**Social Dinner at Glenelg Surf Life Saving Club (hosted by Hully)**

CONFERENCE PROGRAM

Friday 8 November 2024: Second Day Presentations	
08:30	**Session 5** Opening Announcements Presentation of papers 25-32 Mentor Summary
10:30	Morning break and refreshments (coffee cart hosted by Insitu Geotech Services)
11:00	**Session 6** Gold Sponsor acknowledgement (Beca) Presentation of papers 33-38 Mentor Summary
12:30	Lunch
13:30	**Session 7** Presentation of papers 39-44 Mentor Summary
15:00	Afternoon break and refreshments
15:30	**Session 8** Gold Sponsor acknowledgement (Keller) Presentation of papers 45-46 Mentor Summary
16:00	**Heritage Time Capsule (HTC) session** Field trip overview & H&S briefing Closing announcements
17:00	Second Day Presentations conclude
19:00	**Conference Dinner at Stamford Grand Room Colley 1-2 (hosted by WSP)** Presentation of awards

Saturday 9 November 2024: Field Trip (hosted by Keller)	
	Check-out of Stamford Grand Adelaide Hotel prior to 8:30am (attendees to either store bags at hotel reception or load into bus if going to the airport)
08:30	Board bus from reception
09:00	Hallet Cove geology tour
10:30	Board bus to Wirra Wirra Winery
11:00	Wirra Wirra Vineyards wine tasting tour and lunch
12:30	Board bus to Stamford Grand Adelaide Hotel
13:30	Return to Stamford Grand Adelaide Hotel Optional bus to Adelaide Airport by 2pm
14:00	Conference concludes

HERITAGE TIME CAPSULE (HTC)
FOCUS FOR THE FUTURE 100 YEARS

Arrangements are underway for a physical time capsule cube of 1m x 1 m x 1m, to be assembled and sealed at the occasion of the 21st International Conference on Soil Mechanics and Geotechnical Engineering (21st ICSMGE), to be held in Vienna, Austria, in 2026. The time capsule will be housed in a technical museum where visitors can view it. However, once sealed, its contents will remain inaccessible until 2126, i.e., 100 years from when it was sealed.

What will "they", geotechnical engineers and scientists of 2126 and later years, say about our achievements in the second 100 years of geotechnical engineering, after sealing of the time capsule? To address this and other future focus thoughts, the Heritage Time Capsule (HTC) has been initiated and launched by the International Society for Soil Mechanics and Geotechnical Engineering (ISSMGE) with the following three objectives:

Learn about each other ***Tell the world about us*** ***Develop a future focus***

Various cohorts of the ISSMGE, including Member Societies, Technical Committees, Past Presidents/ Champions, Key Persons, Vice Presidents, Corporate Associates, and Board Level Committees, have contributed since 2020 to the development of a "virtual time capsule", now housed in the HTC website, https://htc.issmge.org/

Each individual member of the ISSMGE can submit discoverer reports, to be hosted on the HTC website. The role of the discoverer report is to shine a spotlight on one or more contributions. The HTC website contains further details on the preparation of discoverer reports. The HTC Design Team can be contacted for help via the contact page of the HTC website: https://htc.issmge.org/contact

The critical task for the HTC team leading to 2026, is to develop a focus for the future. The diagram here shows the five elements that form a future focus framework. The HTC team will develop these elements with the help various ISSMGE cohorts to:
a) help with deciding what should be placed in the physical time capsule, and,
b) to prepare an ISSMGE strategy and action plan for the second 100 years of geotechnical engineering, to be re-assessed on a decade-by-decade basis.

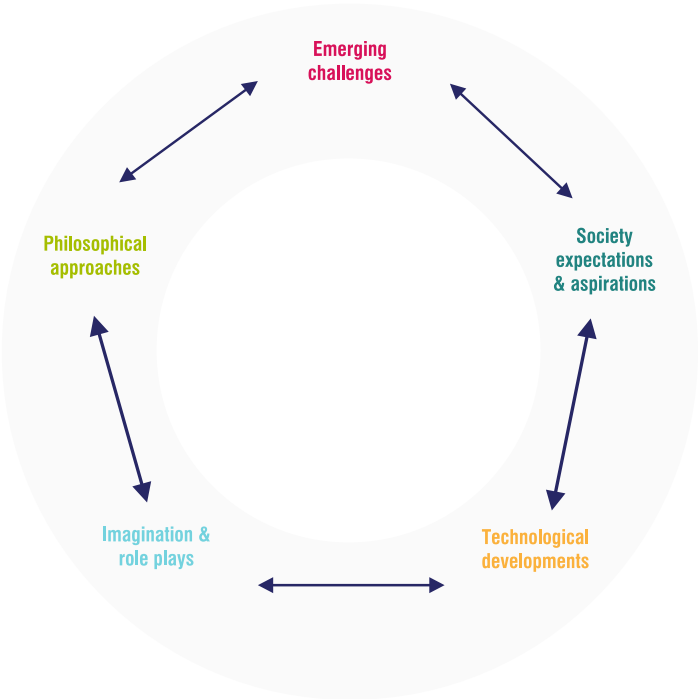

Join us on this exciting journey!

We are excited to host an interactive session during the 15YGPC to contribute to the HTC project and contribute to the future of geotechnics.

References

- Pathmanandavel, S., Bilotta, E., MacRobert C.J, Chung, C. (2024) HTC - Creating and discovering the ISSMGE Heritage Time Capsule, Proceedings of the XVIII ECSMGE, Lisbon, 26-30 August 2024
- Pathmanandavel, S., Bilotta, E., Bouazza, A., Shahien, M., Poulos, H. (2024) - The ISSMGE Heritage Time Capsule Project – Future Focus, Proceedings of the 18th ARCSMGE, Algiers, 6-9 October 2024 (in press)

TABLE OF CONTENTS
TECHNICAL PAPERS

TABLE OF CONTENTS
TECHNICAL PAPERS

TABLE OF CONTENTS
TECHNICAL PAPERS

NUMERICAL MODELLING COMPARISON OF LARGE STRAIN TAILINGS CONSOLIDATION

Daniel Pham
WSP Australia

ABSTRACT

Consolidation of mine tailings can take extended periods of time due to their high water content and relatively low permeability which can affect the storage capacity of the tailings storage facilities (TSFs) during the Life of Mine (LoM), and the timeline to start their rehabilitation at closure. A clearer understanding of the tailings consolidation behaviour during TSF planning stages is therefore critical to achieve efficient and sustainable mine waste management during operations and prior to closure. This can be accomplished by a combination of laboratory testing and numerical modelling prior to the commencement of tailings deposition.

A numerical modelling comparison of large strain tailings consolidation was undertaken between three software packages Plaxis LE, FSConsol and MinTaCo that are commonly used by tailings practitioners. The objectives of the study were to provide the advantages and limitations of each software to assist with selecting the appropriate numerical modelling program corresponding to the project budget, complexity, anticipated effort, and outputs required. This paper presents a case study involving consolidation modelling undertaking on an in-pit tailings storage facility based on laboratory testing results using the software considered for both single and multiple filling scenarios as well as with and without the effects of evaporation.

1 INTRODUCTION

Tailings have been generated in large volumes worldwide as by-products of ore beneficiation from the process plants in the mine sites. Tailings are generally deposited in the form of slurry either on perimeter dykes constructed from their coarser fraction i.e., waste rock above ground, or within the inactive open pits. These structures are called tailings storage facilities (TSFs). Settling and consolidation processes of mine tailings can take a long time which reduces the storage capacity of the TSFs due to the conventional tailings characteristics of high water content and low hydraulic conductivity. As such, a combination of laboratory testing and numerical modelling is usually required prior to the commencement of tailings deposition to achieve effective planning and management during TSF operations and prior to closure.

Numerical modelling on tailings consolidation has evolved over the years with multiple software available both commercially and for educational purposes focussing on one-dimensional configuration. Each software has its own advantages, limitations, functions as well as variability in costs and model configurations. This study presents a comparison between three modelling software that have been used by tailings practitioners to model large strain tailings consolidation which are Plaxis LE, FSConsol and MinTaCo.

2 BACKGROUND

2.1 FINITE STRAIN CONSOLIDATION

The consolidation of tailings can be broken down into three components:

1. Self-weight consolidation occurs following deposition and is the result of settling of the tailings solid particles without additional loading.
2. Primary consolidation follows self-weight consolidation and is the result of dissipation of pore-water pressure generated by an increase in vertical effective stress.
3. Secondary consolidation (or creep deformation) continues in the long-term following primary consolidation and under a state of relatively constant stress. Note that secondary consolidation was not considered in the study presented herein due to its limited settlement magnitude in comparison to self-weight and primary consolidation.

During self-weight consolidation, tailings will undergo large deformations due to low effective stress and high void ratio in the early stage of tailings matrix (i.e., particle fabric) development. The hydraulic conductivity of tailings

decreases as the density changes with increased thickness of the deposit during tailings deposition. Therefore, the conventional Terzaghi consolidation theory becomes invalid due to the inherent assumptions of infinitesimal strains and constant hydraulic conductivity. To capture the high nonlinearity due to initial large volume change at high void ratio of tailings, a finite strain consolidation theory for self-weight consolidation involving large strain deformation is required to be adopted.

2.2 NUMERICAL MODELLING SOFTWARE CONSIDERED

2.2.1 Plaxis LE

Plaxis LE is a software for limit equilibrium slope stability analysis and finite element analysis of groundwater seepage. Consolidation is a module within Plaxis LE that solves coupled hydro-mechanical processes that are available separately in the Groundwater and Stress software packages. The large strain consolidation is modelled following the non-continuum mechanics in the Lagrangian coordinate system developed by (Bonet, 2008). The software has the capability to model both small strain (constant soil properties) and large strain (nonlinear soil properties) consolidation problems in both 1D and pseudo-3D (i.e., coupled 3D slurried tailings deposition scenario with the effects of saturated 1D columns) configurations. Note that the software was originally developed by SoilVision, a geotechnical engineering software provider that was acquired together with Plaxis by Bentley Systems in 2018.

2.2.2 FSConsol

FSConsol is a 1D consolidation program that uses the Finite Strain Consolidation Theory developed by (Gibson, 1967) to determine the rate and magnitude of consolidation of soil slurries such as mine tailings, deltaic deposits, and other soft soils. The software can model a variety of consolidation problems ranging from a step loaded laboratory consolidation test to a complex mine tailings pond scenario with varying filling rates, changing pond areas, and changing soil properties.

2.2.3 MinTaCo

MinTaCo is a 1D numerical modelling program developed by the University of Western Australia (UWA) in 1996. MinTaCo has the capability to incorporate the effects of drying on the conventional large strain consolidation process (Seneviratne, Fahey, Newson, & Fujiyasu, 1996). It iteratively applies different suction values to the surface of the tailings to achieve a specific evaporation rate for the material. This iterative adjustment in suction continues until the layers reach the shrinkage limit density which is assessed by laboratory consolidation testing.

3 MULTI CRITERIA ASSESSMENT

A basic multicriteria assessment (MCA) was conducted with the key criteria summarised in Table 1. Note that the full MCA is not included in this paper due to page constraint. The main advantage of MinTaCo in comparison to the other two software is the ability to model unsaturated conditions such as the inclusion of evaporation during consolidation. Its major drawback is the lack of the functional graphical user interface (GUI) which can create many difficulties for first time users. Plaxis LE has the benefits of having the ability to do 3D modelling which is more suitable for data visualisation, and a well and fully developed GUI that is more appealing to the users.

Table 1: Summary of key outcomes from the multi criteria comparison

Criteria	Plaxis LE	FSConsol	MinTaCo
Ease of use	Advanced graphical user interface (GUI)	Basic GUI	No GUI available
Model configuration	1D & Pseudo-3D	1D	1D
Available license	Network	USB dongle	License is not required
Soil saturation conditions	Saturated only	Saturated only	Saturated & unsaturated

4 CASE STUDY

4.1 BACKGROUND

Consolidation modelling has been undertaken using the three software packages mentioned herein on an in-pit TSF (IPTSF) called De Grey pit which is located in Western Australia (WA) as a case study. De Grey is an inactive open pit and is part of the Shovelanna complex. The pits are located approximately 35 km east of Newman within the Pilbara region of Western Australia. The Hamersley Range and Fortescue Plains subregions (where the pits are located) are typified by an arid and tropical climate, with hot wet summers and cool dry winters. Average annual rainfall is typically 300 mm, most of which falls during the summer because of rain depressions and cyclones. Hot, dry, and sunny conditions in the Pilbara lead to an average annual evaporation rate of typically 3200 mm.

De Grey and Swan pits have been identified as the candidates for short-term tailings management solution with tailings deposition planned to commence in mid-2026 when the process plant is commissioned. The tailings deposition strategy selected was 2 weekly rotated deposition cycles between the two pits to improve consolidation during the operational periods. Note that only the consolidation modelling for De Grey pit is presented in this paper.

4.2 CONSOLIDATION MODELLING

4.2.1 Basis of design

Table 2 presents the adopted design inputs in relation to the IPTSF operations for consolidation modelling.

Table 2: Design basis of the IPTSF operations

Design Parameter	Design Input
Available capacity in pit	13.78 Mm^3 at maximum designed tailings elevation.
Commencement of tailings generation	1 August 2026 (FY27).
Tailings solids generated	5.89 Mtpa on average from FY27 to FY51.
Deposition approach	Slurry deposition by spigots. Two deposition point locations adopted in Swan and De Grey pits (the second deposition point is included for contingency).
Tailings deposition strategy	Multiple filling phases over the LoM and 2 weekly rotated deposition cycles between De Grey and Swan pits.
Representative tailings samples	Average Blend for the first three years of operations followed by High Dales during the LoM.

4.2.2 Laboratory testing and material input parameters

Tailings parameters for input to the models in Plaxis LE, FSConsol and MinTaCo were estimated and calibrated based on laboratory classification and consolidation testing results of Average Blend and High Dales samples. They were used to establish the following:

- Relationship between void ratio and effective stress (fitted extended power function as presented in Figure 1)

$$e = 2.954(\sigma'_v + 0.11)^{-0.155} \ (\sigma'_v \ in \ kPa) \text{ (Average Blend)} \quad (1)$$

$$e = 3.006(\sigma'_v + 0.051)^{-0.149} \ (\sigma'_v \ in \ kPa) \text{ (High Dales)} \quad (2)$$

- Relationship between permeability and void ratio (fitted power function as presented in Figure 2)

$$k_v = 1.0 \times 10^{-9}(e)^{3.047} \ (k_v \ in \ m/s) \text{ (Average Blend)} \quad (3)$$

$$k_v = 9.0 \times 10^{-10}(e)^{2.806} \ (k_v \ in \ m/s) \text{ (High Dales)} \quad (4)$$

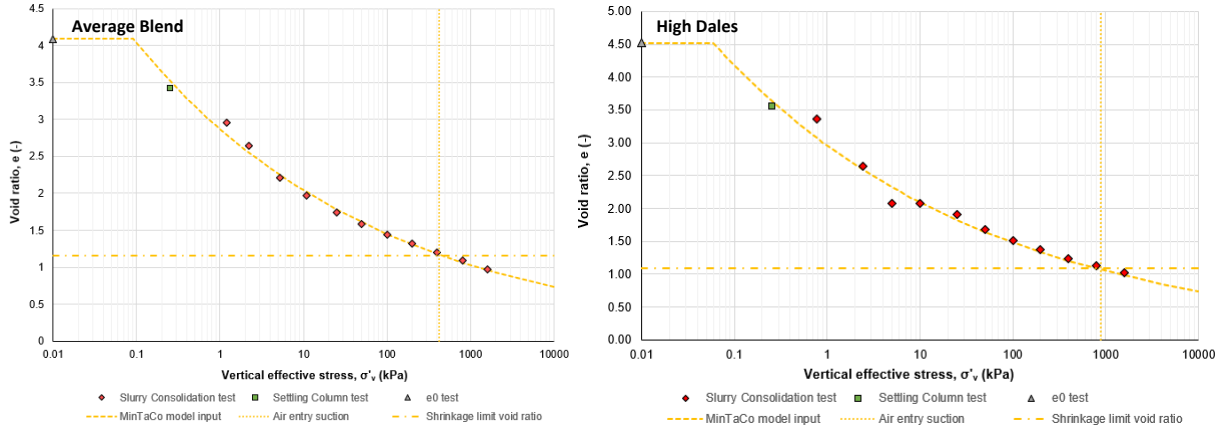

Figure 1: Laboratory test results and functions adopted for void ratio (e) vs. vertical effective stress (σ'v)

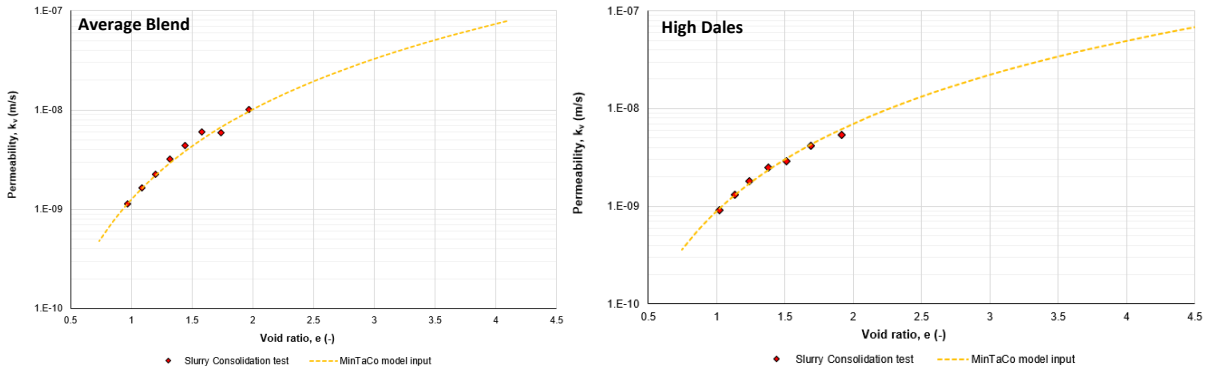

Figure 2: Laboratory test results and functions adopted for permeability (kv) vs. void ratio (e)

4.2.3 Modelling assumptions

The following key assumptions were incorporated in the models:

- A Poisson's Ratio of 0.3 is assumed for both Average Blend and High Dales tailings. This is considered appropriate for iron ore tailings as suggested by (Priestley, 2011).
- An average annual lake evaporation rate of 5.9 mm/day (or 2.2 m/year) was adopted to simulate evaporation in the models. This is equivalent to a coefficient of conversion between A-Pan and the lake evaporation of 0.65. The data was extracted from SILO using Morton's shallow lake evaporation rates at the stations where De Grey pit is located.
- A conservative assumption of no flux at the lower boundary of the models (i.e., zero seepage with only upward drainage allowed).
- Zero excess pore water pressure at the upper boundary to allow for water to drain at the surface. Tailings are assumed to remain fully saturated which is representative of supernatant pond removal through decanting.

4.2.4 Modelling results

Consolidation modelling for the single filling was undertaken adopting the following scenarios and software: Plaxis LE, FSConsol, MinTaCo without evaporation and MinTaCo with evaporation.

For the multiple filling phases, only Plaxis LE (without evaporation) and MinTaCo (with evaporation) were considered. Note that an average tailings settlement magnitude of 5 m was assumed to be the target for tailings deposition restart following the fallow periods.

The results of single filling and multiple fillings are summarised in Table 3 and Table 4, respectively. The outcomes indicate the following:

Single filling

- A storage life of 3.5-3.7 is achieved consistently considering the scenario without evaporation using the three software.
- The incorporation of evaporation using increases the storage life slightly to 3.9 years.

- The expected settlement within De Grey pit is approximately 55-58 m. Note that due to only one tailings sample was adopted for FSConsol, the results of settlement post deposition are not included for comparison purposes.

Multiple fillings

- An overall storage life of ~7 years is anticipated to be achieved incorporating evaporation in MinTaCo in comparison to ~5 years in Plaxis LE without evaporation, which is an increase of ~40% in storage life during operations.
- A reduction total tailings settlement is anticipated when evaporation is considered, from 48 m to 39 m.
- MinTaCo takes longer to reach 90% settlement in approximately 80 years from FY51 in comparison to 51 years using Plaxis LE.

Table 3: Modelling results for the single filling phase

Parameters	Plaxis LE	FSConsol	MinTaCo (without evaporation)	MinTaCo (with evaporation)
Estimated storage life (years)	3.6	3.45	3.7	3.9
Total estimated settlement post-deposition (m)	55	N/A	54	58
Approximate time to reach 90% settlement from end of deposition (years)	47	N/A	44	44
Average stored dry density at the end of deposition (t/m3)	0.83	0.83	0.84	0.85

Table 4: Modelling results for multiple filling phases

Parameters	MinTaCo	Plaxis LE
Estimated storage life at the end of the initial deposition phase (years)	3.9	3.6
Estimated total storage life at the end of the final deposition phase (years)	7	5
Total estimated settlement post-operations (m)	39	48
Settlement ratio (%)	37	46
Approximate time to reach 90% settlement from FY51 (years)	80	51

The results of 1D modelling are representative for a single location within the pit, where settlements are expected to be the greatest. It is expected that the average settlement across the pits' area will be less due to changes in the pit geometry. Pseudo-3D consolidation modelling has been undertaken to provide a better understanding of the tailings settlement profile in three dimensional configuration. Note that pseudo-3D does not consider horizontal dissipation of pore pressure, lateral deformation, and the effects of evaporative desiccation.

The results of pseudo-3D consolidation modelling are presented in Figure 3 showing the estimated final tailings surfaces at the end of consolidation. The results of the pseudo-3D modelling indicate that:

- The settlement profiles at the deepest locations within the two pits are aligned with the 1D modelling results with a total estimated post-deposition settlement of ~50 m in De Grey pit.
- The magnitude of settlement reduces with reducing pit depth/height of tailings column. As such there is likely to be less settlement around the edges of the pits than in the centre, creating a dished tailings surface profile.

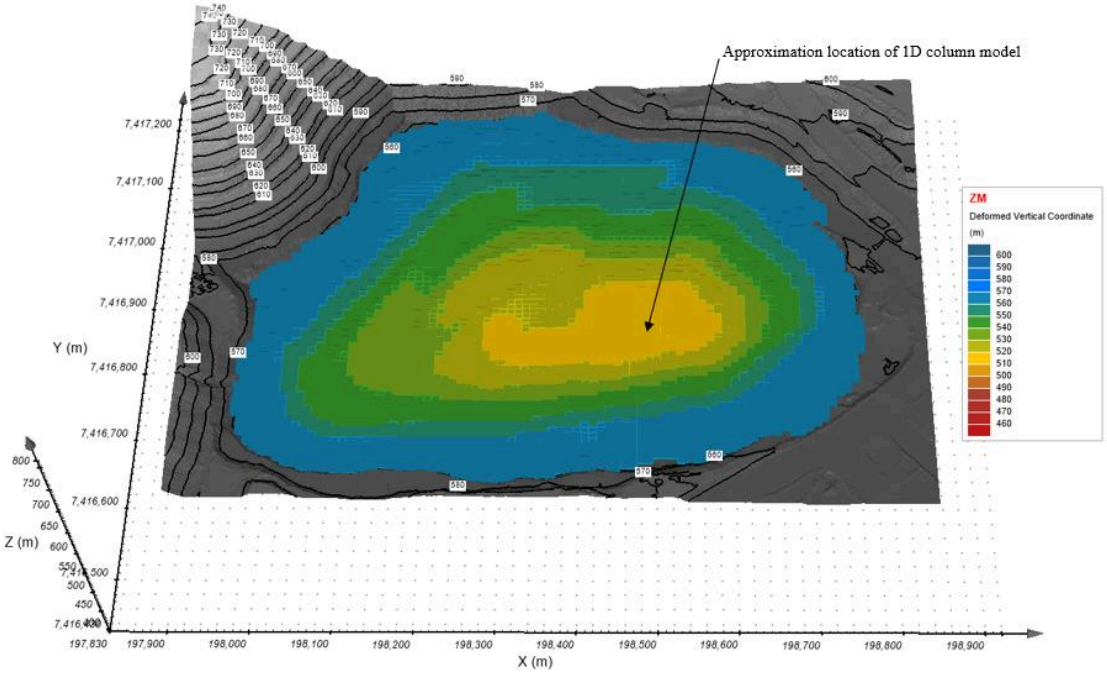

Figure 3: Pseudo-3D surface of total estimated tailings settlement in De Grey pit

5 CONCLUSIONS

A numerical modelling comparison of large strain tailings consolidation was undertaken between three software packages Plaxis LE, FSConsol and MinTaCo that are commonly used by tailings practitioners. The following conclusions can be made based on the outcomes of the study:

- FSConsol has been primarily used by tailings practitioners in the industry for consolidation modelling due to its relatively basic GUI and the ability to model creep deformation. This is suitable for 1D consolidation models having simple TSF geometry with limited inputs required. Plaxis LE has a more sophisticated GUI and advanced functions which allow the users to model complex TSF geometry based on the actual site topography in both 1D and pseudo-3D configurations. However, this will normally require the users to have a relatively advanced modelling skill with some background knowledge on 3D modelling. In comparison to Plaxis LE and FSConsol, MinTaCo has the advantage of being able to incorporate climatic conditions such as evaporation. The major drawback with MinTaCo is the lack of a user-friendly GUI and the ability to model pseudo-3D.
- The case study presented a consistent similarity between the outputs of estimated initial storage life, settlement magnitude and average stored density at the end of the initial deposition phase between the three software programs. FSConsol showed instability in its model solver as it was not able to handle two tailings materials in comparison to Plaxis LE and MinTaCo, even though FSConsol allows to enter over 30 different material types. The results of pseudo-3D modelling in Plaxis LE were consistent with the 1D outcomes. When incorporating evaporation in multiple filling scenario, MinTaCo illustrated a significant increase in storage life of the TSF which emphasises the importance of climatic conditions to tailings consolidation process.

6 REFERENCES

Bonet, J. (2008). Nonlinear Continuum Mechanics for Finite Element Analysis. Cambridge: Cambridge University Press.

Gibson, R. E. (1967). The theory of one-dimensional consolidation of saturated clays - Finite non-linear consolidation of thin homogeneous layers. Geotechnique.

Priestley, D. (2011). Modeling Multidimensional Large Strain Consolidation of Tailings. The University of British Columbia.

Seneviratne, N. H., Fahey, M., Newson, T. A., & Fujiyasu, Y. (1996). Numerical modelling of consolidation and evaporation of slurried mine tailings. International Journal for Numerical and Analytical Methods in Geomechanics, 647-671.

A FRAMEWORK FOR ASSESSING SUBGRADE SHRINK SWELL POTENTIAL FOR NEWLY CONSTRUCTED PAVEMENTS ON EXPANSIVE SOILS IN ADELAIDE, SOUTH AUSTRALIA

Jim Nguyen[1], Lauren Amato[1], Paul Bailie[1], Peter Mitchell[2]
1: Arup, 2: Aurecon

ABSTRACT

In South Australia, the Department for Infrastructure and Transport (DIT) Master Specification RD-EW-D1 Design of Earthworks for Roads requires the calculation of seasonal or long-term road surface movements to be in accordance with AS 2870: Residential slabs and footings. This approach, based primarily on the instability index, is different to the soaked CBR approach followed in many other states, and requires a degree of adaptation and interpretation in its application.

This paper provides a review of the assumptions and methodology for calculating surface movements for recent highway projects in Adelaide, South Australia. Detailed calculation procedures, including the determination of characteristic surface movement and adjustments for South Australia ground conditions, are presented alongside solutions for more sustainable design. The findings of this study offer valuable insights into pavement design considerations, highlighting potential cost savings and performance improvements compared to conventional treatments. By addressing the implications of tree root suction on subgrade movement as a contributor to pavement performance, this paper contributes to the development of more resilient and sustainable urban infrastructure. This research is essential for engineers and practitioners involved in pavement design, facilitating informed decision-making and optimal infrastructure investment.

1. INTRODUCTION

In arid and semi-arid regions around the world, the problematic shrink-swell behaviour of expansive soil due to seasonal changes in moisture content is often exacerbated by the presence of tree roots reaching deep into the ground to find water. This behaviour can lead to significant pavement damage due to volumetric changes in the expansive soil sub-grade material under the pavement. To deal with this, the South Australian Department for Infrastructure and Transport (DIT) published the Master Specification for Design of Earthworks for Roads (RD-EW-D1) which sets the sub-grade volumetric assessment criteria and asks designers to follow the assessment approach set out in AS 2870-2011: Residential slabs and footings. The South Australian method to volumetric assessment is less well-known when compared to other applications commonly used in Queensland and Victoria like the California Bearing Ratio (CBR) based approach (Road and Maritime Services, 2018; VicRoads, 2018), and still poses some ambiguities in its application (Cowan & Gibbons, 2018a; Sagun et al., 2023). This paper aims to clarify some of these ambiguities by providing a simplified framework to assess the shrink-swell behaviour of pavement subgrade and identifying gaps in the literature for further research.

2. BACKGROUND

2.1 Literature Review

As noted by Fityus et al. (2005), assessments of soil volumetric expansion are thought to have commenced in Australia in the late 1960s, led by the work by Aitchison and Woodburn (1969). In the 1980s a methodology for calculating vertical soil displacement based on changes in suction (related to moisture content) using the instability index I_{pt} (defined as the ratio of vertical strain to suction change) was proposed (Mitchell & Avalle, 1984). Despite noting that the core shrinkage test measured under unconfined condition provides a lower bound estimate of I_{pt}, these authors recommended that this test method is appropriate for determining the swell of a confined soil profile in the field because of confinement being offset by the suppression of swell from an increase in confining pressure.

The sensitivity of the core shrinkage test to initial moisture content (wet samples show shrinkage over a range of moisture contents while dry samples exhibit little shrinkage) led to the development of the shrink-swell test to understand the swell potential of soil over a standard suction range (Fityus et al., 2005). The shrink-swell test (described in AS 1289.7.1.1-2003) involves adding the axial strain measurement from a swell test saturated in a consolidation cell under a vertical stress of 25kPa (ε_{sw}) to the axial strain measured from an unrestrained core shrinkage test (ε_{sh}). Factors to account for the lateral restraint to the swell component and for the estimated suction range tested are noted in Equation (1) to calculate the shrink-swell index (I_{ss}) in terms of percentage strain per pF change in suction:

$$I_{ss} = \frac{(\varepsilon_{sw}/2) + \varepsilon_{sh}}{1.8} \quad (1)$$

To convert I_{ss} to I_{pt} for use in vertical soil displacement calculations, an alpha (α) factor needs to be applied to account for the effects of *insitu* lateral confinement and surcharge, as per Equation (2). The selection of an appropriate α value

considers the depth of shrinkage cracking (H_{cr}) where there is no lateral soil confinement, and the lateral and vertical restraint in the uncracked zone assuming movements reduce to zero at a depth of 10m (Fityus et al., 2005).

$$I_{pt} = \alpha * I_{ss} \quad (2)$$

Assessing expected changes in soil suction requires an understanding of the effects that result in moisture content changes within the soil, including effects such as seasonal climatic variation, presence of trees, extent of sealed surfaces or access to water (e.g. well-watered lawns). Mitchell (1984) noted that the presence of trees near structures leads to soil shrinkage over time due to the root structure drawing out moisture from the soil, with the observed impact on soil suction measurements with depth shown in Figure 1.

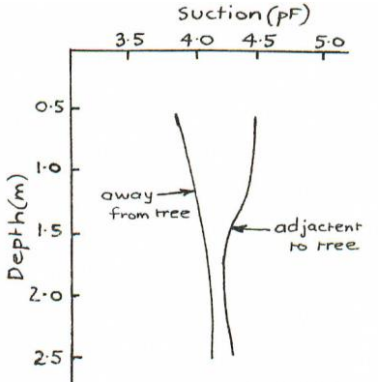

Figure 1: Measured soil suction adjacent to and away from trees (Mitchell, 1984)

2.2 Australian Standard AS 2870: Residential Slabs and Footings

AS 2870 was originally developed for the design of residential housing slabs and footings with contributions from many of the authors noted above and includes a method for calculating the characteristic surface movement and total surface movements accounting for tree effects based on the instability index following the approach outlined by Mitchell & Avalle (1984). The following table summarises the key aspects of the AS 2870 approach and requirements:

Table 1: AS 2870-2011 Summary for subgrade shrink-swell assessment

Item	Description
Characteristic surface movement calculation, y_s (AS 2870 Section 2)	y_s is a function of the sum of y_s for each soil layer, up to a limiting depth of the soil suction profile using Equation (3): $$y_s = \frac{1}{100}\sum_{n=1}^{N}(I_{pt}\bar{}\Delta u\ h)_n \quad (3)$$
Instability index, I_{pt}	I_{pt} is a function of soil shrinkage index (I_{ps}) and lateral restraint factor, α. α is used to account for the cracked and uncracked conditions of the subgrade material: • α = 1.0 cracked zone (unrestrained) • α = 2.0 – z/5 uncracked zone (z = depth below finished ground level)
Soil suction profile, H_s and Δu	H_s, Δu vary based on climates (indexes by Thornthwaite Moisture Index). For Adelaide, H_s= 4.0m considering bedrock and groundwater table (Figure 2). $\Delta u_{surface}$ = 1.2pF.
Differential movement (AS 2870 Appendix F)	For raft footings, the differential mound movement (y_m) can be taken as: • For centre heave: 0.7y_s (both Walsh and Mitchell method) • For edge heave, on initially dry site: 0.5y_s (Walsh) OR 0.7y_s (Mitchell)
Tree-induced movement (AS 2870 Appendix H)	The additional tree-induced movement (y_t) depends on the tree height (HT), arrangement (single or groups of trees), distance from tree to considered building (or pavement area) (D_t) and maximum lateral reach (D_i) and depth of the drying influence of tree (H_t) using the Equation (4), where y_{tmax} is calculated on the same principles as y_s (Equation 3) using the suction change due to trees and depth of soil cracking equal to H_t (i.e. α = 1.0): $$y_t = \{1 - [\frac{\frac{D_t}{HT} - 0.5}{\frac{D_i}{HT} - 0.5}]\}\ y_{t\max} \quad (4)$$ For Adelaide, H_t = 4.0m for a single tree or 4.5m for a tree group, and extra suction change (refer to Figure 2) Δu_{base} = 0.43pF for a single tree or 0.55pF for a tree group.

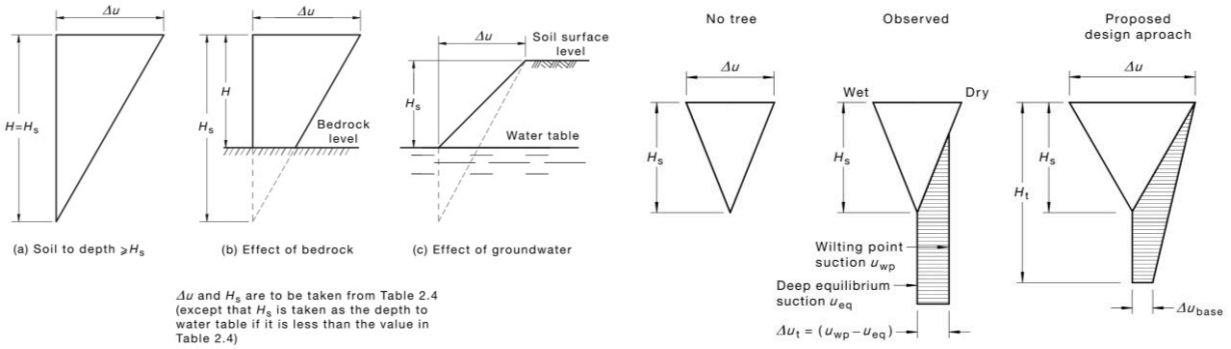

Figure 2: Soil suction profile and effect of bedrock/groundwater level (left), and (right) suction change profile with and without tree effects (extracts from AS 2870-2011)

A commonly accepted approach to derive I_{pt} is to assume that $I_{ps} = I_{ss}$ (Hargreaves, 2007) which aligns with the guidance from Fityus et al. (2005) noted above, with additional consideration for I_{ps} correlations to soil index testing.

2.3 DIT Master Specification RD-EW-D1: Design of Earthworks for Roads (South Australia)

In 2014, DIT started to refer to AS 2870 as its preferred approach for pavement shrink-swell assessment following poor performance of pavement constructed in areas with expansive soils (DPTI, 2014). The latest revision of RD-EW-D1 (DIT, 2022) sets out the requirements and methodology for shrink-swell assessment as follows:

Table 2: Summary of subgrade shrink-swell assessment following RD-EW-D1 Section 5

Item	Description
Characteristic surface movement calculation, y_s	In accordance with AS 2870 characteristic surface movement (y_s) calculation, covering completion of construction and end of the defects liability period stages.
Instability index, I_{pt}	y_s calculations to use I_{pt} as per AS 2870. α factor to be calculated in accordance with AS 2870 section 2.3.2 with the additional stipulation that α must not be less than 1.0.
Soil suction profile, H_s, H_{cr} and Δu	H_s = 4.0m from the top of pavement; this is in accordance with AS 2870 for Adelaide ground conditions (Thornthwaite Moisture Index, TMI ≥ -40 to ≤ -25). H_{cr} = 3.0m from the top of pavement with consideration of depth of cut within previous 2 years (in line with AS 2870: $H_{cr} = 0.75H_s$ in Adelaide). Δu = 0.6pF; in contrast with AS 2870 which recommends Δu = 1.2pF for Adelaide.
Differential movement	Differential mound movement (y_m) taken as equal to y_s unless it can be shown that a reduction is possible due to the extent of the sealed surfaces surrounding the pavement.
Tree-induced movement	Both existing and planned trees and other vegetation shall be considered for design in accordance with the "Special Provisions" document of the Footings Group, South Australia, which in turn refers to AS 2870 Appendix H

RD-EW-D1 requirements are in accordance with AS 2870 with the exception of the soil suction change at surface reduction from 1.2pF to 0.6pF, understood to be based on the work of Aitchison and Richards (1965) as cited in Cowan & Gibbons (2018b). Additionally, RD-EW-D1 set out performance criteria for volumetric assessment (Table 3). Rehabilitation projects may forgo a volumetric assessment where existing pavement can be shown to meet these criteria:

Table 3: RD-EW-D1 Performance criteria for subgrade volumetric changes

Element	Surface Movements	Performance Criteria
Flexible Pavement	Total Movement	Maximum heave or settlement at any point: • Within any 12-month period post-construction < 20mm • Within design life < 50mm
	Differential Movement	Maximum difference in pavement surface level for 2 points 10m apart: • Expressways (including ramps) < 20mm • Urban and Rural Arterials and Connectors < 25mm • Access Roads < 30mm

3. METHODOLOGY

The total surface movement of pavements constructed over expansive soils is calculated in accordance with RD-EW-D1 and AS 2870 by summing the characteristic surface movement (y_s) as well as the tree-induced movement (y_t) where trees are present in the vicinity of the pavement. Figure 3 provides a summary of the necessary input parameters, while Figure 4 sets out a simplified framework for surface movement calculations. The characteristic surface movement (y_s) calculated following this approach (without reduction factor) can be used to classify the site in accordance with AS 2870 as per Table 4 based on the expected level of ground movement.

To reduce both the characteristic and tree-induced movements to an acceptable level (meeting the required performance criteria) it is often necessary to excavate and replace natural soil with controlled fill e.g. Type A material (low permeability engineered fill). The minimum depth required for excavation and replacement is determined by including the pavement and controlled fill layers in y_s calculations with appropriate I_{ps} parameters (0%/pF for granular pavement materials and 0.4%/pF for Type A material in accordance with DIT Master Specification RD-EW-C1: Earthworks).

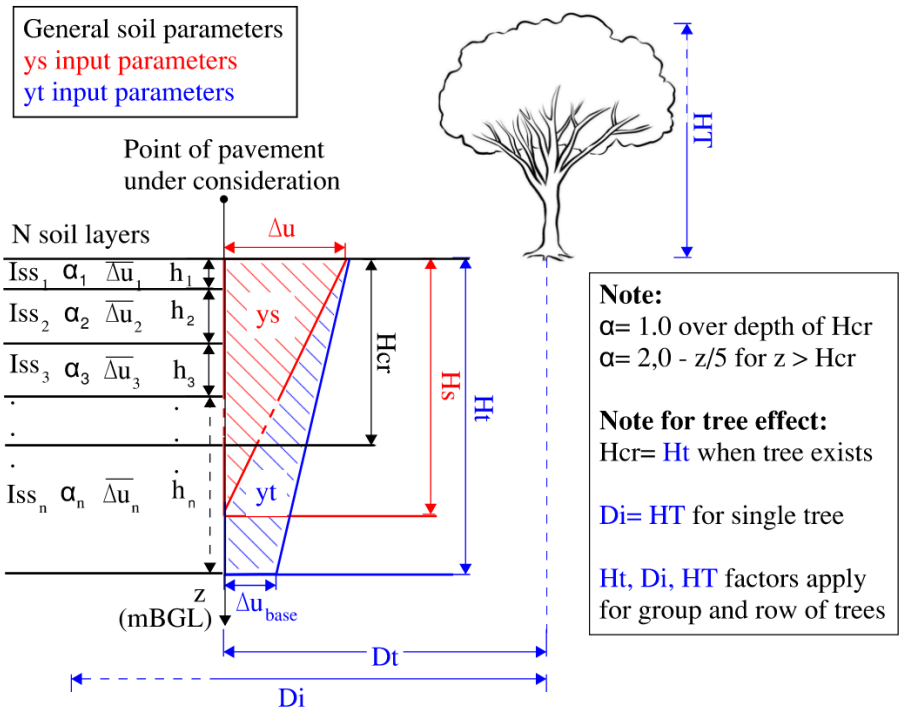

Figure 3: Parameters used in surface movement calculations, simplified for the case of a single tree

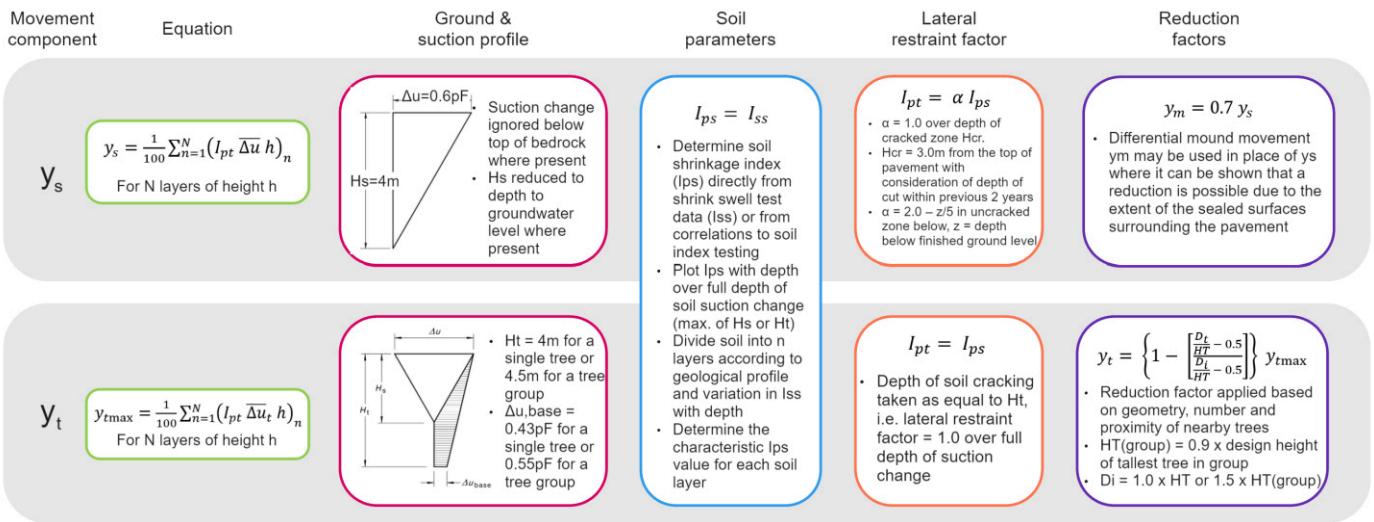

Figure 4: Simplified framework for surface movement calculations

Table 4: AS 2870-2011 Site classification based on characteristic surface movements

Site classification to AS 2870		y_s (mm)
S	Slightly reactive clay sites which may experience slight ground movements	$0 < y_s \leq 20$
M	Moderately reactive clay sites which may experience moderate ground movements	$20 < y_s \leq 40$
H1	Highly reactive clay sites which may experience high ground movements	$40 < y_s \leq 60$
H2	Highly reactive clay sites which may experience very high ground movements	$60 < y_s \leq 75$
E	Extremely reactive clay sites which may experience extreme ground movements	$y_s \geq 75$

4. APPLICATION AND DISCUSSION

4.1 Recent project experience

Volumetric assessment of pavement subgrade was carried out on two recently completed road projects in South Australia following the methodology described above and in accordance with AS 2870 and RD-EW-D1. The subgrade materials for the Regency Road to Pym Street (R2P Alliance, 2020) and Ovingham Level Crossing Grade Separation (PTP Alliance, 2021) projects fell in the range of 'slightly to highly reactive' classification, with y_s ranging between 5mm to 50mm (R2P) and 15 to 30mm (PTP). Both projects followed the process outline in this paper, adopting several generalised ground models along the project alignment to calculate site specific y_s values. I_{pt} was derived from a combination of I_{ss}, plasticity index and soil descriptions, with preference given to I_{ss} data from shrink-swell laboratory tests.

On these projects, it was accepted that the total movement performance criteria permitted 20mm heave or settlement within any 12-month period post-construction (i.e. total of 40mm range of movement), on the basis that the whole pavement subgrade would be expected to either shrink during summer or swell during winter, rather than shrink in some parts and swell in others (excluding anomalies such as leaking services). In addition, while tree effects were identified as a significant factor in the surface soil movement calculation, this movement was not considered to be cyclic due to the suction component of y_t building up gradually over the lifetime of the tree after planting and was taken into account when assessing total or differential movements over the design life of the project. This is illustrated in Figure 5, where it should be noted that this behaviour is expected to reduce with distance from the nearby trees, therefore tree planting arrangement is an important consideration.

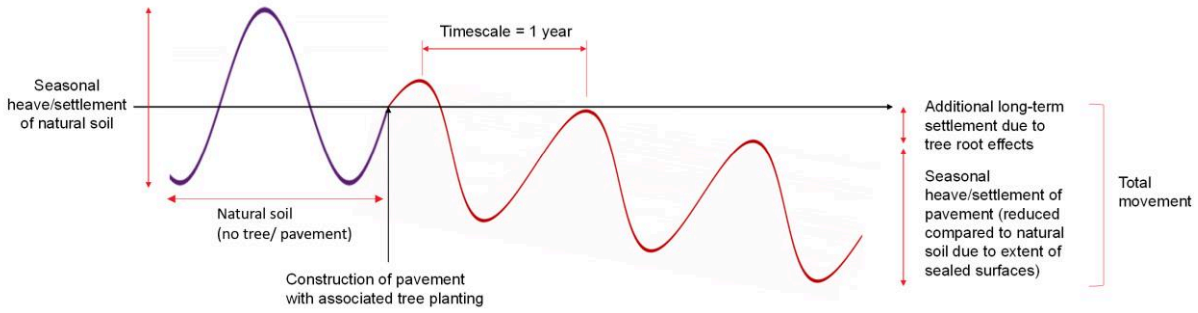

Figure 5: Assumed seasonal and total movements resulting from soil suction changes

4.2 Further considerations

In the methodology and project experience summarised above, tree-induced movements were assumed to be a result of tree planting causing long-term suction increase and settlement, however the opposite effect could occur on an initially vegetated site where trees are removed. It is therefore important to consider the most onerous conditions affecting soil suction change and subgrade movements over the design life of a project, against both the seasonal and long-term total and differential movement performance criteria. It is often found that the differential movement criteria across the pavement is the most onerous condition to be satisfied, from unsealed, vegetated verge to sealed centre of pavement.

To reduce the cost and environmental impact of large volumes of excavation and replacement to satisfy these criteria, adjustments to the landscaping layout (size and location of trees) or adopting species of trees that require less water should be considered, such as plane trees in place of eucalyptus and maple trees (Jaksa et al. 2002). Comparably, where existing pavement is deemed within performance criteria, and no new trees are proposed in the final landscape design, a detailed volumetric assessment is typically foregone and accepted as in compliance with DIT requirements.

RD-EW-D1 notes that differential mound movement (y_m) should be taken as equal to y_s unless it can be shown that a reduction is possible due to the extent of the sealed surfaces surrounding the pavement. As y_m is normally taken as $0.7y_s$

in residential construction where the extent of sealed surfaces is generally less than for road construction, a reduction factor on y_s of 0.7 is considered justifiable for pavement subgrade assessments. However, Cowan & Gibbons (2018b) note that this reduction is valid for the central part of the pavement only, while stating that when using $\Delta u = 0.6pF$ in accordance with RD-EW-D1 (reduced from 1.2pF in AS 2870) then no reduction factor on y_s should be used.

Further work would be beneficial to confirm the volumetric calculation approach and to validate and refine the assumptions noted above, with the aim of driving more sustainable project outcomes. For instance, there is an opportunity to compare the recently completed designs to surface movement measurements of the constructed pavements through review of available field monitoring data or use of remote monitoring technology such as satellite based InSAR data. This would also help to build up an empirical data base to compare AS2870 method performance against CBR-based methods that also have back-up empirical data to compare and validate, as suggested by similar work from Tseng et al. (2018).

5. CONCLUSION

This paper presents a simplified framework to assess subgrade shrink-swell behaviour for newly constructed pavements following the South Australian Master Specification RD-EW-D1 and Australian Standard AS 2870-2011, with an emphasis on South Australian use of the instability index I_{pt} derived from the shrink-swell test. The framework includes consideration for tree-induced movements, which are combined with characteristic surface movements to assess against DIT performance criteria for seasonal and long-term movements for roads projects. The study also highlights further opportunities to review and refine key assumptions as applied in recent and local South Australian pavement projects, where back analysis and comparison of monitored pavement movements against recently completed designs would pave the way for more resilient and sustainable infrastructure design and construction.

6. REFERENCES

Aitchison, G. D. & Richards, B. G. (1965). *A Broad-scale Study of Moisture Conditions in Pavement Subgrades throughout Australia.* Parts 1 - 4. Butterworths, Sydney.

Aitchison, G.D. & Woodburn, J.A. (1969) *Soil Suction in Foundation Design* Proc. 7th Int. Conf. Soil Mech. & Found. Eng., Mexico City vol. 2, 1-9.

Cowan, S. and Gibbons, P. (2018a). *Subgrade treatment design for expansive soils in Adelaide using Australian Standards AS 2870 – Is this the right approach?* Australian Geomechanics Society SA Chapter: Design and construction of earthworks and pavements on expansive clay Adelaide, vol 53, no 1, 97-106.

Cowan, S. and Gibbons, P. (2018b). *The application of AS 2870 for subgrade treatment design of expansive clay in Adelaide*. Australian Geomechanics Society SA Chapter: Design and construction of earthworks and pavements on expansive clay Adelaide, vol 53, no 1, 107-114.

Department for Infrastructure and Transport (2021). *Roads Master Specification RD-EW-C1 Earthworks*, Government of South Australia.

Department for Infrastructure and Transport (2022). *Roads Master Specification RD-EW-D1 Design of Earthworks for Roads*, Government of South Australia.

Department for Planning, Transport and Infrastructure (2014). *DPTI Design Standard EW100: Earthworks for Roads*, Government of South Australia.

Fityus, S. G., Cameron, D. A., and Walsh, P. F. (2005). *The shrink swell test*. Geotech Test J, 28(1), 92-101. DOI: 10.1520/GTJ12327.

Hargreaves, B. L. (2007). *The examination of a possible relationship between the liquid limit and soil shrink index*, 10th Australia - New Zealand Conference on Geomechanics, Brisbane.

Jaksa, M. B., Kaggwa, W. S., Woodburn, J. A., Sinclair, R. (2002). *Influence of large gum trees on the soil suction profile in expansive soils*, Australian Geomechanics Society SA Chapter, March 2002.

Mitchell, P. W. (1984). *The design of shallow footings on expansive soil*. PhD Thesis, University of Adelaide.

Mitchell, P.W. & Avalle, D.L. (1984). *A Technique to Predict Expansive Soil Movements*, Proceedings 5th International Conference on Expansive Soils. Adelaide.

PTP Alliance (2021). *102-60 Pavements Design Report Final Design,* Ovingham Level Crossing Grade Separation Project, Author commercial access.

R2P Alliance (2020), *Technical Note: Pavements – Shrink Swell Assessment*, Regency Road to Pym Road Project, Author commercial access.

Roads & Maritime Services (2018). *Roads and Maritime Supplement to Austroads Guide to Pavement Technology Part 2: Pavement Structural Design*. NSW Roads and Maritime Services, Sydney.

Sagun, S., Rahman, M., Karim, R., Nguyen, H. B. K. (2023). *Review of pavement construction on expansive soil in Australia*. Proceedings of the 14th Australian and New Zealand Conference on Geomechanics, Cairns.

Standards Australia (2003). *Australian Standard AS 1289.7.1.1-2003: Soil reactivity tests - Determination of the shrinkage index of a soil – Shrink-swell index*.

Standards Australia (2011). *Australian Standard AS 2870-2011: Residential slabs and footings*.

Tseng, T., Cocks, G., Verheyde, F. (2019). *Cover requirement over expansive soils in flexible pavement design in Western Australia*, Australian Geomechanics Society, vol 53, no 4, 59-70.

VicRoads (2018). *Code of Practice - Selection and Design of Pavements and Surfacings.* Department of Transport, Melbourne.

CYCLONE GABRIELLE: A COLLABORATIVE APPROACH TO RECONNECTING COMMUNITIES

R Till
Beca Ltd, Wellington, NZ
rebecca.till@beca.com

ABSTRACT

Recent experience in the aftermath of Cyclone Gabrielle on the East Coast of New Zealand highlighted the importance of collaboration during the immediate response to natural disasters. The cyclone resulted in extensive damage to the State Highway network, leading to multiple, extended closures of key regional connections. Given the large-scale recovery, close collaboration between New Zealand Transport Agency Waka Kotahi (NZTA), Higgins Ltd and Beca Ltd, allowed for swift community reconnection. As part of this project, innovative standardised buttress remedial solutions were developed that could be implemented at underslip sites to rapidly reinstate and support the road network. Slope failure causes varied across the network and included river toe scour, concentrated stormwater, soil saturation and stormwater infrastructure failure. Each of these causes needed to be considered in the formulation and application of these standardised buttress solutions to each specific site. On-site geotechnical professionals worked closely alongside contractors to communicate design intent, continuously made site specific adjustments, and provided feedback to the design team on constructability issues allowing the standardised buttress solutions to be rapidly updated for wide use on the network. These geotechnical professionals were able to assess the implementation of these standardised buttress remedial solutions, making sure they have addressed the root cause of failure. The collaboration between NZTA, Higgins, and Beca in developing these standardised buttress solutions demonstrated increased efficiencies and better outcomes for the community.

1 INTRODUCTION

On February 14th, 2023, Cyclone Gabrielle hit the east coast of New Zealand's North Island, resulting in widespread damage throughout the Hawkes Bay and Tairawhiti regions. Cyclone Gabrielle was a significant rain and wind event with the Glengarry rainfall site on the Napier to Taupō road recording 546mm of rainfall over the Cyclone, with almost 400mm falling within 12 hours over the 13th and 14th of February (Hawkes Bay Regional Council, 2023). The daily rainfall gauge at Glengarry can be seen below in Figure 1, highlighting the rainfall in February but also the significant rainfall in the month prior, resulting in saturated ground conditions. This extreme rainfall resulted in widespread damage to the road infrastructure, housing, agricultural land, and industrial businesses throughout the region.

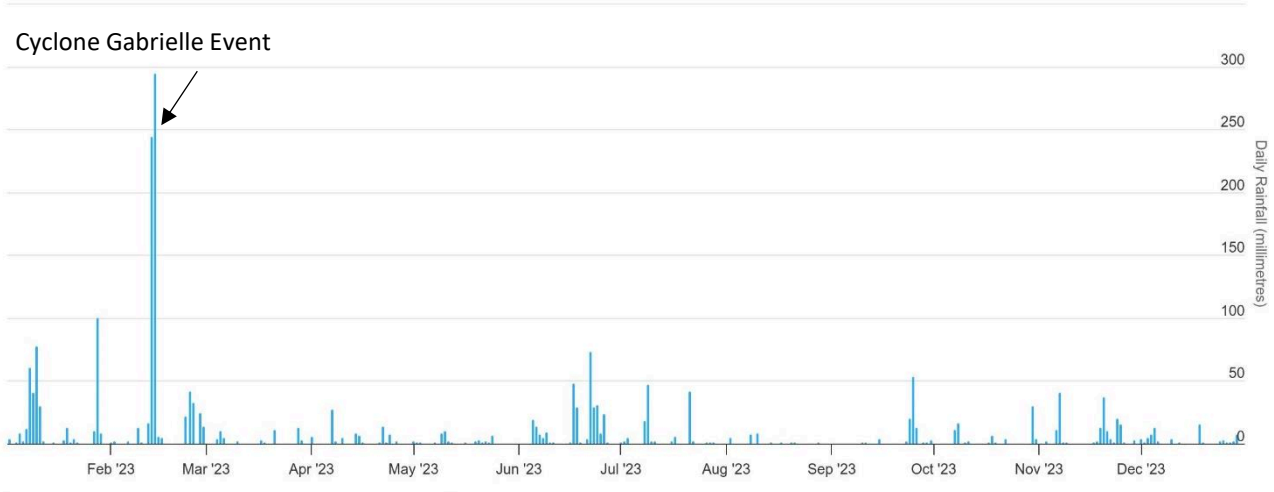

Figure 1: Daily Rainfall Measured at Glengarry Rainfall Station 2023 (Hawkes Bay Regional Council)

2 SETTING

2.1 STATE HIGHWAY NETWORK

The New Zealand Transport Agency Waka Kotahi – Hawkes Bay Network Outcomes Contract (HB NOC) is the road assessment management contract covering the Hawkes Bay region. The HB NOC covers 480km of road, the extent of which can be seen in Figure 2 below.

Road networks provide a vital lifeline to society and, their availability is essential for emergency response and recovery after major events. Cyclone Gabrielle caused a large amount of damage to the Hawkes Bay roading network and resulted in closures of SH2 Napier to Gisborne, SH5 Napier to Taupō, SH38 Wairoa to Lake Waikaremoana and sections of SH51, SH50 and the Hawkes Bay Expressway south of Napier.

In the immediate aftermath of Cyclone Gabrielle, key stakeholders in the Hawkes Bay NOC, New Zealand Transport Agency Waka Kotahi (NZTA), Higgins Ltd and Beca Ltd, worked collaboratively to swiftly reconnect communities and reinstate the road network.

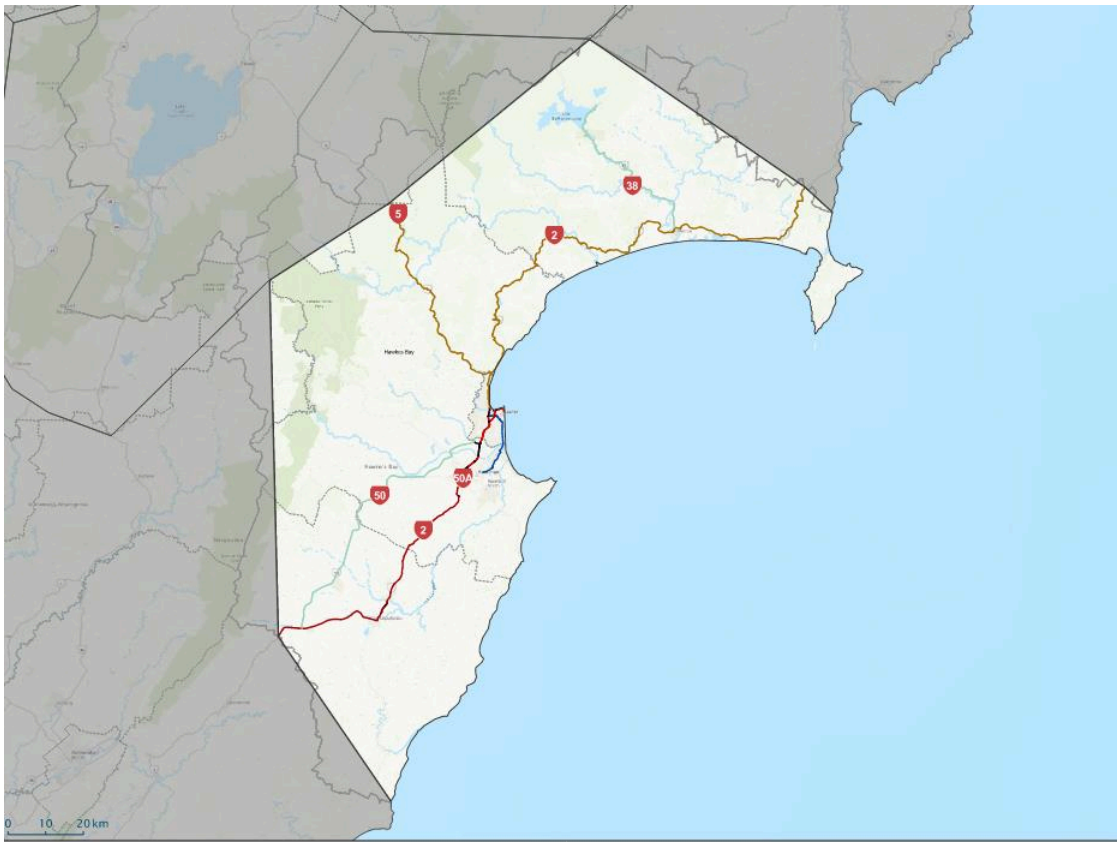

Figure 2: Hawkes Bay Network Outcomes Contract Map. (NZTA Waka Kotahi, 2023)

2.2 GEOLOGY

The geology of the Hawkes Bay region is controlled by the subduction of the Pacific Plate beneath the Australian Plate. Due to the wide geographical area, the geology changes significantly throughout the State Highway Network. The majority of the network tends to be founded on interbedded limestones, mudstones and sandstones overlaid by colluvial materials. On SH5, the Napier to Taupō road, the geology is predominantly ignimbrite and pumice formations of the Taupō Volcanic Zone. The Hawkes Bay Region is an area of rapid uplift associated with the plate boundary. This has resulted in young weak rocks being exposed in steep mountainous country that is easily weathered and eroded by high water flow.

In addition, Hawkes Bay is in a high seismicity region due to its proximity to the Hikurangi Trench (GNS, 2022). There are several faults that cross through the Hawkes Bay region including the Mohaka Fault and the Poukawa Fault that produced the Napier 1931 earthquake. This provided an additional challenge during the recovery of Cyclone Gabrielle, with more extensive designs required to withstand this high seismicity for long term solutions.

3 RESPONSE

3.1 ASSESSMENT

Following Cyclone Gabrielle, a project team was established which included the Beca Geotechnical team, the HB NOC Contractor (Higgins Ltd), the NZTA Waka Kotahi Network Manager and the NZTA Waka Kotahi Geotechnical Subject Matter Expect (SME). The Geotechnical team conducted network wide assessments of all sites, to allow for categorisation and prioritisation, and enable quick decision making within the project team.

The network-wide assessment identified over 250 geotechnical failure sites across the Hawkes Bay State Highway network. These sites had a range of failure causes including river toe scour, concentrated stormwater, soil saturation and stormwater infrastructure failure. The damage to the road network varied, with some complete loss of multiple lanes, shoulder loss, guardrail support loss and stormwater infrastructure damage.

Given the large number of sites, there was an opportunity for standardised remedial solutions, as many of the sites shared similar characteristics.

3.2 DEVELOPMENT

During the initial assessment stage, the scale of the damage to the network and the fragility of the remaining roads was quickly realised. This led to the need for rapidly implementable solutions to reinstate the road network. Standardisation of the field assessment, design and construction phases led to rapid prioritisation and increased efficiencies network wide. In addition to this, the preference for judgement-based solutions allowed for reduced design timelines.

The standardised remedial solutions had a range of requirements to ensure they would be widely applicable in the region. The development of these solutions considered:

- Material flexibility. Material availability was considered a significant factor during the development of these standardised buttress solutions. Understanding which materials were readily available in the region allowed for increased sustainability with reduced carting distances. It also ensured that the standardised solutions had flexibility in the materials used, which was essential for the longevity of solution usage as material availability is likely to change over time.
- Remedial solution adaptability. Having a standardised solution that could be adapted to site-specific conditions allowed for a wider range of sites to implement this standardised solution. This could include site-specific conditions such as slip dimensions, slope geometry, and foundation ground conditions. In particular, due to the lack of ground investigations at most sites, ensuring that the solution could be adapted to different ground conditions during construction was essential.
- Remedial solution applicability criteria. Ensuring that the remedial solutions addressed a large number of failure mechanisms was essential in ensuring they were fit for purpose. Understanding which types of failures the remedial solutions could not address was equally important. Having criteria for each site to meet for implementing these designs was important to prevent inappropriate installations, especially in cases where the installation of a standardised solution could decrease stability, such as in the case of global failures.

Once the remedial solution requirements were understood, three standardised buttresses were developed based on engineering judgement, by experienced geotechnical professionals. It was particularly important that senior design verifiers were involved, who were familiar with the region, sites and solutions, when using these standardised remedial solutions to confirm the applicability and site-specific variations. These standardised buttresses were developed in close collaboration with the NZTA SME and Higgins Construction team, to ensure an agreed and readily constructable remedial solution.

Three standardised buttress solutions were developed and adapted to meet site-specific requirements. All three were rock filled buttresses, with geofabric and subsoil drainage, but each solution had a few variations to be applied depending on the site. These standardised buttress remedial solutions can be seen below in Figure 3 and Figure 4.

- Standardised buttress type A was a gravel buttress, with some scour protection at the toe.
- Standardised buttress type B was a gravel buttress with geogrid reinforcing and gabion wall facing.
- Standardised buttress type C was a gravel buttress with a rip rap facing.

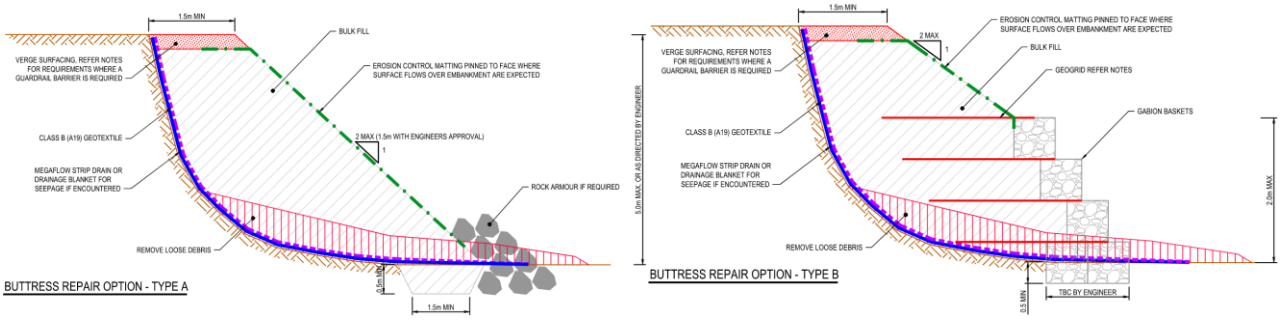

Figure 3: Standardised Buttress Type A (left) and B (right)

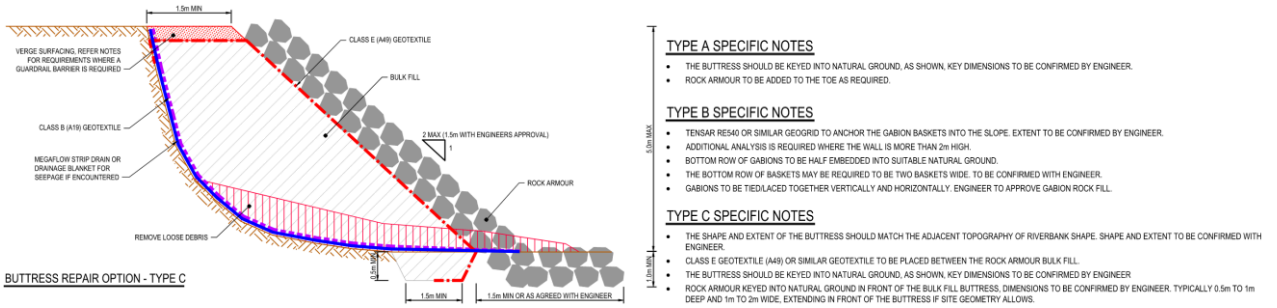

Figure 4: Standardised Buttress Type C (left) and Specifications(right)

There was still a number of known risks associated with the use of these standardised buttresses, due to the lack of ground investigations and design analysis. Communication within the project team ensured that these risks were understood, and the residual risks were known and accepted by the asset owner. There were still some unknowns with the performance of these standardised buttress solutions which may result in some buttresses requiring 'topping up' or additional design measures for longer-term resilience.

3.3 IMPLEMENTATION

A robust process was required to assess the applicability of these standardised buttress designs to ensure they are implemented appropriately. The Geotechnical team conducted desktop studies for each site, which highlighted historic aerial photos, geology, failure mechanisms, and stormwater infrastructure to assess whether the standardised buttress designs would be effective. This assessment also highlighted some sites which may not have been appropriate for the standardised buttress designs, such as deep-seated global failures, deep soft material at the toe of the slip, or significant amounts of groundwater or stormwater flow. The desktop study formats were also standardised for use at all sites during the recovery, aiding in swift communication of risk and information to the project team. The project team used the desktop studies alongside any constructability or material availability considerations to decide which standardised design could be constructed. In some cases, shallow ground investigations such as hand augers and DCP scala tests were carried out to confirm the depth to competent ground.

Once it was established that a standardised buttress was applicable for a site, a walkover would occur with a member of the Geotechnical team and the construction team to determine any site-specific requirements such as extents, stormwater infrastructure, or toe key depth. This was also an opportunity to plan any construction monitoring requirements and any hold points that the Geotechnical team would need to be on site for. A verifier who was familiar with remedial solutions was always involved to ensure that the buttresses were appropriately implemented.

During construction, the Geotechnical team worked in a high-trust environment with the contractors on-site, with regular meetings with the wider project team and personnel stability adding to this trust. This close working relationship allowed for quick assistance with any queries during construction and increased the experience of the site teams. The repetition of buttress construction led to a greater understanding of the requirements of the standard solutions. Construction included stormwater infrastructure reinstatement or improvement to ensure that the root cause of the failure had been addressed.

As construction progressed, the standard solutions were continuously refined based on site requirements and underwent many iterations. One example of this was the Standardised Buttress Type B, which was initially designed as a geogrid reinforced gravel buttress with a gabion basket facing. Throughout the construction process, the project team found that sourcing gabion basket fill was challenging in the Hawkes Bay region, and therefore the Type B solutions was often not preferred. This design was often implemented as a geogrid reinforced gravel buttress with a rip rap facing. It was also found that some remedial solutions were more applicable for certain types of failure mechanisms than others. Standardised

Buttress Type C was our most widely used standardised remedial solution as the rip rap facing protected the buttress from erosion. This was particularly used for sites which had failure mechanism of river scour and stormwater overtopping.

An example of this standardised buttress remedial solution implementation was a site on SH5 which had been caused by scour from the Mangakōpikopiko Stream. This was an underslip where the shoulder had been eroded up to the road edgeline and a solution was required to support the road. Through the desktop study and project team discussions it was decided that a Standardised Buttress Type C solution was applicable for this site. Site photos can be seen below in Figure 5.

Figure 5: Mangakōpikopiko Stream Scour February - May 2023

The Geotechnical team provided guidance and support to the site team during the construction of the buttress. The flexibility of these standardised buttress designs meant that questions often arose regarding the extent of the buttress, materials to be used, and constructability issues, which the project team collectively addressed. This collaborative approach resulted in a successful outcome, with the swift implementation of the buttress preventing further erosion into the road corridor and enhancing support for the road network.

A further case study below shows the remediation of an underslip along Waikaretāheke Stream on SH38 between Wairoa to Waikaremoana. Site challenges included the variable stream height due to the proximity to Waikaremoana dam, and also the isolated nature of the site, with limited reception and long travel times. Site-specific modifications were made to the standardised buttress as shown in Figure 6, to allow for construction under variable stream heights. Repetition of the buttress construction at multiple faults along SH38 allowed for a high trust environment with the local contractors to be established, an important relationship considering the isolated nature of the site.

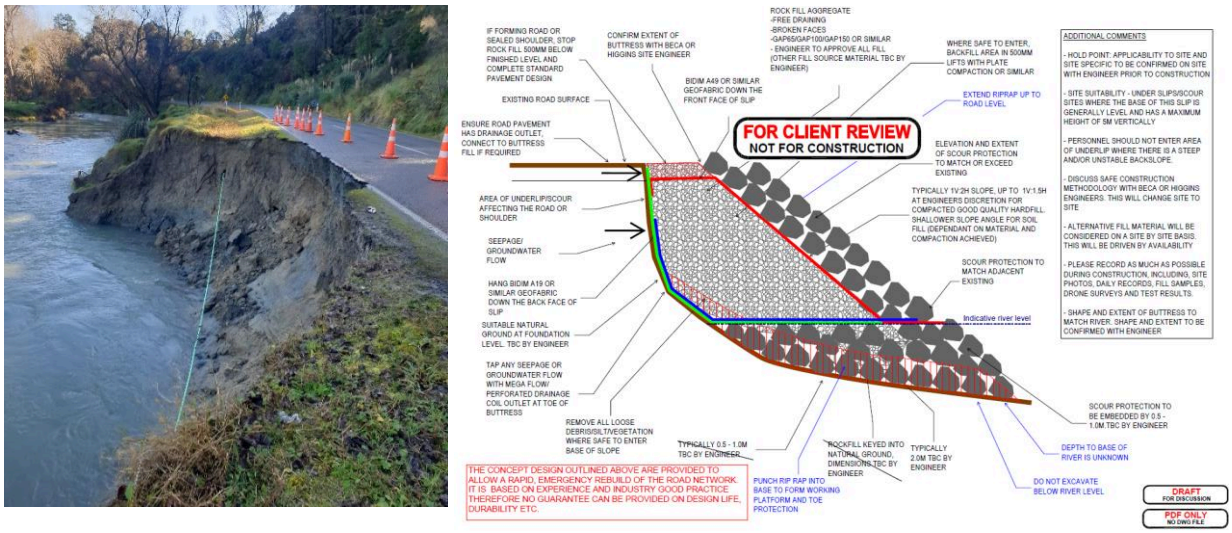

Figure 6: Waikaretāheke Stream Underslip June 2023 (left) and Site-Specific Standardised Buttress Solution C (right).

Figure 7: Waikaretaheke Stream construction photo (left) and completed photo (right)

4 OUTCOME

The standardised buttress remedial solutions were implemented at many underslip sites on SH2, SH5 and SH38 throughout the Hawkes Bay region and provided support to the fragile road network. The buttresses have continued to be monitored for settlement or any signs of instability within the road corridor and have found minimal movement over the past year since construction.

Due to the large scale of rebuild and resilience work that was required following Cyclone Gabrielle, NZTA Waka Kotahi and Kiwi Rail set up the Transport Rebuild East Coast Alliance (TREC) to continue to support the region during their recovery in both Hawkes Bay and Tairāwhiti. The Hawkes Bay NOC was brought into the TREC Alliance with many of the personnel continuing to work in the region. The standardised buttress designs are continuing to be used within TREC and are being further developed around the Tairāwhiti and Hawkes Bay Regions. The standardised buttress designs could be further developed for implementation throughout New Zealand, enabling a prompt recovery from future natural disasters.

The close collaboration between NZTA Waka Kotahi, Higgins Ltd, and Beca Ltd in developing these standardised buttress remedial solutions demonstrated increased efficiencies and better outcomes for the community. The trust and engagement from all members of the project team was essential in the successful reinstatement of the State Highway Network.

5 ACKNOWLEDGEMENTS

The author wishes to thank the New Zealand Transport Agency Waka Kotahi and Higgins Ltd for their permission to publish this paper. The author would also like to acknowledge Joe Cant, Adam Akehurst, Sigfrid Dupre, and the many colleagues who have assisted with this work.

REFERENCES

GNS (September 2022). 2022 National Seismic Hazard Model: Hawke's Bay region. NSHM Info sheet - V1 Sept 2022.

Hawkes Bay Regional Council (retrieved April 2024). Rainfall data shows intensity of Cyclone Gabrielle. https://www.hbrc.govt.nz/home/article/1415/rainfall-data-shows-intensity-of-cyclone-gabrielle-

JET GROUTING CAMPAIGN TO MINIMISE TUNNELLING RISKS IN COODE ISLAND SILT

Erich Kaese and Ashkan Shafee
Delve Underground

ABSTRACT

Melbourne Water's Hobsons Bay Main Sewer Project will divert around 30 percent of Melbourne's wastewater and enable remediation of the existing sewer that was built in the 1960s. This upgrade includes a connection tunnel between the upstream connection utility hole on the existing main sewer and the siphon inlet vortex, which connects to the on-grade conduit under the Yarra River. This upstream connection will enable isolation and flow diversion between the existing conduit and new siphon. Site investigations indicated very soft to soft Coode Island Silt in the tunnelling zone on the Yarra River East bank, necessitating measures to mitigate substantial tunnelling and ground settlement risks. The short drive length for the connection tunnel made tunnel boring machines (TBMs) and pipe jacking cost-prohibitive and impractical, and although Victoria's history includes weak soil tunnelling with cast-iron shields and hand excavation, safety awareness has made that approach effectively obsolete. Moreover, Victoria's recent expertise in larger diameter tunnelling is generally through siltstone and occasionally in more competent soils. Given these constraints, jet grout columns were installed to create a grouted mass in the tunnelling zone prior to sequential excavation method (SEM) tunnelling. The tunnel temporary support design accounted for two scenarios: (1) fully treated and (2) major zones of untreated ground underneath an abandoned sewer above the tunnelling zone. Inspections were undertaken after every excavation advance to observe ground improvement quality and predict support type selection. This paper summarises this portion of the project from initial design through design development and construction.

1 INTRODUCTION

1.1 PROJECT BACKGROUND

The Hobsons Bay Main Sewer is a critical part of Melbourne's sewer network, transferring around 30 percent of Melbourne's wastewater to the Western Treatment Plant. The existing sewer was first constructed in the 1960s, it is now reaching the end of its service life and requires rehabilitation, including re-lining the conduit to provide additional protection against concrete deterioration and reinforcement corrosion. The sewer is located under the Yarra River between Port Melbourne and Spotswood. To rehabilitate the existing sewer, a duplicate sewer was constructed to allow sewage flows to be diverted during rehabilitation works. The project, being delivered by John Holland on behalf of Melbourne Water, began in September 2021 and is expected to be completed in late 2024. Delve Underground was appointed by John Holland to provide temporary works design and impact assessment.

The new sewer and existing sewer will work together to transfer the wastewater flows and the duplication has been designed to accommodate flows projected for the year 2071. This paper outlines the overall scope of this project and discusses design and construction of the SEM tunnel in between the shafts located on the East bank and draws conclusions on the adequacy of ground improvement works in conjunction with temporary tunnel support.

1.2 PROJECT LOCATION

The project is located within the estuarine environment of the Hobsons Bay area, approximately 9 km southwest of the Melbourne central business district (CBD). The works for the project consist of an approximately 678 m long siphon tunnel beneath the Yarra River with siphon inlet and outlet structures on either riverbank. On the East bank, the existing sewer system will be intercepted by a new upstream connection structure (UCS) to enable isolation and permit flow diversion to the new siphon inlet structure (SIS) by a short tunnel of about 25 m in length. On the West bank, the siphon tunnel connects into the new siphon outlet structure (SOS) and then into the new downstream connection structure (DCS) on the existing North Yarra main sewer (NYM).

The sequential excavation method (SEM) tunnel on the Yarra River East bank between UCS and SIS is shown in red in Figure 1. The land on the East bank is relatively flat with an approximate elevation of 2 m Australian Height Datum (AHD).

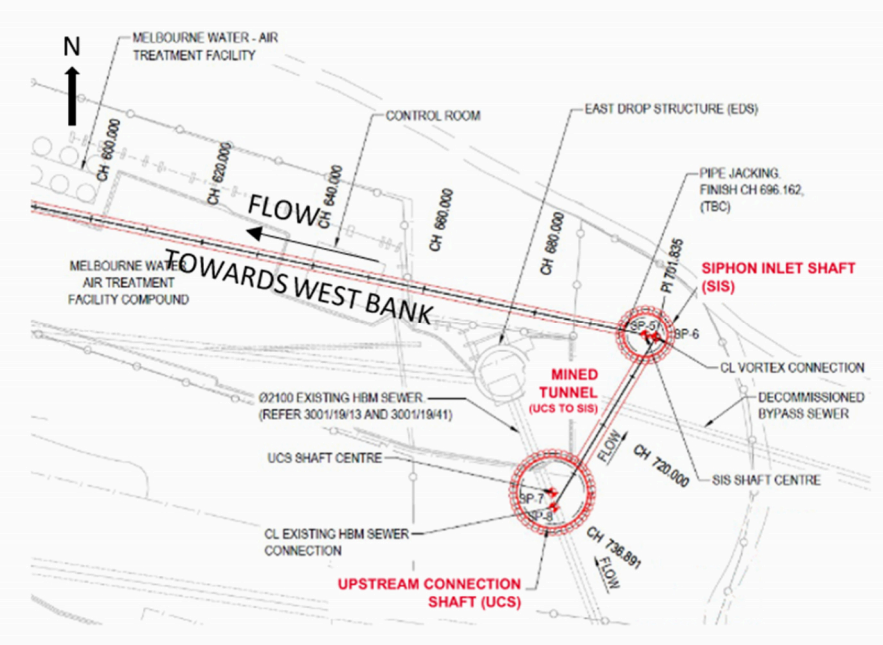

Figure 1: Hobsons Bay main sewer tunnel alignment and eastern bank shaft locations (in red) (Menard 2022)

1.3 EXPECTED GEOLOGY IN TUNNELLING ZONE

The Geotechnical Interpretive Report (GIR) for the project (WSP Australia 2022) outlines the geology of the East bank site as underlain by varying amounts of fill, overlying a sequence of Quaternary sediment deposits. Notably, the tunnel between UCS and SIS was expected to be excavated entirely within Coode Island Silt, described as dark grey to black, very soft to soft, normally to slightly overconsolidated silty clay. Geotechnical properties for Coode Island Silt were derived from an extensive site investigation program, including cone penetration tests (CPT), standard penetration tests (SPT), and a series of unconsolidated undrained (UU) and consolidated undrained (CU) triaxial tests on laboratory samples, suggesting undrained shear strength values of 20 to 75 kPa, effective friction angle of 28 to 35 degrees, and an elastic modulus of 7.2 to18 MPa, calculated from CU tests (WSP Australia 2022).

2 DESIGN

2.1 RISKS ASSOCIATED WITH TUNNELLING IN SOFT SOIL

Soft soils, such as Coode Island Silt, commonly have very little to no standup time, which means SEM tunnel passive support, consisting of a layer of sprayed concrete, has inadequate time to cure to sufficient strength and abate the movement of the soil caused by the opening. Tunnel pre-support, installed prior to tunnel excavation via grouted spiles or grouted canopy tubes in combination with steel sets and a thick, passive, sprayed concrete (shotcrete) lining, can stabilise more competent ground temporarily. Nevertheless, it has not been widely shown to satisfactorily mitigate the excavation-associated risks in material as soft as Coode Island Silt within the safety constraints required by modern Australian civil engineering construction standards. Additionally, the method can be both costly and, at times, ineffective. Another significant risk in SEM excavation through saturated soft soils is that it can lead to groundwater table lowering and considerable surface settlements. It may be noted that Victoria's tunnelling history does include soft soil tunnelling with cast-iron shields and hand excavation. However, today's workforce safety culture has made that approach effectively obsolete.

2.2 DESIGN DEVELOPMENT

Tunnelling via TBMs, where the time between excavation and lining placement is considerably less than SEM, or cut and cover excavations, where the soil is completely excavated prior to tunnel construction and then backfilled, are two methods well-suited to soft soils as they minimise the ground collapse and movement risk in these ground conditions. Pipe jacking is also an option in these soils, depending on the size and extent of the excavation.

However, TBMs are usually cost-prohibitive for short drive lengths—as was the case on this project—and with the tunnelling depth needed for this project, the cut and cover approach had the potential to result in very high movement

magnitudes near the ground surface, necessitating high stiffness cut and cover support elements. The degree of cut and cover ground support was cost-prohibitive for this project, as was pipe jacking due to the short drive length.

Given these constraints, a relatively new option for Victorian tunnelling was considered: ground improvement via jet grouting in the tunnelling zone prior to tunnel excavation. This approach enables adequate standup time of the surrounding ground with a relatively dry face and controlled water ingress inside the tunnel, substantially mitigating the inherent risks of tunnelling through soft soil if paired with a robust passive support system. SEM tunnelling through treated ground has been successfully used in the construction of select cross passages for Melbourne Metro (Vincent et al. 2020).

2.3 FINAL DESIGN

With the very soft to soft Coode Island Silt expected in the tunnelling and shaft base zones, ground treatment in the form of jet grouting at the base of the UCS and SIS shafts and along the tunnel alignment in between shafts was adopted. The primary aim of the jet grouting campaign was to mitigate the risk of hydraulic ground failure at the base of the shafts, potential excessive groundwater ingress into the excavations, and large tunnel deflections, as well as to prevent groundwater table drawdown which could result in consolidation of the silt layer, leading to considerable settlement of the ground surface.

Menard Oceania was appointed by the principal contractor John Holland to complete the detailed jet grout design and construction of the ground improvement works after Delve Underground completed the concept and tender ground treatment design and project specifications. The jet grouting specifications which were prepared by Delve Underground required a minimum 1.5 MPa unconfined compressive strength at 28 days, 16.0 kN/m^3 treated ground unit weight, 1.0 × 10^{-7} m/s treated ground maximum hydraulic conductivity, and 250 MPa elastic modulus of the treated ground (Menard 2022).

Jet grouting along the tunnel alignment between the shafts was designed to create a 7.0 m × 7.0 m × 23 m block of treated ground around the tunnel with 1.9 m diameter overlapping vertical jet grout columns at a maximum spacing of 1.35 m. The challenge in achieving such a treated ground block was a 2.95 m outside diameter abandoned diversion sewer located approximately 1.5 m above the excavation line (E-line) of the SEM tunnel starting from chainage 4.5 m to 8.0 m measured from the tunnel portal in the SIS shaft, as shown in Figure 2. The decision was made to add inclined 2.4 m diameter jet grout columns in the design so that within the tunnelling zone at the underside of the abandoned sewer, the maximum ground extent could be jet grouted. However, this inevitably led to a V-shaped potentially untreated zone just beneath the sewer. Still, this untreated area was significantly smaller in volume compared to the potentially untreated zone if only vertical jet grout columns were constructed.

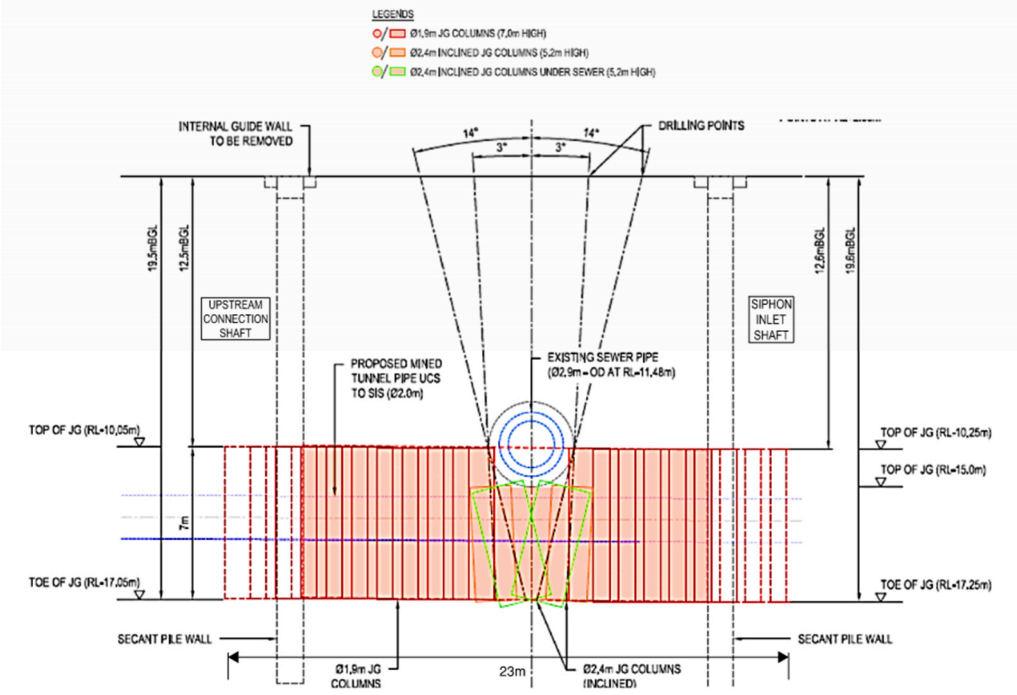

Figure 2: SEM tunnel treatment block with inclined jet grouting column underneath the abandoned sewer (Menard 2022)

Consequently, the SEM tunnel temporary support design accounted for two scenarios: (1) fully treated and (2) major zones of untreated ground. The tunnel support design for the treated ground zone (support type I) demonstrated, from design calculations, that the treated ground is generally self-supporting and only a thin 100 mm layer of shotcrete is sufficient for supporting potential grout blocks/wedges. On the other hand, tunnel support for the zone with major untreated ground extents (support type II) included pre-support in the form of 6 m long face dowels at 750 mm spacing, 6 m long hollow spiles at 200 mm spacing, and a passive support system in the form of steel sets at 1 m spacing with a 200 mm layer of shotcrete. Excavation advance lengths were limited to 1 m. Design calculations and soil-structural interaction analysis will be discussed in detail with comparison to monitoring data in a future study.

2.4 UNCERTAINTIES TO BE RESOLVED DURING CONSTRUCTION

Tunnelling projects, due to their lengths, are usually characterised by complex subsurface settings, making it difficult or impossible to propose a single geological model for excavation and support design. Accordingly, the approach known as the observational method was developed, where the relevant support design to be installed in the next excavation advance is selected, based on the encountered conditions, from a predesigned tool chest of engineering designs that address all possible geological conditions documented in the project's GIR (Peck 1969). Hence, with a continuous, managed, and integrated process of design, construction control, monitoring, and review, greater overall project cost-effectiveness can be achieved without compromising safety. The observational method has been widely used in many major Australian tunnelling projects in the past decades. In this case, the design's success depended on the observational method, given the uncertainty of the ground improvement condition under the sewer. This necessitated having geotechnical engineers and a geotechnical engineering manager be on site to confirm support types, collect water ingress data, and assess the ground conditions through probe holes and visual inspections of the face, crown, and sidewalls.

3 CONSTRUCTION

3.1 PRODUCTION OF JET GROUT COLUMNS

Before beginning the production of jet grouting columns, a test program was performed to adjust parameters for the jet grouting campaign, where necessary, and satisfy quality control requirements. Following the completion of the trial jet grout columns and relevant tests, maximum centre-to-centre spacing of the jet grout columns was optimised, and unconfined compressive strengths of the cored samples from trial columns exceeded the design specification of 1.5 MPa. Jet grouting column installation was initially completed for the SIS invert zone and, thereafter, the connection tunnel zone block. The Issued for Construction (IFC) drawing for the jet grout columns at column (i.e. treated ground block) base level, presented in Figure 3, demonstrates the installed hexagonal pattern layout of overlapping columns for optimised ground improvement coverage.

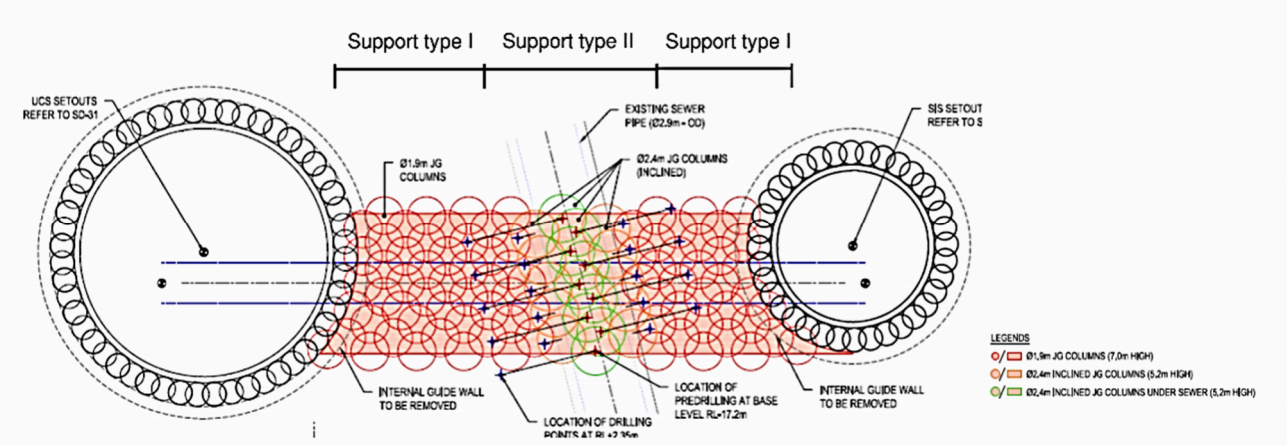

Figure 3: Plan view at jet grout base level (Menard 2022)

3.2 SEQUENTIAL EXCAVATION OF THE TUNNEL

SEM tunnel construction commenced with cutting the secant wall piles in the SIS shaft, followed by drilling six probe holes through the tunnel portal to assess the treated ground conditions and measure water ingress. The jet grouted mass appeared homogenous, without significant discontinuities or clear delineations between grout and soil within the grouted mass. Only minor moisture seepage was observed in the probe holes; however, polyurethane sealant was injected into the probe holes to reduce potential water ingress at the treated ground/shaft interface. The excavation and support cycle started with support type I with the first 1 m long advance showing successfully jet grouted tunnel face, crown, and sidewalls with maximum scattered < 5% untreated soft silt or clay masses (i.e. inclusions). The same observations were made during the next two cuts. At approximately 1.5 m from the abandoned sewer, another set of six probe holes was drilled; water ingress was observed in four of the holes, with an average ingress rate of 97 millilitres/minute and a maximum ingress rate of 250 millilitres/minute. The probe holes were all grouted with polyurethane sealant as a measure to reduce the observed ingress.

Based on the observations, the support type was changed to support type II, which included preliminary support in the form of face dowels and spiles, and passive support of steel sets with shotcrete. The excavation progressed under the abandoned sewer in potentially semi-treated ground. Field observations at these cuts showed that tunnel face, crown, and sidewalls included about 15 to 20% untreated inclusions primarily concentrated in the crown. While no running water was observed, the temporarily exposed surfaces, both at face and excavation perimeter, were highly damp compared to being relatively dry in the cuts prior to reaching the sewer. Nevertheless, support type II was adequate for preventing any instability arising from the semi-treated zone in the crown. Location of support type I and II are shown in a plan view in Figure 3.

Figure 4 compares a typical tunnel face observation away from the abandoned sewer (i.e. successfully grouted) and the tunnel face with considerable inclusions in the crown. The untreated Coode Island Silt inclusions appear as dark grey to black zones in contrast against the pale grey to grey zones of the successfully jet grouted ground.

(a) (b)

Figure 4: Comparison of ground improvement conditions; (a) underneath the sewer and (b) within the treated block away from the sewer

When the tunnel face advanced about 1.5 m beyond the sewer, a third round of probe holes was drilled. The magnitude of water ingress observed had decreased since the last round of probe holes; water ingress was observed in just two of the holes, with an average ingress rate of 38 millilitres/minute and a maximum ingress rate of 140 millilitres/minute. The observations were reviewed, and the decision was made to switch back to support type I.

Tunnel face, crown, and sidewall inspections continued with every 1 m advance, and average scattered <5% inclusions were observed. The fourth and fifth round of probe holes showed reduced water inflow. In two of the final three tunnel advances, the maximum scattered inclusions were estimated to be about <5%, with the penultimate cut estimated at <10%. From there, the tunnel reached the UCS piles, which were subsequently cut from within to enable tunnel breakthrough into the UCS shaft.

4 CONCLUSION AND FUTURE STUDY

The Hobsons Bay SEM tunnel represents a successful implementation of soft soil ground improvement via jet grouting and subsequent tunnelling through the grouted mass. It is among the first projects to integrate the two in Victoria's tunnelling history. As demonstrated, observations and measurements from the tunnel confirmed that the ground improvement campaign readily minimised the risks of tunnelling through saturated, highly compressible soil, even underneath the existing sewer at about 1.5 m clearance. It is the authors' belief that this demonstrates the viability of future projects to follow a similar program to manage soft soil tunnelling.

As a future study, the authors plan to conduct a three-dimensional numerical modelling back-analyses of design calculations and as-built shaft movements assuming similar levels of silt inclusions to those observed on site and further substantiate the viability of larger SEM tunnels and advance lengths via the same approach.

5 ACKNOWLEGMENTS

The authors wish to sincerely thank Mr. Michael Behrens (principal engineer at Delve Underground) for his insights, consultation, and review of this work and Mr. Paul Ostens (associate engineer at Delve Underground) for his site support and management.

6 REFERENCES

(Unpublished) Menard (2022). Hobsons Bay Main Sewer Yarra River Duplication Project, *Ground treatment design and construction method report*.

Vincent, P., Hubaut, A., Chan, S.P., and Auvergne, S. (2020). Cross passages ground treatment for Melbourne Metro tunnel project. *Australian Geomechanics Society Sydney Chapter Symposium,* November 2020, pp. 17-30.

Peck, R. (1969). Advantages and limitations of the observational method in applied soil mechanics. *Géotechnique*, Volume 19, Issue 2, pp. 171-187.

(Unpublished) WSP Australia (2022). Hobsons Bay Main Sewer Yarra River Duplication Project, *Geotechnical Interpretive report*.

INFLUENCE OF CLIMATIC FACTORS ON PAVEMENT MOISTURE AND LONG-TERM PERFORMANCE OF UNBOUND PAVEMENT WITH SPRAYED SEALS

Dr. Chathuri Maha Madakalapuge[1], Dr. Troyee Tanu Dutta[2], Prof. Jayantha Kodikara[3]

[1]Beca Pty Lt. Sydney, Australia, [2]Indian Institute of Technology Kharagpur, India, [3]Monash University, Australia

ABSTRACT

Road pavement rehabilitation entails substantial costs for governments worldwide, with annual expenditures reaching billions of dollars. Moisture infiltration emerges as a primary cause of road failures. In Australia and New Zealand, a major share of surfaced roads is constructed with sprayed seals or chip seals due to their cost-effectiveness. However, the permeable nature of these seals renders the pavements susceptible to moisture-induced degradation. Moisture exchange through these seals, influenced by prevailing climatic conditions, triggers temporal moisture variations in pavement layers throughout the service life. These fluctuations, induced by climatic effects, detrimentally affect the shear strength and stiffness properties of pavement materials, leading to road failures. Consequently, incorporating these temporal moisture dynamics into pavement design becomes imperative. Yet, the current Australian pavement design framework lacks advancement in addressing climatic influences, constituting a primary limitation. The absence of precise models to forecast long-term. moisture variations, considering climatic factors, underscore this deficiency.

To address this gap, the authors developed a computer model integrating daily climatic variations to predict moisture fluctuations in unbound pavements with sprayed seals, by capturing the essential physics of unsaturated soil mechanics. This paper elucidates a long-term pavement performance analysis utilizing the developed model. It evaluates the effect of daily climatic conditions on long-term pavement performance, based on numerical results obtained for three climates in Australia. Moreover, it reveals moisture variation patterns in terms of Degree of Saturation (S_r) and (s) over a 10-year service life and evaluates key parameters defining the pavement's service moisture condition and temporal fluctuations of pavement layers.

1. INTRODUCTION

In Australia, approximately 90% of surfaced roads consist of unbound pavements with sprayed seals (Austroads, 2017), which are common in rural areas and similar regions like New Zealand (where they are known as "chip seals") and South Africa (Ball and Patric, 1998; Tower and Ball, 2001). The primary advantage of this pavement type is its low initial cost. Unbound pavements typically comprise four layers: the wearing course (sprayed seal), base, subbase, and subgrade. The structural integrity of unbound pavements relies heavily on the base and subbase layers, commonly composed of materials such as crushed rock (CR), gravel, soil aggregates, and granular stabilized materials. CR is notably prevalent in Australia due to its ease of compaction and mechanical stability, resulting from a well-graded particle size distribution. It is classified into four classes per VicRoads specifications, with Class 1 and 2 used for high-traffic base courses and Class 3 and 4 for subbase layers under reduced stress.

After compacting the base layer, a seal is applied to prevent moisture infiltration. Single-single sprayed seals, involving a layer of hot bituminous binder and aggregates, are most common. Despite efforts to construct impermeable seals, practical limitations mean some moisture ingress occurs, reflected by the seals' saturated permeability ranging from 10^{-5} to 10^{-9}m/s. This moisture ingress significantly affects pavement layers over their service life. Moisture conditions in pavement layers fluctuate with climatic factors such as precipitation, evaporation, relative humidity, and temperature. Studies, including those by Kodikara (Kodikara, Islam T and Sounthararajah A, 2018) and Alonso (Alonso, 1998), have qualitatively illustrated these moisture variations. Figure 1 illustrates the quantitative behaviour of how moisture condition at a certain depth in a pavement layer changes over time after the construction of pavement.

As illustrated in Figure 1. The moisture condition (expressed as moisture content w) at a given depth of pavement layers eventually reaches an equilibrium moisture content (i.e., w_{eq}) following the construction of the pavement. The initial moisture condition (w_i) may be higher or lower than the equilibrium moisture condition depending on the moisture condition at the compaction of each layer at the construction. This initial moisture condition eventually reaches the equilibrium condition by initial drying or wetting after the construction of the pavement during the time noted as t_{eq} (time to reach the equilibrium). Even after reaching the equilibrium condition, moisture condition in pavement layers fluctuates depending on the ambient climatic conditions. Refer to the seasonal wetting (Δw_{wet}) and drying (Δw_{dry}) cycles marked in Figure 1.

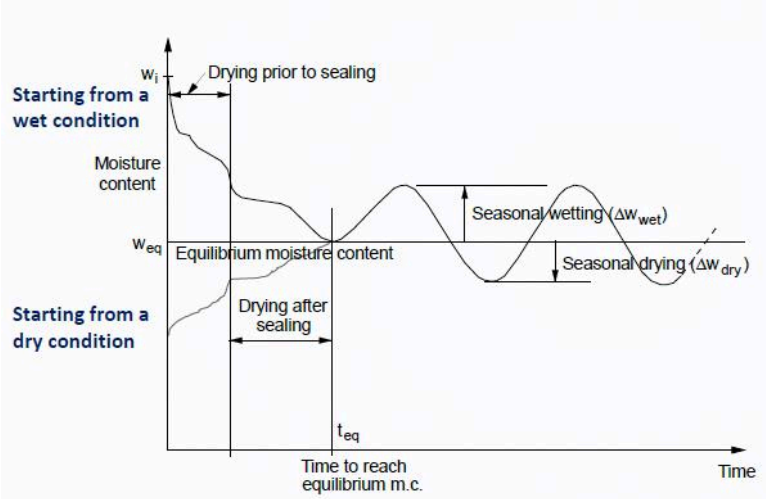

Figure 1: Schematic representation of progressive moisture variation of subgrade after compaction (Kodikara (2018)

These temporal moisture variations, induced by the prevailing climatic factors such as precipitation, evaporation, atmospheric temperature, and relative humidity significantly affect the structural performance of the pavement layers. Particularly, when the degree of saturation (S_r) of unbound granular material exceeds 70% or more specifically the optimum degree of saturation ($S_{r\ opt}$), the material can experience significant performance losses (Austroads, 2008). Moreover, as the moisture content changes, so do the shear strength and stiffness properties of subgrades. Hence, the temporal moisture variations that occur during the service life are essential to account in the pavement design stage to achieve better long-term pavement performances, avoiding moisture-related road failures.

However, the current Australian pavement design (Austroads, 2017) is yet to be advanced to incorporate climatic effects into the pavement design. Aiming to advance the current pavement design by filling this crucial gap, the authors of this paper developed a computer model to predict/simulate the climatic-induced moisture variations of pavement layers, by capturing essential physics of unsaturated soil mechanics and advanced numerical modelling methods. This model simulates the degree of saturation (S_r) at different depths of base, subbase, and subgrade layers of unbound pavements with sprayed seal, by methodology incorporating the daily variations of rainfall, evaporation, relative density, and temperature. The development of this model is published in Maha Madakalapuge et al. 2022 (Maha Madakalapuge *et al.*, 2022) and further validation of the model is published in Maha Madakalapuge et al (2023) (Maha Madakalapuge *et al.*, 2023).

It has been identified that there is a limited understanding of the performance behaviour of unbound pavements with thin seals under different climatic zones, and a significant knowledge gap exists regarding the evaluation of the effects of climate change on long-term pavement performance. Therefore, the primary aim of this paper is to investigate how moisture conditions in pavement layers vary under different climatic conditions and how these variations affect long-term pavement performance. This study utilizes the S_r variations simulated by the computer model developed by the authors (Maha Madakalapuge *et al.*, 2022) in their previous research.

2. METHODOLOGY

2.1. NUMERICAL MODELLING

The S_r variations of pavement layers were simulated using the computer developed in the authors' previous studies. A cross-section of a typical pavement (Figure 2) was modelled under three different climatic conditions, two Melbourne Climates and the Adelaide Climate. Moisture flows through all pavement layers were simulated considering daily variations of climatic factors such as precipitation, evaporation, relative humidity, atmospheric temperature, and water table depth. The details of the equations solved in the numerical modelling are presented in Maha Madakalapuge *et al.*, 2022. The primary model parameters required for the numerical modelling were each material's soil water retention properties and permeability functions. The van Genuchten - Mualem model (van Genuchten M, 1980), was employed to define those two functions for all the pavement layers in the numerical modelling.

A Class 2 crushed rock material was selected for the base material as it is one of the most commonly used base materials in Australia. Carteret (Carteret RS de, 2015) characterised this material and determined the SWRC experimentally in their

studies. The authors of the current study tested a few actual sprayed seal samples collected from a pavement in New South Wales, Australia, to determine the saturated permeability, void content, and SWRC (Maha Madakalapuge *et al.*, 2023). A sprayed seal represents an average K_s value in the range of 10^{-7} m/s was considered in this study. It can be considered as a relatively permeable seal. A sandy clay material tested in a previous study (Carteret RS de, 2015) was selected as the subgrade of the pavement modelled. Model parameters for all three layers are summarised in Table 1.

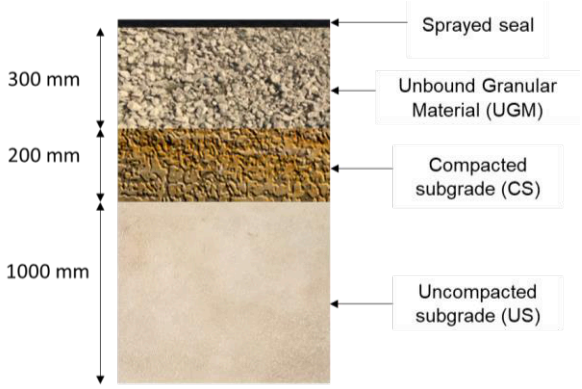

Figure 2: Cross section of the pavement modelled

Table 1. Model Parameters

	θ_r	θ_s	α (1/mm)	n	K_s (m/s)
Sprayed seal	0.028	0.08	0.002	1.17	1.8×10^{-7}
Base (UGM)	0	0.26	0.005	1.150	4×10^{-5}
Compacted subgrade	0	0.27	0.0005	1.175	1.15×10^{-9}
Uncompacted subgrade	0	0.38	0.001	1.275	3.85×10^{-9}

2.2. SELECTION OF CLIMATES

The primary objective of this analysis is to investigate the influence of climate on moisture variations in pavement layers and, subsequently the pavement performances in the long run. Hence, three locations were selected in a way that they represent dry to wet climatic conditions. A summary of the selected three climates is shown in Table 2.

Table 2. Details of climates selected.

No	Location	Coordinates	State	Annual Rainfall (mm)	Annual potential evaporation (mm)
C1	Cranborne botanical garden	38.13 °S, 145.26 °E	Victoria	791.6	1437
C2	Melbourne regional office	37.81°S,144.97 °E	Victoria	525.4	1207
C3	Adelaide	35.00 °S, 138.75 °E	South Australia	256.7	1915

Selected climates vary from wet to dry, with C1 being the wettest and C3 being the driest. Both C1 and C2 climates are classified as mild climates according to National Construction Code (NCC) climate zone classification whereas C3 is categorised as a warm temperate climate. Even though both C1 and C2 are located in the same climatic zone, the annual rainfall is significantly higher in the C1 climate than in C2. C3 illustrates the maximum annual potential evaporation due to the dry nature of the climate. The average temperature is higher in C3 than in C1 and C2. Daily climatic data namely, precipitation, pan evaporation, relative humidity and atmospheric temperature for all three locations were collected from weather station data from the Bureau of Meteorology (BOM) and MeteoBlue databases from 2010 to 2020.

The top boundary of the pavement was modelled as a time-dependent atmospheric boundary condition, which is defined by daily precipitation, pan evaporation, relative humidity and atmospheric temperature. Further details on the equations solved and numerical modelling of boundary conditions can be found in Maha Madakalapuge et al.(Maha Madakalapuge *et al.*, 2022). In defining the bottom boundary condition, the water table depth was assumed to be at 3 m depth from the surface for all the three climates selected. The temporal moisture variations at the top, middle and bottom of each layer

were simulated in terms of S_r and S by using the model developed (Maha Madakalapuge *et al.*, 2022), incorporating climatic factors by employing Hydrus 1D software and internally developed MATLAB codes.

3. RESULTS AND DISCUSSION

The S_r and s variations of the pavement modelled under C1, C2 and C3 climates are shown in Figures 3, 4 and 5 respectively. The initial S_r, which represents the moisture condition immediately after the construction, was kept similar for all three climates. In general, pavement layers are compacted at optimum moisture condition ($S_{r\ opt}$) to achieve the maximum dry density during the construction. It is a common practice in Australia to dry back each layer before placing the next layer down to 60% to 70% $S_{r\ opt}$ (Bodin D, 2017). Hence, Initial S_r of 0.5 was selected to represent the dried back condition of pavement layers in this analysis.

The UGM and compacted subgrade (CS) layers have wetted up within the first few months and reached an equilibrium condition. Then the moisture condition fluctuates around the equilibrium value. This behaviour is similar in all three climates. For example, S_r at the middle of the UGM layer under the C1 climate has reached an average value of 0.8 within around 3 months. Hence, equilibrium S_r ($S_{r\ eq}$) for the middle of the UGM layer is considered as 0.8 in the C1 climate. S_r at the middle of CS takes around 11 months to reach $S_{r\ eq}$ of 0.92. After reaching their equilibrium conditions, S_r of both layers fluctuate around that value. The suction, s also equilibrate accordingly in all the layers. After than only temporal fluctuations are evident.

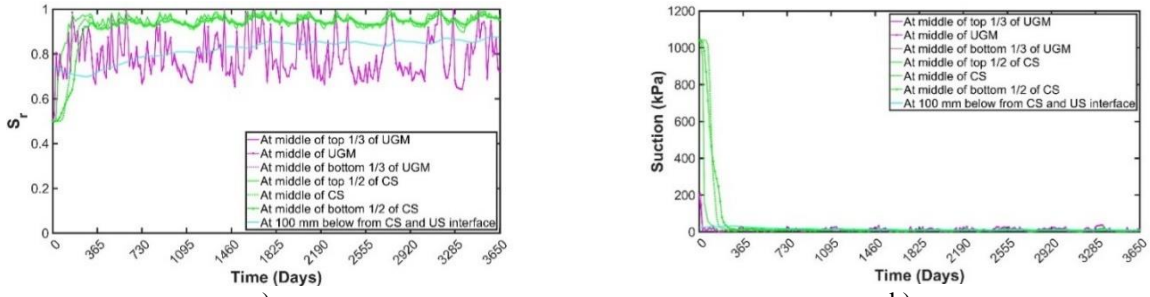

a) b)

Figure 3. Modelled temporal moisture variation of pavement layers under Melbourne Botanical Garden (C1) over 10 years climate a) S_r variations b) Suction (s) variations

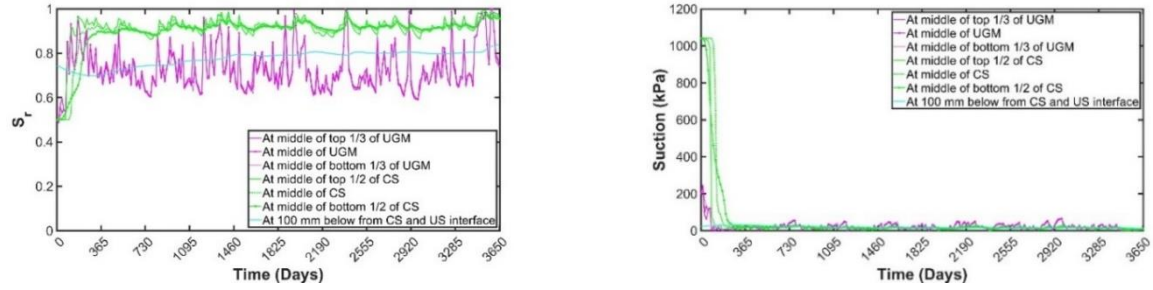

a) b)

Figure 4. Modelled temporal moisture variation of pavement layers under Melbourne Regional Office climate (C2) over 10 years climate a) S_r variations b) Suction (s) variations

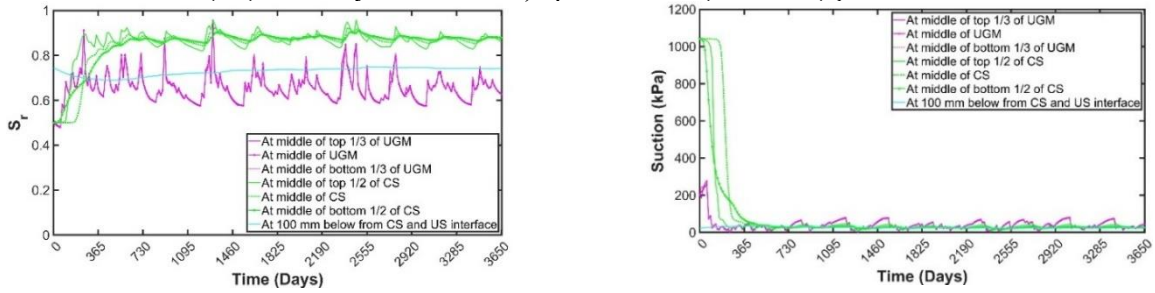

a) b)

Figure 5. Modelled temporal moisture variation of pavement layers under Adelaide (C3) over 10 years climate a) The a) S_r variations b) Suction (s) variations

3.1. INFLUENCE OF CLIMATE ON EQUILIBRIUM CONDITION

Figure 6 compares the $S_{r\ eq}$ at the middle of UGM and CS under all three climates. It can be seen that the value of all pavement layers is influenced by the climate. In wetter climates' climate equilibration takes place at relatively higher values, whereas pavement in dry climates reaches relatively lower values. The UGM layer is significantly more affected by the climate than the subgrade layers are. It shows that the time taken to reach equilibrium is longer in dry climates than in wet climates. For example, the UGM layer reaches equilibrium within around 3 months under C1, the wettest climate, whereas it takes around 7 months to reach equilibrium for the UGM layer under C3, the driest climate. Moreover, CS takes a relatively longer time to reach equilibrium compared to the UGM layer in all three climates.

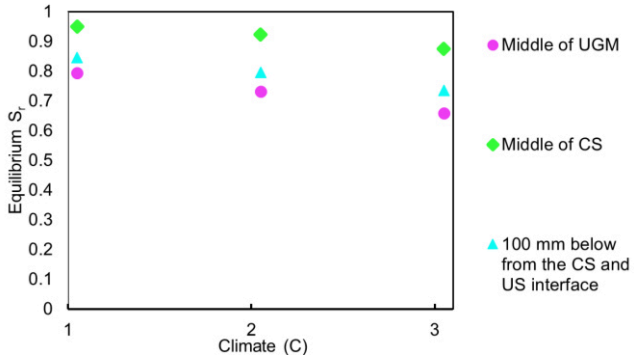

Figure. 6. Comparison of $S_{r\ eq}$ of pavement layers vs Climate

3.2. INFLUENCE OF CLIMATE ON TEMPORAL MOISTURE FLUCTUATIONS

After reaching the equilibrium condition, both fluctuate around the equilibrium value in all the layers. When Figures 3, 4 and 5 are compared, it is clear that the temporal of S_r fluctuation behaviours in both UGM and CS change with the climate. As all other parameters are identical except climate, this result highlights the fact that temporal moisture fluctuations in pavement layers are primarily induced by the climate.

During the pavement's service life, pavement layers wet up and dry out alternately in response to the prevailing climatic conditions. Pavement layers get wetted out easily in wet climates, while drying becomes easy in dry climates. Wetting event intensities are significantly higher in C1 and C2 than in C3. Under both C1 and C2, the UGM layer reaches almost full saturation in many instances. However, in C3, the UGM layer has not reached a fully saturated condition at all. The UGM layer experiences more intense fluctuations than the CS layer. The maximum and minimum S_r values that occurred during 10 years in both UGM and subgrade layers for all three climates are shown in Figures 7 and 8.

The maximum S_r of all the layers increases when the climate becomes wetter. On the other hand, the minimum S_r reduces when the climate becomes drier revealing that it is easier to dry out pavement layers in a dry climate than in a wet climate. The primary structural layer of unbound pavement with a sprayed seal is the unbound granular layer (i.e. UGM). The structural performance of UGM is highly dependent on its moisture condition. More specifically, the resilient modulus (M_R) of UGM reduces when moisture content increases (Cliatt, Plati and Loizos, 2016) resulting in a significant loss of structural capacity of the whole pavement structure.

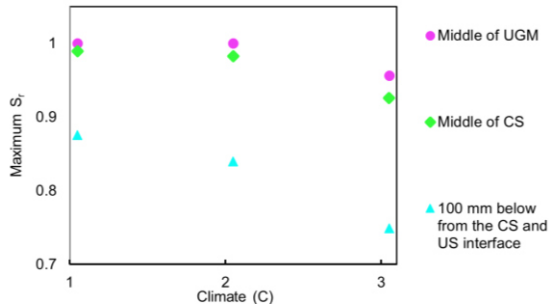

Figure 7. Maximum S_r values occurred during 10 years in both UGM and subgrade layers for all three climates

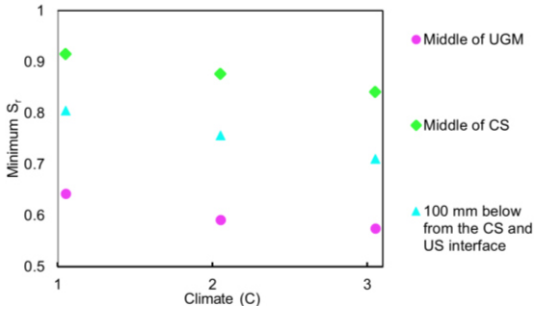

Figure 8. Minimum S_r values occurred during 10 years in both UGM and subgrade layers for all three climates

3.3. INFLUENCE OF CLIMATE ON PAVEMENT PERFORMANCE

Results indicated that S_r in UGM varies according to the prevailing climatic conditions. In wet climates, S_r in the UGM layer reached high saturation conditions during the service life along with intense fluctuation, with where S_r was close to 1. Hence, in those instances, it is possible to reduce the structural strength of pavement layers. In contrast, the moisture conditions in pavement layers are relatively drier in arid climates. It can expect lesser performance losses in dry climates than in wet climates.

4. CONCLUSIONS

This paper investigates the moisture variations in pavement layers that occurred during the service life as a result of environmental interactions under different climates. In this study, a numerical model developed to predict moisture variations in pavement layers is used to simulate the degree of saturation variations of a typical sprayed-seal pavement in three different Australian climates, ranging from wet to dry. Based on the findings, the moisture fluctuations were assessed in terms of equilibrium, minimum, and maximum S_r, and subsequent pavement performances were reviewed.

This investigation showed that the surrounding climate has a significant impact on the moisture conditions in both the unbound granular layer and the subgrade. Unbound granular layers' moisture conditions stabilise under comparatively dry conditions in dry regions, whereas pavement layers' equilibrium state stabilises under wetter conditions in wet climates. It is evident that pavement layers can easily dry out when the surrounding climate is relatively drier.

Furthermore, the model developed has the capacity to assess how climate change will affect pavement performance over the long term. Based on the findings, it is possible to predict that the moisture condition in the pavement layers of unbound pavements with sprayed seals will remain relatively dry as climates become drier as a result of global warming. The authors of this paper will address the effect of climate change on moisture variations and subsequent long-term pavement performances extensively in their future works of this study.

5. REFERENCES

Alonso, E. (1998). 'Suction and moisture regimes in roadway bases and subgrades', *International Symposium on Sub-drainage in Roadway Pavements and Subgrades*. Granada, Spain, pp. 57–104.

Austroads (2008). Guide to Pavement Technology Part 4A. Granular Base and Subbase Materials.

Austroads (2017). Guide to Pavement Technology Part 2.

Ball, G. and Patric, J. (1998). Flushing Processes in Chipseals: Effects of Trafficking, *Transfund New Zealand Research Reports.*

Bodin D (2017). Improved Laboratory Characterisation of the Deformation Properties of Granular Materials.

Carteret RS de (2015). Environmental salinity and bitumen-sealed unbound granular road pavements. *The University of Newcastle.*

Cliatt, B., Plati, C. and Loizos, A. (2016). 'Investigating Resilient Modulus Interdependence to Moisture for Reclaimed Asphalt Pavement Aggregates', in *Procedia Eng*, pp. 143:244–51. Available at: https://doi.org/10.1016/j.proeng.2016.06.031.

Kodikara, J., Islam T and Sounthararajah A (2018). 'Review of soil compaction: History and recent developments', *Transportation Geotechnics,* 17:24–34. Available at: https://doi.org/10.1016/j.trgeo.

Maha Madakalapuge, C. et al. (2022). 'Numerical evaluation of temporal moisture variations in unbound pavements with thin seals', *Transportation Geotechnics*, 35(100787). Available at: https://doi.org/10.1016/j.trgeo.

Maha Madakalapuge, C. et al. (2023). 'Experimental and numerical investigation of moisture variation in unbound pavements with sprayed seals during drying and wetting', *Transportation Geotechnics [Preprint]*.

Towler, J.I. and BALL, G. (2001) 'PERMEABILITIES OF CHIPSEALS IN NEW ZEALAND', in *ARRB Transport Research Ltd Conference*, 20TH, 2001, MELBOURNE, VICTORIA, AUSTRALIA, p. 16.

van Genuchten M (1980) 'A Closed-form Equation for Predicting the Hydraulic Conductivity of Unsaturated Soils', *Soil Science Society of America Journal*, 44. Available at: https://doi.org/10.2136/sssaj1980.03615995004400050002x.

DEVELOPMENT ON LARGE SCALE FOLIATION-CONTROLLED LANDSLIDES IN THE WAKATIPU BASIN

Jacob Johnson, Blake Hoare,
ENGEO Limited

Address: 219 Lower Shotover Road, Queenstown 9371, Phone: 0277735810, Email: jjohnson@engeo.co.nz

ABSTRACT

Geotechnical engineering in the Wakatipu Basin is unique, with the area posing a variety of geomorphological environments where practitioners need to thoroughly understand the geological history and genesis to provide robust engineering solutions. Glacial processes and waning of the last glacial maxima have resulted in a spectrum of terrains, from flat benign terraces to undercutting of schist bedrock cliffs, and everything in between. The region has undergone unprecedented urban growth where geotechnically simple sites are becoming limited. Continued pressure for development has led to expansion into more geotechnically challenging terrain.

This paper focuses the Coronet Peak Landslide Complex (CPLC) which extends from Arthurs Point towards Arrowtown. It is an example of regional dip-slope foliation induced landslides which typify the southern slopes of the Wakatipu Basin. These macro-scale landslides are initiated by glacial de-buttressing during and prior to the last glacial maxima (~20,000 years ago). The CPLC surface geomorphology is dominated by hummocky terrain with a series of secondary reactivations. Typical landslide geomorphology is prominently observed on the slopes of Mt Dewar (Figure 1), with multiple foliation landslide scarps observed at the crest of Mt Dewar. The CPLC has been subject to various studies since the 1990's and is widely considered suitable for development with no significant global movement observed within recent records.

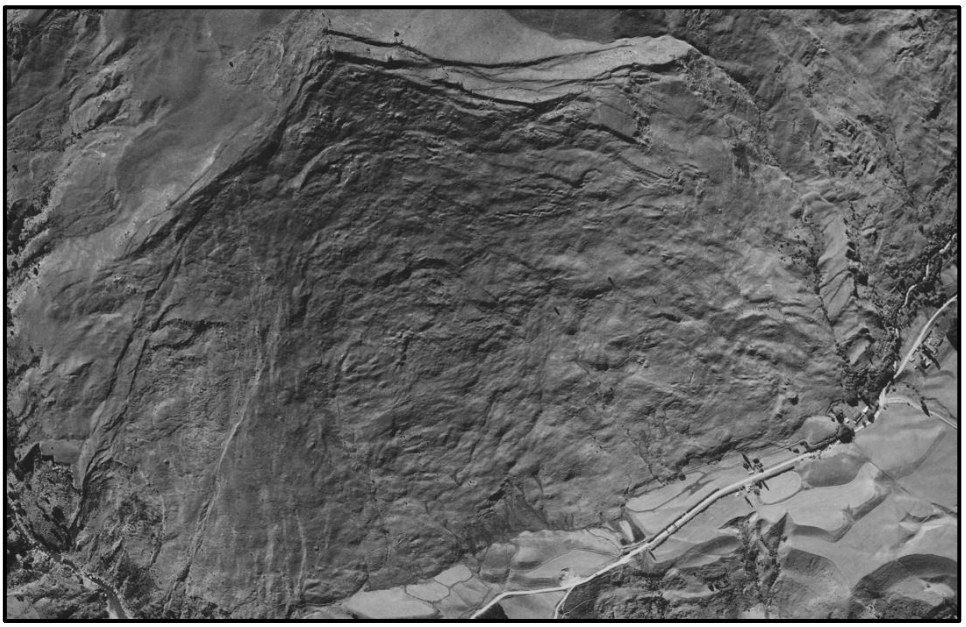

Figure 1: 1956 historical aerial image of Mt Dewar Landslide (Retrolens).

1 INTRODUCTION

To service the growing population demand in the Wakatipu Basin there is increasing pressure to develop on steep slopes. Understanding these slopes from an engineering geological perspective is critical as large-scale landslides are common within the basin given the glacial history and underlying schist geological structure. Outside of the CPLC, examples of these landslide locally include the K9 Landslide within the Kawarau Gorge (Bell, 1992), The Queenstown Hill Landslide (Gnesko, 2020), The Gibbston Slide (Johnson, 1986) and the numerous landslides associated with the stabilisation measures of Lake Dunstan as part of the Clyde Power Project (Macfarlane et al, 1995).

Slope instability and landslide geomorphology are common on aspects where foliation dips out of slope. The Wakatipu Basin is marked by asymmetrical valleys dominated by dip-slope landslide geomorphology on slope aspects with adverse foliation orientations, and rockfall topple type failures on slopes with favourable foliation orientations. Landslides are

generally translational, with basal shear surfaces along foliation layering within schist bedrock (Stossel, 1999). The geology is variable, highly deformed and coupled with a complex compartmentalised groundwater system. An understanding of the past glacial processes and geotechnical issues associated with anisotropic bedrock is paramount to providing robust engineering designs.

This paper presents development of an engineering geological model of the CPLC, focusing on the Mt Dewar landslide and discussion around the geotechnical challenges of development within these macro-scale landslides. The aim of the study is to further develop an understanding of the geotechnical issues and refine engineering geological methodologies which best enable assessment of the risks associated with future development on the lower slopes of the CPLC.

2 GEOLOGICAL HISTORY

The basement geology of the CPLC consists of Otago Schist, an ~150 km structural arch of schist with metamorphic facies varying from prehnite-pumpyite to greenschist. Bishop (1972) and later Craw (1984) refined this arch into four Textural Zones (I-IV), separating the geology into various types of pelitic, psammitic and greenschist. The CPLC is mapped with Textural Zone IV and is described as *"very well foliated and laminated: abundant pelitic and subordinate psammitic greyshcist: minor greenschist and metachert"* (Turnbull, 2000).

Foliation controlled landslides are a common occurrence in alpine environments of anisotropic rock which have experienced prolonged topographic and changes in stress regime due to topographic development (Agliardi et al, 2019, Crosta et al, 2013, Ridl, 2021). The geological history of these environments is marked by dramatic changes in stresses due to tectonics, glaciation and long-term climatic conditions. The stability of these slopes is closely tied to the geological history. The Wakatipu Basin has been through at least four periods of glaciation within the last 350,000 years (Suggate, 1990) with the CPLC being correlated with the Waimea Glaciation (~135 ka) (Willets, 2000), and the Otiran Glaciation (~74 – 11ka) (Shulmeister et al., 2019). The timeline of glacial advances is still poorly understood due to lack of dating, however what is apparent is that the CPLC has undergone multiple periods of both stability and instability associated with glacial advancement and recession.

During glaciation, mass erosion of low-lying parts of the landscape occurs, modifying or removing any existing surficial deposits, and further eroding the schist bedrock. As a result, , toe buttressing by the surficial material in valley floors is eroded, leaving these slopes unsupported and prone to instability. During glaciation these slopes are buttressed by 100's of meters of ice, however as the glaciers wane these slopes become unsupported, and initiate periods of instability. As further waning occurs mass deposition by meltwaters infill valley floors gradually re-buttressing the slope toe. This process is repeated with every glacial advance, inducing landslides on dip-slope aspects and deposition of glacio-fluvial materials.

The extent of glacio-fluvial materials deposited within the CPLC area is apparent from mapping by Barrell (2001). Figure 2.1 below (left) represents the maximum extent of ice at the peak of the last glaciation (~18,000 years ago). It shows the lower slopes of the CPLC likely covered by 100s of meters of ice with an outwash plain from the Shotover River carrying meltwater from the glaciers and its headwaters. Figure 2.2 below (right) indicates the interpreted landform around 14,000 years ago, showing Shotover alluvial terraces forming to the east, abandoning its previous course down Malaghan Road Valley (northwest corner of Figure 2.2). The geomorphology of Malaghan Road Valley suggests ice was still occupying the basin while fan-delta alluvium was accumulating (as shown in orange).

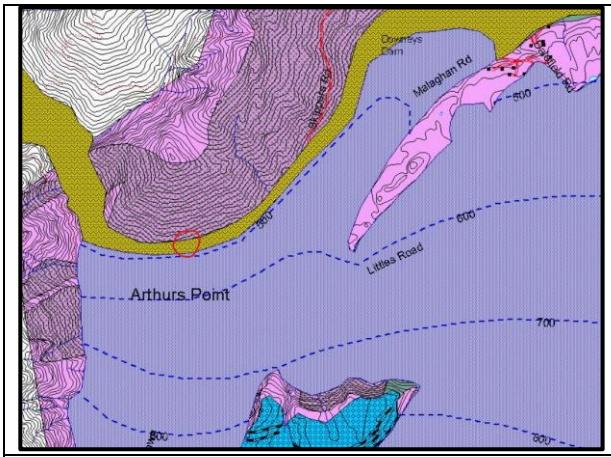

Figure 2.1: Landform reconstruction ~18,000 years ago (site shown in red)

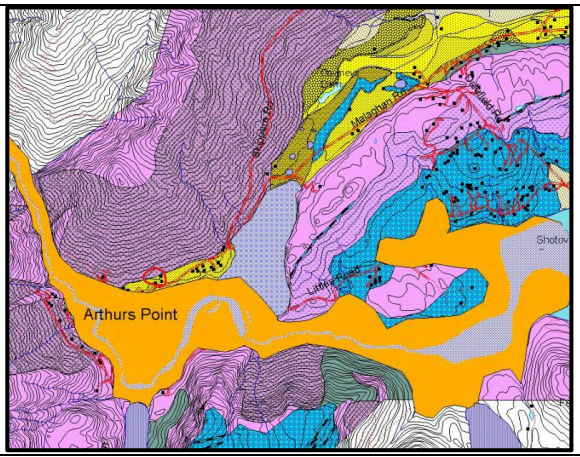

Figure 2.2: Landform reconstruction ~14,000 years ago following ice retreat

3 CORONET PEAK LANDSLIDE MODEL

The CPLC complex is largely a translational failure estimated to include 2700 Mm^3 of material along a basal shear surface comprising foliation surfaces and other defects parallel to foliation (Willets, 2000). The CPLC is dominated by hummocky terrain, degraded scarps, sackung features and deeply incised gulley drainage systems. Extensional sackung features are well documented and easily recognisable through aerial imagery, however compressional deformations are less exposed and less understood. A simplified cross section of the Arthurs Point Woods development is displayed below in Figure 4.

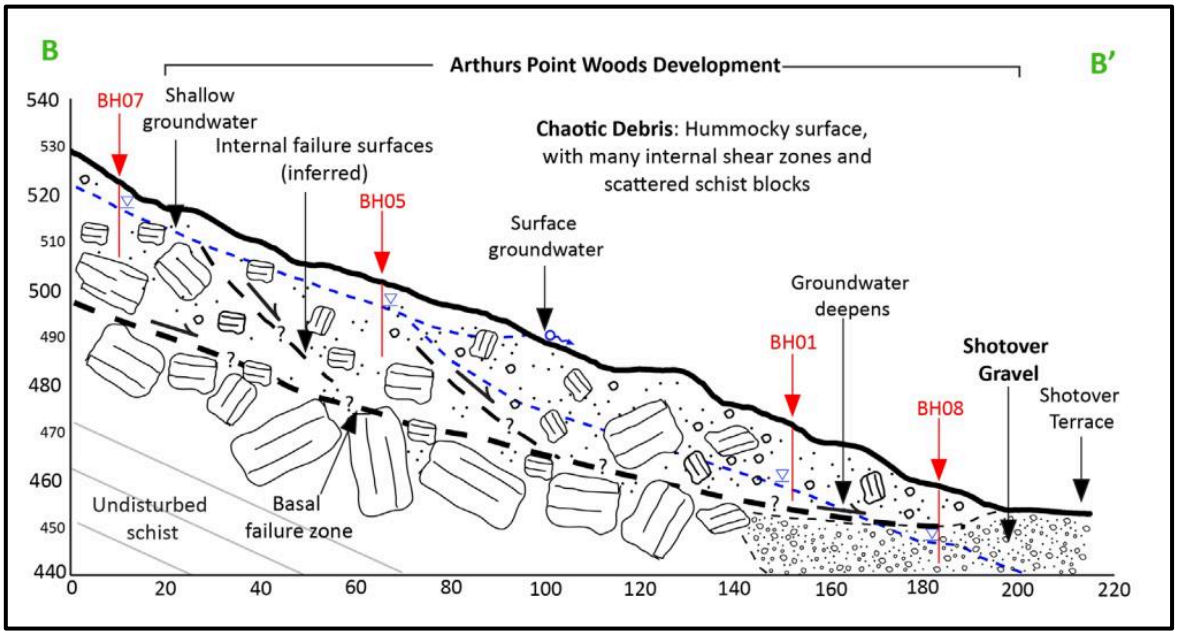

Figure 4: Generalised cross section of the Arthurs Point Woods Development (Rozmus, 2023).

Geomorphic mapping observed over-steepened slopes, scarps, stepped scarps and progression of smaller scale landslides active within the wider failure mass. Compressional deformations are typically located in the lower slopes expressed as bulging, intense rock fracturing and kink folding which characterise the slope toe. Although the region has been subject to numerous Alpine Fault earthquake events (every ~300 years) and heavy rainfall events (Bell, 2018), no significant movement has been recorded within the larger mass. The CPLC is therefore widely considered stable and suitable for development. Hadley Consultants in 2010 completed re-survey of over 20 cadastral survey markers across the CPLC ranging from 3 to 28 years old. Resurvey did detect minor deflections differences, but these were within survey error (140 to 300 mm), further affirming no major movement in recent history. Secondary reactivations from increased local slope angles from reactivations within the larger mass and springs are considered the most active region of the landslide.

The interpretive ground model comprises *in-situ* schist rock at depth (unknown) and a spectrum of landsides masses separated by numerous shear surfaces. The landslide mass materials can be categorised on a scale relative to the extent of deformation which the material has experienced. For the purposes of characterising the landslide mass for the CPLC, we have adopted a similar approach by MacFarlane (1992), established for schist landslide debris within Cromwell Gorge. Beyond *in-situ* schist bedrock the scale starts at Disturbed Schist and grades to Chaotic Landslide Debris. Typically, the higher level of deformation is seen nearer the surface or distally away from the head scarp. Table 1 below illustrates the spectrum of material observed.

Table 1: Spectrum of materials observed across the lower slopes of the CPLC in line with classification by MacFarlane (1992).

Term	Mass Description	Typical Displacement	Photo
Chaotic Landslide Debris	Predominantly matrix supported material comprising schist debris broadly graded from silt to large blocks of schist. Blocks generally have reduced rock mass quality and form a soil like rock material with relic rock fabric. Foliation within schist blocks randomly orientated in relation to *in-situ* schist.	10's to 100's of m	
Blocky Landslide Debris	Predominantly block supported material comprising large schist blocks, with finer schist debris infilling cavities between blocks. Sheared zones, crushed zones and gauge seams may be present within the debris, with foliation often randomly orientated in relation to *in-situ* schist.	m's – 10's m	
Displaced Schist	Rock mass with joints and possible other defects visibly open due to gravitational displacement, possibe minor crushed zones.	mm's – cm's	

4 CONCEPTUAL GROUNDWATER MODEL

Given the conceptual ground model of the CPLC, the groundwater system is complex and doesn't conform to standard hydrostatic groundwater behaviour. Rather, groundwater is inherently linked to the geology of the landslide often manifesting as perched isolated groundwater pockets and springs at the surface. Aquifers are known to exist within both the landslide debris and competent schist layers (Belcher, 2009). Low angle faults or shears subparallel to slope create impermeable barriers further compartmentalising the groundwater system.

Where groundwater is encountered, it has been shown to insensitive to rainfall recharge as piezometers installed across the landslide complex have shown to display static groundwater levels (Figure 4). This is consistent with conclusions by Blecher throughout the CPLC, where significant lag time between rainfall and increased spring discharge was observed. Additionally, based on our limited testing, these groundwater systems do not exhibit excess pore water pressure, indicating excess pressures (if any) are dissipated either by surface expression as springs or into dissipate into deeper groundwater systems.

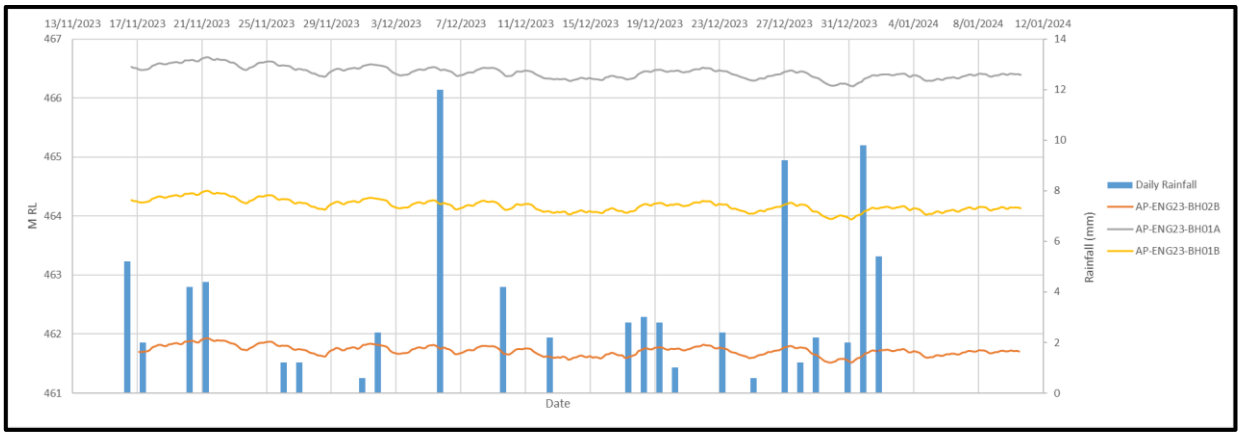

Figure 4: Groundwater levels against rainfall at 117 Arthurs Point Road.

5 SLOPE STABILITY

Although at a macro scale the CPLC is considered stable, the geology presents it's own engineering challenges. As detailed above, the lower slopes generally comprise the widest spectrum of material with investigations to date exposing materials akin to those of the McFarlane classification as described above.

Given these materials, the application of standard geotechnical failure criteria becomes difficult. Quantifying GSI and intact rock mass strength becomes complicated for the generalised Hoek-Brown failure criterion, which is not intended for anisotropic rock masses. Furthermore, the use of cohesion and angle of friction for Mohr-Coulomb doesn't account for the extent of rock fabric and anisotropy that persists even in the more degraded Chaotic Landslide Debris materials.

As the lower slopes of the CPLC are dominated by the 'soil like' chaotic landslide debris we progressed with Mohr-Coulomb. This is also consistent with the approach applied in the Cromwell Gorge by Smith & Salt (1991) where they back analysed a variety of schist landslide debris. We have done the same for the CPLC. Figure 4 presents the results of a parametric back analysis of a stable 12 m, ~ 40 deg slope comprised of materials logged as Chaotic Landslide Debris. The slope was chosen for the back-analysis as it was excavated several years ago, had showed no signs of displacement, and a local piezometer measured groundwater levels below the analysed section.

Back analysis used various circular and non-circular methods and were parametrically plotted out in terms of Cohesion (c) with ϕ = 38° remaining constant (Figure 4). Generally, cohesion of 3 kPa was in the middle for a Factor of Safety (FoS) of 1 or marginally more than 1 (~1.1). On that basis, we adopted c=3, ϕ=38° for parameters across the site as a representation of landslide materials.

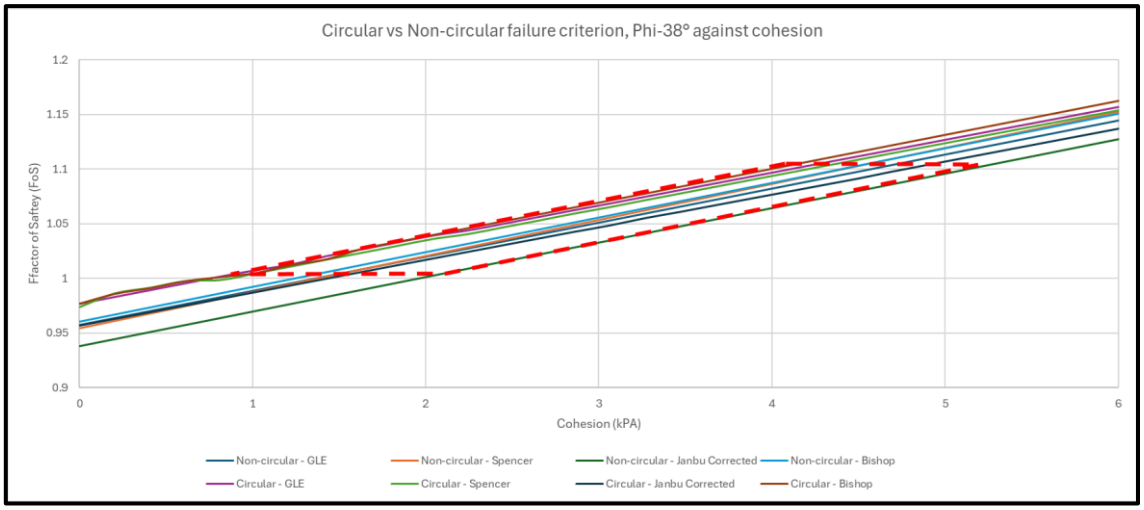

Figure 4: Back analysis of cohesion using circular vs non-circular methods for a local slope at Arthurs Point Woods.

Our back analysis was generally in keeping with the work completed by Smith & Salt (date) who analysed similar soils in the Cromwell Gorge akin to chaotic landslide debris. Their analysis derived parameters up to c-12 and ϕ=36° for low to moderate normal stresses. Incorporating groundwater into slope stability assessments for the CPLC was equally as difficult due to compartmentalised nature of the systems. It is common for groundwater to manifest at surface through springs and at depth in perched isolated pockets. In the case of Arthurs Points Woods bulk earthworks had been undertaken for the development and allowed for adoption of an observational case by case approach in stability modelling.

6 CONCLUSIONS

This study highlights the inherent challenges of engineering within landslide terrain and the difficulty in defining representative engineering parameters to the complex geology. Also highlights the limited applicability of traditional numerical stability analytical methods in this type of geological setting, and the importance of tempering results with engineering judgement. Groundwater although underpins slope stability is compartmentalised and unpredictable leading to challenges in applying these groundwater systems in traditional stability modelling methods. Consequently, slope stability must be approached with conservatism to account for the spectrum of materials.

7 ACKOWLEDGEMENTS

The authors would like to acknowledge the help and support of ENGEO in the preparation of the work present within this paper.

8 REFERENCES

Agliardi, F., Riva, F., Barbarano, M., Zanchetta, S., Scotti, R., and Zanchi, A., (2019), Effects of tectonic structures and long-term seismicity on paraglacial giant slope deformations*: Piz Dora (Switzerland): Engineering Geology,* v. 263, p. 105353

Barrell, D. (2001). Origin of Landforms in the Arthurs Point Area, Wakatipu Basin.

Belcher, D. M., (2009), The Stable Isotopic Variations and the Hydrogeology of the Coronet Peak Ski field, Queenstown.

Bell, (1992), Geomorphic evolution of a valley system: the Kawarau Valley, Central Otago: Landforms of New Zealand. *Longman Paul, Auckland,* p. 317-341.

Bishop, D., (1972), Progressive metamorphism from prehnite-pumpellyite to greenschist facies in the Dansey Pass area, Otago*, New Zealand: Geological Society of America Bulletin,* v. 83, no. 11, p. 3177-3198.

Craw, D., (1984), Lithologic variations in Otago Schist, Mt Aspiring area, northwest Otago*, New Zealand: New Zealand journal of geology and geophysics,* v. 27, no. 2, p. 151-166.

Crosta, G., Frattini, P., and Agliardi, F., (2013), Deep seated gravitational slope deformations in the European Alps: Tectonophysics*,* v. 605, p. 13-33.

Gnesko, L., (2020), Geomorphology and geotechnical characterization of the Queenstown Hill landslide.

Johnson, J.D. (1986). The Gibbston Valley slide, Kawarau Valley, Central Otago: A thesis submitted in partial fulfilment of the requirements for a degree of Master of Science in Engineering Geology in the University of Canterbury.

Macfarlane, D., Pattle, A., and Salt, G., (1992) Nature and identification of Cromwell Gorge landslides groundwater systems, *in Proceedings International symposium on landslides*, p. 509-517.

Macfarlane, D., Riddolls, B., Crampton, N., and Foley, M., (1995) Engineering geology of schist landslides, Cromwell, New Zealand*, in Proceedings International Symposium on Landslides*, p. 2137-2144.

Ridl, R. N., (2021), Evaluation of buckling deformation in the schist of the Cromwell Gorge, New Zealand.

Rozmus, K (2023) Engineering Geology and Geomorphology of the Coronet Peak Landslide at Arthurs Point, Queenstown, New Zealand.

Smith & Salt (1991) Clyde Power Station Reservoir, General Report on Geotechnical Materials involved in landsliding, mineralogy, shear strength and related properties. Volume 2 – Appendices, Report EGI 89/049

Shulmeister, J., Thackray, G. D., Rittenour, T. M., Fink, D., and Patton, N. R., (2019), The timing and nature of the last glacial cycle in New Zealand, *Quaternary Science Reviews*, v. 206, p. 1-20.

Stossel, D. L., (1999), The engineering geology of Frankton Arm.

Suggate, R., (1990), Late Pliocene and quaternary glaciations of New Zealand*, Quaternary science reviews*, v. 9, no. 2-3, p. 175-197.

Turnbull, I. M., (2000), Geology of the Wakatipu area, *Institute of Geological & Nuclear Sciences.*

Willetts, A. J., (2000), The geology and geomorphology of the Coronet Peak and Arthurs Point landslide complexes.

APPLICATION OF GEOSYNTHETICS FOR ENHANCED PERFORMANCE OF TRANSPORTATION INFRASTRUCTURE

Joseph Arivalagan[1], **Buddhima Indraratna**[2], **Cholachat Rujikiatkamjorn**[3]

[1]*Tonkin + Taylor, Unit 11, 1 Metier Linkway, Birtinya, Queensland, 4575, Australia, PH (61) 468490625; Email: JArivalagan@tonkintaylor.com.au*

[2]*Transport Research Centre, University of Technology Sydney, 15 Broadway, Ultimo, New South Wales, 2007, Australia, PH (61) 400213046, Email: Buddhima.Indraratna@uts.edu.au*

[3]*Transport Research Centre, University of Technology Sydney, 15 Broadway, Ultimo, New South Wales, 2007, Australia, PH (61) 401206959, Email: Cholachat.Rujikiatkamjorn@uts.edu.au*

ABSTRACT

The highway embankments and railway tracks constructed on soft soils are particularly vulnerable to increased cyclic stress, which can cause uncontrolled deformation, undrained failure, migration of fines and associated mud pumping. This paper presents a significant contribution to the field by reporting the effectiveness of geosynthetics in mitigating fluidization potential of soft soil. Laboratory experiments were undertaken using a dynamic filtration apparatus (DFA) and a cyclic triaxial apparatus (CTA) to analyse the cyclic response of soft subgrade under impeded drainage conditions. This study critically evaluates the role of geosynthetics in controlling the occurrence of soil fluidization by assessing the build-up of excess pore water pressure (EPWP), the variation in particle size distribution (PSD) and the moisture content (MC). The outcomes of this study reveal that prefabricated vertical drains (PVDs) are effective in alleviating the EPWP developed in middle or deeper soil layers, whereas geocomposites can facilitate surficial drainage. This paper emphasizes the practical implications and the significance of improved drainage and swift dissipation of EPWP on low-lying saturated soils for enhanced track design.

1 INTRODUCTION

The rise in demand for vehicle transportation has led to higher axle loads, impacting the stability of railway and highway embankments, especially under poor drainage conditions. In railway tracks, wheel imperfections or flat wheels can generate large impact dynamic stress, leading to up to 400 kPa of vertical stress at the ballast layer, compared to the typical wheel load-induced stress of 150-220 kPa (Indraratna et al., 2010a). As a result of increased dynamic stresses at the subsurface level, fine particles can be pumped up into the overlying layers, a phenomenon known as 'mud pumping' (Arivalagan et al., 2022). When fine particles move upwards into the coarser ballast particles or compacted capping material, it cannot provide adequate structural stability. Vertical drains (PVDs) can enhance the stability of foundations built on soft ground and provide a viable solution to poor drainage commonly encountered in low-permeability soft soils. PVDs are cost-effective and can be easily installed in moderately to highly compressible soils to significant depths. The installation of wick drains can drastically reduce the critical pore pressure by activating the radial drainage path, thus assisting in soil consolidation under train loading (Arivalagan et al., 2022). Most significantly, PVDs can be swiftly installed without excessive environmental impact or extensive quarrying requirements. In recent decades, geogrids have been widely used to alleviate cyclic stress transferred to subsoil strata and to reduce the potential of subsoil problems associated with lateral confinement. Geotextiles and geocomposites can be used to alleviate the excess pore water pressure (EPWP) at the subgrade interface, provide adequate drainage and mitigate excessive fine migration into capping material (Kermani et al., 2018). This paper presents the effectiveness of geosynthetics in mitigating subsoil fluidization and the use of wick drains to enhance the stability of railway and highway embankments by facilitating adequate drainage at shallow layers.

2 EXPERIMENTAL ANALYSIS

Cyclic triaxial tests and dynamic filtration tests were conducted on remoulded soil samples under different cyclic loads to identify the primary factors inducing mud pumping. Figure 1 (a) and (b) show schematic diagrams of dynamic filtration apparatus (DFA) and conventional cyclic triaxial apparatus (CTA) respectively. As shown in Figure 1(a), DFA has seven key components: (1) a load cell and linear variable differential transformers (LVDTs), (2) a hydraulic actuator, (3) miniature pore pressure transducers (MPTs), (4) body pressure transducers (BPTs), (5) amplitude domain reflectometry probes (ADRs), (6) a data logger, and (7) a computer (PC). The test setup includes a 13 mm thick hollow cylindrical cell, equipped with an array of instruments located at different depths, allowing for the measurement of EPWPs, cyclic

deformation and changes in soil porosity. It has four MPTs, installed at the centreline at depths of 20, 40, 80, and 120 mm and six BPTs (with an accuracy of 0.5 kPa) positioned at 25, 55, 85, 115, 145, and 175 mm from the subgrade surface. Figure 1(b) shows conventional CTA, which can simulate various loading and drainage conditions. The CTA has five key components, (1) a load frame and a dynamic actuator, (2) a triaxial cell, (3) pressure/volume controllers, (4) a pore pressure transducer and (5) a data logger and software program.

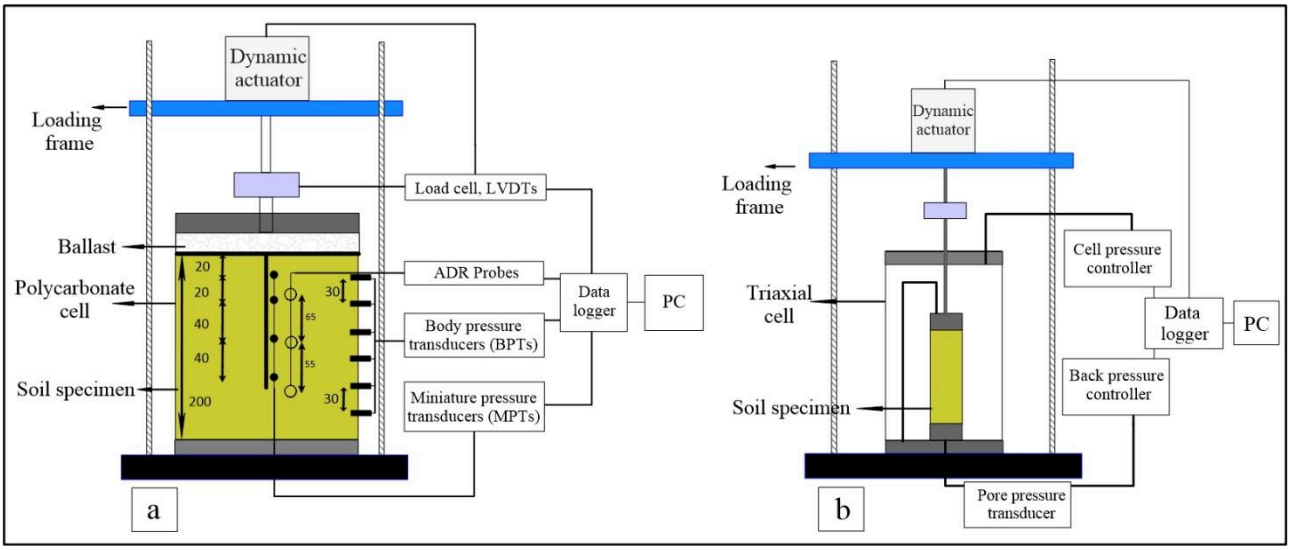

Figure 1: Schematic layout of (a) Filtration Apparatus (DFA) and (b) Cyclic Triaxial Apparatus (CTA)

2.1 PROPERTIES OF SOILS AND GEOSYNTHETICS

Previous studies reported that various soil samples collected at the mud pumping sites near the South Coast Line in NSW had a plasticity index (PI) ranging from 10 to 20 (Nguyen and Indraratna 2021). In this study, soil samples were collected from two mud pumping sites near Wollongong City. Basic geotechnical tests were undertaken at the University of Wollongong and the University of Technology Sydney. The soil properties for both dynamic filtration and triaxial tests are reported in Table 1. A geocomposite with a filter membrane (GC) and a wick drain (P) was adopted for dynamic filtration tests and their properties are listed in Table 2.

Table 1: Basic geotechnical characterisation of subgrade

Soil properties	Soil specimens used for dynamic filtration tests	Soil specimens used for cyclic triaxial tests
Liquid limit, LL	42%	31%
Plasticity index, PI	16%	11%
In-situ moisture content, MC	32%	20%
Specific gravity, G_s	2.59	2.64
Maximum dry density, MDD	1682 kg/m^3	1798 kg/m^3

Table 2: Properties of tested geosynthetics

Geocomposite (GC)	Value	Vertical drain (P)	Value
Tensile strength (kN/m)	50	Drain grab strength (N)	2500
Pore opening size of filter membrane and nonwoven geotextile layer O_{95} (μm)	<10 and 75	Flow discharge at 200 kPa (m^3/yr)	2800
CBR resistance (kN)	10	Filter pore size O_{95} (μm)	75
Thickness (mm)	4.5	Drain width and thickness (mm)	100 × 3.4

2.2 EXPERIMENTAL PROCEDURE

2.2.1 Undrained cyclic triaxial tests

To examine soft soil fluidization, an array of undrained tests were carried out using remoulded specimens, each 50 mm in diameter and 100 mm in height. To mimic undrained or extremely poor drainage conditions, the top and bottom drainage valves remained closed throughout the cyclic tests. A detailed methodology can be found elsewhere Abeywickrama et al. (2021). Soil specimens were subjected to a cyclic load with a sinusoidal waveform (up to 50,000 cycles) under undrained conditions. The cyclic stress ratio (CSR) can be calculated from the following Equation (1):

$$CSR = {}^{q_c}/_{2\sigma_3^{'}} \tag{1}$$

where q_c is the cyclic deviator stress and $\sigma_3^{'}$ is the confining pressure.

In this study, the CSR varied from 0.2 to 0.8, while the confining pressure ranged between 20 and 30 kPa, representing a shallow subgrade behaviour in the field. The frequency for the cyclic triaxial tests was in the range of 1 to 5 Hz.

2.2.2 Dynamic filtration tests

The detailed test method mainly discusses five major steps, (1) compaction, (2) saturation, (3) consolidation, (4) surface preparation/installation of geosynthetics, and (5) cyclic loading. The target bulk density of 1600kg/m^3 and moisture content of 17% were achieved by compacting to the required soil volume. A geocomposite layer was positioned between the ballast and subgrade. The diameter of the current dynamic filtration setup is 240 mm, and it would result in a much smaller drain spacing of 0.24 m if a singular drain were installed. Therefore, a vertical drain with a rescaled size was incorporated (17.3 mm x 3.4 mm). This modification was adopted based on the time factor provided and the average degree of soil consolidation observed both in-field and in laboratory tests. The effectiveness of a geocomposite (Test GC), and a PVD-geocomposite system (Test P+GC) was evaluated under various axle loads and train speeds. The hydraulic actuator (DFA) can apply a uniform normal stress as a minimum, along with a sinusoidal cyclic stress (σ_{min} = 30 kPa and σ_{max} = 70 – 140 kPa) which further mimics an axle load of 25-40 tonnes. The frequency of 1.0 to 5.0 Hz was adopted for cyclic tests using DFA. The detailed laboratory testing procedure has been provided elsewhere Arivalagan et al. (2022). The EPWP recorded by BPTs can be used to measure the normalized excess pore pressure gradient (dimensionless) among distinct soil layers and it can be calculated from the following Equation (2):

$$EPPG = {}^{dU_e}/_{dL} \tag{2}$$

where dU_e is the changes in the excess pore pressure head (m head) and dL is the distance between two locations (m).

3 RESULTS AND DISCUSSIONS

3.1 CYCLIC TRIAXIAL TESTS

Figure 2 shows how the mean EPWP ratio increases with an increasing number of cycles under undrained conditions.

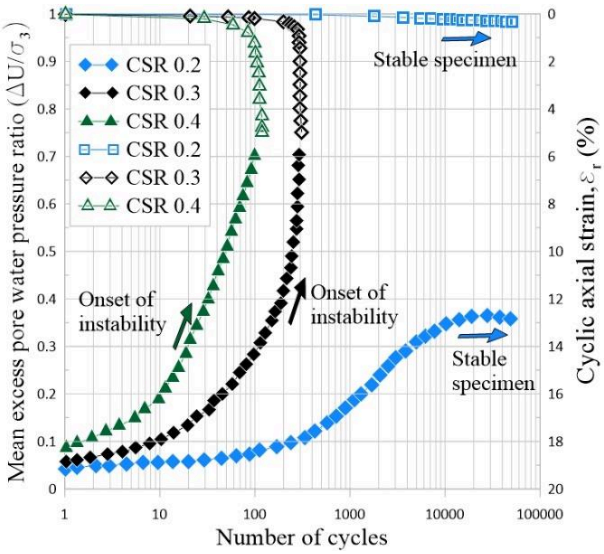

Figure 2: Undrained cyclic tests (a) Mean EPWP ratio and (b) Cyclic axial strain (Abeywickrama et al., 2021)

The EPWP increases steadily and reaches a peak before reaching a constant level (without failure) in stable specimens, whereas the mean EPWP ratio is under 0.36 until the end of the cyclic test. However, soil specimens subjected to a higher cyclic stress ratio (i.e., CSR > CSRc) failed with a sudden increase in EPWP and axial strain. Subsequently, the specimen was prone to early softening, and the topmost part of the specimen became slurry. These findings suggest that mud pumping can occur under undrained or impeded drained conditions (e.g., over-compacted capping material or clogged geotextile or blocked drainage layer) when the subgrade soil is subjected to a large degree of cyclic stress generated by heavy haul trains. As expected, the residual axial strain increases with the number of cycles. A stable specimen was observed when CSR was below 0.2, whereas the specimen subjected to a fluidised state under critical loading conditions. The laboratory results show a gradual increase in cyclic axial strain when CSR is equal to 0.2 (Figure 2). After 50,000 cycles, the maximum residual axial strain that a stable specimen can reach is still less than 0.4%, whereas the specimen under higher CSR rapidly increased to 0.8% only after 70-200 cycles.

3.2 DYNAMIC FILTRATION TESTS

This section reports the performance of a geocomposite (Test GC) and a PVD-geocomposite system (P+GC) under dynamic load. As Figure 3(a) shows that EPWPs rapidly increased beyond 32 kPa within 500 cycles in Test GC, and they continued to decrease over time. All MPTs readings were below 25 kPa after 10,000 cycles, and GC could further reduce EPWPs to under 10 kPa at the end. This confirms that although Test GC cannot dissipate the generated EPWPs at the start (within a few train passages), it helps to alleviate them gradually as the number of cycles increases. Although Test GC indicates a maximum EPWP of more than 35 kPa within 1000 cycles, there is around a 65% reduction in EPWPs due to the inclusion of the PVD.

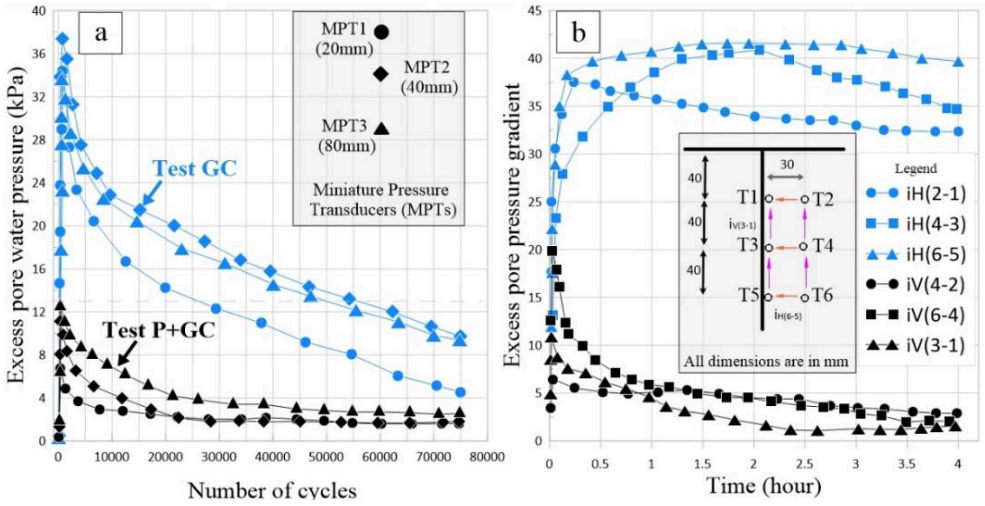

Figure 3: (a) EPWP (Tests GC and P+GC) and (b) EPPG – Test P+GC (modified after Arivalagan et al. (2022))

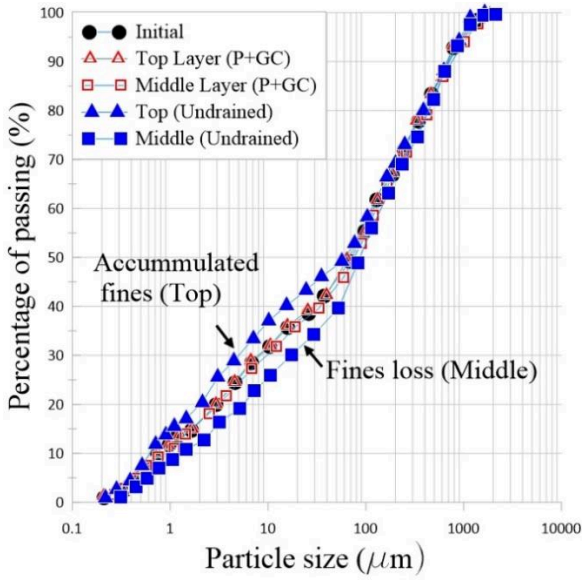

Figure 4: Particle size distribution – Undrained Test and Test P+GC (modified after Arivalagan et al. (2022))

As Figure 3(a) shows, the EPWPs developed at MPT2 and MPT3 are also consistently below 13 kPa in Test P+GC. This confirms that a wick drain and geocomposite system can mitigate the fluidization potential by continuously dissipating EPWPs, unlike undrained or partially drained tests with a geocomposite layer. The MPTs placed at various locations (T1-T6) were also used to measure the time-dependent EPPG in both vertical and horizontal directions as shown in Figure 3(b). In this specific scenario, radial drainage became the dominant factor, with lateral EPPGs swiftly escalating to over 20 within five minutes of cyclic loading (Figure 3(b)). Furthermore, deep soil horizontal EPPGs ($i_{H(6-5)}$) rose to higher values compared to topsoil region ($i_{H(2-1)}$). The horizontal EPPGs maintained above 30 until testing concluded, and they were around ten times the vertical EPPGs. Such findings suggest that wick drains facilitate radial drainage, thereby mitigating the generation of critical EPWPs.

Figure 4 shows the accumulated fines towards the top layer in undrained tests (fine loss in the middle region). However, particle pumping is effectively controlled in Test P+GC as no significant changes are observed in PSD curves compared to the initial test. In other words, the PSD of the top and the middle regions remain the same until the end of the cycle test. This proves how effectively a P+GC system could mitigate fine migration under cyclic loads.

4 A FULL-SCALE FIELD STUDY OF GEOSYNTHETICS

This section looks at two real-life trials using geosynthetics at Chullora Rail Technology Precinct and Sandgate Rail Grade Separation Project, in NSW. The fully instrumented track was built at the Chullora technology precinct, and it includes various sections, including geotextile, geocomposites and rubber geogrids. As Figure 5(a) shows, a geocomposite layer was installed on the subgrade surface to mitigate critical EPWP generation and control subsoil fluidization. If the cyclic stress that is transferred to underlying sub-soil strata is within a permissible range, geocomposite (GC) can be used to prevent excessive migration of fine particles and subsequent soil softening (Arivalagan et al., 2022; Kermani et al., 2018). As Figure 5(b) shows, rubber geogrids made of recycled conveyor belts were installed beneath the ballast layer in one of the sections (Indraratna et al., 2024). They have a similar capacity to conventional high-density polyethylene geogrids and have an energy-absorbing capacity attributed to increased damping. Indraratna et al. (2024) reported that the installation of rubber geogrids resulted in a reduction of vertical stresses at the base of the ballast layer by more than 30% compared to the control section. Moreover, rubber girds can provide effective lateral confinement.

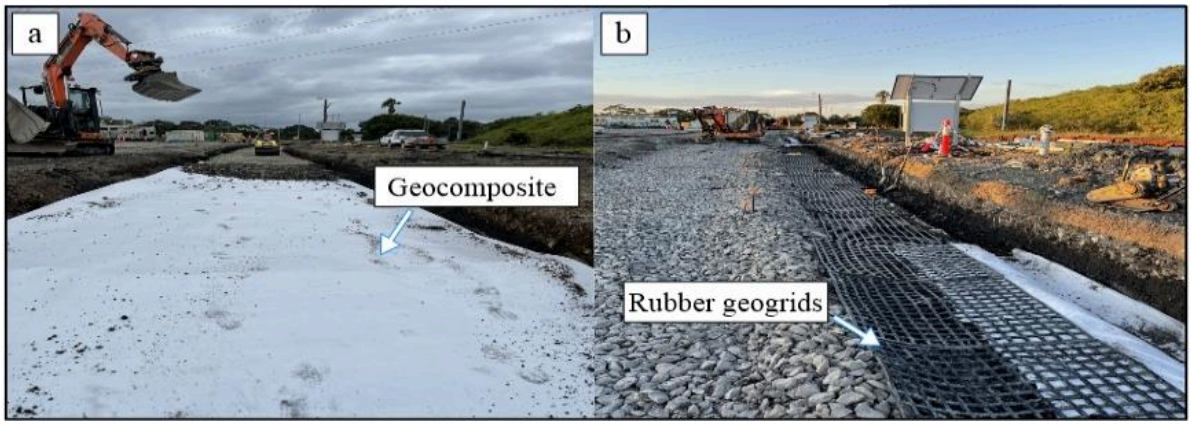

Figure 5: Installation of (a) geocomposite and (b) rubber grids at Chullora rail technology precinct, NSW

Indraratna et al. (2010b) reported the effectiveness of short wick drains at the Sandgate Rail Grade Separation Project. The railway tracks were built immediately after the PVD installation (8m long PVDs at 2m spacings). The track elevation and alignment were maintained during train passages at reduced speeds, even without establishing pre-loading techniques. Class A predictions, in conjunction with field monitoring, revealed that short vertical drains in embankments can successfully alleviate EPWPs and curtail excessive lateral displacement and thus help to stabilize track foundations that are built on soft soils (Indraratna et al., 2010b).

5 INDUSTRY IMPACT

This study presents significant findings that are valuable for geotechnical practitioners. The laboratory results show that soils with a low plasticity index, typically ranging from 10 to 20, can be highly susceptible to subgrade fluidization. Therefore, further assessment is required to stabilize the track foundation when tracks are built over low-lying soft ground and coastal areas. While soft soils with low to medium plasticity exhibit clear signs of early softening, cohesive soils with high plasticity characteristics may not experience fabric instability under similar loading conditions. The study illustrates that mud pumping often occurs at shallower depths due to the high concentration of dynamic stress that is transferred from freight trains. A comprehensive investigation is required for increased axle load and vehicle speed, as alterations in these two mutually influencing factors can lead to critical soil responses. For instance, even a reduced train speed

(<70km/h or 1-3 Hz of frequency) can initiate mud pumping under impeded drainage conditions. Geosynthetics can be a viable solution to enhance track stability by mitigating the migration of fines and dissipating EPWPs generated at shallow depths. Geocomposites designed with an effective filter membrane can serve a dual role as a filter and a separator, preventing excessive fine migration and allowing sufficient drainage. However, the application of geotextiles/geocomposites without adequate drainage and filtration properties can induce instability due to severe clogging. From a practical perspective, the combination of wick drains and effective geocomposites can mitigate fluidization potential and associated track failures. In other words, the introduction of short vertical drains can significantly prevent or delay rapid EPWP generation, while geocomposite or an effective filter can enhance surficial drainage. Note that the laboratory equipment can only accommodate small-scale soil specimens when compared to real-world field scales, and these anomalies or boundary effects will slightly affect laboratory results corresponding to the typical field behaviour.

6 CONCLUSIONS

This paper reported some innovative ways of using geosynthetics to prevent mud pumping in soft subgrades. The effectiveness of wick drains (PVDs) and geocomposites (GCs) in enhancing the stability of weak subgrade subjected to cyclic load was investigated. The key findings from this study are as follows:

- Cyclic frequency (or speed) and cyclic stress ratio (CSR) are key parameters that influence the cyclic behaviour of the subgrade. The undrained cyclic tests show that mud pumping would occur if the CSR exceeds the critical CSR (CSRc). For instance, when the CSR exceeds a certain threshold, such as CSR > 0.3, there is a rapid increase in EPWP and axial strain which makes the soil susceptible to fluidization.
- The inclusion of PVDs rapidly dissipates the EPWPs by activating the radial drainage paths. This is evident from the rapid spike in horizontal EPPG, which could facilitate radial drainage and diminish the critical generation of EPWP at shallow and deeper soil regions.
- Test results highlighted that soft soils can be fluidised under critical hydro-dynamic conditions and the PVD-geocomposite system can be used to effectively control the rapid buildup of EPWP under repetitive cyclic loading. This suggests that subgrade instability due to critical EPWP development can be mitigated by incorporating a combined vertical drain and geocomposite system in vulnerable soils.

7 ACKNOWLEDGEMENT

The financial support provided by the Australian Research Council's Industrial Transformation Training Centre for Advanced Technologies in Rail Track Infrastructure (ITTC-Rail) and Global Synthetics is acknowledged. The technical assistance from the University of Wollongong and the University of Technology Sydney is greatly appreciated. The first author would like to thank Dr Aruni Abeywickrama for her support in writing this paper. Some of the contents produced in this paper have been reproduced with kind permission from the Geotextiles and Geomembranes Journal.

8 REFERENCES

Abeywickrama, A., Indraratna, B., Nguyen, T. & Rujikiatkamjorn, C. (2021). Laboratory Investigation on the use of vertical drains to mitigate mud pumping under rail tracks. *Australian Geomechanics Journal*, 56, 117-126.

Arivalagan, J., Indraratna, B., Rujikiatkamjorn, C. & Warwick, A. (2022). Effectiveness of a Geocomposite-PVD system in preventing subgrade instability and fluidisation under cyclic loading. *Geotextiles and Geomembranes*, 50(4), 607-617, https://doi.org/10.1016/j.geotexmem.2022.03.001.

Indraratna, B., Arachchige, C.M.K., Rujikiatkamjorn, C, Heitor, A., & Qi, Y. (2024). Utilization of Granular Wastes in Transportation Infrastructure – A Circular Economy Perspective. *Geotechnical Testing Journal*, 47 (1), https://doi.org/10.1520/GTJ20220233.

Indraratna, B., Nimbalkar, S., Christie, D., Rujikiatkamjorn, C. & Vinod, J. (2010a). Field assessment of the performance of a ballasted rail track with and without geosynthetics. *Journal of Geotechnical and Geoenvironmental Engineering*, 136(7), 907-17, https://doi.org/10.1061/(ASCE)GT.1943-5606.0000312.

Indraratna, B., Rujikiatkamjorn, C., Ewers, B. & Adams, M. (2010b). Class A prediction of the behaviour of soft estuarine soil foundation stabilized by short vertical drains beneath a rail track. *Journal of Geotechnical and Geoenvironmental Engineering*, 136(5), 686-96, https://doi.org/10.1061/(ASCE)GT.1943-5606.0000270.

Kermani, B., Xiao, M., Stoffels, S.M. & Qiu, T. (2018). Reduction of subgrade fines migration into subbase of flexible pavement using geotextile. *Geotextiles and Geomembranes*, 46(4), 377-83, https://doi.org/10.1016/j.geotexmem.2018.03.006.

Nguyen, T.T. & Indraratna, B. (2021). Rail track degradation under mud pumping evaluated through site and laboratory investigations. *International Journal of Rail Transportation*, 10(1), 44-71, https://doi.org/10.1080/23248378.2021.1878947.

KIWIRAIL NORTH AUCKLAND LINE RECOVERY PROJECT: A CASE STUDY ON DESIGN AND CONSTRUCTION AT NAL 147.145KM

Monique Gainsborough-Waring
Tonkin & Taylor Ltd

ABSTRACT

The KiwiRail North Auckland Line (NAL) recovery project was initiated in response to land damage across Auckland and Northland caused by two large storm events during January and February 2023. These events resulted in damage across the NAL line including scour, erosion and landslides. Tonkin & Taylor (T+T) was engaged by KiwiRail to undertake the investigation, design and construction monitoring at seven sites along the NAL. This paper focuses on the damage encountered at chainage NAL 147.145 km, near Maungaturoto, Northland, New Zealand. The damage manifested as a 60 m long rotational landslide along the rail embankment positioned above a 15 m deep fill embankment transecting a broad valley feature. T+T produced a geotechnical risk assessment heat map to highlight over steepened embankment slopes and identify areas at risk of potential future instability beyond the visible damage, which aided discussions with KiwiRail to determine an appropriate design solution and extent. The design solution adopted by KiwiRail was a 10 m deep, 110 m long partial rail embankment replacement. Challenges were encountered when unexpected fill materials were found within the embankment during excavation. The final design remediated the landslide damage, ensured safe temporary working conditions during construction and re-used all site-won material within design, which provided the client cost and sustainability benefits.

1 INTRODUCTION

Tonkin & Taylor (T+T) worked with KiwiRail on the North Auckland Line (NAL) Recovery Project at seven different sites between Wainui, Auckland and Maungaturoto, Northland. The KiwiRail NAL Recovery Project was an emergency response project that sought to repair and remediate land damage to the NAL in Auckland and Northland caused by two significant storm events: Auckland Anniversary Flooding (27-28 January 2023) and ex-Tropical Cyclone Gabrielle (12-14 February 2023). Both events brought over 200 mm of rain within 24 hours to Auckland, with Whangarei also experiencing a similar rainfall volume during the February cyclone (NIWA, January 2023; NIWA, February 2023). This paper focuses on the major damage at chainage NAL 147.145 km, 3 km southeast of KiwiRail's Maungaturoto yard, approximately 90 km north of Auckland CBD. T+T was engaged to provide consultancy services including geotechnical, stormwater and ecological assessment for this site. This paper focuses on the geotechnical aspect of the work, including geotechnical investigations, development of concept design options, detailed design in consultation with KiwiRail and support through the construction phase by providing engineering inspections and completion documentation for geotechnical elements.

1.1 SITE DESCRIPTION

The rail line at NAL 147.145 km is located on a 15 m high, 200 m long fill embankment that transects a gully feature. The site damage (Figure 1) manifested as a 60 m long rotational landslide on the western side (LHS) of the tracks with the headscarp running parallel to the tracks adjacent to the sleepers. The upper section of the fill embankment (top 6 – 8 m) slopes at an angle of approximately 35° with localised over steepened areas up to 40°. The lower section of the embankment slopes at a gentler gradient (10 - 15°).

Floodplain extents were mapped using local council GIS Hazard Maps (NCR, 2020) and T+T undertook an ecological assessment to identify wetlands within the surrounding area. A large floodplain is located on the western side of the embankment extending along approximately 95 m with wetlands mapped within. An existing concrete arched culvert (1.8W m x 1.5H m) with the inlet positioned on the western side promotes flow of surface water from the upstream area and floodplain. The culvert is approximately 100 m long and runs beneath the embankment, with a true left bend, and outlets on the eastern side of the embankment onto a second floodplain extending 20 m along the embankment towards the south.

Historical landslide features were identified on the surrounding natural slopes in vicinity to the site, typically oriented east-west. Besides the landslide damage seen at NAL 147.145 km, there were no obvious signs of recent, large scale landslide movement in the embankment or on the nearby slopes.

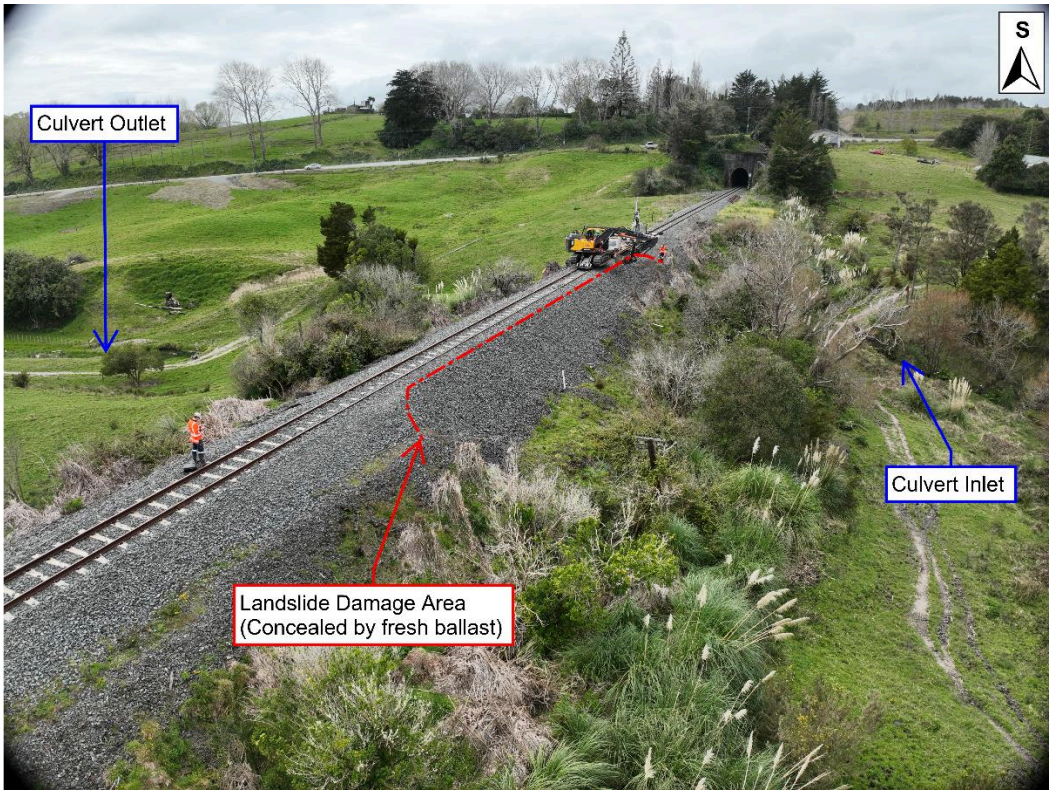

Figure 1: Aerial view, facing south of the western side of the NAL at 147.145 km captured by UAV.

2 INITIAL ASSESSMENT & GEOTECHNICAL INVESTIGATIONS

Tonkin + Taylor undertook a geotechnical site investigation that included one machine borehole, three hand augers and five test pit excavations. Geomorphic mapping and a desktop study were carried out in parallel, which provided insight into the site's geological history and supported development of the ground model.

The regional 1:250,000 geological map (Edbrooke & Brooke, 2009) for the area presents undifferentiated Melange and Mahurangi Limestone of the Northland Allochthon as the basement geological units for the site. Overlying these Northland Allochthon units are younger landslide deposits. The machine borehole completed by T+T encountered 15 m of fill (described as clayey SILT) overlying a thin (<1 m) layer of alluvium over pervasively sheared mudstone of the Northland Allochthon. The geotechnical investigations appear to align well with the expected regional geology.

Geomorphological assessment and knowledge of relevant geological units present revealed the site location had a large-scale stability risk. Mangakahia Complex of the Northland Allochthon, part of the undifferentiated Melange, has a low residual friction angle (between 10° to 13°), and subject to soil creep as ‘lobes’ of this unit progressively readjust to maintain equilibrium (Winkler, 2003). In addition, nearby sections of the NAL with similar geologic and topographic conditions show evidence of large-scale historical landslides and instability. However, we found no conspicuous signs of recent landslide movements at the site linked to deeper historical landslide activities and deemed these features inactive.

Inspection of the landslide showed a 60 m headscarp adjacent to the sleepers in parallel to the tracks with the toe bulge 8 m below the track and 12 m out from the centre of the embankment within the fill material, signs of a complex rotational failure.

3 DESIGN

This section provides an overview of the steps taken to address the embankment instability. A back analysis was first completed that allowed us to utilise these insights to develop a design solution and risk assessment of the site area that formed an approach that considered the past, the present instability and future risk.

3.1 BACK ANALYSIS

The ground model for the rail embankment was back-analysed using Slope/W software (GeoStudio 2023) to establish the material parameters for the soil and determine the failure. Our initial assessment and back-analysis concluded that the

damage was due to a rotational slope failure within the fill embankment and did not extend into the natural ground. The embankment failure was likely triggered by an elevated groundwater level caused by heavy and prolonged rainfall, rather than a deep-seated creep type failure in the underlying Northland Allochthon rock (Winkler, 2003).

3.2 ENGINEERING DESIGN

During the design of the remedial options, slope stabilisation measures were included into the Slope/W model. Two concept remedial designs were developed that included a retaining wall option and an earthworks option. The proposed engineering solutions were to repair the embankment failure and did not consider site wide global stability associated with failure in the Northland Allochthon rock. Based on the remedial solutions analysed, we developed two concept design options and presented them to KiwiRail. The design options had both opportunities and threats which were presented to KiwiRail, summaries of these are presented in Table 1 below.

Table 1: Summary of opportunities and threats associated with the concept options presented to KiwiRail.

Solution	Opportunities	Threats
A) Retaining wall (to support the embankment)	1) Possible to construct post re-opening of the line (subject to KiwiRail accepting suitability of line for rail traffic in current state). 2) Minimal earthworks required (reducing work with floodplains). 3) Reduced construction timeline. 4) Less susceptible to weather conditions.	1) High number of elements involved (piles, walers, anchors and drainage) – time-consuming, complex procurement and specialised contractors. 2) Ongoing maintenance throughout the design life. 3) Required structural design input. 4) Pile embedment may face difficulties due to obstructions within the embankment fill. 5) Installation of tie-back anchors require complete removal and reinstatement of the formation.
B) Earthworks - reconstruction of the failed embankment slope, western side, at 1.5H:1V, with a shear key at the toe of the slope	1) Minimal maintenance required after construction. 2) Repurposes the excavated embankment fill. 3) Readily available and locally sourced materials, reducing procurement issues. 4) No specialist contractors required.	1) Extent of earthworks would be substantial. 2) Significant volume of work to remove and rebuild the embankment (including in mapped floodplain zones). 3) The undercut and backfill volume could potentially increase due to deeper/wider excavations than anticipated. 4) Timeline is reliant on good weather conditions; any wet weather could cause delays in the programme. 5) Must be completed before the line reopens.

After a careful assessment of the opportunities and threats listed above, KiwiRail's preferred option was to develop the earthworks option. The design of the earthworks option was an iterative process with inputs from KiwiRail, the Contractor and T+T. The concept design was developed further to best optimise the re-use of existing materials, minimise the existing slope risks and the construction costs.

To assess the existing slope risks a geotechnical risk assessment heat map was produced (Figure 2), part of the multi-criteria analysis (MCA), to decide how far we would extend the remedial works. The embankment height and slope angle were determined using Global Mapper 24.0 and a risk matrix was developed, by using back analysed soil properties of the existing embankment fill and historical LiDAR, to determine the risk of future instability of the embankment. Sections of the embankment were assigned if they were low, medium or high-risk using this matrix. The results illustrated localised over-steepened slopes with medium to high risk of potential future slope instability on both sides of the embankment and extended beyond the observed failure area.

This heat map was used in the MCA to assess the need to repair both sides of the embankment rather than focus on just the failed side as it showed the opposite side with a high risk of slope instability. In addition to addressing potential future instability, repairing both sides of the embankment rebuild would open up the site to create easier/safer access for the rebuild. In addition, access to the site was enabled from the eastern (non-failed) side of the embankment which made construction of the repair to both sides more straightforward.

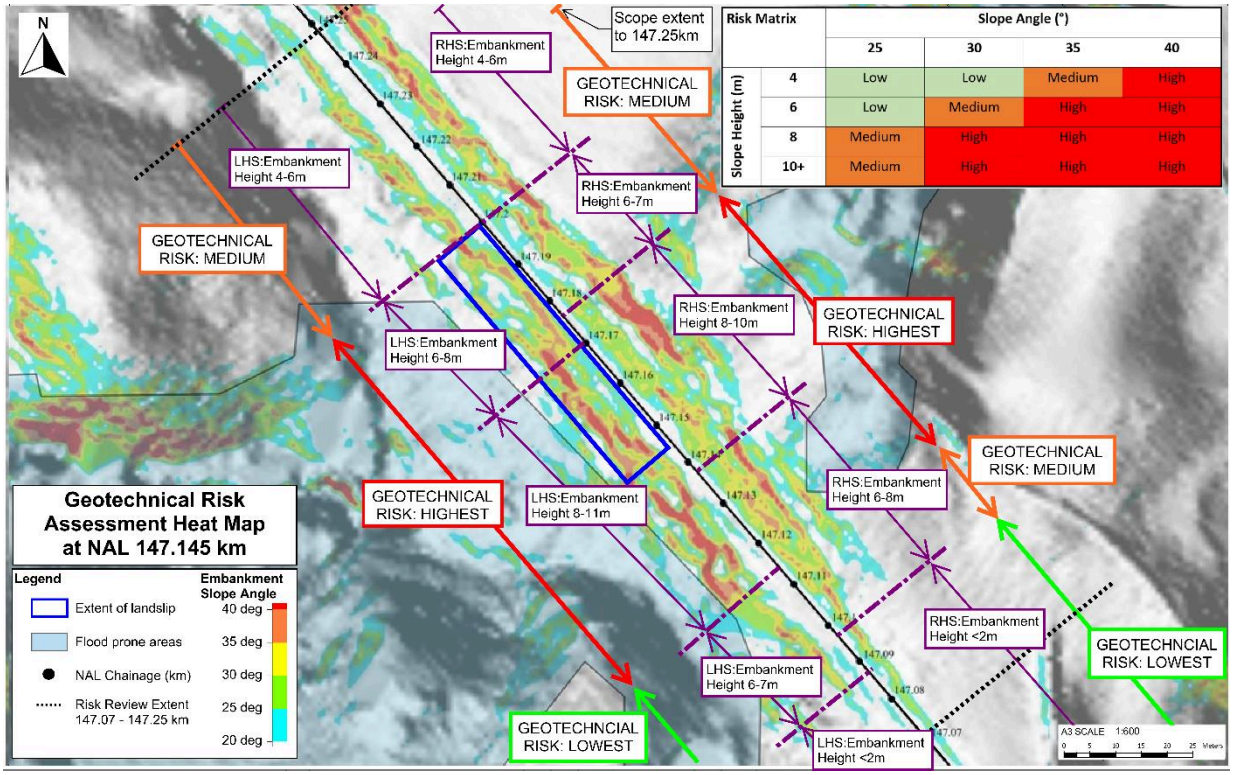

Figure 2: Geotechnical risk assessment heat map of chainage NAL 147.07 – 147.25 km and risk matrix.

3.3 FINAL DESIGN

The final design adopted, presented in Figure 3, incorporated the following elements; a granular core to support the rail track (width of sleepers at top of embankment) constructed at 1.2H:1V and buttressed for additional stability using site-won fill underlaid by a >1m thick drainage layer, as the embankment is located on a floodplain. The design incorporated both sides of the embankment and extended beyond the initial concept solution, which focussed on the failed western embankment, to capture the high-risk zones identified by the geotechnical risk assessment heat map.

The extension of the design provided safe temporary working conditions as the excavation profile would descend progressively in a benched approach and tied the new design with the existing embankment profile. The embankment re-build re-purposed the excavated site-won material which provided a sustainable approach.

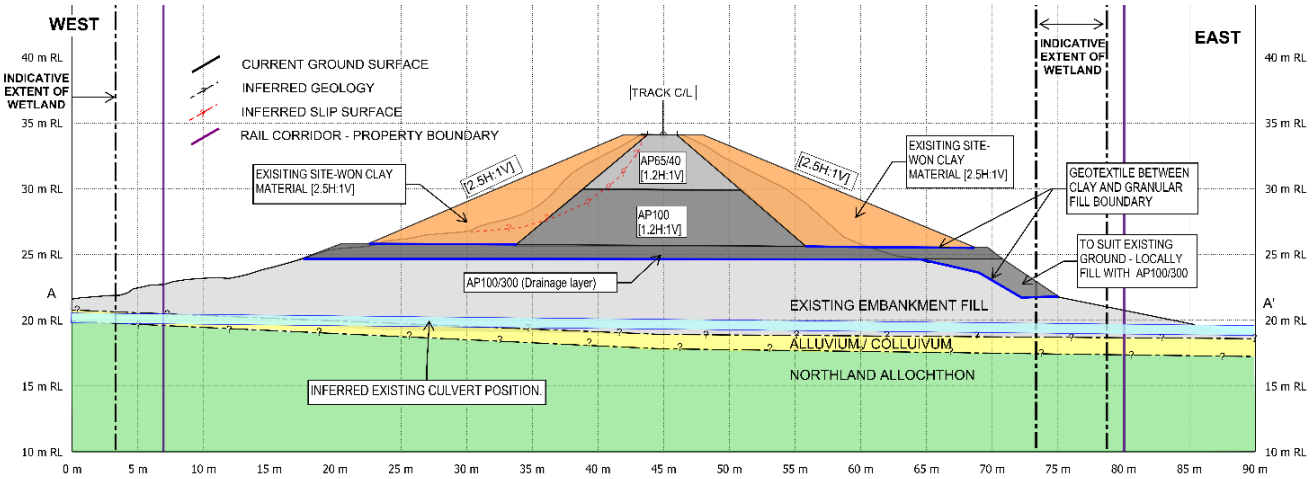

Figure 3: Earthwork solution for the embankment re-design to address instability within the embankment and maximise the re-use of existing materials.

4 EARTHWORKS

4.1 EXISTING EMBANKMENT EXCAVATION

The first phase of the project was to excavate the existing embankment. Excavated material was stockpiled on the adjacent farmer's property within their quarry, reducing transportation and storage costs.

4.1.1 Unexpected Material

During embankment excavation, a wide range of materials were encountered, these comprised of variable fill materials consisting of scoria, old ballast and boulders up to the depth of 7 m below the tracks at the southern end of the landslide extent. This contrasted with the cohesive fill at the northern end of the site. Blocks of concrete and cement-stabilised fill were also scattered within the cohesive material at the site's northern end, extending to depths of up to 10 m below the rail line. The cement stabilised fill comprised large blocks of cement, ballast and rockfill and appeared to be an earlier attempt to stabilise the rail formation in the embankment. The blocks were many meters long (Figure 4) and had to be broken up by the excavators before they could be removed. The unexpected fill materials raised questions about how best to use all these varying materials in the embankment re-build as the original design had assumed clay fill as the buttress material. Collaborating with the contractor, we re-evaluated the situation and amended the design to ensure we reused all the excavated material in a systematic way. The different materials were separated out and placed into different stockpiles around the site. The contractor was able to crush large concrete pieces into <300 mm size to allow re-use of this material. The granular site-won fill was to be used as the base of the buttress fill with the cohesive site-won fill to sit above it.

Figure 4: Blocks of cement stabilised fill encountered at NAL 147.145 km.

4.1.2 New embankment Subgrade Testing

At the base of the embankment rebuild, the subgrade was tested for soft material. The subgrade on-site generally met the required specifications, and any soft zones identified required an undercut. Some organic soils and old sleepers within the subgrade were encountered and removed before construction.

4.2 EMBANKMENT REBUILD

The basic design for the earthwork rebuild was for a granular core under the centre of the embankment, to support the rail line, and buttressed on either side with the existing materials from the old embankment.

To build the drainage layer, AP65/300 greywacke was used, sourced locally from Atlas Quarries at Brynderwyn Hills' (Auckland side). Standard NDM testing was inadequate due to the material size and a compaction trial, including a proof roll, was undertaken to determine compaction methodology, to ensure the material interlocked effectively and achieve satisfactory compaction with no deflection witnessed (NZGS Specification, 2022).

PAP65 rockfill was used to build the granular core which replaced the concept design AP100 rockfill, as it was more readily available and sourced from the same local quarry. The construction of the core progressed in 300 mm loose lifts.

The buttress fill, that supported the granular core, was divided into the western and eastern side and repurposed the site-won materials. Lower lifts used site-won granular material, while cohesive material was used for the higher lifts of the buttress. Where the buttress fill overlaid any floodplain/wetland, a granular fill detail was implemented to allow excess water to flow out and not impact the buttress fill's stability. The compaction process for the cohesive buttress fill was

sensitive to weather conditions. Consequently, periods of wet weather led to delays, given the necessity for simultaneous progress of both the granular core and the buttress fill to maintain adequate site accessibility throughout the construction.

The formation design, the upper ~1 m zone beneath the rail line, was based on KiwiRail's standard formation design C-ST-FO-4110 (2019) consisting of a 600 mm structural fill (PAP65) layer with interbedded geogrids, a 150 mm structural fill (PAP40) layer, and topped with a 300 mm thick layer of ballast.

5 FLEXIBILITY & SUSTAINABILITY IN DESIGN

As the project was guided by the need to re-open the railway line as soon as possible flexibility in the design and construction was required to prevent lengthy hold-ups. Unexpected fill materials encountered onsite emphasized the need for flexibility in the embankment design and re-use of materials.

Entering the excavation phase of the embankment, we had little idea of the complexity that lay ahead. The site's long history, marked by numerous repairs and remediation efforts, led to a surprising variety of unearthed fill materials. Our initial design had accounted for cohesive fill, so the granular material we encountered presented a significant deviation from our planned approach. This raised a practical challenge on how we could effectively incorporate all site material into a stable, long-term embankment design. This situation outlined the importance of flexibility when dealing with unforeseen circumstances during construction.

In close collaboration with the contractors, we reassessed and modified our strategy. As designers we were required to amend the design to suit and work with the Client and Contractor to make best use of the site-won materials. The Contractor was required to manage the re-use of different materials and create stockpiles across the site. The materials were stockpiled based on material properties and separated as site-won scoria, clay, scoria/ballast mix and concrete pieces that were crushed into less than 300 mm size for easier re-utilization. Each separate material distinguished underwent laboratory testing and a compaction trial onsite to determine the appropriate methodology, optimum number of roller passes required, to meet a minimum dry density of 95% of the tested material laboratory maximum dry density.

Ultimately, the unexpected materials turned into sustainable opportunity. By assigning the site-won granular fill to form the base of the embankment buttress and placing the cohesive site-won fill above, we successfully repurposed all the excavated material into the design. This eliminated the need for off-site disposal, preventing unnecessary transport to landfills. This approach highlights the need for adaptability in construction projects and reaffirmed the value of reusing material, reducing waste and optimising resources all in line with the principles of sustainable design.

6 CONCLUSION

The successful design and construction of the embankment replacement at NAL 147.145 km has facilitated the re-opening of the rail line by ensuring a design that not only targeted the slope failure because of the 2023 storm events but also for potential future slope instability risks. This project highlights the value of collaboration and flexibility as it has the potential for turning unexpected outcomes into opportunities for sustainable design and construction.

7 REFERENCES

Blue Marble Geographics (2024). Global Mapper 24.0 software.

Brooke, S.W.; Brook, F.J. (comps). (2009). Geology of the Whangarei area. Lower Hutt: GNS Science. Institute of Geological & Nuclear Sciences 1:250,000 geological map 2 68 p + 1 folded map.

GeoStudio (2023). Slope/W software.

KiwiRail (2019). Civil Standard: Formation. Document number: C-ST-FO-4110, Issue 1.0.

NIWA (January 2023). 'Climate Database Statistics Report.'

NIWA (February 2023). 'Climate Database Statistics Report.'

Northland Regional Council (NRC) (2020). 'Natural Hazards' map viewer. Available at https://nrcgis.maps.arcgis.com/apps/webappviewer/index.html?id=81b958563a2c40ec89f2f60efc99b13b

NZGS Specification (2022). NZGS Earthworks & Ground Investigation Specifications, New Zealand Geotechnical Society. NZGS_0510 Earthworks, version 0.2 – Draft38. Available at http://www.nzgs-earthworks-ground -investigation-specification

Winkler, G. E. (2003). Geotechnical engineering of the Northland Allochthon. In: Geotechnics on the Volcanic Edge. Paper presented at the New Zealand Geotechnical Society 2003 Symposium, Tauranga, New Zealand.

IMPLEMENTATION OF DIGITAL TECHNIQUES TO OPTIMISE SLOPE REMEDIATION DESIGN IN QUEENSLAND, AUSTRALIA

Henry Venus, Ryan O'Neill
Arup

ABSTRACT

Throughout early 2022 across Southeast Queensland rainfall events caused significant damage to the region's roads causing several landslips and rockfalls. The State Road authority identified 132 sites (Figure 1) across the region for remediation works, presenting a unique challenge with the sites located over a 1000km² area that required large digital data exports for geotechnical remediation solutions.

The scope of this study encompasses multidisciplinary slope remediation design, incorporating scaling, rock anchors and soil nailing treatments along with drainage and safety improvements. With a vast number of sites to address, efficient data capture and analysis were critical. The challenges posed by the volume of sites necessitated the rapid collection and processing of publicly available information.

Leveraging Feature Manipulation Engine (FME) project specific service tools were created, that allowed the team to export data into the required Australian standard format for use within cross sections and 2D plans for each site. The user-friendly interface allowed exports of up to 3km² including state control lines, one metre contours, digital elevation tiles and state government aerial imagery that was compiled and assembled as project ready data in a few minutes, versus traditional approach of few days/weeks.

This project showcases the successful implementation of digital data capture, GIS analytics, and FME scripting within project delivery, specifically slope remediation design. The results achieved demonstrate the potential of these techniques to revolutionise geotechnical engineering practices and expedite project delivery. The automation within GIS holds promise for continued enhancements, making it an exciting prospect for the engineering community.

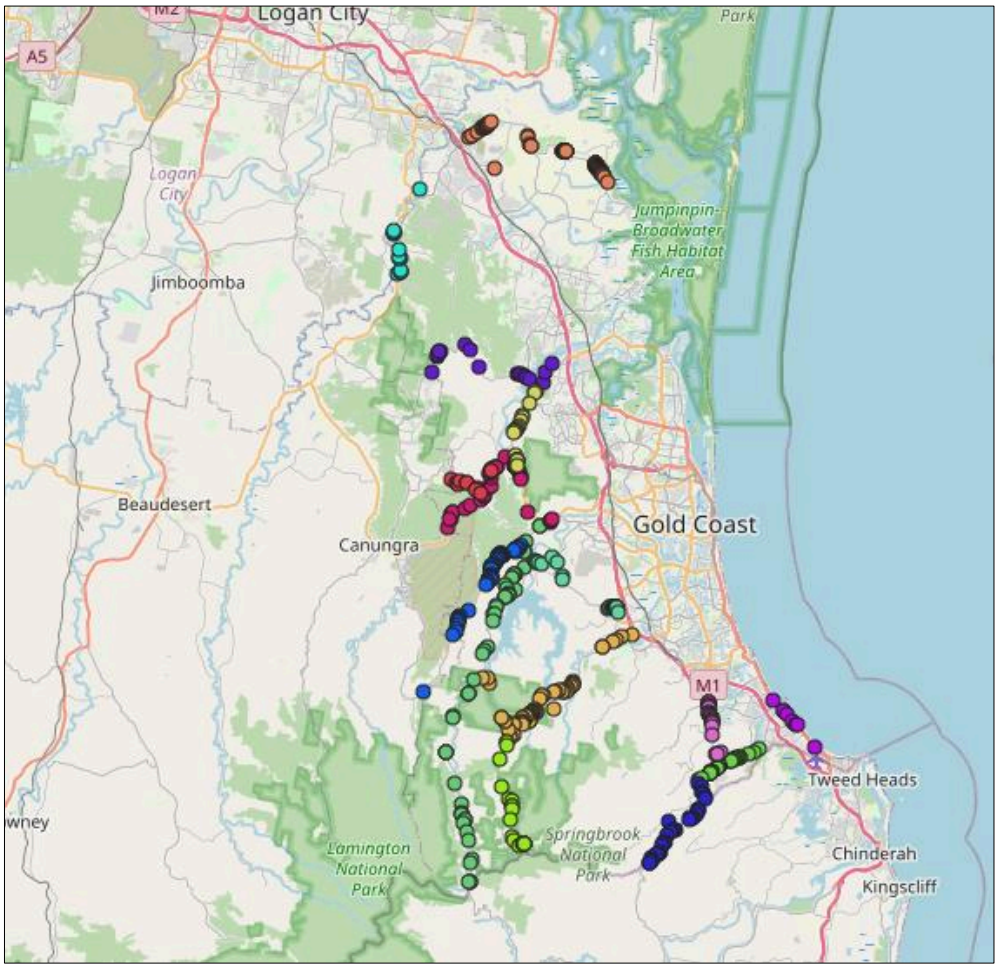

Figure 1: Location of sites involved in project and requiring digital data

1. INTRODUCTION

The Southeast Queensland (SE QLD) roadway network includes a number of range roads in mountainous terrain which are vulnerable to extreme rainfall and bushfire events and there have been several of these extreme events in SE QLD since 2014. Arup were engaged in response to the damage to state road assets as a result of the following severe natural disaster events during 2022:

- **22A** – Central, Southern, Western Queensland Heavy Rainfall and Flooding (10th November / 3rd December 2021);
- **22F** – South-East Queensland Heavy Rainfall and Flooding (22nd February and 7th March 2022); and,
- **22I** – South-East Queensland Flooding (6th May and 20th May 2022).

These events caused significant road damage including numerous landslips, widespread pavement damage and scouring to the road network in Southeast Queensland. Arup were contracted to review, investigate and provide design solutions to remediate damaged assets within the City of Gold Coast Local Government Area (LGA 230).

Our client identified 132 sites across the region for remediation works that required large digital data exports for geotechnical remediation solutions to be developed.

1.1 SITES PACKAGE DESCRIPTION

The roads within the City of Gold Coast Local Government Area (LGA 230) which sustained damage by the 2022 DRFA events and are included in the design package are shown in Figure 2.

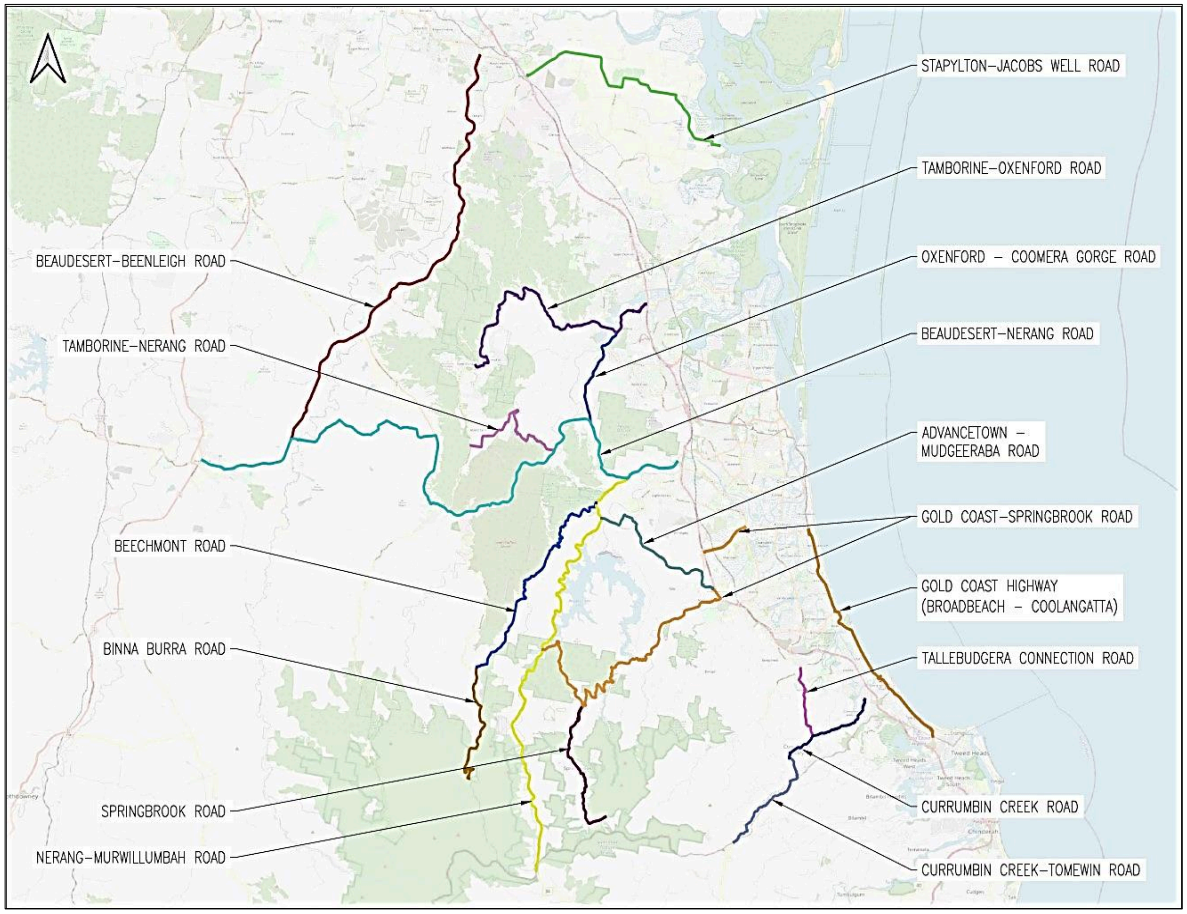

Figure 2: Location of roads within project

The design services were delivered in several packages to accelerate the various technical scope and approvals necessary to deliver the works, these are outlined below:

1. **IRW** – Immediate Reconstruction Works (Roads 104, and 2020);
2. **Urgent REPA** – Restoration of Essential Public Assets (Roads 201, 2001 and 2011); and,
3. **REPA and Betterment Package** – All SCR Roads for LGA 230.

1.2 REPA AND BETTERMENT NON-STANDARD MAINTENANCE SITES

This paper is specific to the REPA and Betterment Non-Standard Maintenance sites and relates to smaller magnitude failures in terms of size as shown in Figure 3.

The project sites included a significant amount of smaller magnitude failures requiring a geotechnical remedial solution with a need for rapid data collection over a large geographic mountainous terrain area.

Figure 3: Example failure types
Images from the REPA and Betterment Package, upslope site on left and downslope site on right.

2. PROJECT DATA

In Queensland digital data is stored across various databases depending on the authority involved. There is publicly available factual data to input to engineering understanding and assessment of sites, but no easy way to access the data for such large areas. In this case for the REPA and Betterment Package located over a 1000km2 area of mountainous terrain (Figure 4).

2.1 REQUIRED PROJECT DATA

For a standard output we require up to date information from across varying database providers and for slope remediation, shown visually in Figure 4 and outlined below:

- **1.0m Digital Elevation Model (DEM) tiles** – downloaded from ELVIS (Elevation Information System) – prepackaged 1x1km Tiff files;
- **State imagery** – on the state's imagery server, access from an API – this is on an esri server open to the public;
- **State road control lines, Digital Cadastral Database (DCDB)** – on the states GIS server (also an esri server); and,
- **State 10m chainage markers** – on the governments states open data portal internet site.

Figure 4: Images of required project data
Left - state imagery / Right - road control line.

2.2 PROBLEM WITH REQUIRED PROJECT DATA

Due to having to access public databases separately / each time the data is required for every site, a number of key problems arose due to the vast number of slope remediations sites requiring treatment within this package, outlined below:

- **1m DEM tiles –** Online system requiring manual input with drawing area online in their portal, tick box), enter your email address and then wait 10-30 minutes for the system to package up a zip download and email you the download link. Across 132 sites traditionally this would have taken over a week of time;
- **State imagery** – Exported as a .tiff format, which is more time consuming for internal teams to process. Traditionally ECW files are used;
- **State road control lines, DCDB** – Queensland sits across a variety of GDA Zones and this data is stored in the state system in a lat/lon format not compatible for a project in GDA2020 Zone 56 coordinate system; and,
- **State 10m chainage markers** – CSV text-based format (with latitude / longitude co-ordinates in the sheet) and 10m markers can sometimes be slightly off from the control line, requiring a manual time consuming process to correct.

3. SOLUTION THROUGH FME SCRIPTING AND GIS ANALYTICS

All of the required project data needs to be downloaded from publicly available databases in more of a time efficient process, then converted and prepared to a usable project specific format.

It was not practical to complete a one-off conversion for the whole state/region/city or even project area as the file sizes would be unworkable with estimated hundreds of gigabytes which would not process in standard software i.e. CAD and/or 12d. Additionally, given the moving scope of project with sites / eligibility criteria /changing site locations and extents; it was also not practical to develop programming script an output of sites and move on.

3.1 ARUP TOOL OVERVIEW

An ARUP in house internal tool (Figure 5) was developed utilising the FME server with self-service functionality, by drawing a box on a map which was a basic leaflet window that allowed users to draw up to 3km² at a time and then send a request to the FME server to prepare the required data. The leaflet window gets the coordinates and sends the request to the server with the user waiting two minutes for the data, which is then provided in a zip folder.

Figure 5: Arup internal self-service tool for extracting project data through an FME server

3.2 DEVELOPMENT OF ARUP TOOL THROUGH FME SCRIPTING

The following stages within the Arup tool were developed within FME server to extract the prerequired data in the correct format suitable for project use:

1. **1km markers and Control Lines** – The first part was the 1km chainage markers, these were reprojected, a cad layer name added, the text label added and then run through to cad file. The downloads the state control lines, reprojects and then adds the layer name before exporting through to the same cad file. In all cases, inputs are only requesting a download from the state server within the bounding box.

2. **DCDB Export** – Same as above, the base parcels from the QLD DCDB gis server are requested. The lot plan text is added and layer names created as attributes before exporting to a usable cad file.
3. **Imagery** – The imagery export uses the states imagery server "export image" function – this allows us to feed lat/lon coordinates at the server and it provides a tiff image. We then reprojected and exported as an ECW for use in CAD.
4. **DEM/Contour** – Now with the initial elvis download providing a significant number of small tiles – we downloaded the entire local government in one go (well over 10GB of tiff elevation files) and merged them into a single large tiff file (Figure **6**). This then allowed FME to go to the large tiff file sitting on our server, clip out the smaller box needed and then convert into both a DEM file (used for 12d – generating cross sections) and the contours in CAD (setup to standard with major/minor lines and correct cad symbology required).

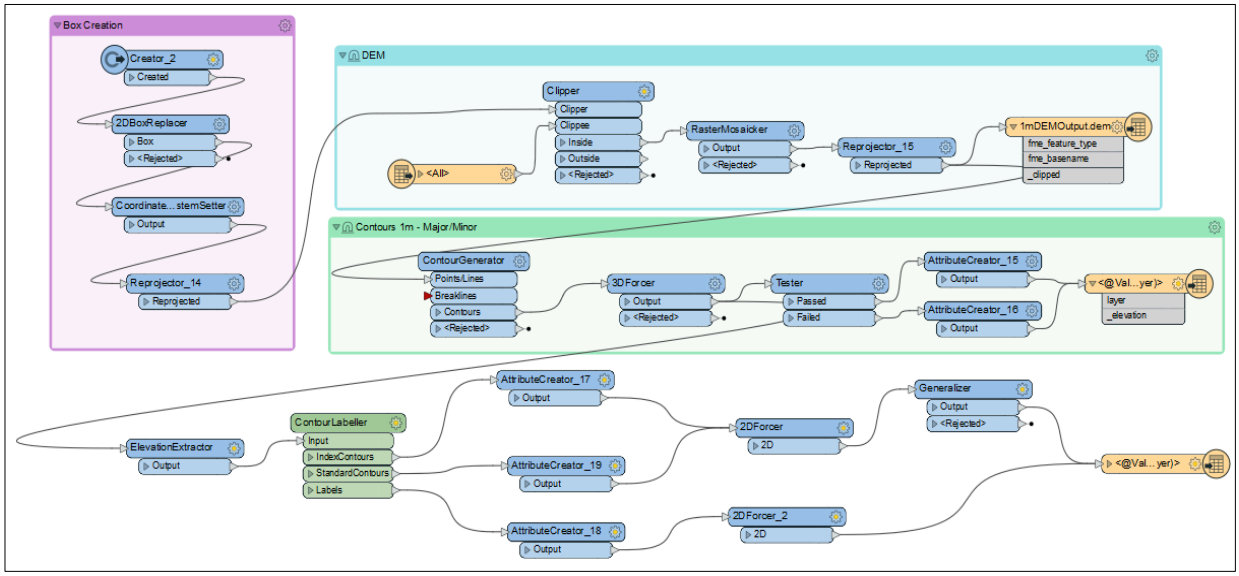

Figure 6: DEM/Contour to CAD file format FME script

5. **10m chainage to CAD file format** – One of the more challenging parts was the 10m chainage files. Design drawings require chainages to be shown with 10m tick marks preferred along the line. These 10m chainages were saved as a CSV file with the latitude / longitude. The developed process, snaps the points to the line, generates the chainage ticks on the line, with the required offset and creates the chainage text for the cad file

4. OUTCOME WITH FINAL DESIGN

Over the course of the project there were 100+ exports successfully completed with an average run time of 2 minutes. Historically the process would have involved a variety of teams including Geotech, GIS and CAD to produce the same results however this had now been streamlined down to a self-request task using a map through a ARUP internal tool.

The output from the streamlined data collection process fed into the design drawings.

4.1 DESIGN DRAWINGS

An example snippet from a design drawing is outlined in Figure 7, it shows an upslope rockfall mesh / anchor solution once1m DEM tiles, State imagery, State road control lines and State 10m chainage markers have been included.

The output of publicly available data in a workable form allowed the multidisciplinary remedial design to take place, however it is important to note there was still significant amount of design work following data output; the process is automating drawings as opposed to automating design. Additionally, the tool had some flaws, outlined below:

- Need for removal of output data with low quality (imagery/DEM etc), triggering need for survey/drones;
- Individual tasks such as manual manipulation of control lines to match aerial centrelines, or to cut cross sections not perpendicular to road were on occasion still required; and,
- Arup internal tool limited to a 3km² square area, requiring multiple requests to extract all project data that was required.

Nonetheless, having this baseline data in workable formats reduced the time to move onto downstream design tasks, and eventually project timelines.

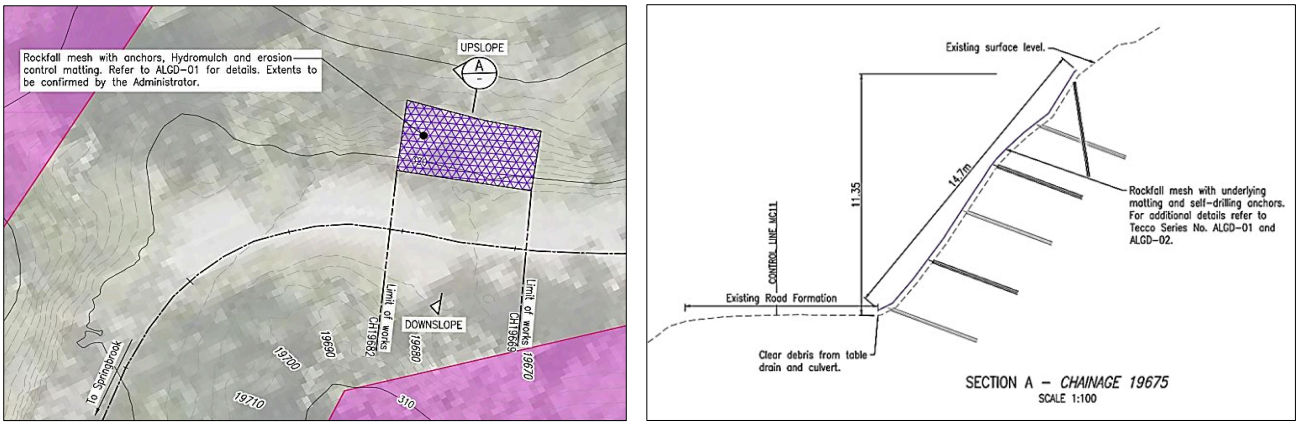

Figure 7: Example design drawing and cross section

5. CONCLUSION

This project showcases the successful implementation of digital data capture, GIS analytics, and FME scripting within project delivery, key outcomes are noted below:

- Streamlined digital process enabled rapid development of engineering solutions reducing project timeframes.
- The results achieved demonstrate the potential of these techniques to improve geotechnical engineering practices.
- The automation within GIS / FME holds promise for continued enhancements, making it an exciting prospect for the engineering / geoscience community.

The south-east Queensland road network includes a number of range roads in mountainous terrain which are vulnerable to extreme rainfall and bushfire events and with climate change and increasing inclement weather anticipated, it is likely there will be additional events requiring rapid response. Utilising automation within digital workflows can streamline data gathering and processing, ultimately leading to this much needed quicker response to facilitate shorter program timeframes.

Initiatives like Digital Atlas of Australia, expected to be fully functional by 2025 will facilitate access to hundreds of trusted datasets on Australia's geography, people, economy and the environment in a central platform and integrating into FME processes will allow for more information to be readily available for use within geotechnical engineering practices.

Additionally, using generative Artificial Intelligence (AI) for geospatial data processing in FME (Warner, T. 2023) will drastically assist in the automation of workflows, to create and train digital models with predictive capabilities to produce an output given varying input parameters / data.

6. ACKOWLEDGEMENTS

Due to the multidisciplinary nature of the work, development of the paper relied on the advice and support of many individuals and teams within Arup, we would like to thank everyone involved across all project teams, this includes Structures, Drainage, Civil, Pavements and most notably GIS and Geotechnical teams.

7. REFERENCES

Digital Atlas of Australia. (2024). Australian Government (*Online)*. Accessed 28th July 2024. Link: *https://digital.atlas.gov.au/*

Warner, T. (2023). Linedin Article. (Online). Accessed 28th July 2024. Link: *Using Generative AI for Geospatial Data Processing in FME (with 6 Examples) | LinkedIn* | LinkedIn

SEISMIC ASSESSMENT OF SOIL ARCHING IN A PILE-SUPPORTED EMBANKMENT: NUMERICAL ANALYSIS

Naveen Kumar Meena[1], Sanjay Nimbalkar[2]

[1]*Geotechnical Engineer, Beca Pty. Ltd., Sydney, NSW 2000, Australia.*

[2]*Associate Professor, School of Civil and Environmental Engineering, University of Technology Sydney, NSW 2007, Australia.*

ABSTRACT

Pile-supported embankments offer viable solutions for railroad construction on soft soil, boasting rapid construction while minimising differential settlements. Within these embankments, the soil arching mechanism plays a crucial role in transferring load from the subsoil to the pile head. To date, numerous finite element method (FEM)-based studies and model tests have explored soil arching under static and traffic-induced cyclic loading conditions. However, the dynamic behaviour of soil arching within these embankments during a seismic event remains uncharted territory.

This paper delves into the dynamic behaviour of soil arching in a pile-supported embankment during a seismic event, employing two-dimensional (2D) plain strain numerical analysis. The findings of the numerical analysis demonstrate the profound influence of earthquakes on soil arching. It is evident that the geosynthetic-reinforced embankment provides a feasible solution for a sustainable and resilient railroad infrastructure in seismically active regions.

1 INTRODUCTION

Over the past decade, investment in transport infrastructures, including railways, roadways, airways, and ports, has been pivotal to the economic growth of the country. In the recent budget of Australia, the Australian government has announced an investment of $16.5 billion in transport infrastructures (2024-25 Australian federal budget). Among all transport modes, railways have been recognised as the most eco-friendly transportation option. Consequently, the construction of railway corridors is experiencing significant growth worldwide (Meena, N.K., 2022). However, the construction of these corridors often encounters poor ground conditions characterised by low strength and high compressibility, and some of these corridors are constructed in seismic-prone regions (Deng et al., 2024).

Various ground improvement techniques have been employed to enhance the engineering properties of unsuitable ground conditions and provide a stable railway subgrade (Arulrajah et al., 2009). Among all ground improvement techniques, the geosynthetic-reinforced pile-supported (GRPS) embankments offer a cost-effective, rapid, and sustainable construction solution that aligns with the United Nations (UN)'s Sustainable Development Goals (SDGs) while maintaining the performance of the overlying railway tracks.

In the GRPS embankments, loads exerted by the embankment, including surcharge, are partially transferred to the rigid concrete piles through a shear resistance (soil arching) mechanism, owing to the stiffness differences between the rigid concrete piles and the surrounding subsoil. Additionally, geosynthetic layers enhance load transfer to these piles via the tension membrane effect. The soil arching mechanism in GRPS embankments is discussed further in the subsequent Section.

The response of the soil arching mechanism in GRPS embankments under static loading and traffic-induced cyclic loading has been assessed in the past (Han et al., 2015; Niu et al., 2018). Han et al. (2015) conducted a series of model tests and numerical analyses to conclude that the reinforcement characteristics and subsoil properties improved the soil arching mobilisation under dynamic loading. Niu et al. (2018) reported that the height of soil arching is reduced under the high-speed train-induced load compared to the static loading condition. However, the earthquake-induced dynamic behaviour of soil arching in pile-supported embankments remains to be fully explored.

Although Australia is widely recognised as a seismically inactive country, small to moderate seismic activities continue to occur (Daniell and Love 2010). The indicative locations of a few earthquakes in Australia to date are shown in Figure 1. Therefore, this study delves into the impact of an earthquake on soil arching mobilisation in a pile-supported embankment, both with and without geosynthetic reinforcement.

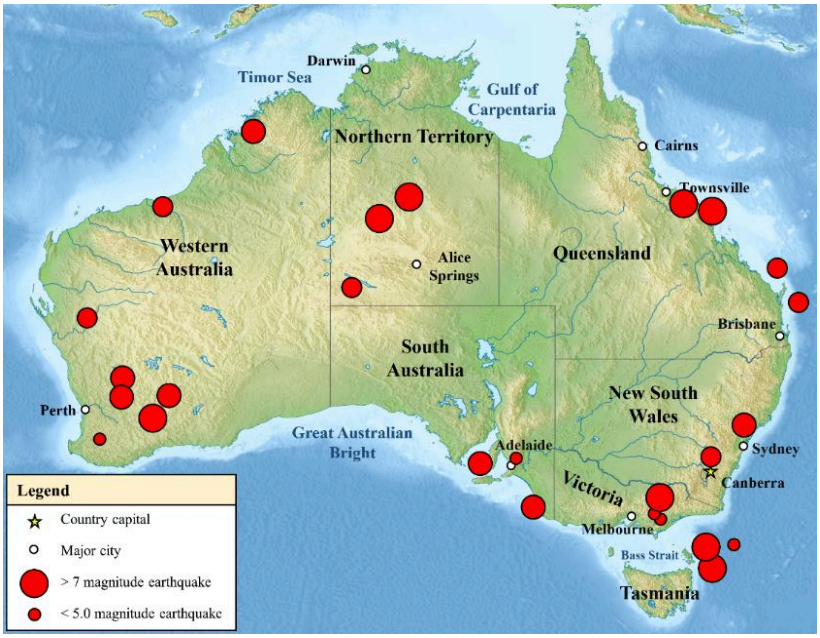

Figure 1: Indicative location of a few earthquakes in Australia and territories (modified from Meena and Nimbalkar 2021)

2 NUMERICAL ANALYSIS

2.1 FINITE ELEMENT (FE) MODEL DESCRIPTION

Nowadays, computational methods can solve complex problems with reasonable accuracy, requiring less time and cost. In this study, finite element (FE) computational software ABAQUS version 2013 (Systèmes, D., 2013) is used to assess the soil arching in a pile-supported embankment adopting two-dimensional (2D) plain strain idealisation. Figure 2 illustrates a schematic diagram of a typical GRPS embankment, including the problem domain chosen for the FE simulation. During the assessment of soil arching, slope of the GRPS embankment is neglected to avoid any complexity of the slip failure.

The FE model comprises a hard stratum (i.e., bedrock) underlain by an 8 m depth of end-bearing piles and subsoil. The pile spacing (s) and pile diameter (D) are fixed at 2.5 m and 1 m, respectively. The embankment height (h) is chosen at 3.5 m, including a 400 mm thick gravel cushion at the base. In the GRPS embankment, a 2 mm thick geosynthetic layer is placed in the middle of the gravel cushion. The FE model is converted from a three-dimensional (3D) to a 2D condition using an appropriate conversion method detailed elsewhere (Meena et al., 2020; Meena et al., 2021).

An infinite element boundary condition is incorporated to minimise the effect of wave reflection from the model boundaries during the dynamic analysis. The four-nodded plane strain element with reduced integration (CPE4R) is used for the finite domain of the numerical model, while the four-nodded plane strain linear infinite element (CINPE4) is used for the infinite domain.

The horizontal acceleration time history of the 2011 Christchurch earthquake is used for the dynamic analysis. This earthquake had a magnitude of 6.3 M_L on the Richter scale and a peak ground acceleration (PGA) of 0.34g for 30 sec. Details of the material parameters, constitutive relationships and model validation are reported in the author's prior works (Nimbalkar and Meena 2021).

2.2 METHODOLOGY

The finite element method of analysis is commenced by establishing the initial stress in the subsoil using the geostatic step. The subsequent steps simulate the installation of the rigid concrete piles and the staged construction of the embankment fill, including the gravel cushion and basal layer of geosynthetic. In the following stage, the earthquake time history is applied at the base of the numerical model after attaining full embankment height.

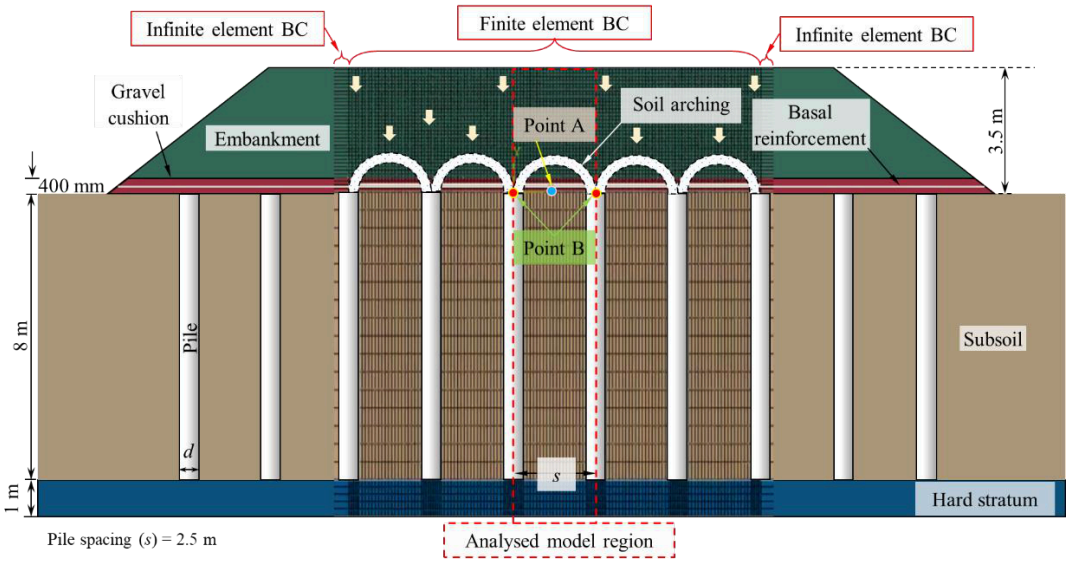

Figure 2: Schematic diagram of a typical GRPS embankment, including mesh profile of FE model

3 RESULTS AND DISCUSSION

3.1 VERTICAL STRESS

Figure 3 shows the time history of normalised vertical stress at Points A and B (refer to Figure 2) for both unreinforced and reinforced conditions. In unreinforced condition, the normalised vertical stress at Point A is observed to be 0.89 at the start of the earthquake (t = 0 sec.). Subsequently, it significantly increases during the 12-14 sec. time frame, coinciding with the peak input acceleration. The maximum normalised vertical stress of 1.70 is reached at the end of the earthquake (t = 30 sec.). Conversely, in the reinforced condition, the normalised vertical stress at Point A decreases by up to 30%. It implies the benefits of basal reinforcement in terms of reducing the vertical stress on the subsoil.

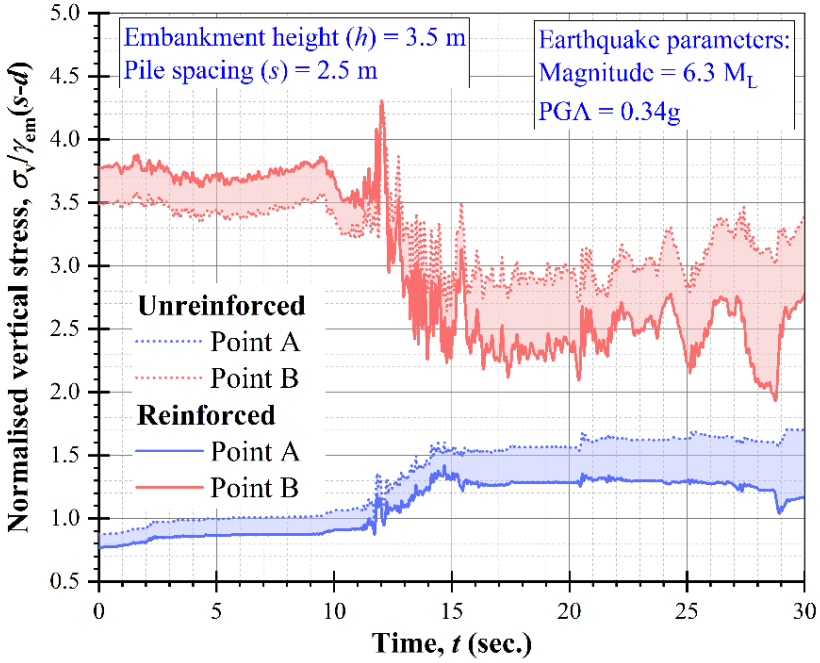

Figure 3: Time history of normalised vertical stress

Further, in the unreinforced condition, the normalised vertical stress at Point B started at 3.5 and fluctuated significantly between 2.7 and 4.3 during the 12-30 sec. time frame. At the end of the earthquake (t = 30 sec.), the normalised vertical stress is 3.4. In the reinforced condition, there is an initial increase of 9% in the normalised vertical stress until 12 sec., followed by a decrease of up to 30% by the end of the earthquake.

It is worth noting that in both unreinforced and reinforced conditions, vertical stress is transferred to the pile before 12 s., while after that the vertical stress on the subsoil and piles is approaching close, hindering the mobilisation of soil arching.

3.2 SETTLEMENTS IN EMBANKMENT

Figure 4 presents the normalised settlement contours along the normalised embankment height for the unreinforced condition at different time instances (t = 0, 13.16, and 30 sec.) and for the reinforced condition at 30 sec. In the unreinforced condition at t = 0 sec., the normalised settlement at Point A is 0.4, while it is negligible at Point B. A uniform settlement plane is observed above the normalised embankment height of 0.8. However, as time progresses, this uniform settlement plane is disrupted, and the normalised settlement increases to 2.52 at the t = 30 sec.

The normalised settlement contour for the reinforced condition at the t = 30 sec. is also compared. In the unreinforced condition at the t = 30 sec., the normalised settlement at Point A is 2.50, whereas with basal reinforcement, it reduces to 2.10. Additionally, the settlement at the top of the embankment is reduced by up to 20%. This indicates that basal reinforcement reduces settlement during the earthquake, which can help prevent potential embankment failure.

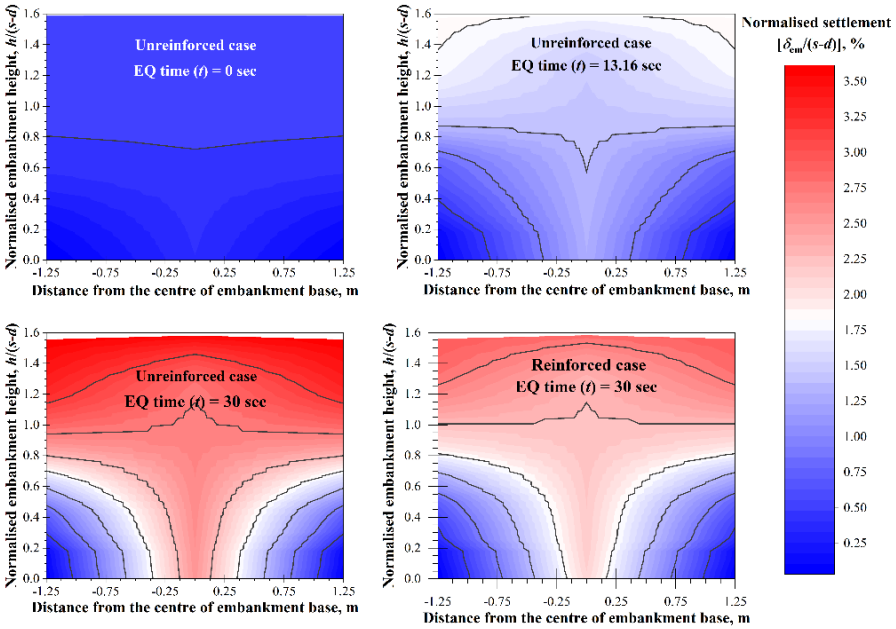

Figure 4: Normalised settlement contours for different time instances in unreinforced and reinforced conditions

3.3 PARAMETRIC STUDY

It is noted that only the geosynthetic case has been considered for the parametric study. The effect of the embankment modulus (E_{em}) on the normalised settlement at point A is shown in Figure 5. The E_{em} has a negligible effect on normalised settlement. The normalised settlement increases by up to 500% with an increase in earthquake time from 0 to 30 sec.

Further, the effect of friction angle of embankment fill is illustrated in Figure 6. The normalised settlement decreases by up to 24% with an increase in the friction angle from 30° to 45°. The reduction in the normalised settlement is more noticeable at the end of the earthquake. Thus, it implies that the friction angle of the embankment material plays a significant role in reducing the settlement on the subsoil even in earthquake conditions.

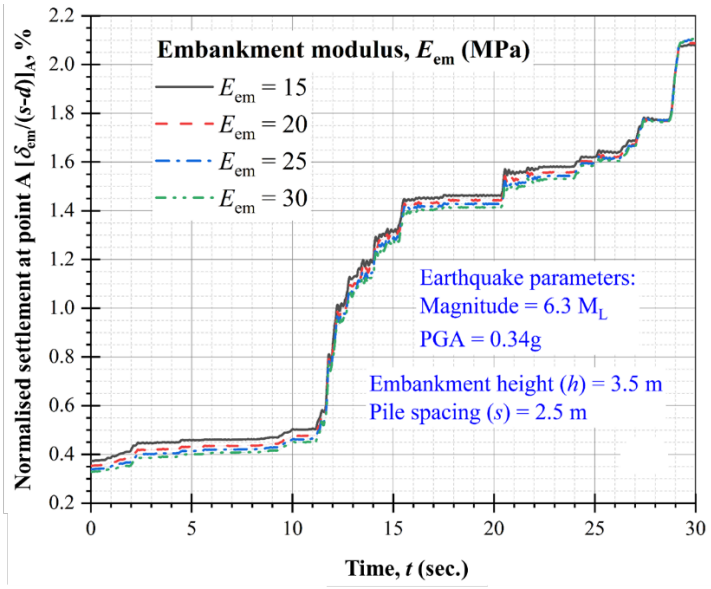

Figure 5: Time history of normalised settlement in a variation of embankment modulus

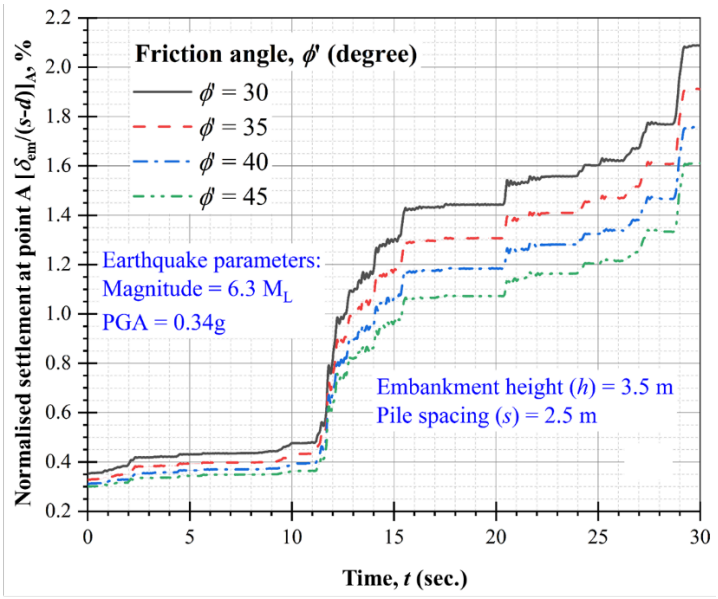

Figure 6: Time history of normalised settlement in a variation of frictional angle

4 CONCLUSIONS

This paper evaluates the dynamic behaviour of soil arching in a pile-supported embankment both with and without basal reinforcement under an earthquake. Based on the findings of this paper, the following major conclusions can be drawn:

- A basal reinforcement layer encourages stress transfer to the pile head through the tension in geosynthetic. It reduces the vertical stress on the subsoil by up to 30%.
- A basal reinforcement effectively reduces embankment settlement during the earthquake, which in turn alleviates the potential risk of embankment failure.
- The friction angle of embankment fill is the most sensitive parameter of a pile-supported embankment which significantly affects soil arching during the earthquake.

5 ACKNOWLEDGEMENT

This paper is part of the first author's doctoral study. The authors extend their gratitude to Beca Pty. Ltd. for providing financial support.

6 REFERENCES

Arulrajah, A., Abdullah, A., Bo, M.W. and Bouazza, A. (2009). Ground improvement techniques for railway embankments. *Proceedings of the Institution of Civil Engineers-Ground Improvement*, 162(1), 3-14. DOI: https://doi.org/10.1680/grim.2009.162.1.3

Australian Federal Government, 2024-25 Federal Budget. Available online: https://www.infrastructure.gov.au/ (accessed on 24 July 2024).

Daniell, J.E. and Love, D. (2010). The socio-economic impact of historic Australian earthquakes. In *Australian Earthquake Engineering Society (AEES) 2010 Conference*, Perth, Australia.

Deng, W., Wang, C., Ou, Q., Ding, X., Luan, L., Xu, Y. and Feng, H. (2024). Seismic response of pile-supported embankment in unequal thickness liquefiable soil with V shape underlying stratum. *Soil Dynamics and Earthquake Engineering*, 182, 108757. DOI: https://doi.org/10.1016/j.soildyn.2024.108757

Han, G.X., Gong, Q.M. and Zhou, S.H. (2015). Soil arching in a piled embankment under dynamic load. *International Journal of Geomechanics*, 15(6), 04014094. DOI: https://doi.org/10.1061/(ASCE)GM.1943-5622.0000443

Meena, N.K. (2022). Assessment of Soil Arching in a Pile-supported Railway Embankment under the Moving Train Load and Earthquake. *University of Technology Sydney* (Australia). http://hdl.handle.net/10453/163832

Meena, N.K. and Nimbalkar, S. (2021). Soil Arching in Geosynthetic-Reinforced Pile-supported Railway Embankments under the Seismic Condition. In *Australian Earthquake Engineering Society (AEES) 2021 Virtual Conference*.

Meena, N.K., Nimbalkar, S., Fatahi, B. and Yang, G. (2020). Effects of soil arching on behavior of pile-supported railway embankment: 2D FEM approach. *Computers and Geotechnics*, 123, 103601. DOI: https://doi.org/10.1016/j.compgeo.2020.103601

Meena, N.K., Nimbalkar, S. and Fatahi, B. (2021). Finite element analysis of soil arching in piled embankment. In *Challenges and Innovations in Geomechanics: Proceedings of the 16th International Conference of IACMAG*, 2(16), 817-824. Springer International Publishing. DOI: https://doi.org/10.1007/978-3-030-64518-2_97

Nimbalkar, S. and Meena, N.K. (2021). Static and Seismic Assessment of Soil Arching in Piled Embankments. In *Civil Engineering for Disaster Risk Reduction*, 263-281. Singapore: Springer Nature Singapore. DOI: https://doi.org/10.1007/978-981-16-5312-4_18

Niu, T., Liu, H., Ding, X. and Zheng, C. (2018). Model tests on XCC-piled embankment under dynamic train load of high-speed railways. *Earthquake Engineering and Engineering Vibration*, 17, 581-594. DOI: https://doi.org/10.1007/s11803-018-0464-7

Systèmes, D., 2013. Abaqus analysis user's manual. Simulia Corp. Providence, RI, USA, 671(40), 672.

United Nations. Transforming Our World: The 2030 Agenda for Sustainable Development. Available online: https://sdgs.un.org/2030agenda (accessed on 24 July 2024).

ROCK MASS CHARACTERISATION OF EXISTING CONCRETE DAMS – MAKING THE MOST OF LIMITED HISTORICAL DATA – TINAROO FALLS DAM

T.K. Winckle[1], G. Dryden[2], A. Duwell[3] and G. Jardine[4]

1. Geologist, Sunwater; 2. Principal Geologist, Sunwater; 3. Principal Engineer – Dams, Sunwater; 4. Jacobs' Technical Director and Global Subject Matter Expert Engineering Geology.

ABSTRACT

Understanding a dam's foundation, including its rock mass properties and the shear strength of its inherent rock defects, is an essential component in ensuring its safety. This paper discusses the use of limited historical data to assess rock mass classification and defect shear strength, which were required as inputs to assess the stability of the concrete monoliths of Sunwater dams, built in the 1950s. The foundations comprise mostly massive granite, but no laboratory strength testing of the foundation rock mass, or its defects have been performed. A review of the dam's foundation including a limited geotechnical drilling program was performed in 2009 to inform dam upgrade works at that time. The current review considered all available geological/geotechnical data, including original investigation borehole and limited geological mapping data, the 2009 data and its assessment, and ultimately contributes to understanding the current overall risk position of the dam. The review aimed to improve estimates of foundation rock mass classification and rock defect shear strength by statistically reviewing the available historical data and applying the methodologies of Barton and Bandis (1990) and Hoek and Brown (1997). The analysis involved assigning three foundation types: sound foundation, hydrothermally altered foundation, and downstream hydrothermally altered. Sensitivity analysis was then performed to account for uncertainties in assigning the various parameters of the foundation rock mass.

1 INTRODUCTION

Foundation strength is one of the key factors that influences the safety of a dam, and instability of a dam may result from pre-existing geological features and/or structures within its foundation. Therefore, understanding a dam's foundation model is a critical input to the assessment of the dam's stability, and other potential failure modes relevant to the dam. As per the ANCOLD guidelines the best way to understand a dam's foundation is through detailed large-scale engineering geological and geotechnical investigations, including in-situ geotechnical investigations and testings (ANCOLD, 2020). However, once a dam has been constructed, the ability to perform these geotechnical and geological investigations increase in difficulty as the foundation is no longer easily accessible. The opportunities to infer the foundation becomes limited to the mapping of downstream exposures and through potentially risky intrusive geotechnical investigations through the dam itself (Lawrence, et al., 2007). This work then needs to be reconciled with available construction records, and other data acquired pre and post construction (Lawrence, et al., 2007).

Tinaroo Falls Dam was built by the Queensland Government in the 1950s and there is limited information available regarding the dam's foundations. Information about the dam is limited to stick logs from construction drawings and few records describing the geology. No laboratory strength testing of the bedrock foundation or its defects has taken place. In 2009 Sunwater completed a geological review of the dam to inform dam upgrade works. The review included a limited geotechnical drilling program and a rock mass characterisation. Given changing standards and approaches to dam management and safety, a re-analysis of the rock mass characterisation was necessary for the foundation conditions of the concrete monoliths. Using the 2009 data and some historical records, the main aim and objective of this review was to inform the estimates of foundation rock mass classification and rock defect shear strength by statistically reviewing the available data. This review applies the Barton and Bandis (1990) and Patton (1966) (hereafter known as Barton-Bandis and Patton) methods for determining rock defect shear strength and the methods of Hoek and Brown (1997) to determine the rock mass strength. In doing so, as some parameters needed to be estimated, the review was conducted via sensitivity analysis, categorising data into different scenarios for the potential foundation conditions of the concrete monoliths.

2 SITE DESCRIPTION AND GEOLOGY: DAM CHARACTERISTICS

Tinaroo Falls Dam is located approximately 14 km east of Atherton on the Barron River, Queensland, Australia. Construction was completed in 1958. The Main Dam is a concrete gravity dam with a centrally located ungated ogee concrete spillway (Figure 1 details the layout of Tinaroo Falls Dam). The dam is underlain by the Late Carboniferous to Early Permian Tinaroo Granite intrusion (GSA, 1978). Across the site, the Tinaroo Granite is seen as coarse-grained and affected by varying degrees of weathering, which is typically more intense along major defects/lineaments. The granite's grain size averages 5 mm, with occasional orthoclase feldspar crystals up to 13.5 mm. The granite is typically high to

very high strength, although this varies due to localised fracturing and hydrothermal alteration. Site inspections of the outcrops located on left and right abutments, and in the downstream channel of the Barron River, have identified a dominant sub-horizontal joint set, and slabbing that suggests a stress relief origin. The stress relief joint spacing across the site ranges from 100 to 400 mm. Information on defects characteristics has been sourced mostly from the 2009 drilling, with no records of defect roughness or shape available from outcrop mapping performed in 2009. However, from inspection of outcrop on site in 2023, subhorizontal defects with large scale undulation were observed. The site geology is further defined in these areas: the left abutment, right abutment, and the downstream channel area.

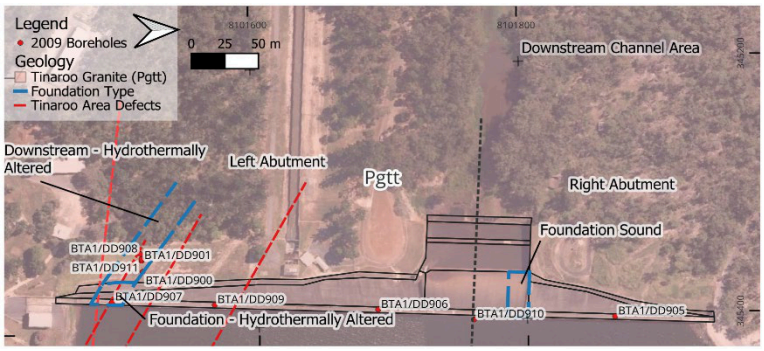

Figure 1: Layout of Tinaroo Falls Main Dam

The left abutment is dominated by granite that is weathered and fractured with varying intensity and overlain by sandy gravelly soil with localised alluvium (Butler & Leamonth, 1960; Sunwater, 2009). The rock strength is high to very high strength with outcrops typically slightly weathered to fresh. When the fracture spacing averages less than 50 mm the intensity of weathering is generally significantly increased to highly weathered, with an accompanying decrease in rock strength (Sunwater, 2009). The right abutment is underlain by granite which contains significantly more defects than the other two domains. There are slabby rock outcrops that have resulted from stress relief jointing bounded by tectonic jointing (Sunwater, 2009). There are granite outcrops downstream of the dam with sheared zones present in the cableway foundation trenches, which are steeply dipping. There are also sub-horizontal defects that are observed to have large scale undulation. The spillway's centre line is orientated parallel to the original channel of the Barron River, and discharges into an area underlain by granite with low angle stress relief jointing. Downstream of the Tinaroo Falls Dam Road bridge there is an area of slightly weathered to fresh, high to very high strength granite. The 2009 inspection identified vertical rock defects in the area with spacings 2.50 to 3.00 m, and stress relief jointing identifiable in the channel area in steps of 200 to 400 mm thickness. There are subhorizontal defects present with dilated slab margins with a persistence of greater than 10 m.

3 METHODOLOGY

This review was performed in three stages: review and statistical analysis of available data, defect shear strength, and rock mass characterisation. Review of available data included rock defect data that was acquired from both boreholes drilled and limited geological mapping that was conducted in 2009. Data available from the 2009 mapping included joint roughness coefficient (JRC), defect dip and orientation, weathering, and rock strength.

3.1 REVIEW AND STATISTICAL ANALYSIS OF AVAILABLE DATA

The 2009 boreholes were assigned to the three foundation types and used as inputs to the rock mass characterisation. These foundation types were based on interpreted geological conditions from historic investigation data. Defects logged as intact (representing veins or rehealed joints) were excluded from the analysis (see cross section in Figure 2). Defects in the uppermost 10 m of the foundation having inclinations between 0° and 20° were analysed as these were considered the most critical for foundation related failure mechanisms. Boreholes BTA1/DD905, 906 and 909 belong to Foundation - sound with BTA1/DD907 classified as Foundation – hydrothermally altered. Foundation – sound and hydrothermally altered contained 52 dominant defects described as undulating rough joints at 5°. BTA1/DD900, 908 and 911 were classified as Downstream – hydrothermally altered and contained 75 dominant defects described as undulating rough joints at 20°.

Defect Roughness Class is no longer a readily used description for defects, however, as it was used in the 2009 study, it was used in this review. Defect Roughness Class was based on AS 1726-1993 (Geotechnical Site Investigation) as a

measure of the inherent surface unevenness and waviness of a discontinuity relative to its mean plane. For the purpose of this review a class of "0" was added for defects that did not have a planarity and roughness described.

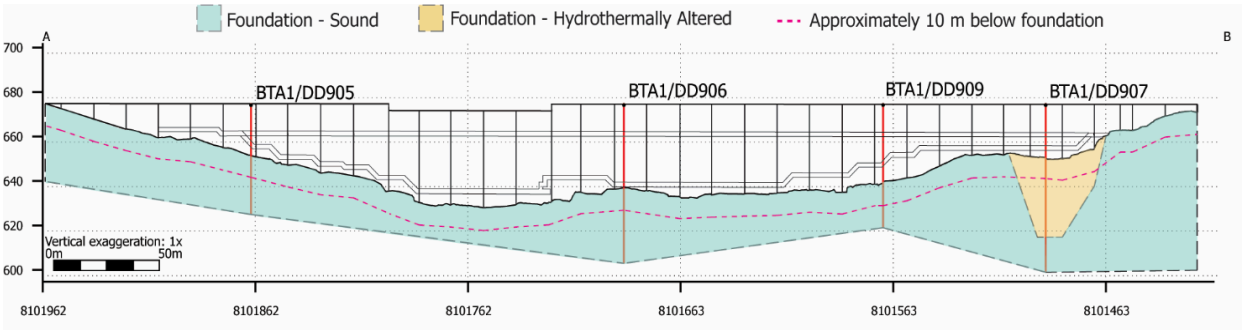

Figure 2: Cross section of Tinaroo Falls Dam with foundation type classification.

3.2 DEFECT SHEAR STRENGTH

The process for defect shear strength analysis was calculated as per ANCOLD (2013). The methods detailed in the ANCOLD guideline use Patton (1966) and/or Barton and Bandis (1990) for the calculation of shear strength. For the analysis, the effective normal stress was assigned as 250 kPa as this is the average effective normal stress for beneath the dam wall. With the equations for the Patton and Bartin-Bandis methods used from Patton (1966) and Barton-Bandis (1990;1982) respectively. As Patton and Barton-Bandis are the accepted methods for calculating shear strength, the scaled effects of JRC and Joint Compressive Strength (JCS) need to be considered. Allowing for the greater possibility of weakness in large surfaces. The equations used to quantify the scale effects are seen in Barton and Bandis (1982). As there has been no recorded surface length or sliding length in previous investigations, L_n and L_0 were defined as 1 m for both variables. JCS required for calculating the scaled JCS was estimated based on field estimates and Hoek (2007). For this review three JCS values were selected due to the original JCS being estimated.

Patton and Barton-Bandis shear strength methods both require an average roughness angle (i), which can be calculated using field or laboratory tests. Due to the absence of the roughness angle data, it is estimated with this term $JRC_n \log_{10}(JCS_n/\sigma)$ from the Barton-Bandis shear strength equation. For Barton-Bandis and Patton shear strength a basic friction angle is required. As there has been no laboratory strength assessment completed on the defects, an estimate was made for a basic friction angle. For sensitivity analysis purposes the basic friction angles are presented in Table 1. The instantaneous friction angle and cohesion were calculated using methods of Hoek (2007).

Table 1: Values for basic friction angle used in shear strength equations. After Hoek (2007) and Barton (1974).

Rock	Description	Peak c' (MPa)	Peak ϕ_b
Granite	Sandy loam fault filling	0.05	40
	Tectonic shear zone, schistose and broken granites, disintegrated rock, and gouge.	0.24	42

3.3 ROCK MASS CLASSIFICATION

GSI was estimated using three different methods: RMR89, the Q method and using the chart for Cai et al (2006). Using different methods for GSI estimation allowed for a greater range of GSI to be considered across the rock mass. RQD was calculated based on the 900 series boreholes. The Hoek-Brown parameters were calculated following the methods of Hoek (2007) and those referenced in Whyllie and Mah (2004). The material constant used in the review was 32±2, although due to the highly weathered nature of the rock mass located in Downstream – hydrothermally altered the lower bound of 29 was used for sensitivity analysis. Originally Butler and Learmonth (1960) suggested the USC of 137.9 MPa (20,000 lb/sq.in.). Lesleighter (2008) adopted a UCS of 150 MPa. Whereas Sunwater (2009) adopted a strength of 100 MPa for fresh rock and 10 MPa for sheared rock. For sensitivity analysis all rock strength values were adopted. The UCS was calculated based on the equation in Marinos and Hoek (2000) utilising the rock strength, material constant and GSI.

4 RESULTS AND DISCUSSION

Defect Roughness Class results indicate that overall foundation rock defects logged in the 2009 boreholes are mostly rough or irregular, stepped and undulating. The distribution of the open defect roughness for the foundation locations,

identified Roughness Classes I and IV as the predominant classes. The roughness is likely related to the coarse grain size of the granite. The defects having a common Roughness Class of I and IV indicate that the potential for sliding on the mean plane is low. For the purpose of GSI calculations, the roughness class of IV was used as it is the most representative Defect Roughness Class for all foundation types. Defect spacing is needed for GSI calculations. As intact defects were excluded in this analysis, the defect spacings from the 2009 boreholes were recalculated. For the review, a geometric mean of 0.66 m was adopted for defect spacing.

Defect orientation data was acquired during the 2009 geological mapping. Table 2 summarises the dominant defect orientations. The shallowest dipping defect set has a dip of 7°, which is interpreted to have developed due to stress relief and is considered the most critical set related to foundation-related failure. The probability of sliding is reduced due to the defects commonly being rough, irregular, stepped and undulating. The results in Table 2 indicate the possibility of rock bridges occurring within the rock mass with the tectonic origin defect sets dipping significantly steeper than the stress relief jointing. Where rock bridges occur, this would reduce the possibility of sliding of the 7° defect set identified as the stress relief jointing.

Table 2: Major defect populations.

Defect Orientation	Dip	Azimuth (True)	Strike (True)	Origin
A	70	080	170	Tectonic
B	79	022	112	Tectonic
C	07	204	294	Stress relief
D1	84	243	073	Tectonic
D2	80	127	217	Tectonic

JRC was estimated in the field during 2009 and assigned to 77 mapped defects. The most common JRC was 8 and this was adopted for the shear strength calculations. Defect shear strength was calculated for foundation - sound based on a defect 5 m below the concrete/foundation interface. This depth was chosen as it is recognised to be the most likely critical depth related to the failure mechanism and rock mass character. The shear strength scenarios have been calculated for initial movement when $\phi b + i$ is at peak.

Both Barton-Bandis and Patton were used in this review as they are the accepted methods in the ANCOLD guidelines for calculating shear strength (ANCOLD, 2013). The results are summarised in Table 6. The results for Barton-Bandis and Patton are the same. This similarity results from the need to calculate the roughness angle *i* in Patton which is equivalent to a term within Barton-Bandis shear strength. A recommendation for future geotechnical investigations including drilling for further understanding of the foundations of the dam has been proposed. This drilling and the potential to relog of original core will aim to identify the roughness angle *i.* Along with calculating the instantaneous friction angle and cohesion, using the methods of Hoek (2007), Barton-Bandis shear failure was modelled for different normal stresses at depth. The results are presented in Table 3, and the six scenarios illustrated in Figure 3. Overall, it is seen that Scenario 6 returned the highest overall shear failure criterion.

Table 3: Summary of results for sensitivity analysis of defect shear strength, instantaneous friction and cohesion.

Factor	Scenario 1	Scenario 2	Scenario 3	Scenario 4	Scenario 5	Scenario 6
JCS (MPa)	40	30	50	40	30	50
Dip (basic friction angle) (°)	40	40	40	42	42	42
i (°)	17.63	16.63	18.41	17.63	16.63	18.41
Barton-Bandis (KPa)	394	398	407	427	410	440
Patton (KPa)	394	398	407	427	410	440
ϕp(°)	54	53	55	56	55	57
c (KPa)	53	50	55	59	56	62

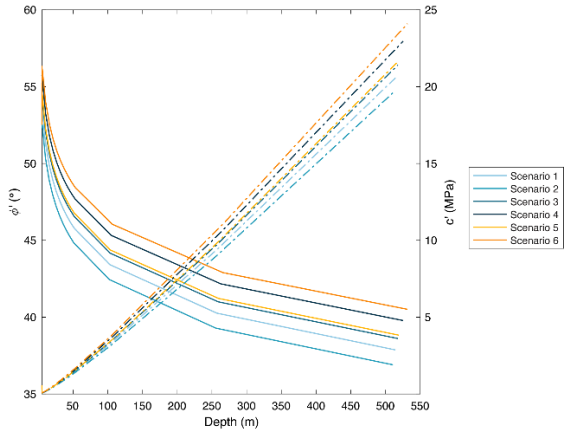

Figure 3: Defect friction angle (ϕ') and cohesion (c') modelled at depth for defect shear strength modelled using methods of Hoek (2007)

The RQD values used for rock mass characterisation were recalculated for GSI estimation based on Deere and Deere (1989), the foundation – sound is classified as excellent quality rock, with foundation – hydrothermally altered and downstream – hydrothermally altered classifying as good and fair respectively. For GSI estimation Jcond89 was utilised as it is used both in RMR89 and GSI when calculated using Hoek's method. Across the locations defined for the rock mass characterisation, RMR ranges from very good to fair rock. The method of GSI chosen for the rock mass strength calculations was estimated based on Cai et al. (2004). The estimation of GSI from this chart was used, as this was how the 2009 rock mass characterisation was completed. Rock mass strength calculations were based on the division of foundation into three types, and then sub-divided scenarios were based on the above statistical review of data. This provides a view of the possible rock mass strengths for the relatively unknown foundation. Key results for the three foundation types are summarised in Table 4.

Table 4: Summary of key results for rock mass strength calculations for foundation type and scenarios.

Factor	Foundation – Sound			Foundation – Hydrothermally Altered			Downstream – Hydrothermally Altered			
	S1	S2	S3	S1	S2	S3	S1	S2	S3	S4
Unconfined compressive strength (MPa)	150	137.9	100	150	137.9	100	150	137.9	100	10
σ'1(MPa)	57	53	31	49	45	26	39	37	22	4
mb	16	16	13	13	13	11	11	11	9	8
s	0.13	0.13	0.07	0.09	0.09	0.05	0.06	0.06	0.03	0.02
a	0.50	0.50	0.50	0.50	0.50	0.50	0.50	0.50	0.50	0.50
σcm (MPa)	92	85	54	80	74	46	71	65	41	4
ϕ(°)	71	71	71	70	70	71	71	71	71	64
c (MPa)	5	4	2	4	4	2	3	3	1	0
Em (GPa)	73	70	45	62	59	38	49	47	30	7

The results for the modulus of deformation (E_m) displays a decrease within rock mass quality. It is noted that the instantaneous friction angles and cohesion are high. As with the defect shear strength, the rock mass was modelled following the methods of Marinos and Hoek (2000) and were used to estimate the Hoek-Brown and Mohr-Coulomb parameters at depth for a range of normal stresses. The results are presented in Figure 4. The figure shows that Scenario One for all three locations produces the highest results, likely due to the high unconfined compressive strength. Overall, the cohesion results are very low for the rock mass parameters, and it would be ideal to recreate this study when more information is available to see how the cohesion is affected.

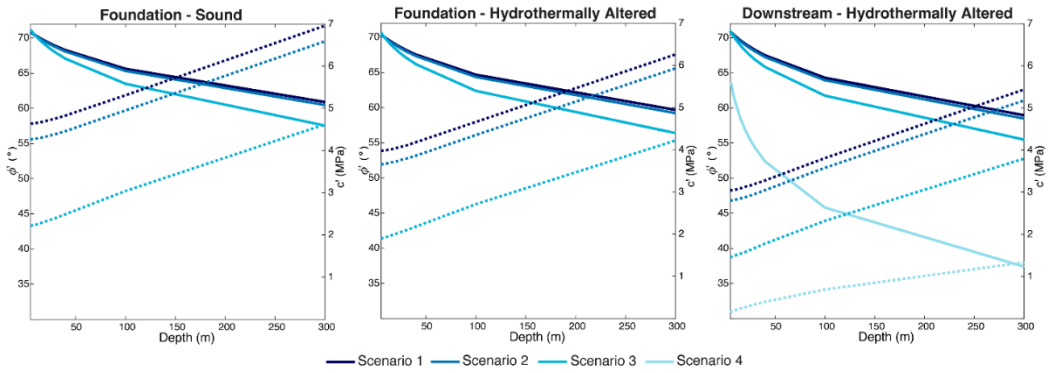

Figure 4: Modelled rock mass friction angle and cohesion for foundation locations using the methods of Hoek et al (2000).

5 CONCLUSIONS

Although there are limitations surrounding the information available for Tinaroo Falls Dam, this review demonstrated how limited data may be used for preliminary assessment of rock mass and rock defect strengths. As rock defect strength is considered the most significant input of most potential foundation related failure modes, recommendations have been made to further understand the dam's foundation and used to further refine this rock mass and defect strength assessment. The following additional geotechnical works are proposed:

- Production of a three-dimensional factual geological and geotechnical model using existing geotechnical data.
- Relog the original rock cores for input and updates to the geological and geotechnical model.
- Perform downhole ATV/OTV in selected foundation drains to determine aperture, dip and dip direction of rock defects present.

6 ACKNOWLEDGEMENTS

We would like to acknowledge and thank Mr. Deryk Forster for his work in 2008 and 2009, and the guidance for this review. Finally, the authors would like to thank Sunwater for permission given to publish this paper.

7 REFERENCES

ANCOLD, 2020. *Guidelines for geotechnical investigations of dams, their foundations, and appurtenant structures*. s.l.: Australian National Committee on Large Dams.

ANCOLD, 2013. *Guidelines on design criteria for concrete gravity dams*. s.l.: Australian National Committee on Large Dams.

Australian Standard, 1993. *Geotechnical site investigation AS1726-1993*. Homebush, NSW: Standards Australia.

Barton, N. & Bandis, S., 1982. *Effect of block size on shear behaviour of jointed rock*. Berkely, California, The 23rd U.S. Symposium of Rock Mechanics (USRMS).

Barton, N. R. & Bandis, S. C., 1990. *Review of predictive capabilities of JRC-JCS model in engineering practice*. Leon, Norway, Rock Joints, proc. int. symp. on rock joints.

Butler, N.J. & Learmonth, F.M., 1960. *Mareeba-Dimbulah irrigation project – design and construction of Tinaroo Falls Dam*. The Institution of Engineers – Australia – The Journal.

Cai, M., Kaiser, P. K., Tasaka, Y., & Minami, M. (2007). Determination of residual strength parameters of jointed rock masses using the GSI system. International Journal of Rock Mechanics and Mining Sciences, 44(2), 247-265. https://doi.org/https://doi.org/10.1016/j.ijrmms.2006.07.005

GSA, 1978. *Excursions handbook third Australian geological convention*. Brisbane: Geological Society of Australia, Queensland Division.

Hoek, E., & Brown, E. T. (1997). Practical estimates of rock mass strength. *International Journal of Rock Mechanics and Mining Sciences*, *34*(8), 1165-1186. https://doi.org/https://doi.org/10.1016/S1365-1609(97)80069-X

Lawrence, M. S., Martin, C. D. & Moore, D.P., 2007. *Estimating rock mass strength for a concrete dam founded on good rock: Blind Slough Dam*. Vancouver Canada, 1st Canada – U.S. Rock Mechanics Symposium.

Lesleighter, E., 2008. *Tinaroo Falls Dam – Review of hydraulics and potential for erosion downstream of Tinaroo Falls Dam*, s.l.: Lesleighter Consulting.

Marinos, P. & Hoek, E., 2000. *GSI: a geologically friendly tool for rock mass strength estimation*. Melbourne, ISRM International Symposium.

Sunwater, 2009. *Tinaroo Falls Dam geological review of foundation*, Brisbane: Sunwater.

Whyllie, D. C. & Mah, C., 2004. Rock slope engineering. 4th ed. London: CRC Press.

EXPLORING THE IMPLICATIONS OF SOIL WEIGHT DENSITY IN ROUTINE DESIGN

Jay Lobwein
Tonkin + Taylor

ABSTRACT

It is becoming more important for practicing engineers to consider the sustainability impacts and potential improvements on all aspects of their designs. For geotechnical engineers, due to the inherent uncertainty in the ground, designs are often too conservative with suggested parameters adopted with limited data available or not utilised most effectively. The dry, saturated, or partly saturated soil weight density (or unit weight) is frequently only suggested and often overlooked as an important parameter in common geotechnical problems. Rather it is the focus on the derivation and characterisation of strength and stiffness parameters which almost always take priority in routine design. The typical methods used to obtain the soil weight density are reviewed with potential improvements provided. The primary objective of this paper is to present parametric studies from common geotechnical stability problems to show the importance of the soil weight density parameter in routine design and the potential opportunities and pitfalls geotechnical engineers may face in practice.

1 BACKGROUND

The world is undergoing the most disruptive economic transformation since the Industrial Revolution to decarbonise our economies. Australia's Net Zero Plan aims to reduce our greenhouse gas emissions by 43% below the 2005 levels by 2030 and reach net zero emissions by 2050 (DCCEEW 2024). The master plan will be supported by six sectoral emission reduction plans: electricity and energy, transport, industry, agriculture and land, resources, and the built environment. The wide scope of civil engineering may cover all these sectors. For each sector, the Australian government has outlined five major steps to decarbonise our economy, the first of which, and one that can be acted upon immediately by engineers, is to increase the materials and energy efficiency of our economy. All engineers will play a major role to ensure material efficiency becomes a permanent part of the economy with the once celebrated conservative designs now under scrutiny. To formalise this change, the Institute of Structural Engineers (IStructE) is now calling for mandatory legal limits to embodied carbon that can be emitted on a project (Kanaris 2024). The question arises, what can geotechnical engineers do now to support the plan to net zero emissions?

2 A GEOTECHNICAL DESIGN CHALLENGE

Due to the aleatory and epistemic uncertainties in the ground, it seems geotechnical engineers have missed the opportunity to present the positive impact on transitioning to a net zero economy. On one hand, this comes as a surprise as the coefficient of variation (COV) of common geomaterial properties have shown to be higher than anthropogenic materials (e.g., steel and concrete) leading to potentially larger material efficiencies in design (Bond and Harris 2008; Duncan 2000). However, on the other hand, it comes as no surprise as geotechnical engineering spreads itself across numerous sectors often as an unfortunate afterthought rather than as an opportunity for reduced embodied carbon emissions. The well-known geotechnical sales pitch, "you will pay for a site investigation, whether you have one or not", may be taking on a new meaning focusing on embodied carbon emissions, rather than geotechnical failures.

Nonetheless, without regulatory oversight in a commercially competitive market the geotechnical engineer is often left with no choice but to adopt conservative estimates based on limited data available under a tight construction programme. At a minimum the geotechnical parameters required to determine the stability of a geotechnical structure includes the strength and density properties of the geomaterials. As the soil weight density typically shows little variation (i.e., smaller COV) compared to the well-known strength parameters, and coupled with the uncertainty in the ground, it is often overlooked as being an important piece of the design puzzle.

The suggested soil weight densities provided in codes, standards, and guidelines do not help with this sustainability design challenge, as shown in BSI (2020), CIRIA (2017), and Standards Australia (2002). Generally, the recommendations are that suggested values may be used in the absence of reliable data. Inadvertently, the recommendations are often overlooked to reduce investigations. Ultimately, this leads to conservative designs with the opportunity missed to reduce the embodied carbon emissions from man-made and/or natural materials in construction. This paper aims to re-emphasise the importance of the soil weight density parameter and encourage engineers to reconsider their investigations and designs in a transitioning economy.

3 TYPICAL SUGGESTED SOIL WEIGHT DENSITIES

Design codes, standards, and guidelines provide suggested soil weight densities, however there are discrepancies between each of them. The designer is left with a choice of a characteristic value that is either dry, moist, saturated, or one that is above or below the groundwater table. This may cause confusion when selecting a soil weight density parameter in routine design. Many values may be selected for each material layer; however, it is typical to select one value per layer.

In addition to the inferred moisture condition, the suggested soil weight density is typically a function of consistency for cohesive materials, and particle size, grading, and relative density for granular materials. Generally, other intrinsic properties (e.g., clay mineralogy, plasticity, particle density and angularity) are not considered. A selection of suggested values from the Australian Standard (AS) for Earth-retaining structures (AS 4678–2002) is provided below in Table 1. Notably, the cohesive soil weight densities do not change between moist and saturated conditions, however for granular materials of the same relative density the values change by up to 4 kN/m^3. In summary, selecting the soil weight density on limited information alone may ultimately lead to inaccurate designs.

Table 1: Suggested soil weight densities of soils (Standards Australia 2002)

Material	Moist Bulk Weight (kN/m^3)		Saturated Bulk Weight (kN/m^3)	
Cohesive				
Organic clay	15.0			
Soft clay	17.0			
Firm clay	18.0			
Stiff clay	19.0			
Hard clay	20.0			
Stiff or hard glacial clay	21.0			
Granular	**Loose**	**Dense**	**Loose**	**Dense**
Gravel	16.0	18.0	20.0	21.0
Well-graded sand and gravel	19.0	21.0	21.5	23.0
Coarse or medium sand	16.5	18.5	20.0	21.5
Well-graded sand	18.0	21.0	20.5	22.5
Fine or silty sand	17.0	19.0	20.0	21.5
Rock fill	15.0	17.5	19.5	21.0

4 TYPICAL SOIL WEIGHT DENSITY TEST METHODS

There are many methods to determine the bulk soil weight density in the field and laboratory. Following determination of the bulk density it is typical to calculate the moisture content and hence the dry density. The sample should be preserved in the field to avoid any loss of water for laboratory testing typically with a porous fabric (e.g., muslin) and molten microcrystalline wax (e.g., paraffin wax). Brief descriptions of the typical bulk soil weight density test methods for either natural or compacted soils are provided below.

4.1 CORE CUTTER

This field method is for cohesive soils free from coarse-grained sized particles. The procedure involves driving or pushing a greased cylindrical core cutter of known mass and internal volume, typically with a length of 130 mm and an internal diameter of 100 mm, into a small area of soil. Once the surrounding soil is trimmed away, the core cutter is weighed to determine the soil weight density.

4.2 SAND REPLACEMENT

This field method may be used for both fine and coarse-grained soils, however unsuitable for soils containing a large proportion of particles larger than coarse gravel. The procedure generally involves laying a metal tray with a hole centred of 150 mm or 200 mm diameter on the test surface, excavating the soil through the hole to a maximum depth of 250 mm, and weighing the excavated material. Subsequently, a dry clean uniformly graded silica sand of known density is poured from a cylinder into the hole with the amount of sand required to fill the hole weighed. The soil weight density of the soil is then calculated by knowing the mass of the sand infilling the hole and the pre-calibrated soil weight density of the sand.

4.3 WATER REPLACEMENT

This field method is typically used for coarse-grained soils, including the larger coarse gravel and rock fill. The procedure consists of excavating a large hole using a circular density ring typically ranging from 500 mm to 2.5 m as a function of the largest particle. Subsequently, the hole is lined with a flexible sheet to retain water and determine the excavated hole volume. The soil weight density is calculated by determining the volume of the hole and mass of the excavated material.

4.4 NUCLEAR

This field method is typically used for compacted fine and coarse-grained soils. The calibrated nuclear surface moisture-density device uses radioactive material to quickly measure both soil weight density and moisture content. The procedure typically involves drilling an access hole of at least 16 mm diameter and inserting the probe into the hole to the required test depth typically between 50 mm and 300 mm for a count time of not less than 1 min.

4.5 LINEAR MEASUREMENT

This laboratory method is for cohesive soils of regular shape, normally in the form of either rectangular prisms or right circular cylinders from block samples or sampling tubes. The soil weight density is directly calculated by determining the volume and mass of the formed specimen.

4.6 IMMERSION IN FLUID

This laboratory method is typically used for lumps of soil that are preferably cubical or cylindrical in shape, but without any re-entrant angles. The procedure to prepare the specimen includes trimming the sample until each dimension is typically at least 100 mm, weighing the specimen, filling the surface air voids with a material (e.g., wax or putty), reweighing the specimen, coating the specimen completely with moltefmann wax, and finally reweighing the specimen again. Subsequently, the specimen is placed in a cradle which is then submerged into a fluid container (usually of water) and suspended from a supporting frame attached to weighing scales to determine the buoyant mass. The soil weight density is calculated by knowing the density of the waxes and fluid, and the masses sequenced without filling, with filling, with coating wax, and with coating wax submerged in fluid.

4.7 FLUID DISPLACEMENT

Similar to the immersion in fluid method, this laboratory method is typically used for lumps of soil with comparable specimen preparation procedures to form the wax coated specimen. The procedure involves lowering the specimen completely into a fluid filled container to measure the displaced water via a siphon tube. The soil weight density is determined by knowing the density of the waxes, and the masses sequenced without filling, with filling, with coating wax, and displaced water from specimen submergence.

5 POTENTIAL IMPROVEMENTS

There are many improvements that can be implemented by geotechnical engineers throughout the design process from scoping the fieldwork activities, scheduling the laboratory tests, deriving the characteristic soil weight density parameters, and finally designing the proposed works. Recommended design steps include the following:

- Position the exploratory holes to encompass the entire location and depth of the proposed design scenarios.
- Select suitable drilling techniques to maximum the chances of obtaining representative samples.
- Specify adequate sampling from each of the material layers.
- Schedule a variety of field and laboratory tests for increased reliability.
- Weigh, measure, and preserve both the tubes and undisturbed samples for direct testing and logging on site.
- Weigh, measure, and preserve lumps of soil in preparation for laboratory testing.
- Estimate the excavated volumes from shallow exploratory holes incrementally using mobile technology.
- Weigh the associated excavated material incrementally for direct testing and logging on site.
- If field testing is not possible, test all tube and block samples in the laboratory routinely.
- Utilise all the available data from other element laboratory tests (e.g., shrink-swell, oedometer, triaxial tests).
- Calculate and plot the bulk, dry, and saturated densities to identify trends and omit any outliers.
- If there are many proposed design scenarios, provide a range of characteristic soil weight densities.
- Adopt the correct characteristic soil weight density for the proposed design scenario.
- Evaluate the impact of other design inputs on the soil weight density for the proposed design scenario (if any).

6 ENGINEERING IMPLICATIONS

To assess the impact of the soil weight density (unit weight) in routine design, three parametric studies were carried out on a shallow strip foundation, a gravity retaining wall, and an earth structure. The studies focused on bearing failure for the shallow strip foundation, toppling failure for the gravity retaining wall, and global rotational failure for the earth structure. To further simplify the studies, only effective stress conventional methods were adopted with no surrounding surcharges, groundwater pressures (i.e., dry conditions), effective apparent cohesions or other specific design inputs considered. Each study adopted typical soil weight densities ranging from 14 kN/m^3 to 22 kN/m^3 and effective angles of shearing resistance ranging from 15° to 35°. Global factors of safety across the range of densities and strengths have been determined for each failure mechanism. The aim of these studies is to show the potential material efficiency opportunities facing engineers if careful consideration of the unit weight parameter is undertaken throughout the design process. Importantly, the factors of safety presented below are not intended to be used in design and each geotechnical problem faced should be considered accordingly.

6.1 SHALLOW FOUNDATION

The general shear bearing failure mechanism was analysed for a rough shallow strip foundation with an embedment depth of 0.9 m and a width of 0.4 m. The ultimate bearing capacity was determined using Terzaghi's (1943) equation following the Reissner (1924) analytical solution extended from Prandtl (1921). The Hijaj et al. (2005) soil weight density bearing capacity factor was adopted for the analyses. The bearing pressure was adjusted until the factor of safety equated to approximately 2 with a constant soil weight density of 18 kN/m^3 and an effective angle of shearing resistance (φ′) of 25°. The remaining cases inputted the fixed bearing pressure. The results shown below in Figure 1 delineate a linear increase in the factor of safety with increasing soil weight density. Furthermore, as the soil strength reduces there is a significant reduction on the impact of the density in the design.

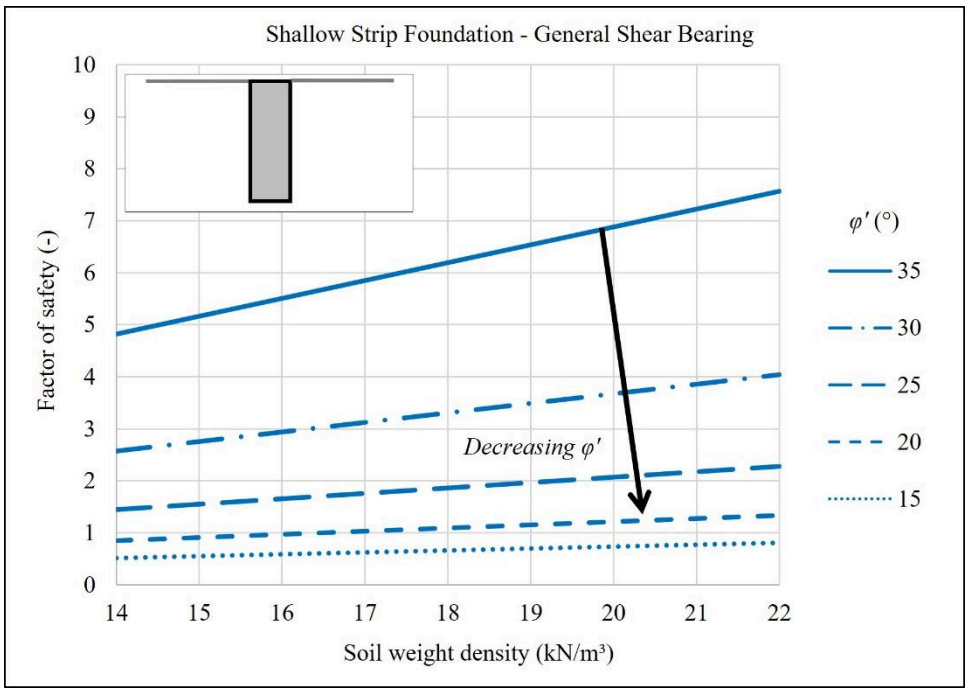

Figure 1: Parametric study results for bearing failure of a shallow strip foundation

6.2 GRAVITY RETAINING WALL

The toppling failure mechanism was analysed for a gravity retaining wall 1.2 m wide and 2.7 m high with no embedment. The equivalent Coulomb (1776) and Rankine (1857) limiting active earth pressure coefficients for a frictionless wall were adopted in the study. The dimensions of the wall were adjusted until the factor of safety equated to approximately 2 with a constant soil weight density of 18 kN/m^3 and φ′ of 25°. Conversely, the results shown below in Figure 2 delineate a near linear reduction in the factor of safety with increasing density. In addition, as the soil strength reduces there is a slight reduction on the impact of the density in the design.

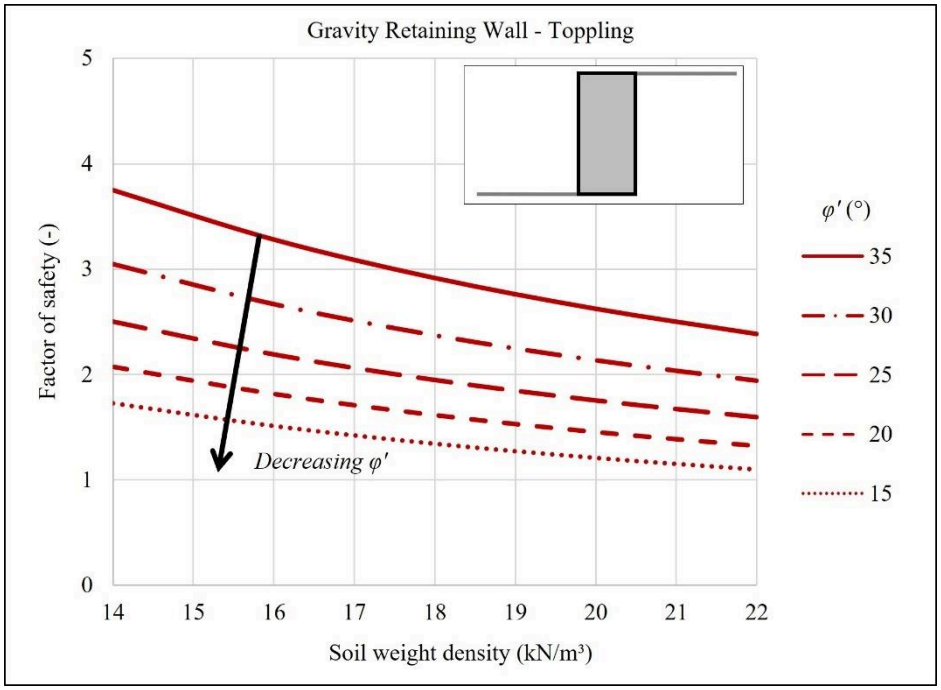

Figure 2: Parametric study results for toppling failure of a gravity retaining wall

5.3 EARTH STRUCTURE

The global rotational failure mechanism was analysed using Slide2 (Rocscience v9.028 2023) for a 4 m high earth structure with batters 1:4 (v:h). The Morgenstern and Price (1965) limit equilibrium method was adopted to determine the critical slip surface. The geometry of the slope was adjusted until the factor of safety equated to approximately 2 with a constant soil weight density of 18 kN/m^3 and φ′ of 25 °. Figure 3 presents no change in the factor of safety with change in density. Lastly, as the soil strength reduces there is no change on the impact of the density in the design.

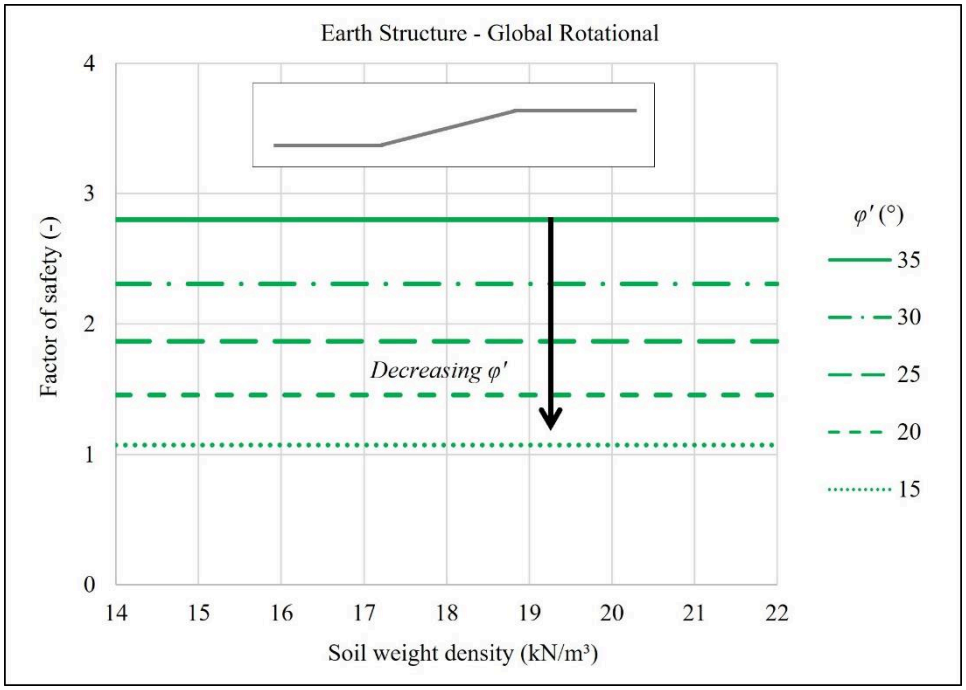

Figure 3: Parametric study results for a global rotational failure of an earth structure

7 CONCLUSIONS

As the economy continues to transition to net zero, designers need to assess the potential material efficiencies available. For geotechnical engineers, suggested soil weight densities are often relied upon without appropriate investigations, which ultimately leads to conservative designs. To add confusion, there are discrepancies between the codes, standards, and guidelines when selecting soil parameters based on limited information in routine design. Recommended steps for improvement have been provided that can be implemented from the early scoping of fieldwork activities to the later designing of the proposed works. Execution of these steps will provide the designer more confidence in selecting a characteristic soil weight density parameter to reduce the required man-made and/or natural materials. Three parametric studies were undertaken on isolated failure mechanisms of specific design scenarios to show the impact the soil parameter has in common geotechnical problems. The results show the factor of safety varies with increasing soil weight density; the bearing failure of a shallow strip foundation increases linearly, the toppling failure of a gravity retaining wall reduces near linearly, whilst the global rotational failure earth structure does not change. Furthermore, as the strength of the soil reduces there are varying impacts of the density in the design; the bearing failure of a shallow strip foundation shows a significant reduction, the toppling failure of a gravity retaining wall shows only a slight reduction, and the global failure of an earth structure delineates no impact at all. These contrasting results reaffirm the importance of investigating and adopting the correct characteristic soil weight density parameter relevant to the design scenario and highlights the opportunity for material efficiency if appropriate steps are undertaken throughout the design process.

8 ACKNOWLEDGEMENTS

The author would like to acknowledge the ongoing support and guidance of colleagues at Tonkin + Taylor, especially Dr Joseph Arivalagan for the countless conversations.

9 REFERENCES

Bond, A. and Harris, A. (2008) Decoding Eurocode 7, Taylor & Francis, Abingdon, UK, https://doi.org/10.1201/9781482265873.

BSI (British Standard Institution). (2020) Code of practice for foundations, BS 8004:2015+A1:2020, London, UK.

CIRIA Construction Industry Research and Information Association. (2017) Guidance on embedded retaining wall design, London, UK, https://doi.org/10.1680/jgere.18.00039.

Coulomb, C.A. (1776) Essai sur une application des règles de maximis et minimis quelques problèmes de statique, relatits à l'architecture. *Memoires de Mathématique de l'Académie Royale de Science 7*, Paris, France.

DCCEEW Department of Climate Change, Energy, the Environment and Water. (2024) Net Zero. https://www.dcceew.gov.au/climate-change/emissions-reduction/net-zero.

Duncan, J.M. (2000) Factors of safety and reliability in geotechnical engineering, *Journal of Geotechnical and Geoenvironmental Engineering*, 126(4), pp. 307-316, https://doi.org/10.1061/(ASCE)1090-0241(2000)126:4(307).

Hjiaj, M., Lyamin, A.V. and Sloan, S.W. (2005) Numerical limit analysis solutions for the bearing capacity factor Nγ. *International Journal of Solids and Structures*, 42(5-6), pp. 1681-1704, https://doi.org/10.1016/j.ijsolstr.2004.08.002.

Kanaris, S. (2024) Legal Limits. *New Civil Engineer*, March 2024, pp. 44-45.

Morgenstern, N.R. and Price, V.E. (1965) The analysis of the stability of general slip surfaces. *Géotechnique*, 15(1), pp. 79-93, https://doi.org/10.1680/geot.1965.15.1.79.

Prandtl, L. (1921) Über die Eindringungsfestigkeit (Härte) plastischer Baustoffe und die Festigkeit von Schneiden. *Zeitschrift für Angewandte Mathematik und Mechanik*, 1(1), pp. 15–20.

Rankine, W. (1857) On the stability of loose earth. *Philosophical Transactions of the Royal Society of London*, 147.

Reissner, H. (1924) Zum Erddruckproblem. In: Biezend, C.B., Burgers, J.M. (Eds.), *Proceedings of the first International Congress for Applied Mechanics*, Delft, Netherlands, pp. 295-311.

Standards Australia. (2002) Earth-retaining structures, Australian Standard 4678–2002, Sydney, NSW, Australia.

Terzaghi, K., 1943. Theoretical Soil Mechanics. John Wiley & Sons, New York, USA.

GEOTECHNICAL DESIGN AND CONSTRUCTION METHODOLOGY OF STRUCTURAL ELEMENTS ON NEAR VERTICAL CLIFF FACES

Rachel Kraak
EDG Consulting Pty Ltd, Brisbane, Australia

ABSTRACT

Unusual geotechnical challenges are faced when designing and constructing structures on near vertical cliff faces. On a recent project for a public climbing attraction, typical processes for geotechnical assessment and design, such as rock mass characterisation, stability hazard identification, rock dowel design and construction phase services required bespoke solutions and considerable forethought to overcome access limitations. This paper presents an overview of the geotechnical design, construction methodology, and verification process tailored for the development of multiple structural elements connected to the cliff face utilising rock dowels on near-vertical rock faces.

The design approach includes a thorough site investigation process, including geological mapping, rock mass characterisation, and hazard susceptibility zoning. Combining rope access assessments, unmanned aerial vehicle (UAV) based LIDAR (light detection and ranging) and digital imaging allowed for a detailed assessment of the stability and rock mass behaviour of the face at broad and local scales.

The proposed methodology comprises dividing the site into zones characterised by mass/material characteristics, hazard susceptibility, access similarities, structural constraints, and client priorities to optimise the concept design development. Special attention was given to analysing the complex interactions between structural elements and the surrounding rock mass to maintain long-term stability at multiple scales coupled with structural integrity.

The construction phase encompassed a staged approach, utilising advanced rope access drilling and anchoring techniques, and precision instrumentation for rock dowel testing. Collaboration between the asset owners, geotechnical engineers, structural designers, and construction professionals is emphasised throughout the program to address unforeseen challenges in the design and construction of the structures.

1 INTRODUCTION

Construction on near vertical cliff faces is a rare occurrence in Australia, presenting significant design and construction difficulties. Its complexity is heightened by its scarcity of implementation in Australia, stemming from both limited demand and opportunity. This not only reduces the availability of design examples but also results in a lack of relevant standards or guidelines. A recent design and construct project of a public climbing attraction serves as a prime example of one of these rare instances for design of structures located on a near vertical face.

The climbing attraction comprises numerous separated structures over a 250m span of the cliff face at varying elevations. The structural elements are horizontally fixed to the cliff face via rock dowels. Some elements are interconnected by flexible components such as tensioned steel wires and flexible rock dowel connections. Each structure is unique in purpose and composition resulting in varied loads and constrained location options on the cliff face's irregular profile. For instance, the placement of an 80-meter-long zip line's launch and landing pads is restricted by the allowable grade of the zip line and availability of mid span support locations. The suitability of a chosen location is further influenced by the area-specific rock properties and larger scale hazards. Hazards being either external, like falling blocks, or intrinsic, such as widespread instability within the rock mass.

The project was delivered within a collaborative framework comprising the asset owners, structural and geotechnical designers and specialist contractors. Collaborative and ongoing interactions between the parties were required to overcome the unique challenges of the project where their spheres of expertise overlapped. Regular meetings between all relevant parties proved to be effective in communicating updates and outlining the responsibilities of each group. Due to the uniqueness of the project, it was critical to invest time into delineating each step of the methodology to ensure clarity on potential consequences and efficiency in project staging. The project schedule included an iterative process, whereby various stages were either confirmed or re-assessed following new information gained from on-site observations, additional scaling works, drone imagery, and rope access investigations.

2 GEOLOGICAL SETTING

The project site is situated in south-eastern Queensland (QLD) where the regional geology is characterized by a series of lava flows some 23 million years ago (Blewett 2012). The site is situated in the middle of a rainforest, which experiences high rainfall and occasional bush fires. The extent of the site ranges approximately 540m AHD (Australian Height Datum) to 700m AHD with a typical slope of 65° to 80°. The outer portion of the cliff line and face comprises columnar jointed rock formed by a major Rhyolite flow. However, at certain locations, the columns have collapsed to expose massive rock behind. The series of vertical cooling joints forming the rhyolite columns define the rock mass's most prominent structure set and are typically spaced between 2.2-2.8 m. There are also several sub-horizontal to dipping (approx. 0-30°) defects which cut through the columns to likely form the base of previously formed rockslides and wedge failures.

Understanding the area's geology and geomorphology was fundamental to inform critical decisions requiring engineering and geological expertise (Baynes, 2021). To better gain this understanding of the site conditions, an Engineering Geological model (EGM) was developed. The EGM combines and evaluates all relevant available input data to produce an interpretive understanding of the site engineering geological conditions (IAEG, 2021). The developed EGM for the project informed rock mass characterisation, natural hazards and identification of geotechnical instability mechanisms, erosion patterns, feasibility of structure locations, and qualitative risk assessments. EGMs are live models which are continually developed and improved with data points captured at various stages throughout the entire design and construction of the project.

3 PROJECT DELIVERY METHODOLOGY

3.1 DATA REVIEW

The project concept was simple, consisting of four structures proposed to be horizontally attached to the cliff face which had recently been exposed during a bushfire event 3 years prior. As the project progressed, additional structures and adventure elements were added to eventually comprise: ziplines structures, suspended 'wobbly' bridges, multiple additional climbing routes with anchorages, support ropes and multiple wire bridges.

An initial desktop review of the available geotechnical and geological data was carried out to assess the project constraints. The data assessed included geological setting, historical information on rock mass instability, natural disasters, and current use of area and surrounds. From this data a preliminary EGM was developed.

3.2 INITIAL SITE WORKS

An initial geotechnical site visit was then carried out to assess site conditions and structural location feasibility through geological mapping of the rock mass from rope access and site walkovers above and below the face. High resolution photographs of the whole site were captured using a unmanned aerial vehicle (UAV). This survey method obtains geospatial images to produce a realistic textured photogrammetry model. UAVs are beneficial in overcoming the limitations of traditional surveying methodologies, especially when dealing with difficult-to-access rock faces. A direct rock mass survey is a beneficial addition to either UAV or traditional surveying methods for a more realistic interpretation of digital results, when feasible (Pappalardo, 2020).

3.3 PRELIMINARY GEOTECHNICAL ASSESSMENT

A thorough knowledge of the geological conditions is required when interpreting the various forms of data to accurately assess instability mechanisms, hazards and potential solutions. The UAV digital data and results from physical site assessments were compared to conclusions from the data review to expand upon the existing EGM. Continually developing and optimising the EGM throughout the entire project lifecycle adds to the model's reliability and comprehensiveness and allows for further analyses like hazard susceptibility.

Based on the developed EGM, a high-level qualitative hazard susceptibility assessment was carried out to inform the concept designs and positioning of various structures. The assessment identified four key hazards with potential to affect the proposed infrastructure or pose significant risk to life. These were categorized based on size and included: small scale colluvial rockfall/slides (block sizes < 0.5m^3), toppling / falling of individual boulders/blocks (0.5 m^3 to 20 m^3), toppling/sliding of one or multiple columns (100 m^3 to 500 m^3), and rockslides and rock falls involving numerous columns with a volume (>500 m^3). To assess susceptibility, the cliff face was divided into broad zones classified by the potential for presence of hazard and consequence of its instability. Each zone was denoted either low, medium, or high susceptibility, and then further evaluated for a more detailed zonation of specific features affecting the stability of the

face. Remediation measures were then identified to reduce the likelihood of instability with comment on practical and economic feasibility.

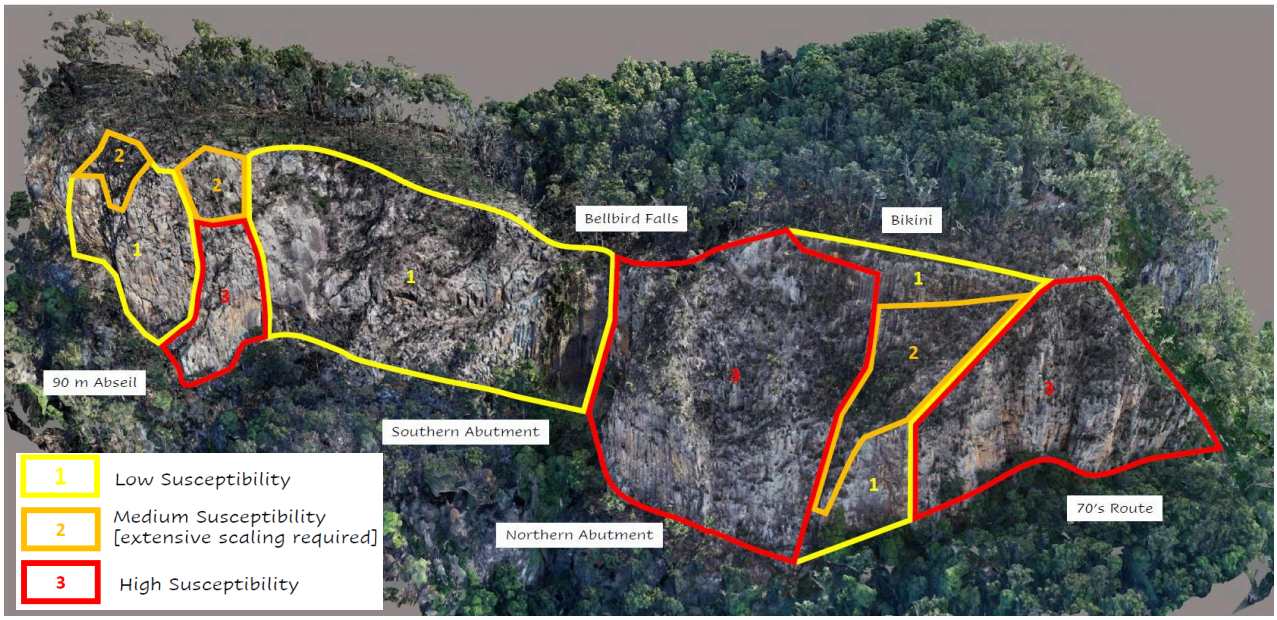

Figure 1: Example of initial hazard susceptibility zoning

Preliminary rock dowel bond material properties were assessed and provided to the structural engineers for their preliminary design. Hilti RE 500 Epoxy Chemset was nominated for the rock dowel installation grout and according to the manufacturer's specification, requires over 20MPa UCS bonding material. The assessment of the grout-rock bond strength of the site's in-situ rhyolite initially adopted 10% of its assessed Uniaxial Compressive Strength (UCS) for calculations. The grout/rock bond strength was to be confirmed in the construction stage of the project through pull out testing of sacrificial anchors. Alternative considerations for grout material selection included the provision of acceptable corrosion protection. To this purpose the addition of an HDPE sheath, or a "duplex" coating comprising both galvanising and epoxy was nominated.

The EGM, hazard zoning, and preliminary rock dowel bond material properties were presented to the client, structural designer and the specialist contractors for collaboration on determining structure's location and arrangement. The critical considerations included access constraints, purpose of structure, feasibility and hazard susceptibility and removal/remediation options (scaling, rockfall netting mesh, rockfall fence/ canopy, boulder pining). It was highlighted that the location of the dowels should avoid the top of blocks where toppling could be induced via lever effect.

3.4 DETAILED DESIGN PHASE

A robust and detailed approach to design was required due to the individuality of each rock dowel brought about by localised rock mass properties, geometry, and loading. The structural designers provided the predicted structural actions, fixity requirements (rock dowels with fixed head or flex-head connections), and arrangement for each structure at their structure-rock connection points. The provided preliminary forces were resolved into maximum shear and tensile components at ultimate limit state. The maximum shear force was assessed from either the provided force acting in the shear plane or the resultant shear force acting between external planes. The UAV procured digital data within the EGM provided initial estimates on the orientation and dip of the face at the rock dowel locations.

The design of dowels and bond material was undertaken along with a geotechnical rock mass classification and kinematic assessment to inform potential failure mechanisms (bearing failure, grout-ground bond failure, tensile failure in steel, grout-bar bond failure, shear failure and cone pull out) as depicted below in Figure 2.

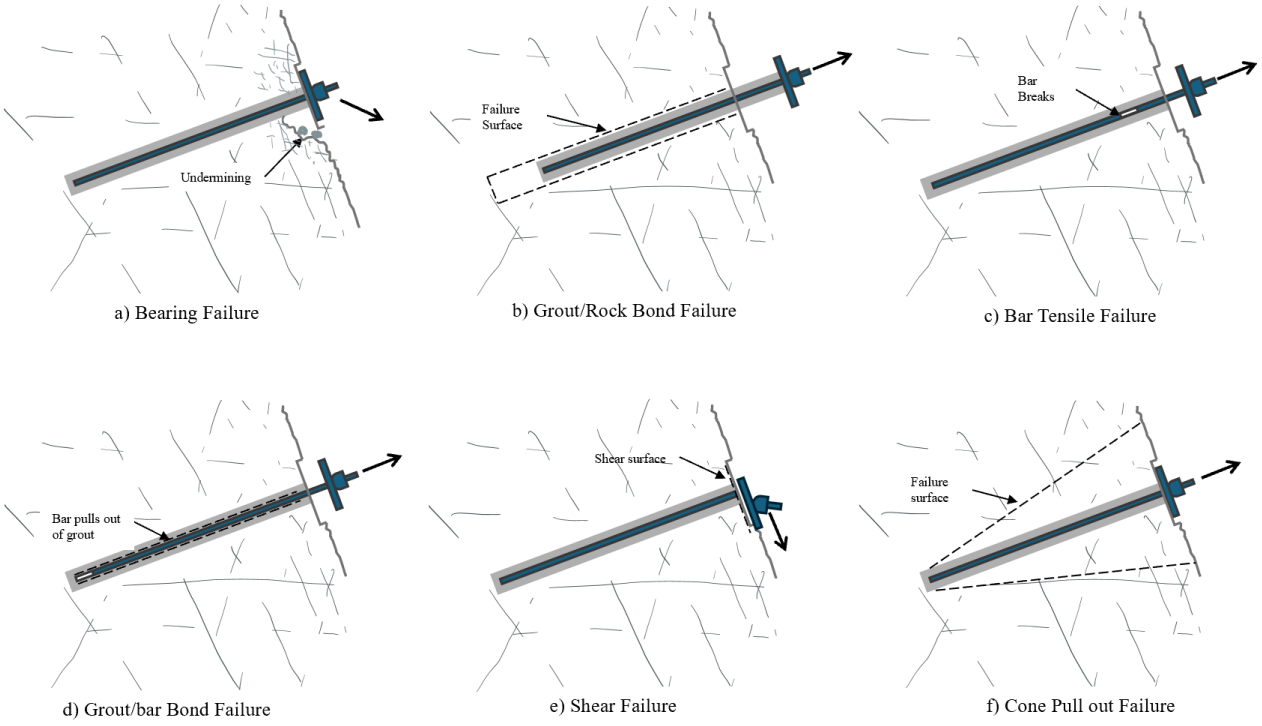

Figure 2: Potential failure mechanisms of rock dowels (sketched by author)

The design of grout material considered grout/ground and grout/bar bond design requirements. Rock dowel connection design was completed for rigid or flexible connections and dictated by degree of rotation in the connection and loads. The rock dowel bar design considered tensile and shear failure of the bar from the applied loads. Stainless steel bars were adopted to eliminate the requirement for large hole diameters which would otherwise be required to achieve suitable corrosion protection through grout cover and corrosion of exposed steel surface outside the rock mass. The required embedment design/minimum bond length considered the provided design actions, grout/rock bond strength (Hilti RE 500 Epoxy Chemset) and outcomes of the kinematic assessment. The failures mechanisms from the kinematic assessment relevant to embedment design included: failure along the grout/rock contact, failure along localised defects within the surrounding rock mass (cone pull out), and failure along the larger defects which define the individual blocks and columns.

To gain confidence in the achieved bond stress between grout/rock interface, pull out tests were conducted to cover the range of rock material strengths. The methodology outlined in the standards of Queensland Rail Civil Engineering Standard Specification (Ref: QR-CTS-Part 37 – Passive Anchors) was nominated to test the rock dowels. The test method includes testing for ultimate strength, suitability, and acceptance.

- Ultimate strength tests (pull out or proof tests) are sacrificial and conducted prior to the construction of any working dowels to gain an ultimate bond strength for a specific in situ material. The test comprises loading a vertically installed rock dowel till the dowel's head has undergone a permanent displacement of at least 50 mm.
- Suitability tests are conducted on working dowels and to assess the long-term performance of the in ground elements. The dowels are incrementally loaded over three 15 minute cycles to 150% the design working load. The test is considered successful if the total measured displacement of the rock dowel head after the three cycles is less than 0.1% bar length plus 10mm and less than 2mm per log cycle of time rate of creep at the maximum test load. Failing the creep condition, the test time for the failed cycle can be increased to an hour to potentially stabilise and pass. Suitability tests were nominated to be conducted on the first 5 working dowels at each structural climbing element location followed by one every 20 dowels installed thereafter, as a minimum.
- Acceptance tests comprised one cycle of the suitability test and were required for 20% of all working rock dowels and at a minimum of two per structure element. Suitability tested dowels are accepted towards the minimum requirements for acceptance tests.

This rigorous testing gave confidence that the rock dowels had adequate capacity to support the structures and that the construction methodology adopted was satisfactory.

3.5 VISUAL ASSESSMENT AND VERIFICATION OF CONNECTION LOCATIONS

The primary driving factor of rock dowel failure was assessed to derive from the condition of the rock mass and discontinuities present at each rock dowel location. As such, each individual rock dowel location was visually assessed, via rope access, prior to rock dowel construction. This assessment was conducted for the purpose of gaining confirmation on the rock dowel location suitability with respect to the rock structure and mass scale features / geo-hazards which may pose risks during construction or long term use.

The nominated rock dowel locations were locally evaluated for feasibility by undertaking a high level qualitative assessment for large and localized geohazards in the surrounding area. Rock mass observations were recorded and comprised: validation of rock material strength, block size, installation, and orientation / dip at the individual rock dowel points. An assessment of these observations gave an interpretation of the rock mass characteristics to confirm that the basis of design was satisfied.

The rope access works adopted a dynamically adaptable staged approach. Due to the changing perspective during a drop, the assessors had to be continuously vigilant throughout each drop and be prepared to change route (if safe) to further assess identified geohazards. Rock dowel locations flagged unfeasible or with intolerable risk were deemed unsuitable and new locations were immediately proposed and investigated to efficiently make use of each drop and assessor's time.

Information regarding the findings was systematically captured on site through notes and photographs. The identified hazards were collated in a presentation that locates the hazard on the cliff face and includes a localised picture for reference. The observations made were summarised in brief tables, grouping together the individual structures and commenting on the presence of hazards (referencing the hazard identification presentation) and feasibility of design and/or installation. An example of the table is given below in Table 1.

Table 1: Example of spot assessment structure suitability

Zipline Platform – Not Suitable					
Rock dowel point	**Mass Scale Features. Geohazards[1]**	**Rock dowel Location Suitability**			
		Rock dowel Suitability	**Large Scale Issue**	**Small Scale Issue**	**Details**
12JJ	-	yes	-	-	
12KK	H8	yes	-	-	Potentially pin boulder above. To be further assessed during construction phase services
12NN	-	yes	-	-	
12MM	-	No	Yes		Rock dowels potentially drilled into block
12LL	-	yes	-	-	
12PP	-	Not Assessed	-	-	Could not assess due to hazardous block – to be assessed following scaling

The mitigation of risk is generally assessed based on two general strategies: hazard and/or consequence/risk reduction. Hazard reduction is comprised mainly of the removal or stabilization of potential hazards, thereby reducing the likelihood of an instability to initiate in the future. On the other hand, risk reduction can be achieved by controlling the effects of an instability, i.e., eliminating negative consequences. (Marinos, 2017). Based on this theory, the rock dowel location either underwent remedial measures for risk reduction or relocation of structure. Necessary relocation of rock dowel points was communicated to the structural designers to either adjust the structure or to move it entirely. Following rock dowel relocation, the new rock dowels points underwent the same process of design, assessment, and validation as previous.

3.6 CONSTRUCTION PHASE

Construction works commenced after design finalization of structural elements, foundations and rock dowel locations. Additional scaling works was required to provide access, remove identified hazards, and localised rockface manicuring for rock dowel installations. A Menzi Muck spider excavator, equipped with advanced drilling technologies, was used to drill the rock dowels. This machine's alterable legs, rotating chassis, and telescopic drilling arm enabled it to adapt to the sites challenging terrain (Menzi Muck Machinery, 2023). Rock dowel installations and testing was conducted through rope access methods. Testing adhered to the Queensland Rail Civil Engineering Standard Specification with 10% of the tests observed by a geotechnical engineer to confirm compliance.

4 CONCLUSION

Construction on near vertical cliff faces presents unique challenges and requires a collaborative approach combining structural and geotechnical expertise with innovative surveying and construction techniques. Success relies heavily on thorough geological assessments, hazard zoning, and dynamic adaptability in design processes. Advanced technologies like UAV photogrammetry facilitate data collection efficiently and was corroborated with localised in-person visual assessments to develop a robust and detailed EGM. Detailed geological and geotechnical assessments were fundamental in informing critical decisions, thereby ensuring the safety and feasibility of the construction.

The design approach of zoning a large area into smaller manageable sections (big to small) allowed the design of numerous independent and dependent structures to progress concurrently. Proof methods and field trials ensured compliance with safety standards and provided confidence on design outcomes prior to construction. This increased the projects efficacy in construction advancement and design confirmation. Clarity and efficiency throughout the project was ensured through regular transparent interdisciplinary communication. This project's findings will hopefully provide valuable knowledge for future cliff face construction endeavours.

5 REFERENCES

Baynes, F. J. and Parry, S. (2022). Guidelines for the development and application of engineering geological models on projects. *International Association for Engineering Geology and the Environment (IAEG)* Commission 25 Publication No. 1, 129 pp. DOI: https://doi.org/10.1007/s10064-014-0576-x.

Baynes, F. J., Parry, S. and Novotný, J. (2021). Engineering geological models, projects and geotechnical risk. *Quarterly Journal of Engineering Geology and Hydrogeology*, Volume 54. DOI: https://doi.org/10.1144/qjegh2020-080

Blewett, G. and Geoscience Australia (2012). *Shaping a nation: A geology of Australia.* Canberra: Geoscience Australia And Anu E-Press. DOI: http://doi.org/10.22459/SN.08.2012

Marinos, V., Prountzopoulos, G., Asteriou, P., Papathanassiou, G., Kaklis, T., Pantazis, G., Lambrou, E., Grendas, N., Karantanellis, E., & Pavlides, S. (2017). Beyond the boundaries of feasible engineering geological solutions: Stability considerations of the spectacular Red Beach cliffs on Santorini Island, Greece. Environmental Earth Sciences, Volume 76, pp. 513. DOI: https://doi.org/10.1007/s12665-017-6823-2

McElroy, C.T. (1963). *The geology of the Clarence-Moreton basin*. Department of Mines, New South Wales. DOI: https://doi.org/10.1080/14400956908527969

Menzi Muck Machinery (2023) Brochure Menxi Muck M5x. Available at: https://menzimuck.com/en/product/walking-excavator/menzi-muck-m5x/ (Accessed: 3 Jun. 2024).

Pappalardo, G., Mineo, S., S. Imposa, Grassi, S., Leotta, A., F. La Rosa and Salerno, D. (2020) A quick combined approach for the characterization of a cliff during a post-rockfall emergency. *Landslides*, Volume 17(5), pp. 1063–1081. DOI:10.1007/s10346-019-01338-w

Wang, S., Ahmed, Z., Hashmi, M. Z., & Pengyu, W. (2019). Cliff face rock slope stability analysis based on unmanned aerial vehicle (UAV) photogrammetry. *Geomechanics and Geophysics for Geo-Energy and Geo-Resources*, Volume 5, pp. 333–344. DOI:10.1007/s40948-019-00107-2

Zaruba, Q. and Mencl, V. (1976). *Engineering Geology*. Elsevier, Amsterdam. DOI:10.1017/S0016756800041054

FOUNDATION CORRECTION WORKS ON SOFT SOIL: INSIGHTS FROM PRACTICE

Manamea Koteka
Tonkin & Taylor Ltd

ABSTRACT

Peat/organic soils are characterised by low undrained shear strength, high compressibility and are susceptible to significant ground settlements, creating challenges for engineers and developers. Since construction in 2015, a housing subdivision in Auckland, has been impacted by ground settlement and distortions to foundations and superstructures. The pattern of distortions are indicative of differential settlements resulting from mixed foundation types, being part-piled and part-ground bearing over soft compressible peat.

Mixed foundations are sometimes used where dwellings are built adjacent to or over services, with piles being used to transfer loads to below the level of the services. A number of dwellings within the subdivision, which were constructed with mixed foundation types, have required regular intervention works to maintain dwelling serviceability. Foundation distortion correction works were trialled on one damaged property with the purpose of proving the adopted remedial methodology and substantiating future foundation performance.

The remedial works involved disconnecting piles and implementing staged and cycled surcharge loading with water tanks on the foundation slab. This method was used to verify the performance of the slab and to measure the dwelling response to the change of support. Water tanks were positioned near the locations of the most significant distortions and subjected to loading cycles over several weeks while monitoring changes in floor distortion. The trial results successfully demonstrated compliance of the corrective works with the performance expectations of the New Zealand Building Code.

This paper presents the challenges and solutions implemented on the trial property during the foundation distortion correction works.

1 INTRODUCTION

New Zealand is enduring rapid expansion and population increase, thus spurring the demand for land development. A general scarcity of high-quality land has resulted in investment and development of land with less favourable geotechnical characteristics, including over soft soils. Soft soils are commonly associated with poor geotechnical performance characteristics, including low strength, high compressibility (often with slow consolidation rates) and susceptibly to creep related movement; they may be organic or inorganic in nature.

This paper presents a case study from one such development over soft organic soils where dwellings have experienced long term differential settlements, principally arising from the use of mixed foundation types (piles and ground bearing elements). Whilst the dwellings have performed reasonably well (no loss of structural integrity but some serviceability issues), it is likely that without any intervention ongoing settlement would result in more significant damage, likely requiring substantive repairs and/or rebuild works.

The trial intervention works aimed to:

1. Reduce current distortions in the building foundation to more acceptable and stable levels.
2. Substantially reduce the risk of the need for future structural interventions over the dwelling's design life.
3. To mitigate the need for ongoing repair and maintenance requirements to a level akin to routine homeowner maintenance operations, accommodating expectations for ageing and wear and tear of fabrics.
4. Prove the suitability of the interventions works and demonstrate compliance of the dwelling performance to the requirements of the New Zealand Building Code.

2 BACKGROUND

The trial property was constructed in 2015 and comprises of a 4 bedroom, single-storey dwelling constructed on a rib-raft slab foundation covering an area of approximately 157 m^2 with two piles along the north-eastern corner of the property (in proximity to a buried service line) as shown in Figure 1. The dwelling superstructure is of timber frame construction, with a metal tile roof with mixed, weatherboard and brick veneer, cladding.

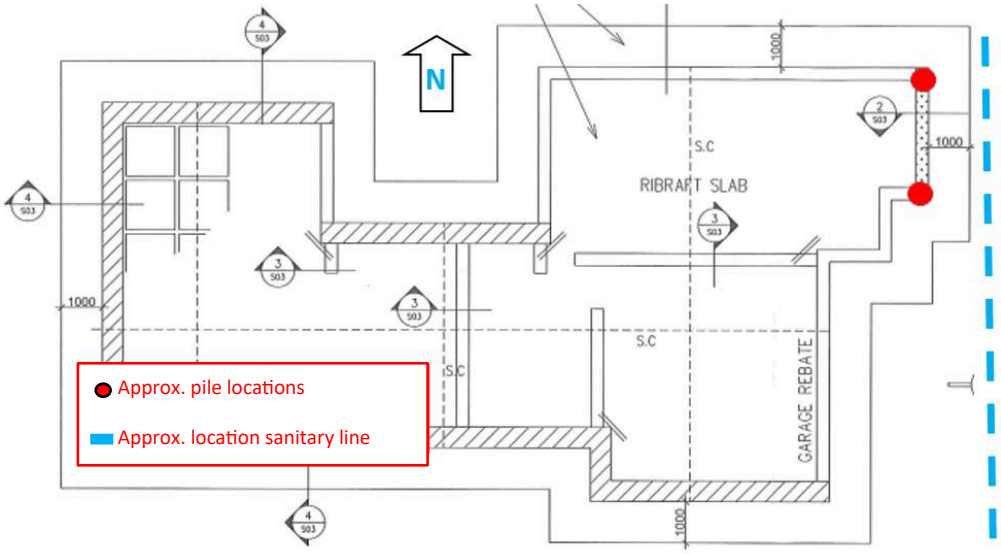

Figure 1: Floor plan layout annotated with pile and sanitary line location

Published geological mapping indicates that the trial property is underlain by alluvial sediments of the Tauranga Group, comprising Holocene-age and Pleistocene-age soils. These sediments comprise a combination of organic/peaty soils (Holocene-age) and pumiceous (inorganic) clays, silts, and sands (Pleistocene-age). The subdivision area is therefore underlain by relatively compressible soils that are susceptible to consolidation and creep settlements and to seasonal shrink-swell movement. Site investigations undertaken have identified an approximately 10 m thick layer of these compressible soils.

3 TRIAL WORKS

Before initiating any physical works on the trial property, a comprehensive investigative process was carried out. The following steps were taken in this process:

3.1 VISIBLE DAMAGE ASSESSMENT

The history of the maintenance works that have been required on the dwelling are consistent with the effects of differential foundation movements, in particular differential foundation movement focussed on the north-eastern edge of the property where the foundation transitions from being supported on piles to being ground bearing.

Prior to the commencement of the trial interventions, a comprehensive visual inspection was conducted on the property. Internally the damage observed at the property is generally confined to the area where differential distortions have arisen due to mixed foundation support types (i.e. piled foundations and ground bearing raft). Internal damage included cracking of gib boards and linings, particularly within 2 m to 3 m of the piled locations, with cracking generally being diagonal and emanating from corner openings in the timber frames (i.e. doors and windows). Door and window frames were out of plumb or had apparent maintenance adjustments to hinges (Figure 2) and trimming of door panels associated with planar distortions of the framing around openings. Localised bowing of gib-bracing sheets, which were orientated perpendicularly and close to the line of the pile support area, also provided evidence of local distortion but no actual structural rupture. The internal gib board and bracing around the front of the property were removed to allow visual inspection of the timber framing. No damage to the timber framing was observed, it was noted that some local and minor separation between the base plates and the top of the floor slab had locally occurred.

Externally there was no apparent damage to external weatherboards or brick cladding (the latter being remote from pile locations). Evidence of distortional movements within the internal building fabric over areas of the dwelling remote from the piles (i.e. >3 m distant from pile locations) has been identified but was of very minor nature.

At the location of the piled foundations, a gap had developed between the underside of the rib-raft foundation and the soil surface. The gap extended approximately 2 m distant from the location of the piles back into the dwelling footprint (i.e. the floor slab was acting in a suspended mode in this locality). However, remote from the piles, the foundation slab and superstructure have performed well with no apparent evidence of distress or significant foundation distortions. It is therefore likely, where the slab is not distorted by differential settlements associated with mixed foundation types (i.e. adjacent ground bearing and piled elements), the effects of settlement and shrink-swell are within design performance expectations.

Figure 2: (a) Adjusted door hinge showing clear signs of movement and (b) Garden edging detached from slab and settlement adjacent to pile locations

3.2 INVESTIGATIONS

3.2.1 Floor Level Survey

The profile of the foundation slab was evaluated through laser survey measurement of relative levels of the surface of the rib-raft foundation.

Recorded differential levels across the entire dwelling footprint were of the order of 90 mm. No significant cracking or step changes in the floor slab profile were identifiable. The absence of damage around the majority of the property demonstrates general resilience of the timber frame superstructure and it is likely that some of the apparent local distortions in the floor slab may have been built out as the building construction proceeded. Maximum tilt on the surface of the floor slab was assessed to be (locally) up to approximately 1 Vertical: 50 Horizontal.

3.2.2 Intrusive Investigations

Boreholes and Coreholes

Boreholes were drilled as part of a broader investigation of the subdivision, and logs confirm the local geological profiles are generally consistent across the wider development and consistent with previous investigations and expectations from published geological mapping.

Several coreholes were drilled through the floor slab to identify the potential for local yielding or damage within the slab as a consequence of the observed distortions.

CCTV – sanitary water pipeline

A sanitary water pipeline which runs along the eastern boundary of the lot was inspected by CCTV survey before and following completion of the foundation distortion correction works.

Terrestrial Survey and INSAR

Terrestrial survey monitoring has been undertaken at a select number of locations across the broader sub-division area. This monitoring covers an eleven-month period from October 2021 to September 2022. The resulting survey data suggest that seasonal shrink-swell movement occurs within a range of approximately +/-5 mm. There is also evidence within the data of an overall underlying settlement trend of up to approximately 7 mm/year (likely survey tolerance of +/-2 mm) for the subdivision.

Additionally, to provide supplementary assessment of the longer-term settlement trends across the subdivision, satellite Interferometry data (INSAR) has also been acquired and analysed. The INSAR data demonstrates that, over the period 2016 to 2021, settlements within the broader area have been continuing to develop, albeit at rates which are diminishing with time.

The settlement trends apparent from both the terrestrial and INSAR are generally compatible and confirm that the overall subdivision is subject to both local and area wide settlement trends (including seasonal shrink-swell movements). The INSAR data is presented below in Figure 3.

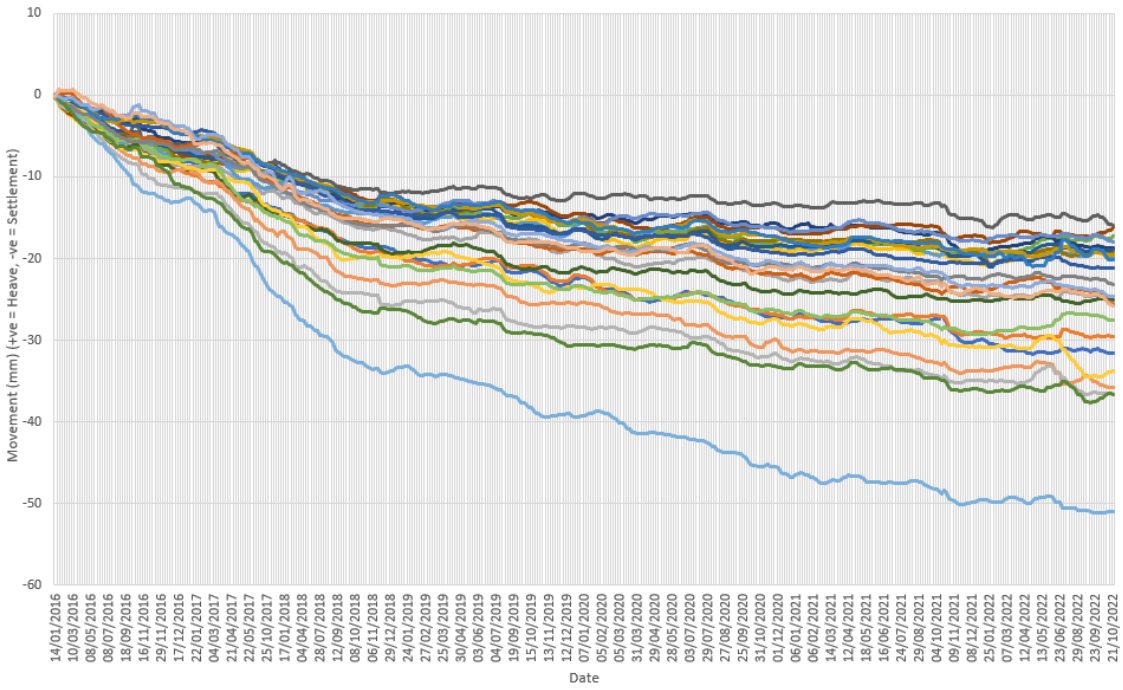

Figure 3: Ground Movement versus using INSAR data

3.3 THEORETICAL EVALUATION

The floor surface profile for the trial property was measured to perform a theoretical evaluation of the structural performance of the foundation slab. This evaluation aimed to assess the risk of unseen plastic deformation or cracking in the floor slab. The calculations suggested a risk that the floor slab might have yielded. However, it was also recognised that the theoretical assessment was sensitive to several critical assumptions, and it didn't correlate with any physically observed damage to the floor slabs.

To address this potential theoretical failure (which would necessitate structural remedial works to the floor slab structure, if confirmed), coreholes were drilled through the concrete floor slab to confirm yielding. Observations from these cores revealed very minor hairline cracking but no signs of actual structural damage. Therefore, it was concluded that the physical performance observations of the distortions in the structure and slab were more reliable than theoretical assessments that also accounted for several unknown variables or assumptions.

3.4 PHYSICAL WORKS

The trial works were designed to correct distortions and allow the slab freedom to self-correct, under the self-weight and targeted surcharging, by disconnecting the piles that support the north-eastern elevation of the property. The works included the staged and cycled surcharge loading (water tanks) of the slab to verify the performance of the slab and dwelling response to the change of support.

3.4.1 Preparation Stage

The trial remediation programme for this structure involved fixing a temporary support beam to the lower portion of the timber piles and placing jacks between the beam and the underside of the rib-raft foundation. Once the foundation load had been released from the top of the piles; by engaging the jacks, a short sectional length of pile was cut out and the jacks were lowered. Prior to the pile cut, the internal gib-bracing panels were slackened to promote the shape correction.

Figure 4: (a) Jacks between jacking beam and underside of the rib-raft foundation and (b) Pile Cut

The raft responded to the release of the hydraulic jacks by settling immediately by approximately 20 mm to 25 mm. However, the gap between the underside of the rib-raft foundation and the soil surface did not close completely and the gap between the cut surfaces of the piles also remained open.

3.4.2 Loading Stage

As a supplementary stage of the trial, water tanks were then placed within the front portion of the house (between the location of the piles and the area of maximum angular distortion in the slab). The three tanks were progressively filled with water and then the loading cycled over a number of weeks whilst changes in the distortion of the floor slab were monitored. The impact of the cutting of the piles on the shape of the floor slab was observed by monitoring the distance between marker pins fixed to the upper and lower sections of the pile and intermittent checks on the level profiles on the surface of the rib-raft foundation. The load cycling initially induced approximately a further 5 mm – 10 mm of settlement towards the front of the property.

4 TRIAL WORKS RESULTS

The overall changes in the ground floor profile achieved by these works are illustrated in Figure 5 by the following 3-D representations of the floor surface within close proximately to the piled area before and after the works were started/completed.

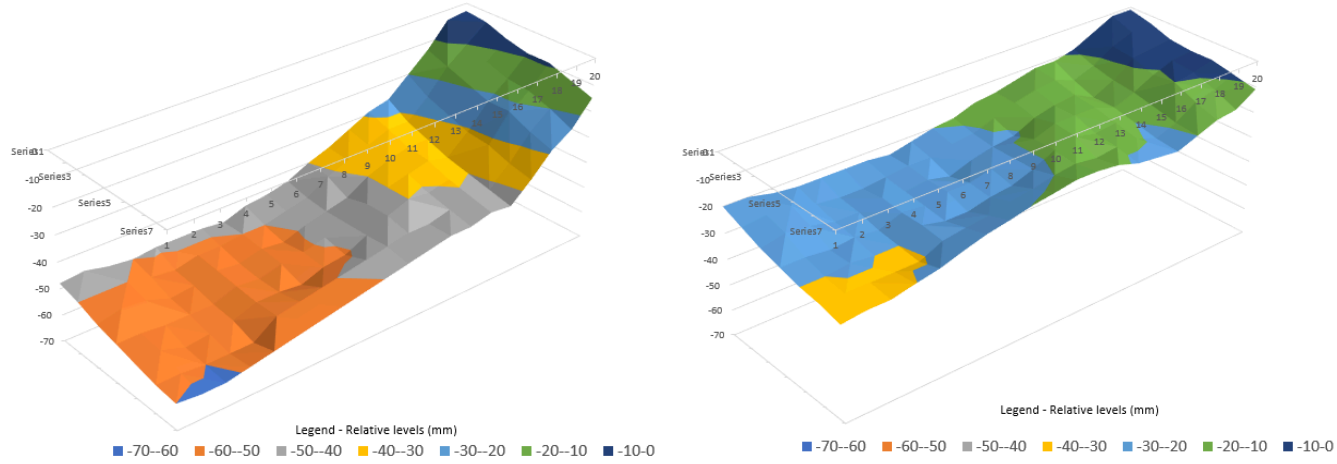

Figure 5: Floor slab profiles (a) before pile cutting, and (b) after pile cutting

It is considered that movement response to the imposed floor loading (water tanks) indicated that the slab remained and performed in an elastic mode during the load-reload cycles, despite the imposed floor loading exceeding the design floor loading of 1.5 kPa and the slab apparently cantilevering in excess of 2 m.

Based on the results of the trial, there was a reduction in differential settlement of the order of 30 mm and with no further damage to the fabric of the dwelling. This outcome indicates that the composite performance of the slab and superstructure

is resilient and can continue to function without the support of the piles. i.e. the performance of the structure does not rely on the piles and the performance of the buried sanitary pipe is unlikely to be impacted by bearing pressures from the foundation slab itself.

It required a significant period of monitoring (>1 year) to evaluate and gain confidence in long term estimates of settlement and building performance in this area. However, extrapolation of the INSAR data (Figure 3) indicates that further settlement of approximately 40 mm over the next 50 years is credible. Therefore, the following three potential performance scenarios have been considered:

1. All movement comes to an abrupt halt. This is an unlikely scenario. If this were the case, there is a very low residual risk of re-intervention works being required.

2. Movement continues uniformly beneath the entire structure, at or below the currently identified diminishing settlement rates (INSAR data), until such point that the pile ends re-engage. Provided total movements remain consistent beneath the floor plan then no further damage is likely.

3. As a result of the new loading regime, the area of the house in the vicinity of the piles would undergo a short-term acceleration in rates of settlement compared to the rear of the house. In this case, existing differential settlements in the critical areas at the front of the house should continue to diminish but may require further ongoing and short-term maintenance interventions (i.e. gib/doors) because of the higher initial rate of localised movement after the internal finishes are reinstated.

Following the completion of these works, the house underwent refurbishment, which included the fitting of gib, tidying up, re-setting of door and windows and decorating. The dwelling is now occupied. Observations over the last year, post-reinstatement, points to a notable improvement in performance with no evidence of further damaging distortions. There is no discernible ongoing differential settlement, indicating the effectiveness of the trial works.

5 CONCLUSION

The interventions, which involved disconnecting piles and implementing staged and cycled surcharge loading with water tanks, satisfied and met the objectives of the trial. Along with predictions of future performance (based on post remedial observations to date and predictions of long-term settlement from INSAR data) the works have been used to demonstrate that the performance requirements of the New Zealand Building Code have been met and will likely be satisfied for a further 50 years.

The trial demonstrated the challenges and unique geotechnical issues posed by construction on soft soils particularly if mixed foundation systems are utilised. While some degree of settlement is likely to continue, it is anticipated to diminish over time and remain manageable within the scope of standard homeowner maintenance following the correction works. The findings from this study can provide insights into similar situations, particularly in dwellings within this subdivision displaying compatible construction forms and distortions (albeit mixed foundation types should generally be avoided). The results from the trial interventions also prove the feasibility and effectiveness of foundation correction works as a robust strategy to mitigate substantial potential future settlement damage in such terrains.

PERFORMANCE AND STABILITY OF SHORT PILES IN CRACKED DESICCATED SOIL

H.S Thomas[1], D.W Airey[1]
[1]*The University of Sydney, NSW, Australia*

ABSTRACT

Many solar farms use solar panels supported by pile foundations. The required load capacities are small, but often design leads to a requirement for long piles because of reactive soil concerns. This situation is partly a consequence of limited evidence on the performance of piles in reactive soils, particularly when desiccation cracks are present. There is ambiguity regarding the influence of swelling and shrinkage on the strength of soil and its effect on soil-structure interaction that lead to practical challenges and disagreements in the design of short piles for solar farm foundations where economy favours pile termination within the active zone. While it is certain that cracks reduce the capacity, improved understanding in quantifying crack depth and the changes in soil stiffness and strength would reduce uncertainties required for cost effective design of foundations for solar farms in arid regions of Australia where expansive clays are encountered. A series of laboratory experiments have been performed using small scale model piles in expansive clays and sand-bentonite mixtures to understand the behaviour of piles under cycles of wetting and drying in the presence of cracks. These are to complement a full-scale test program underway in Adelaide. The load-displacement responses are compared with finite element simulations to quantify pile performance. Finite element simulations on scaled piles were performed to study performance variation in saturated and partially saturated conditions and results are presented.

1 INTRODUCTION

Sizeable, under-utilised land areas in Australian territories are often associated with highly plastic expansive clayey soils. The ground movements associated with seasonal moisture changes in expansive soils (Ito and Wagai, 2017) and desiccation cracking during summers present many challenges to foundations built on them. Recent focus in developing large-scale solar farms in Australia necessitates huge land areas, where the Photo-Voltaic (PV) panels supported by steel pile foundations track and harness solar energy. The frames supporting PV panels are relatively flexible and hence larger foundation movements can be tolerated than conventional structures. When the depth of soil affected by seasonal changes is large, as is the case in many parts of Australia, there can be a requirement to ignore any capacity derived from the active zone of the soil resulting in long and costly piles. As large solar farms involve many thousands of piles (Surjadinata et.al, 2021, Kelly et.al, 2021) (W 6x8.5 or 150 UB 14 H-section being the common section), a small change in pile length could translate to thousands of meters in total pile length and this can dictate project economics. For short piles in the active zone consideration must be given to unsaturated soil behaviour which presents a major challenge for the geotechnical engineer. As drying and desaturation of soil are associated with shrinkage, separation could occur between pile and soil. Since the tension or pull-out resistance of pile depends on normal stresses on the shaft, it is conceivable that stresses could reduce to zero at segments of the shaft undergoing separation. Experiments on drilled shafts in expansive soil (Johnson and Stroman, 1981) have encountered desiccation cracks down to 7m in depth with no shaft resistance, and Crilly and Driscoll (2000) recommend ignoring shaft friction in design in active zones. Several studies have investigated the axial response of piles in expansive soils in both laboratory (Challa and Poulos, 1991) and field using timber piles (eg: Cameron and Walsh,1983; Fityus and Delaney,2001) and concrete piles (Crilly and Driscoll, 2000). These studies show an initial movement of piles accompanied by the swell of soil, though the relative movement of pile with further shrink-swell cycles of soil remains relatively small; the studies however did not consider the effects of uplift or lateral forces on the piles which are necessary for understanding the response of short piles in solar farms. It is expected that the suction generated during drying near the soil surface should increase the soil strength thereby improving the lateral and uplift capacities, provided that the separation between pile and soil doesn't occur, since the behaviour of short piles are greatly dependent on mechanical properties of soil at shallow depths. Recently numerical studies (Cheng and Vanapalli, 2021; Lalicata et.al, 2021) have incorporated the effect of suction to predict the performance of piles in unsaturated soil conditions. However, these are not validated, and little consideration was given to the desiccation cracks generated under drying. This paper analyses observations from a set of laboratory experiments carried out to understand the behaviour of laterally loaded small-scale piles in expansive clays (Niu, 2022). The results are then compared to numerical simulations to understand the effects of partial saturation and desiccation cracks on pile capacity.

2 EXPERIMENTAL PROGRAMME

A set of laboratory tests of laterally loaded scaled model piles in high plasticity expansive clay subjected to sequential drying and wetting were performed at the University of Sydney (Niu, 2022). A naturally occurring residual soil sourced from Western Sydney airport site was dried, crushed and reconstituted at its optimum moisture content. The reconstituted soil was compacted in layers in containers, 310 mm in diameter, and subjected to sequential wetting and drying.

Instrumented model aluminium piles, with hollow circular sections of uniform thickness 2.4mm were installed into the soil samples after initial moisture equilibration. These piles were subjected to lateral and uplift forces at different stages of drying and final wetting of the soil, with the applied head load and pile head displacements being monitored. The moisture content of the soil within each container was measured before each testing stage and photographs taken to observe the cracking pattern on the surface (Figure 1). The soil is classified as high plasticity clay and meets the requirements to be considered as expansive (Liu et.al, 2019; Burton et.al, 2014; Mitchell, 2013). Properties of the clay obtained following Australian Standard procedures are listed in Table 1. Three soil tanks with compacted soil were used for the study; once compacted, the samples were left open to room temperature to allow drying for a period of seven days, after which all samples were wetted. This was considered to represent one cycle of drying and wetting. Instrumented piles were then installed at a steady speed using a motorised drive mechanism. Dimensions of the model piles are detailed in Table 2. The soil containers A, B and C had the same diameter of 310mm but varying soil depths 175mm, 185mm and 225mm respectively. The arrangement of piles can be seen in Figure 1; a single central pile was used in container A and B while two piles were embedded in container C. The dimensions of pile or soil containers were not scaled based on field scale piles; however, the selection of sizes of piles and soil samples enabled a series of tests to be conducted within a fixed period of time, allowing for observing response of pile interface in soil undergoing desiccation cracks.

Table 1: Soil Classification Results

Soil Properties	
LL (%)	61
PL (%)	20
PI (I_P)	41
G_s	2.67
OMC (%)	21
USCS	CH

The performance of both piles from container C were essentially identical, hence only one is reported here. It is acknowledged that piles are installed closed to the boundary this and could influence the results, particularly the lateral capacity and crack pattern. Once the piles were installed, the soil samples were allowed to dry with lateral loading being performed after three days and then after three weeks of drying, constraining the displacement at pile head to 1.5mm, which was monitored by an LVDT. The soil samples were then allowed to hydrate by addition of water after which a third and final episode of loads were applied, two weeks post wetting. The loading times are denoted T_1, T_2 and T_3. The moisture contents of the soil were obtained by extracting small diameter core samples at different depths before each stage of loading and results are presented in Figure 2. The trends from containers A and B are similar with high moisture contents after initial wetting at T_1, large reductions in moisture content, most pronounced at the surface after drying at T_2, and then significant increases in the final wetting. Container C has a similar pattern but much smaller changes at all depths. It is believed this is related to different desiccation crack patterns at depth in this deeper container. For analysis it has been assumed that undrained strength can be estimated directly from moisture content using a correlation between liquidity index and undrained strength (Wood, 1991). The liquidity index correlation has been used as it provides a simple and reasonable indication of the large changes in soil strength associated with wetting and drying. The undrained strength profiles calculated using the correlation are presented in Figure 3.

2.1 OBSERVATIONS

The formation, propagation and partial healing of desiccation cracks due to drying and wetting are illustrated through Figure 1. The moisture profiles from container B and C at T_2 and T_3 shows that an active zone formed. The seepage of water through the cracks closes the gap at the pile annulus, however not all desiccation cracks close up quickly due to the time required for water to penetrate intact clay. After three weeks of drying (T_2), the surface moisture content drops below the plastic limit in containers A and B. At this stage significant suctions in the clay and air entry to the soil are expected.

Table 2: Pile Dimensions

Pile Dimensions (mm)	P_A	P_B	P_C
Total Length	220	220	220
Outer Diameter	25	25	25
Embedded Length	120	160	200

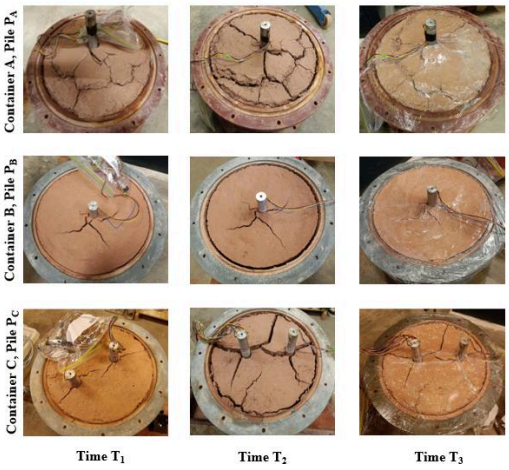

Figure 1: Embedded pile(s) in soil containers through different phases of drying and wetting

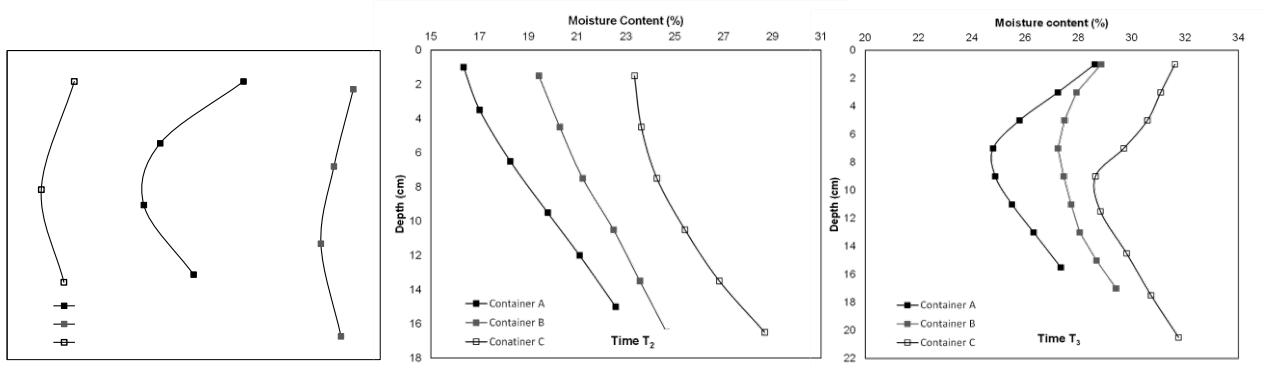

Figure 2: Moisture content along depth of containers A, B and C at times T_1, T_2 and T_3

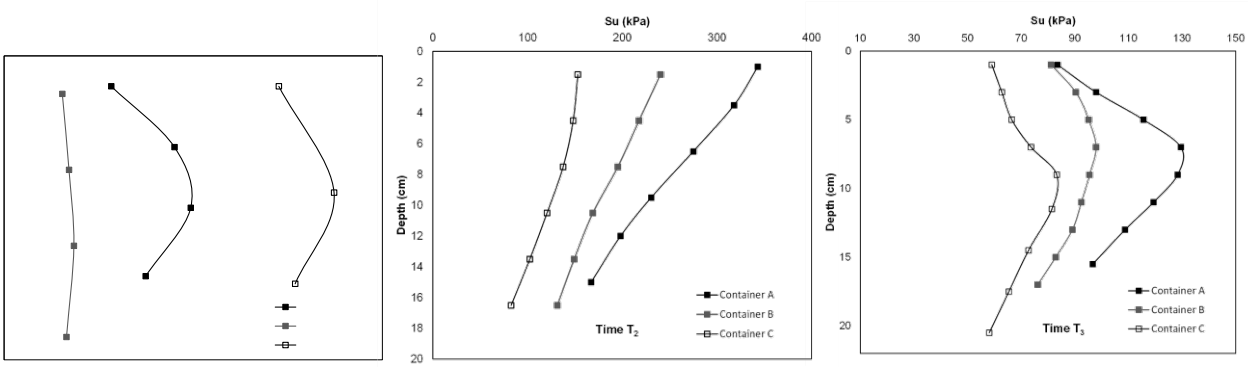

Figure 3: Undrained strength profile of soil (containers A, B and C) at times T_1, T_2 and T_3

The data from the applied load at pile head against observed head deflection for piles embedded in three containers are presented in Figure 4. As evident from Figure 1, the soil in Container B experienced minimal cracking within the soil mass and at the pile anulus, whereas soil in containers A and C experienced significant desiccation cracks and partial healing by wetting. The response of piles P_A and P_C at T_2 are like their initial responses, despite the formation of cracks, which suggests an improvement in the strength of the soil near the pile due to drying. The subsequent reduction in lateral load capacity on wetting indicates that only partial healing has occurred. The higher resistance of P_B at T_2 supports the argument that soil strength and hence lateral capacity is increased by suction and partial saturation. Figures 1 and Figure 4 suggest that desiccation cracks are primarily responsible for the reduction in capacity, and that this can be partially countered by the unsaturated state which increases soil strength. In container A, some recovery in pile capacity can be observed, however, in container C, with pronounced cracking the least recovery is observed. The lack of recovery may be because insufficient time was provided for swelling, but it appears unlikely that the initial resistance would have been recovered. For design it is required to quantify the reduction in strength associated with the developing cracks. This will depend on their depth and surface pattern which are both difficult to measure and predict.

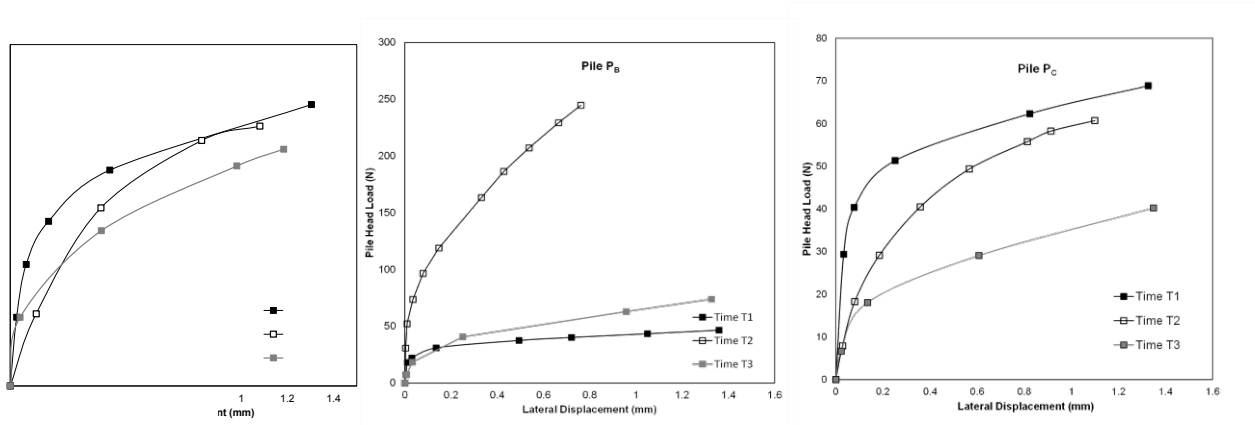

Figure 4: Pile Head Load-Lateral Displacement response of P_A, P_B and P_C at times T_1, T_2 and T_3

3 NUMERICAL SIMULATIONS

Several studies have been performed to numerically simulate the effect of partial saturation on the axial response of piles have been performed (Mohamedzein et.al, 1999; Liu and Vanapalli, 2021; Georgiadis et.al, 2003). Fewer numerical studies have investigated the lateral response of short piles under partially saturated soil conditions (Lalicata et.al, 2021) and only limited soil conditions have been studied. The simulations detailed here were performed in ABAQUS using the in-built Cam-Clay model to study pile-soil interaction under lateral loading for saturated and partially saturated soil states. The Modified Cam-Clay model (MCCM) is an effective stress based elasto-plastic model that was originally developed to capture saturated behaviour of clays. To account for unsaturated soil behaviour ABAQUS makes use of Bishop's (1959) definition for effective stress in unsaturated soil given by Equation (1), where the parameter χ varies from 0 for dry to 1 for saturated states.

$$\sigma' = (\sigma - u_a) + \chi\,(u_a - u_w) \tag{1}$$

where σ' is the effective stress, (σ-u_a) the net stress, χ the effective stress parameter and (u_a- u_w) the matric suction (or measured suction, denoted as $\boldsymbol{s}$). It is assumed that $\chi = S_r$, S_r being the degree of saturation. Analyses using partially saturated soil require a relation between suction ($\boldsymbol{s}$) and degree of saturation ($\boldsymbol{S_r}$), often referred to as the soil-water retention/ characteristic curve (SWCC or SWRC). The ABAQUS in-built module was used to incorporate the SWCC, were the S_r-$\boldsymbol{s}$ relation developed for the Western Sydney Clay sample in laboratory were used as the input. The model parameters for the Cam-Clay model are listed in Table 3. The values of λ, κ and η are derived from 1-D oedometer and triaxial tests performed by the authors on saturated specimens of reconstituted Western Sydney clay. The wet yield surface (β) and flow stress ratio (K) values were assigned the default value of 1; values for the SWCC parameters were obtained from curve fitting to the results of filter paper tests shown in Figure 6(b).

Table 3: Mechanical Parameters of the Modified Cam Clay Model

Parameter	Description	
λ	Slope of NCL in *e: ln p'* plane	0.209
κ	Slope of URL in *e: ln p'* plane	0.05
η	Stress Ratio	0.98
ρ	Density (t/m^3)	1.8
ν	Poisson's Ratio	0.28

3.1 NUMERICAL MODEL

The 3D model represents half of the cross-section of the pile and soil, utilising the symmetry along the vertical plane containing the force, as shown in Figure 6(a). The soil model has a diameter of 310mm and thickness of 225mm with pile embedment of 120mm, similar to the experimental pile P_A. The FEM modelled pile has the same diameter and flexural rigidity E_pI_p as the experimental pile. The initial void ratio and yield surface are chosen to give an undrained strength, S_u= 40kPa, to reproduce the estimated strength at time T_1 in container A. The soil block is discretised with three-dimensional solid continuum porous elements C3D8P and modelled as an elasto-plastic material, while C3D8 3D stress non-porous

elements are assigned to pile, which is modelled as linearly elastic material with rigid head. Timoshenko beam elements (B32) with null stiffness (E=1kPa) were constrained to the centre of the pile to effectively obtain the deflection profile along the pile length (Lalicata et.al, 2021). All displacements at the base of the model were restrained, while normal displacements were prevented on the lateral boundaries. At the soil-pile interface interaction is purely frictional with an assumed friction angle, $\delta=\phi'/2$. The pile is wished in place and is initially in geostatic equilibrium with the soil saturated and the water table at the base of the model. For the saturated analysis the pile is then displaced laterally. For the unsaturated analysis a suction of 100 kPa is applied to the soil surface before the lateral pile loading. As observed from Figure 6(b) the soil has a high air entry value (AEV) close to 8MPa, requiring large suctions to generate partial saturation. When combined with $\chi = S_r$ this leads to unreasonably high effective stresses. To provide more reasonable results analyses have been run using lower applied suction values. The response of soil-pile system would depend on the AEV of the soil, applied suction and loading conditions. The effect of hydraulic hysteresis has been ignored in the analysis, as only the main drying path is considered.

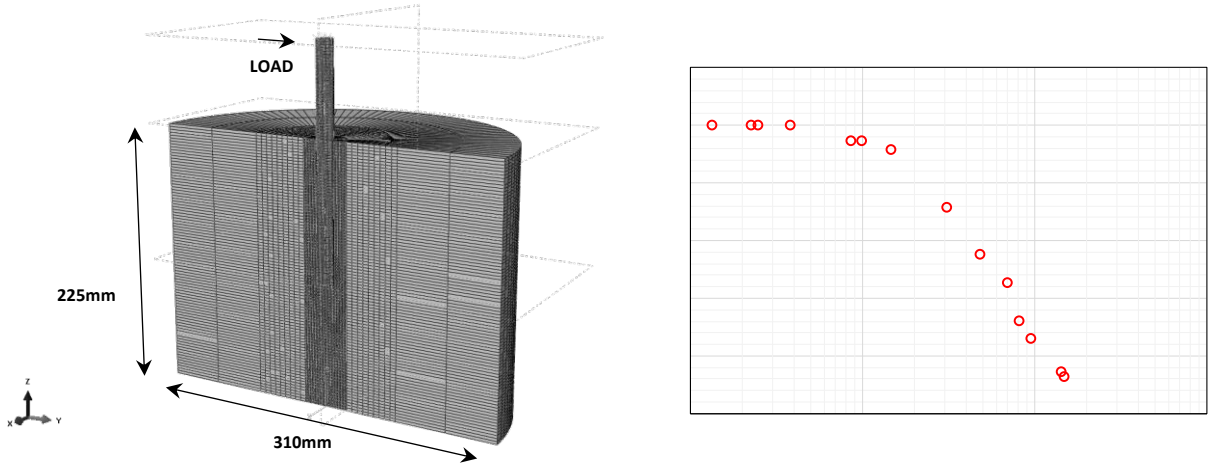

(b

Figure 6: (a) Finite element mesh of the three-dimensional model, (b) SWCC for Western Sydney Clay

3.2 RESULTS

Validation of the saturated model response is achieved by comparing simulation results to the response of pile P_A at time T_1. Since saturated soil state ensures complete contact between the pile shaft and soil, a strength comparable to response at T_1 is expected. Figure 7(a) shows that the numerical simulations significantly overestimate the experimental result, which is believed to be a consequence of not modelling the crack separation between pile and soil. The numerical simulation of the partially saturated soil shows an increase in lateral resistance. This was expected because the suction increases the effective stresses in the soil and hence the stiffness. The effect of suction is not as marked as shown for pile B because only a limited suction was applied. It was also observed that the suction application caused the soil to separate from the pile as a result of the soil shrinkage, and this may have contributed to the relatively small increase in lateral resistance when suction applied. The bending moment (BM) profiles from the simulations are presented in Figure 7(b). With suction application the bending moments increase which is related to the greater soil reaction and resistance to loading.

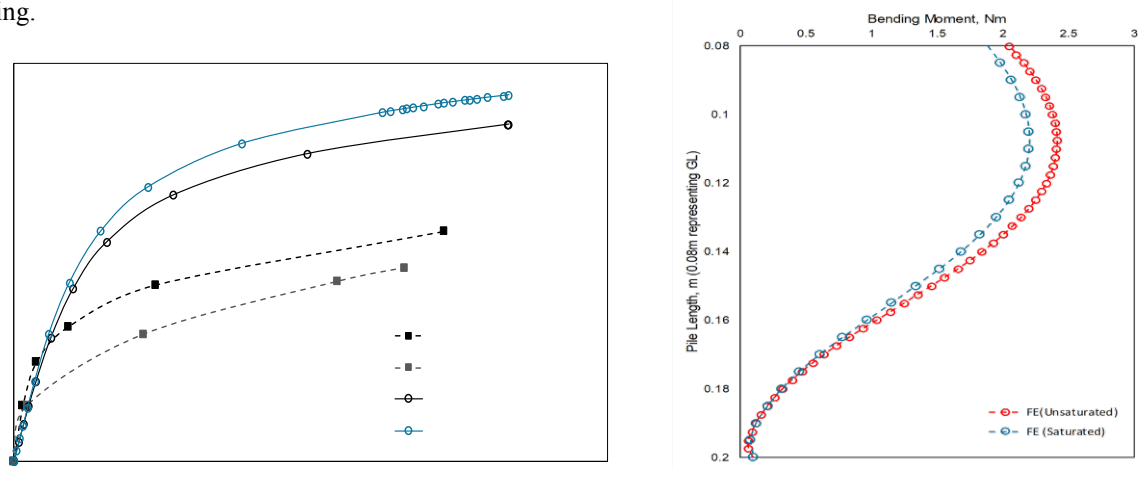

(b

Figure 7: (a) Load-displacement response, (b) BM profile along the length of pile

4 CONCLUSIONS

A series of lateral tests performed on model scale piles embedded in expansive high plasticity clay subjected to cycles of wetting and drying and results are reported. A reduction in pile capacity is observed in the cycle of drying and wetting. Numerical simulations on saturated and unsaturated soil were performed using the built-in framework of ABAQUS to investigate the lateral pile responses. The Cam-Clay model with $\chi = S_r$ formulation and SWCC can capture the stiffness and saturation variations under application of suction and mechanical loading. The simulations showed improved performance of pile-soil system in partially saturated conditions. The response of pile depends on formulation of effective stress parameter χ, applied suction, air entry value of the soil and most importantly on the presence of desiccation cracks. The numerical analyses allowed separation between the pile and soil but did not consider cracks within the soil mass. While the soil strength is expected to increase under the effect of negative pore pressure, the cracks at pile annulus and within the soil could reduce these advantages, making development of cracks under drying crucial in pile performance. Further studies to explore response of piles under cyclic loading conditions under multiple cycles of swell and shrink are necessary. A field study to understand performance of solar farm scale piles is underway in Adelaide. This could bring out effect of response of short piles embedded within the active zone of soil under cycles of loading, where soil is open to changes in moisture content and desiccation cracks.

5 ACKNOWLEDGEMENT

This study was conducted at The University of Sydney, NSW, Australia and was supported by Australian Research Council (ARC) under grant DP220103611. The authors are grateful to ARC for the financial support. The authors are grateful to Mr. Gang Niu for sharing laboratory experimental results.

6 REFERENCES

ABAQUS Theory Manual Version 6.6

Bishop, A.W. (1959). The principle of effective stress, *Teknisk Ukeblad 106 (39), 859-863.*

Burton, G.J., Sheng, D., Airey, D. (2014). Experimental study on volumetric behaviour of Maryland clay and role of degree of saturation. *Can. Geotech. Journal, 51, 1449–1455*

Cameron, D.A., Walsh, P.F. (1983). The timber pile experiment in a swelling clay, *CSIRO Division of Building Research*

Challa, P.K., Poulos, H.G. (1991). Behaviour of single pile in expansive clay, *Geotechnical Engineering (2), 189-216*

Cheng, X., Vanapalli, S.K. (2021) Prediction of the nonlinear behaviour of laterally loaded piles in unsaturated soils. *Comput. Geotech., 140,104480*

Crilly, M.S., Driscoll, R.M.C (2000). The behaviour of lightly loaded piles in swelling ground and implications for their design, *Geotechnical Engineering, 143, 3-16*

Fityus, S.G., Delaney, M.G. (2001). Timber pile foundations for expansive soils, *Australian Geomechanics (46), 3-16*

Georgiadis, K., Potts, D.M., Zdravkovic, L., (2003). The influence of partial soil saturation on pile behaviour, *Geotechnique 53 (1), 11-25.*

Ito, A., Wagai, R., (2017). Global distribution of clay-size minerals on land surface for biogeochemical and climatological studies, *Scientific Data*, 4:170103.

Johnson, L.D., Stroman, W.R. (1984). Vertical behaviour of two 16-year-old drilled shafts in expansive soil, Analysis and Design of Pile Foundations (ed. Meyer), ASCE, 154-173

Kelly, R., Huang, J., Poulos, H.G., Stewart, M. (2021). Geotechnical and structural stochastic analysis of piles solar farm foundations, *Computers and Geotechnics, 132, 103988*

Lalicata, L.M., Rotiscani, G.M., Desideri, A., Casini, F.,(2021). A Numerical model to study the response of piles under lateral loading in unsaturated soils, *Geosciences (12)*

Liu, X., Buzzi, O., Yuan, S., Mendes, J., Fityus, S., (2016). Multi-scale characterisation of retention and shrinkage behaviour of four Australian clayey soils, *Can. Geotech. Journal, 53, 854-870*

Liu, Y., Vanapalli, S.K., (2017). Influence of lateral swelling pressure on the Geotechnical Infrastructure in Expansive Soils, *J. Geotechnical and Geoenvironmental Engineering, ASCE, 143, 6, 04017006*

Mitchell, P.W., (2013). Climate change effects on expansive soil movements, *Proceedings of the 18th International Conference on Soil Mechanics and Geotechnical Engineering, Paris*

Mohamedzein, Y.E.A., Mohamed, M.G., El Sharief, E (1999). Finite element analysis of short piles in expansive soils, *Computers and Geotechnics 24 (3), 231-243*.

Niu, G., (2022). Uplift Resistance of short pile within the expansive soil in solar farm, *Masters Thesis*, University of Sydney

Surjadinata, J., Airey, D., Khoshghalb, A., Hsi, J.,(2021). Challenges for solar farm pile design in reactive soil., *Australian Geomechanics (56), 107-114.*

Wood, D.W., (1990). Soil Behaviour and Critical state soil mechanics, Cambridge University Press, UK.

MATERIAL RE-USE AND IN-SITU STABILISATION OF SAND AND CLAY MIXTURES FOR RAIL FORMATION IN SOUTH-EAST MELBOURNE

Nick Withers[1]
[1]*WSP Australia*

ABSTRACT

As part of the Level Crossing Removal Project in Victoria, Australia, the Southern Program Alliance (SPA) is removing numerous level crossings along the Frankston line in South-East Melbourne. At Parkdale, two level crossings have been removed and replaced with a rail viaduct (rail over road) solution.

The surficial geology of the Parkdale site consists of aeolian sands underlain by sand and clay of the Sandringham Sandstone formation. An important component of rail viaduct solutions is the earthworks associated with backfilling of approach embankments to the viaduct, and the formation earthworks associated with tying into the existing rail network. The SPA implemented an approach to re-use material from large excavations as select backfill for the approach embankments, and proposed lime and cement stabilisation of in-situ materials for rail formation, to attain time, cost and sustainability benefits to the project. This paper summarises key investigation and design considerations of soil compaction and strength behaviour identified in laboratory testing, along with anecdotal construction commentary, to promote the benefits and discuss the challenges of material re-use and stabilisation in large rail infrastructure projects.

1 INTRODUCTION

Since inception in 2017, the Southern Program Alliance (SPA), comprising the Level Crossing Removal Project (LXRP), WSP, Acciona/Coleman Rail, and Metro Trains Melbourne (MTM) has removed 17 level crossings in the South-East suburbs of Melbourne, and are in the detailed design phase of the removal of five additional crossings across wider Melbourne. At Parkdale, the site of the Additional Works Package 6 (AWP6) project, the scope of works for the SPA included replacing level crossings at Warrigal Road and Parkers Road with a rail over road solution, including a rail viaduct spanning approximately 1150m, a new station at Parkdale and other infrastructure including local intersections, parking and paths. The two rail tracks were elevated onto a rail viaduct supported by piers and Continuous Flight Auger (CFA) piles, with the inclusion of L-Shaped reinforced concrete and post and panel wall supported rail embankments, which raise the rail from existing grade level to the rail viaduct. Both Warrigal Road and Parkers Road were rebuilt at existing grade level (underneath the rail viaduct).

As with all rail projects, a significant design and construction element of the project is the rail formation, both in the sense of the material required to be imported into the project to serve as capping and other structural fill layers, and the suitability of the existing underlying material when subjected to rail loading. With rail viaduct solutions, the former consideration is particularly important when considering the typical height, width and grade of compliant rail embankments, as they require large volumes of structural fill with strict performance requirements. Moreover, specific to the Parkdale site, the existing rail network south of the proposed viaduct required upgrade and additional infrastructure, which added approximately 650m of upgrade works to the original SPA scope. When combining this consideration with the significant volume of material required for the proposed rail embankments, and the practical constraints associated with working in a rail corridor, the earthworks component of the project presented a major cost and sustainability item.

This paper presents the methodology undertaken by the SPA to assess the potential to re-use natural soil material generated from large excavations (that were scheduled to be undertaken outside of rail occupation to reduce program risk) as select backfill for the approach embankments, whilst also using lime and cement stabilisation to improve the properties of in-situ materials to be utilised for rail formation, to attain significant time, cost and sustainability benefits to the project.

2 GEOLOGICAL CONTEXT

2.1 GEOLOGY AND HYDROGEOLOGY

The geological conditions at the Parkdale site are typical for that of South-East Melbourne, whereby a thin to intermittent coverage of Quaternary aged aeolian deposits overlie Tertiary aged sediments to significant depths. The geological units at the site are relatively uniform in layering sequence, thickness and strength properties. More specifically, the relevant geological and hydrogeological conditions of the site include:

- Fill (designated Unit 1) of varied composition, but typically less than 0.5m thick.
- Intermittent coverage of Quaternary age aeolian deposits, which are typically a thin layer of fine to medium grained windblown sand. For the purposes of design, this unit was designated as Unit 2A – Quaternary Sands.

- Tertiary Age Sandringham Sandstone Deposits (formerly Brighton Group). The Sandringham Sandstone is often delineated into subdivisions of the Red Bluff Sands and the Black Rock Sandstone.
  - The Red Bluff Sands subdivision of the Sandringham Sandstone is described to be deposited in partly fluviatile and partly near-shore lagoonal environments, comprising carbonaceous sands that generally transition to clayey and silty sands or sandy clays with decreasing depth, where iron staining is not uncommon (Kenvall, from Peck et al, 1992, VandenBerg, 1971). This sub-division was further split for the purposes of design into Unit 3Ai – Upper Red Bluff Clays (typically 2m to 3m thick), Unit 3Aii – Upper Red Bluff Sands (typically 4m to 5m thick) and Unit 3B – Lower Red Bluff Sands.
- The Upper Tertiary aquifer (fluvial) (UTAF), of importance to the overall design, but less so for the earthworks, was typically observed at 7m to 9m below exiting ground level.

The geotechnical investigation at the site included boreholes to varied depths, Cone Penetration Tests (CPT), test pit/shallow auger locations and groundwater monitoring wells, coupled with laboratory testing inclusive of index testing, Oedometer testing and triaxial testing, compaction and California Bearing Ratio (CBR) testing, and dispersivity testing. This investigation and testing allowed each unit to be characterised for engineering design.

2.2 RELEVANT UNITS FOR RAIL FORMATION DESIGN

Whilst the Unit 1 – Fill and Unit 2A sands were somewhat relevant to rail formation design (depending on the thickness and continuity of the materials), the main design unit of interest for rail formation was the Unit 3Ai – Upper Red Bluff Clay as it was more often the natural subgrade material at the proposed basal level of structural fill. The unit generally consisted of a stiff to very stiff, orange-brown and grey sandy clay, with medium to high plasticity fines and fine to medium grained sands. The unit typically either outcrops or directly underlies the Unit 1 or 2 materials. Figure 1 shows the typical particle size distribution (PSD) for Unit 3Ai, with typical Unit 3Aii values for context. Corrected SPT values typically increased with depth, generally correlating with increasing sand content and reducing plasticity within the unit. Typical cone resistance values show good agreement with consistency from SPT correlations. Soil Behaviour Type (SBT) plots from CPT's give insight to the interbedded nature of sands and clay within the unit (varying from clay and silty clays, sands and silty sands). Standard compaction and CBR results within this unit typically range from maximum dry density (MDD) between 1.5t/m^3 and 1.8t/m^3, optimum moisture content (OMC) between 15% and 30%, CBR values of 3% to 6% (lower to upper quartile), and CBR swell between 0 and 2.5%. The heterogenous nature of the material (interbedded sands and clays, although predominantly a sandy clay) was not considered an issue for the subgrade to be considered appropriate to be use as a founding layer for structural fill. However, this heterogeneity would subsequently create complications in the proposed composition of in-situ stabilisation.

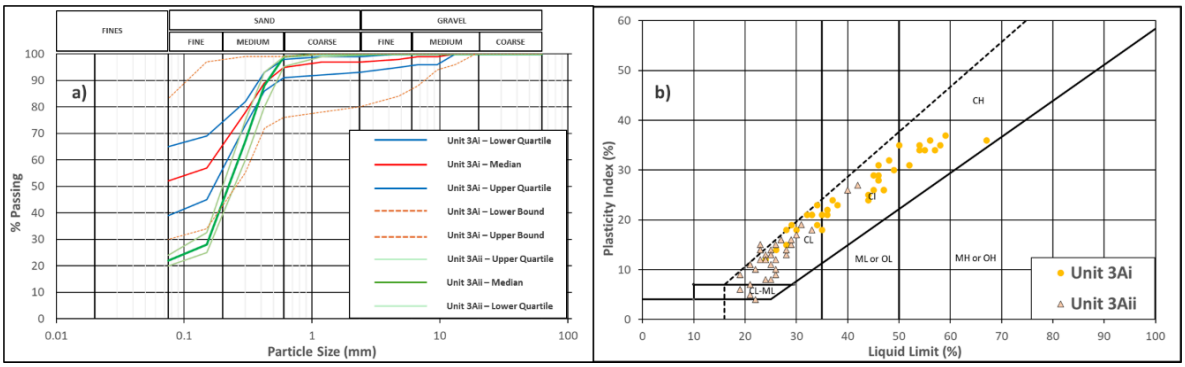

Figure 1: PSD (Figure 1a) and Atterberg Limit (Figure 1b) testing for Unit 3Ai and Unit 3Aii

3 TRACK FORMATION DESIGN

Track formation typically consists of a ballast layer over a capping layer and subsequent structural fill layer (and general fill if required, which is typically of a lower strength and less strict grading criteria to that of structural fill), to distribute the train loading from the rail to the underside of the sleeper and subsequently to the top of the subgrade, to prevent shear failure and excessive settlement under repeated loading. The design bearing pressure is obtained by factoring the subgrade ultimate bearing capacity by a load factor and a settlement factor to arrive at an allowable bearing pressure (design limit) used for design purposes. Whilst undertaken by the designers, the analysis undertaken to assess rail performance (settlement) is not discussed herein.

3.1 SOLUTION AT THE COMPLETION OF DESIGN

As with many rail authority standards, the MTM earthworks and formation specification and standards A1392 and A1537 respectively make use of the CBR of the capping layer, structural fill or subgrade as the primary means for control of load-settlement performance. Other requirements for assessing the materials include providing bounds for particle size, plasticity, material swell, organic content and dispersivity of the proposed fill or subgrade, to ensure that the material has suitable compaction (and potentially permeability) performance, is not prone to significant seasonal movements and is not subject to scour and/or erosion. Of note, the following requirements (amongst others) dictated the design solution for this project:

- For general fill, a soaked CBR of 3% Min (for 4-day soak and 13.5kg surcharge, and at a density ratio of 98% of the MDD at OMC), maximum of 2.5% CBR Swell and a Plasticity Index (PI) of between 9% and 20%;
- For structural fill, a soaked CBR of 8% Min (for 4 day soak and 4.5kg surcharge, and at a density ratio of 100% of the MDD at OMC), maximum of 1.5% CBR Swell, Dry Density of minimum 1.8t/m^3, a maximum PI of 20% and maximum Liquid Limit (LL) of 40%.

With construction input throughout the detailed design process, a solution in general accordance with A1392 and A1537 was proposed such that where the rail formation was to be constructed "at-grade" (i.e. not on fill imported to build up the embankments) and the encountered subgrade was of Unit 3Ai material:

1. Subgrade to be excavated and replaced with structural fill of up to 300mm depth (with standard subgrade preparation details). In this instance, the subgrade will need to comply with the general fill criterion.
2. Placement of 150mm of capping material atop the structural fill.

The general design philosophy for importing general fill into embankments to the underside of structural fill was similar to the "at-grade" solution, noting that the proposed general fill material would be reviewed by the design team prior to use.

3.1.1 Potential Value Add Options Explored

Whilst the design solution already provided cost benefit compared to the tender solution, the SPA queried if a more sustainable and cost-effective solution could be achieved rather than the removal of in-situ material, which would need to be undertaken during rail occupation. Through collaborative meetings between design and construction teams, an option to adopt soil stabilisation was proposed.

Furthermore, the design team reviewed test results from various sites and suppliers, and accompanied the construction team to prospective sites where general fill may have been sourced to fill the embankments. For a variety of reasons, the prospective sites were deemed unsuitable, or added constructability risk to the project. Throughout the discussions between design and construction, the possibility of utilising excavated material from viaduct pile caps, surficial drainage and other miscellaneous structures (which would be progressively excavated and stockpiled outside of rail occupation) was raised. This review led to a change in the proposed imported fill strategy.

3.2 ADOPTED DESIGN SOLUTION

A two-fold design approach was adopted to reduce the amount of material both removed from site and excavated during rail occupation. The approach was as follows:

1. Where rail formation requires construction at grade, and within rail occupation, the subgrade material was to be tested for an appropriate stabilisation technique (i.e. adding lime, cement or both). The intent of this testing was to assess if the existing subgrade could be improved to remove the need for the structural fill layer (i.e. only place 150mm capping atop the improved subgrade). The testing regime required additional site investigation to be undertaken within the rail corridor, with additional laboratory tests to assess the appropriate amounts of lime or cement. Based on the aforementioned plasticity of the material and with reference to industry standards such as AustStab Technical Notes No. 4 and No. 5, it was hypothesised that at a minimum an addition of lime was required to reduce the natural water holding capacity of the soil, followed by additions of cement to gain the additional strength to achieve the CBR required for structural fill in accordance with A1392 and A1537.
2. Where the rail formation is to be built upon rail embankments, site won material, predominantly from pile cap excavations and a newly incorporated civil drainage underground storage tank (UST), was to be utilised as general fill. With all the proposed excavations being undertaken in areas known to penetrate into the Unit 3Ai layer (and potentially into Unit 3Aii), the focus of further assessment was on stockpiles of excavated material and within the extents of the proposed UST excavation.

4 RESULTS OF ADDITIONAL INVESTIGATIONS AND LABORATORY TESTING

4.1 IN-SITU STABILISATION

Without specific guidelines within documents A1392 and A1537, DTP (previously known as VicRoads) test method RC301.04 guidelines for the design CBR and swell values of stabilised existing material were adopted. These standards specify the design CBR and swell values shall be considered as 1/3 and 2 times the values obtained from laboratory testing, respectively. Whilst not explicitly mentioned, it is inferred that a (not *the*) reason for this recommendation is due to the difference in control conditions for mixture heterogeneity (both in terms of sample size and external site conditions) in the field and the laboratory. Therefore, a minimum CBR value of 24% and a maximum swell of 0.75% for the stabilised material was considered as the laboratory test design requirements previously outlined for structural fill.

Laboratory testing utilised Hydrated Lime ($Ca(OH)_2$) and General Purpose (GP) Cement for stabilisers, with mixing and curing times, and also curing temperatures consistent with the recommendations of DTP standards.

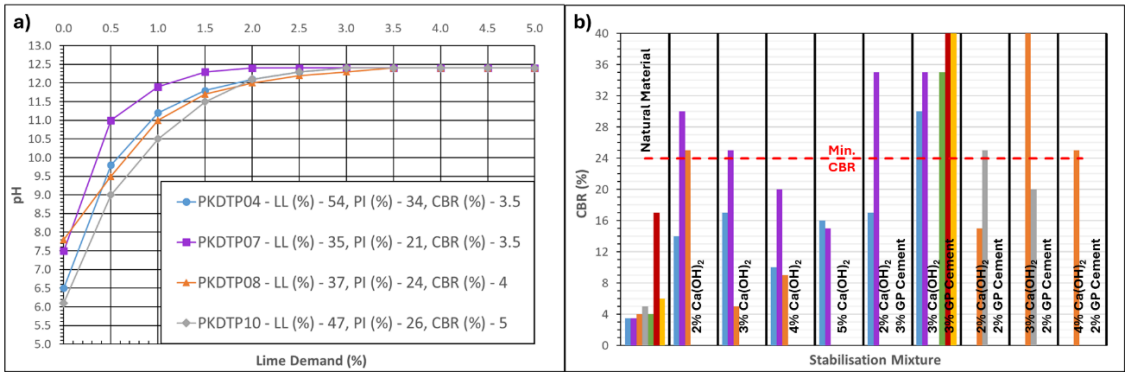

Figure 2: Lime Demand (Figure 2a) and Soaked CBR (Figure 2b) results for stabilisation mixtures.

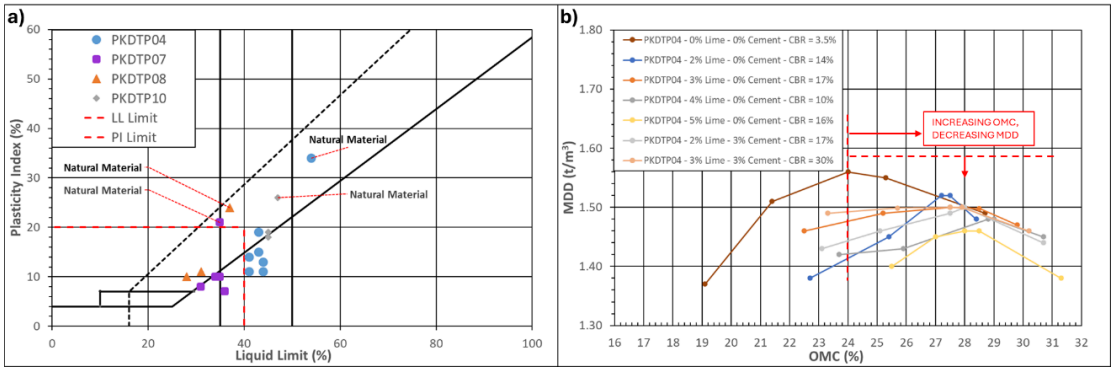

Figure 3: Atterberg limit testing (Figure 3a) and compaction curves (Figure 3b) for stabilisation mixtures.

The initial locations for bulk CBR sampling (allowing for numerous compositions of lime and cement additions to be tested upon the same material) presented a cross-section of the Unit 3Ai material, with material of low, medium and high plasticity tested, and fines content of between 25% and 66%. This variability was also demonstrated in the results of Lime Demand testing, where the results ranged between 1.5% to 3%. Moreover, the compaction curves (an example of one sample location is presented in Figure 3b) demonstrate how the curves become much "flatter" with the addition of Hydrated Lime ($Ca(OH)_2$), with the inference of clay particles becoming flocculated and behaving more in line with that expected of a silt material (Bell, 1996, AustStab, 2010), which is in agreement with standards and published literature. Of note, the OMC was increased from the "natural" result with the addition of lime, coupled with a reduction in MDD. Both of these phenomena typically continued to increase and decrease respectively, with increasing hydrated lime content. A further observation was the reduction in LL and increase in PL, resulting in substantial decreases in the PI of the samples tested (as shown in Figure 3a). The introduction of hydrated lime sparked immediate change in plasticity characteristics for all samples, however unlike for the compaction tests, increasing lime content did not result in significant change in PI following the initial introduction of lime. These observations demonstrate the effect of hydrated lime in reducing the water carrying capacity of the soil, and typically agree with the results of similar published literature such as Bell, 1996.

As expected, using lime stabilisation alone did not provide sufficient improvement of the material in terms of CBR strength, although did provide substantial strength increase. The addition of General Purpose (GP) cement along with

lime, significantly and consistently improved CBR strength, whilst no detrimental change in the compaction characteristics and index properties were observed. Therefore, to achieve the desired CBR strength in accordance with RC 301.04 guidelines, a blend of 3% Hydrated Lime and 3% Medium setting GP cement was proposed as the design solution. Additional sampling and testing from the samples demonstrated in Figure 2a was undertaken to demonstrate the repeatability and consistency of results following the adoption of a proposed stabilisation mixture, as shown within Figure 2b.

Further testing of triaxial tests and uniaxial compressive strength tests were undertaken on the aforementioned samples, however the results of which are proposed to be the topic of a separate paper.

4.2 EXCAVATED MATERIAL RE-USE

Throughout the course of the construction of the rail viaduct, material from pile caps, drainage and other structures was progressively screened and taken to a stockpile area on the site. The site team ensured that unsuitable fill and topsoil, much of which was already removed from site during the construction of a piling hardstand, was separated from the stockpile material. This process resulted in stockpiles of approximately 3 metres high, 8.5 metres wide and greater than 100 metres length, at the time of stockpile investigations. Given the extent of site investigation undertaken at the site, the SPA considered that the stockpiles of site-won material should be suitable for use as general fill. Of importance to the design team however was verification that the stockpiles were relatively homogenous, so that any sampling would be representative of the entire stockpile and were free of organic, foreign or generally unsuitable material.

Investigations in the stockpile confirmed the material to be a mixture of grey sands from Unit 2A (albeit with limited evidence of this material), materials from Unit 3Ai and Unit 3Aii inclusive of ferruginous nodules of medium grained gravel size, as well as inferred hardstand gravel material, which was angular to sub-angular and grey imported fill. Furthermore, investigations at the UST, just south-west of the viaduct alignment encountered a thinner Unit 3Ai layer, which resulted in collected bulk samples being of the Unit 3Aii material, and thus having lower plasticity fines, lesser fines content and higher CBR values than the typical Unit 3Ai material.

Figure 4: Site photographs of stockpiles and excavated test pits within the stockpile (with commentary).

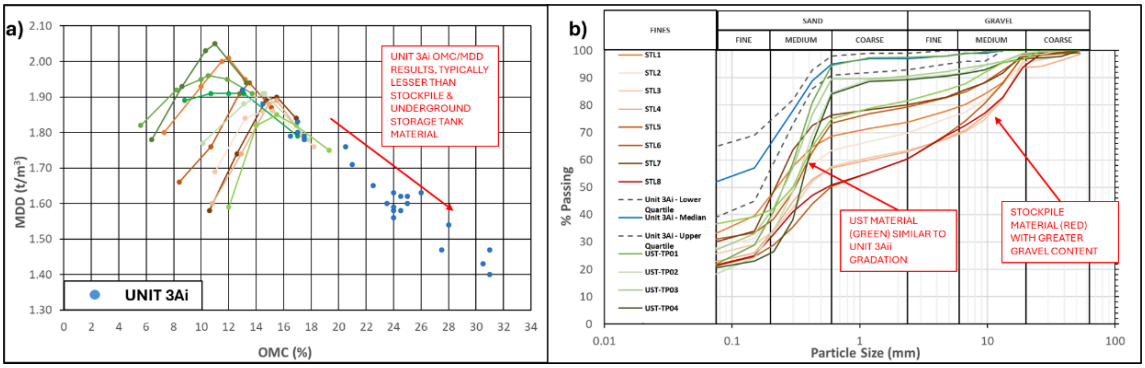

Figure 5: Compaction testing (Figure 5a) and PSD gradings (Figure 5b) of the Stockpile and UST material.

The result of sourcing material from numerous separate excavations, across an alignment of greater than a kilometre, with probable "incidental mixing" through moving and unloading spoil into a stockpile, was that sampled material in the stockpiles represented mixtures of gravel, sand and fines. Subsequently, CBR results and MDD and OMC values are

representative of a more granular material, compared to the typical results of Unit 3Ai. Whilst the material was typically suitable for general fill (and in some instances also suitable for structural fill), it was still considered a risk that sections of the stockpile may have greater proportions of fines and higher plasticity material, and as such the recommendation remained only to utilise the site won material as general fill. Therefore, the 300mm layer of structural fill was still required to be placed atop the finished compacted surface of the placed site-won material within the rail embankments. A minor exceedance of the PI criterion for general fill was also encountered from stockpile material. However, the overall risk of unsatisfactory performance of this material was considered to be low, given the load-settlement characteristics, the confinement of the material within a retaining wall, the overlaying structural fill and capping layers, and suitable track and sub-soil drainage systems. It is also noted that organic matter testing undertaken on stockpile material gave good confidence that the risk of unsuitable material being used as general fill was mitigated.

5 CONSTRUCTION COMMENTARY

Despite the significant design and construction effort to undertake soil stabilisation techniques, inclement weather conditions including rain delays and high winds caused delay in the program which subsequently meant that stabilisation could not be completed within the rail occupation. Much to the disappointment to those who investigated the soil stabilisation proposal, the original proposal of "excavate and replace" was adopted. Whilst considered, tested and thought feasible during the soil stabilisation proposal for Parkdale, the Author recommends others who are considering undertaking soil stabilisation for rail formation under rail occupation to consider the timeframe and contingency required.

The stockpiled material and excavated material from the UST were successfully re-used as intended, with the entire southern approach embankment for the rail viaduct and a portion of the northern embankment filled with general fill sourced from site-won material. Whilst this portion of the scope was a success, the Author would recommend that increased site supervision during the stockpiling process may be prudent for other projects that wish to utilise a similar methodology. An increased supervision at this stage may alleviate some of the potential uncertainty surrounding stockpile heterogeneity.

6 CONCLUSION

The re-use of natural material excavated from shallow excavations across the site to construct rail embankments for the elevated rail viaduct produced significant cost, time and sustainability benefits for the project. Through investigation, supervision of stockpiles and good engineering judgement, the re-use of site won material was undertaken in a compliant and successful manner. Moreover, despite the removal of the in-situ stabilisation scope from the rail formation works at the Parkdale site, the benefit of improving the engineering properties (with respect to compaction) of soil from the Sandringham Sandstone formation, a material that is not typically stabilised in large infrastructure projects, through the addition of lime and cement was shown through extensive laboratory testing.

7 ACKNOWLEDGEMENTS

The author would like to acknowledge WSP colleagues Chandra Balasundrem, Bhupatindra Vaidya, Sutha Visvalingam, Nancy Bower, Jason Ly and Anton Perera for their continued support, mentorship and comradery throughout the project, along with Stuart Colls for the valuable assistance in review of this paper. Moreover, the author would like to thank Matt Gillard, David Moore, Nic Fyfield, Adam Goulding, Stu Smith, Callum Strack and Kobe Davies from SPA for their great inputs, support and feedback on constructability throughout the project. In particular, the Author would like to thank Nic Fyfield for first challenging the alliance to look into alternate solutions, in the pursuit of best for project outcomes.

8 REFERENCES

AustStab.(2010). What is Lime?. Document Number: Technical Note 4. *AustStab Technotes*

AustStab.(2012). Cement Stabilisation Practice. Document Number: Technical Note 5. *AustStab Technotes*

Bell, F. G. (1996). Lime stabilization of clay minerals and soils. *Engineering Geology,* 42, 223-237

Metro Trains Melbourne (MTM).(2023). Earthworks and Formation Specification: A1392. *MTM Controlled Documents: Requirements: Engineering – Track and Civil*, 3.

Metro Trains Melbourne (MTM).(2023). Earthworks and Formation Standard: A1537. *MTM Controlled Documents: Requirements: Engineering – Track and Civil,* 4.

Peck W., Nielson, J., Olds, R., and Seddon, K.. (1992). Brighton Group – Geology. *Engineering geology of Melbourne*. 1, 191-196.

Vandenberg, M. (1971). Explanatory Notes on the Ringwood 1:63 360 Geological Map, *Geological Survey Report*, 1971/1.

VicRoads (2017). Lime Stabilised Earthworks Materials – Available Lime, Assigned CBR and Swell: RC 301.04, *VicRoads Standard documents*

USING PROBABILISTIC SEISMIC HAZARD ANALYSES TO OPTIMIZE GROUND IMPROVEMENT

Ben McKay, Kori Lentfer and Harshad Phadnis
CMW Geosciences

ABSTRACT

As development across New Zealand continues to spread beyond existing city limits, geologically/geotechnically complex development locations are increasingly selected due to their vicinity to existing population centres. One of the major challenges in many of these locations in New Zealand is seismic risk and associated hazards like liquefaction, cyclic softening, seismic instability including flow failure and lateral spreading. Design seismic loading is routinely obtained from national standards or equivalent documents.

A Probabilistic Seismic Hazard Analysis (PSHA) can be performed to provide seismic input including design seismic loads. A PSHA is usually performed for critical infrastructure, rather than for residential or even industrial development.

This paper presents a case study of a residential land development project in Cambridge, New Zealand, where a PSHA was performed based on which the peak ground acceleration for the ULS loading (1-in-500 years event) was reduced from 0.28g to 0.17g. The resultant modelling of the site indicated a significant reduction in calculated lateral spread and slope instability risk, which lead to substantial construction cost savings and reduced carbon emissions associated with the development. This was a critical part of the development design, which ultimately allowed the project to proceed from a feasibility study to construction.

1 INTRODUCTION

Geotechnical earthquake engineering practice in New Zealand has been evolving rapidly over the last few years based on our understanding of earthquake hazard risk following events such as the Canterbury 2010-2011 earthquakes or the Kaikoura 2016 earthquake. These changes have been reflected in various versions of the MBIE/ NZGS Guidelines that are adopted by geotechnical and structural engineers when performing engineering analyses in New Zealand e.g. the Earthquake Geotechnical Engineering Practice. However, the seismic source model and the supporting ground motion model has not been updated since 2004.

This paper examines the role site-specific probabilistic seismic hazard analysis (PSHA) might have when undertaking geotechnical analysis and design for residential or industrial development. PSHAs are usually only performed for critical infrastructure projects in New Zealand due to the associated cost and complexity. This paper presents a case study of a residential subdivision in Cambridge, New Zealand, where geotechnical analysis and design was carried out as per the New Zealand Standards and PSHA-determined seismic loading parameters, and how the seismic loadings from the PSHA affected the ground improvement requirements and the economic feasibility for the development. Some the lessons from this example could be used for other development projects.

The National Seismic Hazard Model (NSHM) presents the likelihood and magnitude of earthquake shaking that is predicted to occur across New Zealand over various return periods based on numerous research studies conducted over the last few years, including key changes to the components of the seismicity rate model and the ground-motion characterisation model. The NSHM represents the latest seismic knowledge for New Zealand and is a fundamental revision of the national seismic hazard model, which was last updated in 2010. The PSHA was performed before the NSHM results were made public in 2022.

2 INTRODUCTION TO PROBABILISTIC SEISMIC HAZARD ANALYSES

A PSHA is a well-accepted method of determining site-specific seismic response and has been used for the last 60 years for real-world applications and design (Bradley et al. 2022). The basic steps of a PSHA were originally proposed by Cornell (1968) and have largely remained the same in the industry, however, the steps can be refined based on the complexity of the project. A PSHA routinely provides the design peak ground acceleration, magnitude and response spectra for various return periods, which are useful to engineers. Deaggregation is also performed to understand scenarios that contribute the most to seismic loads e.g. source-to-site distance, earthquake magnitude.

3 CASE STUDY

3.1 INTRODUCTION TO CASE STUDY AREA

The case study site is located in Cambridge, Waikato and comprises an area of approximately 9.2 Ha.

The pre-development landform, together with associated features located within and adjacent to the site, is presented on Figure 1. Nearly 100 residential lots were proposed to be developed, along with associated local roading and infrastructure. Part of the development included a 8.9m-high road fill embankment connecting the lower and upper terraces, and multiple residential lots over weak alluvial materials adjacent to a modified watercourse.

The site topography is dominated by a relatively level upper terrace at RL60m to RL64m. A steep (approximately 25 to 32 degrees) east-facing natural escarpment extends through the centre of the site. The escarpment bends to become north facing in the southern portion of the site. A lower terrace to the west of the escarpment is located at RL40.0m to RL44.6m.

The eastern side of the site is bound by an existing stream gully system, with a relatively shallow pond located at the base of the gully (<2.0m deep as indicated by survey data). The pond is present due to historical damming of the gully to create the water feature. Details of pond construction are unknown, but its presence is indicated in the earliest historical photographs for the area circa 1939.

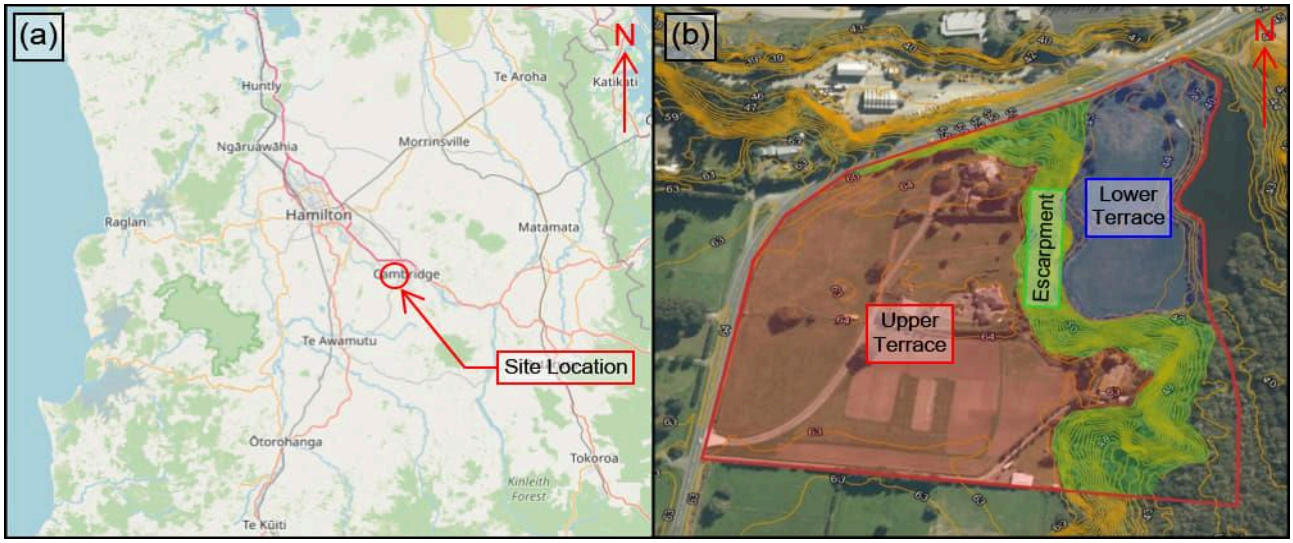

Figure 1: Case study site location (a) and contour data (b) with site area identifications. Basemap imagery sourced from Openstreetmap (2024) and Waikato Regional Council (2024).

3.2 GEOLOGICAL SETTING

3.2.1 Regional Geology

The case study area is within the Hamilton Lowlands, which comprises a wide alluvial plain with multiple low hills, approximately 30-70m above the plain level. Late quaternary volcanic-sourced alluvium forms the bulk of the near-surface material throughout the plain, where pumice-rich sands, silt and gravels have been deposited by the wandering Waipa and Waikato River systems over the last 100,000 years. The early quaternary low hills are comprised of a sequence of tephra beds, alluvial clays and non-welded distal ignimbrites. The Waikato River has slowly cut into the alluvial plain surface on its present-day path for the last 22,000 years. Previous to this, the ancestral Waikato river flowed through the Hauraki Basin (Lowe, 2010).

3.2.2 Site Geology

The local geology map (Edbrooke, 2005) for the case study area depicts the upper terrace as comprising cross-bedded pumice sand, silt and gravel with interbedded peat of the Hinuera Formation (12,000-27,000 years old). Holocene River Deposits (<11,000 years old) consisting of alluvial and colluvial soils are mapped in the lower eastern part of the site. Recent Taupo Pumice Alluvium (14,000-800yrs old) is mapped in the northern-most lower terrace area. Recent peat soils up to 5m thick were present in the southern part of the lower terrace overlain by uncontrolled fill.

3.3 GROUNDWATER TABLE

The regional groundwater table was encountered between RL 43m to RL 40m i.e. approximately 1m to 4m bgl beneath the lower terrace.

3.4 OBSERVATIONAL GROUND MODEL

The observational ground model developed for the subject site is presented in Figure 2 below.

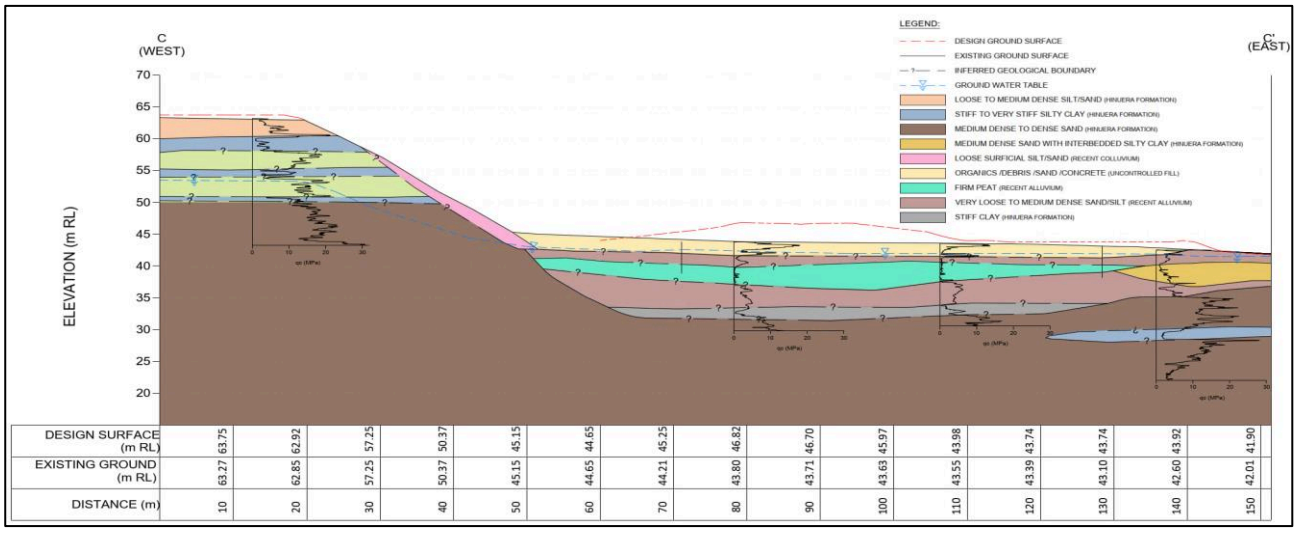

Figure 2: Observational ground model for subject site, including geological units and groundwater layout during prevailing slope conditions.

3.5 ANALYSES AND RECOMMENDATIONS USING NZ STANDARD

Geotechnical design parameters were determined based on field investigation results, local experience, and back analysis of several slope cross-sections modelled under high-ground water conditions.

Initial geotechnical analyses were carried out by CMW Geosciences in 2022 before the NSHM results were made public using Peak Ground Acceleration (PGA) values from MBIE Module 1 (2021). The Importance Level for the proposed residential development was IL2. PGA values for the serviceability (SLS1) and ultimate (ULS) limit states were 0.07g and 0.28g respectively.

The geotechnical analyses methods, findings and resultant recommendations using the MBIE Module 1 derived PGA values are outlined in Table 1. Note that temporary surcharge filling was placed and monitored to mitigate static settlement within the peat and uncontrolled fill.

Table 1: Geotechnical Analyses, Findings and Recommendations based on MBIE Module 1 PGA Values

Analysis Type	Software, Methods and Assumptions	Findings	Recommendations
Liquefaction-induced ground deformations	• Geologismiki CLiq software (V3.3.3.2) • Boulanger and Idriss (2014) method • Idriss and Boulanger (2008) clay like behaviour • Fines according to Robertson and Wride (1998) • Settlements according to Zhang et al (2002) • N_{kt} of 12	<u>Upper Terrace</u>: • <5mm settlement under SLS1 and ULS loading. • Negligible lateral spread risk.	• No further design actions required for residential development. • TC1 site classification.
		<u>Lower Terrace</u>: • <5mm settlement under SLS1 conditions. • 5-150mm settlement under ULS loading. • Widespread liquefaction triggering and lateral spread risk.	• Ground improvement (either anchored ultra-high strength geotextile or continuous flight auger piles/deep soil mixing) required to control lateral spread. • Hybrid TC2/TC3 foundations required for each dwelling.
Slope Stability	• RocScience Slide2 software used • Morgenstern-Price (1965) method, circular and translational slip surfaces • Newmark sliding block (1965) analysis for slope displacement magnitude	• Factor of Safety (FoS) under ULS seismic load between 0.2-0.8 across escarpment. • Lateral movement calculated at 50-200mm within 10m of escarpment	• Building restriction zone (BRZ) of 10m from escarpment crest and toe.

3.6 DRIVERS FOR PSHA APPLICATION

Following the analysis and recommendations made for the lower terrace, a cost/benefit analysis of multiple options was carried out by the CMW project team. These indicated that the lowest cost option for development of the lower terrace would be to install ultra-high strength geotextile to control lateral spread of the lower terrace, and then all residential structures would require hybrid TC2/TC3 foundations to sustain liquefaction-induced vertical settlements as per the Canterbury Earthquake Guidance which is widely used throughout New Zealand.

Due to the design levels of the proposed infrastructure which were governed by existing council infrastructure at lower levels, and the proposed fill levels, it was only going to be possible to place a single layer of geotextile, with a required strength of 1400 kN. A specialty PET-based woven reinforcement geotextile that would be suitable was identified, however the cost to manufacture and ship the material on site was anticipated to exceed NZD$2.2M. The anticipated cost for contractor labour and geotextile anchorage was to be a minimum of ~NZD$1.0M, in addition to the material cost.

Other practical challenges related to using a high-strength geotextile were identified. These included clashes with future hybrid TC2/TC3 foundations for residential structures, fabric tensioning issues due to consolidation of peat materials, and service penetrations, which included concerns about future serviceability of any lines penetrating the geotextile.

The combined financial factors and construction complexity indicated that the lower terrace would be very expensive to develop, whilst also significantly increasing the developer's exposure to construction risk. Accordingly, a sensitivity analysis was undertaken to determine how much liquefaction triggering could be expected for different PGA values at the site. This was supported by CMW's past experience in the region, where reduced ULS PGA seismic loads were calculated for other sites based on PSHA's.

Significant reductions in liquefaction triggering over the lower terrace could be expected when PGA values under 0.20g were used in analyses, which would lead to reduced ground improvement requirements. A PSHA was recommended at this point, as it was recognised there was potential to have a significant impact on the economic feasibility of the development and to reduce construction risk.

3.7 PSHA FINDINGS

A PSHA was carried out for the subject site by CMW Geosciences using the McVerry 2006 ground motion model, which indicated that the site-specific PGA for the IL2 SLS1 and ULS seismic design events were 0.05g and 0.17g respectively. The PSHA was reviewed by an external peer reviewer. Note that MBIE Module 1 (2021) guideline recommends the design ULS PGA should not be less than 0.19g. A sensitivity analysis showed that using either 0.17g or 0.19g had the same design outcome i.e. design recommendations in Table 2 could sustain both 0.17g and 0.19g ULS loads.

3.8 ANALYSES AND RECOMMENDATIONS USING PSHA PARAMETERS

Geotechnical analyses for the site were re-performed with the alternative SLS1 and ULS PGA values as per Section 3.6. The geotechnical analyses methods and assumptions were consistent with those outlined in Table 1. The findings and resultant recommendations are outlined in Table 2.

Table 2: Geotechnical Analyses, Findings and Recommendations based on PSHA-derived PGA Values

Analysis Type	Findings	Recommendations
Liquefaction-induced ground deformations	Upper Terrace: • <5mm settlement under SLS1 and ULS loading. • Negligible lateral spread risk.	• No further design actions required for residential development. • TC1 site classification (MBIE, 2012).
	Lower Terrace: • <5mm settlement under SLS1 conditions. • <25mm settlement under ULS loading for all lots with exception of one lot. • Sensitivity analysis performed by varying PGA values. • Isolated liquefaction triggering. Lateral spread risk is low.	• No ground improvement required to mitigate lateral spread risk. • All lots within limits for TC1 site classification with exception of one lot, which required hybrid TC2/TC3 foundations (MBIE, 2015).
Slope Stability	• Factor of Safety (FoS) under ULS seismic load >1.4 across escarpment. • Lateral movement calculated at <10mm within 10m of escarpment	• BRZ of 10m from escarpment crest maintained. BRZ at toe of slope removed.

4 DISCUSSION

4.1 CASE STUDY DISCUSSION

The PSHA indicated a lower design PGA for the SLS1 and ULS cases for the subject site, which reduced the assessed liquefaction susceptibility at the site. Liquefaction-induced vertical settlements due to liquefaction triggering was <25mm in all but one of the lots on the lower terrace in the ULS case. The significantly reduced liquefaction mitigation for these lots meant that the land was less costly and more feasible to develop.

Lateral spread risk over the lower terrace was assessed to be negligible as liquefaction triggering was anticipated to occur in thin, laterally discontinuous bands in the ULS case. As a result, costly lateral spread mitigation was not required.

With acceptable Factors of Safety calculated for the toe of the slope in the static and ULS seismic case, and only minor shallow movement expected on the existing escarpment, it was deemed appropriate to optimise the building restriction zone at the toe of the slope. The building restriction zone of 10m from the escarpment crest was maintained. This meant that the lots had additional area along the toe of the slope that was suitable for development without the need for specific analyses and design by a geotechnical engineer, thus reducing development cost and increasing flexibility in land use.

A part of the southern end of the lower terrace was still prone to some liquefaction effects in the ULS case. This area contained a single residential lot and the road embankment between the upper and lower terrace. A hybrid TC2/TC3 foundation was recommended for this residential lot. The road embankment was to be vested with the local council, and the requirements for a non-critical road embankment as per the Bridge Manual were achieved without the use of any geotextile. See Figure 3 for an illustration of the reduction in ground improvements under the reduced seismic loading.

All of the above lead to positive financial and programme impacts including reduced earthworks and construction scope, reduced construction materials required to develop the site, less material handling issues, shorter timeframes to construct the development, and overall less construction cost. Environmental benefits included a reduction of embodied carbon to develop the land due to reduced material requirements as well as associated reduced transportation costs.

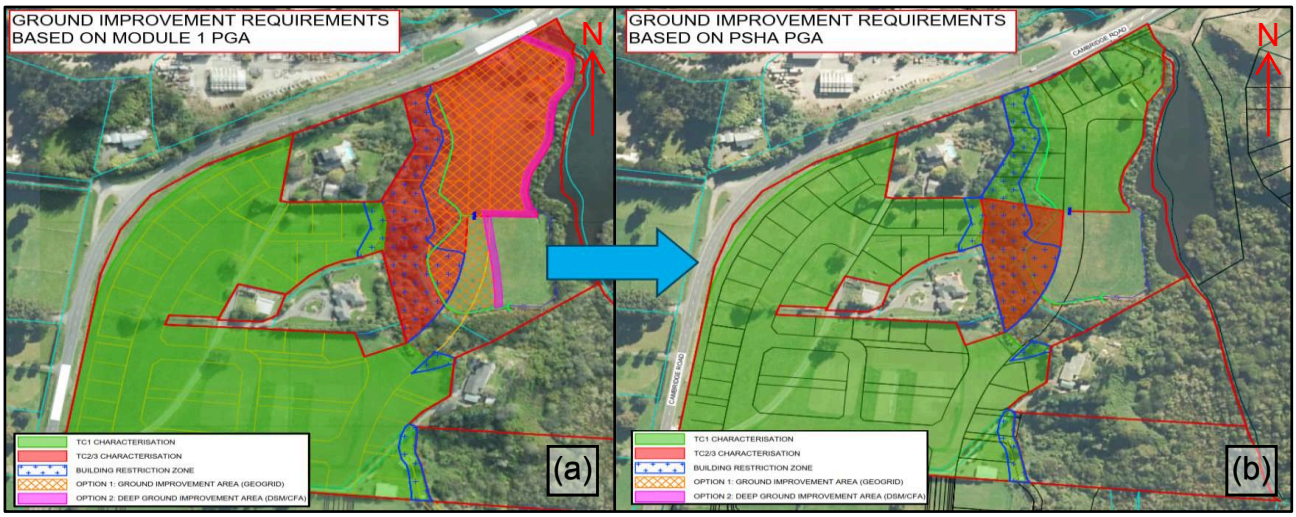

Figure 3: Ground improvement requirements for the case study area with PGAs from the (a) Module 1 guidance document and the (b) PSHA.

4.2 DISCUSSION RELATING TO NSHM UPDATE

In 2022, GNS released the NSHM for public access. The NSHM was also the basis for the recently released draft TS1170.5 'Structural design actions: Part 5: Earthquake actions – New Zealand'. The TS1170.5 document will be codified no earlier than 2027. Given these updates, a question arises regarding the usefulness of a site specific PSHA. Following the NSHM release a PSHA is less likely to be beneficial for residential development (IL2) projects in general. It is important to note that the PSHA provided benefit for the proposed development because the PSHA was carried out by CMW Geosciences before the NSHM results were made public in 2022. Refer to Table 3 below for design PGA loads for NZGS Module 1, the NSHM & the subject PSHA.

Table 3: PGA based on Specification Document or Analysis

Document/Analysis	SLS1 PGA (g) and Magnitude (M)	ULS PGA (g) and Magnitude (M)
NZGS Module 1	0.07, 5.9M	0.28, 5.9M
NSHM	0.04, 6.7M	0.20, 7.0M
PSHA	0.05, 6.5M	0.17, 5.8M

A PSHA is still likely to be beneficial to critical projects (IL3 to IL5) or when the site-specific hazard is sought e.g. to account for surficial soil response or when other intensity measures are required e.g. significant duration of shaking, PGV, Arias intensity, etc. A PSHA also provides useful information to support a non-linear structural analysis by providing site-specific response spectrum as well as deaggregation results by fault, magnitude, distance, directivity, etc. This results in better understanding of the seismic sources which dominate the seismic hazard, and which can be used to provide a suite of ground motions. For more critical projects particularly IL4 or IL5 structures, the steps in the PSHA following the Cornell 1968 method can also be refined, however this is likely to require involvement of geotechnical engineers, geologists and seismologists, and will then have to be peer reviewed.

5 CONCLUSIONS

This paper presents a case study of a residential subdivision in the Waikato region, where a PSHA indicated a lower design SLS1 and ULS PGA for the subject site which reduced the assessed liquefaction susceptibility at the site. The lowered design PGA resulted in reduced ground improvement saving the project millions of dollars, programme time, and had environmental benefits including a reduction in the materials and transport costs required to develop the site.

6 REFERENCES

Boulanger R. and Idriss, I. (2014). *CPT and SPT Based Liquefaction Triggering Procedures*, Report No. UCD/CMG–14/01, Dept. of Civil & Environmental Engineering, University of California at Davis.

Bradley, B., Cubrinovski, M., and Wentz, F. (2022). Probabilistic seismic hazard analysis of peak ground acceleration for major regional New Zealand locations. *Bulletin of the New Zealand Society for Earthquake Engineering,* 55(1), 15-24.

Cornell, C.A. (1968). Engineering Seismic Risk Analysis, *Bulletin of the Seismological Society of America*. Vol. 58, No. 5, 1583–1606.

Edbrooke, S. (2005). *Geology of the Waikato area: Scale 1:250 000*. Institute of Geological and Nuclear Sciences Limited, Geological Map 4.

Idriss, I.M. and Boulanger R.W. (2008). Soil Liquefaction during Earthquakes. MNO–12, Earthquake Engineering Research Institute.

Lowe, D.J. (2010). *Introduction to the landscapes and soils of the Hamilton Basin*. In: Lowe, D.J.; Neall, V.E., Hedley, M; Clothier, B.; Mackay, A. 2010. Guidebook for Pre-conference North Island, New Zealand 'Volcanoes to Oceans' field tour (27- 30 July). 19th World Soils Congress, International Union of Soil Sciences, Brisbane. *Soil and Earth Sciences Occasional Publication*, 3, Massey University, Palmerston North.

McVerry, G. H., J. X. Zhao, N. A. Abrahamson, and P. G. Somerville (2006). New Zealand acceleration response spectrum attenuation relations for crustal and subduction zone earthquakes, *Bulletin of the New Zealand Society for Earthquake Engineering*. 39, no. 1, 1–58.

Ministry of Business, Innovation & Employment (2021). Earthquake Geotechnical Engineering Practice – Module 1: Overview of the Guidelines, *Earthquake Geotechnical Engineering Practice Series*.

Morgenstern, N. and Price, V. (1965). The Analysis of the Stability of General Slip Surfaces. *Géotechnique*, 15, 79-93.

Newmark, N. (1965). Effects of earthquakes on dams and embankments. *Géotechnique*, 15(2), 139–160.

Robertson, P.K. and Wride, C.E. (1998). *Evaluating Cyclic Liquefaction Potential Using the Cone Penetration Test*. Canadian Geotechnical Journal, 35, 442–459.

Waka Kotahi NZ Transport Agency. (2022). *Bridge Manual*, Third Edition, Amendment 4.

Zhang, G., Robertson, P., and Brachman, R. (2002). Estimating Liquefaction-induced Ground Settlements from CPT for Level Ground. *Canadian Geotechnical Journal*, 39, 1168–80.

THE APPLICATION OF 3D FINITE ELEMENT METHOD IN THE ANALYSIS OF SLOPES UNDER EXTERNAL LOADS

Aria Moradshahi[1], and Kaveh Ranjbar Pouya[1]
[1] FSG Geotechnics & Foundations, Melbourne, Australia

ABSTRACT

The majority of slope stability assessments in geotechnical engineering practice are typically carried out using two-dimensional plane strain analyses. However, there are instances where the results from 2D plane strain and 3D analyses can significantly differ. One such scenario arises when a slope is subjected to concentrated external surcharges, such as those exerted by cranes, piling rigs, and other construction equipment. A common practice is to convert these concentrated surcharges into equivalent infinite strip loads for analysis in a 2D plane strain context. While historically regarded as a conservative approach, the suitability of this conservatism can be questioned from a design standpoint. This paper presents a comprehensive parametric study comparing 2D and 3D slope stability analyses, focusing on factors such as surcharge loading magnitude, configuration (dimension and offset), slope angle, and width of the slope mechanism. The analyses utilise the elastoplastic finite element method employing the strength reduction technique. Comparisons are made in terms of safety factors, shear failure mechanisms, and deformation behaviour. The results underscore the significance of employing 3D FEM analysis for slopes experiencing highly concentrated surcharge loads, particularly those associated with crane lifting operations. Furthermore, it was demonstrated that in scenarios involving such concentrated loads, stress distributions and potential failure mechanisms could be complex and are better evaluated within a 3D FEM framework. This approach leads to an optimised design solution without compromising safety, especially in construction operations adjacent to existing slopes.

1 INTRODUCTION

Slope stability is a critical aspect of geotechnical engineering, influencing the safety and design of various structures. Traditionally, the assessment of slope stability has relied on 2D plane strain analyses. While effective in many scenarios, 2D analyses can fall short when addressing complex loading conditions, such as concentrated external surcharges from construction equipment. These loads are often converted into equivalent strip loads (e.g. CIRIA), a simplification that may not fully capture the three-dimensional nature of the problem. It should be noted that although the CIRIA guidance is specifically for embedded retaining walls, it is common practice in the industry to apply reduction factors based on CIRIA for plane strain analysis, due to the lack of other comprehensive references. This paper explores the application of 3D Finite Element Method (FEM) in slope stability analysis under external loads, emphasising the benefits over traditional 2D analyses in terms of accuracy in stress distribution and failure mechanism prediction. The reliance on 2D plane strain analyses in geotechnical engineering is primarily due to their ease of use and lower computational demands and commercial constraints. However, these methods often fail to accurately reflect the real-world conditions of slopes under complex loading scenarios. Research has shown that 3D analyses can provide more accurate assessments of slope stability, particularly when dealing with irregular load distributions and geometries (e.g., Baligh and Azzouz, 1975). Unlike 2D models, 3D FEM can account for spatial variations in load distribution, soil properties, and slope geometry, providing a more realistic assessment. This is particularly important for scenarios involving heavy construction equipment, where the loads are highly localised and can significantly impact the stability of the slope. In these situations, three-dimensional analyses may be warranted.

2 COMPARATIVE ANALYSIS OF SLOPE STABILITY UNDER SELF-WEIGHT

Consider a simple slope with a height of 9.0 m and an angle of 33.0°, as illustrated in Figure 1. The soil has a unit weight of 20 kN/m³, a friction angle of 28.0°, and a cohesion of 15 kPa. For slopes with regular geometry and uniform soil properties, 3D FEM analysis using PLAXIS typically identifies a failure mechanism similar to that of an infinite slope under plane strain conditions. However, other methods, such as 3D Limit Equilibrium Method (LEM), are sensitive to the model boundaries. Studies like those by Griffiths and Marquez (2007) indicate that depending on the model's dimensions parallel to the slope, a distinct 3D failure mechanism may emerge from a circular search in 3D LEM, which can significantly differ from the failure mechanism assumed for slopes infinitely long in the direction perpendicular to the plane of interest. In this study, we use Strength Reduction Method (SRM) within a 3D FEM framework, making the model boundaries less critical.

The results from FEM using the strength reduction technique are highly sensitive to mesh design and its density. To ensure an accurate comparison between 3D and 2D analyses of locally loaded slopes, we validated the mesh size by matching the FOS for slopes under self-weight in both 2D and 3D. This approach minimises the influence of mesh density

in all subsequent parametric analyses. The below figure compares the incremental shear strain contours from 2D and 3D analyses.

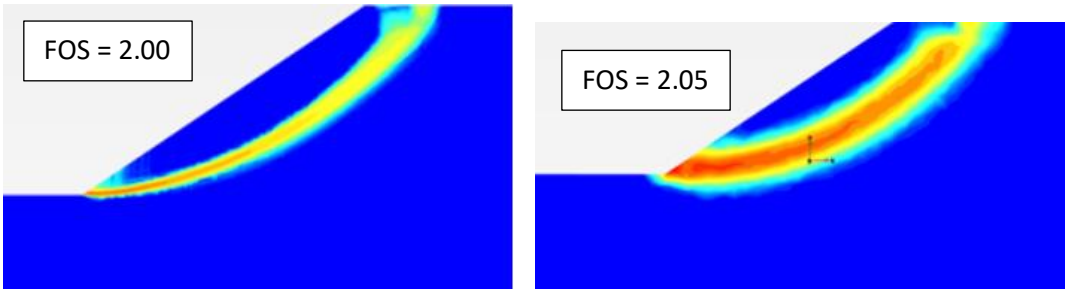

(a) **(b)**

Figure 1: Incremental shear strain contours for a slope under its self-weight (a) FEM 2D; and (b) FEM 3D

As shown above, under self-weight conditions, the FOS derived from both 2D and 3D analyses is nearly identical in terms of the calculated FOS and the identified failure mechanism (critical slip surface in 2D and critical soil mass in 3D).

3 STABILITY ANALYSIS FOR A LOCALLY LOADED SLOPE

3.1 APPROPRIATENESS OF 2D PLANE STRAIN ANALYSIS

Baligh et al. (1975) identified two failure modes for slopes under surcharge loads: (a) Bearing capacity failure, where the shear surface is confined near the load and doesn't intersect the slope, and (b) Slope failure, where the critical shear surface extends beyond the crest, involving part of the slope. Most 3D slope stability analyses in the literature focus on 3D effects, soil strength heterogeneity, boundary conditions, and complex geometries (Griffiths and Marquez 2007; Li et al. 2009, 2010). However, the impact of concentrated loads on 3D slope stability has not been extensively investigated.

3.2 COMMON INDUSTRY PRACTICE

In practice, 2D plane strain analysis is often used due to its simplicity and efficiency for slope stability assessments. When a slope experiences a concentrated, localised load, designers often use reduction factors to account for 3D effects on slope stability. These factors, typically based on experience or engineering judgment, commonly range from 0.7 to 0.67. Alternatively, some refer to the reduction factors provided in CIRIA guidelines to account for load dimensions and offset to the crest of the slope. These reduction factors are intended to prevent over-design and excessive conservatism when assessing the stability of a slope under concentrated loads coming from footings or construction plants such as outriggers, crawler cranes, or piling rigs. However, in the authors' view, these reduction factors are specifically tailored for the design of retaining walls rather than for slope stability assessments. A primary objective of this study is to assess the appropriateness of these reduction factors for slope stability analysis through 3D FEM analysis. According to CIRIA, surcharges of limited extent can be represented as equivalent infinite strip loads, as presented below:

$$Q_L = Q_C/(2A + L) \quad (1)$$

where, *Qc* is the concentrated load (kN), *QL* is the equivalent line load (kN/m), *A* is the minimum distance of the loaded area from the wall, and *L* is the lateral extent of the loaded area, which in the case of a point load will be zero. Based on Figure 2, a concentrated load (Q_c) spreads outward at a 45-degree angle as it intersects the slope. This spreading increases the load's effective width from *L* to *L+2A*, accounting for the additional width gained on both sides. This assumption provides a simplified yet conservative estimate of the load's impact on slope stability.

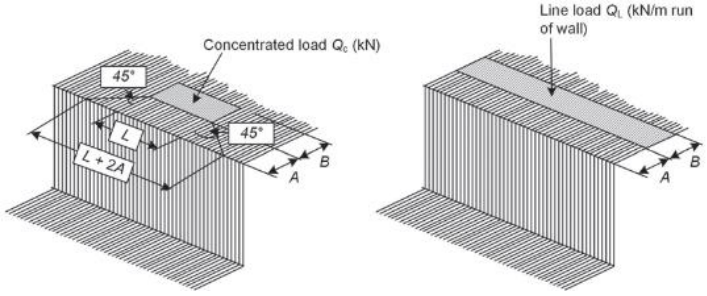

Figure 2: Concentrated and line load surcharges (from Williams and Waite, 1993)

3.3 PARAMETRIC STUDY

The parametric study involved a comprehensive assessment to evaluate the accuracy and applicability of load reduction factors derived using the CIRIA method. Initially, a 3D Finite Element (FE) analysis was conducted, incorporating a concentrated load on the slope to establish a baseline for stress distribution and failure mechanisms. The soil properties are the same as those indicated in Section 2. To achieve this objective, we considered a track load with dimensions of 11 m x 2 m and a load intensity of 200 kPa, which is representative of typical crane loads operating in Australia. Subsequently, a corresponding 2D FE analysis was performed using identical geometric parameters, with the primary aim of calibrating the load reduction factor necessary to align the 2D results with those from the 3D analysis. This calibration process enabled a direct comparison between the CIRIA-derived reduction factor and the factor obtained from the calibrated FE analysis. The procedure was systematically applied to investigate the effects of varying slope height-to-load width ratios, different load offsets, and varying slope angles. Figure 3 shows the schematic of 3D and 2D geometries considered in this analysis.

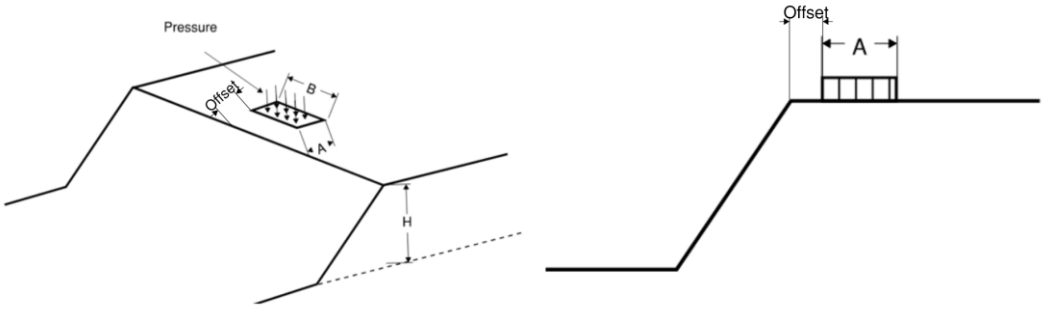

(a) **(b)**

Figure 3: (a) Schematic diagram of the 3D; and (b) 2D FE analysis

3.3.1 Effect of slope height to load width ratio (H/B)

The effect of different slope heights to load length parallel to the slope ratio (H/B) on the global stability of the slope was investigated for four different ratios: 0.2, 0.4, 0.6, and 0.8. In this analysis, the load track dimension was assumed to be 2 m by 11 m, with B = 11 m. Two different offsets, 1 m and 4 m were used in both 2D and 3D analyses to better compare the impact of localised loads in 2D and 3D.

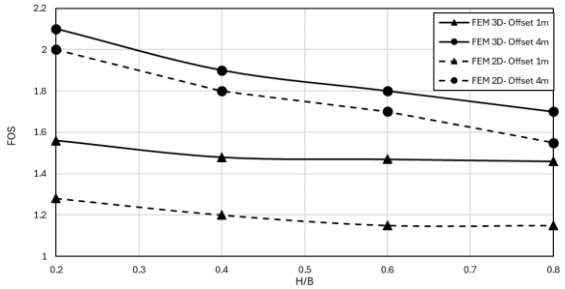

Figure 4: Effect of slope height to load width ratio on the global stability

Figure 4 shows the influence of the H/B ratio on the FOS for both 2D and 3D FEM analyses at offsets of 1 m and 4 m. The results indicate that the FOS decreases as the H/B ratio increases, demonstrating that slopes with greater heights (relative to load length) exhibit reduced stability

The 3D FEM analysis consistently shows higher FOS values compared to the 2D analysis, regardless of the offset, indicating that 3D analysis provides a more comprehensive understanding of the slope's stability under localised loads. The difference between 2D and 3D results is more pronounced at smaller H/B ratios, highlighting the limitations of 2D analysis in scenarios involving slopes with greater heights with concentrated loads.

Comparing the two offsets, the achieved FOS is generally higher for the 4 m offset in both 2D and 3D analyses, indicating that increased distance between the load and the slope crest improves stability. However, the gap between 2D and 3D results narrows as the offset increases, suggesting that for larger offsets, 2D analysis becomes more conservative but still

less reliable than 3D analysis. However, both FEM models show that the collapse of a slope involves a combination of both translational and rotational failure mechanisms.

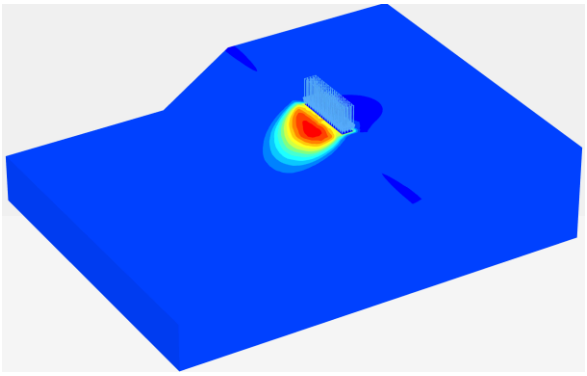

Figure 5: Critical soil mass from 3D FE model for H= 9 m and offset of 1 m

3.3.2 Effect of offset

The effect of the offset of the edge of the tack to the crest of the slope has been investigated for four different offsets of 1 m, 2.5 m, 4 m, and 5.5 m. For each of these offsets, two methods have been considered:

a) Calculating the reduction factor based on CIRIA (Equation 1)
b) Calibrating the reduction factor required for 2D FEM analysis based on FEM 3D analysis using a concentrated load

Figure 6a highlights that the CIRIA reduction factors are notably more conservative for smaller offsets, showing significantly higher values compared to the FEM-calibrated factors. However, as the offset increases, the CIRIA reduction factors gradually converge towards the FEM-calibrated values. Additionally, comparing the two different height-to-width ratios (H/B = 0.6 and H/B = 0.4), it can be observed that for smaller offsets, larger slope heights require higher reduction factors, emphasising the importance of considering slope geometry in load reduction.

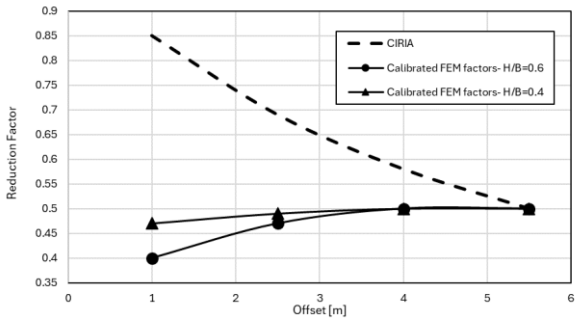

(a)

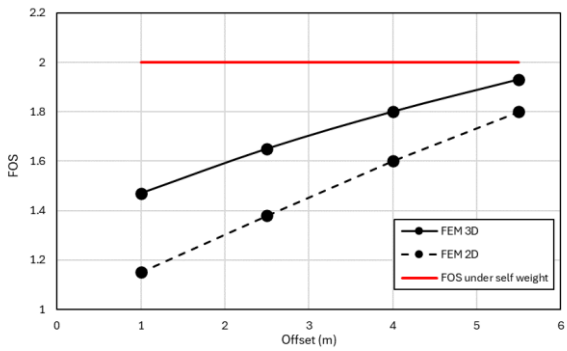

(b)

Figure 6: Effect of offset on (a) FEM and CIRIA calibrated reduction factors; and (b) derived FOS from FEM 3D and FEM 2D with consideration of CIRIA reduction factors

Figure 6b illustrates how the FOS is influenced by offset distance for both 2D and 3D FEM analyses. The solid line represents the 3D FEM results, while the dashed line shows the 2D FEM results. As the offset increases, the FOS is also observed to rise in both cases, indicating improved slope stability. However, the 3D FEM consistently provides higher FOS values than the 2D FEM, emphasising the limitations of 2D analysis and the importance of 3D analysis for a more accurate assessment, particularly under localised loading conditions. Once a concentrated load is applied to the top of the slope, the failure mode may shift from 2D to 3D. This load should be substantial compared to the weight of a soil mass that could be mobilised under the self-weight of the slope. In contrast, a small load applied at a distance from the slope, such as from a footing or outrigger load, might only cause a local bearing capacity failure and should be differentiated from the case of a locally loaded slope.

3.3.3 Effect of slope angle

Three different slope angles of 1H:1V, 1.5H:1V, and 2H:1V were considered for an offset of 2 m and H/B of 0.6 to compare:

a) Reduction factors calculated using CIRIA and reduction factors calibrated for performing 2D FEM analysis based on 3D FEM analysis to ensure similar FOS values between 2D and 3D FEM analyses.
b) The FOS for 2D FEM analysis based on CIRIA reduction factors and 3D FEM analysis.

Figure 5 shows the relationship between the FOS and reduction factors with the load aspect ratio (A/B) for slopes with various angles. B is the length parallel to the slope, while A is the length perpendicular to the slope.

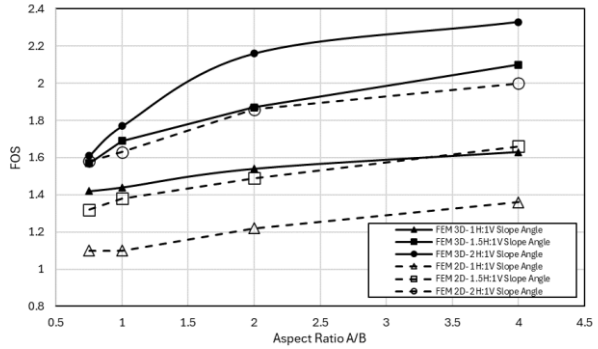

(a)

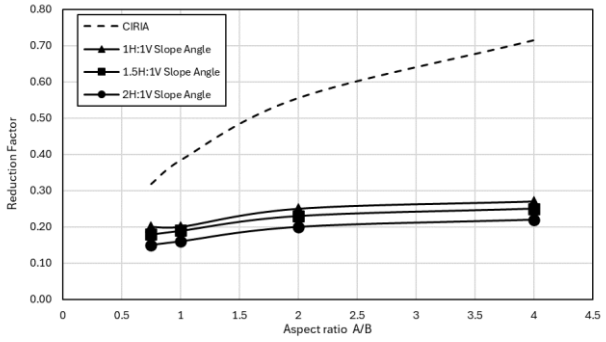

(b)

Figure 7: Effect of angle slope on (a) FEM calibrated reduction factors; and (b) derived FOS from FEM 3D and FEM 2D with consideration of CIRIA reduction factors

Figure 7(a) compares the reduction factors calculated using CIRIA methods with those calibrated for the 2D FE model based on the 3D FE model. As shown in this figure, CIRIA reduction factors are significantly higher than those derived from the 2D FE model, indicating that the CIRIA method produces more conservative results. Additionally, lower reduction factors are required for gentler soil slopes, suggesting that the CIRIA method may be overly conservative in these cases. For larger aspect ratios, the gap between the calibrated reduction factors and CIRIA reduction factors increases, highlighting that the CIRIA reduction factors become less reliable for larger load aspect ratios.

Figure 7(b) shows the relationship between the FOS and the aspect ratio for slopes with varying angles. Solid lines represent 3D FEM analyses, while dashed lines depict 2D FEM analyses. The 3D FEM analysis consistently predicts

higher FOS values compared to 2D FEM, emphasising the importance of 3D modelling for accurate assessments, especially under localised loading conditions. Additionally, steeper slopes require higher load aspect ratios to maintain a stable FOS, indicating that a wider base is essential for stability in such cases.

4 CONCLUSION

This study underscores the importance of using 3D FEM analyses in evaluating slope stability under concentrated external loads, such as those from cranes and piling rigs. Through a series of parametric studies, it is evident that 3D analyses offer more realistic assessments compared to traditional 2D methods, especially under localised loads.

The base case analysis, involving a uniform pressure equivalent to a piling rig load near a batter slope in stiff clay soil, reveals significant differences in FOS between 2D and 3D analyses. The 3D model's ability to capture true spatial stress distribution and potential failure mechanisms highlights the necessity of 3D analysis for precise geotechnical assessments.

While the findings of this study support the efficacy of 3D FEM in slope stability analyses for scenarios involving concentrated loads, it's important to acknowledge the potential limitations of this approach in other contexts, such as very long tracks or cohesionless slopes. Further research is needed to assess the applicability of 3D FEM across a wider range of slope conditions.

For slopes that are not subjected to external loads, the failure mechanism tends to align with a plane-strain condition when using the strength reduction method in FEM. However, three-dimensional analysis becomes beneficial when dealing with localised loading on the slope.

For the case with greater height (H=0.8B), for offsets exceeding a certain value, the FOS calculated from the 2D FE model did not depend on the track location as the track was outside the failure surface zone.

5 REFRENCES

Azzouz, A. S., & Baligh, M. M. (1983). Loaded Areas on Cohesive Slopes. Journal of Geotechnical Engineering, 109(5).

Baligh, M. M., & Azzouz, A. S. (1975). End Effects on the Stability of Cohesive Slopes. *Journal of the Geotechnical Engineering Division*, ASCE, 101(GT11), 1105-1117.

CIRIA, 2017. *Guidance on embedded retaining wall design.*Fredlund, D. G., & Krahn, J. (1977). Comparison of slope stability methods of analysis. Canadian Geotechnical

Journal, 14(3), 429-439.

Griffiths, D.V. & Marquez, R.M. 2007, 'Three-dimensional slope stability analysis by elasto-plastic finite elements', *Géotechnique*, vol. 57, no. 6, pp. 537-546.

Li, A.J., Merifield, R.S. and Lyamin, A.V., 2009. Limit analysis solutions for three-dimensional undrained slopes. *Computers and Geotechnics*, 36(8), pp.1330–1351. https://doi.org/10.1016/j.compgeo.2009.06.002.

Li, A.J., Merifield, R.S. and Lyamin, A.V., 2010. Three-dimensional stability charts for slopes based on limit analysis methods. *Canadian Geotechnical Journal*, 47(12), pp.1316–1334. https://doi.org/10.1139/T10-030.

Li, S., Huang, M. & Yu, J., 2019. Continuous field-based upper-bound analysis for the undrained bearing capacity of strip footings resting near clay slopes with linearly increased strength. *Computers and Geotechnics*, 105, pp.168–182. doi:10.1016/j.compgeo.2018.10.002.

Leshchinsky, D., & Baker, R. (1986). Three-Dimensional Slope Stability: End Effects. *Soils and Foundations*, 26(4), 98-110.

Michalowski, R. L., & Drescher, A. (2009). Three-dimensional stability of slopes and excavations. *Géotechnique*, 59(10), 839-850.

Michalowski, R.L. 2010, 'Limit analysis and stability charts for 3D slope failures', *Journal of Geotechnical and Geoenvironmental Engineering*, vol. 136, no. 4.

Tschuchnigg, F., Schweiger, H. F., & Sloan, S. W. (2015). Slope stability analysis by means of finite element limit analysis and finite element strength reduction techniques. Part I: Numerical studies considering non-associated plasticity. *Computers and Geotechnics*, 70(1), 169-177.

Wei, W. B., Cheng, Y. M., & Li, L. (2009). Three-dimensional slope failure analysis by the strength reduction and limit equilibrium methods. *Computers and Geotechnics*, 36(1-2), 70-80.

Zhang, Y., Chen, G., Zheng, L., Li, Y., & Zhuang, X. (2013). Effects of geometries on three-dimensional slope stability. *Canadian Geotechnical Journal*, 49(1), 1-10.

ON PRACTICAL APPLICATIONS OF THE SOIL NAIL OPTIMISATION TOOL IN CYCLONE RECOVERY

Evangeline Alterman
Mott MacDonald

ABSTRACT

Cyclones often inflict severe damage on soil structures, necessitating swift and effective recovery efforts. However, they also create multiple constraints for geotechnical engineering design solutions and construction, such as limited timeframes, and constrained budgets. Soil nailing reinforces unstable soil slopes, which have been crucial for restoring infrastructure post-disaster.

This paper investigates the practical applications of the Soil Nail Optimisation Tool (SNOT) developed by Michael Crisp (Crisp and Davies, 2024), particularly in the recovery work after Cyclone Gabrielle struck Auckland, New Zealand, in February 2023. The SNOT integrates Python coding and geotechnical data to facilitate the selection of soil nail lengths optimised for the site's specific conditions. It reduces the time and cost of geotechnical design and, through optimisation, lowers construction costs. A case study based in the Waitākere Ranges in Auckland demonstrates how optimisation tools expedited recovery efforts while ensuring long-term stability. Furthermore, this paper discusses challenges and opportunities in implementing this tool, including cost considerations and technological advancements. This research underscores the significance of employing the SNOT in cyclone recovery projects, helping geotechnical engineers, disaster response agencies, and policymakers mitigate the impact of natural disasters on infrastructure and communities.

Cyclones profoundly influence infrastructure and soil stability, posing significant challenges to disaster preparedness response and recovery efforts. Effective mitigation measures are essential for reducing vulnerability and enhancing resilience to cyclonic hazards.

1 INTRODUCTION

Soil nailing involves installing closely spaced steel bars (nails) into the ground, typically in a grid pattern, to improve the stability of soil or rock formations. The process begins with drilling holes into the unstable mass and inserting grouted steel. These soil nails are anchored within the soil or rock mass, effectively reinforcing it, and providing stability against gravitational and lateral forces. The concept of soil nailing originated in Europe in the 1960s, initially as a temporary stabilisation measure for construction sites (GEO, 2017). Over the decades, advancements in materials, equipment, and design methodologies have transformed soil nailing into a widely accepted and preferred solution for permanent slope stabilisation, landslide mitigation, and excavation support in geotechnical engineering. Soil nailing offers a range of advantages over traditional stabilisation methods such as retaining walls or ground anchors. They are quick to install, requiring minimal excavation and disturbance to the surrounding environment. Additionally, soil nailing systems are flexible and adaptable, making them suitable for various soil types, slope angles, and project requirements. Moreover, the cost-effectiveness of soil nailing, particularly in comparison to conventional techniques, has contributed to its widespread adoption in geotechnical engineering projects worldwide. The effectiveness of soil nailing depends on numerous factors, including soil properties, nail design, installation techniques, and environmental conditions. Geotechnical engineers employ rigorous analysis and design procedures to optimise soil nail configurations and ensure reinforced structures' long-term stability and performance.

In recent years, soil nailing has extended beyond routine construction projects to encompass emergencies such as natural disasters. Cyclones, hurricanes, earthquakes, and other catastrophes often result in widespread soil erosion, slope failures, and infrastructure damage. Soil nailing is a valuable tool in post-disaster recovery efforts, facilitating the rapid stabilisation and restoration of critical infrastructure in affected areas. Against this backdrop, developing and implementing advanced optimisation tools for soil nail design have emerged as a priority in geotechnical engineering research and practice. These tools leverage computational algorithms and modelling techniques to enhance soil-nailing solutions' efficiency, and cost-effectiveness, particularly in challenging environments such as cyclone-affected regions. This paper focuses on the practical applications of one such optimisation tool, the SNOT, which integrates with the Rocscience software, Slide2, to analyse the slope stability in cyclone recovery scenarios (Rocscience, 2022). A case study analysis demonstrates the efficacy of SNOT in optimising soil nail designs for enhanced stability in post-cyclone environments. Cyclones are among the most destructive natural phenomena, capable of causing widespread devastation to infrastructure and ecosystems. Their impacts on soil stability and the built environment are multifaceted and catastrophic.

The main effects of cyclones on slope stability are:

- Erosion and soil loss: cyclones cause intense rainfall and winds, often resulting in soil erosion. Soil particles may be carried away, leading to sedimentation in large water bodies and destabilisation of slopes.
- Landslides and slope failures: Heavy rainfall and wind can trigger landslides in susceptible areas. As the soil becomes saturated from the rainfall, it loses strength and frictional resistance, increasing the loading. Landslides can cause devastating damage to public and private property while also risking people's safety.
- Widespread flooding: Floodwaters will saturate the soil, reducing its bearing capacity and compromising foundations and slope stability.

Efficient geotechnical recovery tools are crucial for addressing these challenges and facilitating the restoration of infrastructure and communities (Firoozi et al., 2017).

2 LITERATURE REVIEW

2.1 EXISTING OPTIMISATION TECHNIQUES FOR SOIL NAIL DESIGN

Existing optimisation techniques for soil nail design aim to enhance soil nail reinforcement systems' efficiency, and cost-effectiveness (Imam and Hoseini, 2021). These techniques leverage advanced computational algorithms, numerical modelling, and optimisation methods to optimise various aspects of soil nail design, including nail spacing, length, diameter, orientation, and material properties (Wang et al., 2017). Using Finite Element Analysis (FEA) allows clear visualisations of stress distribution and can identify the locations of critical failure planes (Pang et al., 2024). On the other hand, the flexibility, adaptability, and simultaneous parameter optimisation allowed by Genetic Algorithms (GA) is a massive benefit (Nagaraju et al., 2023). Alternatively, using Particle Swarm Optimisation (PSO) has an ease of implementation and scalability (Kashani et al., 2020). Finally, Response Surface Methodology (RSM) provides a visual representation of the effects of different parameters and allow informed decisions to be made) (Tan et al., 2013) (Benayoun et al., 2021).

In summary, existing optimisation techniques for soil nail design offer diverse approaches to address the complex challenges of geotechnical engineering. By integrating computational modelling, optimisation algorithms, and engineering expertise, engineers can develop optimised soil nail reinforcement systems that enhance stability, durability, and cost-effectiveness in various geotechnical applications (Huang et al., 2020).

2.2 CHALLENGES IN POST-CYCLONE SOIL STABILISATION

- **The need for quick restoration of existing infrastructure.** Cyclones can cause widespread damage to roads, bridges, and other critical infrastructure.
- **Cyclones often cause a loss in soil stabilisation.** This will result in landslides and slope failures.
- **Build Back Better (BBB).** Cyclones and other natural disasters highlight the weaknesses in existing infrastructure. During cyclone recovery, the challenge is to design more resilient infrastructure.
- **Restoration of ecosystems.** The flooding and high winds caused during these events can destroy ecosystems, especially in coastal or floodplain areas.

2.3 SEISMIC CONSIDERATIONS FOR OTHER TOOLS

The seismic scenarios developed during a slope stability analysis conducted to design soil nail slopes can be represented by the following considerations (Palmer, 2019):

- Seismic loading will be applied based on the design life and location of the site. Both factors are considered when developing the horizontal loading applied during a seismic event. This peak ground acceleration (PGA, g) can fluctuate massively across New Zealand. For example, in the Far North, for a 50-year design life site, a PGA of 0.13g is used. However, in Wellington, an Importance Level four, one in 2500 return period, will use a 1.27g PGA (NZTA Bridge Manual, 2022).
- In Slide2, the ground model will consist of undrained materials to model the transient moment a seismic event may occur. This will remove the input parameters of friction angle and cohesion and solely rely on the undrained shear strength, which is user-defined for each material (Rocscience, 2022).
- Temporary live loads are often factored down during seismic events. This prevents overly conservative design as it is highly unlikely that these loads will be acting fully at the time of a seismic event.

3 METHODOLOGY

3.1 INPUT PARAMETERS AND DATA REQUIREMENTS

Slide 2 uses various limit equilibrium methods to analyse the stability of slip surfaces, evaluating the factor of safety based on different load combinations and scenarios. Ground models may be based on ground investigation or a detailed desktop study (Kim et al., 2018) and should be produced by an engineering geologist. The following parameters will be inputted into the Slide2 models:

- Geotechnical parameters (unit weight, cohesion, friction angle)
- Depth and formation of each geotechnical unit
- Groundwater levels and seasonal fluctuations
- Topography of the slope.
- Material/unit dependent bond strengths for grouted nails.
- Soil nail type and available lengths (most contractors will have a preference, and nails will be produced to specific lengths).
- Soil nail parameters (based on type), including tensile capacity, diameter, and plate capacity.
- Soil nail in-plane and out-of-plane spacing and nail angles.
- External loads (temporary live loads, construction loads, dead loads).

The SNOT tool will determine the shortest feasible nail lengths which maintain a compliant design.

3.2 ALGORITHMS AND COMPUTATIONAL MODELS USED

The Python software integrated with Slide2 can efficiently analyse multiple geological sections, construction stages, scenarios (earthquake, flooding, etc.) and different Factors of Safety requirements for each scenario (Python Software Foundation, 2021). The tool solves the problem by determining a soil nail design and optimising across all scenarios and cases simultaneously, and on a row-by-row basis. Here, optimisation minimises soil nail length for a given configuration. The tool is efficient due to its global application to multiple sections globally. Further details of the tool's functionality are included in the paper, '*A tool for soil nail wall design optimisation using Slide2 and Python*' (M. Crisp & O. Davies, 2022). Combinations of parameters may also be assessed automatically to find a globally optimal solution for various scenarios, e.g., high groundwater and seismic (Liu et al., 2021). This tool allows the engineer to identify the influence of critical variables and quickly calibrate the optimised design to the specific constraints of the projects.

3.3 CASE STUDY SITE SELECTION

In West Auckland, the mountain range and national park Waitākere Ranges extend along the west coast of New Zealand. The national park mainly consists of dense bush, remote beaches, and rural winding roads. During Cyclone Gabrielle in February 2023, the Waitākere Ranges saw extensive damage, with rain, flooding, and high winds causing thousands of landslides. Many landslides have caused damage to rural roads and property. The roads were mainly constructed in the pre-1940s, so they are un-engineered and prone to collapse in flooding events. The site chosen for this case study in West Auckland is a road with significant landslides occurring on the leading edge of the road and blocking the road from vehicular and pedestrian traffic. The slip scarps generally extend between 3-4 metres below the road level and extend from 10-30m in length. Soil nails were the preferred remediation technique due to their relative affordability and efficient construction programmes.

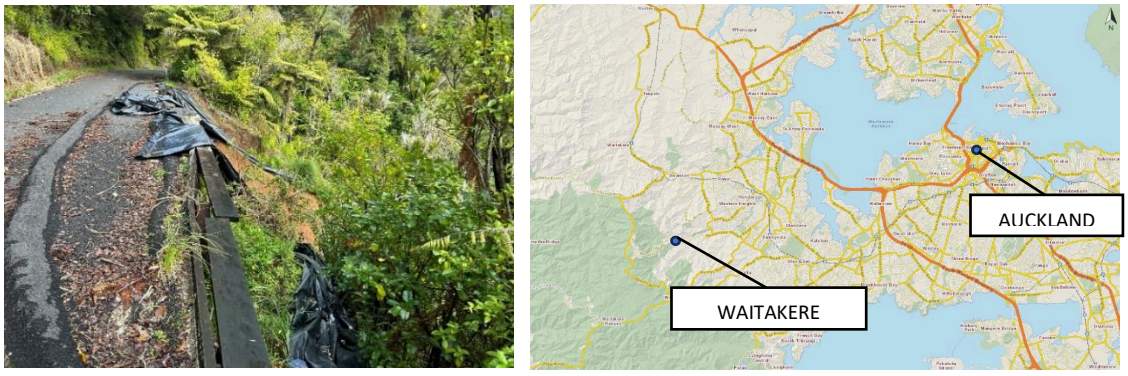

Figure 1: Landslide in the Waitakere Ranges (Alterman, 2024) & Landslide location in Waitakere Ranges, West Auckland (Auckland Council Geomaps, 2024)

3.4 ANALYSIS OF RESULTS

Cost and time values are based on the average 'per site' value provided by the design consultancy and contractor. The contractor costs are the average 'per site' value for all construction (including mobilisation and materials). The 'with python' costs are estimated based on the percentage reduction calculated applied across materials, labour, and design fees.

4 RESULTS

4.1 RESULTS AND ANALYSIS OF SITE PERFORMANCE

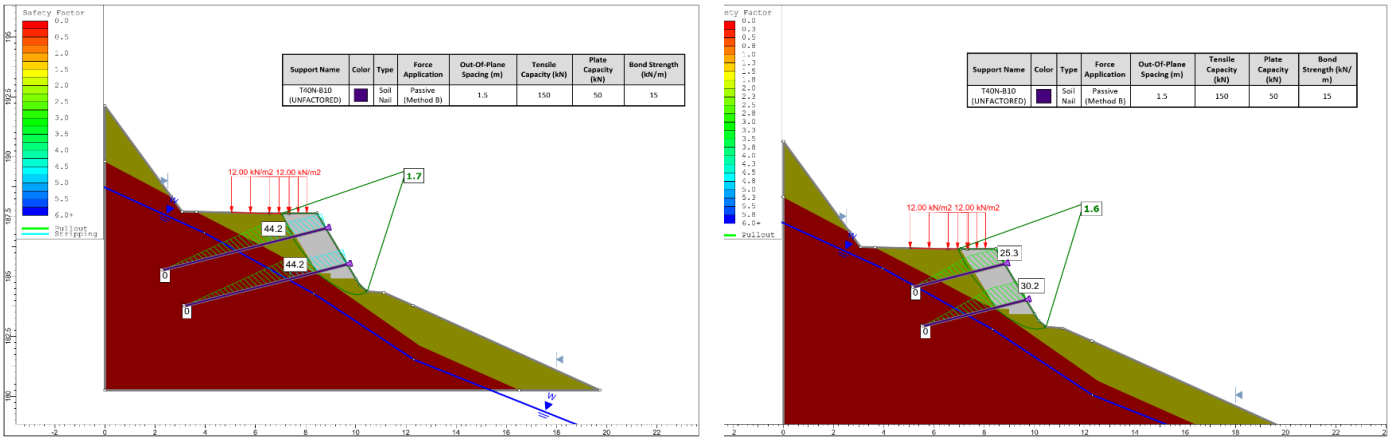

Figure 2: Slide2 outputs with and without the Soil Nail Optimisation Tool.

Figure 2 shows the case study site before and after the use of the SNOT. This example is an unfactored non-circular analysis, targeting a Factor of Safety of 1.5 for long-term groundwater conditions and a 'Normal' traffic loading H_N of 12kPa. The uniform parameters (regarding the soil nails) are highlighted below:

- 1.5m Out-of-Plane and vertical spacing
- The material bond strength is 15kN/m, with a bond strength of 0kN/m within the no-fines concrete buildout (material-dependent).

Although both designs comply with the NZTA Bridge Manual, the Python-optimised design recommends soil nail lengths of 3.8m and 4.3m for layers 1 and 2, respectively (compared to 5.5m for both layers in the manual design) (NZTA Bridge Manual, 2022). The percentage of material saved is 26% from this optimisation. This value is solely considering the materials saved. However, this value could increase significantly when considering the reduction in complexity, an increased efficiency for project management and ease of construction. This, in turn, could reduce contractor labour hours and minimise design hours.

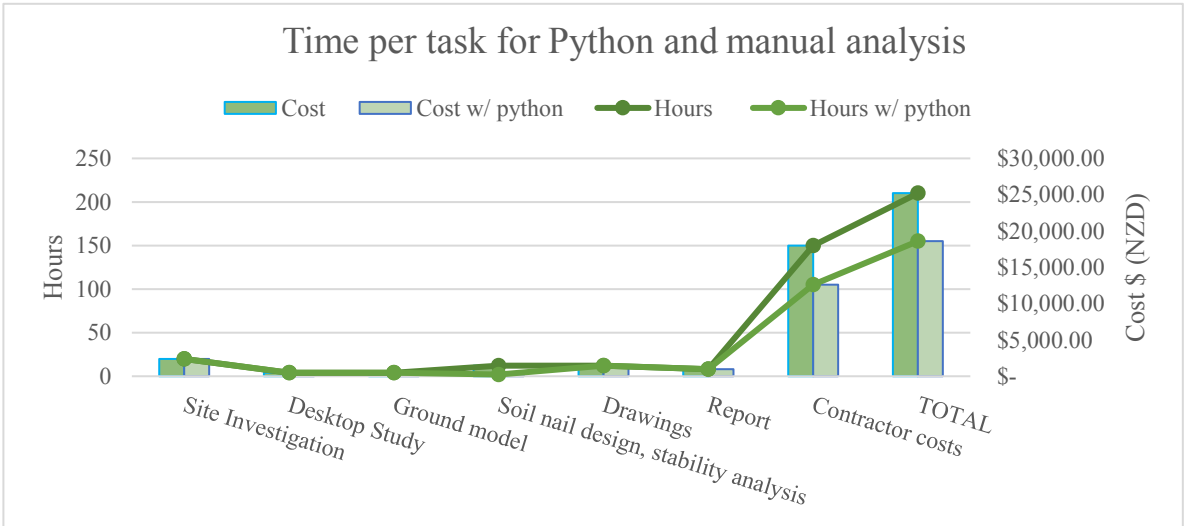

Figure 3: Estimate of costings with and without Soil Nail Optimisation Tool.

Figure 3 shows the cost/time structure of this type of cyclone recovery remediation project. Relatively, the most significant savings can be made by reducing wastage, improving efficiency and optimising on-site. Reducing the design process for geotechnical engineers saves the client money and allows more remediation work to be completed quickly. Through the optimisation of the design and removing wastage from potential solutions, this tool may be applied to projects of all sizes.

5 BENEFITS, IMPACTS AND CHALLENGES

5.1 BENEFITS OF SOIL NAIL OPTIMISATION TOOL

5.1.1 Cost savings and time efficiency

Optimisation tools help allocate resources efficiently (such as labour, materials, and energy). Optimisation algorithms quickly evaluate various scenarios and recommend optimal solutions, accelerating decision-making, especially in complex situations.

5.1.2 Environmental considerations and sustainability

Several environmental considerations are crucial to ensure stability and minimise adverse effects when designing and implementing soil nail systems. Understanding the subsurface soil and rock profiles is essential. Seasonal moisture variations and potential load-bearing demands must be considered. Soil nails are typically grouted into drilled holes within soil or rock, functioning as passive anchors that reinforce the inherent strength of the soil. Protective coatings or stainless-steel materials should be used to prevent corrosion. Proper drainage design helps minimise water infiltration, which can accelerate corrosion. To avoid the negative impact of soil nail slopes on the environment, assessment of the ecological implications of soil nail installation is crucial to avoid disturbing sensitive habitats, vegetation, or wildlife. Implementation of erosion control measures during construction will prevent sediment runoff.

5.2 IMPACTS OF SOIL NAIL OPTIMISATION TOOL

Ability to produce geotechnical designs for cyclone recovery quicker and cheaper while maintaining the safety and standard of the design.

5.3 CHALLENGES OF USING THE SOIL NAIL OPTIMISATION TOOL

This paper demonstrates the vast potential of this tool in cyclone recovery work. However, several aspects could be improved by this tool. To run the analysis with this tool, the model needs to be set up in a particular way:

- Ground model, unit, and soil nail parameters must be pre-determined and manually entered.
- Nail spacing and out-of-plane spacing need to be pre-determined.
- Loading and scenarios must be pre-programmed, e.g. seismic loads, traffic loads, and groundwater fluctuations.

These conditions require the user to have a full understanding of the functionality of the software to benefit from its efficiency. This may in turn limit its accessibility if training is limited. A large majority of the parameters need to be pre-determined before this tool may be employed, which reduces its efficiency and allows for human error to be a factor.

6 FURTHER WORK

The tool is currently available as an internal executable. All users need a certain amount of coding experience to access it and to program the required outputs. By developing an app, with a more comprehensive interface, this programme will be more readily available for those using Slide2 for soil nail design.

Further functionality will ensure two things: not only will the design be the most optimised version possible, but secondly, the iterative process of adjusting vertical/horizontal spacings, angles and lengths will be compacted into a simple analysis and will drastically reduce the time taken to produce the most optimal design.

As this tool is currently in its trial period, further trials over slope stability projects, with varying complexity and variations to surface and analysis methods, are required to show this tool's full range and capacity. Upon further trials, the aim is to develop further the program to create a more efficient and widely accessible tool.

7 CONCLUSION

In conclusion, the research presented in this paper highlights the critical role of the SNOT in post-cyclone recovery efforts, particularly following Cyclone Gabrielle in Auckland, New Zealand. The tool’s integration of Python coding and geotechnical data has proven to offer a streamlined approach to soil nailing that significantly reduces both the time

and costs associated with design and construction. The case study in the Waitakere Ranges demonstrates the practical benefits of this tool, highlighting how it can optimise design efforts while ensuring the long-term stability of restored infrastructure. The SNOT has shown that efficient and effective solutions are achievable. Moreover, this research underscores the importance of continued innovation and technological advancement in geotechnical engineering. By leveraging tools like the SNOT, engineers, disaster response agencies, and policymakers can better mitigate the impacts of natural disasters on infrastructure and communities, contributing to more resilient and sustainable recovery efforts. This paper's findings advocate for the broader adoption of optimisation tools in geotechnical practices, emphasizing their potential to transform disaster recovery projects.

8 REFERENCES

Alterman, E.A (2024*). Landslide in the Waitakere Ranges*. [Photograph].

Auckland Council. (2024). *Geomaps mapping service*. Available at: https://www.aucklandcouncil.govt.nz/geospatial/geomaps/Pages/default.aspx

Benayoun, F., Boumezerane, D., Bekkouche, S. & Ismail, F. (2021). *Optimisation of geometric parameters of soil nailing using response surface methodology*. Arabian Journal of Geosciences, Volume 14.

Crisp, M.P. and Davies, O. (2024). *A Tool for Soil Nail Wall Design Optimisation Using Slide2 and Python.* ResearchGate. Available at: https://www.researchgate.net/publication/378336998_A_tool_for_soil_nail_wall_design_optimisation_using_Slide2_and_Python.

Firoozi, A.A., Olgun, C.G., Firoozi, A.A. and Shojaei Baghini, M. (2017). *Fundamentals of soil stabilization*. International Journal of Geo-Engineering. Available at: https://link.springer.com/article/10.1186/s40703-017-0064-9

GEO (2017). *Guide to Soil Nail Design and Construction (Geoguide 7)*. Geotechnical Engineering Office, Civil Engineering and Development Department, HKSAR Government. Available at: https://www.cedd.gov.hk/filemanager/eng/content_117/eg7_20170918.pdf

Huang, J., and Li, X. (2020). *Numerical analysis and optimisation of soil nail walls in sandy soils.* Computers and Geotechnics, 123, pp. 103561.

Imam, R. and Hoseini, S.S. (2021). *Design and optimization procedure for composite soil nail-anchor walls*. Japanese Geotechnical Society Special Publication. Available at: https://www.jstage.jst.go.jp/article/jgssp/2/45/2_IRN-12/_pdf

Kashani, A.R., Chiong, R., Mirjalili, S. and Gandomi, A.H. (2020). *Particle Swarm Optimization Variants for Solving Geotechnical Problems: Review and Comparative Analysis.* Archives of Computational Methods in Engineering. Available at: https://link.springer.com/article/10.1007/s11831-020-09442-0

Kim, Y., and Jeong, S. (2018). *Performance-based design optimisation of soil-nailed slopes.* Geotechnical and Geological Engineering, 36(5), pp. 3085-3098.

Liu, H., and Zhang, L. (2021). *Reliability-based optimisation of soil nail walls considering spatial variability.* Soils and Foundations, 61(4), pp. 1010-1022.

Nagaraju, T.V., Sireesha, M., Sunil, B.M. and Alisha, S.S. (2023). *A Review on Application of Soft Computing Techniques in Geotechnical Engineering*. Proceedings of The 5th International Conference on Advances in Civil and Ecological Engineering Research. Available at: https://link.springer.com/chapter/10.1007/978-981-99-5716-3_26

Pang, C.Y., Liang, M., Yang, Z. and Boon, C.W. (2024). *Intelligent Framework for Finite Element Analysis with Machine Learning and Back-Analysis Capabilities for Geotechnical Engineering.* Proceedings of the 5th International Conference on Geotechnics for Sustainable Infrastructure Development. Available at: https://link.springer.com/chapter/10.1007/978-981-99-9722-0_138

Python Software Foundation (2021). *Python Language Reference*. [Online] Available at: http://www.python.org/

Palmer, S. (2019). *Seismic Assessment of Existing Buildings Geotechnical Considerations.* New Zealand Geotechnical Society. Available at: https://www.nzgs.org/libraries/seismic-assessment-of-existing-buildings-geotechnical-considerations/

Rocscience (2022). *Slide 2 - 2D Limit Equilibrium Analysis for Slopes.* [Online] Available at: https://www.rocscience.com/software/slide2

Tan, X., Shen, M., Hou, X., Li, D. and Hu, N. (2013). *Response Surface Method of Reliability Analysis and its Application in Slope Stability Analysis.* Geotechnical and Geological Engineering. Available at: https://link.springer.com/article/10.1007/s10706-013-9628-4

Waka Kotahi NZ Transport Agency (2022). *Bridge manual (SP/M/022)*. 3rd ed. [online] Available at: https://www.nzta.govt.nz/resources/bridge-manual/ [Accessed 28 July 2024].

Wang, J., and Zhang, L. (2017). *Optimization of soil nail length and spacing for slope stabilisation.* Engineering Geology, 228, pp. 1-10.

THE DANGERS OF RESTRICTING ACCESS TO RESIDENTIAL HOUSING FOLLOWING LANDSLIDES

Jesse Beetham & Nick Rogers
Tonkin & Taylor Ltd.

ABSTRACT

Following the damaging climate related rainfall events in Aotearoa in early 2023, regulatory controls that come into play during and after state of emergencies resulted in legally enforced, restricted access to more than 2000 private houses (Television New Zealand 1 News, 2023).

Many of these restrictions were placed on private houses in the form of Red Placards or Dangerous Building Notices as a result of landslides that either damaged or had a perceived risk of damaging the residential houses which could result in deaths or serious injuries to the occupants.

The purpose of these restrictions, which are applied under the Civil Defence and Emergency Management (CDEM) Act 2002 and 2016 Amendments or the Building Act 2004, is to ensure the safety of people living in the affected houses and/or the public and/or adjacent buildings. The impact on the occupants of the forced evacuation is, however, traumatic, which raises a number of important issues around both the process and the outcome.

This paper sets out the issues around restricting access to houses when property damaging landslides occur or are considered likely to occur and presents some suggestions as to how these situations could be better managed in future events. This paper draws from the authors' experiences and observations in responding to landslide events across New Zealand, assessing resultant damage, and managing the removal of red placards from residential dwellings.

1 INTRODUCTION

A year after the devastating rainfall events of the Auckland Anniversary weekend storm (27/01/2023), which was closely followed by Cyclone Gabrielle (11/02/2023 to 17/02/2023), the Auckland Mayor said that using emotive language like an “intolerable risk to life” was unhelpful in the context of a complex and very expensive recovery effort.

However, eighteen months after those events, many people are still out of their homes because the risk to them reoccupying their homes has been assessed as being intolerable.

The involuntary removal of people from their houses should be something that is only undertaken in exceptional circumstances, but unfortunately this practice is becoming more common. The current process that is displacing people from their houses (owned or occupied) is in our opinion, resulting in more harm to people than the natural disaster that has long since passed.

Government-driven policies and processes associated with natural disaster response need to be updated based on our recent experiences with natural disasters. However, before we embark on a new path, it is crucial to understand how we arrived at our current situation.

2 NATURAL DISASTER RISK

In Aotearoa it is not possible to live in a residential dwelling and be at no risk from natural hazards. The best one can do is choose the hazard(s) one is most comfortable living with. Safety used to be a relative, not an absolute, term when it came to living with natural hazards which were generally described as being high, medium or low risk.

When we first constructed our pā and our houses in Aotearoa, we did not completely understand the risks that landslides presented. For example, historical records suggest that in 1760, 135 fatalities were recorded as a result of a landslide and debris flow that occurred at Omoho Pā, Waihi, Lake Taupō (Bruce, 2022). Thankfully, these mass fatality landslide events in Aotearoa have not been frequent, however, smaller scale landslides have also caused fatalities in many locations across New Zealand, some of which have occurred within populated areas and affected residential properties. We repeatedly see the same question asked after every natural disaster event, why did the territorial authority allow the affected homes to be constructed in these areas with landslide risks?

A recent publication by the Crown Research Institute GNS Science (GNS) states that, over the past 160 years, landslides in Aotearoa have resulted in more fatalities than from earthquakes, volcanoes and tsunamis combined (de Vilder, et al.,

2024). This suggests that we have been building in landslide prone areas and, seemingly unknowingly, been putting homes and people in harms way. This also feeds into the narrative that we need to protect people during and after landslide events even if this means affecting their human and property rights in the name of intolerable risk to life safety.

Regulations around building in areas of natural hazard risk in New Zealand have been in place for a long time. Since the introduction of the Local Government Amendments Acts in 1978 and 1979, Territorial Authorities have been required to manage natural hazards so that they do not endanger people or property by refusing to permit subdivision or building in areas of natural disaster risk unless the risk was mitigated.

However, since 1981 with the introduction of Section 641A of the Local Government Act (and subsequently Section 36(2) of the Building Act 1991 and Section 72 of the Building Act 2004) Territorial Authorities have been able to issue residential building consents in hazard prone areas and not be under any civil liability. Under this provision, Territorial Authorities are also required to place a notice on the property title which essentially states that the building consent applicant has agreed to accept the natural disaster risk so future owners of the subject property are also aware of the risk. A Section 72 notice typically means that the notified property will generally not be insured for the natural hazard specified on the title, and banks may not provide mortgage finance. This also means that tenants should check a property title before occupying such a property.

As a consequence of the requirements of Territorial Authorities to manage natural disaster risk, very few people have been killed or injured by landslides in their residential homes over the last 50 years. The evidence base indicates that Territorial Authorities have not been reckless in allowing urban development in landslide prone areas. Living in legally consented residential dwellings in Aotearoa seemingly does not present an intolerable life safety risk. Which raises the question, why then are Territorial Authorities removing some people out of their homes after landslide events?

3 RED PLACARDS AND DANGEROUS BUILDING NOTICES

Following natural disaster events in New Zealand, Territorial Authorities are required to assess the life safety risk to the occupants of buildings under the Civil Defence and Emergency Management (CDEM) Act 2002 and 2016 amendments (the most common are structural assessments of visibly damaged buildings after an earthquake event). Depending on the severity of a natural disaster event, the CDEM Act 2002 allows delegated representatives from territorial authorities to declare a "state of local emergency". Emergency powers come into play under a state of local emergency which enable directive management of people and buildings. One of these emergency powers is known as the Rapid Building Assessment Placarding System. The purpose of this system is to indicate "whether or how a building may be used" following a significant weather event or natural disaster and to visually assess the risk against safety and life of people using the affected building, which can include residential buildings.

There are three different types of placards used in a Rapid Building Assessment following a weather event or natural hazard, those being white, yellow and red. A white placard means that the subject building can be occupied, a yellow placard means the subject building has restricted/controlled access and a red placard means that access to the subject building is prohibited, as the building may pose "a significant risk to public safety, health, and wellbeing" (Ministry of Business, Innovation & Employment, 2023).

Another example of the Rapid Building Assessment Placarding System was observed in the Port Hills, Christchurch, following the 2010 and 2011 earthquake events. The seismically induced landslides and rockfalls in February 2011 were dramatic and damaged many homes in the area, which resulted in red placards being placed on approximately 500 homes (Canterbury Earthquake Recovery Authority, 2011). However, many undamaged properties in the same area were considered to be in danger of damage and as a result, red placards were also placed on those houses. Due to the process in which the Rapid Building Assessment Placarding System is implemented, there is often different perspectives and risk interpretations that result in some controversial placard placements.

Under the Rapid Building Assessment Placarding System, red and yellow placards do not automatically expire, however their intention is still to assess the immediate risk to life. Currently, the process to remove a red or yellow placard is onerous, and usually falls on the affected property owner to engage professionals to "provide advice on building usability and options to address any damage, e.g., repair or demolition" (Ministry of Business, Innovation & Employment, 2023). This is normally a time consuming and expensive process and more often than not, affects buildings that have legally been consented by a territorial authority in the first place. It is important to recognise that red placards are different and separate from dangerous building notices (Section 121 of the New Zealand Building Act 2004). Although, one can often lead to the other and both prohibit occupation of a building.

Under Section 121 of the New Zealand Building Act 2004, "a building is dangerous for the purposes of this Act if in the ordinary course of events (excluding the occurrence of an earthquake), the building is likely to cause injury or death (whether by collapse or otherwise) to any persons in it or to persons on other property". In practical terms, the meaning of Section 121 was the subject of a Determination which found that a Section 124 notice is justifiable only if the risk of

injury or death for people living in the houses is so high that, in the public interest, the building owner cannot be allowed to take that risk, and that injury or death is likely in the ordinary course of events (Department of Building and Housing , 2006). This is a very high bar, as it should be, as it affects both property and human rights, just like a red placard.

There are many reasons why it is desirable to get displaced occupants back into their homes as soon as possible following a natural disaster or weather event. The main reason being the social and emotional connection that most humans have with their personal homes. The ties humans have to their personal spaces can be profound. Personal homes are often the basis for memories, serve as a familiar space providing comfort and stability, and function as the focal point of social interactions. Displacement from these personal spaces can induce stress and anxiety, exacerbating the trauma already associated with natural disasters. Alternative accommodation in disaster areas is also usually in short supply, and often required by personnel responding to the disaster and looting of unoccupied houses is also a common problem.

4 REPONSE TO AND RECOVERY FROM RAINFALL INDUCED LANDSLIDE EVENTS

While an extreme weather event is unfolding, and conditions are chaotic and often assessed during darkness, it is a rational response under such circumstances to be cautious and risk adverse. The occupants of damaged houses, and those above and below areas of landsliding, are often advised or ordered to evacuate their houses, and red or yellow placards are placed on the doors of the houses assessed as being unsafe to occupy.

Once the weather event has passed, it used to be normal practice to re-evaluate the affected properties as soon as possible to see if the previously placed placards could be removed and the houses could be reoccupied. The test for this was to evaluate whether the risk had essentially returned to that which existed before the weather event/disaster occurred, and where the risk was considered acceptable.

Up until 2010, no New Zealand government had intervened in the natural disaster recovery of residential property following natural disaster events, leaving this task to the insurance industry (including the governments Natural Disaster Insurance Scheme administered by the Earthquake Commission, now the Natural Hazards Commission) and local authorities to manage.

Following the 2010 earthquake in Christchurch, the recovery objective to rebuild everywhere after the disaster changed after the smaller magnitude but much more destructive earthquake on 22 February 2011. The scale of the liquefaction related residential land and building damage was such that rebuilding everywhere was no longer an option. The decision to withdraw from the flat land was not based on an unacceptable or intolerable life safety risk. It would just take too long to raise or improve the ground and rebuild the buildings and infrastructure in the worst affected suburbs.

In June 2011, the New Zealand Government offered to purchase 7,346 of the most severely damaged residential properties on the liquefaction prone flat land (Canterbury Earthquake Recovery Authority, 2016), involving the retreat of some 20,000 people. That area of land designated for withdrawal became known as the Residential Red Zone (RRZ).

The RRZ government purchase was essentially a one-off transaction, undertaken under the Canterbury Earthquake Recovery Act 2011. However, since that time many property owners who have been through subsequent natural disasters believe that if they cannot occupy their homes because they are deemed to be dangerous (red placards or dangerous building notices) by the local authority, then their properties should be “red zoned”. By that they mean that someone will pay for their properties to be taken off their hands.

In 2011, Cyclone Wilma caused widespread flooding and landslides in both the North Island and the top of the South Island. In Nelson, Emergency Managers placed red placards on houses and the local council issued many at risk properties with dangerous building notices, but upon a return to normal conditions (the ordinary course of events) most of these red placards and dangerous building notices were removed on the advice of experienced geotechnical specialists. One particular property in Nelson suffered a landslip on the rear lawn, several metres distance from the corner of the house. A local engineer assessed that the undamaged house was at risk from land slippage, and the local council issued a dangerous building notice. These actions confirmed to the property owner that there was no way they would be allowed to, nor would they now want to, occupy the house. A local member of the New Zealand Parliament considered that if it was good enough for the residents of Christchurch to receive compensation in similar circumstances, then it should also apply to the residents of Nelson.

The building in Nelson was undamaged and the risk to the building was uncertain but was in all likelihood at no greater risk of damage than many similarly located residential dwellings throughout Aotearoa. In this case there was no compensation forthcoming from their insurer, or council, or government.

An assessment by another geotechnical specialist considered that the house was not at undue risk and that the dangerous building notice could be removed. This clearly provided a dilemma for the property owner. Without a dangerous building

notice there was little ability to pressure the council or government for the property to be "red zoned". Also, having been told by one engineer that the house was unsafe to live in, it was also difficult for the property owner to believe that it was now sufficiently safe to live in. What if the first engineer was right? Who to believe? Who had the better judgment?

5 LIFE SAFETY RISK

The fundamental driver of red placards, yellow placards and dangerous building notices being placed on buildings is the perceived life safety risk following a natural disaster or extreme weather event. In most instances, this life safety risk is not supported by extensive quantitative risk assessments, but by the judgement of experienced professionals tasked with assessing such situations. However, the most important question that underlies all of this is, what is "safe"?

The assignment of a probability to define acceptable risk arose from work by the Food and Drug Administration (FDA) in the USA in the 1970s, in order to establish the amounts of particular substances that were "safe". "Safe", in the context of developing cancer by ingesting substances, was initially put at a probability of 1 in 100 million (1×10^{-8}) by the FDA in 1973, but this was changed in 1977 to be 1 in 1 million (1×10^{-6}). These numbers had no scientific basis but were merely considered to be "essentially zero" (Kelly, 1991).

Prior to the Canterbury Earthquake Sequence, GNS had been proposing that Local Authorities adopt a risk-based approach to their management of natural hazards, including criteria where the risk to life would be intolerable, or unacceptable (Glavovic, et al., 2010). After the February 2011 earthquake in Canterbury, geotechnical specialists in the Port Hills looked to remove previously placed red placards as they had done in Nelson in March 2011. However, in April 2011, GNS reportedly suggested that to get a red placard removed from undamaged houses in the Port Hills a geotechnical specialist would need to state that the occupants would not get killed by a 1 in 2500-year earthquake event. This would require a quantitative risk assessment, not the judgement (described by GNS as "gut feel") of experienced geotechnical professionals.

In April 2011 GNS specialists provided Christchurch City Council and Environment Canterbury with information on tolerable risk definitions that Council might want to adopt as the basis for the planned risk-based approach to repatriation or retreat of evacuated homes in the Port Hills suburbs (Taig, et al., 2012). Council would eventually decide that an intolerable life safety risk was one that had an annual individual fatality rate less than 1 in 10,000 (1×10^{-4}). Although no communities had ever agreed that this was an appropriate threshold for life safety risk in New Zealand from natural hazards, Christchurch City Council adopted this value.

In 2012 GNS undertook quantitative life safety risk assessments in the Port Hills and many undamaged properties assessed to be at an intolerable life safety risk were abandoned and purchased under an agreement between Council and Government. The uncertainty around the actual risk value did not appear to be taken into account.

The expertise of professional geotechnical judgement was critically underestimated by those in governmental environments, being disparagingly referred to as subjective or haphazard decision-making. In response to the council's decision regarding the intolerable life safety risk, only a very small number of red placards were removed from undamaged houses in the Port Hills. This would be repeated in Kaikoura in 2016 and 2017, and again in the wake of Cyclone Gabrielle in Northland, Auckland, Coromandel, Bay of Plenty, Te Tairāwhiti and the Hawkes Bay in 2023 and 2024. How many of the homes damaged by landslides caused by Cyclone Gabrielle had an intolerable or unacceptable risk to life before the event took place? Is it reasonable to place a red placard or yellow placard on a home if the risk to life has not changed significantly post-event?

6 RECENT RESPONSE TO CYCLONE GABRIELLE IN 2023

Following the residential property damage from the Auckland weather event in January 2023 and the more widespread residential property damage from Cyclone Gabrielle a few weeks later in February 2023, the Government eventually decided that their involvement in financially supporting Territorial Authorities with cyclone damage recovery in their communities would be based on life safety risk. Following Cyclone Gabrielle, the government announced a land categorisation system, known as the Future of Severely Affected Land (FOSAL), to deal with the risks from future severe weather events on affected properties (many of which were affected by landslides).

As part of the FOSAL system, the Government provided a framework for territorial authorities to follow to allow affected properties to be classified as one of three risk categories. Properties where the life safety risk was assessed to be tolerable would be assigned Category 1. Buildings or properties with an intolerable risk to life would be Category 2 (practical and economic measures available to reduce the life safety risk) or Category 3 (intolerable life safety risk unable to be mitigated). Unlike placards these categories assess the future risk to life. Category 2 was then split into whether property specific (P) or community based (C) mitigation measures were available, or whether further assessment (A) was required (Beehive.govt.nz, 2023). FOSAL category 3 properties were offered a voluntary buy-out option that was co-funded by

local authorities and the crown. It is likely that in most instances, the properties that were categorised as FOSAL 3, would have previously been red placarded, yellow placarded, or subject to a Dangerous Building Notice.

Many of the intolerable life safety risk properties (FOSAL Category 3) in Auckland and elsewhere in New Zealand resulting from the 2023 weather events are those affected by landslides.

7 A DIFFERENT PATH

The placing of Red Placards, Dangerous Building Notices or FOSAL Category 2 or Category 3 status to undamaged residential buildings immediately after rainfall/cyclone triggered landside events on the basis of an intolerable life safety risk needs to be critically examined.

After the onslaught of the Auckland Anniversary Storm and Cyclone Gabrielle, many property owners in New Zealand find their situation mirroring that of their counterparts in Nelson in 2011, as well as others throughout Aotearoa who have experienced similar flood and landslide events caused by rainfall in the past. A significant number of these properties retain red placards or dangerous building notices or have been classified as FOSAL Category 2 or 3. This implies that these structures and/or properties have been deemed dangerous, posing an unacceptable risk to human safety.

Once a territorial authority informs a property owner or occupier that their undamaged house is at "a significant risk to public safety, health, and wellbeing" or is "dangerous", and prevents the building owners or occupiers from accessing that building for a considerable period of time, they quite reasonably do not want to live in that house ever again. However, many now find themselves under severe duress, with no or insufficient financial support from their insurers, council or government.

The current processes require re-evaluation to better achieve fairness. An overhaul is needed to change the way we assess risk in the aftermath of natural disaster events. A more balanced approach is needed, one that equally considers the needs and interests of residential property owners and occupiers, along with those of local authorities, who at some point in time, legally consented the dwellings in the first place. We consider that there are two issues that need to be addressed:

- The assignment of a residential house as dangerous to the occupants in the first place (whether this is by way of a red placard, a dangerous building notice or a category 2 or 3 assignment), and
- The assessment that the building is not, or is no longer, dangerous as a result of the event.

Historic events and firsthand experiences prove that it is far too easy to state that a house is dangerous, and far too hard, if not impossible, to state that the same house is not, or is no longer, dangerous. The current process all too easily enables local authorities to take away the rights of the owners or occupants of residential houses, but then places the virtually impossible onus on these displaced and traumatised owners or occupiers to prove that their buildings or homes are in fact safe to occupy.

Owners and occupiers of residential properties in Aotearoa have become the unwitting victims of risk, not natural disaster risk but territorial authority risk aversion. The path that we have followed since 2012 is resulting in unnecessary distress to people already traumatised by natural disasters. When disaster strikes it must be made more difficult for local authorities to force people out of their houses and made much easier to get these same people back into those houses. Judgement must be a factor that is weighed as much as numerical analyses. The criteria for natural disaster recovery assistance could be:

- Any property that has a house with a red placard or a dangerous building notice remaining after 12 months should be bought out by the local authority who placed the placard.
- Any property that requires consenting for repairs under Section 72 (likely to be damaged by a natural disaster) should be bought out by the council if that council issued a building consent for the house to be built in the first place.

These criteria would incentivise local authorities to be more prudent in issuing building consents in hazard prone areas in the first place and would focus the recovery on the subjects such as human rights, property rights, and the availability of insurance and bank finance.

8 REFERENCES

Beehive.govt.nz, 2023. *Update on assessment of affected properties post Cyclone and flooding.* [Online] Available at: https://www.beehive.govt.nz/release/update-assessment-affected-properties-post-cyclone-and-flooding [Accessed 15 July 2024].

Bruce, Z. R. V., 2022. *Version 1 of the New Zealand landslide fatalities database*, 1760 - 2020, Lower Hutt, New Zealand: The Institute of Geological and Nuclear Sciences Limited (GNS Science). DOI: 10.21420/SW43-TJ28.

Canterbury Earthquake Recovery Authority, 2011. *Port Hills risk notices to be replaced*. Wellington, New Zealand: Canterbury Earthquake Recovery Authority.
Canterbury Earthquake Recovery Authority, 2016. *Residential Red Zone Survey (of those who accepted the Crown Offer)*, Wellington, New Zealand: Canterbury Earthquake Recovery Authority.
de Vilder, S. J. et al., 2024. *Landslide Planning Guidance: Reducing Landslide Risk through Land-Use Planning,* Lower Hutt, New Zealand: The Institute of Geological and Nuclear Sciences Limited (GNS Science).
Department of Building and Housing, 2006. *Determination 2006/119 - Dangerous building notices for houses in Matata, Bay of Plenty,* Wellington, New Zealand: Department of Building and Housing (Ministry of Business, Innovation & Employment).
Downes, G. et al., 2005. *EQC Project 03/490 - Understanding local source tsunami: 1820s Southland tsunami, Lower Hutt, New Zealand*: Institute of Geological & Nuclear Sciences and Niwa: Taihoro Nukurangi.
GeoNet, 2011. *M 6.2 Christchurch Tue, Feb 22 2011*. [Online] Available at: https://www.geonet.org.nz/earthquake/story/3468575 [Accessed 4 July 2024].
Glavovic, B. C., Saunders, W. S. A. & Becker, J. S., 2010. *Land-use planning for natural hazards in New Zealand: the setting, barriers, 'burning issues' and priority actions*. Natural Hazards, pp. 54: 679-706. DOI: 10.1007/s11069-009-9494-9.
Kelly, K. E., 1991. *The Myth of 10-6 as a definition of acceptable risk*, Vancouver, Canada: Air & Waste Management Associated.
Manatū Taonga — Ministry for Culture and Heritage, 17 July 2023. *Eruption of Mt Tarawera.* [Online] Available at: https://nzhistory.govt.nz/eruption-of-mt-tarawera [Accessed 4 June 2024].
Ministry of Business, Innovation & Employment, 2023. *Building Performance - Rapid building assessment placarding system*. [Online] Available at: https://www.building.govt.nz/managing-buildings/managing-buildings-in-an-emergency/rapid-building-assessment-placarding-system [Accessed 11 July 2024].
Taig, T., Massey, C. & Webb, T., 2012. *Canterbury Earthquakes 2010/11 Port Hills Slope Stability: Principles and Criteria for the Assessment of Risk from Slope Instability in the Port Hills, Christchurch*, Lower Hutt, New Zealand: The Institute of Geological and Nuclear Sciences Limited (GNS Science).
Television New Zealand 1 News, 2023. *Over 2100 properties red, yellow stickered post-cyclone.* [Online] Available at: https://www.1news.co.nz/2023/03/07/over-2100-properties-red-yellow-stickered-post-cyclone/ [Accessed 4 July 2024].
The New Zealand Government, 2002. *Civil Defence Emergency Management Act 2002*. Wellington, New Zealand: Government of New Zealand.
The New Zealand Government, 2004. *Building Act 2004.* Wellington, New Zealand: Government of New Zealand.
Thomas, K.-L., 2018. *Research to inform Community-Led Action to Reduce Tsunami Impact, Wharekauri-Rekohu-Chatham Islands, Aotearoa-New Zealand*, Christchurch, New Zealand: University of Canterbury.
Worksafe - Mahi Haumaru Aotearoa, 21 February 2024. *Prosecutions: Whakaari/White Island.* [Online] Available at: https://www.worksafe.govt.nz/laws-and-regulations/prosecutions/whakaari/ [Accessed 4 July 2024].

ENHANCING GEOTECHNICAL DESIGN EFFICIENCY IN COMPRESSIBLE SOIL WITH ARTIFICIAL INTELLIGENCE USING GENETIC ALGORITHMS

Ye Win (Douglas) Tun

WSP, 900 Ann St, Fortitude Valley QLD 4006, douglas.tun@wsp.com

ABSTRACT

This paper presents an unconventional approach to optimise geotechnical designs in compressible soil using Genetic Algorithms (GA), a subset of Artificial Intelligence (AI) algorithms. GA enhances the efficiency of two geotechnical designs: a parametric study and geometric optimisation in this paper. Geotechnical engineers primarily rely on empirical and analytical approaches over Finite Element Modelling (FEM) due to their computational efficiency and extensive literature. However, FEM holds excellent potential for future geotechnical design due to its ability to capture complex geometry, consider soil-structure interaction, and benefit from tremendous improvements in computational speed. GA integrates with the FEM software PLAXIS2D using the Python programming language and proposes an efficient method for design optimisation in this paper. It explores constrained optimisation approaches tailored to project-specific requirements and facilitates the exploration of various design cases, presenting results in a four-dimensional interpretation. The advantages and drawbacks of the methodology are highlighted through two case studies. This approach aims to advance the integration of AI-driven optimisation methods among geotechnical engineers, paving the way for efficient and sustainable geotechnical solutions.

1 INTRODUCTION

In geotechnical engineering, ground conditions with compressible material layers (clay, silt, and organic soils) can lead to design challenges due to low strength and high compressibility. These conditions can cause excessive settlements and stability issues without appropriate ground treatment. Ground improvement techniques can enhance the mechanical properties or properly control the natural soil variation while ensuring the safety and stability of the design. Traditional approaches include preloading or excavating and replacing techniques.

Geotechnical investigation (GI) and laboratory testing are the industry standard approaches to derive geotechnical design parameters. The primary disadvantages of GI and laboratory testing in compressible soil are the cost and the significant duration required to complete the test, especially when collecting a representative sample for testing. Back analysis using settlement plates is often considered a cost-efficient approach compared to extensive laboratory tests. Settlement plates provide real-time, in-situ data on soil behaviour under actual load conditions with an interpreted soil profile from GI, which can significantly enhance the accuracy of design parameter prediction (Biram, 2019). Australian Government Geoscience Australia (AGSA) also encourages innovative approaches like InSAR, which has excellent future potential for monitoring the settlement.

These monitoring data can be used to perform back analysis, in which monitored settlement data are compared to initial predictions, and soil parameters are adjusted accordingly. This iterative process helps refine the geotechnical model without the need for extensive laboratory testing. The challenge of back analysis is fitting settlement plate data with the calculated settlement results from the estimated consolidation parameters. This repetitive task of estimating consolidation parameters to match the calculated results with monitoring data can be done with the help of a Genetic Algorithm (GA).

In recent years, the integration of Artificial Intelligence (AI), Machine Learning (ML), and Deep Learning (DL) into engineering applications has shown great potential in enhancing the efficiency and accuracy of design processes (LeCun et al., 2015). AI is the overarching field that includes both ML and DL, where ML provides the framework for learning from data. DL extends this framework to more complex, layered neural networks for handling intricate and large-scale data-driven tasks. AI is often more suitable than ML and DL in day-to-day geotechnical engineering problems. This is mainly due to the spatial variation and uncertainties in geotechnical design properties as well as the limitations and reliability of the data in the geotechnical engineering industry.

The convenience of not requiring gradients is commonly appreciated by users of genetic algorithms. In the case of multiple design solutions, GAs have an advantage because they can handle multimodal problems as well. Other common optimisation methods in engineering are particle swarm optimisation (Reale, 2015), ant colony (Kahatadeniya, 2009), and some nature-inspired algorithms (Yang, 2014).

In this paper, the Python programming language was used to integrate GA with the FEM software PLAXIS2D to propose an optimisation methodology for geotechnical designs. Two case studies are presented in the paper. Case Study 1 focuses on the parametric study of the soft soil design parameters, whereas Case Study 2 emphasises optimising the design geometry. Alternative software with different programming language platforms can be used with the proposed method.

2 METHODOLOGY

Elastic settlement in compressible soil refers to the immediate deformation in soil when it is subjected to a load (embankment or structure). It happens instantly after the load is applied, reflecting the soil's immediate response to the stress due to the Soil's Elasticity (Young's Modulus *'E'* and Poisson's ratio '*v*'). Either the applied load is not removed, or the water table is lowered, and the subsurface profile experiences additional stresses beyond the existing overburden stresses. The pore water pressures initially resist these additional stresses. However, these excess pore water pressures dissipate, and the load is gradually transferred to the soil skeleton, increasing the soil's effective stress equivalent to the dissipated excess pore water pressure, known as primary consolidation (Ameratunga, 2021).

The following parameters are the critical geotechnical design parameters for the primary consolidation assessment in this paper: Compression Ratio ($CR = C_c/(1+e_0)$), Recompression Ratio ($RR = C_s/(1+e_0)$), coefficient of consolidation (C_v) or permeability ($k_v \approx 0.5k_h$), and Pre-consolidation Pressure (σ'_p). C_c and C_s are the Compression index and Swelling index, respectively. These indexes can be converted to the corresponding ratio by dividing with ($1+e_0$), where e_0 is the initial void ratio. Generally, pre-consolidation pressure can be considered in the calculation using the Over-consolidation Ratio (OCR) or Pre-overburden Pressure (POP) (Das, 2008). C_v dictates the consolidation rate, which is influenced by soil permeability. There are different approaches to correlating the coefficient of consolidation (C_v) and permeability (k_v). A common method that uses a fundamental theoretical relationship is presented in Eq.1. (Ameratunga, 2021)

$$k_v = xk_h = \frac{C_v\gamma_w}{M_v} = C_v.\gamma_w.m_v = C_v.\gamma_w.\frac{0.434CR}{\sigma'_{avg}} \quad (1)$$

where γ_w is the unit weight of water, M_v is the coefficient of compressibility, m_v is the coefficient of volume compressibility, σ'_{avg} is the average vertical normal stress during consolidation, and x is assumed to be 0.5.

The subsequent stage of this time-dependent process is secondary compression or creep. Creep involves a readjustment of soil particles under a constant load and occurs over an extended period. In traditional Terzaghi's consolidation theory (1943), creep is often accounted for using the secondary compression index ($C_a = C_{ae}(1+e_0)$), which characterises the volume change rate during the secondary consolidation phase. Mesri and Godlewski (1977) studied the secondary compression of various soils and provided empirical relationships in determining C_a. This paper used PLAXIS2D with the Soft Soil Creep (SSC) Constitutive Model.

2.1 Genetic Algorithm 'GA'

GA uses an analogy to Darwin's theory of evolution, aiming to improve a set of parameters to obtain even better sets according to a particular goal. GA's ability to function without gradient information is highly valued among users, especially for parametric studies in geotechnical design (Tun et al., 2018). GA approach is advantageous in geotechnical engineering, where the design space is complex, and the traditional methods may not capture the optimal solution. GA is particularly effective in handling the non-linear and multi-modal nature of geotechnical optimisation problems (Tun et al., 2018).

Figure 1(b) presents the non-linear function 'Shekel' for typical geotechnical design illustration purposes. It presents many similarities with geotechnical problems in terms of complexity and non-linearity. Geometric inputs like *the length* and *the embedment depth* may lead to several *settlement* results. This scenario can be defined as a non-linear optimisation problem in numerical terms. Suppose the objective is to achieve the design-specific *settlement*. In that case, the standard approach is to use the geotechnical engineer's previous design experience and several trials and errors while running numerous modelling simulations. This can be more challenging if the problem is a parametric study. There is no guarantee that the results are the optimum solution. It can be time-consuming to solve, and the potential for better design options may be limited to the engineer's previous design experience or creativity.

This paper presented parametric and geometric studies without relying on existing data, making GA particularly suitable. A genetic algorithm aims to evolve a set of parameters (individuals) to obtain better individuals. The integration of GA and PLAXIS2D is illustrated in the flowchart in Figure 1(a). All the annotations related to the GA algorithm will be defined with the $_{GA}$ subscript to differentiate them from Geotechnical-related parameters. GA started with the *Individuals and Population* stages, where potential parameters, 'P_{GA}', are randomly generated within the range selected by the geotechnical engineer. This P_{GA} is a set of consolidation parameters in Case Study 1 and geometric parameters in Case Study 2.

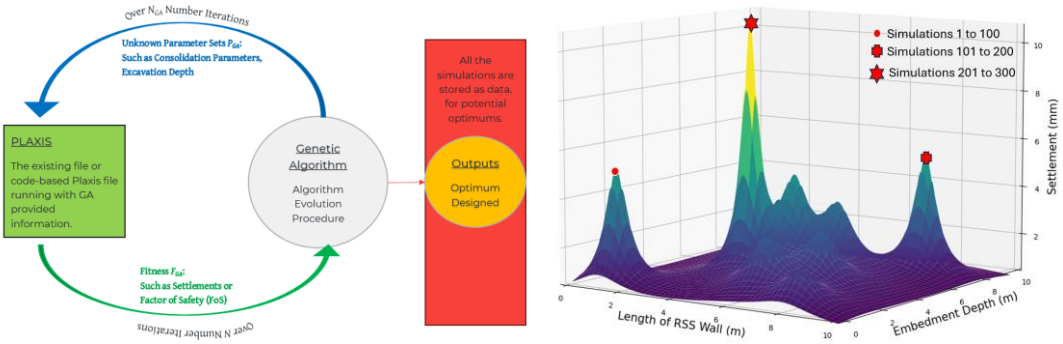

(a) (b)

Figure 1: (a) Flowchart for the Integration of GA and PLAXIS2D. (b) An example of a Geotechnical problem as the Shekel Function and how mutation works (illustration purpose only)

GA needs the potential parameter ranges for P_{GA}, which is known as a constrained optimisation approach. P_{GA} is then used in the PLAXIS2D file. After running all the numerical simulations with P_{GA}, the results are extracted to calculate the fitness value 'F_{GA}' using the fitness function 'F_{PGA}'. The aim is to minimise the F_{GA}. The detailed GA procedure can be found in Tun (2018). GA continues to iterate through these stages until a stopping criterion is met or arrives at a fixed number of defined iterations, 'It_{GA}', and each iteration is a defined number of simulations ($N_{Sim,GA}$).

Mutation is one of the critical components of the GA. It is applied to the $P_{GA,\ New\ Gen}$, occasionally with provided probability, introducing random changes to individual genes to maintain genetic diversity and prevent premature convergence to local optima. Figure 1 (b) shows the first 100 simulations showing the local optimum. Once the mutation is provided, the chance of moving from local to global optimum will increase. Without mutation, the algorithm will stay in the local optimum and may not be able to arrive at the global optimum.

3 CASE STUDY 1 – PARAMETRIC STUDY WITH GA

This project is in a large landfill area that was previously designed using the surcharge loading technique for several decades. The settlement plate records the data throughout the surcharge loading period at the project location. In recent years, the existing infrastructure at the site location needs to be upgraded with a new additional structural load for the existing pile foundation system. The scope of work was to assess the design adequacy of the existing pile from the additional loads.

Existing geotechnical information from the 1970s shows that the ground stratigraphy comprises various layers of the study area. Starting from the top is a FILLS (Loading Material) layer, followed by the Upper Clay Layer (UCL) (approx. 5m thick), clayey SAND, and Lower Clay Layer (LCL) (approx. 7m thick). A thick silt, sand, and gravel stratum is between the LCL and Rock Layer. Due to project site restrictions, geotechnical borehole drilling was challenging. Conducting back analysis with numerical models at the early design stage was done to gain confidence in the design parameters. The nearest old CPT data was used to interpret the ground profile. The back analysis involved a comprehensive evaluation of PLAXIS2D parameters using the surcharged load history.

In settlement design cases, back analysis fits two curves plotted in two axes (Figure 2(a)). These curves are plotted between settlements (y-axis) against the time (log) (x-axis). It is challenging for engineers or GA to define which parameters are calibrated well, or in other words, what calibration gives the best Fitness value (F_{GA}). This paper proposes that the fitness value F_{GA} can be calculated by the Fitness function (F_{PGA}) shown in Eq.2.

$$F_{PGA} = \frac{\sum_0^{n=number\ of\ data\ poitns} |s_{\ Settlement\ Plate} - s_{PLAXIS2D}|}{n=number\ of\ data\ points} \quad (2)$$

First, 'Δs' calculates the difference between Settlement '$s_{Settlement\ Plate}$' from settlement plate data and PLAXIS2D 's_{PLAXIS}' results for each date ($t_1, t_2, t_3, \ldots, t_n$). Then, divide the absolute value of $|\Delta s|$ by the total number of recorded dates (total data points). This will be the Fitness function 'F_{PGA}'. GA will minimise the F_{PGA}, closing the gap between the $s_{Settlement\ Plate}$ and s_{PLAXIS}. This parametric study used UCL and LCL consolidation parameters to match the settlement plate data against the PLAXIS2D results. These consolidation parameters can be denoted as P_{GA} in GA.

Four cases with different ranges were studied to check the robustness of GA. In the first two cases (RID 1 and 2), consolidation parameters for both UCL and LCL were used. The remaining cases (RID 3 and 4) only consider the UCL consolidation parameters. RID 1 and 2 have ten unknowns, but RID 3 and 4 have five unknowns. Also, RID 1 and RID 3 have a more comprehensive range than RID 2 and 4. These ranges of consolidation parameters were provided by the

project-wide design parameters and literature. All the available information was correlated to PLAXIS2D input parameters to provide an acceptable value. The optimised design parameters with the lowest fitness are stated in Table 1.

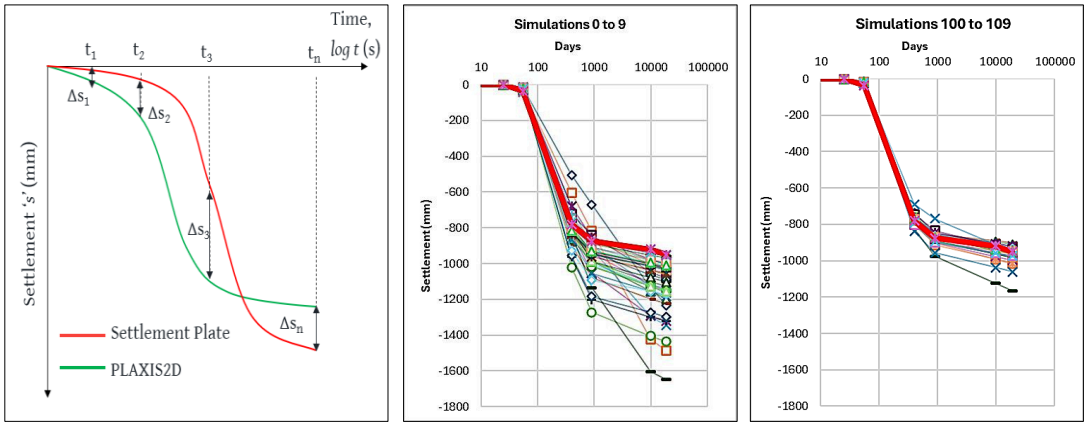

(a) (b) (c)

Figure 2: (a) Fitness Calculation F_{PGA} for the CS1 from Eq.2. (b and c) Evolution of fitting the Settlement Plate (red line) with GA (b) First 10 Simulations and (c) After 100 simulations.

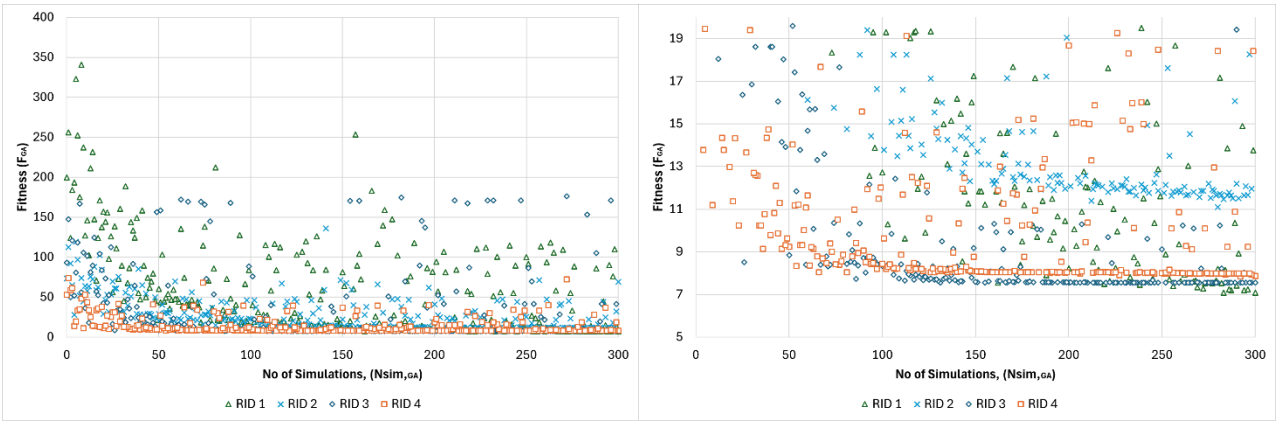

(a) (b)

Figure 3: (a) Summary of all the Fitness 'F_{GA}' from all the cases, and (b) Fitness value between 5 to 20

Iteration 'It_{GA}' and several populations '$Pop_{P,GA}$' were initially set. In CS1, 30 iterations with ten populations were used, giving 300 numerical simulations '$N_{Sim,\ GA}$'. The goal was to minimise the value of F_{GA} in the provided $N_{Sim,GA}$. Figure 3 presents all the RIDs' results, where their F_{GA} values decreased with the increasing number of simulations. In Figure 3 (a), all the F_{GA} values were very high at the first 0 to 75 simulations, and then the F_{GA} values were significantly lower. Figure 3 (b) focuses on the F_{GA} values between 5 to 20. Figure 3 (b) shows that RID 3 and 4 converged faster than others. The fitting plots from early and late simulations from GA are presented in Figure 2.

Table 1: CS1 Optimised Design Parameter for UCL and LCL.

		UCL[2]					LCL[3]				
Range ID (RID)	F_{GA} (mm/data)	C_c	C_s	C_{alpha}	k_v (m/day)	OCR	C_c	C_s	C_{alpha}	k_v (m/day)	OCR
1	6.5	0.503	0.0799	0.021	1.06E-04	1.35	0.955	0.100	0.023	6.64E-05	1.50
2	10.3	0.553	0.0799	0.020	1.30E-04	1.33	0.901	0.085	0.020	4.34E-05	1.47
3	7.5	0.590	0.0705	0.020	1.29E-04	1.47	0.910[1]	0.090[1]	0.020[1]	5.26E-05[1]	1.46[1]
4	7.9	0.539	0.0789	0.022	1.16E-04	1.36	0.910[1]	0.090[1]	0.020[1]	5.26E-05[1]	1.46[1]

Note: 1 The parameters do not vary for optimisation. 2 Void radio for UCL is 1.5. 3 Void radio for UCL is 1.7.

As illustrated in Figures 2(b) and (c), the GA estimation initially did not fit well with the settlement plate data (red line). However, it got better with the increasing number of simulations. Although the GA's predictions were closer to the data, several cases were significantly far from the actual data. This was due to the mutation stage of GA, which helps the algorithm avoid the local optimum and move toward the global optimum. In general, the proposed approach's limitation is that there are many combinations of parameters to match a settlement plate with the calculated settlement. The number of combinations can significantly increase with more compressible layers or unknown parameters. Therefore, engineering judgment is required to provide a realistic parameter range.

4 CASE STUDY 2 – GEOMETRIC OPTIMISATION WITH GA

Case Study 2 (CS2) represents several areas of the project site from one of the major road transport projects. It is in the greenfield area with compressible soil layers (Figure 4). The compressible soil ranges from soft to firm clay, varying from one site location to another. The compressible material has a similar range of parameters as the UCL material mentioned in Table 1, whereas the Engineering Fill is Class A material from Queensland Transport & Mains Road-MRTS04. Other materials' parameters have high stiffness, and most of their settlement is due to the elastic settlement.

This proposed GA assessment was done at the early stage of the design for option engineering. One option was to remove the compressible soil and replace it with a non-compressible engineering fill. This assessment did not design the mechanical strength inside the RSS wall. The design only considered the settlements and factor of safety (FoS) when placing the RSS Wall and engineering fill materials (grey colour in Figure 4). The primary objective of the GA application was to reduce the length of the RSS wall, utilise the engineering fill and minimise the excavation depth. The extent of the RSS wall depends on several factors, including the ground profile, wall height, loading conditions, and local design standards. The design-specific settlement is 150mm, and the minimum factor of safety (FoS) value is 1.5.

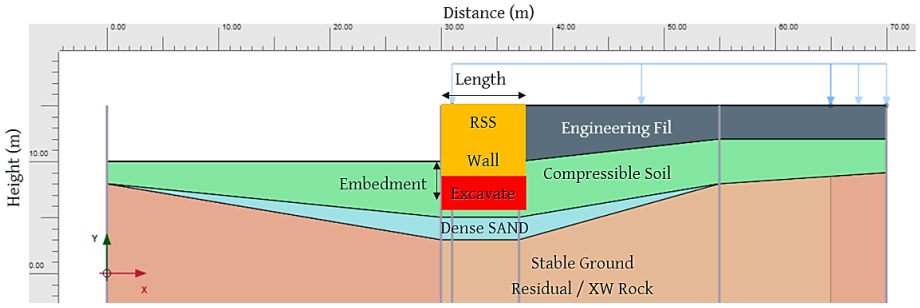

Figure 4: The ground profile and RSS wall

$$F_{PGA} = |s_{PLAXIS} - 150| + f(RSS_{unknowns}) \quad (3)$$

The fitness function is presented in Eq. 3, where s_{PLAXIS} is the settlement results at the top of the RSS Wall from PLAXIS2D. Introducing $f(RSS_{unknowns})$ can minimise the size of the RSS wall and excavation depth, which is the additional fitness component function with the weighted factors for RSS wall geometry. The optimisation speed depends on the assumed weighted factors. A similar methodology can be found in Tun et al. (2018).

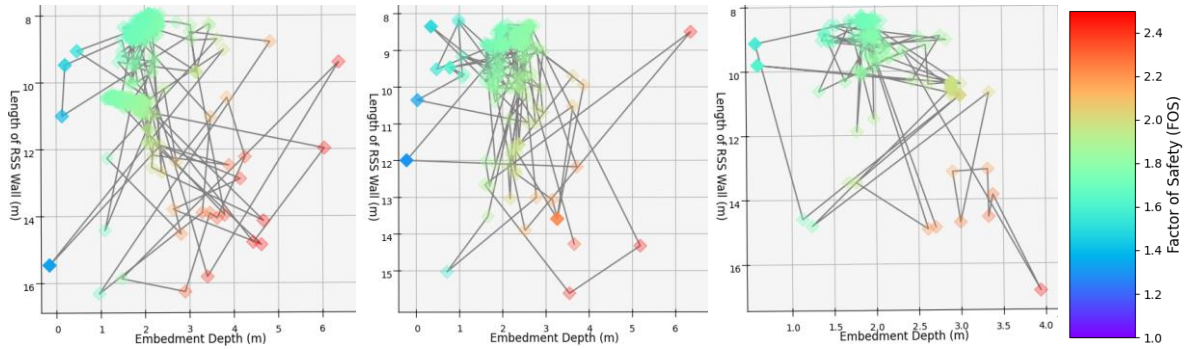

(a) (b) (c)

Figure 5: GA's optimisation evolution path with increasing simulation: (a) Trial A, (b) Trial B, and (c) Trial C. Factor of Safety Contour Bar (Purple = 1.0, Blue = 1.5, Green = 3.0 and Red = 5.0)

The fitness function from Eq.3 was used to find all the potential combinations of RSS wall size that can lead to a settlement of 150mm during the design life. Three trials were done; the results are presented in Figure 5 (a) to (c). These figures show the GA optimisation path during the evolution of 200-300 simulations. The data points are colour-coded, representing the FoS values ranging from 1 to 2.5. Different embedment depths and lengths of RSS wall ranges were investigated, and they were named Trails A, B, and C. Trial A had the most comprehensive range, and Trial C had the lowest range. Figure 5 (a) to (c) shows that FoS 1.5 to 2 were concentrated in the area between approximate embedment depth from 1.5 to 2.5m, and the length of the RSS wall varies between 8 to 9m.

The results from all the data combinations in Figure 5 were combined and highlighted in Figure 6. Figure 6 (a) highlights that most of the combinations show a settlement of 150mm. GA also converged these combinations to the smaller RSS wall size by concentrating all the data points in 1m to 2m embedment with an 8m long RSS wall length in Figure 6 (b).

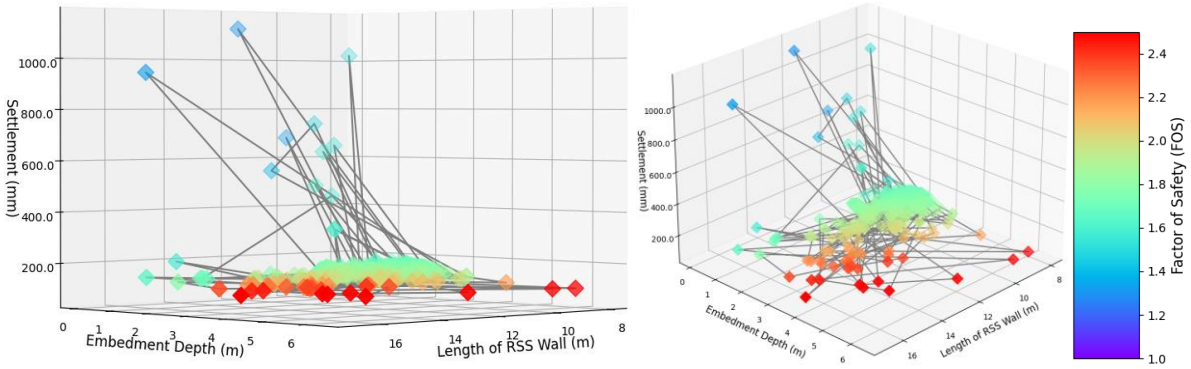

(a) (b)

Figure 6: GA's optimisation evolution path with increasing simulation: (a) Highlighting Settlement, and (b) Four-Dimensional (4D) Interpretation – FoS Colour Bar, Settlement, RSS Wall Length, and Embedment Depth.

5 CONCLUSION

The integration of GA with FEM for geotechnical design in compressible soils offers a promising approach to enhance design efficiency and optimise complex engineering problems. However, it is crucial to understand that this methodology should serve as an assisting tool only and not to replace essential engineering concepts and judgment. The GA approach is more suitable when addressing complex problems, like those in Case Studies 1 and 2, where trial and error may be time-consuming or unachievable with manual input approaches. Automation approaches should be considered before applying GA or other AI algorithms. The proposed methodology holds excellent potential for the future of geotechnical engineering. Other alternative AI optimisation techniques like particle swarm, cuckoo, and ant colony optimisation are recommended for future studies.

6 REFERENCES

Ameratunga, J. (2021). *Soft Clay Engineering and Ground Improvement*, CRC Press.

Back, T. (1996). *Evolutionary algorithms in theory and practice,* Oxford University Press.

Biram, K. (2019). Surcharge design using a probabilistic framework. In: *Proceedings of the 13th Australia - New Zealand Conference on Geomechanics*, Perth, Australia. Theme 6: Soft Soil Engineering. Golder Associates Pty Ltd, Brisbane, Australia.

Das, B.M. (2008). *Fundamentals of Geotechnical Engineering*. 3rd ed. Boston: Cengage Learning.

Kahatadeniya, K. Nanakorna, P. Neaupane, K.M. (2009). Determination of the critical failure surface for slope stability analysis using ant colony optimisation, *EngGeol*, 108:133–41. https://doi.org/10.1016/j.asoc.2024.111927.

LeCun, Y., Bengio, Y. and Hinton, G., (2015). Deep learning. *Nature*, 521(7553), pp.436-444. https://doi.org/10.1038/nature14539.

Mesri, G. and Godlewski, P.M. (1977). 'Time and stress compressibility interrelationship.' *Journal of Geotechnical Engineering Division*, 103(GT5), 417–430.

Reale, C. Xue, J. Pan, Z. Gavin, K. (2015). Deterministic and probabilistic multi-modal analysis of slope stability. *Computer Geotech*, 66:172–9. https://doi.org/10.1016/j.compgeo.2015.01.017.

Terzaghi, K. (1943). *Theoretical Soil Mechanics*. John Wiley & Sons.

Tun, Y. Llano-Serna, M.A., Pedroso, D.M. and Scheuermann, A. (2018). Multimodal reliability analysis of 3D slopes with a genetic algorithm. *Acta Geotechnica*, 14(1), pp.1-17. http://dx.doi.org/10.1007/s11440-018-0642-9.

Yang, X. (2014). Nature-inspired optimization algorithms. Amsterdam. *Elsevier.*

REMEDIATION OF CAVES BELOW PRINCES HIGHWAY WEST, YAMBUK, VIC

Aleksandar Radmanovic
Department of Transport & Planning, VICTORIA, AU

ABSTRACT

This paper presents a hazard assessment, construction methodology, and investigation for remediating an extensive shallow cave system within a Pleistocene calcarenite geological unit that partially closed the A1 Princes Highway West in Yambuk, South-western Victoria. In January 2023, a road grader unintentionally punctured a 0.5 m thick roof slab of a previously unidentified shallow karst cave with a vertical cavity dimension of 3 m during road widening works on the A1 Princes Highway West. The cave posed a safety risk for the highway, which is a freight route, requiring an extensive sub-surface investigation to assess the extent of the cave and to develop a de-risking rehabilitation (or remediation) methodology. The investigations revealed a 'domed' fanning cave which formed part of a multilevel chamber system and an extensive network of corridors. Void volumes affecting the highway exceeded 3000 m^3. Close inspection and collaboration with the contractors allowed for excavation of the cave roof, deemed necessary due to the collapse caused by the grader. A first principles approach was adopted to predict the consequence of cave subsidence and helped delineate the excavation area prior to implementing a 'cave-plugging' remedy. The remedy included the compaction of engineered fill. Additional cost-effective treatments adopted included compaction of pockets of the excavated calcarenite and infilling the caves with mass concrete through 300 mm diameter 'entry' cored holes to avoid large volumes of excavation. Drainage blankets and geotextile layers were used to minimise the impact on subsurface hydrogeology and prevent wash-out of the plug. The construction approach was considered cost-effective and lessened structural impacts to the surrounding cave structures.

1 INTRODUCTION

1.1 PROJECT HISTORY

Princes Highway West is a key arterial freight route which services the most populous regional towns of western Victoria, being Colac, Warrnambool, and Portland. The route is necessary for the transit of OSOM (Over Size Over Mass) vehicles such as wind turbine components transported from the Port of Portland to regional wind farms. The Department of Transport and Planning (DTP) regularly undertake re-surfacing, shoulder widening and road widening to allow for safer turning lanes along this route. This paper discusses caves encountered during a shoulder and turning lane widening highway upgrade project at the intersection of Princes Highway West and Greens Road, 2 km west of the small township of Yambuk. A sub-surface investigation, consisting of 10 test pits excavated in the pavement and adjacent grassed verges using a 5-tonne excavator was conducted in mid-2021 to inform the pavement design. Each test pit refused on rock material at depths of between 1 m and 3 m, with no evidence of underlying cavities. In early 2023 during the highway upgrade works, a 20-tonne grader punctured the roof slab of a cave at the Greens Road intersection when compacting a sub-base crushed rock layer. The puncture was excavated to reveal a cave with a void thickness of 2-3 m, a width of 7 m, a length of 20 m and a roof thickness of 0.5-1 m.

1.2 FIRST RESPONSE & PROJECT DIRECTION

The DTP Project team and its internal Design Services (which the author is a part of) responded to the cave puncture by stopping works throughout the project area until the risk posed by the caves was mitigated by:

- understanding the extent of the caves beneath the site by exposing the full extent of the punctured cave and any connecting caves
- attempting to understand the cave roof behaviour prior to designing the remedial works (an engineered plug)

Design Services could not source a proven methodology to assess the behaviour and stability of the cave; developed and proven methodologies such as the Q and RMR methods (Bieniawski, 1976) show how to assess the relationship between ground defects and engineered support systems (e.g. rock bolts) for man-made excavations such as tunnels and open pits. These methods were not used by Design Services because (i) natural cave structures are not man-made excavations and (ii) nor could the caves be accessed in a way which allowed for installation of engineered support systems as outlined in those methods. Design Services instead adopted first principle approaches to (i) choose investigation methods suitable

for determining the extent of the cave system, (ii) understand and predict the behaviour of the cave roof supporting the overlying road, (iii) assess and assign a level of risk, and (iv) develop a remediation detail to 'plug' any caves or excavated areas with engineered fill.

2 GEOLOGY

2.1 GEOLOGICAL SETTING

The 1:250,000 Seamless Geology Map No. 48 Warrnambool-Mortlake (Welch et al., 2011) shows that the site is underlain by the Pleistocene-age Bridgewater Formation (BWF). The BWF is a bioclastic calcarenite (aeolianite) formed by deposition of dune sediments (quartz sand) in shallow tidal, dune and lagoon environments during sea-level fluctuations throughout the Pleistocene (~2.6 Ma to ~12,000 years ago). It is a geological unit that extends along the southern Australian coastline from Victoria to South Australia. The thicknesses of the BWF varies between 5 m and 45 m but is typically 15-25 m. The BWF is weakly cemented but is moderately cemented where caves have formed, with up to 30% of the composition being cement. The Bridgewater Formation is highly variable in carbonate content (varying from 26% to 96% carbonates, and 5% to 73% sub-rounded quartz in Bats Ridge) across southern Victoria (Lipar and Webb, 2015). Regional dating indicates deposition of the BWF between 230,000 and 250,000 years ago (White, 2000).

2.2 CAVE FORMATION AND STRUCTURE

2.2.1 Cave Speleogenesis

Drilling investigations (see Section 3.2) showed that the Greens Road cave roof is shallow (void appears as little as 1 m depth below road surface), linear, multi-entranced, multi-level (excavations indicated level thicknesses of 2-3 m) and with a length of at least 30m which spans across the highway reserve and continues below private properties. The cave roof is a calcrete capping layer or 'caprock', a competent layer formed by precipitation of calcium carbonate ($CaCO_3$) (White, 1994). During the induced collapse of the cave roof, the caprock was found to comprise high strength calcrete typically 2 m thick.

2.2.2 Cave Structures – Dome chambers, Flatteners and Pillars

Figure 1 below shows the photographed cave structures below Greens Road. The most common cave structures are 'flatteners' which are voids characterised as being flat, wide and typically 0.5 m - 1.5 m thick (White, 1994). The 'flat' shape of the Greens Road cave ceiling means the cave was possibly formed at the top of an old water table within a syngenetic cave system, characterised as a shallow horizontal cave system, comparable to the flat ceiling discovered in the limestone cave of Bats Ridge, Victoria (Grimes, 2006). The observed flatteners are located 2 m above the existing water table, meaning they likely were formed sometime in the Plesitocene period when sea levels were 2 m higher. Flatteners served as passages which connect multiple dome chambers. Dome chambers were measured to be 1.5 m - 2.5 m thick, 3-5 m in diameter and were characterised by collections of rockpiles at their base. Two key cave pillars (Figure 1c) were found to support the eastern and northern sides of the Greens Road excavated area. All structures were sighted from the perimeter of the Greens Road main excavation.

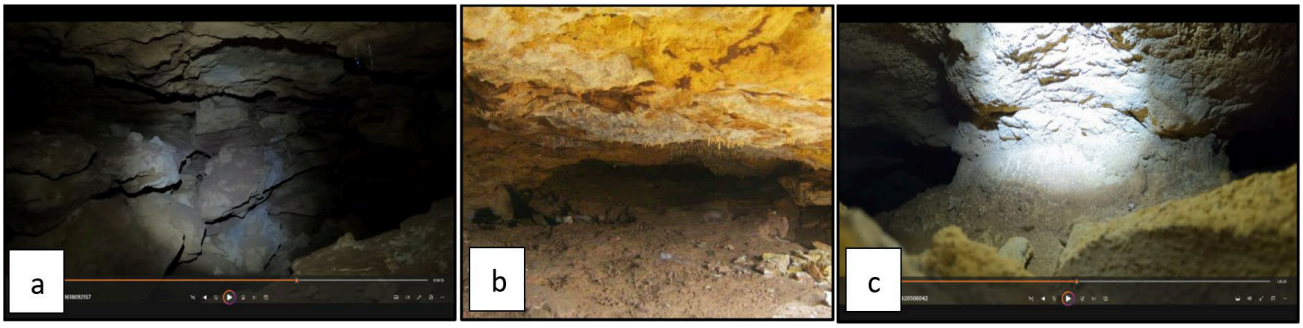

Figure 1: GoPro photographs showing cave structures: Dome Chamber (a), Flattener (b), Pillar (c)

3 INVESTIGATIONS

A combination of destructive and non-destructive exploratory investigations were conducted throughout the project area to reassure the project team that any sub-surface cavities would be discovered, cavity volumes estimated, and the associated risks mitigated. Targeted investigations were undertaken around the Greens Road intersection.

3.1 SEISMIC SURVEY

A Multichannel Analysis of Surface Waves (MASW) seismic survey was undertaken by Black Geotechnical Pty Ltd throughout the Project area. MASW survey limitations include that (i) the velocity data does not indicate size of voids but rather that it indicates possible existence of them, and (ii) that the geophones' influence perpendicular to the survey alignment was approximately 1 m. Correlation between confirmed voids (visuals, drilling) and MASW seismic data should be undertaken to assist with interpretation of MASW data where voids are not yet confirmed. General agreement was found between the confirmed presence of dome chambers 2 m - 3 m thick and 3 m - 4 m wide below 2 m of caprock, and the MASW velocity inversion from 400 to 700 m/s (inferred as caprock) to less than 300m/s (inferred as void) in two key locations. The MASW data captured on site appeared to show that caves did not extent throughout the remainder of the project area, which was supported by the subsequent drilling campaigns discussed in section 3.2.

3.2 DRILLING INVESTIGATIONS

Three week-long borehole drilling campaigns were undertaken with the assistance of Pells Sullivan Meynink (PSM) using two drill rigs on site. Eighty-three (83) boreholes were HQ cored throughout the Project area to depths of 3 m to 5 m, with a typical depth of 4 m. Approximately forty (40) boreholes were drilled at the Greens Rd Intersection, as shown in Figure 2 below. Borehole locations are shown using red and green dots, where a red coloured dot indicates presence of voids, and the green dot does not. A GoPro camera and light was attached to a hand-held pole and inserted into each borehole to capture images as shown in Figure 1. A 'targeted' drilling investigation was planned for areas inferred to have a high likelihood of caves. This planning was done by (i) interpolating a sub-surface profile between existing boreholes using logs and images and (ii) sighting the Greens Road excavation perimeter to approximate a cave trajectory and size beyond the line of sight. The targeted investigation allowed for boreholes 2.5-5 m apart (boreholes denoted by the capital 'T', i.e. T04), resulting in the discovery of multiple dome chambers around the excavation perimeter. Boreholes denotated by 'N' and 'S' represent the highway's north and south carriageways.

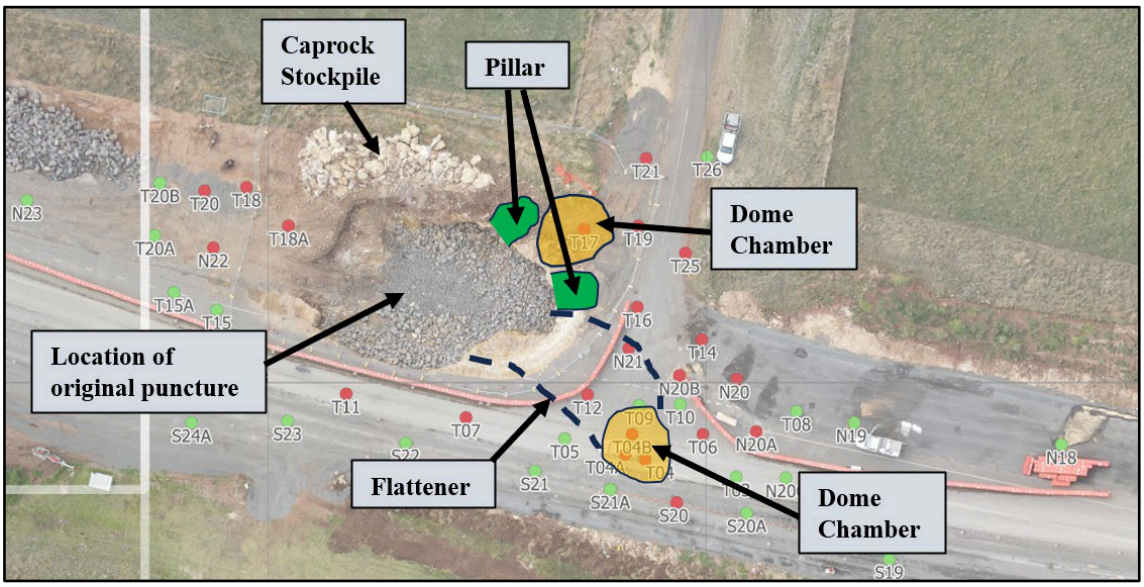

Figure 2: Greens Road Intersection – Main Excavation, Borehole Locations and Cave Structure Map

Typical rock cores were described as having 1-3 m of calcrete cap rock of HIGH strength, underlain by aeolianite comprising cemented sand. Uniaxial Compression Strength (UCS) testing undertaken on the caprock and a high variance in test results was found with results ranging between 0.6 MPa and 60 MPa (typically 20 MPa); however, test results between 2 MPa and 10 MPa were absent. Common failure modes included 'diagonal shearing and splitting' for >2 MPa samples, and 'disintegration' for <2 MPa samples. It was determined that UCS testing of the cave roof was not a reliable indicator of cave roof strength and stability due to a large variance in UCS for boreholes only 2-3 m apart.

3.3 EXPLORATORY EXCAVATIONS

Exploratory excavations were undertaken using two 30-tonne excavators with rock breaking attachments. The main purpose of the excavations was to collapse the 0.5-2.5 m thick cave roof west of the Greens Road intersection, around the location of the original cave roof puncture. The secondary purpose was to explore and reveal adjacent cave structures prior to using the Hazard Assessment (see Section 4) to 'chase' caves deemed required for remediation (excavation and backfilling).

3.4 LEARNINGS – INVESTIGATIONS

The following learnings were made from the investigations:

- 2-3 m deep test pits excavated with a 5-tonne excavator are not favourable for finding voids in the BWF.
- Drilling at intervals of 20-25 m (in each direction of highway) proved useful in locating voids/cave systems over a scale of hundreds of metres to 1-2 km.
- Targeted drilling (5 m intervals) in the BWF proved successful in locating and quantifying the size of sub-surface cavities in areas inferred to have a high likelihood of having cave structures.
- The MASW seismic survey data showed good correlation in predicting existence of dome chamber caves, later confirmed via borehole drilling. MASW data should be correlated with caves confirmed via boreholes or excavations. Nighttime MASW surveying may be needed to minimise disruptions to the geophone sensors from passive noise sources such as nearby vehicles or operations from nearby fuel stations.

4 HAZARD ASSESSMENT

4.1 AGS RISK ASSESSMENT

DTP's Roadside Geotechnical Hazard Management Plan (RGHMP) guidelines adopted a simplified version of the Australian Geomechanics Society (AGS) 2007 landslide risk assessment (AGS Landslide Taskforce, 2007) to undertake a risk assessment of the caves. The risk assessment was used to assign a risk level for vertical road steppings that could be caused by the collapse of a cave roof based on (i) locations of the steppings on the road and (ii) the speed and number of vehicles driving over the steppings. DTP's RGHMP guidelines do not permit vehicles at speeds of over 80 km/hr impacting a vertical surface step of greater than 200 mm, therefore the adopted treatment sought to eliminate any hazard (i.e. void below the road) which could result in a 200 mm vertical stepping at the road surface. The locations of the possible road steppings is imporant information to be inputted into the risk assessment because it shows that voids below a running lane will have greater risk level than the same voids below a road shoulder (because of a reduced traffic count and/or reduced vehicle speed on the road shoulder).

4.2 HAZARD ASSESSMENT

Detailed modelling of the cave, including accurate mapping of the rockmass defects (joints and bedding planes) below the road, was not considered feasible with the technologies known to be readily available. With the structural strength of the cave roofs below the road surface not being able to be determined, the project team conservatively assumed that each identified cave roof would eventually collapse, and the underlying void would be filled in by the collapsed material. Thus, the resulting vertical stepping at the road surface dictates whether the cave should be considered for treatment. A vertical stepping can be estimated using the following information: (i) the thickness of the void, (ii) the thickness of the roof material overlying the void, and (iii) a bulking factor of the roof material. A bulking factor of 1.33 for the aeolianite and caprock was adopted after measuring the slow collapse of the open cave perimeter after months-long exposure. Collapse of the BWF aeolianite appeared to be predominantly dictated by separation along the bedding planes, with defects normal to the bedding planes controlling the dimensions of the collapsed block(s). The typical block was noted to be tabular in shape, 0.2-0.5 m thick and 1-1.5 m long and wide, which is comparable to the size of the older detached blocks sighted at the floor of the domed chambers.

An example of using the Hazard Assessment is as follows: Acknowledging that a vertical step of less than 200 mm is acceptable at road level, it was estimated that a 1.2 m thick void below 3 m of unstable BWF rock would result in the void being filled by 1 m as the 3 m of collapsed material would bulk to roughly 4 m; leaving a 200 mm step at the road surface. Using this sexample, it's evident that either a thicker void or a thinner overlying roof would leave a surface step greater than 200 mm, thus resulting in the cave roof requiring excavation and a 'plug' treatment (see Section 5).

4.3 LEARNINGS – HAZARD ASSESSMENT

The following learnings were made from the hazard assessment:

- Detailed rock mass modelling could not be undertaken due to the impracticality of mapping rock defects that control the structural stability of the caves, and therefore modelling could not be used to inform a Hazard Assessment.
- Design Services assumed that the cave roof above each cave structure would eventually collapse. A Bulking Factor of 1.33 was applied to BWF material collapsing into an underlying void, resulting in a vertical stepping in the overlying road surface. The resulting displacement/settlement at the road surface was calculated and compared against the stepping allowable by DTP's RGHMP using a modified version of the AGS landslide risk assessment.

5 THE TREATMENT

5.1 THE 'PLUG'

The total volume of cavities at Greens Road was estimated to be approximately 3000 m^3 by a combination of interpolating cavity thicknesses recorded in boreholes and recording cavity measurements during surveillance of the exploratory excavations. It was decided to remediate the caves by (i) collapsing the roof of the caves were determined by the Hazard Assessment, (ii) excavating the base and perimeters of the cave to form a uniform base and batter slopes and (iii) filling in all excavated areas with an engineered fill 'plug'.

Figure 3a shows rocky fill used as 'plug' material for the lower half of the excavation (2-3 m in height), and the upper half of the excavation being filled with a Type A (DoT, 2015) clayey rock spalls material sourced from a local quarry and compacted using a developed site-specific method specification. Figure 3b shows design details implemented at the base and perimeter of the cave excavation. Bidim A64 geotextiles were installed at the base and side batters of the excavation to prevent the migration of the plug material into any connecting cave tunnels, with a basalt drainage blanket installed at the cave floor to allow the cave to maintain some of its hydrology.

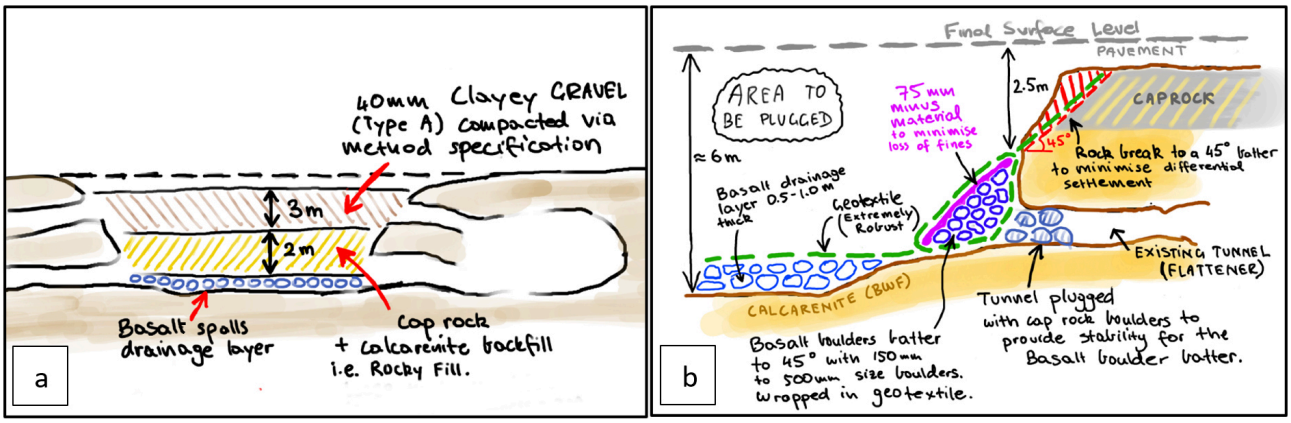

Figure 3: Backfill 'plug' materials (a), Design details at excavation base and perimeter (b)

Figure 4a shows the fracturing aerolianite rock blocks failing along the cave perimeter, and Figure 4b shows aeolianite and caprock material being reused as backfilling material to plug the excavated areas. Figure 4c shows the selection of 500-1500 mm wide aeolianite and caprock rock blocks for rock-breaking and down-sizing into smaller particles with the use of a 100 mm diameter hydraulic rock breaking chisel attachment. The caprocks were downsized to a 'rocky fill' composed of 100-300 mm (up to 500 mm) diameter rocks and sand particles. Pockets of excavated silty cemented material were not reused as plug material. Loose layers 400 mm thick were compacted to a final thickness of 300 mm. A 16-tonne vibrating padfoot roller required approximately 8 passes (4 up and 4 down) to achieve the final thickness, with powerful return-vibrations from the roller being indicative of an achieved high relative density.

Figure 4: Failing aeolianite blocks (a), Aeolianite and caprock used as the 'plug' backfill (b) and (c)

300 mm diameter holes cored through the caprock were used to pour 15 MPa Mass Concrete to fill-in small dome chambers. Pours were as quick as 15 minutes per truck. Holes were drilled adjacent these to assess the effectiveness of the concrete treatment using a down-the-hole camera. Pours were made in hourly stages, allowing initial pours to set rather than to potentially continue flowing into connecting tunnels.

5.2 LEARNINGS – THE TREATMENT

The following learnings were made during planning and construction of the treatment:

- A drainage layer (below the 'plug') should be provided to allow for relief against hydrogeological impacts caused by the excavation and backfilling works, and for drainage of the caves during flood events. Basalt rock spalls were used during this project as they are expected to be durable in saturated environments.
- A clayey rock spalls layer was seen as the preferred backfill material because it behaves as a 'plug' to slow the speed of surface water entering the upper cave areas. Surface water entering the cave is expected to be relieved via the basalt spalls drainage layer, with geotextiles placed around the plug to prevent loss of fines.
- The excavated BFW was able to be reused as 'plug' material by breaking the rock into a 'rocky fill' material with particle sizes ranging from 100-300 mm. The reuse of the BFW allowed for cost savings for the Project.
- A 45-degree batter was formed between the 'plug' backfill material and the adjacent in-situ ground (typically caprock) to minimise differential settlement along the contact between the in-situ ground and backfill plug.
- The backfilling of small dome chambers using mass concrete as described above was successful used to 'plug' a dome chamber in the centre of the highway in two days using 60 m^3 of concrete.

6 SUMMARY

Caves below Princes Highway West in Yambuk were identified and investigated during highway project works using a combination of destructive digging, closely spaced borehole drilling in high-risk areas, and non-destructive MASW seismic survey and widely spaced (>25 m) boreholes in the remainder of the project areas. A a conservative approach that did not assess whether a cave would collapse, but rather what the resulting vertical stepping at the road surface would be when collapse occurred, was used to determine which caves required treatment. The treatment of caves primarily included the battering of the caves' perimeter, and backfilling using a combination of Type A engineered fill, re-worked aeolianite and caprock material excavated during the investigation phase, and mass concrete poured through entry holes cored in the caprock. On-going visual monitoring of the Project area is planned to assess the efficacy of the remedial works. An inventory for arterial roads with potential for karst collapse is planned by DTP and will assist it with future investigations. Regionally, such areas include southwest Victoria, the Great Ocean Road, the Mornington Peninsula, Sale and Bairnsdale.

7 ACKNOWLEDGEMENTS

The author would like to thank the DTP for permission to publish this paper. The views expressed in this paper are those of the author and do not necessarily reflect the views of DTP. The author also wishes to thank the following: DTP Barwon Southwest Region, PSM, Black Geotechnical, Dr. Susan White from Wakelin Associates, Mibus Bros Contractors, and the Eastern Marr Aboriginal Corporation and the Gunditj Mirring Traditional Owners Aboriginal Corporation.

8 REFERENCES

Australian Geomechanics Society (AGS) Landslide Taskforce. (2007). Guideline for Landslide Susceptibility, Hazard and Risk Zoning for Land Use Management. *Australian Geomechanics, Vol 42, No. 1*.

Bieniawski, Z.T. (1976). Rock mass classification in rock engineering. *In Exploration for rock engineering, proc. of the symp*, 1, pp. 97-106.

Department of Transport (DoT) (2015). Section 204 – Earthworks. Department of Transport. Victorian Government. https://webapps.vicroads.vic.gov.au/VRNE/csdspeci.nsf/webscdocs/9C4882FDC5886201CA257BF900198C3E?OpenDocument

Grimes, K.G. (2006). Syngenetic Karst in Australia: a review. *Helictite*, 39(2), pp. 27-38. https://www.researchgate.net/publication/263467394_Syngenetic_karst_in_Australia_A_review

Lipar, M., Webb J.A. (2015). The Middle-Late Pleistocene Bridgewater Formation on Cape Bridgwater, South-western Victoria: Chronostratigraphy and Palaeoclimatic Significane. *The Royal Society of Victoria*, 127, pp. 81-91. https://www.publish.csiro.au/RS/pdf/RS15020

Welch, S.I., Higgins, D.V., Callaway, G.A. (2011). Surface Geology of Victoria 1:250,000. Geological Survey of Victoria, Department of Primary Industries. http://earthresources.efirst.com.au/product.asp?pID=1086&cID=16

White, S. (1994). Speleogenesis in aeolian calcarenite: A case study in Western Victoria. *Environmental Geology*, 23, pp. 248-255. https://link.springer.com/article/10.1007/BF00766739

White, S. (2000). Thermoluminescence dating of dune ridges in western Victoria. *Helictite*, 36(2), pp. 38-40. https://helictite.caves.org.au/pdf1/36.2.White.pdf

DYNAMIC ASSESSMENT OF JOINTED ROCK SLOPE STABILITY: FLAC MODELLING AND CONSTITUTIVE MODEL COMPARISONS

Ri Hong Kee (Cyrus), Neil Korte, Dan Andrews, Ananth Balachandra
Tonkin and Taylor, Auckland New Zealand
Geotechnical Engineer, Tonkin and Taylor, Auckland New Zealand, 1 Fanshawe Street, Auckland CBD, Auckland 1010, +64 022 0358 279, email: ckee@tonkintaylor.co.nz

ABSTRACT

This paper presents a dynamic stability analysis of jointed rock masses subjected to seismic loading using the FLAC finite volume method. Three constitutive models—Mohr-Coulomb, Hoek-Brown, and Bilinear Strain-Softening/Hardening Ubiquitous-Joint (SUBI)—were evaluated for their ability to simulate seismic responses in rock slopes. Ground motion data was derived from the Tokachi-Oki earthquake, and dynamic material properties were modelled based on field data and geotechnical testing. The study found that the SUBI model effectively captures strain-softening behaviour and jointed rock mass deformation under seismic conditions, offering more realistic displacement profiles compared to simpler models like Mohr-Coulomb and Hoek-Brown. This work highlights the importance of considering joint strength degradation in seismic slope stability assessments, informing future engineering practices for infrastructure design in seismically active regions.

1 INTRODUCTION

Rock slope failures during seismic events pose significant risks to infrastructure, as demonstrated by the Canterbury Earthquake Sequence (CES) and the Kaikōura earthquake in New Zealand (Heron et al., 2014; Massey et al., 2018). These events highlighted the impact of seismic shaking on jointed rock masses, where discontinuities such as faults and joints play a critical role in slope stability (Che et al., 2016). The complexity of these geological structures necessitates advanced numerical modelling techniques to accurately predict failure mechanisms during seismic loading.

This study focuses on evaluating the effectiveness of three constitutive models—Mohr-Coulomb, Hoek-Brown, and Bilinear Strain-Softening/Hardening Ubiquitous-Joint (SUBI)—in simulating the dynamic behaviour of jointed rock slopes. Unlike previous work that primarily used simplified assumptions, this research seeks to provide a comparative analysis of these models under realistic seismic conditions. By investigating how each model handles discontinuities and strength degradation, this paper aims to inform more accurate assessments of slope stability in seismically active regions

2 LITERATURE REVIEW

This section provides a brief background on dynamic stability of jointed rock slopes, emphasizing seismic wave propagation, the impact of rock discontinuities, and the application of numerical models for analysing seismic loading.

2.1 SEISMIC WAVE PROPAGATION IN THE JOINTED ROCK MASS

Seismic shaking at a site is influenced by the seismic source, distance, propagation path, and site-specific conditions. These factors determine the amplitude, frequency, and duration of ground motion, which are critical for evaluating slope stability (Kramer, 1996). High-amplitude ground motions, characterized by Peak Ground Acceleration (PGA), shaking duration, and frequency content, significantly impact slope stability under seismic loading (Jibson & Harp, 2016).

Topographic amplification, caused by seismic waves interacting with irregular surface topography, intensifies ground motion and contributes to landslides (Sepúlveda et al., 2005). Material contrasts within the rock mass, such as variations in stiffness and density, also affect wave amplification, influencing slope stability (Kramer, 1996). Discontinuities like joints and faults alter seismic wave propagation, acting as planes of weakness and critically impacting the dynamic response of rock slopes (Bai et al., 2019).

2.2 A REVIEW OF CONSTITUTIVE MODELS

Understanding the behaviour of rock masses under seismic loading requires an assessment of their elastic properties, such as Young's Modulus and Poisson's ratio, along with strength parameters (Itasca, 2019). Failure criteria like Mohr-Coulomb and Hoek-Brown define failure envelopes based on principal stresses and material constants, aiding in rock failure prediction (Hoek & Brown, 1997).

Rock joint strength is commonly characterized by the Mohr-Coulomb and Barton-Bandis criteria. This study utilizes a Mohr-Coulomb slip contact model to define joint strength, employing a bilinear failure criterion to represent joint shear strength. Post-peak strength behaviour in rock masses can be classified into four types: brittle, plastic, strain-softening, and strain-hardening (Wyllie, 2017). Brittle materials exhibit a rapid decrease in strength post-peak, while plastic materials maintain strength as strain accumulates. Strain-softening and strain-hardening describe reductions or increases in strength with increasing strain, respectively.

The Bilinear Strain-Softening/Hardening Ubiquitous-Joint (SUBI) Model is employed to simulate the behaviour of rock masses with a single preferential discontinuity set. This model captures the transition from peak to residual strength through strain-softening or hardening, providing a more accurate representation of rock mass behaviour during and after seismic events (Hudson et al., 2016). The different stress-strain behaviours mentioned above are illustrated in Figure 2.1.

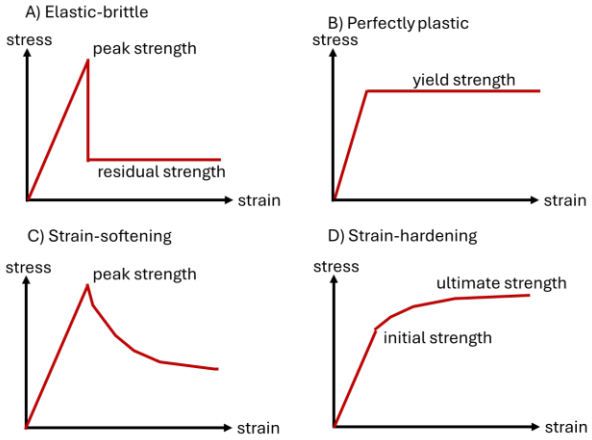

Figure 2.1: Stress-strain material behaviour (after Wyllie, 2017)

3 METHODOLOGY

3.1 STUDY AREA

The study area selected for this research is located within a seismically active region known for its complex geological structures, specifically in Hawke's Bay on the east coast of New Zealand's North Island.

3.1.1 Geological setting

The study area is underlain by the Matahorua Formation, comprising marine siltstone with interbedded sandstone and tephra beds. Major rock defects and joints identified during site investigations impact slope stability. Figure 3.1 shows the geological map, highlighting key formations and faults that influence seismic behaviour, while Figure 3.2 provides the stratigraphic column illustrating the rock layers that affect seismic response.

The area lies on the Hikurangi subduction zone, where the Pacific plate subducts beneath the Australian plate at 40mm/year (Stirling et al., 2012), contributing to its high seismic activity, as shown in Figure 3.1.

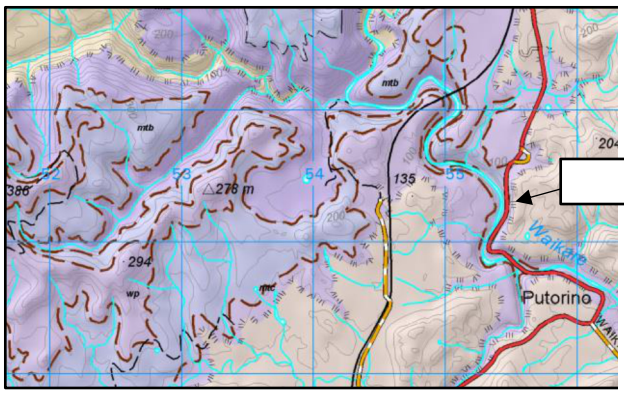

Figure 3.1: Geological map from Bland (2006)

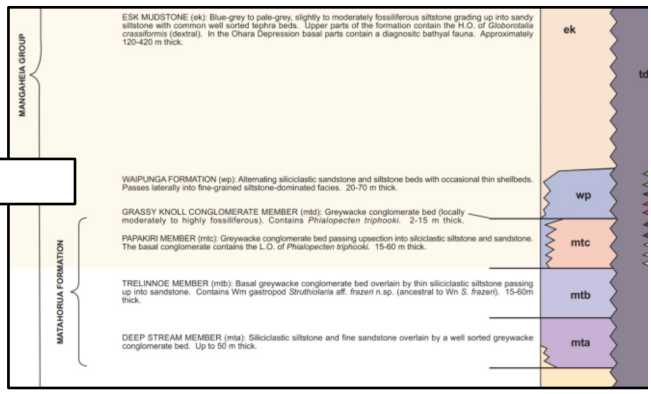

Figure 3.2: Stratigraphic column from Bland (2006)

3.2 MODELLING APPROACH

Ground motion data was derived from the Tokachi-Oki earthquake (RSN4032552), scaled by a factor of 0.96. The earthquake had a magnitude of Mw 8.3, with a total duration of 28 seconds, and peak ground acceleration (PGA) applied to the base of the model. Ryleigh damping of 1% critical damping was applied, and model boundaries were set at twice the slope width to reduce boundary effects (Itasca, 2019).

Free-field boundary conditions with a rigid lower boundary were employed for dynamic analysis, and the earthquake's acceleration history was applied. The models evaluated include Mohr-Coulomb, Hoek-Brown and Bilinear Strain-Softening/ Hardening Ubiquitous-Joint (SUBI) constitutive models. Monitoring of wave propagation, acceleration, velocity, and displacement was carried out at fifteen points across the slope, including shallow points near the crest surface to ensure proper observation of the slope's shallow behaviour.

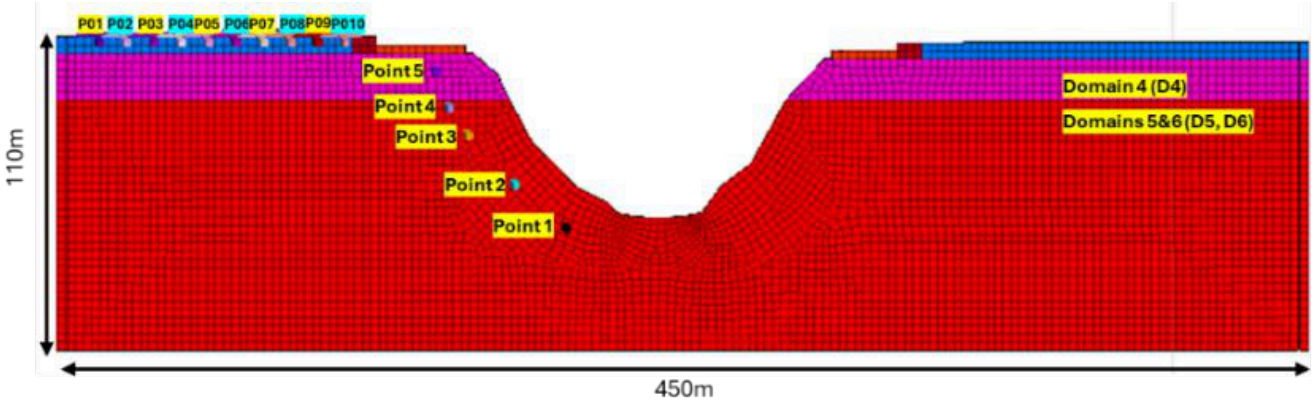

Figure 3.4: FLAC3D model and geometries of the rock slope

3.2.2 Material properties

Rock mass parameters were obtained from geotechnical testing and geophysical surveys, as shown in Tables 3.1 and 3.2 for the three models. Joint strength values are listed in Table 3.3. In the SUBI model, cohesion degradation is used to simulate the brittle behaviour of certain rock types: Domain 4 (slightly to moderately weathered, weak to moderately strong sandstone and siltstone), Domain 5 (highly weathered, very weak brown sandstone with siltstone beds), and Domain 6 (slightly weathered, very weak sandstone). This degradation is based on strain measurements from Unconfined Compressive Strength tests, as shown in Figure 3.5.

Table 3.1: Rock mass properties for MC and SUBI models

Constitutive model	Material	Density (kg/m3)	Friction angle (°)	Cohesion (kPa)	Bulk modulus (MPa)	Shear modulus (MPa)
Mohr-coulomb	D4	2100	35	300	417	192
	D5 & D6	2000	41	150	167	100
SUBI	D4	2100	35	Refer Fig. 3.5	417	192
	D5 & D6	2000	41	Refer Fig. 3.5	167	100

Table 3.2: Rock mass properties for Hoek-Brown model

Constitutive model	Material	Density (kg/m3)	Hoek-Brown Constant			Unconfined compressive strength, σ_{ci} (MPa)
			mb	s	a	
Hoek-Brown	D4	2100	4.9	0.06	0.5	4.5
	D5 & D6	2000	4.9	0.06	0.5	1.0

Table 3.3: Properties of joints for SUBI model

Constitutive model	Material	Joint dip (°)	Joint friction angle (°)	Joint cohesion (kPa)
SUBI	D4	North side 85 South side 85	30	15
	D5 & D6	North side 67 South side 52	30	15

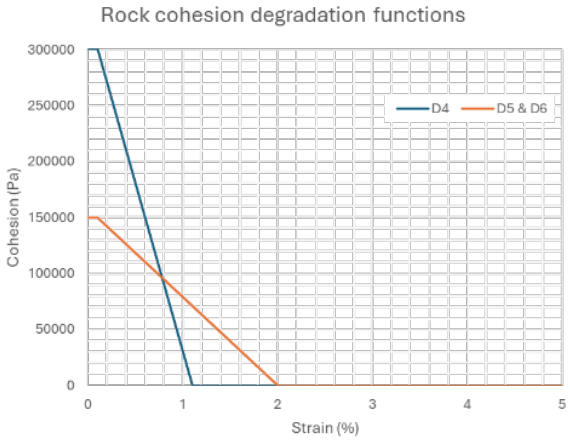

Figure 3.5: Rock mass cohesion degradation applied for SUBI model

4 RESULTS

The results show significant differences in the predicted displacement profiles between the three models. Figures 1, 2, and 3 display the horizontal displacement profiles for the SUBI, Mohr-Coulomb, and Hoek-Brown models, respectively.

- Figure 4.1 shows the displacement profile using the SUBI model. The SUBI model demonstrates significant variability in horizontal displacement across the monitoring points, with the highest displacements occurring near the toe of the slope. Progressive failure mechanisms are observed as the deformation propagates along weak joint planes, consistent with strain-softening behaviour (Song et al., 2020).
- Figure 4.2 shows the horizontal displacement profile from the Mohr-Coulomb model. Displacement is relatively uniform, with minor plastic deformation. This model does not capture the progressive failure mechanism seen in the SUBI model, indicating that the assumption of homogeneity in the rock mass oversimplifies the actual behaviour during seismic events.
- Figure 4.3 shows the horizontal displacement profile using the Hoek-Brown model. Similar to the Mohr-Coulomb model, the Hoek-Brown model exhibits limited deformation, with peak displacements occurring early in the simulation and then plateauing. This model also fails to account for joint strength degradation, leading to an overestimation of the rock mass's overall strength.

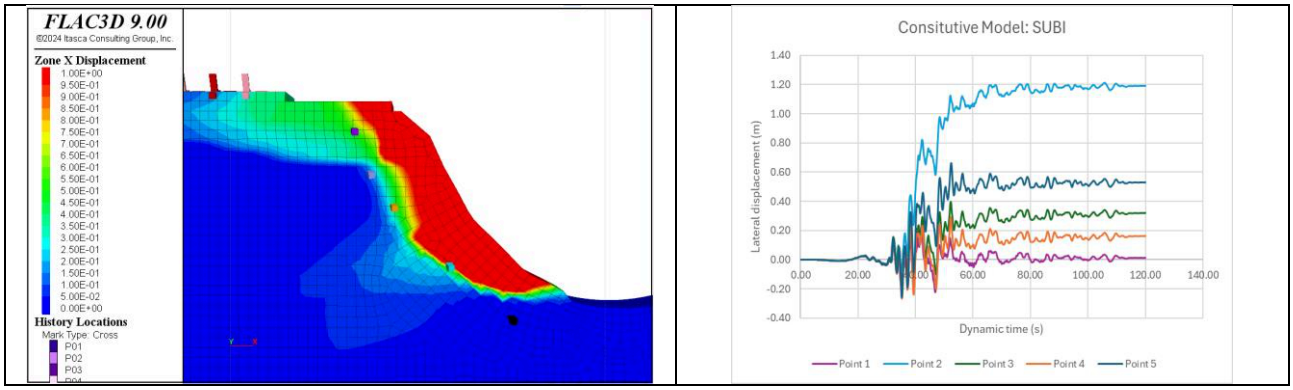

Figure 4.1: Horizontal Displacement profile using SUBI model

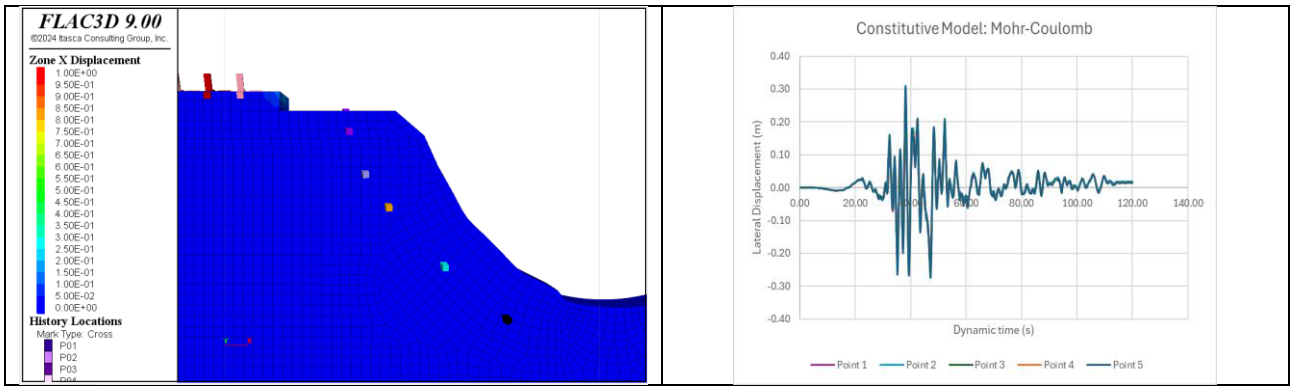

Figure 4.2: Horizontal Displacement profile using Mohr-Coulomb model

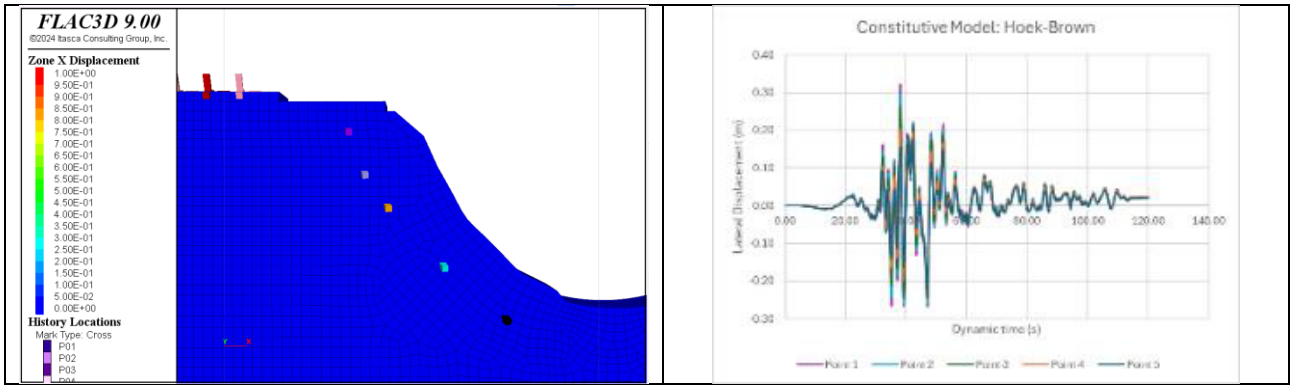

Figure 4.3: Horizontal Displacement profile using Hoek-Brown model

4.2 SPECTRAL ACCELERATION COMPARISON

Spectral acceleration comparisons (Figures 4.4 and 4.5) show notable differences between the three models.

- Figure 4.4 compares the spectral acceleration at the slope's top surface for the three models. The SUBI model shows the lowest spectral acceleration, indicating significant energy dissipation within the fractured rock mass. This behaviour is due to wave scattering along joint planes and strain-softening, reducing the overall seismic response at the surface (Song et al., 2020).
- Figure 4.5 shows the spectral acceleration response at one of the monitoring points near the slope's crest. The Mohr-Coulomb and Hoek-Brown models exhibit higher spectral accelerations, suggesting less wave energy dissipation. These models assume more uniform rock mass conditions, leading to an overestimation of surface acceleration during seismic events.

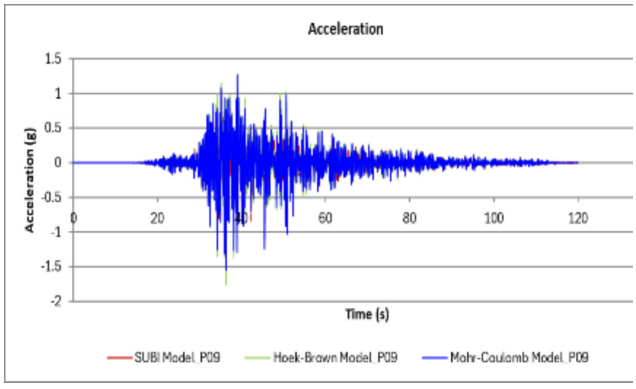

Figure 4.4: Ground motion response at history P09

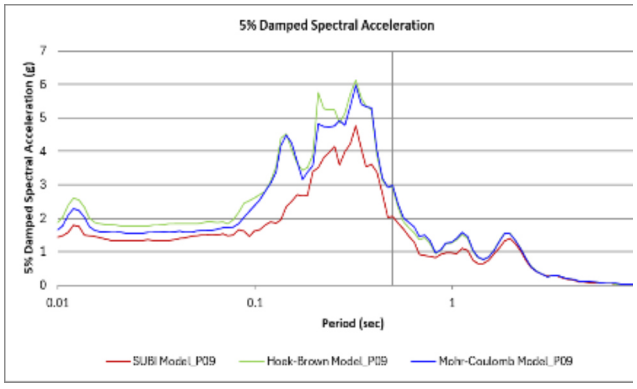

Figure 4.5: Spectral acceleration at history P09

5 DISCUSSION

The SUBI model demonstrated the highest level of accuracy in simulating the complex deformation patterns in jointed rock masses during seismic events. As illustrated in Figure 4.1, the SUBI model's ability to simulate strain-softening and joint strength degradation resulted in more realistic displacement profiles. These findings are consistent with previous research, which showed that discontinuities in rock masses can significantly alter wave propagation and seismic response (Song et al., 2020).

The Mohr-Coulomb and Hoek-Brown models, as shown in Figures 4.2 and 4.3, failed to capture the progressive failure mechanisms that are crucial in jointed rock slopes. The uniform displacement profiles and lack of strain-softening effects in these models highlight their limitations in representing the true behaviour of fractured rock masses under seismic loading. Both models underestimate the potential for progressive failure, which is critical for assessing slope stability (Hoek & Brown, 1997).

In terms of spectral acceleration, Figures 4.4 and 4.5 demonstrate the importance of accounting for discontinuities and energy dissipation mechanisms in jointed rock masses. The lower spectral acceleration observed in the SUBI model (Figure 4.4) reflects the complex wave interactions and energy redistribution caused by jointed rock formations. In contrast, the higher spectral accelerations in the Mohr-Coulomb and Hoek-Brown models overestimate the seismic response due to their oversimplified assumptions about rock mass homogeneity.

These results underscore the need for more advanced modelling techniques like the SUBI model when assessing seismic slope stability. Joint strength degradation and strain-softening behaviour play a critical role in determining the failure mechanisms and overall stability of slopes during earthquakes. Future studies should focus on validating these findings against field data and exploring the applicability of the SUBI model to other geological settings.

6 CONCLUSION

This study highlights the superiority of the SUBI model in simulating jointed rock slope behaviour during seismic events, particularly in capturing the effects of strain-softening and joint degradation. The results emphasize the need for advanced models in seismic slope stability assessments, as simpler models like Mohr-Coulomb and Hoek-Brown may fail to predict progressive failure mechanisms. Future research should focus on validating the SUBI model against real-world data and exploring its applicability to a wider range of geological condition

7 REFERENCES

Bai, B., Xu, C., Liu, M. & Li, X. (2019). A hydro-fracturing tester for rock saturated with controlled two-phase pore fluids. *Rock Mechanics and Rock Engineering*, 52(10), 4147–4154. https://doi.org/10.1007/s00603-019-01813-9.

Bland, K.J. (2006). Analysis of the central Hawke's Bay sector of the Late Neogene forarc basin Hikurangi margin, New Zealand. PhD thesis, Department of Earth and Ocean Sciences, University of Waikato.

Che, A., Yang, H., Wang, B. & Ge, X. (2016). Wave propagations through jointed rock masses and their effects on the stability of slopes. *Engineering Geology*, 201, 45–56. https://doi.org/10.1016/j.enggeo.2015.12.018.

Heron, D., Lukovic, B., Massey, C., Ries, W. & McSaveney, M. (2014). GIS modelling in support of earthquake-induced rockfall and cliff collapse risk assessment in the Port Hills. Christchurch. *Journal of Spatial Science*, 59(2), 313–332.

Hoek, E. & Brown, E.T. (1997). Practical Estimates of Rock Mass Strength. *International Journal of Rock Mechanics and Mining Sciences*, 34(8), 1165-1186. https://doi.org/10.1016/S1365-1609(97)80069-X.

Hudson, J.A., Harrison, J.P. & Xia-Ting, F. (2016). Engineering rock mechanics: An introduction to the principles. Elsevier.

Itasca (2019). FLAC3D — Fast Lagrangian Analysis of Continua in 3 Dimensions, Ver. 7.0. Minneapolis: Itasca.

Massey, C., Townsend, D., Rathje, E., Allstadt, K.E., Lukovic, B., Kaneko, Y., Villeneuve, M. (2018) 'Landslides Triggered by the 14 November 2016 Mw 7.8 Kaikōura Earthquake, New Zealand', Bulletin of the Seismological Society of America, 108(3B), pp. 1630-1648. doi: 10.1785/0120170305.

Song, D., Chen, Z., Chao, H., Ke, Y., & Nie, W. (2020). Numerical study on seismic response of a rock slope with discontinuities based on the time-frequency joint analysis method. *Soil Dynamics and Earthquake Engineering*, *133*, 106112. https://doi.org/10.1016/j.soildyn.2020.106112

Stirling, M. et al. (2012) 'National seismic hazard model for New Zealand: 2010 update', Bulletin of the Seismological Society of America, 102(4), pp. 1514-1542.

Wyllie, D.C. (2017) Rock Slope Engineering - Civil Applications (5th ed.). CRC Press.

WHY UNDERSTANDING GEOLOGY MATTERS FOR ENGINEERING DESIGN

Tom Montgomery

Senior Engineering Geologist

Ground and Underground Engineering (GUGE), Aurecon, 25 King Street Bowen Hills 4006, Queensland

ABSTRACT

Engineering projects worldwide rely on the sub-surface as their foundation, yet our understanding of the geological subsurface characteristics is limited. Each soil particle, pebble, and boulder carry an origin story, and understanding how material came to its current state profoundly impacts the performance of the structures. Overlooking geological history can lead to incorrect identification of geological characteristics during the design, which could affect the intended performance of the structures, examples include, subsidence in structures, dam failures and slope failures.

It is documented that one third of failed dams worldwide are linked to poor geological understanding at the site (P. Adams, 2024). Additionally, many dams remain unfilled and underutilised due to unforeseen geological complexities during construction and operation, elevating the risk of failure if used at full capacity. Further, poor understanding of the geological conditions in steep environments can lead to slope instability. This instability can affect infrastructure such as roads, retaining walls and bridges especially if these structures are built on deep-seated colluvium and unstable material. By comprehending regional and site-specific geology, we gain important insights and can develop solutions to mitigate these risks.

This paper explores the synergy between geological understanding and engineering design in addressing these challenges with two case studies. The case studies look at the geological aspect of why a design failed and what might be missed or overlooked without geological understanding.

1 INTRODUCTION

Civil engineering infrastructure projects globally depends on its foundations which in turn are dependent on the geology they are founded on. The case studies outlined below aim to identify two examples of how the engineering design was not suited for the geological conditions present. By incorrectly assessing a structure's foundation infrastructure is likely to have a considerably shorter lifespan or not be able to function at full capacity as designed. To understand geology, we must first understand its history. Asking questions about the geology is a critical step in this process. How did this rock type get here? Why are there fractures through these rocks? Is this colluvium or sediment? How old is this rock? What are the clues showing us? If you don't know the answers, ask someone who can find out. By understanding the geological history, it can point the engineering design down the correct path from the beginning, and avoiding the mistakes which seem so obvious in hindsight.

2 CASE STUDIES

2.1 DAM FAILURE – MALPASSET DAM (FRANCE)

Often by nature, dams are built in deep valleys with narrow passes providing cost effective material inputs vs reservoir size. However, these deep valleys with narrow passes are there for a reason, extreme geological settings with a history of stress, deformation, faulting and compression are often the reason.

Located in the South of France constructed in the préalpes (alpine foothills) ~7km North of Fréjus, the Malpasset Dam was a concrete arch dam built across the Le Reyran River which failed in 1959 resulting in the deaths of 421 people (Mary, 1968). An inquiry followed the disaster and made the following findings about the human and natural causes to the failure. Initial geological mapping was completed at the dam site in the local area. Two geological reports were

produced prior to construction and a further 3 reports were completed during the construction. Critically no plan, sections or borehole logs were included in any of the reports. Communication between different teams was poor, each working independently and not collaborating effectively. The geological language used was not fully understood by the design engineers and the geologists used in these mapping exercises had little experience or understanding of the type of structure. The dam design and location also changed between some of the mapping and construction. The geologists were not privy to the foundation designs of the dam structure. No mention of forces and direction of forces, stresses or deformation were found to be present in the subsequent inquiry. Thus, collection of geological data without the consideration of what the data will be used for is of little use. The inquiry found that the geologists needed to use non-scientific language and to write simply and concisely to convey the geological conditions effectively (Larouzée, 2019).

Igneous and metamorphic rocks such as the gneiss found onsite are considered "strong enough for dam foundations" (Larouzée, 2019). This is because they typically are impervious to water ingress and are hard enough to withstand weathering and to support heavy structures. The hard gneiss rock located on the left abutment contained a narrow but persistent crushed seam only 25-50mm wide parallel to the dam wall some meters downstream. This crushed seam indicated a fault which dipped ~45° towards the dam passing below its foundations at approximately 15m deep, as can be seen in Figure 1 below.

After completion of the dam, it took 5 years to fill due to the small catchment. Filling the reservoir increased the water load on the wall. This load on the dam wall was transferred into foundations as designed. But as the dam approached capacity during a high rainfall event the weight and pressure of the water on the dam wall foundations thrusted the rock block between the downstream fault and the dam toe upwards. The movement occurred along the downstream fault resulting in cracking and a catastrophic failure of the thin concrete structure. At the time the Malpasset Dam was the thinnest concrete arch dam in the world (Ross, 1984).

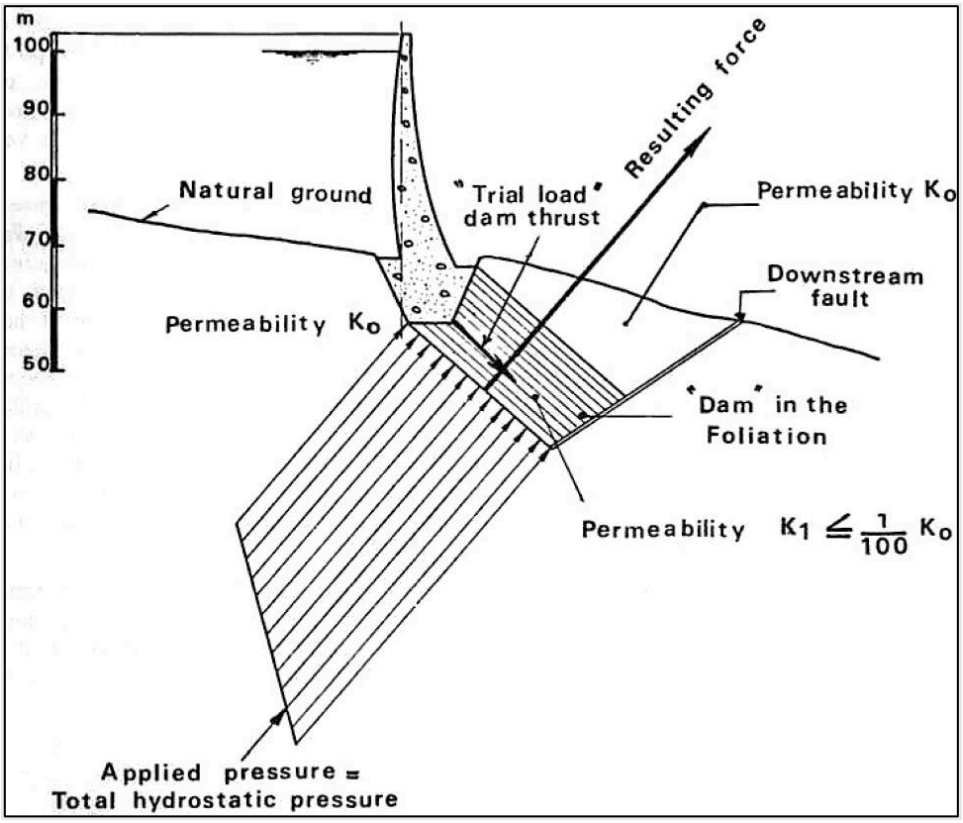

Figure 1: Cross section through the left abutment of Malpasset Dam (Duffaut, 2013)

The wedge below the dam had not been considered a valid failure method at the time. This fault was dipping favorably (towards the structure) so in normal circumstances should not move. However, with the combination of the hydrostatic pressure underground and the dam wall load, enough force was exerted on the fault to thrust it upwards (Duffaut, 2013).

Figure 2 below taken after the failure clearly shows the fault plane dipping (from right to left) beneath the dam wall foundations on what remains of the left abutment.

Figure 2: Malpasset Dam remains of the left abutment (Mary, 1968)

Numerous lessons have been learnt from this unusual failure type. The inquiry made after the disaster pointed to several issues within the internal structure of the design and geology teams working on the project, most notably their communication methods. The metamorphic geology of this site was suitable by type (gneiss) but contained numerous faults and foliations through the rock in numerous directions and orientations which were not fully understood by the designers. This disaster highlights the importance of understanding what the geological mapping needs to be targeting and where the detail needs to be focused. It also highlights the importance of clear information transferral and of communication between teams.

2.2 SLOPE INSTABILITY – HIDDEN UNITS (AUSTRALIA)

A misunderstanding of geological maps can have significant implications on engineering projects. For example, published geological maps show surface geology only, and do not always contain a section. Therefore, the reader may overlook the presence of geological units that do not appear at the surface.

By the end of the Mesozoic, Queensland was distant from any plate margins or subduction zones and deposition of sediments in the Great Australian Superbasin had ceased early in the Late Cretaceous. Over the next 65 million years, Queensland was in a mild epeirogenic and extensional tectonic setting (Jell. P.A. et al, 2013). Many small and discrete Paleogene and Neogene sedimentary basins, including the Petrie Basin, Oxley Basin, Booval Basin, Redbank Plains Basin, Darra Basin…and so on… have been identified and their contents recorded to uncomfortably overlie Paleozoic and Mesozoic geology and sometimes underlie later basalt flows.

One basin unit, known locally as Undifferentiated Tertiary Sediments (UTS); that is a sedimentary basin without a formal name, has been found in parts of Great Dividing Range of Southeast Queensland, Australia. The UTS is a narrow grouping of sedimentary layers that behave in a similar geotechnical manner. However, the presence of this unit does not appear on state or published surface geological maps and could therefore easily be missed in a generic desk study or even site walkover. In fact, the unit has previously been mislabeled in the Toowoomba region as a Jurassic aged Marburg Formation, Walloon Coal measures or as the Eurombah Formation (Yago J. a., 1996) and (Willey, 2020).

The UTS is found to sit below the Tertiary aged basaltic flows of the Main Range Volcanics and unconformably above the Mesozoic aged sedimentary rocks of the Marburg formation. It is comprised of mainly claystone and mudstone, with minor sandstone, siltstone, carbonaceous shale and coal. The colors range from orange, light pink, reddish-brown to greenish grey, light and dark grey, white and black. Generally, these rocks are poorly consolidated and show strong development of slickensided joints and fractures (Denaro, 1985). The UTS is typically extremely to very low strength material and unweathered. When exposed to the atmosphere and water it breaks down rapidly, it is highly susceptible to slaking and to a lesser degree dispersion (Denaro, 1985).

Most rocks within the UTS are believed to be the product of low energy depositional environments such as lakes, slow moving streams and swamps (PJT. Donchak, 2007). These environments have resulted in the formation of thin successions of low strength sedimentary rocks, potentially deposited over unconsolidated residual soils (Denaro, 1985). The unit is found to be discontinuous and variably thick, and because these units may be somewhat diagenetically or lithologically immature (i.e. may not be fully lithified and structurally incompetent), they are easily broken down. Also, when un-weathered the UTS can easily be confused with the weathered top of the Mesozoic sedimentary rocks below, due to alteration from overlying basalt lava which has cooked the surface of the UTS.

The presence of UTS material within road or rail cuttings may prove problematic from a slope stability point of view. The relative weakness of the UTS and its susceptibility to weathering (Figure 3) may result in the relatively competent rocks above overhanging and eventually being undermined, should the UTS material not be protected. Ultimately, this could result in progressive rock fall-type failure.

Pictures of a fresh cutting in Southeast Queensland exposing the UTS before and after rain are shown below:

Fresh cutting (note clean benches)

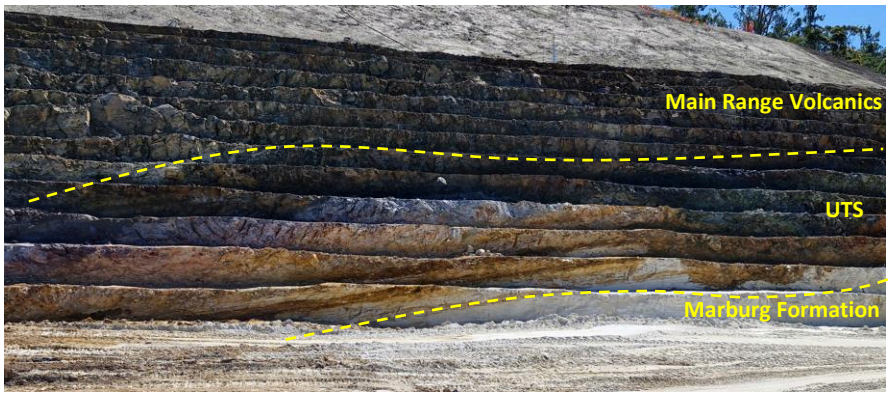

Post rain event (note debris on each bench)

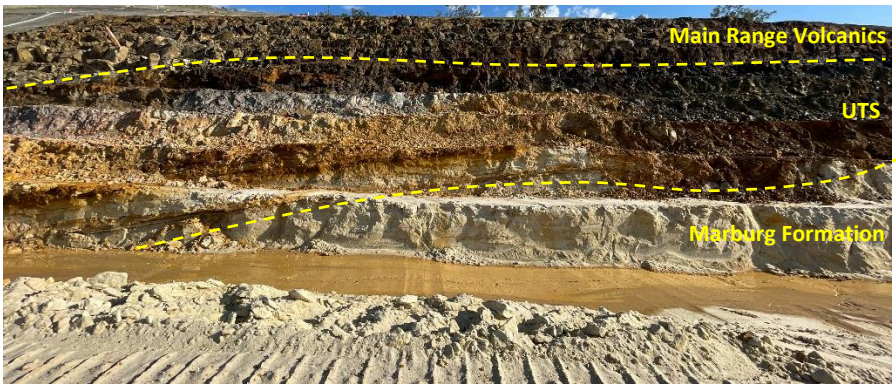

Figure 3: Exposed UTS cutting

If an inexperienced geotechnical professional were to construct a ground model with the available published geological maps, with limited or no intrusive ground information and a limited understanding of the local geological history in an area such as this, it is entirely probable that the resulting ground model might miss this geotechnically important, narrow unit (UTS). This could result in the implementation of an incorrect engineering design with the problems that flow on from that. This is why understanding geology matters for engineering design.

Understanding the local geological history and how the units are deposited can give us a deeper understanding of what we might be looking at or building on. Once we've made this first critical step, we can then start asking ourselves questions like: What can we do better to improve engineering outcomes for infrastructure in these environments? Where else might I expect to find poor conditions such as these? How can I have a more conservative design with this in mind? Where can I make cost savings and where can't I afford to cut corners?

3 CONCLUSION

Geology is an integral part of civil infrastructure which can be overlooked or allocated insufficient budget consideration in engineering design. For any civil engineering project, getting the foundations correct is critical, and understanding the geological history of a site will guide the design toward the best outcomes. The addition of a geologist to a major construction design team will not nullify geotechnical or geological risks. For a successful outcome, a robust strategy with clear communication between the teams should be established and maintained throughout a project. Constant feedback and communication with the addition of flexible design to allow for changes during construction are important.

Often during a project more information becomes available than was initially used to create the design. For example, an excavation may reveal a completely different rock type than expected. The case studies discussed above point out what can happen when the geology of a site is overlooked or not fully understood. Taking time aside to learn the geological history and conditions needs to be forefront of major civil projects. Engineers and geologists working together in a unified team from the beginning of a project can go a long way to identifying and solving these geotechnical problems before it's too late.

4 REFERENCES

Association of State Dam Safety Offical s . (1984). Retrieved from Lessons Learned From Dam Incidents and Failures: https://damfailures.org/case-study/malpasset-dam-france-1959/

Association of State Dam Safety Officials . (2020, 7 20). *Dam: Failures Modes and Their Possible Solutions*. Retrieved from Association of State Dam Safety Officials : https://damsafety.org/dam-failures

Barker, R. (1982). *Buderim Sewerage, geotechnical report on the Coolum View reticulation area and the Price Lane escarpment crossing.* Brisbane: Geological Society of Queensland.

Coffey, C. a. (1981). *Landslip Occurrence at Buderim Mountain.* Brisbane: Coffey & Partners.

Denaro, T. (1985). *Toowoomba Range Railway Tunnel Geological Report.* Toowoomba.

Duffaut, P. (2013). The traps behind the failure of Malpasset arch dam, France, in 1959. *Journal of Rock Mechanics and Geotechnical Engineering Volume 5, Issue 5*, 335-341.

Geoscience Australia. (2024, 09 07). *Geoscience Australia*. Retrieved from Geoscience Australia Stratigraphic Units Database: https://asud.ga.gov.au/search-stratigraphic-units

Jell. P.A. et al. (2013). *Geology of Queensland.* Geological Survey of Queensland: ISBN 9781921489761.

Larouzée, P. D. (2019). Geology, Engineering and Humanities: three sciences behind the Malpasset dam failure (France, 2 December 1959). *Quarterly Journal of Engineering Geology and Hydrogeology*, 445-458.

Mary, M. (1968). *Arch Dams, history, accidents and incidents.* Paris: Dunod.

P. Adams, e. a. (2024, 7 20). *How Dams Fail*. Retrieved from Probe International: https://journal.probeinternational.org/2008/05/01/how-dams-fail-2/

PJT. Donchak, R. B. (2007). *Geology and mineralisation of the Texas Region, South-Eastern Queensland.* Brisbane: Queensland Geology 11.

Ross, S. (1984). *Construction disasters: Design failures, causes and prevention.* New York: McGraw-Hill.

Willey, E. (2020). *Rocks and Landscapes, Toowoomba District.* Brisbane: Geological Society of Australia, Queensland Division.

Yago, J. a. (1996). Sedimentology of the middle Jurassic Walloon Coal Measures . *Mesozoic geology of the Eastern Australia Plate* (pp. 574 - 575). Brisbane: Geological Society of Australia .

Yago, J. V. (1994). Depositional styles of channel & overbank deposits, Clarence-Moreton basin, NSW, Advances in the study of the Sydney Basin. *Proceedings of the twenty eighth symposium.* Newcastle: University of Newcastle.

NOVEL APPROACH FOR INVESTIGATING SOFT SOILS USING THE MEDUSA DMT

Kayne Allen
SMEC Australia

ABSTRACT

The majority of invasive geotechnical investigations through soil stratigraphy in Australia typically fall into one of two categories: conventional drilling (auger/wash-boring/mazier) with Standard Penetration Tests (SPTs) and undisturbed tube sampling, or direct push static probing (Cone Penetrations Tests, Flat Dilatometer Tests). Conventional drilling methods rely on visual, tactile logging and rudimentary penetration tests, whereas push probe methods capture continuous geotechnical data whilst often omitting sampling. Whilst both methods typically capture the necessary data, they are most often used exclusively, due to the additional time and costs incurred when used in conjunction. SMEC Australia recently undertook a geotechnical investigation in a soft soil environment and derived a methodology to incorporate both investigation methods at a singular investigation point, therefore increasing data reliability in a time and cost-effective manner.

This paper describes this methodology in detail, discussing how it optimises geotechnical investigations. It also includes a comparison between DMT test results and laboratory results.

1 INTRODUCTION

It has long been regarded that the assessment of soil properties and behaviour is the most important part of geotechnical design (Janbu, 1975). Geotechnical site investigations are an integral part of any new civil engineering project and should be one of the first tasks undertaken. The data collected from geotechnical investigations is important in to evaluate the ground conditions, assess spatial variability and derive design parameters. Spatial variability within stratigraphy can contribute to design and construction challenges, which could lead to poor or overly conservative geotechnical design.

Typically, in Australia, geotechnical site investigations will fall into one of two categories, conventional drilling, or direct push static probing and can be undertaken at any stage throughout the project. Both categories require the use of specialised equipment, with each having category having benefits over the other. Both types of geotechnical investigation will provide necessary data required to derive basic geotechnical design parameters, such as unit weight (kN/m^3), internal friction angle (ϕ') and undrained shear strength (Cu) to varying degrees.

2 TYPES OF INVESTIGATION

2.1 STANDARD PENETRATION TESTS

Conventional drilling with Standard Penetration Tests (SPTs) and/or undisturbed tube sampling is arguably the most prominent type of geotechnical investigation for assessing soil stratigraphy within Australia.

The SPT has a number of favourable benefits:

- Relatively cheap and robust equipment
- Highly repetitive
- Allows for visual/tactile logging of soil descriptions
- Allows for sample collection
- SPT N-Value is used to interpret many soil geotechnical parameters
- Can test very dense granular layers with minimal impact to equipment

However, the SPT also has a number of downfalls:

- Unlikely to be replicated
- Typically undertaken at predefined intervals, and not changes in stratigraphy
- Incongruous for very soft to soft clays
- Lacks accuracy
- Is over 120 years old (was developed by the Raymond Piling Company in 1903)

Incorporating undisturbed tubes with conventional drilling provides better data for very soft and soft clays, as Pocket Penetrometer and hand vane tests can be undertaken in the base of the sample. These tests provide congruous shear strength values.

2.2 CONE PENETRATION TESTS

Cone Penetration Tests with a piezo-cone (CPTu) has been used in Australia since the turn of the century and is very popular when investigating very soft to firm soil sites. As with conventional drilling, it also has its own set of benefits and downfalls:

- Highly repetitive and replicated
- Obtains a continuous profile of soil
- Precise, delineates thin strata and presents accurate depth where strata changes
- Can measure in situ permeability via the dissipation test
- Unable to collect soil samples
- Geotechnical parameters are still interpreted through correlations
- Generally unable to penetrate dense to very dense granular layers
- Equipment requires frequent calibration off site to ensure reliable data is obtained
- Requires precise and continuous probing

2.3 FLAT PLATE DILATOMETER TEST (DMT)

The DMT is a relatively new (1980) type of static probe test which is well suited for classification of soil sites (Marchetti, 1980). A DMT blade can be pushed into the ground using typical CPT hydraulic rams, or even a drill rig.

The DMT was not often used for very soft soil sites in Australia due to the high dexterity required by the operator during the test cycle and potential for human error. However, a recent update allows for the testing to be fully automated using a “Medusa” DMT (Marchetti, 2018), which completely removes any human error which may have crept into test results, and thus enhancing the sensitivity when testing very soft to soft soils

The DMT has similar benefits and downfalls as CPTu, however does not require precise and continuous probing due to tests being undertaken at set intervals (ASTM D6635, 2015), and calibrations are undertaken during each test without the need for additional equipment, reducing the chance of poor data acquisition from uncalibrated cones.

The Medusa DMT has also been shown to provide high quality shear strength data in very similar ground conditions, when compared to CPT (3MPa cone) and an A.P van der Berg electronic vane shear system (Marchetti & McConnell, 2023).

3 RECENT INVESTIGATION APPROACH

SMEC recently was engaged to undertake a geotechnical investigation for a proposed upgrade to a bridge protection structure in disrepair. These investigations were required to be undertaken within a busy marine thoroughfare.

3.1 GEOLOGICAL SETTING

The site is located within Sydney Harbour and is underlain by Holocene Age Estuarine Deposits overlying Tertiary Age Hawkesbury Sandstone. Nearby investigations for the Sydney Metro West (Golder/Douglas Partners JV, 2022), indicated that the Estuarine deposits were up to 25m thick, with up to 10m of very soft to soft clay immediately below seafloor.

Geophysical seafloor mapping using a multibeam echosounder, also undertaken during the Sydney Metro West investigations (GBG, 2022), indicated that the seabed around the bridge site was littered with debris, likely fallen timber piles from the deteriorating bridge protection structure.

3.2 INVESTIGATION AIM AND SCOPE

The initial aim of the investigation was to assess the shear strength of the marine soils, as well as the strength of the upper 15m of sandstone, to allow for future foundation design. The initial tender scope was for the investigation to be undertaken over two mobilisations, the first being conventional drilling to sample the marine sediments and core through the rock, with CPTu being undertaken during the second mobilisation to capture a full profile of the soil. Both investigations were to be carried out from a jack up barge.

However, during a detailed assessment of the site, numerous challenges arose, namely being:

- The proposed investigation locations were underlain by numerous underwater cables, which would be costly and time consuming to locate for each mobilisation of the barge.
- Unknown consistency of the upper region of the marine sediments. The previous overwater investigations for Sydney Metro West (Golder/Douglas Partners JV, 2022) did not focus on testing the soil strength, and in some locations the barge was unable to jack up form the seafloor.
- Likelihood of encountering seafloor debris.
    - Would the barge legs punch through wooden piles during a load test and create a safety hazard?
    - CPTu unable to advance past the timber piles, and movement of barge required
- If the barge was unable to jack up during this investigation, how reliable would the CPT data be if the barge was floating and moving with the tide and marine vessel wash?

Given challenges posed in setting up a suitable barge, and potential for poor data capture from CPTu if a floating barge was required, it was proposed that the CPTu tests be swapped with DMT tests, with a Medusa DMT being advanced using a geotechnical drill rig at the same location as the conventional borehole. DMTs have commonly been advanced using drill rigs in Europe, however, is not something which is common in Australia. Due to the DMT also not requiring to be penetrated at a constant rate (unlike CPTu) data would not be compromised if the investigation were to be undertaken form a floating barge.

The Medusa DMT was advanced for a maximum stroke length of 3m, with DMT soundings being undertaken at 200mm centres. Following the completion of the DMT sounding at the end of the stroke length, the DMT blade was removed, and the borehole advanced using conventional rotary drilling techniques, and casing reset at the depth of last DMT sounding. This allowed for visual tactile logging of the soil units to present on a typical geotechnical engineering log. Once casing had been set in place, sampling was able to be undertaken. Another benefit of having DMT soundings immediately above the sample location, was the ability of the operator to select the most appropriate sampling type: piston sampling (if the soil was cohesive and very soft to firm), thin wall undisturbed u-tube sampling (TWT, 75mm diameter) (if the soil was cohesive and firm to stiff) and split spoon sampling using the SPT (if the soil was granular or very stiff to hard cohesive).

This method provided an improved resolution of all soil units, allowed for visual tactile logging, as well as collection of undisturbed and disturbed samples.

By using DMT for the investigation, most of the challenges posed were mitigated: only one mobilisation and set up would be required per test location, and barge selection (i.e. jack up or floating) become a non-issue.

Due to the challenges posed by the site, SMEC devised the following methodology to both mitigate the risk of poor data capture (if the barge was unable to jack up, encountering early refusal) and accomplish the aims of the investigation (assess the full profile of the soil):

- A barge, supporting a geotechnical drill rig was mobilised to site
- Once safely set up over the proposed investigation point, the drill rig drills out the upper 1-2m of soil (depths which are typically ignored in pile design), to drill through any potential debris, which may hinder the advancement of a DMT blade
- Casing is set at the base of the drilled section, and DMT blade lowered down, through the casing and commences testing 0.4m past the bottom of casing
- DMT probe readings taken at 0.2m intervals, for a maximum stroke length of 3m
- Once the 3m stroke length is reached, the DMT blade extracted, the tested soil length over drilled and casing reset at the new depth
    - The over drilling of the soil column allowed for visual tactile logging of the soil column
- Upon casing being reset, and prior to recommencing DMT probing, a sample was obtained, either a piston tube sample (75mm diameter), undisturbed tube sample (75mm thin-walled u-tube), or SPT sample.
    - The lower DMT probe results could be assessed in the field to best determine the most suitable type of sampling at the base of the borehole.
    - Samples were also able to be undertaken at differing intervals, such as change in strata, based on the DMT probe results
- Upon DMT or sampler refusal, typical diamond coring techniques progressed the borehole through rock.

4 RESULTS

Shear strength of cohesive soil was calculated by the formula derived by Marchetti (Marchetti, 1980) and has been compared against undrained unconfined triaxial tests on samples collected by both piston tube samplers and thin-walled u-tubes (TWT). Results of the laboratory triaxials, on both TWT samples and piston tube samples, have been plotted on

each DMT plot as shown in Figures 1 to 5. Corrected hand shear vane test results have also been plotted. The gaps in DMT data represent depths where samples were taken, or granular material was encountered.

Results varied, with triaxial tests undertaken on piston tube samples showing a shear strength much closer, ie within 3kPa, to that recorded by the DMT (BH02, BH05). Triaxial tests undertaken on thin-walled samples (BH01, BH04) typically were up to 50kPa lower than the shear strength derived from the DMT, with one TWT triaxial returning a shear strength within 9kPa of that derived by the DMT.

Hand vane tests, undertaken in the field, returned results much closer to the derived shear strength from the DMT with variability of up to 8kPa.

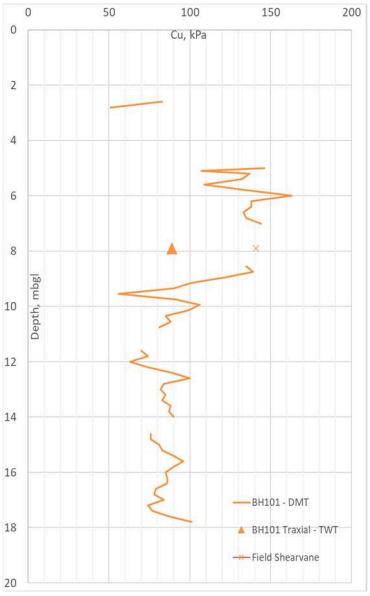

Figure 1: Recorded shear strengths from DMT, laboratory triaxial tests and hand shear vanes, BH01

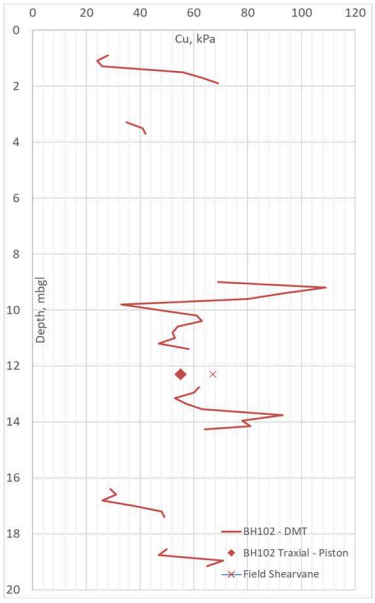

Figure 2: Recorded shear strengths from DMT, laboratory triaxial tests and hand shear vanes, BH02

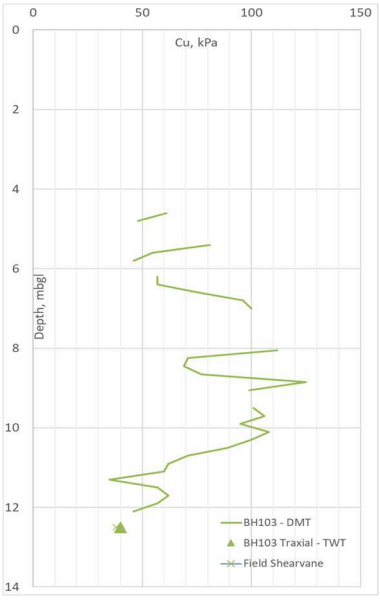

Figure 3: Recorded shear strengths from DMT, laboratory triaxial tests and hand shear vanes, BH03

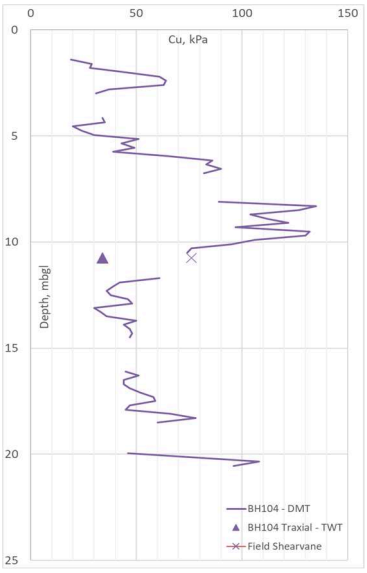

Figure 4: Recorded shear strengths from DMT, laboratory triaxial tests and hand shear vanes, BH04

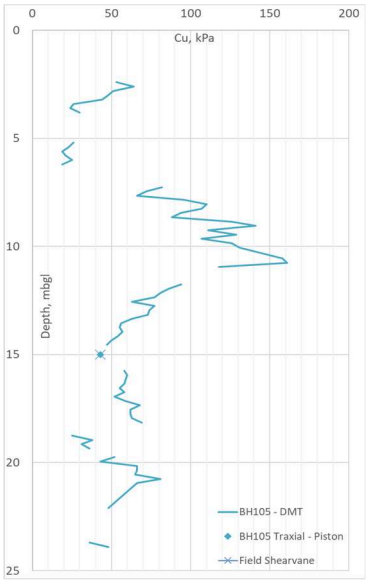

Figure 5: Recorded shear strengths from DMT, laboratory triaxial tests and hand shear vanes, BH05

5 DISCUSSION

The results show some variability between the laboratory triaxial testing and in situ testing. The main outliers from triaxial testing were from thin-walled samples, whilst tests where DMT readings were very similar to triaxial testing were performed on samples obtained from the piston tube sampler.

Hvorslev (1949) introduced a concept that samples collected from push in tube samples experience disturbance due to the elongation of the soil inside the tube. Both Hvorslev (1949) and De Groot (2005) have observed that by using a piston sampler (i.e. to restrict the movement of the soil within the sampler) reduces disturbance in clay samples.

Rowe (1972) in the Twelfth Rankine Lecture discusses the quality of different sampling techniques for cohesive soils. Piston sampling is given a "Quality Class" of 1 and pressed in thin-walled tubes given classification of either 2 or 3, subject to the permeability of the soil. It is proposed that shear strength testing only be undertaken on samples of Quality Class 1 (Rowe, 1972) (ISO 22475-1, 2021) due to the likely less disturbance on the sample. This suggests that the samples collected for BH101 and BH104 may have been disturbed by the sampling technique.

It is likely that sampling methodologies impacted the sample integrity, especially as the medusa DMT has been shown to capture high quality shear strength data (Marchetti & McConnell, 2023) in similar depositional environments to this investigation.

It is unlikely that the investigation methodology disturbed the soil whilst in situ. The methodology undertaken for the investigation provided excellent results, when a higher quality sampling technique was implemented.

6 CONCLUSION AND RECOMMENDATIONS

A new methodology for testing the geomechanical properties of soil, was developed on a recent investigation within Sydney Harbour. The methodology combined both conventional drilling and direct push static probing with excellent results. Dilatometer readings, with conventional geotechnical drilling and sampling techniques provided a near continuous strength profile of the soil, based on Dilatometer and laboratory test results. This approach allowed for higher quality data acquisition as well as conventional geotechnical logging, and negated project specific risks such as overwater CPTs from a floating barge. Reflecting on the investigation undertaken, the author draws the following conclusions and recommendations for future investigations:

- Substantial project savings (both cost and time) can be achieved by using this methodology, and shows that the best outcomes occur when "the right tool for the job" approach is adopted.
- In field assessment of the DMT data allowed for the appropriate sampling methodology to be selected (i.e. undisturbed sample, SPT).
- Careful consideration of undisturbed sampling (i.e. selection of piston sampling) should be undertaken for sites where assessing the shear strength of soils is critical.
- Laboratory testing may not be indicative of the in situ characteristics of the soil, and laboratory results assessed in conjunction with all available site data.

7 REFERENCES

ASTM D6635, 2015. Standard Test Method for Performing the Flat Plate Dilatometer. West Conshohocken, PA, USA: ASTM International.

De Groot, D. J., Poirier, S. E. & Landon, M. M., 2005. Sample disturbance-soft clays. Studio Geotechnica et Mechanica, 27(3), pp. 91-105.

GBG, 2022. Sydney Metro West Marine Geophysical Investigation - Johnstons Bay & Darling Harbour, Sydney, NSW: s.n.

Golder/Douglas Partners JV, 2022. Final Geotechnical Data Report 2, Sydney Metro West Geotechnical Investigation - Eastern Tunnelling Package, Sydney, NSW: s.n.

Hvorslev, M., 1949. Subsurface exploration and sampling of soils for civil and engineering purposes, Vicksburg, USA: American Society of Civil Engineers.

ISO 22475-1, 2021. Geotechnical investigation and testing - Sampling methods and groundwater measurements - Part 1: Technical principals for teh sampling of soil, rock and groundwater. Second ed. s.l.:International Standards.

Janbu, N., 1975. "Discussion" ASCE Specialty Conference on In-situ Measurement of Soil Properties. North Carolina, Caolina State University.

Marchetti, D., 2018. Dilatometer and seismic dilatometer testing offshore: available experience and new developments. Geotech. Testing, 41(5), pp. 967-977.

Marchetti, D. & McConnell, A., 2023. Medusa DMT for Automated Dilatometer Testing - A major advance in geotechnical in situ testing. Cairns, ANZ2023.
Marchetti, S., 1980. In Situ Tests by Flat Dilatometer. Geotechnical Engineering , 106(GT3), pp. 299-321.
McConnell, A., 2006. Soft soil site characterisation by In Situ testing. Sydney, Sydney Chapter 2006 Symposium, pp. 55-62.
Rowe, P., 1972. The relevance of soil fabric to site investigation practice. Géotechnique, 22(2), pp. 195-300.

APPLICATION OF ELECTRO-OSMOSIS TO THE CONSOLIDATION OF SAND QUARRY TAILINGS

Xiyang Chen[1], Mark Jaksa[2], An Deng[2], Fereydoon Pooya Nejad[2]
[1] WSP Australia, [2] School of Architecture and Civil Engineering, University of Adelaide

ABSTRACT

ABSTRACT: The need for an effective and efficient consolidation method for mine operations has significantly increased throughout the past decade. In comparison to inefficient, conventional consolidation methods, electro-osmosis consolidation has shown great potential in consolidating tailings, with measured benefits demonstrated from laboratory experiments and some civil engineering applications. However, in order to achieve large scale field implementation in mining operations, a comprehensive, optimised electro-osmosis operation procedure is required. The aim of this paper is to examine the efficiency and effectiveness of the electro-osmosis consolidation method with respect to sand quarry tailings. This laboratory-scale study is the initial part of a larger research endeavour which seeks to upscale the findings to operational quarries. In this paper, experiments were undertaken on sand quarry tailings in testing tanks at two different scales, containing approximately 0.06 m^3 and 1.07 m^3 of tailings. Tests were conducted using steel electrodes. The results indicate a positive outcome of using electro-osmosis consolidation, and a more optimised outcome may be achieved with the implementation of intermittent current and polarity reversal.

1 INTRODUCTION

1.1 BACKGROUND

Tailings produced by the quarrying of sands present a significant engineering challenge for its storage. Tailings storage facilities (TSFs), where the tailings are stored in-situ, are a particular challenge for quarry operators, both operationally and environmentally. In circumstances when the TSFs are reaching capacity or closure, consolidating the existing tailings would expend the storage capacity, hence life, of the TSF and increase the factor of safety (FoS) of the facility after decommission. However, consolidating tailings is challenging because of the significant time needed, which is usually in the order of several years, due to its low permeability and low strength, combined with its high water content.

1.2 ELECTRO-OSMOSIS

Conventional consolidation methods, namely surcharge and vacuum preloading consolidation, have been proven, by numerous research studies, to perform poorly in low permeability, fine-grained soil. Both kinds of the preloading methods involve the use prefabricated vertical drains (PVDs) for water drainage, which relies on the soils' hydraulic permeability (Kaniraj et al. 2010, Liu et al. 2017). Disadvantages of the application of PVDs in fine grained tailings or soil also include 'clogging' or 'caking', resulting in unsatisfactory consolidation outcomes (Cai et al. 2017).

In contrast, the electro-osmosis (EO) consolidation method offers the potential for dewatering and consolidating fine to ultra-fine soils, such as mine tailings. Instead of relying on the hydraulic permeability of the soil, EO consolidation mostly relates to a soil's electrical conductivity and electro-osmosis permeability, which are less influenced by grain size, therefore making the dewatering of fine-grained soils much more feasible than conventional methods (Lamont-Black et al. 2016).

It may be summarised that there are two main goals in achieving successful electro-osmosis consolidation: (a) Prolong the effective consolidation period prior to cracking; and (b) Optimising energy consumption. Subdividing these goals further, reveals three key aspects of electrode-osmosis research: (1) Electrode material; (2) Electrical techniques; and (3) Optimisation with the combination of other techniques or consolidation methods.

1.2.1 ELECTRODE MATERIAL

The electrode material is one of the key aspects for the efficient operation of EO consolidation. Conventional metallic materials, such as iron, copper, steel and brass, experience corrosion due to electrical-chemical reactions and require ongoing replacement in long-term dewatering projects that run for months. On the other hand, according to Fourie et al. (2007), electrokinetic geosynthetics (EKGs) have shown promise for long-term EO consolidation applications. EKGs are non-metallic based electrically conductive materials, that have shown great potential in solving the corrosion problem. Experiments on different fine tailings indicated high durability against corrosion with an extremely long operation time (Fourie et al. 2007, Fourie and Jones 2010).

1.2.2 ELECTRICAL TECHNIQUES

The electrical techniques applied to the EO consolidation method is another key aspect impacting energy consumption and dewatering efficiency. The voltage gradient is usually expressed in the form of the applied voltage divided by the distance between the electrodes, using the units of V/m or V/cm. Commonly agreed theories established by Bjerrum et al. (1967) and Lockhart (1983), which were later confirmed by Fourie et al. (2007), suggest that a low voltage gradient generally tends to result in low energy consumption.

Two electrical techniques, that many studies have demonstrated improving electro-osmosis effectiveness, are intermittent current and polarity reversal. Intermittent current (IC) is the application of current in discrete intervals, as opposed to it being applied continuously. In theory, IC may reduce the power consumption while maintaining a relatively efficient dewatering rate. Polarity reversal (PR) involves switching the polarity of the electrodes in the experiment within a predetermined schedule.

2 AIMS

From the previous section, it is evident that many of the previous studies have been confined to the experimental domain and at a relatively small scale. This begs the question: "How can findings from small, lab-scale experiments be transferred to the larger, operational scale, which eventually leads to engineering application?"

The aims of this paper are to: (1) Examine experimentally, at laboratory- and meso-scale, the efficacy of EO in construction and silica sands tailings; and (2) Examine upscaling from the laboratory scale to a meso-scale application.

3 METHODOLOGY

This research project incorporates two scales of laboratory experiments: laboratory-scale and meso-scale, and the dimensions are presented in Table 1.

Table 1: Size differences between laboratory- and meso-scale experiments

Experimental scale	Lab-scale	Meso-scale
Plan dimensions (m)	0.5 × 0.5 (square)	0.6 (diameter)
Depth (m)	0.25	0.60, 0.95
Volume (m^3)	0.06	0.68, 1.07

In order to maintain compatibility between the two scales of experiment the following remain the same across the experiments: the tailings sample, steel electrodes, hexagonal electrode arrangement, drainage method, and data acquisition devices. The tailings used in this study were acquired from a sand quarry tailings storage facility, located in Golden Grove, Adelaide, South Australia, the properties of which are given in Table 2.

Table 2: Geotechnical properties of sand quarry tailings

Soil type	Grain size	Specific gravity	Liquid limit	Plastic limit	Water content
Silty CLAY	95% < 0.075 mm	2.60	55%	23%	130–168%

3.1 LABORATORY SCALE EXPERIMENTS

The lab-scale experiments included 8 separate tests, which examined the EO consolidation performance by the following variables:

1. Apply a low voltage gradient (LV1);
2. Apply an intermittent current with two different time intervals (IC1 and IC2) at the same low voltage gradient and intermittent ratio;
3. Alternate the electrode polarity with different reversal time intervals (PR1 and PR2) at the same low voltage gradient and polarity ratio; and
4. Optimise the consolidation by changing the applied electrical technique and its detail settings (Opt1, 2 and 3) at the same low voltage gradient.

Details of each experiment are given in Table 3, and there are a few points to note:

(a) The intermittent ratio is defined as the ratio between the powered ON time divided by the powered OFF time;

(b) The polarity ratio is defined as the ratio between the normal polarity runtime divided by the reversed polarity runtime;

(c) Experiments Opt1, 2 & 3, which are the optimisation trials, only intermittent current was implemented due to the results of the polarity reversal experiments deemed to be suboptimal. Opt3 doubled the voltage gradient, with full power on for the first half, and intermittent current was applied for the remainder of the test; and

(d) The initial water content of all the tests is set between 69% to 71% to facilitate effective comparison.

Electro-osmotic performance was evaluated in terms of the amount of water removed from the tailings slurry, soil surface settlement and electrical energy consumption.

Table 3: Laboratory-scale experiment details

Experiment No.	LV1	IC1	IC2	PR1	PR2	Opt1	Opt2	Opt3
Intermittent ratio	–	1.5	1.5	–	–	1.5	1.5	1.5
Intermittent ON time (hours)	–	3	14.4	–	–	14.4	3	3
Polarity ratio	–	–	–	0.2	0.1	–	–	–
Polarity ON time (hours)	–	–	–	12	13	–	–	–
Voltage gradient (V/cm)	0.1	0.1	0.1	0.1	0.1	0.1	0.1	0.2
Effective runtime (days)	15							

This series of experiments was conducted using a square acrylic tank, with dimensions given in Table 1. An hexagonal arrangement of electrodes was adopted. Drainage occurred through the central hollow cathode by gravity to an outside beaker which was continually weighing using a load cell. The cathode was wrapped with layers of geotextile acting as filter. To minimise variations in evaporation, the ambient temperature was controlled to between approx. 20°C to 25°C.

3.2 MESO-SCALE EXPERIMENTS

The meso-scale experiments were conducted to examine the efficacy of an optimised solution in an upscaled scenario, and to study scaling effects. Two experiments were conducted using a cylindrical tank, with a diameter of 1.2 m and height of 1.2 m. The setup includes 5 laser transducers placed between the electrodes. In addition, water content was measured by 6 volumetric water content (VWC) sensors, and pore water pressure was measured by 3 pore water pressure probes. Due to space constraints, the pore water pressure measurements will not be presented.

Meso1 adopted the LV1 experiment setting and served as a preliminary experiment for later iterative improvements. The voltage gradient was set to 0.1 V/cm, with the experiment running for 28 days.

Meso2 sought to improve dewatering by using a higher voltage gradient. A voltage gradient of 0.4 V/cm was adopted and the experiment ran for 78 days. To study scaling effects, the meso-scale experiments adopted the same hexagonal electrode arrangement, steel electrodes, gravitational drainage system and geotextile filter as the lab-scale experiments.

4 RESULTS

4.1 LABORATORY-SCALE EXPERIMENTS

The results of the laboratory-scale experiments are presented in Table 4, where water removal percentage is defined as the percentage of water removed, by weight, against the initial total weight of the tailings; surface settlement is the final average soil settlement across the 6 laser measuring points; and energy consumption is the total cumulative electricity usage, in Wh, over 15 days of runtime. In summary, with a higher voltage gradient, hence higher energy consumption, enhanced dewatering occurs with greater soil surface settlement, as one might expect.

Table 4: Results of laboratory-scale EO experiment

Experiment No.	LV1	IC1	IC2	PR1	PR2	Opt1	Opt2	Opt3
Water Removal Percentage	33.0%	20.9%	20.2%	18.8%	17.1%	21.6%	19.0%	30.5%
Settlement (mm)	27.6	30.9	45.2	44.7	37.9	49.2	44.0	62.2
Energy (Wh)	57.0	32.4	37.0	54.0	51.0	40.6	39.5	77.5

In order to facilitate effective comparison between tests, the laboratory experiments included almost the same amount of tailings, with an initial water content varied between 69% to 71%. At a low voltage gradient of 0.1 V/cm, all experiments demonstrated enhanced dewatering due to EO consolidation, with varying degrees of efficiency. This is clearly demonstrated by comparing the performance of EO against natural drainage (red line in Figure 1), and as a result, EO is highly effective.

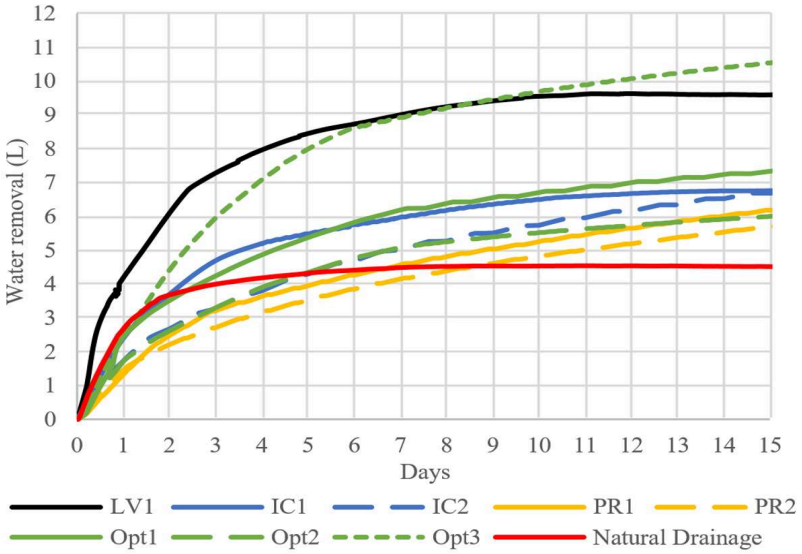

Figure 1: Water removal from laboratory-scale experiments

The electrical techniques also demonstrate various outcomes. IC dewaters the tailings at a rate of approximately 65–70% of that with continuous EO (i.e. LV1), whilst consuming 60–80% of the energy. At the same intermittent ratio, a longer power-on time interval results in superior performance. PR demonstrated less efficient performance with respect to dewatering, which was not unexpected. EO at a relatively low voltage gradient demonstrated satisfactory performance in relation to dewatering at lab-scale, and both IC and PR have shown positive results.

The soil settlement measured by laser transducers suggest it is strongly correlated to water removal, whereby the overall settlement follows a similar, but delayed trend (approx. up to 5 hours), with respect to the water removal results. The total average soil settlements were approximately 40 to 45 mm (i.e. 16–18%). Soil cracking appears to be an important factor affecting EO performance, and was observed in all of the experiments. Major cracks formed between the electrodes and compromised the EO process.

Energy consumption, is reduced with the adoption of both IC and PR. However, in order to minimise cracking, PR sacrifices energy consumption. In addition, for those tests that incorporated IC and PR, a greater water removal rate is observed at the end of the experiments, when compared against the flattening slope in the natural drainage and LV1 tests. Note, in the first half of experiment Opt3, the same power-on setting as LV1 was adopted, hence it follows a similar trend, as expected. However, in the second half of Opt3, the intermittent current was applied at two times of the voltage, hence the significantly higher energy consumption. By doubling the voltage applied, the amount and rate of water removal are both higher than the other experiments that used IC. This indicates that the application of a higher voltage in conjunction with IC produces superior performance.

The electrical consumption with respect to water removal is summarised in Table 5, where E/W refers to the energy consumption versus water removal, in Wh/L. When comparing the electrical energy consumption to the amount of water removal, conclusions can be made which are similar to those given previously in §4.1.1, that a longer IC time interval generates more efficient energy usage with respect to water removal.

Table 5: Electrical energy consumption versus water removal

Experiment No.	LV1	IC1	IC2	PR1	PR2	Opt1	Opt2	Opt3
E/W (Wh/L)	5.7	4.8	5.6	8.7	9.0	5.5	6.6	7.3

4.2 MESO-SCALE EXPERIMENTS

The meso-scale experimental results are presented in Table 6 and Figure 2. The results demonstrated general similarities, with more significant surface cracking after the upscaling. The results suggest that: (1) upscaling is non-linear; and (2) soil cracking and surface deformation are more significant.

Comparing the water removal and energy consumption associated with Meso1 with the laboratory-scale experiments, it is observed that the larger scale results in diminished performance. For example, when comparing the energy consumption versus water removal factor, E/W, for LV1 and Meso1 (Tables 5 and 6), which were performed at the same voltage gradient without IC and PR, Meso1 yields 12.4 Wh/L, which is much greater than the 3.9 Wh/L obtained for LV1. This suggests that, when upscaling, the EO voltage gradient is not the only factor that needs to be considered, as the soil depth and volume also affect performance. While the same voltage gradient was applied, Meso1 did not achieve the same level of dewatering as at the lab-scale. The water removal curve given also supports this conclusion. For example, in Fig. 1, LV1 exhibits a water removal curve which plateaus after approx. 7 days, whereas in Fig. 2, Meso1 has a relatively linear water removal curve. In addition, as shown in Table 6, Meso1 removed a lower percentage of water (25.1%) when compared against LV1 (33%) in Table 4. Therefore, in the next test iteration, for Meso2, the power input was increased by adopting a higher voltage gradient.

Table 6: Results of Meso-scale EO consolidation experiment

Experiment No.	Initial Water Content	Water Removal Percentage	Surface Settlement (mm)	Energy (Wh)	Energy/Water (Wh/L)
Meso1	176.4%	25.1%	134.9	1738	12.4
Meso2	129.6%	45.4%	> 400	38,495	102.3

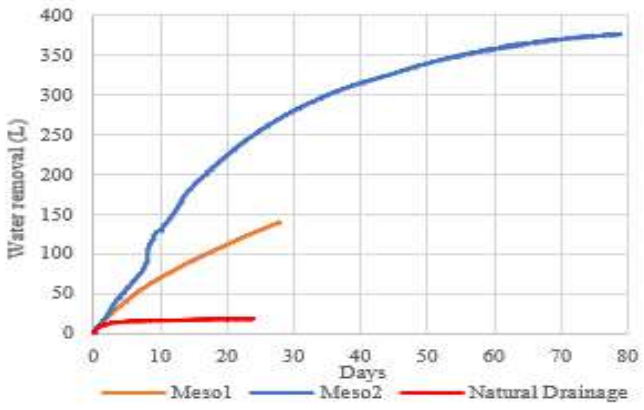

Figure 2: Water removal from meso-scale experiments

As can be seen from Table 6 and Fig. 2, the volume of water removed by Meso2 increased significantly due to the higher voltage gradient, which also led to a greater surface settlement and energy consumption. At the time of writing, IC and PR had not been applied at the meso-scale. As a result, further testing is required to confirm whether or not the parameters applied to Meso2 are optimal or not.

When comparing Meso1 with Meso2, the following were observed in both: (1) the over-saturated initial water content diminishes the effectiveness of EO, in which the design voltage gradient was unable to be achieved until preliminary dewatering reduced the water content to some degree; (2) as observed in the lab-scale experiments, significant soil cracking formed vertically along the electrodes and horizontally between the anodes and the cathode; and (3) the energy consumption of both Meso1 and Meso2 was significantly greater and less efficient when compared to the lab-scale experiments.

When comparing LV1 with Meso2, both of which were continually powered during the experiments, the following conclusions in relation to the EO upscaling effects were deduced:

(1) The effectiveness determined by the energy consumption versus water removal factor, E/W, reduced significantly in both the 15-day and 80-day periods (see Table 7);

(2) The significantly reduced EO effectiveness is likely not to be the result of drainage clogging or a drop in permeability, since samples from adjacent to the Meso2 cathode were soft and saturated, with no evidence of clogging;

(3) Upscaling increases the physical size and quantity of the tailings but not the particle and void sizes. Hence, the reduced E/W is the result of significantly higher energy consumption and reduced water drainage effectiveness. As shown in Table 7, the drainage path is the longest horizontal distance that a water molecule travels in the tailings which, in the laboratory-scale is half of the diagonal length, and in the meso-scale is the radius of the chamber (i.e. 0.35 m and 0.6 m, respectively, Table 7). The combined effect of the increased tailings volume and the increased drainage path length contribute to the reduction in the effectiveness of the drainage; and

(4) Drainage at the cathode in the experiments presented in this study may be considered sufficient as no water accumulation was observed, but the drainage path length could be further optimised with respect to the different scale.

Table 7: Results of Meso-scale EO experiment

Experiment No.	Tailings (m^3)	Drainage Path (m)	Energy/Water 15 days (Wh/L)	Energy/Water Total (Wh/L)
Meso1	0.06	0.35	5.70	5.70
Meso2	1.07	0.60	60.68	102.30

In summary, the meso-scale experiments demonstrated promising potential for dewatering sand tailings with the application of EO when compared against natural gravitational drainage.

5 CONCLUSONS

This paper has presented the results of ten EO consolidation tests performed on silica sand quarry tailings. Tests were performed at two different scales. At both experimental scales, the application of EO consolidation was found to enhance and accelerate water removal significantly, and it shows promise at the operational scale of a TSF. When translating the results of the lab-scale tests to those at the meso-scale, it was observed that upscaling was not linear and further work is needed to determine the nature of the upscaling relationship. In addition, soil cracking was observed at both scales, and this was shown to reduce the overall efficacy of EO consolidation. Further work is needed to refine the EO parameters in order to optimise the energy consumption versus volume and rate of water removal. Finally, larger field scale testing is needed to inform the operational characteristics of EO consolidation.

6 REFERENCES

Bjerrum L., Moum J. and Eide O. 1967. *Application of Electro-Osmosis to a Foundation Problem in a Norwegian Quick Clay. Géotechnique*, 17 (3), 214–235.

Cai Y., Qiao H., Wang J., Geng X., Wang. P. and Cai. Y. 2017. *Experimental tests on effect of deformed prefabricated vertical drains in dredged soil on consolidation via vacuum preloading. Engineering Geology*, 222, 10–19.

Fourie A., Johns D. and Jones C. 2007. *Dewatering of mine tailings using electrokinetic geosynthetics. Canadian Geotechnical Journal*, 44 (2), 160–172.

Fourie A. and Jones C. 2010. *Improved estimates of power consumption during dewatering of mine tailings using electrokinetic geosynthetics (EKGs). Geotextiles and Geomembranes*, 28 (2), 181–190.

Kaniraj S., Huong H. and Yee J. 2010. *Electro-Osmotic Consolidation Studies on Peat and Clayey Silt Using Electric Vertical Drain. Geotechnical and Geological Engineering*, 29 (3), 277–295.

Lamont-Black J., Jones C. and Alder D. 2016. *Electrokinetic strengthening of slopes – Case history. Geotextiles and Geomembranes*, 44 (3), 319–331.

Liu J., Lei H., Zheng G., Zhou H. and Zhang X. 2017. *Laboratory model study of newly deposited dredger fills using improved multiple-vacuum preloading technique. Journal of Rock Mechanics and Geotechnical Engineering*, 9 (5), 924–935.

Lockhart N. 1983. *Electroosmotic dewatering of clays. I. Influence of voltage. Colloids and Surfaces*, 6 (3), 229–238.

SETTLEMENT PREDICTION OF AXIALLY LOADED PILED RAFT FOUNDATIONS USING ADVANCED FINITE ELEMENT ANALYSIS

Parisa Rahimzadeh Oskooei[1], and Kaveh Ranjbar Pouya[1]
[1] FSG Geotechnics & Foundations, Melbourne, Australia

ABSTRACT

Piled raft foundations are an advanced engineering solution designed to improve safety against a potential bearing capacity failure or more importantly to mitigate the risk of excessive total or differential settlement and the generated flexural stresses in the raft. In a piled raft system, a concrete raft acts as the primary load-distribution platform and piles are installed into deeper, more stable soil strata to control settlements. This design approach facilitates economic design without compromising the safety and performance of the foundation. Several simplified methods are available in the literature to estimate piled raft settlement; however, these methods possess limitations in terms of simulating the realistic soil-structure interaction and load-sharing behaviour among the piles and the raft in complex ground conditions particularly for soils with highly variable strength and stiffness parameters. In addition, these methods lack accuracy when dealing with non-typical pile arrangements or piled raft geometries. This study utilises the finite element method as an advanced tool to investigate the non-linear load settlement behaviour of a piled raft. A series of parametric studies have been conducted to explore the soil-structure interaction problem and identify the impact of influential parameters on piled raft settlement, including piled raft geometry, pile spacing, number of piles and the depth to a stiff layer. The findings from this study offer valuable insights into the design and analysis of piled raft foundations, as well as a deeper understanding of the load-sharing mechanisms within these systems.

1 INTRODUCTION

Piled raft foundations are advanced engineering techniques increasingly used to support buildings and heavy industrial facilities. The inclusion of piles in these foundations can help to reduce both average and differential settlements of the raft, offering a cost-efficient design that maintains the safety and performance of the foundation. Piled raft foundations consist of three main elements: soil, raft, and piles where a concrete raft acts as the primary load-distribution platform and piles are installed into deeper soil strata to control settlements. The design of a piled raft foundation generally assumes that the majority of the load from the structure will be carried by the piles, while the raft provides a rigid platform to accommodate the piles and distribute the load among them. Therefore, it is of great importance to understand the load transfer mechanism in a piled raft and to accurately estimate the differential and total settlements of the foundation.

There are several design approaches and calculation methods for analysing the behaviour of piled raft systems and predicting the settlements (Randolph 1994, Poulos 2001, Clancy and Randolph 1993, Horikoshi and Randolph 1998); however, most of these approaches used simplified assumptions and cannot consider an accurate interaction of piles, raft and the surrounding soil. Poulos (2001) and Lee et al., (2010) suggested that using advanced numerical methods such as Finite Element Methods (FEM) can offer a better understanding of the behaviour of piled rafts and consider the pile-soil and pile-raft interactions. Despite the number of studies in this area, research into investigating the performance of the piled rafts appears limited. In addition, hand calculation and analytical methods are often unable to account for the presence of two distinctly different soil layers and other types of soil heterogeneity. This study aims to investigate the settlement behaviour of a piled raft under vertical loading using an advanced three dimensional (3D) finite element method and compare the results with commonly used analytical methods. In addition, several parametric checks have been undertaken in this study to identify the impact of several factors (i.e. depth to a stiff soil layer, piled raft geometry, pile spacing, and the number of piles) on the settlement behaviour of a piled raft system.

2 EMPIRICAL METHODS

Several empirical and conventional methods are being widely used in industry to calculate the settlement of piled rafts. Tomlinson (1994) proposed the Equivalent Raft method to calculate piled raft settlement. In this method, the piled raft is simulated as a raft placed at a depth of one-third of the pile length above the toe and the load at the surface is distributed into the soil at a slope of 4V:1H. To account for the presence of a stiff layer and the effects of embedment, influence factors I_f and I_s, as suggested by Fox (1948) and Steinbrenner (1934), can be applied in conjunction with the Equivalent Raft method. Poulos and Davis (1980) proposed the Equivalent Pier concept, in which a single equivalent pier is used to substitute the piles and the soil between them. Considering the Equivalent Pier concept, Horikoshi and Randolph (1999) and Poulos (2001) proposed simplified design methods to calculate the settlement of piled rafts, which are based on pile-

raft interaction. The equivalent pier may have an equivalent length and the same size in the plan of the group, or the same length and an equivalent diameter.

The Equivalent Raft method is preferred for large pile groups, or more precisely for groups where the raft width (*B)* is larger than the length of the piles (*L)*, while the Equivalent Pier method is more suitable for *L>B*. Randolph (1994) proposed an aspect ratio (R) and suggests using the Equivalent Raft method for an aspect ratio of *R*>4, and the Equivalent Pier method for *R*<2. While the suggested method and other empirical approaches in the literature can provide estimates of piled raft settlements, recent studies have demonstrated that the complex interactions between piles, soil, and the raft demand more rigorous analytical techniques. Therefore, sophisticated numerical analysis is required to accurately model the load distribution within pile groups and rafts, and to account for variations in pile actions due to the load distribution and pile locations.

3 NUMERICAL ANALYSIS

A 3D FEM model was developed using commercially available software PLAXIS 3D to investigate the behaviour of piled raft foundations in both infinite and finite soil conditions. Ideally, modelling piles as volume elements in 3D analysis is beneficial for providing the most accurate representation of the physical problem, particularly with regard to soil-structure interaction; however, due to associated computation costs and effort, volume elements can be replaced by embedded beam elements in PLAXIS 3D software. The embedded beam is particularly beneficial in cases of modelling large numbers of piles. Using embedded beam elements, the pile is represented by beam elements, while soil–pile interaction along the pile shaft and at the pile tip is described by special interface elements that are constructed based on node-to-node, non-linear coupling springs. In order to ensure that a realistic pile geotechnical capacity can be reached, PLAXIS 3D assumes an elastic zone around each embedded beam element in which soil plasticity is entirely excluded. This elastic zone allows the embedded beam to approximate the behaviour of a volume pile of the same diameter. However, it is crucial to verify that the embedded beam model performs as expected, without responding too softly or too stiffly compared to the volume pile model. Therefore, the performance of a single pile modelled as both a volume pile and as an embedded beam element was compared as shown in Figure 1. The load-displacement behaviour of these two models demonstrates a close agreement, indicating that the embedded beam can effectively replicate the performance of the volume pile with minimal discrepancies.

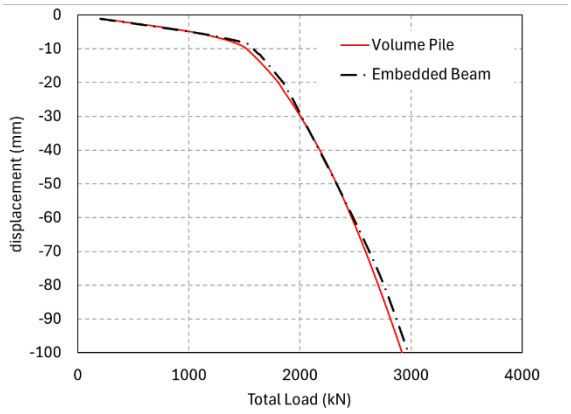

Figure 1: Comparison between the load-settlement behaviour of a single pile modelled as volume pile and embedded beam

As shown in Figure 2, a series of geometric parameters have been considered to investigate the impact of several influential factors on the settlement behaviour of piled raft foundations. Numerical analyses were carried out on piled rafts with varying pile numbers, lengths, spacings, and configurations, as shown in Figure 2. In the base case, the piles have a diameter of 750 mm and a length of 12 m (floating piles). The piled raft for the purpose of this study has been assumed to be rigid with a thickness of 0.5 m.

It is well understood that for flexible piled rafts (relatively thin and large rafts), the settlement estimates and the load-sharing behaviour between the piles and the raft can be significantly influenced by the type of loading. While uniform loading may be sufficient for the preliminary design purposes of large flexible rafts, it is considered to be inadequate for a more detailed design. However, in this study, a rigid raft that is not subjected to differential bending has been assumed to eliminate concerns related to the influence of loading types and a concentrated load (i.e., point loading) was applied at

the centre of the raft in all parametric analyses. Additionally, a 3x3 flexible piled raft was modelled to compare the impact of the area ratio against the rigid piled raft. Instead of applying a point load, the load was distributed as an equivalent uniform pressure over the raft area for all flexible piled raft cases, ensuring that the load distribution remained consistent and prevented unrealistic localised effects on the piled raft system. The soil material properties were selected based on industry experience and typical design values for stiff clay. A linear elastic perfectly plastic soil constitutive model with the Mohr-Coulomb failure criteria was adopted. All analyses were conducted under drained conditions. As such, a hydrostatic water pressure distribution was assumed, with the groundwater table at 4 m below ground surface.

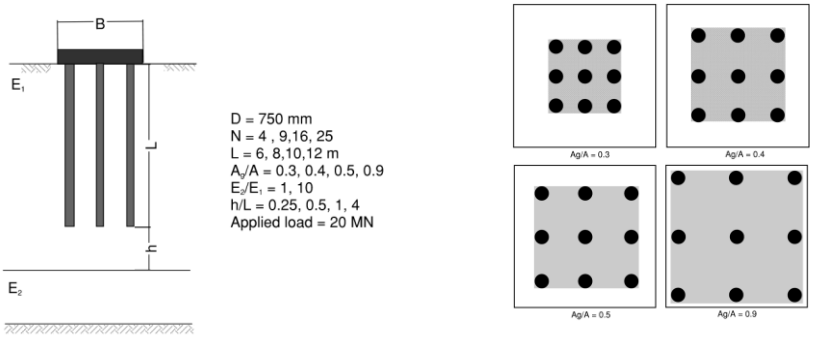

Figure 2: Variables considered for the parametric study

4 RESULTS AND DISCUSSION

Figure 3 presents a comparison between conventional methods for calculating piled raft settlement and FEM analysis. The results show that both the Equivalent Raft and Equivalent Pier methods generally predict higher settlements, often overestimating the settlement of a piled raft foundation. This observation is consistent with findings from previous studies (Viggiani et al., 2014), which suggest that analytical methods like the Equivalent Raft and Equivalent Pier methods tend to be conservative in their settlement predictions. However, previous studies have typically focused solely on comparing settlement estimates across different methods without considering the critical roles of load sharing between the piles and the raft, as well as the pile utilisation ratio relative to their ultimate geotechnical capacity. As shown in Figure 3(a), although analytical methods show higher settlement estimates (conservative) for piled raft configurations with 9, 16, and 25 piles, when piles are working harder (with more than 90% utilisation), such as in a 4-pile arrangement, FEM analysis reveals significantly greater settlement, challenging the validity of the previous assumptions.

As noted by Mondolini et al. (2005), the ratio of the area occupied by the piles to the raft area (for simplicity, referred to as the area ratio, Ag/A, hereinafter) is one of the critical factors in the design of piled rafts, influencing both differential and total settlement. However, as shown in Figure 3(c), the Equivalent Raft method does not account for the impact of the area occupied by the piles in the piled raft (A_g) and thus predicts a constant settlement for various A_g/A ratios. This limitation points to the method's inability to accurately reflect the distribution of load between the piles and the raft based on the piles' coverage area. Figure 3(d) further demonstrates the shortcomings of the Equivalent Raft method when combined with Steinbrenner's (1934) influence factor for the presence of a stiff layer with a stiffness 10 times higher than the soil above. The method generally underestimates settlement, particularly as it assumes a uniformly rigid layer beneath the raft without accounting for variations in stiffness. For small h/L ratios, the settlement predictions from the Equivalent Pier method and FEM analysis are comparable. However, as the depth to the stiff layer ratio increases, the discrepancy between the settlements predicted by these two methods becomes more pronounced, underscoring the limitations of the Equivalent Raft method in scenarios involving deeper stiff layers. These findings reinforce the conclusions of Randolph (1994) and Viggiani et al., (2014) that the Equivalent Raft method is more suitable for large pile groups with an aspect ratio of $R > 4$.

Figure 4 compares the settlement of a rigid piled raft and the piled raft coefficient (Q_p/Q_t) as functions of the number of piles and the area ratio. As illustrated in Figure 4 (a), there is a critical threshold for the number of piles beyond which adding more piles becomes less effective in terms of settlement reduction under constant vertical loads on the raft. Once the number of piles surpasses this critical threshold, additional piles result in only marginal decreases in settlement. This suggests that optimising the number of piles within this critical range can lead to significant cost savings without compromising the overall performance of the foundation system.

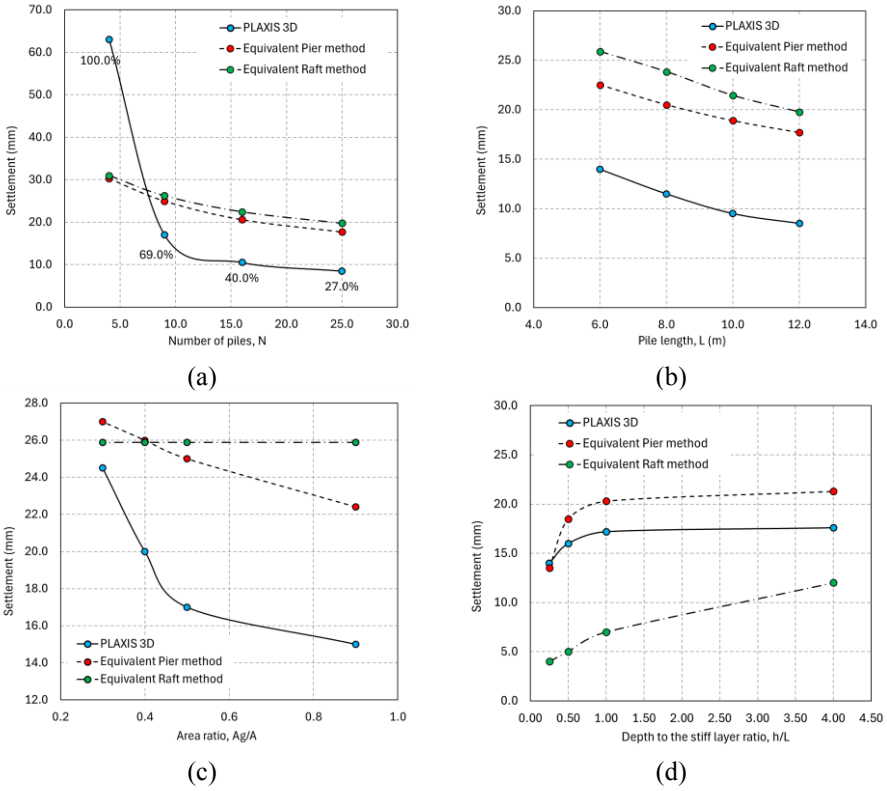

Figure 3: Effect of (a) Number of piles, (b) Pile length, (c) Area ratio, and (d) depth to the stiff layer on the piled raft settlement (data labels indicate the pile utilisation)

Figure 4 (b) further illustrates the relationship between the area ratio and the settlement behaviour of the piled raft. The results indicate that as the piled raft area ratio increases, the piled raft coefficient (Q_p/Q_t) also increases, suggesting a greater contribution of the piles to load transfer compared to the raft. This implies that the piles are taking on a larger share of the load as the area ratio increases. Therefore, designing a small rigid piled raft with a higher area ratio (A_g/A between 0.7 and 0.9) can not only effectively control settlements but also result in a higher piled raft coefficient, indicating more efficient load distribution within the foundation system.

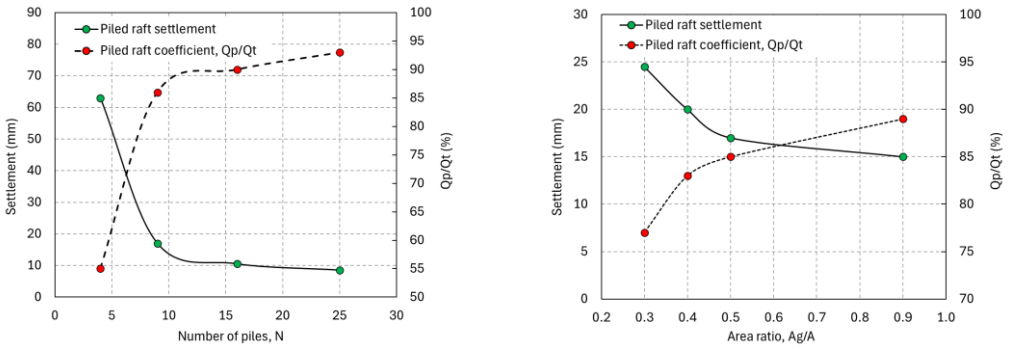

Figure 4: Piled raft settlement and piled raft coefficient as a function of (a) number of piles, and (b) area ratio

A piled raft foundation is commonly employed to mitigate differential settlement across the raft particularly when it is relatively flexible. To evaluate the impact of the area ratio on differential settlement, a 3x3 flexible piled raft was modelled with four different A_g/A values. As shown in Figure 5, the differential settlement ratio, defined as the ratio of settlement at the raft corners to the settlement at the raft centre, increases as A_g/A values increase. However, there is a threshold beyond which as piles are spaced further apart, the central piles become less effective at controlling the bending of the raft. This can lead to increased dishing, which in turn reduces the mobilisation of the corner piles, results in higher loads being transferred to the central piles and increases contact pressure in the central zone of the raft. The findings are consistent with the recommendations of Mondolini et al. (2005), who suggested that the optimal performance of a piled

raft is achieved when the piles are centrally located at an A_g/A of about 0.2 to 0.45. This is also consistent with the findings of Fleming et al., (1992) who discussed using the effectiveness of a central group of piles to reduce differential settlement. It is important to note that the optimal design is not always achieved by minimising differential settlement alone. A holistic approach considering maximum settlement, differential settlement, and the piled raft coefficient is necessary to determine the most efficient pile arrangement for the specific conditions of the foundation system.

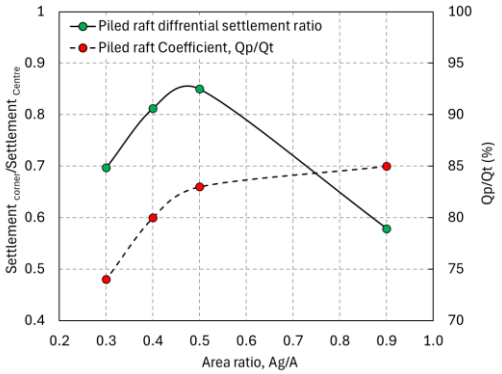

Figure 5: Differential piled raft settlement and piled raft coefficient as a function of area ratio - flexible piled raft

The load-displacement behaviour of the piles within a 5x5 rigid piled raft is illustrated in Figure 6 (a). It is evident that at the same displacement value, the corner piles experience a load larger than the average, while the central piles carry a load smaller than the average, and the peripheral piles fall somewhere in between. This behaviour can be attributed to the soil movement around each pile, as demonstrated in the corresponding vertical displacement contour plot. As shown in Figure 6(b), the soil mass enclosed inside the piles raft settles much more compared to the soil mass outside the footprint of the piled raft. Due to the relative rigidity of the raft, the absolute settlements of all piles are very similar; however, the corner piles experience higher differential settlement relative to the soil which results in the mobilisation of higher shaft resistances in these piles causing these piles to carry larger loads compared to the other piles. On the other hand, the soil mass inside the piled raft undergoes a larger settlement and the displacement of the centre pile relative to the soil is correspondingly lower; hence, less resistance is mobilised in the centre pile. The findings are consistent with the conclusions of Ranjbar Pouya et al. (2021). However, it should be noted that as the applied load increases gradually, the corner piles may reach their ultimate capacity. Once this happens, additional loads will be transferred to the peripheral/central piles. As a result, at a certain ultimate load level, all piles may experience similar axial loads.

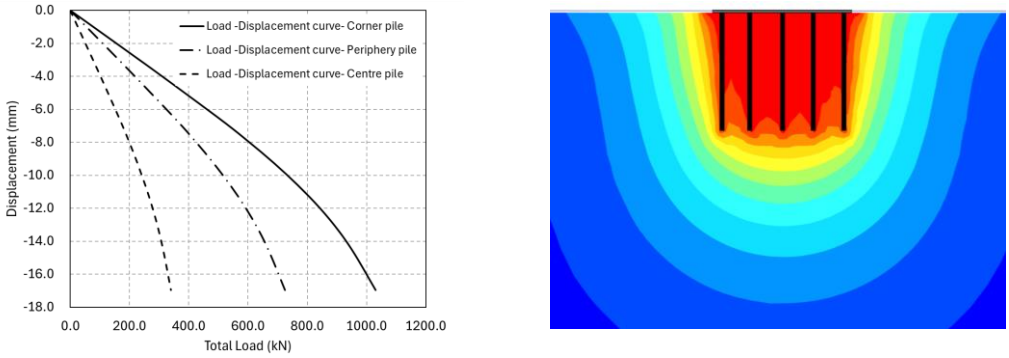

(a) (b)

Figure 6: (a) Effect of pile location on the load-displacement behaviour of a rigid piled raft; (b) Schematic view of vertical displacement contour of a 5x5 rigid piled raft

Figure 7(a) shows the load-displacement behaviour for a 3x3 flexible piled raft. Compared to the rigid raft with an A_g/A ratio of 0.5, as shown in Figure 5, this configuration was identified as the most effective in controlling differential settlement. The flexible raft exhibits a more uniform load distribution among the piles. The vertical displacement contours also highlight that although the corner piles settle less than the centre pile, the amount of mobilised shaft resistance is higher in these piles as they experience higher differential settlement relative to their surrounding soil. It is important to emphasise that these results are contingent upon selecting an A_g/A ratio that minimises dishing in the raft. Should excessive dishing occur, the corner piles may experience reduced load-bearing capacity and become less utilised.

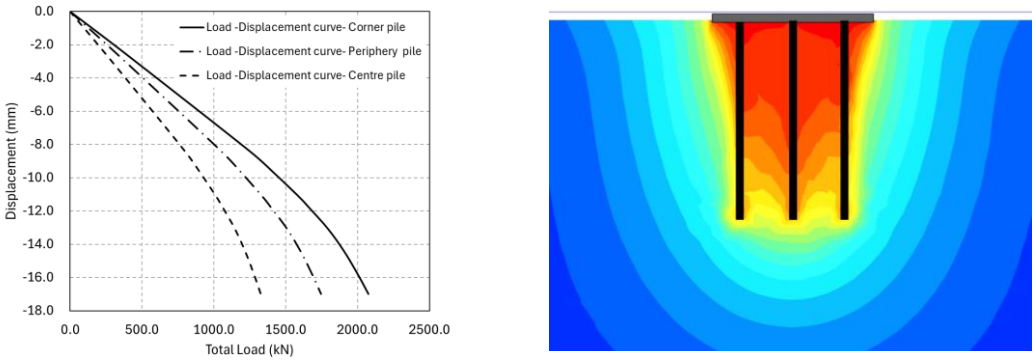

(a) (b)

Figure 7: (a) Effect of pile location on the load-displacement behaviour of a flexible piled raft; (b) Schematic view of vertical displacement contour of a 3x3 flexible piled raft

5 CONCLUSION

This study has demonstrated the effectiveness of using advanced FEM analysis in more accurately predicting the settlement behaviour of axially loaded piled raft foundations. By exploring various influencing factors, such as pile length, spacing, and the depth to a stiff soil layer, the research provides a deeper understanding of the complex soil-structure interactions influencing settlement outcomes. The finding of this study highlights the importance of optimising the pile arrangement rather than merely increasing the number of piles or their length. This study emphasises the need for a strategic approach to pile layout that maximises load distribution efficiency while controlling settlement. In conclusion, while the traditional empirical methods can be a useful tool for predicting the settlement of piled raft foundations, it is crucial to carefully consider the relation between settlement behaviour, the piled raft coefficient, and pile utilisation which are governed mainly by the strategic arrangement of the piles, rather than solely concentrating on the number of piles and pile lengths for the settlement control. Moreover, the study challenges the misconception that analytical methods always provide conservative settlement estimates. For example, when piles are heavily utilised, FEM analysis shows greater settlement compared to the Equivalent Pier and Equivalent Raft methods. This observation suggests that while these methods are useful tools for conceptual design and preliminary sizing of the raft and pile layout, they should be used with caution. For more reliable settlement estimates, in particular, for settlement-sensitive structures, an advanced 3D FEM analysis may be required.

6 REFERENCES

Clancy, P. and Randolph, M. F. (1993): "An approximate analysis procedure for piled raft foundations," *Int. J. Numer. Anal. Methods Geomech*., Vol. 17, pp. 849-869, DOI:10.1002/nag.1610171203.

Fleming, K., Weltman, A., Randolph, M. and Elson, K., 2008. Piling engineering. CRC press.

Fox, E. N. (1948). "The Mean Elastic Settlement of a Uniformly Loaded Area at a Depth below the Ground Surface," Proceedings, 2nd International Conference on Soil Mechanics and Foundation Engineering, Vol. 1, pp. 129–132.

Horikoshi, K., Randolph, M.F., (1998). A contribution to the optimum design of piled rafts. *Geotechnique* 48 (2).

Horikoshi, K. and Randolph, M.F., (1999). Estimation of overall settlement of piled rafts. *Soils and Foundations*, 39(2).

Lee, J., Y. Kim, and S. Jeong, Three-dimensional analysis of bearing behavior of piled raft on soft clay. *Computers and Geotechnics*, 2010. 37(1-2): p. 103-114, DOI: 10.1016/j.compgeo.2009.07.009.

Mandolini, A., Russo, G. and Viggiani, C., 2005. Pile foundations: Experimental investigations, analysis and design. In Proceedings of the 16th International Conference on Soil Mechanics and Geotechnical Engineering (pp. 177-213).

Poulos, H. G. and Davis, E. H. (1980). *Pile Foundation Analysis and Design,* John Wiley and Sons, New York.

Poulos, H., (2001) Piled raft foundations: design and applications. *Geotechnique*. DOI: 10.1680/geot.2001.51.2.95

Poulos, H.G., 2005. Piled raft and compensated piled raft foundations for soft soil sites. *In Advances in designing and testing deep foundations: In Memory of Michael W. O'Neill*, DOI: 10.1061/40772(170)

Randolph, M. F. (1994): "Design methods for pile group and piled rafts," *Proc. 13th Int. Conf. on SMFE*, New Delhi.

Ranjbar Pouya, K., Collingwood, B., and Judi, A., (2021) The Application of 3D Finite Element Method in the Design of a Large Piled Foundation System - Case Study: Melbourne Cement Facility. *AGS Victorian symposium: Innovation in geotechnical design.*

Steinbrenner, W. (1934). "*Tafeln zur Setzungsberechnung*," Die Strasse, Vol. 1, pp. 121–124.

Tomlinson, M., (1994). *Pile design and construction practice.* 4th edition, London.

Viggiani, C., Mandolini, A. and Russo, G., 2014. Piles and pile foundations. CRC Press.

BRIDGING THE GAP: ESTABLISHING A FRAMEWORK FOR SLOPE STABILITY SITE WALKOVER ASSESSMENTS IN NEW ZEALAND

Callum Sands[1]

[1] Hawthorn Geddes Engineers & Architects Ltd, 7 Selwyn Ave, Whangarei, New Zealand; email: cbs@hgcs.co.nz

Abstract:

The site walkover assessment is an essential skill for geo-professionals, serving as the initial step in identifying potential geohazards, and assessing project risk. Site walkover assessments lay the foundations for more detailed geotechnical assessments, providing valuable insight to guide decision-making. Despite the significance of this assessment, there is a notable absence of published guidelines and literature in New Zealand.

Currently, the skills and knowledge for undertaking an effective walkover assessment are primarily passed down through in-house mentorship from senior geo-professionals. As the profession grapples with an ageing demographic and a shortage of new talent, there is a genuine concern that this skill and expertise may be lost. This is particularly worrisome in more remote regions and smaller engineering firms where access to senior mentorship and training resources is limited.

Formal guidelines on such are needed to establish consistency and promote best practices within the industry, ultimately better serving the wider community. This paper seeks to address this gap by exploring the components of an effective site walkover assessment, serving as a quick guide/resource for young engineers who may lack direct access to senior mentorship. This paper has a focus on slope stability, stemming from the author's first-hand experience navigating their career with a lack of senior mentorship, whilst working in the challenging Northland geological environment.

1 INTRODUCTION

Geotechnical engineering fundamentally seeks to interpret the past, recognise the present, and predict the future behaviours of the landscape around us, and the impacts of this on society and infrastructure. Geotechnical hazards can include, but are not limited to, slope instability, liquefaction, lateral spreading, ground settlement, rock fall, mine collapse, and karsts. To ensure long lasting and safe infrastructure, geo-professionals must in the first instance correctly identify the signs of a geological hazard (Benson & Yuhr 2016).

Published geological maps and databases, Light detection and ranging (LiDAR) data, Digital Elevation Models (DEMs), and Geographic Information Systems (GIS) are used to develop engineering geological models (EGM), at the desktop stage. Site observations, subsoil stratigraphy, and other data are then later used to refine this model. The EGM is a ground model used to conceptualise geological conditions, and the interaction with our infrastructure, and assess the risk to human safety (Baynes & Parry 2022). These models are initially developed based on a desktop assessment and later refined in the field. The initial site walkover assessment provides an opportunity to conceptualise the preliminary EGM and to identify any potential hazard(s) present on the site. Often it is during this assessment that we begin to conceptualise mitigation measures. Adequate time must be allowed to undertake this assessment.

This paper presents a preliminary framework for conducting geotechnical site walkover assessments, focusing on land stability and landslide identification; including essential pre-visit research and what observations could be made on site. It is purposed to serve as a quick reference guide, aimed at young geo-professionals who may lack years of experience, extensive geological backgrounds, and/or access to senior mentorship.

The author of this paper has spent his career in Northland, New Zealand, working out of Whangarei, a region plagued with the complex geological unit Northland Allochthon. This geological formation is prone to movement even on gentle slopes, creating significant design challenges due to frequent landslides and unstable ground conditions. Drawing from the author’s extensive hands-on experience in this geologically complex region, this paper presents a framework for addressing slope stability, a critical issue exacerbated by recent natural events in the Northland region.

2 LITERATURE REVIEW

2.1 LANDSLIDES

Landslides are the dynamic (downward and outward) process involved in forming the earth's surface. Landslides can be defined as one of six classifications, namely falls, topples, slides, spreads, flows and a combination of two or more.

Landslide classification is the identification of the mass movement, material, rate of movement, failure geometry, causation, geographic location, degree of development and state of activity (Varnes 2020).

Slides are generally classified as either rotational or translational movements. Rotational slope movement is characterised by the detachment and subsequent downslope movement of a mass of soil or rock along a curved or concave failure surface. The triggering mechanisms often involve factors such as increased pore water pressure due to heavy rainfall, saturation of the soil matrix, and geological weaknesses such as the presence of a weak layer or discontinuity within the slope. On the surface, this type of failure manifests as a distinctive concave-shaped headscarp or scar at the uppermost part of the slope. Below the headscarp a displaced block forms, featuring an irregular and rugged surface morphology, Figure 1 below. This surface disruption results from the non-uniform deposition of material during its downward movement, leading to a hummocky and undulating terrain through the main body of the slip (Varnes 2020).

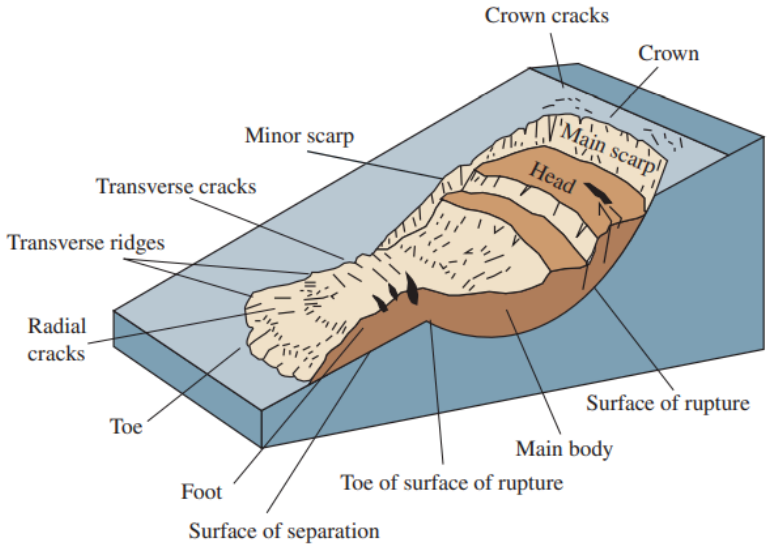

Figure 1: Common labelling of a rotational slide (Coastal and Marine Hazards and Resources Program 2004)

Translational slope movement occurs when a relatively coherent mass of soil, rock, debris, or combination, moves downslope along a nearly planar surface. In simpler terms, it's when a chunk of the hillside breaks away and slides downhill in a flat, sheet-like manner, without much rotation or tumbling. This type of movement is typical to occur over a shear plane, whereby there is a notable difference in soil/rock mass and strength. These slides can occur at immense scales and are not always self-stabilising (Varnes, 2020).

On a smaller scale, terracettes are evidence of shallow translational movement, also known as soil creep, generally occurring in the upper 0.5 to 1.0 m of the soil horizon. This can occur due to soil saturation, high rainfall, oversteepening of slopes (gravitational), and/or soil shrink/swell processes.

3 GEOTECHNICAL REPORTING IN NEW ZEALAND

3.1 LEGISLATIVE REQUIREMENTS

When assessing applications for building consent, regulatory authorities must be satisfied on *reasonable grounds* that all building works comply with the provisions of the Building Code, outlined under Section 71 of the Building Act 2004 (BA 2004) (New Zealand Government 2004). In the case of land development, the same is outlined in Section 106 of the Resource Management Act 1991 (RMA 1991) (New Zealand Government 1991). Both pieces of legislation define natural hazards that must be assessed, including slippage.

3.2 ENGINEERING STANDARDS & DISTRICT PLAN REQUIREMENTS

In New Zealand, District Plans and Engineering Standards are used to manage and regulate the use of natural resources and infrastructure. Each jurisdiction (district) has its own District Plan and Engineering Standard, the two serving complementary roles. A District Plan is a statutory document prepared under the RMA 1991, setting out the objectives, policies, and rules for land use and development within a given district. Engineering Standards are technical documents that provide detailed specifications for the design, construction, and maintenance of infrastructure.

The above generally requires that a site-specific geological/geomorphological hazard assessment is undertaken by a suitably qualified geo-professional, comprising the following:

- Assessment of the site and surrounding geomorphological processes,
- Definition of subsoil conditions, including the material strength, and likely slippage depth/planes,
- Analysis of potential failure mechanisms (typically a numerical slope analysis)
- Likely remedial measure, and any development restrictions.

To conduct a numerical analysis of a subject site, geo-professionals commonly rely on a numerical back analysis of nearby landslides to determine material strength and slippage planes. Often there is no immediate feature to undertake this back analysis, and geo-professionals may need to rely on visual inspection to define the continuity of the subsoil strata only. Similarly, visual slope identification is required to appropriately and accurately undertake a qualitative risk assessment. Therefore, a well-detailed and documented desktop and site walkover assessment is essential.

3.3 CURRENT PRACTICES

NZGS has recently released the first unit of seven in a series of guidance notes for geotechnical engineering. This document touches on techniques and methods for landslide identification, referring the reader to the IAEG Commission 25 guidelines (NZGS, 2023). The IAEG document provides a comprehensive framework for developing an EGM, however, it generally glosses over the site walkover assessment, suggesting it should be undertaken by a *"competent engineering geologist"* who relies on *"knowledge and experience."* (Baynes & Parry 2022). While these are reasonable statements, it is not always practical, particularly outside large consultancies where resources are limited. Future guidelines by the NZGS should include prescribed procedures for conducting landslide assessments, as well as for other geohazards. These procedures should incorporate detailed checklists, step-by-step instructions, and illustrative examples to ensure consistency and promote best practices.

4 SITE WALKOVER METHODOLOGY

A geotechnical site walkover assessment is generally undertaken to better understand the geomorphological process of a site, determine potential development sites, and/or assess the extent of a landslide(s).

4.1 DO YOUR HOMEWORK

The first step to undertaking a successful geotechnical site walkover assessment is to do your homework. This should comprise a detailed desktop assessment of all available data online, including a review of published geological mapping, online geotechnical database, aerial imagery, LiDAR data, and online GIS mapping. The desktop assessment serves as a virtual tour of the site's geomorphological history, developing an understanding of the site's behaviour. Much of this data is publicly available and should be utilised by geo-professionals.

Google Earth provides historical aerial imagery dating back to 1985 for New Zealand, allowing users to toggle between different periods to observe topographical changes. With the adoption of satellite imagery, the quality and frequency of capture have improved allowing engineers to assess the site under various conditions, such as different times of the day, seasons, or even post-cultivation, revealing indicators of land movement. Older aerial photography can be sought from Retrolens and with the use of stereograms, change in landform can readily be observed.

Free-to-download GIS software packages, such as QGIS can be utilised to process and view DEMs. The use of a hillshade model allows for rapid identification of slope features.

Many regional and district councils in New Zealand have developed and published natural hazard maps for their respective regions., including published reports that provide high-level overviews of the geomorphology of the region and likely hazards. These maps are a good point of reference as to what level of assessment is required.

4.2 ON-SITE OBSERVATIONS

4.3.1 General Walkover Assessment (Establishing Slope Stability Hazards & Development Footprint)

When conducting a general geotechnical site walkover assessment, the primary goal is to identify areas of the site that are currently, potentially, or have historically been subject to land movement that could negatively impact the proposed infrastructure.

Whilst travelling to the site, observe any roadside excavations, these are often over-steepened and not retained, allowing inspection of the wider geological unit. Note the soil type and layering, examine the rock; identify the rock type, and look for bedding, weathering, or fracturing. Look for signs of slope movement, such as longitudinal cracks or separations in the road pavement and leaning power poles, especially around bends and corners that traverse gullies. Observe the location of the existing infrastructure over the surrounding landscape, what is the topography doing, are there any modifications.

The bowing and leaning of trees are a telltale sign of slope movement. Due to phototropism trees will generally grow vertically, and when the root system is subject to movement, the trunk will correct this and grow upward, creating a bow, indicating historic movement. Whereas the leaning of trees indicates more recent slippage. Be cautious when using this method as some trees may falsely suggest slope movement, such as multi-stem trees, mature trees in high wind zones, shallow-rooted trees, or trees beneath a canopy with restricted light. Similar observations can be made with farm fences, which are often installed parallel or tangential to the slope direction, indicating the direction and extent of slope movement.

Water is the primary cause of slope movement, whilst walking over the site look out for areas of ponding and overland flow. Are there areas of concentrated reeds indicating saturated soils? Consider why there is a pond—whether it is anthropogenic or the result of a historic slippage creating a depression (main body - Figure 1).

Examine the appearance of the slopes: do they have a uniform, smooth, and planar surface, a terraced step-like appearance, an undulating rolling hill formation, or a hummocky, irregular, mounded terrain? A planar slope is typically stable, whereas undulating and hummocky slopes suggest varying levels of shallow and active slope movement. Note any cracks in the landscape, including the shape and direction, this could indicate slope movement (crown cracks – Figure 1).

At the toe of steep slopes, streams or creeks are often present. Assess the condition of the stream banks—are they eroded or incised? These conditions can indicate recent, large-scale slope movement, typically translational.

Allocate sufficient time to thoroughly observe your site. While large-scale landslides are usually evident, the previously mentioned indicators can signal less obvious gradual slope movements. It is important to view the site from multiple vantage points and at various times of the day. Variations in perspective and lighting can significantly affect your perception of the terrain. Look for unusual geological conditions that may not fit the general pattern of the landscape. These anomalies can often indicate anthropogenic interference or hidden hazards. Thought as to what slopes you may rely on for a back analysis and soil/rock strength calculation should be made; is the scale of the observed movement sufficient to back analyse the material strengths?

4.3.2 Landslide Assessment/Classification

When making site observations, a geo-professional must accurately identify and document the key geological features to develop the EGM and understand the main hazards and constraints of the site. These may include:

- **Dimensioning**: Measure the height, width, and length of the main scarp, minor scarps, and any crown cracks. Document the overall landslide length from scarp to toe, the length of the depression (main body), and the bulging (foot).
- **Material**: Note the condition of the evacuated material, whether it is moist, wet, or saturated. Is it soil, rock, or a combination of the two?
- **Causation**: Determine the cause of the landslide. Investigate the source of any water, this could be due to overland flow from a large catchment above, from stormwater short-circuiting due to anthropogenic, or natural slope modifications, or the presence of a spring. Has the site recently been felled of pines, resulting in the removal of root systems and significant soil disturbance, or have high winds uprooted trees to the same effect? Has river, or coastal erosion removed the buttressing mass (toe) of a slope, is there construction nearby causing vibration, or has there recently been seismic activity to trigger movement?
- **Vegetation and Weathering**: Vegetation growth and soil/rock weathering are good indicators of the landslides' age. Older movements often have progressed vegetation growth within the scarp. Moss growth and minor vegetation growth may indicate the landslide is not recent, and no more than a few years old. The absence of any growth indicates a more recent movement.
- **Condition of Natural Drainage Paths:** Assess the state of natural drainage paths and any signs of obstruction or diversion caused by the landslide. Where is the landslide debris headed?
- **Scale:** It is important to remember that landslides are often larger than initially perceived. The observable landslide may be part of a large movement.

4.3 DOCUMENTATION & REPORTING

Adequately documenting your site walkover assessment is imperative for future reference by you or other geo-professionals. When taking photographs in the field, take the time to ensure that the intended subject is fully captured

within the frame. Fewer, well-thought-out photos are easier to interpret in the office than numerous poorly composed ones. Think about the angle and framing of the photo so that it may be presentable in your later reporting. Adding a scale or label to photographs is equally important. Additionally, enabling the location setting on your mobile device allows for GPS-referencing the photos back in the office. Videos of topographical features, with voice notes/annotations, are a great way to translate thoughts back in the office. For a wider perspective of the site, drones are a great and cost-effective tool for taking aerial imagery from various angles/perspectives. Caution should be taken when using wide, or fish-eyed lenses in photography/videography as this can distort the landscape, and exacerbate, or hinder slope features.

Taking scaled A3 printouts of a DEM or high-resolution aerial imagery is highly recommended. This practice facilitates geomorphological mapping on-site, allowing for the annotation of key observations and their approximate locations.

5 FRAMEWORK FOR GEOTECHNICAL SITE WALKOVER ASSESSMENTS

Following the site walkover assessment, it is important to take a step back and revisit your findings with a fresh perspective. Having a colleague review your documentation can help identify anything you might have missed, as geotechnical professionals can sometimes convince themselves they see something that isn't there.

When formally documenting your walkover assessment, remember that your client is not a geo-professional. Your report should not only describe the findings but also explain the methodology and reasoning behind them. Write in a way that follows your walkover procedure and thought processes, allowing the reader to understand how you arrived at your conclusions. Simplification, and formalising your site notes on a simplified geomorphological map, in conjunction with annotated photographs of key features is a great way to do this.

The flow chart appended to this paper, Figure 2, illustrates some key steps that could be followed to ensure that a well-thought-out and structured site walkover assessment is undertaken. This flow chart is intended to be a quick-fire guide that may assist a young geo-professional in the field, serving as a reminder as to what key observations should be made.

6 CONCLUSIONS

This paper has explored the critical aspects of conducting a geotechnical site walkover assessment, emphasising thorough preparation, detailed on-site observations, and considered documentation for the identification of slope instability and landslides. Key features such as scarp dimensions, crown cracks, landslide direction, evacuated material state, and vegetation cover have been discussed to aid in accurate classification and impact assessment of landslides.

Before conducting a walkover assessment, young geo-professionals should undertake a detailed desktop study, to ensure they head to the site with a basic understanding of the site geomorphology. During their assessment, they should observe topographical characteristics, and signs of slope instability (active, or historic), document thoroughly with thoughtful photos and EGM annotations, assess water impacts and infrastructure damage, and consider wider geomorphological effects. After the site assessment, it is important to review findings with fresh eyes and seek peer review.

To standardise site walkover assessments in New Zealand, it is recommended that formal guidelines be developed and disseminated within the industry, including detailed checklists, step-by-step procedures, and illustrative examples to ensure consistency and best practices. It is understood that NZGS are in the process of developing this, highlighting the relevance and purpose for which this paper has been written.

Future research will be focused on creating a quick reference guide or handbook for young geotechnical engineers, further elaborating on the content herein.

7 REFERENCES

Baynes, F. J., & Parry, S. (2022). Guidelines for the development and application of engineering geological models on projects. International Association for Engineering Geology and the Environment (IAEG) Commission 25 Publication No. 1. Available at: https://www.iaeg.info/C25EGMGuidelines/.

Benson, R.C. & Yuhr, L.B., 2016. Site Walkover. In: Site Characterization in Karst and Pseudokarst Terrains. Dordrecht: Springer.

Coastal and Marine Hazards and Resources Program 2004, Diagram of deep-seated landslide, USGS Fact Sheet 3004–3072, US Geological Survey, viewed 5 July 2024, https://www.usgs.gov/publications/fact-sheet-3004-3072.

New Zealand Government. (1991). Resource Management Act 1991. Wellington: New Zealand Government.

New Zealand Government. (2004). Building Act 2004. Wellington: New Zealand Government.

NZGS. (2023). DRAFT Guidance Notes for Geotechnical Engineering. New Zealand Geotechnical Society.

Varnes, D.J., 2020. Chapter 2: Slope Movement Types and Processes.

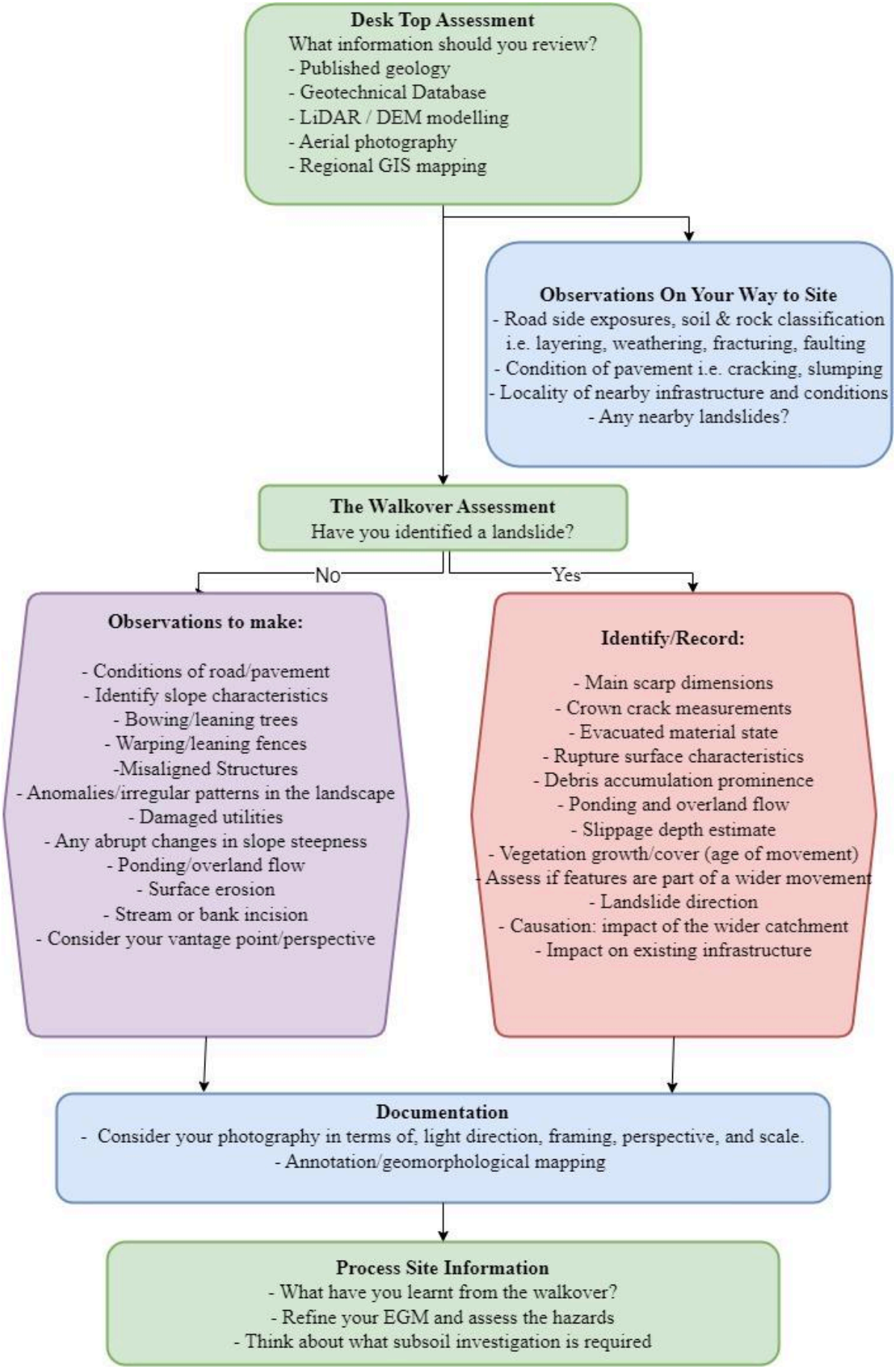

Figure 2: Simplified procedure for undertaking a geotechnical site walkover assessment of slopes/landslides.

APPLICATION OF STRESS WAVE THEORY TO PROVIDE NOVEL INSIGHTS INTO THE DYNAMIC CONE PENETRATION TEST

Edward J Smith
The University of Queensland, Australia

ABSTRACT

The Dynamic Cone Penetration (DCP) test is a relatively simple, cost-effective, and widely adopted penetration test that provides readily interpretable results. It is routinely used from preliminary site investigations through to construction verification. In this study, stress wave theory commonly applied to pile driveability studies and the dynamic testing of piled foundations, is used to provide novel insights into various factors affecting DCP test results. The stress wave delivered to the DCP rods following the hammer impact is modelled, and the stresses that develop in the testing apparatus and the DCP's interaction with the surrounding ground are studied. In examining these aspects, an alternative method for correlating DCP test results to ground strength has been derived, the influence of ground squeezing on the DCP rods examined, and more novel items such as the fatigue life of the DCP apparatus investigated. These insights improve understanding of the uncertainty associated with DCP correlations based on a range of static and dynamic properties, provide a means to isolate DCP rod friction from DCP test results, as well as provide recommendations on maintenance intervals for the DCP apparatus.

1 INTRODUCTION

The Dynamic Cone Penetration (DCP) test provides readily interpretable results that are used throughout the geotechnical industry. The interpretation of DCP test results requires the use of correlations with various engineering parameters, with geotechnical engineers often needing to consider the applicability of and uncertainty within these correlations. In addition, the potential for DCP test results to be affected by rod friction is ever present. Regular users of DCP equipment will also be familiar with the potential for equipment breakage and how this can reduce the efficiency of a testing program.

Stress wave theory has been applied to dynamically installed and/or tested piles for over half a century (Smith, 1960). This study has examined the application of stress wave theory to the mechanically similar, albeit smaller scale, DCP test to provide insights into correlations with undrained shear strength, the effect of rod friction, and equipment breakage.

2 BACKGROUND

2.1 DYNAMIC CONE PENETRATION TEST

The DCP test undertaken in accordance with AS1289.6.3.2 involves repeatedly dropping a 9 kg steel hammer vertically from a height of 510 mm to advance a 20 mm diameter hardened steel cone with apex angle of 30^o ahead of 1 m long, 16 mm diameter mild steel rods (Standards Australia, 1997, 2006). The test result typically reported is the number of hammer blows required to penetrate the rod for each 100 mm into the ground.

Theoretically, the maximum test depth is limited by the number of available rods, with additional rods connected using grub screws as the test proceeds. In reality, as the test depth increases there is increased risk of misleading results due to ground squeeze on the rods and or potential for energy losses due to lateral movement of the DCP rods over their unrestrained length.

The results of DCP tests have been correlated with a variety of parameters of interest to geotechnical engineers including the consistency of cohesive material, density of granular material, California Bearing Ratio and allowable bearing capacity (Look, 2014; Standards Australia, 2006). In this study, the correlation between DCP blow count and undrained shear strength of cohesive material is compared to the results from the application of stress wave theory.

2.2 STRESS WAVE THEORY

As the DCP hammer impacts the head of the rods, a compressional stress wave is introduced which propagates towards the conical tip (Benz Navarrete et al., 2022). An infinitely stiff and strong soil will not displace as the stress wave arrives at the conical tip, resulting in the reflection of a compression wave upwards into the rods, whilst a weak soil exhibiting no resistance will not limit the cone's displacement, and results in the reflection of a tensile wave equal in amplitude to the downwards compression wave. In reality, the nature of the cone-ground interaction will be between these limiting

conditions. The propagation of the stress wave can be modelled using the one-dimensional wave equation (Holloway, 1975). In this study the static and dynamic components of the ground resistance were simulated using the continuum model proposed by Simons and Randolph (1984).

3 METHODOLOGY

3.1 STRESS WAVE MODELLING

In this study, the one-dimensional wave equation was solved to determine the DCP cone penetration resulting from each DCP hammer blow. The simulation is initiated by assigning an initial velocity to the hammer, v_{hammer}, based on the gravitational acceleration (g = 9.81 m/s^2), the drop height (h = 0.51 m) and the assumption of 100% efficiency within the drop system ($\eta = 1$) (Equation 1).

$$v_{hammer} = \sqrt{2gh\eta} \tag{1}$$

This modelling approach has been implemented in a computer program being developed as part of the author's PhD studies, the software has passed preliminary verification studies however detailed verification is ongoing.

3.2 DCP CONE RESISTANCE

The static cone resistance, q_c, can be calculated using Equation 2, where N_c is a cone factor and σ a stress term dependent on the method used to calculate N_c (Baligh et al., 1980). Baligh et al. (1980) group the theories available to assess q_c into three categories: bearing capacity approaches (e.g. Meyerhof, 1961), cavity expansion approaches (e.g. Yu, 1993) and steady penetration approaches (e.g. Baligh, 1975). Using the referenced studies, cone factors ranging between approximately 7 and 20 have been calculated for a DCP cone assuming rigidity index2 (G/c_u) between 50 and 300.

$$q_c = N_c c_u + \sigma \tag{2}$$

3.3 DCP ROD FRICTION

The larger diameter of the conical DCP tip is intended to create a void annulus around the following DCP rods. However, there is potential for the ground to relax into the void annulus, contact the rods, and erroneously increase the penetration resistance. In this study, the effect of rod friction was simulated by running additional simulations with non-zero shaft friction at various rod embedment depths. The shaft friction adopted was based on the α method (Equation 3) (Das, 2015). For simulations considering rod friction, the results presented are for the second DCP blow from the given embedment (as opposed to the first DCP blow) to allow for the development of residual stresses in the rods.

$$q_s = \alpha c_u \tag{3}$$

3.4 STRESSES IN THE TESTING APPARATUS

Regular users of DCP equipment will likely have experienced the occurrence of broken grub screws which are used to connect DCP rods. In this study, the stresses developed in the grub screws were examined by extracting the maximum internal compressive and tensile rod force during a hammer blow and dividing by the cross-sectional area of the grub screw. These locally increased stresses were then compared to established metal fatigue parameters, and the anticipated life span of a DCP grub screw (in terms of DCP blows) was calculated. Consistent with the author's experience, the grub screw is assumed to be UNC 3/8 (7.8 mm minor diameter) made from A2-70 stainless steel.

The explicit modelling of the grub screw was not considered in analysing the stress wave. Consistent with AS1289.6.3.2, it was assumed that the grub screw connecting the rods was suitably tight so that the DCP rod ends were continuous. As they remain in perfect contact there was no change in impedance as a compression wave traversed the connection. For tensile waves, the reduction in impedance at the grub screw would reduce the force transmitted through the screw, such that the forces calculated by not modelling this change in impedance would be conservative (Randolph, 1991).

3.5 MODEL PARAMETERS

The ground models considered by this study are summarised in Table 1, with additional parameters required to undertake simulations described in Table 2. The range of N_c parameters considered were extended beyond the range indicated in Section 3.2, however the considered values were within the bounds that the author has determined from site specific calibrations between instrumented DCPs and in situ shear vane tests. The σ term in Equation 2 was taken as the initial vertical stress. It was assumed that the DCP rods extended 0.5 m above the ground such that the total length of rods for the embedments considered are 1 m, 2 m, and 3 m, respectively.

Table 1: Ground conditions considered in stress wave analysis

Ground Model	γ (kN/m^3)	c_u (kPa)	G/c_u [(1)]	ν [(2)]	α [(1)]	J_{vs} (s/m) [(3)]	N_{vs} (-) [(3)]
1	16	25	50	0.5	0.9	3.1	0.2
2	17	50	150	0.5	0.7	3.1	0.2
3	18	100	250	0.5	0.5	3.1	0.2
4	19	200	300	0.5	0.4	3.1	0.2

Notes: [(1)] Refer to Das (2015). [(2)] Undrained loading. [(3)] Typical values to simulate viscous resistance in clays, refer to Gibson and Coyle (1968).

Table 2: Model parameters adopted in stress wave analysis

Parameter	Value	Comment
Steel Young's modulus, E_{rod}	200 GPa	Typical (Standards Australia, 1998)
Steel density, ρ_{rod}	7850 kg/m^3	Typical (Standards Australia, 1998)
DCP hammer length	0.20 m	Assumed (Deemed typical)
DCP anvil mass	2 kg	Assumed (Deemed typical)
DCP anvil length	0.10 m	Assumed (Deemed typical)
DCP cone length	0.02 m	Typical cone approximately 0.05 m long, shorter length simulated to maintain approximate mass similitude.
Cone factor, N_c	10, 20, 30, 40	Various values for sensitivity assessment
Cone embedment	0.5 m, 1.5 m, 2.5 m	Various values for sensitivity assessment

4 DCP BLOW COUNT TO UNDRAINED SHEAR STRENGTH CORRELATIONS

4.1 CORRELATION WITHOUT DCP ROD FRICTION

The results of driveability simulations that did not include rod friction are presented in Figure 1. Results are presented for a rod embedment of 1.5 m, with similar results obtained for embedments of 0.5 and 2.5 m. The results indicate that adopting N_c = 30 gives simulated blow counts most consistent with the guidance provided by Standards Australia (2006) and Look (2014). This simulated value was higher than the range suggested in Section 3.2 and this result has initially been attributed to some combination of the following,

- The guidance presented by Standards Australia (2006) and Look (2014) may be conservative and the nominated DCP blow counts may be higher than necessary for a particular soil consistency.
- The limiting end bearing resistance that can be attributed to the strength of the soil (as opposed to resistance from energy radiation) is larger in cases of dynamic loading such that larger cone factors should be adopted in driveability simulations.
- The dynamic resistance simulated in the continuum model proposed by Simons and Randolph (1984) may not fully capture the increase in end bearing resistance due to dynamic loading, particularly for the small diameter DCP cone being simulated.
- The driveability analysis assumed 100% efficiency of the hammer release system, and no consideration was made for energy losses at impact. The energy losses associated with these items would be anticipated to reduce the DCP rod penetration.

It is also noteworthy that for c_u = 25 kPa, all simulations indicated > 100 mm penetration per DCP blow, with simulations using N_c = 10 also demonstrating that the ground could not support the DCP apparatus. These results suggest that more sensitive testing equipment (e.g. shear vane, instrumented PANDA® DCP) should be adopted in these materials to obtain reliable measurements of soil strength or a penetration/blow measurement implemented within the DCP test.

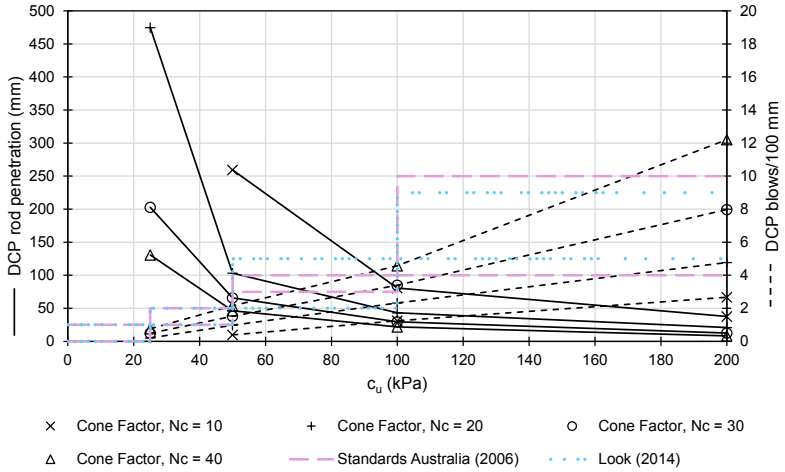

Figure 1: Results of driveability analysis without DCP rod friction (1.5 m embedment)

4.2 CORRELATION WITH DCP ROD FRICTION

The results of driveability simulations that included the presence of rod friction are presented in Figure 2. Results are presented for N_c = 30 and have been normalised against the results in the absence of rod friction. The analysis demonstrates that DCP tests undertaken at greater depths, or in softer soils, are more sensitive to the development of rod friction. However, the following points should be considered when drawing conclusions from Figure 2,

- The driveability analysis did not consider friction fatigue of the shaft material. The occurrence of friction fatigue will likely reduce the shaft friction exerted by the soil, particularly as the embedment increases.
- The driveability analysis assumed that the soil immediately relaxed onto the DCP rod after the cone passed. In reality, this relaxation is likely time dependent and stiffer materials likely have a reduced tendency to fully relax onto the rods.

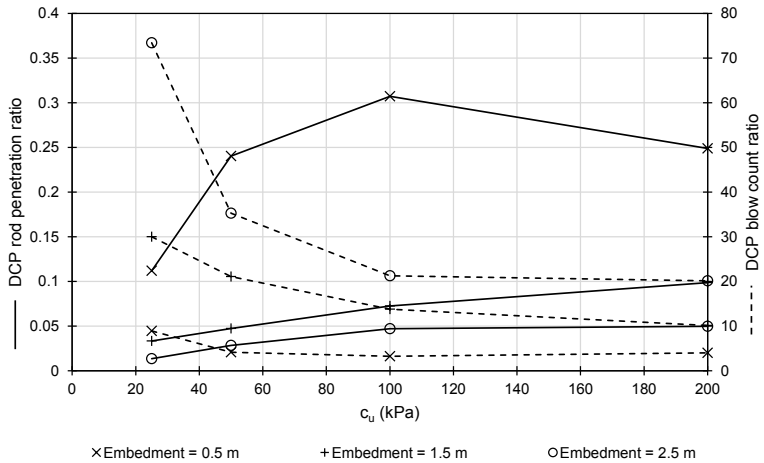

Figure 2: Results of driveability analysis with DCP rod friction presented normalised to simulations without rod friction (N_c = 30)

In light of these points, the results presented in Figure 2 further over-estimate the contribution of rod friction as rod embedment and soil consistency increase. Regardless, the analysis undertaken demonstrates the importance of accounting for the development of rod friction in DCP test results, particularly in weaker soils where the soil is more likely to relax onto the rod shaft and where the correlation with soil consistency is more sensitive to the reported DCP blow count value (per 100 mm rod penetration). Engineers might consider accounting for rod friction in the following ways,

- Vigilance of the DCP operator, ensuring the rods driven into the ground can rotate freely as the test proceeds.
- Applying a reduction factor to DCP blow counts. Whilst Figure 2 may assist in developing such a correction, the analysis underpinning this work was based on crude approximations for demonstration purposes. Site specific reduction factors, or more detailed analysis, may be required to correct for the development of rod friction.

- The development of a site specific correction would likely involve comparative testing with equipment less sensitive to rod friction, for example, an instrumented PANDA® DCP with a sufficiently oversized cone that removed the existence of rod friction.

5 STRESSES WITHIN THE DCP TEST APPARATUS

5.1 STRESSES AT ROD CONNECTIONS

The simulated peak DCP rod stress and the corresponding peak stress in the grub screw for a rod embedment of 1.5 m with N_c = 30 and no rod friction are presented in Table 3. The compressive stresses were larger than the corresponding tensile stresses, highlighting the importance of securely connecting adjacent DCP rods to ensure the rod ends are in intimate contact with each other (i.e., to not concentrate stress onto the grub screw).

Table 3: Peak stresses developed in DCP rod and grub screw for different ground models

Ground model	Peak compressive stress (MPa)			Peak tensile stress (MPa)		
	DCP rod	Grub screw	$N_{f,screw}$	DCP rod	Grub screw	$N_{f,screw}$
1	185	785	910	145	620	2510
2	190	800	830	170	720	1320
3	190	800	830	165	700	1480
4	195	820	750	160	670	1800

5.2 FATIGUE OF METALS UNDER CYCLIC LOADING

In the field of fatigue and fracture mechanics, an S-N curve is used to describe the relationship between the applied stress, $\Delta\sigma$, and the corresponding number of cycles to failure, N_f. Wang et al. (2020) established an S-N curve for A4-70 stainless steel at a 3 Hz loading frequency as described by Equation 4, with additional tests demonstrating no direct relationship between the number of cycles to failure and loading frequency for frequencies between 1 and 5 Hz. Whilst A4-70 stainless steel provides greater corrosion resistance than A2-70 steel, both materials have similar strength and stiffness properties (British Standards Institution, 2020). As such, Equation 4 was deemed appropriate for the purposes of providing general insights into the fatigue life of DCP grub screws for different ground conditions.

$$N_f = \frac{2.7285 \times 10^{15}}{\Delta\sigma^{4.3105}} \tag{4}$$

5.3 RELEVANCE TO DCP TEST APPARATUS MAINTENANCE

The predicted number of cycles to failure based on the peak stresses have been calculated using Equation 4 and are listed in Table 3. The following points should be considered when drawing conclusions from Table 3,

- The analysis undertaken assumes non-eccentric axial loading of the DCP rods. In reality, stress concentrations are likely to occur which will reduce the number of cycles to failure.
- Energy losses within the hammer release system and during impact have not been considered. Energy losses will reduce the stresses in both the DCP rods and grub screws.
- The results demonstrated sensitivity to the mesh discretisation and assumed apparatus geometry. The results should be viewed in terms of the trends they represent, rather than their specific values.

The results indicate that the modelled grub screw should survive between approximately 750 and 910 DCP hammer blows if the grub screw must sustain the compressive stress wave, and between approximately 1320 and 2510 blows if the grub screw only needed to sustain the tensile stress wave. Interestingly, the results suggest that a DCP grub screw can generally sustain more DCP blows as the soil consistency increases (assuming tensile loading only). This finding is consistent with stress wave theory, where the greater resistance offered by the stronger ground reduces the amplitude of the tensile stress wave reflected from the DCP cone (Section 2.2). It is acknowledged that this trend is not supported by simulations involving c_u = 25 kPa, which may be influenced by the mesh discretisation or other attributes of the numerical procedure, and could warrant attention in future work. When rearranged in terms of the number of DCP tests undertaken, 1800 blows corresponds to approximately 15 number of DCP tests to 1.5 m in c_u = 200 kPa ground (approximately 8 DCP blows/100 mm, Figure 1) whilst 1320 blows corresponds to approximately 60 number of DCP tests to 1.5 m in c_u = 50 kPa ground (approximately 1.5 DCP blows/100 mm, Figure 1). When viewed in light of the approximations and assumptions made in the analysis, these results are likely consistent with field experience.

6 CONCLUDING REMARKS

This study has examined the application of stress wave theory to the DCP test. The study was designed to provide general

insights into published correlations between DCP test results and undrained shear strength, the effect of DCP rod friction, and the stresses developed within the grub screws used to connect the DCP rods. The salient conclusions are as follows,

- In the absence of rod friction, the adoption of a cone factor of 30 gave simulated blow counts most consistent with published undrained shear strength correlations. This factor is larger than typically suggested in existing literature and indicates possible scope for the development of dynamic cone factors.
- DCP penetrations in soft soil were significant and emphasised the importance of adopting a more sensitive testing procedure (e.g., shear vane, instrumented PANDA® DCP, measurement of penetration/blow) in these cases.
- DCP test results were more sensitive to rod friction as soil strength reduced or embedment increased. Appropriate measures should be implemented on site to prevent or allow suitable correction for the occurrence of rod friction.
- When the DCP rod ends are not in intimate contact, the number of cycles to grub screw failure reduces. Where the grub screws only need to sustain the tensile wave, the number of blows to failure generally increases with increasing undrained shear strength, however the total number of DCP tests to failure generally decreases.

This study incorporated several assumptions and approximations for the purpose of providing general insights. Users of DCP equipment and/or test results should consider the applicability of the findings to their particular projects and develop site specific correlations and/or equipment maintenance plans as necessary to account for the items considered.

7 ACKNOWLEDGEMENTS

The author prepared this manuscript during their studies at the University of Queensland which are supported by the Australian Government Research Training Program Scholarship and the National Industry PhD Program. The author would like to thank David Lacey and Matthew Stewart, FSG Geotechnics and Foundations, for their encouragement to prepare and time reviewing this manuscript. The author also acknowledges David Williams, The University of Queensland, for his guidance and for supporting the attendance of the author at the 15th Young Geotechnical Professionals Conference.

8 REFERENCES

Baligh, M. M. (1975). *Theory of deep site static cone penetration resistance* (Report No. R75-56). Massachusetts Institute of Technology.

Baligh, M. M., Azzouz, A. S., & Martin, R. T. (1980). *Cone penetration tests offshore the Venezuelan Coast* (Report No. MITSG 80-21). Massachusetts Institute of Technology.

Benz Navarrete, M. A., Breul, P., & Gourvès, R. (2022). Application of wave equation theory to improve dynamic cone penetration test for shallow soil characterisation. *Journal of Rock Mechanics and Geotechnical Engineering*, *14*(1), 289-302.

British Standards Institution. (2020). BS EN ISO 3506-1:2020 - Fasteners - Mechanical properties of corrosion-resistant stainless steel fasteners - Part 1: Bolts, screws and studs with specified grades and property classes: BSI Standards Limited.

Das, B. M. (2015). *Principles of foundation engineering* (7th ed.). Cengage Learning.

Gibson, G. C., & Coyle, H. M. (1968). *Soil damping constants related to common soil properties in sands and clays* (Research No. 125-1). Texas Transportation Institute - Texas Highway Department.

Holloway, D. H. (1975). *Wave Equation Analyses of Pile Driving* (Report No. S-75-5). Soils and Pavements Laboratory - U.S. Army Engineer Waterways Experiment Station.

Look, B. G. (2014). *Handbook of geotechnical investigation and design tables* (2nd ed.). CRC Press, Taylor and Francis Group.

Meyerhof, G. (1961). The ultimate bearing capacity of wedge-shaped foundations. 5th International Conference on Soil Mechanics and Foundation Engineering, Paris, France.

Randolph, M. (1991). Analysis of the dynamics of pile driving. In P. K. Banerjee & R. Butterfield (Eds.), *Advanced Geotechnical Analyses* (1st ed., pp. 223-272). Taylor and Francis Group.

Simons, H. A., & Randolph, M. F. (1984). *New Approach to One Dimensional Pile Driving Analysis* (Report No. CUED/D-Soils TR 159). University of Cambridge.

Smith, E. (1960). Pile-driving analysis by the wave equation. *Journal of the Soil Mechanics and Foundations Division*, *86*(4), 35-61.

Standards Australia. (1997). AS1289.6.3.2 - Methods of Testing Soils for Engineering Purposes: Standards Australia.

Standards Australia. (1998). AS4100-1998 - Steel Structures. Australia: Standards Australia,.

Standards Australia. (2006). HB160-2006 Soils testing. Sydney, Australia: Standards Australia,.

Wang, J., Uy, B., Li, D., & Song, Y. (2020). Fatigue behaviour of stainless steel bolts in tension and shear under constant-amplitude loading. *International Journal of Fatigue*, *133*.

Yu, H. S. (1993). Discussion on Singular Plastic Fields in Steady Penetration of a Rigid Cone. *Journal of Applied Mechanics*, *60*, 1061-1062.

VICTORIAN LAVA CAVES: INVESTIGATION AND RISK MANAGEMENT

Simon Harbig[1], Susan White[2,3]
[1]WSP Australia, [2] Wakelin Associates, [3]Victorian Speleological Association Inc.

ABSTRACT

Small to medium sized subcrustal lava caves occur in Western Victoria in the Neogene to Quaternary Newer Volcanics Basalt. Subsurface voids created by these lava caves and the potential collapse can present a significant risk to developments in areas underlain by the Newer Volcanics. The size, depth and spatial distribution of lava caves can be difficult to determine and investigations in such areas are not routinely designed to detect lava caves. This paper briefly describes lava cave formation in Victoria and resources that inform locations and features of known lava caves. Two case studies are discussed, an investigation of a known lava cave for a proposed development and an unexpected void or blister cave encountered during construction. The paper then discusses strategies to mitigate the risk of encountering un-anticipated subsurface voids or lava caves within the Newer Volcanics Basalt.

1. INTRODUCTION

Victoria's lava caves are located on the Western District Volcanic Province, the world's third largest volcanic plain with an area of ~2.3 million hectares (Romsey Australia, 2011). Formed by a succession of eruptions of basaltic lava flows between about six million to 5,000 years ago, it has over 400 identified eruption points and over 130 known lava caves across the province, many associated with the youngest eruptions, Mt Eccles (Budj Bim) and Mt Napier (Grimes, 2007). Lava caves also exist in the Mt Gambier area, Queensland Cenozoic volcanic provinces (Webb et al 2023) and New Zealand, e.g. Auckland.

Increasing development can result in un-anticipated lava caves or subsurface voids within the basalt presenting risks, for both safety and environmental reasons. Currently there is little publicly available guidance on how to manage these risks. This paper aims to give some guidance to practitioners on how to investigate and manage lava cave risks.

2. LAVA CAVE FORMATION

There are three broad subcrustal lava cave types are linear lava tubes, lava lobes (Peterson et al., 1994) and blister caves (Grimes 2002). These cave types can be broadly described as:

- Linear lava tubes: long, roughly linear lava tubes, associated with a main channel.
- Lava lobes: A series of advancing lava lobes, generally secondary to the main channel.
- Blister caves: isolated small cavities formed by pockets of hot gas or trapped liquid lava that later drains away.

The formation of lava tubes occurs by roofing over a linear surface lava channel or the draining of molten material from under the solidified crust of pahoehoe flow lobes (Peterson et al., 1994) (Figure 1). Roofing occurs when sections of crust break up into solid rafts that may jam at channel constrictions and weld into a solid roof. Fluctuating, rapid and/or turbulent flows form levees from overflow or spatter over channels forming roofs (Figure 1).

Lava lobes form in a series of steps as liquid lava breaks the sidewall of a larger channel creating a smaller channel and caves form in a series of waterdrop shaped lava lobes. Once the lava source is exhausted, the liquid lava in the lobes may move forward, partially draining the lobes behind or draining back into the main channel and a linear feeder tube (Figure 1, Steps 3b and 4) Lava lobe development is associated with less viscous or pahoehoe lava. Local factors including: the type of eruption, lava viscosity; interactions with previous lava flow; geomorphology and geology, may result in varied and complex lava cave systems forming.

Not all tubes are drained, most will remain filled, and later eruptions may flow through an existing open tube causing further evolution of the tube or blockages. Both during active flows or after eruptions have long ceased, collapse of the roof or walls may occur within the cave. (Gunn, 2004). Younger flows break through into lower and older lava flows, filling, partially filling or further eroding them, and complex multilevel systems may develop.

Blister caves are small circular, elongate or irregular cavities not associated with larger lava cave systems. They are isolated low roofed chambers that create crescentic highpoints or 'stoney rises' in the landscape. The chamber roof sags while hot and may later collapse and the void filling with debris. The outer edges of the chambers may be smoothly rounded or form a sharp angle with a nearly flat roof, with lava drips, forming when the lava was plastic (Grimes 2002).

Surface features are an unreliable indication of subsurface lava caves. 'Stony rises' may indicate the presence of blister caves (Grimes 2002). Tumuli are a discrete steep-sided lava crust pressure mounds pushed up above the flat lava surface. Occasionally the liquid core drains back to leave a central subsided hollow (Grimes, et al., 2010). However, the low relief surface topography in Western Victoria, means the topography of sub-surface lava caves is not always evident.

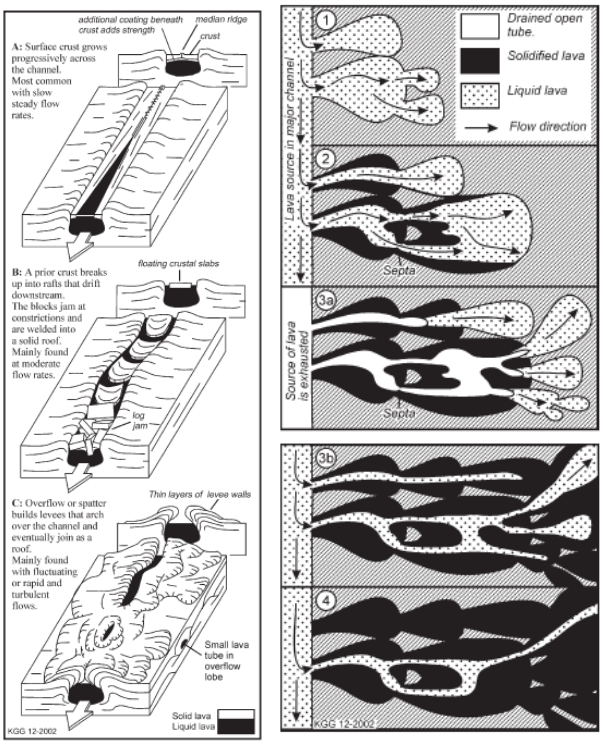

Figure 1 : Linear lava channel formation (left) and lava lobe formation (right) (Grimes, 2002)

3. LAVA CAVE LOCATIONS

There is limited detailed publicly available information on Victorian lava caves. The only extensive and detailed cave records, including surveys and maps, are held by the Victorian Speleological Association (VSA). Cave locations are rarely published, except for tourist caves, to protect the caves and minimise risk of accidents. Across Australia, cave related data is held by the Australian Speleological Federation (ASF) and its various member clubs. ASF has a publicly available Karst Index Database (KID) which includes some information on lava caves available at https://caves.org.au/caves-and-clubs/karst-index-database/. The database generally includes basic cave descriptions and very limited location data. The Geological Society of Australia (Victoria) (GSA-V) maintains the sites of geological significance database for Victoria and other states and territories have state-based records. Both VSA and GSA-V are approachable for information. The Victorian Resources Online (VRO) website contains some information but this data is often out of date. Geological Survey of Victoria's (GSV) maps and reports of an area are useful, especially for identification of lava flows.

4. CASE STUDIES

Two case studies of lava cave investigations are Parwan Lava Cave (3H-4) and a construction site in Truganina.

4.1. PARWAN LAVA CAVE (3H-4)

The Parwan Lava Cave (3H-4) is located at Parwan, Victoria, 1 km southeast of the Parwan railway station. It is assigned as a site of high-level State Geological/Geomorphological Significance by GSA-V as the second oldest known lava cave in Australia, 4.13 million years old (Aziz-ur-Rahman & McDougall 1972, Gibson 2007). The cave is the type locality for the rare Parwanite mineral, a phosphatic mineral formed by the interaction of basalt and bat guano.

4.1.1. INVESTIGATION PROCEDURES

Golder Associates Pty Ltd (WSP Golder), assisted by Wakelin Associates, was engaged to provide recommendations for the ongoing protection of the cave and any geological hazards which may impact a proposed development. These comprised of a desktop study, an upgrade of the 1969 VSA survey of the cave, and a geophysical survey (WSP Golder report 'Parwan Lava Cave – Geotechnical Assessment' (2 June 2023)).

The desktop study collated publicly available information on the cave with information from the VSA and GSA-V. This included the 1969 tape, compass, clinometer with detailed cross sections cave survey conducted by VSA members and detailed descriptive material. WSP Golder plotted the 1969 survey in real space which enabled the mapped extent of the cave to be better understood with respect to the proposed development and assist with subsequent stages of investigation. A survey using a radio direction finder (RDF) device (two radio phones, a transmitter and a receiver) and a distance laser measuring device (Disto) was undertaken. The transmitter emits a radio frequency directionally from one circular antenna which is picked up by the receiver. Transmitting from inside the cave, radio frequencies are transmitted vertically to the ground surface that position can be located by the receiver and a GPS, logging in real-world coordinates. The cave alignment was mapped at surface level by repetition along the direction of the passage. The Disto device was used for accurate internal cave measurements between the various RDF points. The RDF GPS data were plotted with the Disto measurements in 3D space and compared against the underground 1969 map, improving the accuracy of the map. WSP Golder also conducted a geophysical survey comprising of both electrical resistivity tomography (ERT) and seismic refraction tomography (SRT) in a two staged approach. The section west of the entrance of the upgraded survey map was annotated with scan lines. Geophysical scan lines were completed for the section of the cave west of the entrance enabling the geophysical survey to be calibrated against the upgraded survey results. Extra scan lines were conducted to western areas of the mapped cave. A relatively coarse resolution of 1-1.5 m receiver spacing was used.

Comparison between the two surveys indicated that both ERI and SRT techniques were able to identify the lateral extent of the cave. The geophysical survey could not distinguish between open void and areas of rock rubble or loose soil (i.e. collapse material). SRT survey results appear to show the cross-sectional cave shape more clearly. Voids interpreted by the geophysical survey elsewhere were plotted against the 1969 survey (**Figure *2***). The results showed correlation with the 1969 survey but indicated significant voids outside of the 1969 mapped extent.

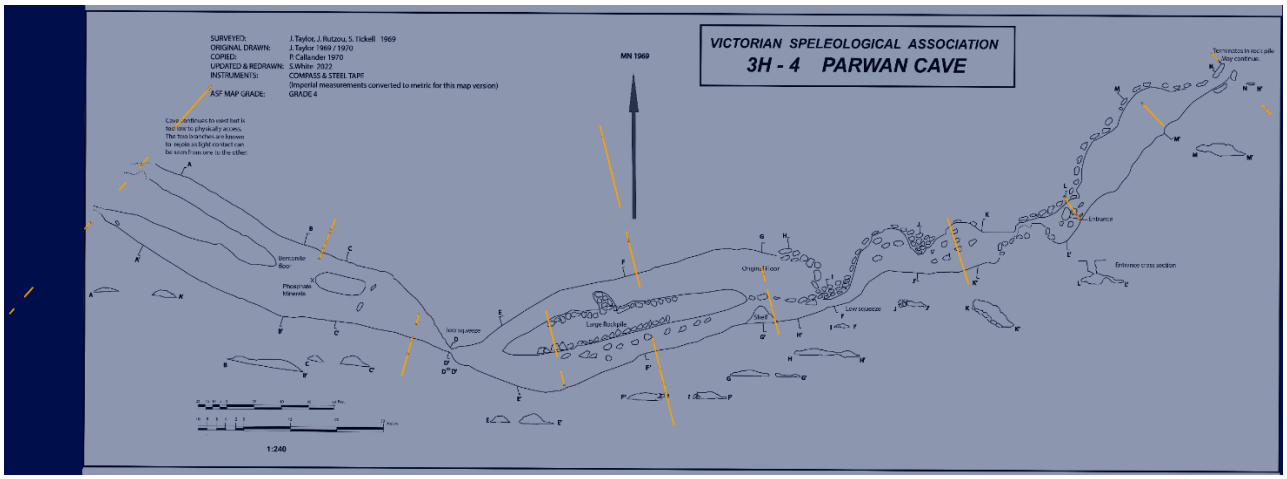

Figure 2: Comparison of voids (orange lines) found by WSP Golder geophysical survey and 1969 speleological survey.

4.1.2 RESULTS AND DISCUSSION

The area is flat with no significant surface depressions; the only known entrance is the collapse entrance (Figure 2). The area is lightly developed (mostly farmland), but other cavities may be present locally and likely to be discovered by excavation (i.e. from development).

The 1969 Parwan Lava Cave map (Figure 2) covers only part of a longer cave system; the extent mapped is the known accessible passage in 1969. The extra passage to the west was too tight to enter. Voids to the north and south indicated by the geophysical survey suggest additional lava tubes or chambers are likely to be present and that the Parwan Lava Cave may be part of a lava lobes style cave system as represented in Figure 1. The 1969 survey gave an understanding of the known cave in size, extent and condition and the results obtained from the upgraded survey gave confidence to the geophysical survey techniques, with SRT giving clearer results (Figure 3 and Figure 4).

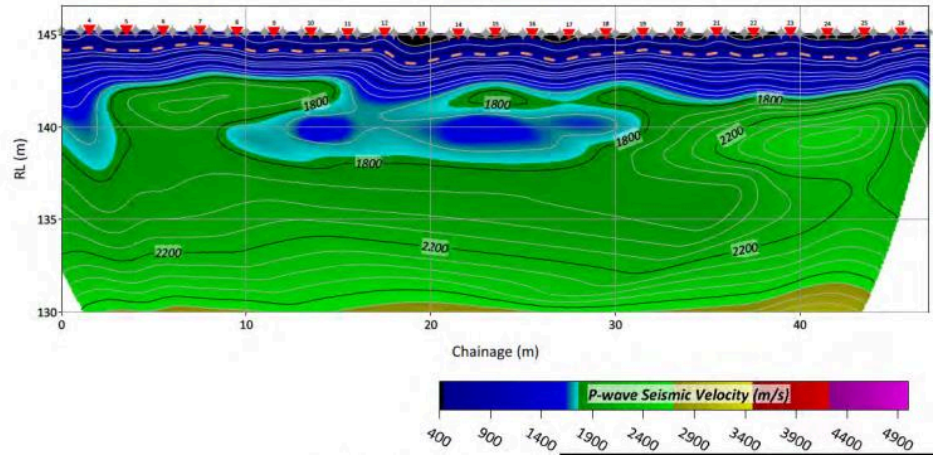

Figure 3: SRT geophysics scan of Parwan Lava Cave. Scan conducted perpendicular to general cave alignment. Sharp velocity gradients (green to blue) indicate areas of void.

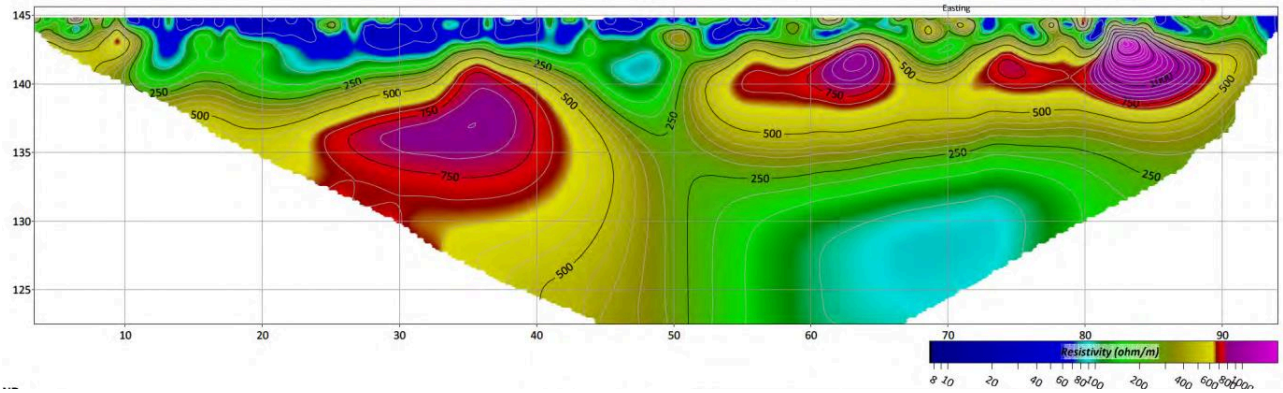

Figure 4: ERT geophysics scan of Parwan Lava Cave. Scan conducted perpendicular to general cave alignment. High resistivity (red to purple) zones indicate areas of void.

The most likely eruption point for the lava is Mount Bullengarook some 30 + kms to the north-east (Roberts 1985). This flow can be mapped from the eruption point to the Parwan area where it has spread out into a fan style feature that may host more voids. The area surrounding the cave comprises Newer Volcanic basalts of similar age to the flow.

4.2. TRUGANINA

During foundation slab excavation in the western Melbourne suburb of Truganina, a significant subsurface void was uncovered. Excavations extended 2 to 3 m below the original ground surface into solid basalt where the void was encountered. The void contained some loose rock and clay. Once cleaned of these, the void was ~6 m deep and ~8 m by ~4 m in plan area. Being located underneath a proposed foundation slab, concerns were raised regarding the extent of the void and potential risk to the proposed foundations. Potential delays in construction activities also created time pressures on investigation and remediation of the void.

This paper gives a brief overview of the investigation methods and remediation undertaken referenced from internal WSP correspondence.

4.2.1 INVESTIGATION PROCEDURES

Loose material present in the void was cleaned out and an earth berm constructed for safety. Multiple basalt lava flows of highly variable thickness, were evident in cuts around the site. Layers 30 cm to a few meters thick being observed. The void appeared to be at the intersection of several flows, with the more deeply weathered rock near the intersection of the flows and a relatively thin but hard ‘ledge’ forming a cap or bridge over the void (Figure 5).

Remediation of the void was needed and concerns were raised that the void may continue beneath the basalt ‘ledge’ and additional larger chambers could exist. Initially to determine the extent of the void, a drone was utilised to photograph in the void, mitigating safety risks of personnel attempting to enter it. The drone footage indicated that the void narrowed to a very small opening but continued, indicating further investigation was required. Lava ‘drip’ features could be seen on the void’s roof which confirmed this void was a natural feature.

Due to time and construction constraints, geophysical survey methods could not be employed around the void, and reverse circulation (RC) drilling was used to drill boreholes in a radial fashion around the void.

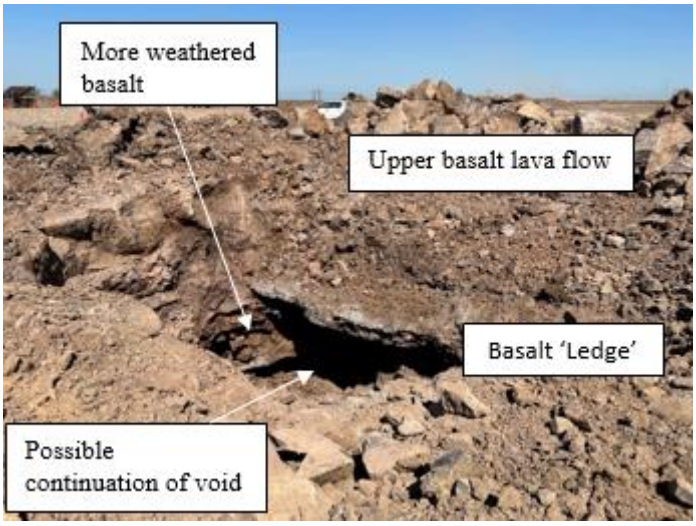

Figure 5: Uncovered void in basalt, loose material has been removed from void.

4.2.2. DISCUSSION

No obvious entry and exit points were observed in the drilling only a small, narrow section of cave was encountered. No other similar features were encountered during bulk excavations leading to the conclusion that this void is probably a localised blister cave (see section 2). Although this void did not extend significantly, the presence of similar blister cave voids has been reported in the flows in the area between western Melbourne and Geelong. In this case there is confidence that this void does not extend significantly further, although other blister caves may exist.

5 LAVA CAVE RISK MANAGEMENT

All caves and voids present risks for construction, health and safety and environmental values. Lava caves present risks to civil projects and developments within the Western District Volcanic Province, especially in the new development areas of Western Melbourne.

The earlier potential lava caves are identified in a project, the risks affect proposed developments place on the lava caves themselves, the more likely are to be able to be avoided and/or mitigated. However, while efforts should be made to investigate the presence of lava caves their presence within the Western District Volcanic Province is not easy to predict; the potential for their presence should be always considered. Techniques described in case studies (Section 4) are valuable methods to employ, but each case will be unique.

5.1 RISK ASSESSMENT

This section has information for projects in Victoria; other states have similar bodies for consultation. Case files presented in section 4 give examples of different methods used to investigate potential lava caves. The types of methods used will largely depend on the project scope and evidence of existing lava caves in the area.

The following questions should be considered:

Are there known lava caves reported in the area? A preliminary desktop study during the planning phase of a project, is valuable and consulting relevant geological maps and reports and contact with relevant cave related organisations (see Sections 3 and 4).

Are there any features in the area that might indicate the potential for lava caves? What are the potential consequences for the proposed development? Consequences for a development are hard to ascertain as it depends on the type of development, phase of the project, location and size and nature of the potential cave. During project planning limits to development boundaries or other requirements on developers to undertake appropriate investigations may be put in place. Lava caves have geological and community significance which can present reputational risk. VSA and GSAV can provide guidance in determining significance. Ignoring the problem will not make it go away and may then become a public relations issue.

What methods are going to be the most appropriate for the project? Site walk overs for features identified in the desktop study by an appropriate geologist and in-cave speleological surveys help understand a cave's condition and extent. Drones can produce useful photos both of surface and underground, especially if a void is hard to access. Appropriate geophysical surveys are a non-intrusive way of investigating sub-surface void although expensive and truthing is still needed. ERI and SRT methods give good results and for large area developments Frequency Domain Electromagnetics or Ground Magnetics with targeted areas of ERI and SRT surveys to give an indication of underground caves and voids. (see Section 4). Benefits of borehole drilling are increased confidence of the nature of voids and surrounding rock encountered. The primary limitation is that a borehole, typically being around 50 mm in diameter, only provides a very small section of the ground profile and it is easy to miss large parts of the cave or the cave entirely. Targeting borehole at anomalies or voids found by a geophysical survey increase confidence in the geophysics results and give a better understanding without needing extensive drilling. Hazard, susceptibility and risk maps may help communicate the potential of geohazards (e.g. sinkholes, karstic ground or landslide potential). The methodology in creating these maps is not discussed in detail in this paper, however there is a framework which could be applied to lava caves. The ability to produce quality mapping relies upon available information obtained through steps outlined in sections 5.1 and 5.2, but often limited available information will impede the practicality of producing a satisfactory hazard, susceptibility or risk map.

The Australian Geomechanics Society Landslide Risk Management Guidelines (AGS 2007) sets out guidelines to estimate landslide risk to people and structures. Theoretically a similar but modified approach could be applied to assess lava cave risk, however, similar to risk mapping, it relies upon good information. Specific risk management guidelines for caves are also available from the ASF website: https://caves.org.au/administration/codes-and-standards/.

6 CONCLUDING REMARKS

Currently there is little publicly available guidance on how to manage lava cave risks in Victoria. It is important that projects located within the Western District Volcanic Province consider the potential for lava caves. Each case will be unique, however case studies and discussion described here may provide some helpful insights.

7 REFERENCES

Aziz-ur-Rahman, A. and I. McDougall. I. (1972) Potassium-argon ages on the Newer Volcanics of Victoria. *Royal Society of Victoria Proceedings 85*. Victoria, pp. 61-69.

AGS 2007d. Commentary on Practice Note Guidelines for Landslide Risk Management (2007). *Journal and News of the Australian Geomechanics Society*., 42(1).

Gibson, D, (2007). Potassium-Argon Ages of Late Mesozoic and Cainozoic Igneous Rocks of Eastern Australia. *CRC LEME Open File Report.*, 193. pp 53.

Golder Associates Pty Ltd. (2023). Parwan Lava Cave Geotechnical Assessment., Melbourne.

Grimes, K. G. (2002). Small Subcrustal Lava Caves: Examples from Victoria Australia. *AMCS Bulletin 19 / SMES Boletin 7*, pp. 35-44.

Grimes, K. G. (2007). Volcanic Caves of Western Victoria. *26th Conference of the Australian Speleological Federation*., pp. 1 - 10.

Grimes, K. G., Hamilton-Smith, E. & White, S. (2010). Field Guide to the Volcanic Caves of Western Victoria. *14th International Symposium on Vulcanospeleology.,* Undara Australia, pp 1 – 40.

Gunn, J. (2004). Encyclopedia of Caves and Karst Science. Great Britain: Fitzroy Dearborn.

Peterson, D.W., Holcomb, R.T., Tilling, R.I. and Christiansen, R.L., 1994. Development of lava tubes in the light of observations at Mauna Ulu, Kilauea Volcano, *Hawaii. Bulletin of Volcanology*, 56, pp.343-360.

Roberts, P.S., 1985. Bacchus Marsh. 1:50 000 geological map. Geological Survey of Victoria.

Romsey Australia (2011). *Wayback Machine*. Available at: https://web.archive.org/web/20110228005429/http://home.iprimus.com.au/foo7/volcmap.html (accessed: 10 August 2024).

Victorian Reasources Online (2018). *L13 - Parwan - Lava Cave*. Available at: https://vro.agriculture.vic.gov.au/dpi/vro/portregn.nsf/pages/port_lf_sig_sites_l13 (accessed: 3 July 2024).

Webb, J. A. (2023). Western Victorian Lava Caves. In: Australian Caves and Karst Systems. *Springer Nature.*, Melbourne, Australia, pp. 245-252.

Webb, J.A., Joyce, E.B. and Stevens, N.C. (1982). Lava caves of Australia. *The Proceedings of the Third International Symposium on Vulcanospeleology*., Oregon, America, pp. 74-85.

SUSTAINABLE DESIGN AND CONSTRUCTION IN WESTERN SYDNEY: REPURPOSING TAILINGS DAMS FOR INDUSTRIAL COMMERCIAL DEVELOPMENT IN WESTERN SYDNEY

Stephanie Salim, Jeremy Toh, David Piccolo
Pells Sullivan Meynink
G3 56 Delhi Road
North Ryde, NSW 2113 Australia
Email: stephanie.salim@psm.com.au

ABSTRACT

Tailings is a waste product of quarrying, and it is typically very soft in consistency, highly compressible and therefore makes it undesirable for any development. Without appropriate treatment, development over tailings likely results in unacceptable settlement under loading. This paper illustrates the design of ground treatment adopted on one of the tailings dams in Western Sydney, which was previously used as settlement ponds for a sand quarry. The adopted ground treatment design comprised a combination of vertical drains/wick drains and preload of varying height depending on the characteristics and thickness of the tailings. The wick drains spacing and preload height were first determined based on the in-situ testing results (i.e. CPT and test pits). The novel approach adopted in the design verification involves utilising the wick drains installation equipment to help characterise the site and confirm the assumptions adopted in the design. The wick drains installation records provide a detailed coverage of the depth of the tailings based on the installation resistance and is a pseudo-indicator of the tailings consistency. Additionally, monitoring results were used to validate the design predictions and inform if any design changes are possible during construction (e.g. shorter preload duration).

1 INTRODUCTION

Along the Nepean River in Western Sydney, a number of sand and gravel quarries had operated in the 20th century. As part of these operations, settlement ponds or tailings dams were created. The tailings which are the waste materials from quarry activities, are stored in the settlement ponds. This material usually makes the land unsuitable for development without any ground treatment. Often these settlement ponds would be capped by some stronger material allowing trafficability on the surface, however leaving the subsurface relatively soft and untreated.

The settlement pond in the subject of this study occupies an area of about 40ha and was proposed to be developed as an industrial development. The industrial development has certain performance criteria that it requires of the sub surface that would not be satisfied without treatment of the tailings.

To achieve the desired performance of the sub surface and to complete it within the desired timeframe a solution was developed involving a system of vertical wick drains, sub horizontal drains on the pre-existing surface (i.e. at the base of the preload), conveying water away from the tops of the wick drains and preload.

To characterise the site, conventionally a number of Cone/Piezo Cone Penetration Testing (CPT/CPTu), boreholes and test pits would be used. This was initially completed at a sparse testing frequency however it was determined that a much larger quantity of investigation would be required to improve our understanding of certain buried features that may impact the sub surface performance, e.g. buried banks or variations in the depth and/or compressibility of tailings may cause issues with differential settlements.

As is often the case, it was considered more economical to use an "observational" method to observe how the subsurface performs and then determine what optimisations can be made to the preload design. The optimisation of preload can be derived from interpreting the results of monitoring data. Such optimisation requires the preload to be built or partially built in order to see how the tailings respond. In this paper, we explore use of the data gathered by the machine used to install the wick drains in order to assess optimisations prior to the commencement of the construction of the preload. In this way, optimisations can be made sooner and also include variations to wick drain spacings and extent.

The general approach undertaken is summarised as follows:

1. Historical characterisation, makes use of historical records and aerial photographs of the site and of nearby sites with similar history to assist in developing a model and identify areas requiring attention in the geotechnical investigation.
2. Geotechnical investigation, used to compliment the historical characterisation and understand the current character of the site.
3. Build a site model which is based on the historical review and geotechnical investigation.
4. Develop a preliminary design noting areas with potential for optimisation.

5. Undertake wick drain installation in areas where CPTu's were completed for calibration between wick drain resistance during installation and cone resistance.
6. Review the characteristics of the potential optimisation areas and make optimisations to the design as appropriate.
7. Install wick drains in areas identified as potential for optimisation. Use installation records to confirm optimisation.
8. Undertake monitoring to confirm design assumptions and further adjust preload design if necessary.

2 SITE CHARACTERISATION

The settlement pond tailings and surrounding material was characterised utilising historical photographs, historical records of the quarry activities, site investigation (completed after the historical review) and available data from nearby settlement ponds of similar history and origin.

2.1 HISTORICAL REVIEW

A review of historical aerial photographs was undertaken to help understand the broad scale extent of the historical settlement ponds, any unique or buried features, the duration of the active settlement ponds prior to backfilling/capping and how long since the capping was completed. Based on the historical photographs, key features of the settlement pond are identified and listed below:

- The quarry activities began around 1986;
- Settlement ponds are observed from 1988 and the tailings have been discharged at multiple points (at least 6);
- A delta in the settlement pond could be observed in 1991, as seen in Figure 1;
- Capping works started between 2001 and 2002, then finished in between 2005 and 2006, as seen in Figure 1; and
- Ponding water observed in some areas in 2009 and 2010 and no major change observed between 2010 and 2020.

Figure 1: Historical photographs (a) the delta formed in the settlement pond in 1991 and (b) capping works finished around 2005 and 2006 (NSW Government Spatial Services 2024)

Historical documents highlight other important features, such as where discharge points are located which allows an initial qualitative understanding of the grain size distribution of the settlement pond. Given the multiple discharge point locations on this site, it makes interpreting the depositional distribution more complex.

2.2 SITE INVESTIGATION

A total of 39 CPTus, were undertaken in the tailings material to understand the character of the tailings and any buried features to assist with the ground treatment strategies. Dissipation testing was undertaken to understand the tailings horizontal coefficient of consolidation, C_h. A number of test pits were also completed to understand the existing capping material and inspect the tailings material. The CPTs, dissipation testings and test pits indicate the following:

- The CPTs indicate the presence of between 1 m and 2 m thickness of capping over the top of the tailings. Some of the areas particularly in the lower-lying north-east portion of the site may not have been capped as they were not trafficable during the investigation (i.e. too soft);
- The bedrock level is typically between 10m to 15m deep and as such the tailings varies up to 15m deep;
- The tailings properties range from a sandy silt to silt and clays; and
- The transition from one end of the settlement pond to the other appears to be overall gradational and appears to be related to the discharge arrangement and distance from the discharge point.

2.3 SITE MODEL

Based on the results of the historical review and the results of the site investigation, the site was categorised into four settlement zones (i.e. S1 to S4) depending on the tailings characteristics and thickness of the tailings, which are described as follows (Refer Figure 2 for plan extents of zones):

1. Area S1 is characterised by
    a. Presence of capping layer over most of the tailings, which comprises of gravelly sand and sand.
    b. Relatively thinner tailings (<4m) due to being located at the edge of the dam.
    c. Indicative average corrected cone resistance 5 to 10 MPa.
2. Area S2 is characterised by
    a. Presence of "better tailings", which typically comprises sandier materials. Thickness of tailings ranges from 4m to 14m. May contain thin layer of "poorer tailings".
    b. The tailings becoming deeper from south to north.
    c. Indicative average corrected cone resistance 2 MPa with peak values up to 4 MPa.
3. Area S3 is characterised by
    a. Presence of "poorer tailings", which typically comprises fine-grained material. Thickness of tailings ranges from 10 m to 14 m.
    b. The tailings directly overlying bedrock.
    c. Indicative average corrected cone resistance 0.2 to 0.5 MPa.
4. The ground conditions in area S4 were less well defined than other areas because access for investigation rigs was unsuitable. Based on the historical records, conditions in S4 were expected to be similar to or worse than area S3.

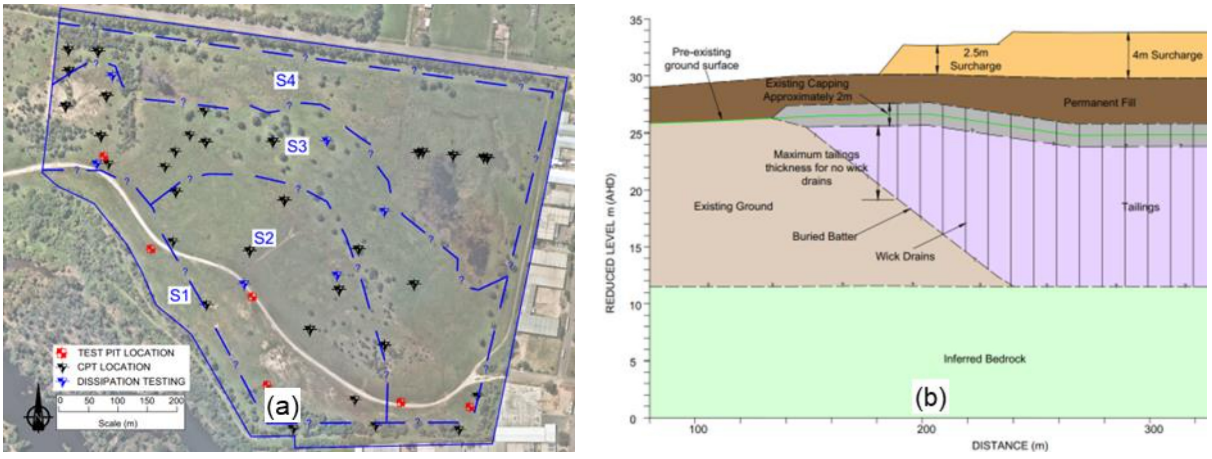

Figure 2: (a) Plan view of the extent of settlement zones and (b) Schematic diagram showing design approach

3 DESIGN APPROACH

3.1 ADOPTED DESIGN FOR DIFFERENT SETTLEMENT ZONES

To achieve the required construction target timeline and post-constructions settlement limits, the adopted design approach comprises a combination of the following to accelerate consolidation and over-consolidate the tailings:

- Wick drains/vertical drains. The adopted spacing is a triangular spacing of 1.5 m x 1.5 m connected together at the surface by horizontal drains;
- Surcharge filling (preload surcharge) above the final landforms. The height of the preload differs for each settlement zone (e.g. S1, S2 etc.); and
- The target preload period is 12 months (not including the time required for filling, and removal of preload).

The selection of the combination of the above is based on the tailings thickness and the design parameters, the adopted design is as presented Table 1. The post construction secondary settlement (creep) is mainly governed by the creep rate and it determines the performance of the site over the 30-year design life. Since the creep rate adopted was based on empirical data, there was a possibility that the creep rate may vary across the site.

The wick drains and preload are only adopted when the thickness of "poorer tailings" exceeds a total of 2 m. Figure 2 shows a schematic diagram of the adopted design approach.

Table 1: Adopted Treatment Method

Zone	Wick drain adopted	Permanent fill height (m)	Preload height (m)
S1	No	1 to 4	No
S2	Yes (1.5m spacing)	1 to 5	2.5
S3 & S4	Yes (1.5m spacing)	1 to 7	3.5 to 4

3.2 WICK DRAIN RIG CALIBRATION AND DESIGN OPTIMISATION

The design is based on a number of assumptions such as the thickness of the tailings, the location and slope of buried features and the consolidation parameters of the tailings. These assumptions are informed by the limited number of tests undertaken during the design phase. The design could therefore be optimised if additional information is collected to further characterise the tailings and improve the confidence in certain parameters.

The wick drain installation rig records information of depth and penetration resistance while installing the wick drains. It was considered that this information may provide additional data with which to optimise the design or at the very least, confirms it.

The wick drain installation equipment is shown in Figure 3. Each installation rig uses a rectangular hollow section (mandrel) to install the wick drains. The mandrel is driven by hydraulic forces to penetrate the soil and is retracted after each wick drain is installed. An anchor plate is also attached to the end of each wick drain to secure the wick drains in place. The anchor plate is made of galvanised steel with approximately 190mm long x 90mm wide and 1mm to 2mm thickness (as per the rig specifications).

Some trial sets of wick drains were installed firstly at the locations of previously completed CPTs. The wick drain rig records the pressure vs depth at a relatively coarse interval of 0.5 m increments. The pressure recorded at each increment is a maximum pressure at the mandrel encountered since the previous record. The results of the wick drain penetration resistance vs depth is compared to the nearby CPT results to calibrate the wick drain resistance with CPT results (Refer to Figure 4). Evident from Figure 4, the top two metres penetrate a capping layer before penetrating softer tailings. It is important to note, that in some instances where the capping layer is too stiff to penetrate, the holes are pre-drilled in the capping layer. This has implications on the installation resistance as the anchor plate located at the tip of the mandrel will retain its shape more before it reaches the tailings. When the anchor plate penetrates the tailings, it is unclear how much the anchor plate deforms. This provides a challenge when considering the results of the wick drain installation rig.

Figure 3: (a) Typical rig setup and (b) Example of mandrel used to install the wick drains

From Figure 4, it is evident on a macro scale that as the CPT resistance increases, the wick drain resistance increases and decreases as the wick drains decrease. However, on a smaller scale, it is clear that a perfect correlation between the two does not exist, i.e. in the deeper tailings. Therefore, the calibration was based on a "screening" type approach.

Our design analysis indicates wick drains are required where the "poorer tailings" exceed 2m in thickness. The "poorer tailings" was categorised as having CPT corrected cone resistance of less than 0.5 MPa. To come up with a conservative general rule we compared the wick drain and CPT data and determined that a wick drain penetration resistance of 10 MPa or less was always correlated to CPT resistances of 0.5 MPa or less. On this basis, the wick drain resistance of less than 10 MPa was considered as reflective of "poorer tailings".

Once the criteria was established, the wick drain installation data could be used to delineate and optimise the boundary zones (e.g. between S1 and S2). Due to how closely spaced wick drains are, they provide a highly detailed coverage on the thickness of the tailings, gradients of buried features and pseudo indication of material consistency. The thickness of tailings with less than 10 MPa wick drain resistance has been utilised to refine the boundary between settlement zones. The refinement of the boundary has resulted in a decrease in treatment of approximately 22,500 m^2, which is equivalent to 10,000 wick drains and cost and time saving.

The wick drain installation record provides the wick drain resistance vs depth and was used to assess the thickness of the tailings (Refer to Figure 4). It is noted that Figure 4 appears to be contour like, however are in fact just many coloured dots with each dot representing one wick drain (i.e. there are over a hundred thousand wick drains installed).

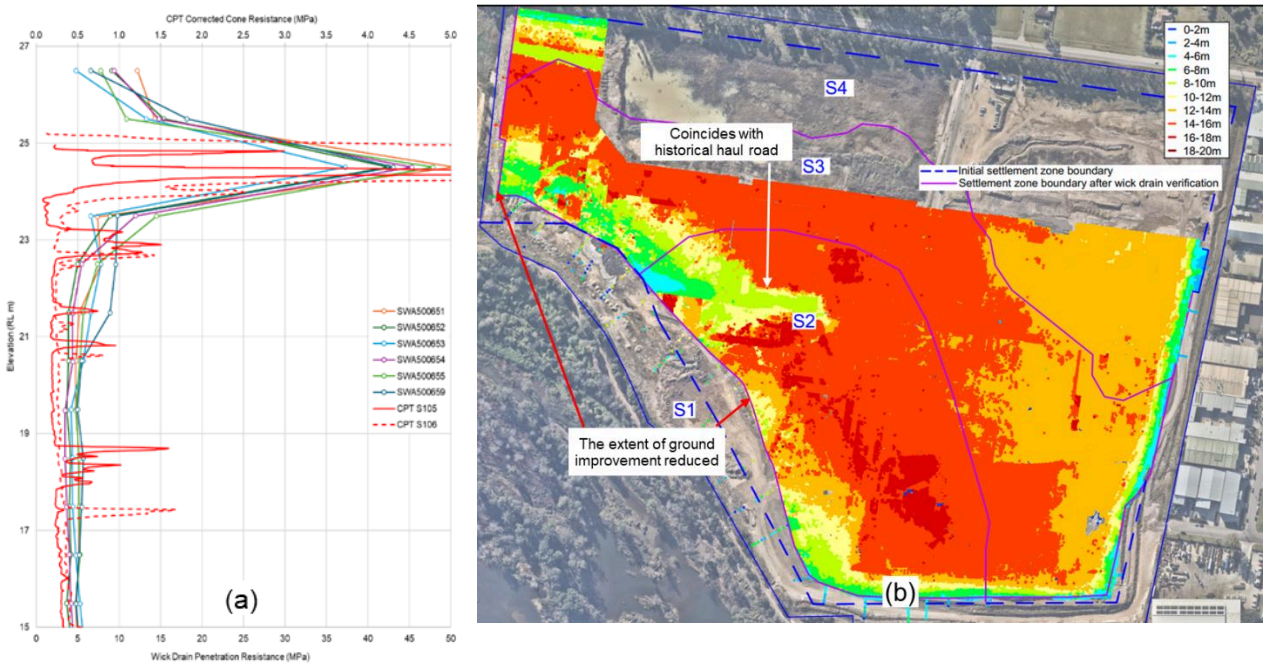

Figure 4: (a) Comparison between CPT tip resistance (red lines) and wick drain resistance and (b) Total thickness of tailings

3.3 LIMITATIONS

The following limitations should be noted:

- The wick drain penetration resistance is recorded at 0.5m depth increments, therefore any local changes between each increment will not be recorded.
- The wick drain penetration resistance requires calibration with CPT or other testing, i.e. it cannot be used independently to assess the soil characteristics.
- No direct correlation has been established, the correlation between the wick drains and CPT results are dependent on the rig configuration, in particular the mandrel and anchor plate geometry.
- The effect of the rig configuration (e.g. mandrel and anchor plate dimensions) on the wick drain resistance have not been investigated, the wick drains in this site have been installed with the same configuration.

4 SETTLEMENT PREDICTION AND MONITORING RESULTS

The use of the wick drain resistance as means of assisting the design, reduced but did not remove the requirements of monitoring to validate the design assumptions. Monitoring of the consolidation are still required to verify:

- Consolidation settlement develops as predicted (rate and magnitude) and hence design parameters are appropriate; and
- Slope stability during construction.

The above is achieved by a combination of instruments such as settlement plates, surface settlement pins/markers and vibrating wire piezometers.

The monitoring data, including the actual filling rate, was used to back-calculate the average compression ratio on each settlement plate location.

Figure 5 presents a comparison between the predicted settlement during the design phase, the actual settlement based on monitoring results during the construction and the updated settlement predictions adopting the actual placement of fill (time and thickness) but still with the original design parameters. Across the entire site, the back-calculated parameters were typically found to be within the range of design parameters.

Using the monitoring results discussed above, the preload thickness was reviewed across the later stages by taking into consideration the back-analysed compression values.

The wick drain installation which provided an extensive coverage of the site, assisted the interpretation and interpolating the monitoring results between the monitoring locations, by giving some indication of the site characteristics between the monitoring locations.

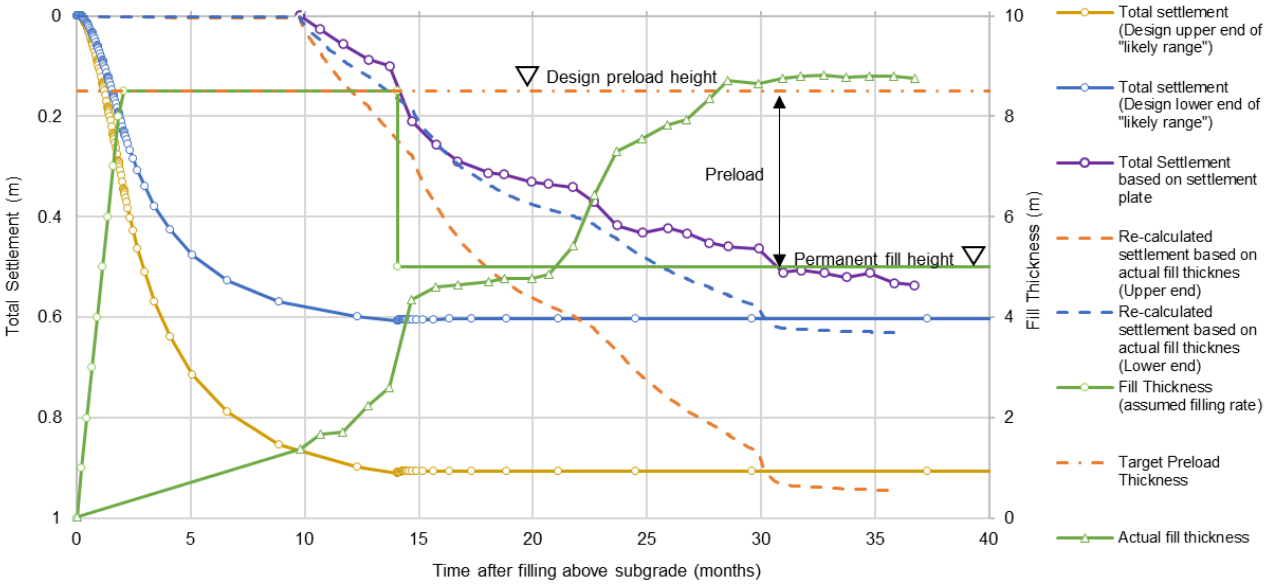

Figure 5: Comparison between predicted settlement during design and actual settlement based on monitoring results and re-calculated settlement based on the actual filling

5 CONCLUSIONS

Historical tailings settlement ponds are typically unsuitable for development without any ground improvement. The ground improvement at this site was undertaken by means of wick drains and preload. The characteristics of this site was originally investigated by review of historical information, as well as typical site investigation such as CPT and test pits, however some variabilities and uncertainties still remain between these test locations.

A novel approach of adopting the wick drain penetration resistance into design validation and optimisation was successfully adopted, at minimal additional cost to the project, but bringing several benefits. In particular, the extent of wick drains and preload were reduced, while the overall settlement performance remained within the design limits.

It is noted that there are many site specific and rig specific factors that might influence the relevance of the wick drain penetration resistance calibration and others using this approach should be careful to consider their specific circumstances.

Monitoring results were used to validate the design predictions and undertake design revisions during later stages of construction (e.g. shorter preload duration). The design revisions were greatly informed from the extensive coverage provided by the wick drain installation records.

6 REFERENCES

NSW Government Spatial Services (2024) *Historical, aerial and satellite imagery*. (Accessed: 22 June 2024)

Soil Wicks Australia (2021). Standard Operating Procedure. Installation of prefabricated vertical drains (PVDs).

LIME STABILISATION OF EXPANSIVE AUCKLAND SOILS

D. R. Tilsley[1], W. J. S. Ritchie[2], and K. L. de Graaf [3]
[1]*ENGEO Limited, 1/314 Maunganui Road Mt Maunganui 3116, +64 7 777 0209, email: dtilsley@engeo.co.nz*
[2]*Tonkin + Taylor, 711 Victoria Street Hamilton 3240, +64 7 834 7320, email: writchie@tonkintaylor.co.nz*
[3]*School of Engineering, University of Waikato, email: kim.degraaf@waikato.ac.nz*

ABSTRACT

Significant areas of Auckland, New Zealand are situated on soils termed at risk of shrink or swell, also known as reactive or expansive soils (Brown, et al., 2008). The movement of buildings as soils shrink or swell can cause structural damage (Elsaidy, et al., 2019). Under NZS 3604:2011, residential building platforms must meet the requirements of 'good ground' conditions; otherwise, a specific engineering design is usually required. This paper considers whether expansive soils in the north and south of Auckland can be stabilised within the top metre using burnt lime (CaO) to meet 'good ground' standards for building construction. This study found that treatment of these specific expansive soils with burnt lime (5%, 7%, and 9% by weight) improved the sample strengths and reduced shrinkage. After 28 days curing, all lime dosage rates effectively brought linear shrinkage to within the NZS 3604 'good ground' threshold. Longer curing times (28 days versus 7 days) resulted in an increased unconfined compressive strength (UCS). The curing time had a greater effect than the lime dosage. There is potential for this methodology to be upscaled and implemented in construction, to improve reactive soils to meet NZS 3604 requirements. This would mean that specific foundation design can be replaced by simple slab-on-grade foundations, as the building is no longer at risk of differential settlement. However, more research is needed to determine the feasibility and costs associated with this approach. Prolonged testing will be needed to determine the longevity of the effects. In addition, environmental impacts should be investigated.

Key Words: Expansive soil, reactive soil, lime treatment, stabilisation, foundation design

1 INTRODUCTION

Auckland is a rapidly growing city, with expectations of an increase in population by 500,000 people in the next 30 years to reach a total population of 2.2 million (Auckland Council, 2023). By 2050 New Zealand is predicted to have a population of 6 million (Statistics NZ, 2020), suggesting that a third of the population will be living in Auckland. This increased population growth will result in more residential subdivisions to accommodate the housing demand. This housing pressure is leading to development in greenfield sites in greater Auckland.

However, significant areas of Auckland are situated on soils termed at risk of shrink or swell, also known as reactive or expansive soils (Brown, et al., 2008). The issue of expansivity within the Auckland region is particularly associated with the shrinkage capability of the expansive soil, due to the climate of Auckland which includes droughts, temperate weather and relatively high levels of rain (de Graaf, et al., 2023). The movement of buildings as soils shrink or swell often results in differential settlements which can cause structural damage (Elsaidy, et al., 2019). To allow building development to be completed in accordance with NZS 3604:2011, residential building platforms must meet the requirements of 'good ground' conditions, generally not the case where expansive soils are encountered and so a designer must refer to AS2870:2011 to work out how expansive the soil at the site is and what foundation options might be appropriate.

A range of measures for soil expansivity are given in various local and international standards. In New Zealand, NZS 3604 outlines that a soil with a liquid limit of over 50% and a linear shrinkage of over 15% does not meet the standard of 'good ground' and is at risk of expansivity. The Australian standard AS2870 then requires the use of the shrink-swell test as a measure of expansivity, but the suitability of using this test in high-rainfall areas (such as New Zealand) is debatable, as highlighted by various authors (Rogers, et al., 2020; Teal & Rogers, 2021; Kaith, 2021; McDougall & Rogers, 2020). Specifically, using the shrink/swell test to determine an appropriate site class for foundation design in Auckland (Kaith, 2021) or certain parts of Australia (Karunarathne et al., 2020) may be unwise due to the shrink/swell test's apparent sensitivity to moisture content. In comparison, in the USA, AASHTO uses a liquid limit threshold of 60% and a plasticity index of 35% to characterise a soil at risk of a high degree of expansion. Under the UK NHBC, a soil with a plasticity index of over 40% is considered to have a high potential for volume change.

This typically results in the requirement of specific engineering design such as waffle slab foundations or piles to reduce the impact of soil movement on residential buildings. Alternatively, in-ground treatment may be an option for expansive soils. This approach has been used in roading for many years. When dealing with a substandard pavement subgrade for example, stabilisation can be achieved by mixing lime and/or cement binders with water to create a slurry, which is then incorporated into the upper layers of the subgrade material (Gray, 2017). The improved subgrade stiffness facilitates the construction of more cost-effective pavements, and typically leads to decreased maintenance requirements throughout the

road's life span. The use of lime (CaO) is most effective at stabilising subgrades consisting of fine particles with >25% passing 75 um and a plasticity index >10% (Kett, et al., 2010).

This paper considers whether potentially expansive soils from the north and south of Auckland can be stabilised within the top metre using burnt lime (CaO) to reduce shrinkage and increase strength, a similar approach to that used for pavement subgrade stabilisation. Specifically, this study refers to soil samples retrieved from a residential and commercial development site in Waiuku (South Auckland), and from a residential development in Albany (North Auckland). This research builds on earlier work undertaken by de Graaf, et al. (2023) who also looked at the treatment of expansive soils in parts of Auckland.

2 SAMPLING, LAB TESTING, AND MIXING METHODOLOGIES

Soil samples were collected from sites located in Waiuku (45 km south of Auckland CBD) and Albany (15 km north of Auckland CBD) in the form of disturbed core retrieved from several 1 m deep hand auger boreholes.

Initial tests were conducted on these samples for identification of reactive soils due to their characteristics and physiochemical properties before treatment. These tests included Atterberg limits, linear shrinkage, particle size distribution, allophane testing, scanning electron microscopy (SEM), and x-ray diffraction (XRD).

The soil samples were amalgamated from similar depths and then treated with CaO at three different dosages. CaO dosages of 5%, 7%, and 9% by weight of the natural soil were mixed with distilled water equivalent to twice the total weight of CaO. After slaking, a mincing grinder was then used to mix the soil and slaked lime into a homogeneous mixture that was then placed into cubic moulds to air dry. The mincer was used to best represent the larger scale rotor equipment that is used in the field for pavement subgrade stabilisation (Gray, 2017).

Laboratory testing was carried out on the air-cured samples after 7 and 28 days. The samples were tested for their unconfined compressive strength (UCS), and then portions of the cube samples were taken for SEM and XRD testing. Post-treatment linear shrinkage was also undertaken on the cured samples, which were ground and remixed with water to form a homogeneous paste at the liquid limit of the treated soil.

3 SOIL CHARACTERISTICS AND EXPANSIVITY

The near-surface samples retrieved from the Waiuku site were classified as stiff to very stiff silty clays and clayey silts of the South Auckland Volcanic Group. These soils had clay content ranging between 17% to 40%, and in-situ moisture content ranging from 39% to 67%.

The Albany soil samples can be described as a stiff to very stiff clay of the Waitematā Group East Coast Bays Formation. The particle size distribution of the Albany soils indicated a clay particle fraction of 14% to 27%, and a natural moisture content between 38% to 40%.

The mineralogy testing showed the Waiuku samples were dominated by halloysite, as indicated by the XRD results and the tubular structures observed in the SEM photos. There was also a suggestion of kaolinite in the XRD results for one Waiuku sample, and some plate structures consistent with kaolinite were observed in the SEM photos. These minerals are not generally considered to be expansive compared with smectites such as montmorillonite (Foster, 1954). There was no sign of montmorillonite in the Waiuku XRD results, although this was found in samples taken nearby in an earlier study in Paerātā (de Graaf et al, 2023). The results of the allophane test showed that the Waiuku samples contained 5% to 7% allophane.

In the Albany soils, montmorillonite was evident throughout the SEM imaging of the samples. Traces of kaolinite, illite, and halloysite were also observed in SEM and XRD results. Unlike montmorillonite, kaolinite and illite are not known to be reactive but are rather sensitive. Allophane was also found to be present in the Albany samples, ranging between 5% to 7%. Example SEM images for both sites are shown in Figure 1 below.

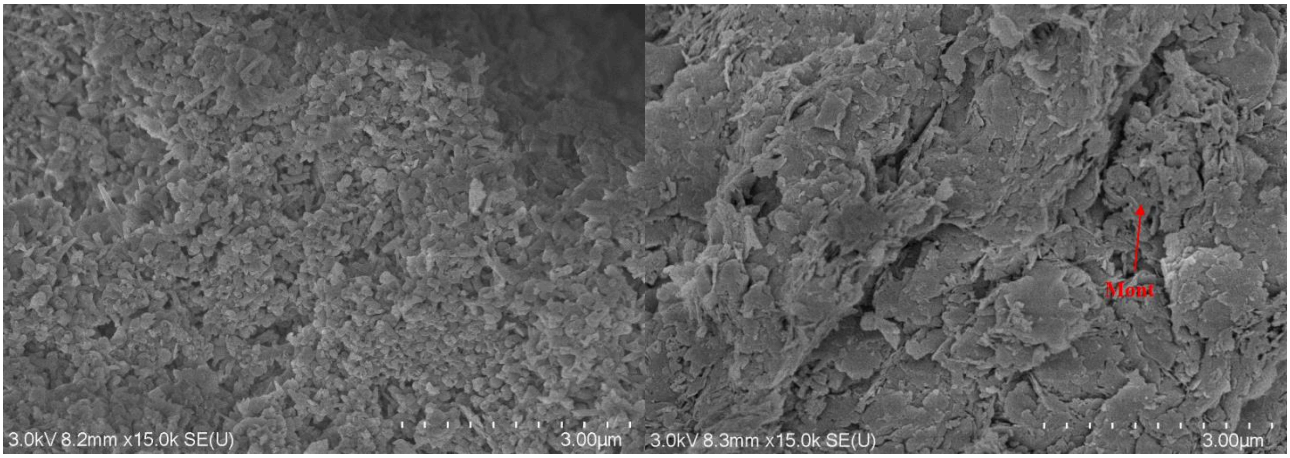

Figure 1: (a) Waiuku sample with halloysite observed (b) Albany sample with montmorillonite observed

Allophane and halloysite are known to attract water and be sensitive to reworking (de Graaf et al, 2023). Halloysite is made up of tubular microstructures which have a strong capillary force to hold onto water; this may then be released when the microstructure is disturbed (Knauf, 2022). If montmorillonite is also present alongside the halloysite, this moisture release could trigger its expansion. This may increase the reactive behaviour of the montmorillonite soils sampled in Albany.

The plasticity indices (PI) for the Waiuku soils ranged from 30% to 69%, and for the Albany soils from 30% to 85%. The corresponding liquid limit (LL) range for Waiuku was 94% to 124%, and for Albany this was 68% to 124%. Linear shrinkage for the untreated Waiuku samples ranged from 21% to 27%, and for Albany it was 17% to 26%.

There is evidence of expansivity in the samples tested from both sites, based on the clay mineralogy, linear shrinkage and Atterberg limit results. The LL and linear shrinkage results all meet the definition outlined in NZS 3604:2011, as shown in Figure 2 below. Figure 2(a) also shows that the samples met the AASHTO LL requirement for a high degree of expansion (LL >60%). However, referring to the UK NHBC and AASHTO standards based on PI displayed in Figure 2(b), only some of the samples were categorised as having a high potential for volume change/ high degree of expansion.

Lime stabilisation is considered effective for soils with clay contents that are greater than 10% and PI ranging from 10% to 50% (Bartley Consultants Limited, 1998). This infers that the sampled soils are suitable for lime stabilisation, excluding the two samples that are greater than 50 % PI, shown in Figure 2 below.

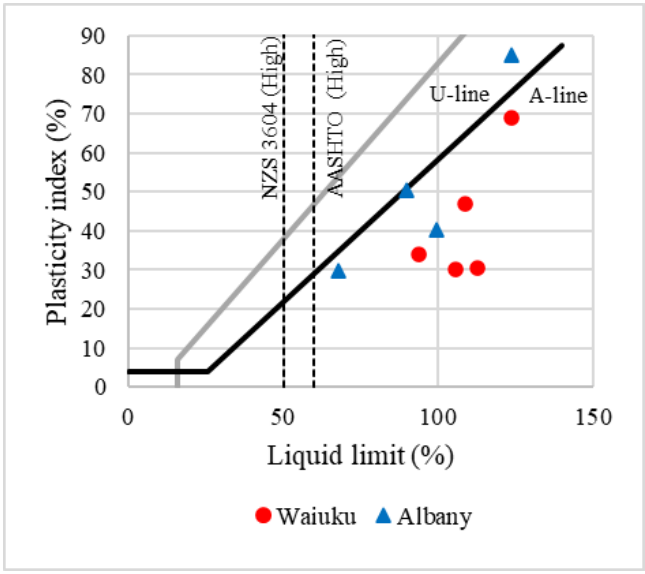

Figure 2: (a) Atterberg limit results for the untreated Waiuku and Albany soils against NZS 3604 and AASHTO criteria

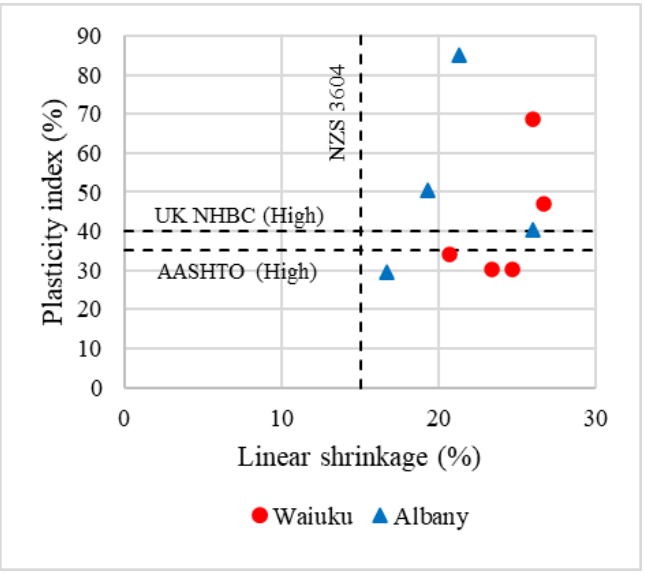

(b) Linear shrinkage and plasticity index results for the untreated Waiuku and Albany soils against NZS 3604, UK NHBC, and AASHTO criteria

4 EFFECT OF TREATMENT

After 28 days curing, the linear shrinkage was significantly reduced (see Table 1), showing that all lime dosage rates effectively brought linear shrinkage to below the NZS 3604 'good ground' threshold of 15%.

Table 1: Linear shrinkage results for untreated and treated soil samples after 28 curing days at 5%, 7%, and 9% lime dosages

Site	Linear shrinkage of untreated samples (%)	Post-treatment after 28 curing days	
		Lime dosage (%)	Linear shrinkage (%)
Waiuku	21 – 27	5	8
		7	4
		9	2
Albany	17 – 26	5	1
		7	2
		9	1

The effectiveness of the treatment was also evaluated by testing the improvement in soil strength (UCS) after treatment when compared with an initial gently compacted sample. The UCS was used due to the rapid hardening of samples after treatment, as it gives insight into the overall stiffness of the soil, which also relates to settlement (Knappett & Craig, 2020). Figure 3 shows the results of the UCS testing for the Waiuku (a) and Albany (b) soils across all dosage rates.

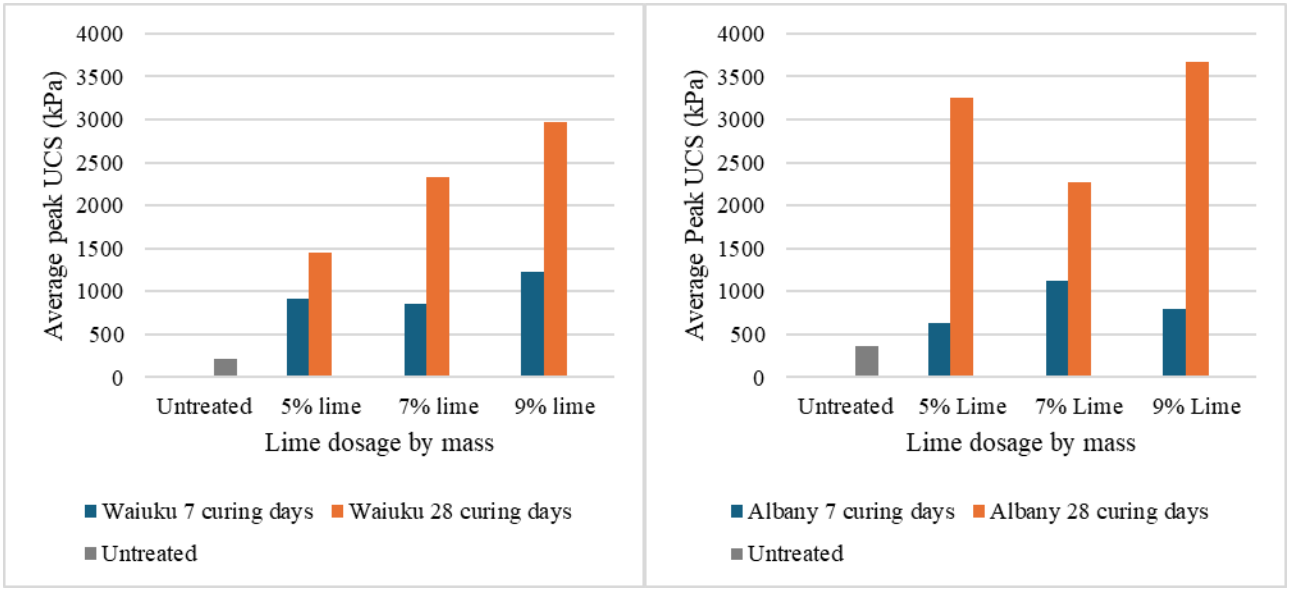

Figure 3: Average peak unconfined compressive strength results for Waiuku (a) and Albany (b) soils before and after treatment at 5%, 7%, and 9% lime dosage

For Waiuku, longer curing times resulted in an increased average peak UCS for the soils. Raising the lime dosage consistently increased the UCS in the 28 curing day samples. However, the 7 curing day samples showed mixed results with increasing lime. Therefore, the curing time had a greater effect than the lime dosage. This is shown in Figure 3(a), where the 9% lime treatments were the most effective dosages, and more markedly so after curing samples for 28 days.

The Albany soils also had a mixed result with the 7% lime treatment (Figure 3(b)). After 7 days of curing the 7% treatment had the greatest UCS improvement. Conversely, the 7% treatment after 28 days showed lower increase in UCS than the 5% and 9% treatments. The 7% treatment anomaly may be attributable to the difference in mineralogy between the soils tested at different lime dosages. The 5% and 9% treatment soil samples, as examined in the SEM displayed evidence of montmorillonite, displayed in Figure 1(b). However, the 7% treatment soil sample predominantly showed kaolinite. Montmorillonite has a high cation exchange capacity compared to kaolinite, which has a relatively low cation exchange capacity (Bell, 1996). This means longer curing times improve UCS of reactive clays with higher montmorillonite content.

Figure 3(b) shows the base material strength was greater in Albany, and this difference carried through with the lime treatment at 5% and 9% following 28 curing days. Once again, the Albany 7% sample was an anomaly, having lower strength than the Waiuku 7% sample after 28 curing days.

5 USE IN RESIDENTIAL HOUSING

The use of burnt lime to increase the compressive strength of subgrades is widely implemented in pavement and road stabilisation. In road stabilisation a tipper truck evenly spreads burnt lime across the surface of the road, followed by a cultivator ripping the top 150 – 300 mm of subgrade, allowing the lime to penetrate beneath the surface. A water truck then disperses water over the applied lime to enhance the pozzolanic reaction (NZ Forest Association Inc., 2020). With pavement stabilisation a single-rotor mixer is used which cuts the soil and mixes the lime into the soil simultaneously.

Kett et al (2010) performed a cost analysis for eight different commonly used binders in pavement stabilisation. They used a performance-based specification for the cost analysis assuming that the compressive strength of the subgrade was maximised to reduce the amount of aggregate used. AUSTROADS (1992) states that a subgrade CBR value of 30 requires a minimal amount of aggregate to be used in a pavement design. The results of the analysis identified that a 3% lime binder achieved a CBR > 30. Using the AUSTROADS (1992) design charts, Kett et al (2010) determined suitable aggregate thicknesses and the total cost for these. They found that the aggregate cost could be reduced by two thirds for binders achieving CBR >30.

Using a Dynamic Cone Penetrometer to CBR conversion chart (NZ Forest Association Inc., 2020), a CBR of 30 approximately correlates (dependent on soil type) to 10 blows per 100mm on a Dynamic Cone Penetrometer. NZ3604 specifies 5 blows per 100mm is the equivalent to an ultimate bearing capacity of 300 kPa. Therefore, the results of the tests from Kett et al (2010) indicate that with the addition of a lime binder of at least 3% to a residential site, a CBR >30 might be achieved which would meet the requirements of NZS 3604 ‘good ground’.

For this same mixing methodology to be applied to the top metre of a residential site, the founding soil must be thoroughly tested. This includes characterisation of the soil itself, to confirm the expansive behaviour of the soil and to determine the correct percentage of lime by weight and curing time needed for any shrinkage to be minimised. The methodology to mix the lime into the soil at a site is considered reasonably achievable with modern equipment (i.e. cultivators, trenchers, and pulverisers). More important for developers is to consider whether this method is more cost-effective than site-specific engineered foundations, particularly given the finding that 28 curing days was needed to maximise the UCS of the reactive soils. Large-scale field testing will be required to perform an in-depth assessment of the improvement over time and a suitable cost-benefit analysis.

6 FUTURE WORK

Further testing is needed to investigate whether the effects found in the laboratory-scale results can be replicated and upscaled in the field. Due to the research being conducted within a span of eight months, the longevity of the improved soil strength and reduction in risk of shrinkage was unable to be assessed. Future work could assess whether the effects of treatment are maintained over a prolonged period (50-year typical design life of a house) when soil is subject to the overburden pressure of a structure. Testing the most efficient and cost-effective dosages should also be carried out to determine the optimal percentage of lime to improve the subgrade to suitable limits under NZS3604 ‘good ground’ in the least amount of time. To do this it is recommended different burnt lime treatment percentages are tested at 2%, 4% and 6% by weight, with additional curing times of 14 and 21 days.

Another aspect for future work is to consider the effect of lime leaching into the surrounding environment, if the site had a high groundwater table or overland flow paths. The addition of lime to soil can raise pH levels possibly creating a toxic environment for organisms.

7 CONCLUSION

The Waiuku and Albany sites both met thresholds used to define expansive or reactive soils. This study found that treatment of these expansive soils with burnt lime (CaO) improved the soil strength and reduced shrinkage.

All treatment dosages decreased linear shrinkage and increased the average peak UCS compared to untreated soils. This was more marked after 28 curing days. There were some mixed results from increasing the lime dosage from 5% to 7% to 9%, with particular variation in the 7% dosage across the different curing times in the Albany soils. This was thought to be due to the variation in montmorillonite content in the soil samples used for the different dosages. The best results were observed at both sites with a 9% lime dosage after 28 curing days, indicating that there is potential for the use of this methodology to be upscaled and implemented in construction. Further research at intermediate dosages and curing

times could ascertain the minimum treatment to achieve 'good ground' required under NZS 3604. This would mean that specific foundation design can be replaced by simple slab-on-grade foundations, as the building is no longer at risk of differential settlement, reducing construction costs.

However, more research is needed to determine the feasibility and costs associated with undertaking this for a construction site. Prolonged testing will be needed to determine the longevity of the UCS and shrinkage effects. In addition, environmental impacts of using CaO should be investigated.

8 ACKNOWLEDGEMENTS

We would like to acknowledge our supervisor Kim de Graaf for her input to the research. The authors also wish to acknowledge the assistance of The University of Waikato laboratory technicians to complete this research. We also appreciate the support of ENGEO for providing background information and access to the sites to undertake sampling.

9 REFERENCES

Auckland Council, 2023. *Tamaki - Whenua Taurikura Auckland Future Development Strategy 2023-2053,* Auckland: s.n. ISBN: 978-1-99-106098-3(Print) / 978-1-99-106099-0(PDF)

Austroads Pavement Research Group, 1992. *Pavement Design,* Sydney: Austroads. ISBN: 978-1-922700-94-0

Bartley Consultants Limited, 1998. *Design of Pavements Incorporating a Stabilised Subgrade Layer,* Auckland: Transfund New Zealand Report No.104 . ISBN: 0-478-11062-6

Bell, F., 1996. *Lime stabilization of clay minerals and soils,* s.l.: Engineering Geology. PII: S0013-7952(96)00028-2

Brooks, S. J., Georgantzopoulou, A., Torum Johanson, J. & M, M., 2020. *Determining the risk of calcium oxide (CaO) particle exposure to marine organisms,* s.l.: Marine Environmental Research. DOI: 10.1016/j.marenvres.2020.104917

Brown, B., Shorten, J., Dravitzki, D. & Goldsmith, P., 2008. *Soil expansivity in the Auckland region,* s.l.: BRANZ Addendum Study Report No 120A. ISSN: 1178-4938

de Graaf, K., Wang, Z., Fuentes, R. & Fletcher, P., 2023. *The effect of lime on the behaviour of expansive soils from the Auckland region.* Cairns: ANZ2023, 14th Australia and New Zealand Conference on Geomechanics.

Elsaidy, H., Yan, M. W. & Pender, M. J., 2019. A novel formula for the prediction of swelling pressure of compacted expansive soils. *Géotechnique Letters, 9(3),* pp. 231-237. DOI: 10.1680/jgele.20.00010

Foster, M. D., 1954. The relation between composition swelling in clays. *Clays and Clay Minerals, 3(1),* pp. 205-220.DOI: 10.3133/ofr5491

Gray, W., 2017. *Best practice guide for pavement stabilization,* s.l.: NZ Transport Agency Research Report No 622. ISBN: 978-1-98-851248-8

Kaith, R., 2021. *Evaluation of shrink-swell testing in selected Auckland soils,* s.l.: Masters Thesis, University of Auckland.

Karunarathne, A. M. A. N., Gad, E. F. & Rajeev, P., 2020. Effect of insitu moisture content in shrink-swell index. *Geotech Geol Eng,* Volume 38, pp. 6385-6392. ISSN: 0960-3182

Kett, I., Evans, J. & Ingham, J., 2010. *Identifying an Effective Binder for the Stabilisation of Allophanic Soils,* s.l.: International Journal of Pavement Engineering. DOI: 10.1080/10298430903033347

Knappett, J. & Craig, R. F., 2020. *Craig's Soil Mechanics Ninth Edition.* New York: Taylor & Francis Group. ISBN: 9781138070066

Knauf, L., 2022. *Site Behaviour and Management of Sensitive Volcanic Soils,* s.l.: NZ Geomechanics News. ISSN: 0111-6851

McDougall, N. & Rogers, N., 2020. Initial moisture content bias in the shrink-swell test maintained. *Australian Geomechanics,* p. 2020. ISSN: 0818-9110

NZ Forest Association Inc., 2020. *NZ Forest Road Engineering Manual,* s.l.: Forest Owners Association. ISBN: 978-0-473-50660-5(Printed) / 978-0-473-50661-2(PDF)

Rogers, N. W. et al., 2020. The Shrink-Swell test: A Critical Analysis. *NZ Geomechanics Iss. 99,* pp. 66-80. ISN: 0111-6851

Statistics NZ, 2020. *New Zealand's population could reach 6 million by 2050.* [Online] Available at: https://www.stats.govt.nz/news/new-zealands-population-could-reach-6-million-by-2050/ [Accessed 9 July 2024].

Teal, J. & Rogers, N., 2021. *Identifying and classifying expansive soils in New Zealand - time to find a better way?* Dunedin, 21st New Zealand Geomechanics Symposium.

CHALLENGES AND LESSONS LEARNED: UPGRADING A SEAWALL ON COMPRESSIBLE CLAYS AT THE PORT OF BRISBANE

Clinton T Chan
Port of Brisbane Pty Ltd, Brisbane, Australia; clinton.chan@portbris.com.au

ABSTRACT

The Future Port Expansion Seawall at the Port of Brisbane was constructed in 2005 directly on the seabed, overlying deposits of highly compressible marine clay up to 27 m thick with undrained shear strengths as low as 5 kPa. The seawall was designed to settle over time and regular upgrades are required, with the first upgrade undertaken in 2013 and the second upgrade completed in 2022. Both upgrades required top-up of the seawall structure crest levels and improvements to the armour rock. A condition and risk assessment were undertaken in 2020 to understand the current and future risk exposure, followed by repair design.

This paper delves into the delivery and construction challenges faced when the Seawall was upgraded in 2022. It outlines the impact of utilising an Early Contractor Involvement phase into the design to validate design feasibility, streamline budgeting, and optimise project timelines. Other construction challenges that are discussed include the criticality in construction sequence due to the requirement for stability berms to be constructed below the tidal zone on soft compressible material, and quality assurance in reusing existing rock armour and core rock. The construction was supplemented by an instrumentation and monitoring regime to observe the deformation and verify the behaviour of the seawall.

The findings of this paper will be beneficial to the development of future seawall projects that are designed to settle over time, and how to mitigate the delivery and construction risks on highly compressible clays in a marine environment.

1 INTRODUCTION

The Port of Brisbane (PoB), situated at the lower reaches of the Brisbane River extending into Moreton Bay, is Queensland's largest general cargo port. Given the anticipated trade growth and increasing population in Southeast Queensland, PoB is currently expanding through the development of the Future Port Expansion (FPE) reclamation area, spanning approximately 224 hectares. This expansion aims to accommodate the future requirements for container terminals and yards.

The FPE seawall is a rubble-mound (rock fill) revetment structure constructed between August 2003 and March 2005 around the 4.6 km long perimeter enclosing the FPE area; the alignment is shown in Figure 1. The original seawall had a crest level of RL 4.0 m and is founded on the natural seabed, with water depths ranging from 1 to 6 meters depending on tidal height and location. Beneath the seawall lie soft, compressible Holocene marine clay layers, varying in thickness from 5 to 27 m, reaching elevations below RL -30 m., as shown in Figure 2. The seawall is divided into three separate bund sections: North Bund, East Bund and South Bund.

To ensure stability, the seawall foundation is reinforced with high-strength basal geotextile, placed directly on the seabed. The design and construction of the seawall, including the underwater placement of the geotextile, were detailed by Ameratunga et al. (2005).

The seawall is designed to settle over time, and thus requires periodic top-ups to maintain its integrity and intent. Based on the initial design, it was identified that the East Bund and short portion adjoining the North Bund would be required to be topped-up around 2011 to 2012. Survey results confirmed that this would be the case, and the first upgrade design was undertaken in 2012 and construction completing in 2013 with crest elevations ranging from RL 3.5 m to RL 4.0 m. The design undertaken in 2012 estimated that the seawall would continue to settle, and it would need to be topped up again around 2019 to 2020. A detailed survey of the seawall was completed in August 2020, where it was identified that some sections of East Bund and North Bund required topping-up again, as per the design undertaken in 2012.

The FPE Seawall Upgrade (Second Top-Up) project commenced in 2021 and completed in 2022, which resulted in a maximum 1 m crest level raise (to RL 3.5 m) for a 1.5 km section bounding the outermost reclamation cell.

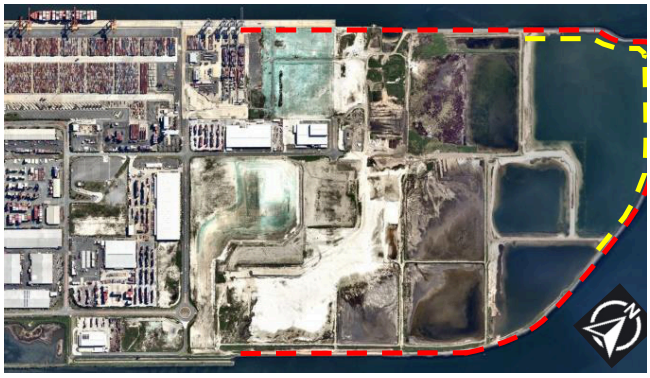

Figure 1: FPE Seawall. The original seawall is shown in red, and the second top-up extents are shown in yellow.

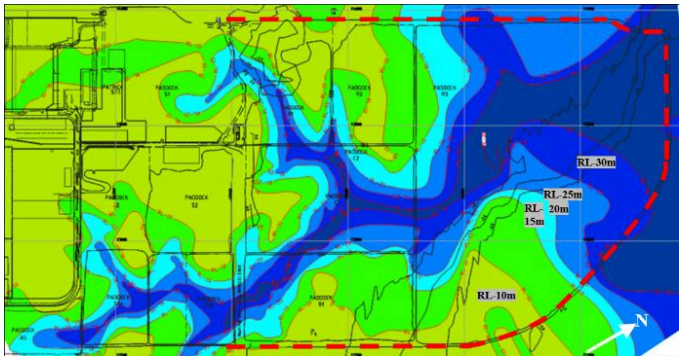

Figure 2: Base of Holocene Contour at FPE. The deeper base of Holocene (dark blue) indicates thicker sections of soft clays, which increases the magnitude of expected settlement.

This paper focuses on the delivery and construction aspects of the FPE seawall upgrade (second-top up). The second top-up geotechnical engineering design was carried out by WSP (formerly Golder Associates) with coastal engineering by Water Technology and construction by Hall Contracting. The findings of this paper are relevant to the geotechnical, coastal and port community dealing seawall, rockwall and revetment structures on challenging ground conditions.

In this paper reduced levels (RLs) relate to Port Datum (PD) at PoB which coincides with Lowest Astronomical Tide (LAT).

2 GEOTECHNICAL CONDITIONS

The ground conditions across Port of Brisbane land were characterised using various ground investigation methods, including boreholes, vane shear tests and cone penetrometer tests with pore pressure measurements (CPTu) supplemented with in-situ CPTu dissipation tests and laboratory tests. The port is located in the lower reaches of the Brisbane River and is founded on soft compressible Holocene materials.

The geomorphology and geological setting at PoB are described in detail in Ameratunga et al. (2010). A brief description of the relevant geological units is summarised in Table 1.

Table 1: Geological Units

Geological Unit	Description / Comments
Upper Holocene	Predominantly very loose or loose sand with some inter-layered soft clays and silts. These sediments were deposited during the most recent rise in sea level, in shallow fluctuating water bodies. In some sections of the alignment (i.e. East Bund) this layer is absent.
Lower Holocene	Normally to slightly over-consolidated, weak, highly compressible, marine clay, laid down in relatively deep stream channels during marine transgression at the end of the last glacial period. The clay is generally unrelieved by sandy layers/lenses.
Pleistocene	Older sediments comprising mainly over-consolidated, stiff to hard clays and medium dense to dense sands. This layer is considered to be incompressible relative to the overlying Holocene deposits.

The Lower Holocene layer posed a significant impact on the seawall upgrade design because the clay layers are soft, creating stability issues, and highly and slowly compressible, leading to large, yet protracted, settlements.

3 ORIGINAL DESIGN AND INITIAL UPGRADE

3.1 ORIGINAL DESIGN

The original seawall design was based on a rock fill embankment founded on high-strength geotextile placed on the natural seabed. For the North and South Bunds, where the Upper Holocene sand layer is present, the geotextile is directly overlain with rock fill. In contrast, the East Bund, with less favourable geotechnical conditions due to a thin or absent Upper Holocene sand layer, features a clean sand fill 'pancake' underlayer up to 4 meters thick beneath the rock fill.

The East Bund had the following key features as shown in Figure 3.

- Basal high-strength geotextile with an ultimate tensile capacity of 700 kN/m;
- Sand pancake wider than the basal geotextile;
- Separation/filtration geotextile to cover the sand pancake and to minimise sand movement due to tides and waves;
- Rock core bund above the sand pancake;
- Armour (secondary and primary) on the flanks.

The East Bund had a nominal crest level of RL 4.0 m in the original design.

Due to the nature of the ground conditions, parts of the seawall settled by up to 1 m during the construction period alone, and it was estimated to settle progressively up to 2-3 m over a period of 10 to 15 years post construction.

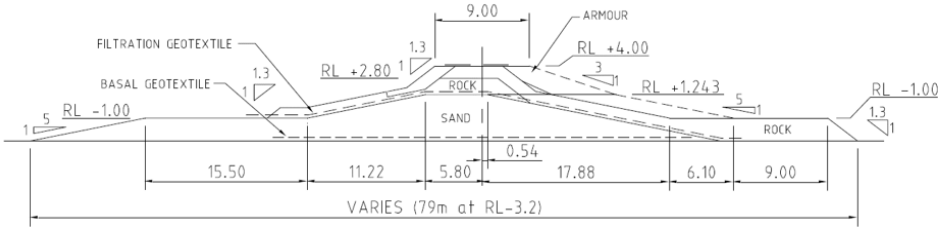

Figure 3 – Typical East Bund Profile (2005 as-built)

3.2 INITIAL TOP-UP

A periodic survey in 2011 revealed that parts of the seawall had settled by approximately 1 m, reducing the crest level to RL 3.0 m. This settlement aligned with initial design predictions. Following an engineering review of stability, settlement, and coastal engineering aspects, topping-up was conducted in mid to late 2013, raising crest levels to between RL 3.5 m and RL 4.0 m. The top-up involved placing rock armour on the crest to cover the exposed core rock along the East Bund.

4 SECOND UPGRADE – DESIGN AND PROCUREMENT (2022)

4.1 CONDITION AND RISK ASSESSMENT

A detailed survey in August 2020 confirmed the seawall's need for another top-up, as predicted by the 2012 design report. Consequently, Port of Brisbane Pty Ltd (PBPL) engaged Golder (now WSP) and Water Technology to undertake a condition and risk assessment. The findings, summarised by Stuer et al. (2021), indicated that parts of the East Bund and North Bund were at moderate risk, necessitating prompt repairs to mitigate the risks to acceptable levels.

4.2 DETAILED DESIGN

The detailed design by Golder and Water Technology aimed to meet both geotechnical and coastal engineering objectives. The details of the coastal and geotechnical designs are summarised in Stuer et al (2021) and Alinur et al (2023) respectively.

As part of the detailed design stage, two options were presented to PBPL to assess their viability. These included raising the crest of the bund to RL 3.5 m or RL 4.0 m. The design intents and challenges of the two options were presented for comparison. For the RL 3.5 m option, the design presented a lower geotechnical risk compared to the RL 4.0 m option, as the additional weight from topping up the crest to a higher level would require additional and larger stability berms. Furthermore, the additional weight from the RL 4.0 m option would accelerate the consolidation settlement of the foundation materials. Conversely, from a coastal engineering perspective, the RL 4.0 m option presented a lower risk on

the condition of the seawall, as it was expected to last longer than the RL 3.5 m option (20 years and 10 years respectively for the next scheduled top-up).

4.3 PROCUREMENT STRATEGY

To ensure a cost-effective and efficient solution for the second upgrade, PBPL adopted an Early Contractor Involvement (ECI) procurement strategy. This approach aimed to leverage the expertise and insights of experienced contractors early in the design process, with the primary objectives including to assess constructability and identify potential construction challenges, obtain accurate cost estimates, develop a realistic construction project schedule and incorporate this feedback into the detailed design.

The preliminary 60% design documentation with a crest design level of RL 3.5 m was provided and submitted to three selected contractors as part of the Early Contractor Involvement. The ECI phase was undertaken over a four-week period where workshops were held with all three contractors. It was identified during this phase to further investigate a solution to raise the crest level to RL 4.0 m and reissued as part of the formal tender process.

Based on the tender submissions for both options by the experienced tenderers, it was assessed that raising the seawall to RL 3.5 m provided the best value for money over raising it to RL 4.0 m, considering both the capital expenditure for the top-up and risk profile for each option. Raising the crest to RL 3.5 m compared to RL 4.0 m also reduced the requirement for wider stability berms, potentially limiting the future use of the seawall for reclamation development. Hall Contracting were chosen as the contractor to deliver the works following a competitive tender process.

The ECI phase provided valuable input into the budgetary, constructability and program input from each of the tenderers, and also allowed for the detailed design to be optimised to achieve best outcomes for the project.

5 SECOND UPGRADE – CONSTRUCTION

5.1 ROCK SELECTION

The selection of armour rock and core rock for the seawall upgrade was guided by technical specifications provided by Golder and Water Technology. Hall Contracting proposed using basalt sourced from the Bromelton quarry in Beaudesert, approximately 90 km from the Port of Brisbane. To ensure the rock's suitability for the project, an initial quarry inspection was conducted with representatives from PBPL, Hall, Golder, and Water Technology in attendance. Additionally, the quarry performed a series of drop tests to assess the rock quality, which were supplemented by laboratory testing conducted in advance of the inspection.

The drop tests revealed the need for corrective actions to align with the technical specifications and establish quality control measures for the armour rock supply. It is recommended to conduct thorough inspections at the project's outset to identify and address any issues before the rock is delivered to the site. This proactive approach minimised the risk of rejecting unsuitable rock on site, an expensive and disruptive process if the rock cannot be repurposed for the project.

5.2 QUALITY ASSURANCE

To ensure that the construction of the seawall met the design intent developed by Golder and Water Technology, it was imperative that quality control measures were implemented successfully. At the beginning of the project, site inspections were undertaken by representatives from PBPL, Golder, and Water Technology on a bi-weekly basis (i.e., twice per week). The intent of the site inspections was to provide feedback to Hall Contracting and rectify any non-conformances as soon as possible, rather than constructing long sections of the seawall that required significant rework. In most instances, the site representatives from Golder and Water Technology were able to guide the contractor in their design intent for the required interlock of the armour rock. Expectations were set early in the construction program, which enabled the contractor to progress through the project with a good understanding of the design intent and what was considered to be acceptable method of rock placement.

5.3 CHALLENGES DURING CONSTRUCTION

5.3.1. Variable existing conditions

As with many projects of this scale, there were variable conditions along the project alignment. One significant challenge was the condition of the core rock during excavation prior to placing the armour rock on the crest of the seawall. The design assumed that the existing core rock would be free of fines; however, during excavation, a layer of “mixed” core rock with silts and clays was discovered, resulting in a clayey sand to gravelly sand layer. This material was deemed unsuitable for direct placement due to poor interlocking properties. This issue may have arisen from construction practices during the 2013 initial top-up or the migration of fines through wave action. Consequently, the unsuitable material had to

be boxed out to 1.35 m below the crest level and replaced with an underlayer (D_{50} of 110 kg), prior to the placement of a double layer of armour rock (D_{50} of 1.7 t) to meet the design intent.

5.3.2. Stability of the seawall

The global stability of the seawall structure was a key consideration that directly influenced the constructability and construction sequencing of the seawall. During the design development, it was determined that the size of an excavator working along the crest line was limited to a 35-t excavator, equating to a 10 kPa uniformly distributed live load considered in the stability analyses. In some cases, trimming of the crest was required to RL 2.24 m and RL 2.7 m to allow an excavator to work along the crest line. Along the North Bund, stability berms were required before raising the crest level to RL 3.5 m due to the unfavourable ground conditions in this section. In these instances, marine-grade geotextile was installed before constructing the stability berms with suitable armour rock. Installation was executed using a combination of a long-reach excavator and professional divers to secure the geotextile in the correct position. Once the geotextile was installed, temporary stability berms were placed using the long-reach excavator from the seawall. The placement of the geotextile and the temporary stability berms was influenced by tides, requiring low tide conditions for the excavator to operate out of the water. Although this method restricted the progress, it was considered favourable compared to marine placement such as barge usage.

To improve productivity along the East Bund, a 50-t excavator was assessed and permitted for use on the southern sections of the East Bund where ground conditions were more favourable. This offset the production losses experienced on the North Bund due to the additional work required for the stability berms. The use of the 50 t expedited the production as it has a higher bucket capacity, in turn being able to place the armour rock more quickly than the 30 t.

The stability of the seawall was highly dependent on the precise geometry of the upgrades and top-up. To achieve this accuracy, the 3D design model was integrated into the excavator's GPS control system. This allowed the operator to receive real-time feedback and place the armour rock with a tolerance of ± 0.2 m. Monthly Unmanned Aerial Vehicle flyover surveys were conducted to further verify the accuracy of the placements, ensuring consistent compliance with design specifications throughout the project.

5.4 SUSTAINABILITY AND ENVIRONMENTAL CONSIDERATIONS

As part of the design process, there was an opportunity to reuse existing armour and core rock. The risk and condition assessment identified that existing rocks were suitable for the seawall's design life, reducing the carbon footprint by minimising the need for new materials and associated transport emissions. Additionally, the design considered climate change impacts, including sea level rise and increased wave heights, ensuring the selected armour rock sizing could withstand these future conditions for the next 50 years.

Another environmental consideration was the timing of the works to minimize impact on migratory birds, particularly the Grey Tailed Tattler, which use sections of the seawall to rest and feed during the summer months. Construction was scheduled for the cooler months to avoid disrupting these birds. Additionally, the selected materials aimed to discourage weed growth, maintaining the habitat for migratory shorebirds.

5.5 INSTRUMENTATION AND MONITORING

To monitor the seawall's performance, four inclinometer casings were installed at critical locations before construction began, which are shown in Figure 4. These inclinometers were used alongside fifteen settlement plates installed along the seawall alignment. A schematic of the instrumentation cross-section is presented in Figure 5. The settlement plates were monitored in real-time using the Kurloo system by Land Solutions, with data fed directly to a web portal. The results, summarized by Alinur et al. (2023), confirmed that the seawall's behaviour generally aligned with design predictions.

The settlement plates and inclinometers will continue to be monitored to create a dataset for the next top-up design and to alert PBPL of any adverse movements post-construction.

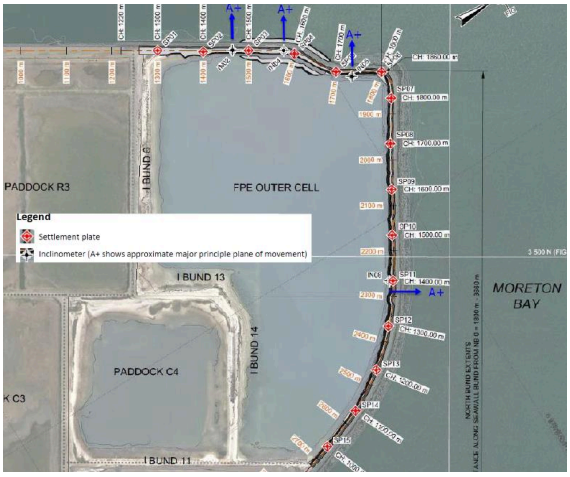

Figure 4: Instrumentation and Monitoring Locations (Inclinometers and Settlement Plates)

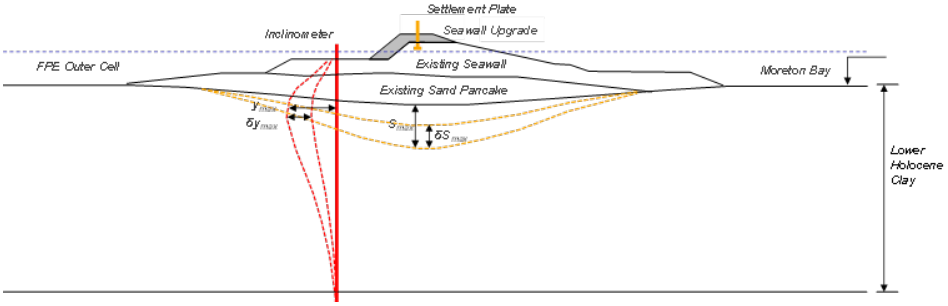

Figure 5: Schematic of lateral displacement (inclinometer) and settlement monitoring (settlement plate)

6 CONCLUSIONS

The FPE Seawall Upgrade project at the Port of Brisbane serves as a vital case study in managing infrastructure on challenging geotechnical conditions. The project, necessitated by ongoing settlement of the seawall foundation, highlights the complexities and technical challenges associated with upgrading marine structures founded on compressible Holocene clay layers.

For complex projects with a number of constraints and challenges, it is recommended that an ECI phase is included as part of the design and project delivery for future upgrades. The project's success also underscores the importance in the necessity of ongoing monitoring to inform future maintenance and upgrades. The FPE Seawall Upgrade project offers valuable insights and lessons learned for the geotechnical, coastal, and port communities, providing a robust framework for similar endeavours in the future. The proactive and adaptive measures employed ensure the long-term stability and functionality of this critical infrastructure, supporting the continued growth and development of the Port of Brisbane.

7 REFERENCES

Alinur, J., Perryman, G., Ng, Z. and Chan, C. (2023). Geotechnical Design and Monitoring of FPE Seawall Upgrade (Second Top-Up), Port of Brisbane. *Australia and New Zealand Conference on Geomechanics 2023*. Cairns, Australia.

Ameratunga, J., Shaw, P., Beohm, W.J. and Boyle, P.J. (2005). Seawall construction in Moreton Bay, Brisbane. *Proc. 16th Int. Conf. on Soil Mechanics and Geotechnical Engineering,* pp 1439-1442 Millpress Science Publishers/IOS Press.

Ameratunga, J., Noyle, P., De Bok, C. and Bamunawita, C. (2010). Port of Brisbane (PoB) clay characteristics and use of wick drains to improve deep soft clay deposits. *Proc. 17th Southeast Asian Geotechnical Society Conf.*, Taipei, Vol I, pp 116-119

Stuer, A., Ng, Z. and Alinur, J. (2021). Port of Brisbane Future Port Expansion Seawall Upgrade. *Australasian Coasts & Ports Conference 2021*. Christchurch, New Zealand.

DESIGN OF SUSTAINABLE COMPACTED SOIL BLOCKS FOR RAISING DYKES ALONG THE NEW BRUNSWICK FUNDY COASTLINE

K. O'Connor [1], S. Bennett[2], M. Taylor[3], N. Tratnik [4], K. Lokken[5]
[1]*Jacobs New Zealand,* [2,3,4,5] *The University of New Brunswick*

ABSTRACT

In Atlantic Canada, dyke systems are used extensively to protect the fertile agricultural land from being damaged by the saline ocean water in coastal areas. Without the 103 km of New Brunswick dyke systems, 14 500 hectares of land would be submerged by the Fundy tidal Fluctuations. The Shepody Dyke Rehabilitation project is required to ensure the land currently used for agriculture, transportation, and energy capture continues to be usable in the future. The original dykelands were constructed when the first Acadian settlements were built over 300 years ago. Due to continually rising sea levels caused by climate change, the dyke systems are currently threatened and require further development.

The Shepody dyke system construction has been a challenge in the past, due to variable site conditions and conventional construction methods requiring footprint extension onto valuable agricultural lands. As a result of this issue, a feasibility study on an innovative compacted soil block method to raise the dyke elevations was completed. By using pre-compacted soil blocks instead of conventional dyke construction methods, it will minimize the amount of heavy machinery required on site and keep construction within the existing dyke footprint. Based on the analysis of the proposed design, it was determined that the compacted soil block design meets the criteria established by the New Brunswick Department of Transportation and Infrastructure. The raised dyke height of 2.5m results in a final elevation of 9.6 metres above sea level. The stability modelling established a minimum factor of safety of 1.6 for the optimal compacted soil block mixture of 2% bentonite 98% natural soils by weight.

1 INTRODUCTION

The chosen location to develop and analyze the compacted soil block dyke construction method is the dykelands in Shepody, NB, Canada. The site location of the study can be seen in Figure 1 below.

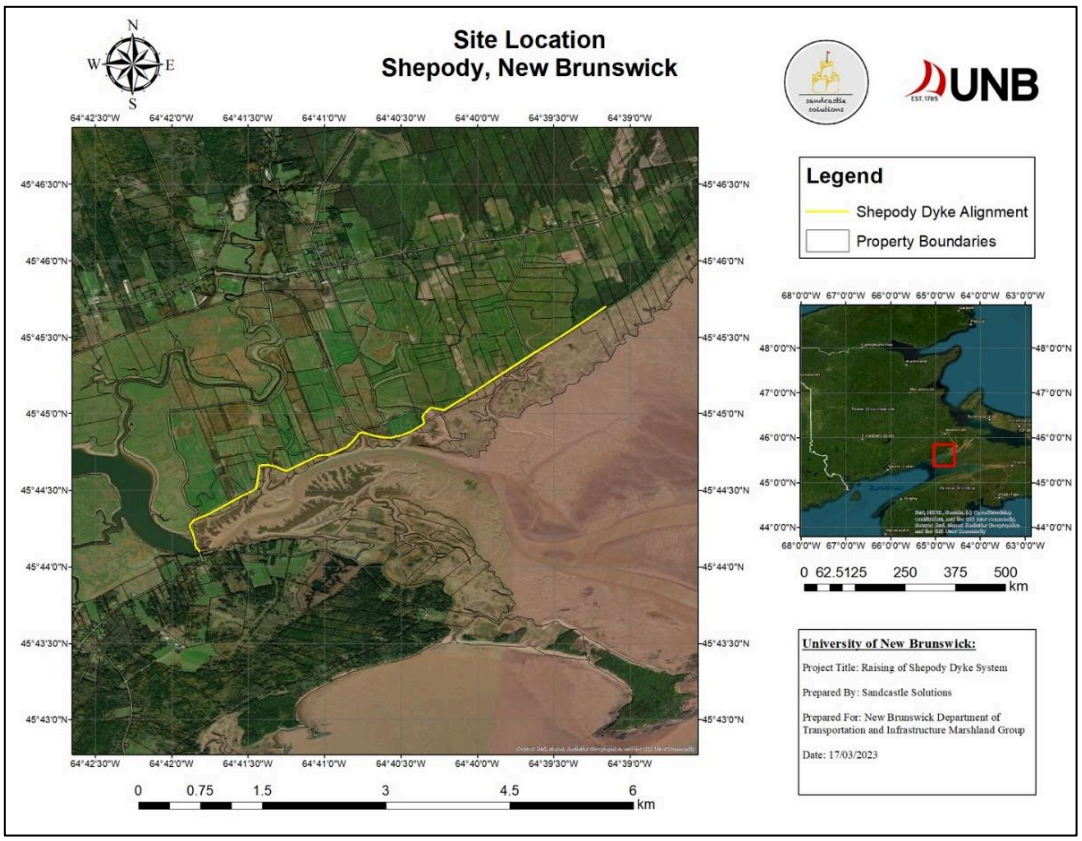

Figure 1: Shepody Dyke Alignment, New Brunswick, Canada.

The location is along the current dyke infrastructure system protecting the local agricultural lands. Due to changing tide levels, a vegetated plain lies between the dyke and the main tidal river channel. As global temperatures continue to rise due to climate change, thermal expansion of ocean waters and the melting of terrestrial ice are causing increased sea levels in Atlantic Canada (Williams & Daigle, 2011). In addition to these factors, Atlantic Canada is currently experiencing isostatic subsidence due to the last glaciation, causing the Bay of Fundy coastline to slowly subside and an increased rate of sea level rise (Williams & Daigle, 2011). As a result, marshland dykes in New Brunswick are being overwhelmed by a rising sea level. To mitigate this, the New Brunswick Department of Transportation and Infrastructure (NBDTI) is currently in the process of adapting their dykelands infrastructure to be able to withstand higher sea level elevations and continue to preserve the valuable agricultural land in the area. The sea level rise in the area for the worst projected case is 9.6 CGVD-2013 (masl). Therefore, the existing dyke structures must be increased to a height of 9.6 meters above sea level (masl) to withstand changing sea level with a one hundred-year life cycle.

Geological and Civil Engineering students from the University of New Brunswick were retained by NBDTI to create a solution to this problem as part of their senior design project which comprised of a feasibility study on the compacted soil block method to raise the dyke elevations. The final deliverable provided includes laboratory data and results, all previous testing and site investigation data incorporated into the design, slope stability analysis, and the finalized design drawings.

2 GEOTECHNICAL LABAROATORY TESTING

2.1 SAMPLING

Two field excursions to the site were completed by the project team on October 5, 2022, and November 5, 2022, to collect soil samples, complete in-situ field testing, and collect geophysical data. During the first site visit, approximately 300 kg of soil was collected from two separate locations at the Shepody Dykelands. The soil samples were collected by hand, using shovels and sample bags. The soil collected on site was then used to undertake geotechnical laboratory testing in order to determine geotechnical properties of the local material. Additional information from a previous site investigation in the area undertaken by WSP was utilized, including geotechnical borehole information and laboratory results for the in-situ material.

2.2 TESTING METHODS

Index testing on the soil samples collected from the site was completed. These tests consisted of Atterberg Limits (ASTM D4318-17e1), specific gravity (ASTM D854-23), Proctor (ASTM D698), and natural moisture content testing. Block compaction was completed based on the maximum dry density and optimal water content results determined by Proctor testing completed by the project team. Direct shear and UCS Testing were conducted on the compacted blocks of four soil and additive mixtures to determine internal friction coefficient and cohesion values.

2.3 SOIL ADDITIVES

Sufficient shear strength for design was not attained through compacted local soils alone, and additives such as bentonite, medium sand, and hay were combined with the local soils to determine the optimal soil to additive mixture. An iterative process for each soil mix was used to construct compacted soil blocks and undergo direct shear and UCS tests. The results of the consolidated drained direct shear test and UCS testing for each additive is presented in Table 1 below.

Table 1: Summary of Consolidated Drained Direct Shear Test and UCS Testing.

Mixture/Additives	Average UCS (kPa)	Average C_u (kPa)	Effective Internal Friction Angle (degrees)	Effective Cohesion (kPa)
Local Soil Only	198.59	99.29	17.52	41.67
5% Sand / 95% Soil	284.15	142.07	24.27	33.78
2% Bentonite/ 98% Soil	**316.32**	**158.16**	**23.18**	**43.6**
Straw/ Soil	369.56	184.78	16.99	45.95

Based on an increased effective internal friction angle and effective cohesion, the 2% bentonite additive with 98% local soil mixture was selected as the design soil mixture for the compacted soil blocks. After the preferred soil mix was selected, Consolidated Undrained Triaxial testing with porewater pressure measurement and flume testing was completed on the bentonite mix only. The parameters obtained from the triaxial test were hydraulic conductivity (k), cohesion (c), and the internal friction angle (ϕ) to be used directly in the slope stability analysis for the compacted block material.

2.3 RESULTS

The results of the Geotechnical Laboratory testing performed on the collected local soil samples and undertaken by the project team are presented in Table 2 below.

Table 2: Summary of Geotechnical Laboratory Testing Results.

Liquid Limit	Plastic Limit	Specific Gravity	Natural Moisture Content	Bulk Unit Weight	Optimal Water Content	Maximum Dry Density
31.7% to 42.1%	20.6% to 23.8%	2.64 to 2.69	26.9% to 65.3%	15.2 kN/m^3 to 17.1 kN/m^3	17.5%	1625 kg/m^3

The Consolidated Undrained Triaxial testing with porewater pressure was completed on the optimal soil mixture of 2% bentonite. Data from the triaxial testing was used to determine the cohesion and internal friction values through the failure envelope plotted with a series of Mohr's Circles. Darcy's Law was used to determine the hydraulic conductivity (k) of each of the soil samples. A summary of the averaged hydraulic conductivity values as well as the values determined from the failure envelope are shown in Table 3 below.

Table 3: Summary of Triaxial Test Result Analysis.

Average k (m/s)	ϕ (^{o})	c (kPa)
2.5x10^{-9}	6	67

3 PHYSICAL DYKE MODEL

The optimum water content for natural soil blocks and maximum dry density were used to calculate the mass of soil and water needed to create a compacted soil block of a desired volume. A steel mold for compacting soil blocks at a size of 225 mm by 112 mm by 70 mm was designed by the project team. The design of this mold consists of five steel plates which bolt together to form a box and a compaction plate which attaches to the Instron Machine. The Instron Machine is a compression and tension machine with a maximum applicable load of 250 kN. This representative soil block is not to scale of a compacted soil block that would be used for construction purposes, and the sizing was controlled by the parameters required to use the Instron machine at the University.

A model of the compacted soil block dyke was constructed in the hydraulic flume at the University of New Brunswick. The purpose of the flume analysis was to visualize the erosion of the soil blocks under simulated tidal fluctuations and wave action. The dyke model constructed of small-scale compacted soil blocks can be seen in Figure 2 below.

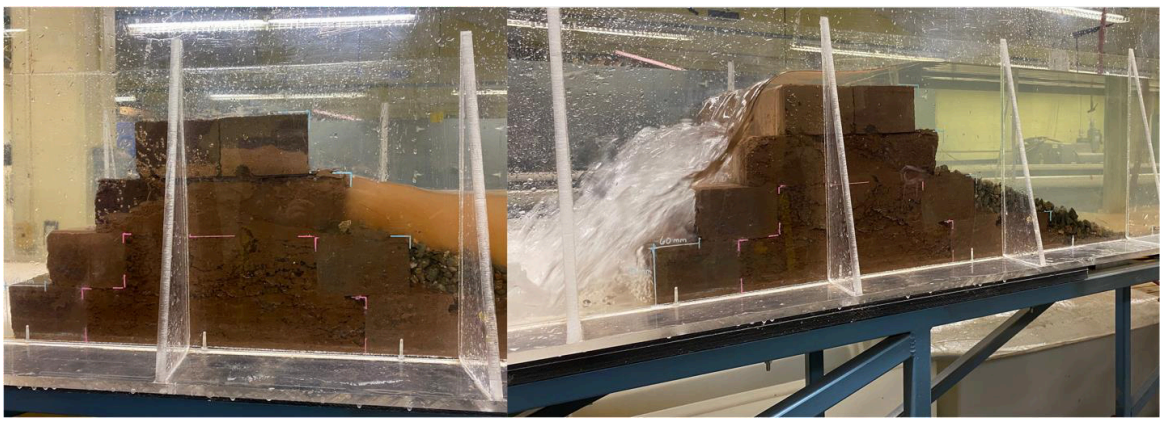

Figure 2: Flume Analysis Using Hydraulic Flume.

During the flume analysis, it was observed that the compacted soil blocks effectively retained water during the tidal fluctuation simulation. After several iterations of fluctuating water levels to simulate a tide, sediment transport and erosion was minimal. The main passage for seepage was through the joints between blocks. An overlapping block pattern could be used in future trials to minimize seepage between the joints. As seepage continued, fine-grained sediments accumulated

and effectively blocked the seepage. During the wave-action simulation and overtopping of the dyke, erosion as well as sediment transportation was also minimal. After overtopping the structure several times, piping began to occur in the joints between blocks. The piping continued until the dyke ultimately failed during overtopping. This scenario simulated extreme storm surge conditions.

4 SLOPE STABILITY ANALYSIS

4.1 OVERVIEW

A slope-stability analysis was performed with GeoStudio 2020 SLOPE/W and SEEP/W on the developed geological model with a dyke raise composed of the designed compacted soil blocks. The slope stability analysis was used to determine the factor of safety for landward and oceanward failures under total stress (short-term) and effective stress (long-term) scenarios.

4.2 ANALYSIS INPUTS

A representative cross section of the geological conditions on site was created using the existing borehole data provided by WSP. This representative cross section was used for the GeoStudio SLOPE/W and SEEP/W analysis. Soil parameters for the foundation soil and existing dyke were provided by WSP. Soil parameters for the compacted soil blocks were determined by the project team through geotechnical lab testing. The geotechnical parameters used in the model are shown below in Table 4, while the GeoStudio slope stability model is shown in Figure 3.

Table 4: Summary of Geotechnical Parameters used in Slope Stability Model.

Unit	Colour	k (m/s)	ϕ' (º)	c' (kPa)	ϕ (º)	c (kPa)	C_u (kPa)	γ (kN/m^3)	Specific Gravity
Compacted Soil Blocks	Red	$2.5x10^{-9}$	23	43	6	67	158	19.5	2.66
Silty CLAY	Pink	$4.8x10^{-9}$	21	25	15	30	16	16.2	2.66
Clayey SILT	Yellow	$4.3x10^{-9}$	36	2	28	8	40	17.9	2.73
Silty SAND	Brown	$7.8x10^{-8}$	31	20	35	40	N/A	17.0	2.68
CLAY	Green	$1.0x10^{-10}$	0	30	0	30	105	18.6	2.8

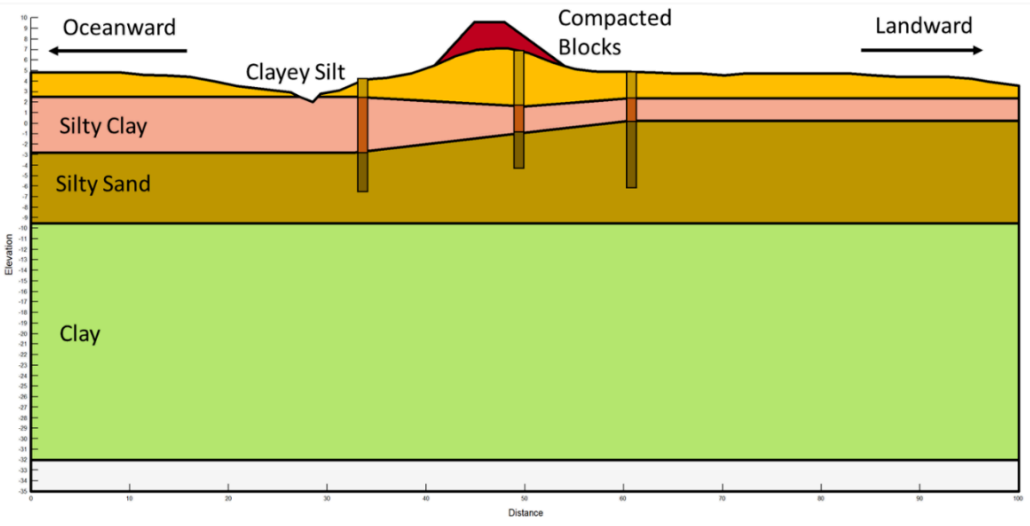

Figure 3: GeoStudio Slope Stability Model.

4.3 ANALYSIS METHODS

Initial water levels are modelled in a steady state system where a reservoir is at the dyke crest (9.6 masl). From this steady state output, a transient SEEP/W model is used for the dyke slope stability analysis (Broaddus, M. R., 2015). This transient analysis is modelled to replicate the daily tide cycle with maximum water level at the dyke crest over 10 days. This results in two full tidal cycles daily, transitioning from a high-tide (9.6 masl) to a low-tide (elevation of 2.5 masl). Boundary conditions have been developed to simulate the conditions on site. The reservoir on the seaward side during steady state modelling starts at 9.6 masl. Landward from the toe of the dyke, a boundary condition of water pressure head equals 0 m was used. All the SLOPE/W analyses used Bishop's method. Slip surfaces from right to left (seaward) and left to right (landward) were analyzed for each model using the grid and radius slip surface method. The default of 30-slices per analysis was used in each model.

4.4 RESULTS

After slope stability modelling with effective stress analysis (long-term model) and total stress analysis (short-term model) was completed on the raised dyke geometry using compacted soil blocks, the lowest FOS was determined to be 1.60. The lowest FOS was a result of effective stress analysis towards the ocean during low tide. The lowest FOS under total stress analysis was 1.79, which also resulted in an oceanward failure during low tide. Therefore, the results of slope stability analysis indicate that the compacted soil blocks can increase the crest elevation of the Shepody Dykelands to 9.6 masl maintaining a FOS of greater than 1.5 under the conditions examined. The Results of the raised dyke geometry model are presented in Table 5.

Table 5: Slope Stability Analysis Results.

Right to Left (Seaward) F.O.S.	Left to Right (Landward) F.O.S.	Model Type	Shear Strength Parameters
1.79	2.43	Short-Term	ϕ and c
1.60	2.38	Long-Term	ϕ' and c'
2.40	2.25	Short-Term	Cu

5 CROSS SECTION DESIGN

A primary objective was the development of a cross-sectional dyke design. The cross-section was developed for dyke construction based on the GeoStudio modelling geometry. This cross-section represents the developed geological model and dyke raise design which meets the project criteria. Design criteria regarding the cross-section was also specified by the client; including determining cross-section dimensions to achieve a crest elevation of 9.6 masl and obtaining a factor of safety (FOS) of at least 1.5.

Results from the slope-stability analysis display a minimum FOS of 1.6 with the chosen cross-section geometry. The design includes a 3.0 m crest width to accommodate vehicle accessibility. The oceanward slope is 4.0 m wide on a 1:1 gradient, while the landward slope extends 7.2 m on a 1.5:1 gradient. The more gradual slope on the landward side allows for maintenance and machinery accessibility. The total dyke raise is 2.5 m from 7.1 masl to 9.6 masl. Figure 4 below displays the proposed dyke geometry using compacted soil blocks on the existing dyke structure. Erosion controls on the ocean side, such as designed vegetation cover or a rip-rap apron, are recommended and require further study.

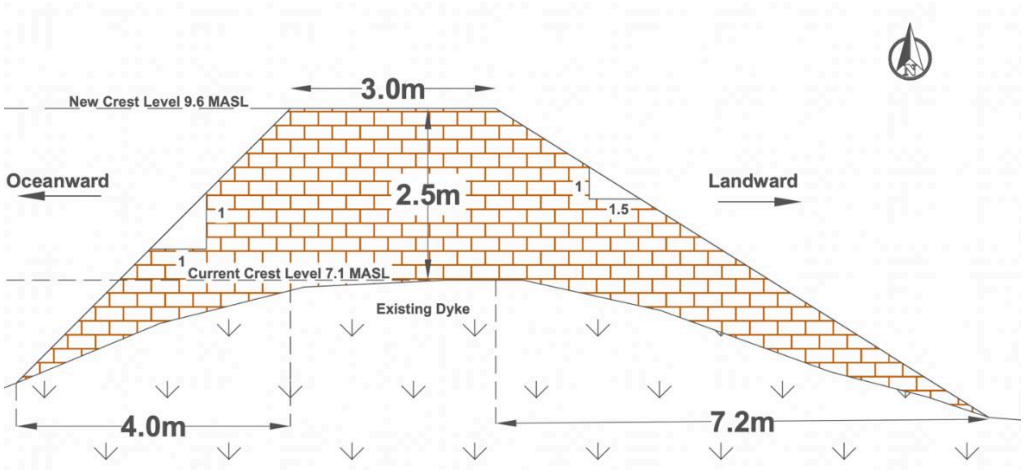

Figure 4: Final Cross Sectional Design of Raised Dykes Using Compacted Soil Blocks.

6 CONCLUSIONS AND RECCOMENDATIONS

The existing dyke structures located along the New Brunswick Fundy Coastline are no longer sufficient due to rising sea levels. Due to challenging site conditions, an alternative dyke construction method is required in order to maintain within the current footprint. The University of New Brunswick Geological Engineering Senior Design team successfully provided a unique solution to this design challenge. This is the addition of pre-compacted soil blocks to raise the height of the dykes to be able to withstand predicted sea level rise. The raised dyke height of 2.5m results in a final elevation of 9.6 metres above sea level. The stability modelling established a minimum factor of safety of 1.6 for the optimal compacted soil block mixture of 2% bentonite 98% natural soils by weight. Based on the analysis of the proposed design, it was determined that the compacted soil block design meets the criteria established by the New Brunswick Department of Transportation and Infrastructure.

Due to limitations such as cost and time, there are several recommendations to improve the future studies of this feasibility project. The project team recommends that SIGMA/W modelling is completed on the slope stability model to account for consolidation and settlement. The effects of freeze-thaw failures (heave failures) on the soil blocks themselves were excluded from the design. Additional research and lab testing are recommended to determine a compacted block dyke construction method and implementation on a large-scale project. Detailed construction costs should be calculated for large scale implementation, which should include specific equipment required to construct the soil blocks in the field.

7 REFERENCES

ASTM D854-23. *Standard Test Methods for Specific Gravity of Soil Solids by the Water Displacement Method.* (2023). https://www.astm.org/standards/d854

ASTM D698. *Standard Test Methods for Laboratory Compaction Characteristics of Soil Using Standard Effort.* (2021) https://www.astm.org/standards/d698

ASTM D4318-17e1. *Standard Test Methods for Liquid Limit, Plastic Limit, and Plasticity Index of Soils.* (2018). https://www.astm.org/d4318-17e01.html

Broaddus, M. R. (2015, August 11). *Performing a steady-state seepage analysis using SEEP/W: a primer for engineering students*.ir.library.louisville.edu/etd. https://ir.library.louisville.edu/cgi/viewcontent.cgi?article=3252&context=etd

Richards, W. & Daigle, R. (2011). Scenarios and Guidance for Adaptation to Climate Change and Sea Level Rise – NS and PEI Municipalities. https://www.novascotia.ca/nse/climate-hange/docs/ScenariosGuidance_WilliamsDaigle.pdf

A DISCUSSION ON STRENGTH GAIN FACTORS FOR COMMON SOIL UNITS IN THE WAIKATO REGION OF NEW ZEALAND

Jessel Ladwa, Harshad Phadnis, Robert Taylor
CMW Geosciences

ABSTRACT

The Cone Penetration Test (CPT) is routinely used to obtain insitu data and to assist in geotechnical analysis and design activities for construction projects. CPT data is also used commonly to evaluate liquefaction potential using empirical correlations developed over the last 50 years using either in-situ or laboratory test data from case histories involving young soil deposits.

Through recent studies, it is shown that liquefaction resistance is increased due to factors such as aging and bonding through the contribution of soil microstructure. To account for this contribution of soil microstructure to liquefaction resistance, several methods are available to derive a strength gain factor, K_{DR}, by combining conventional CPT data with shear wave velocity testing.

This research will look at strength gain factors calculated using two methods for a database of seismic CPTs (SCPT) performed in the Waikato region of the Central North Island. The range of strength gain factors derived for different geological formations will be presented along with an interrogation of any general trends observed.

1 INTRODUCTION TO MICROSTRUCTURE AND STRENGTH GAIN FACTOR

The Cone Penetration Test (CPT) is routinely used to obtain insitu data and to assist in geotechnical analysis and design activities. CPT data is also used commonly to evaluate liquefaction potential using empirical correlations developed over the last 50 years using either in-situ or laboratory test data from case histories involving young soil deposits.

Through recent studies, it is shown that liquefaction resistance is increased through the contribution of soil microstructure. Microstructure is a term used to describe mechanisms that reinforce the links between soil particles commonly observed in aged or cemented soils (Hatanaka and Uchioda 1995, Goto et al 1992). Eslaamizaad and Robertson (1996) showed that the contribution of microstructure can be assessed using seismic CPTs (SCPT) based on the small-strain shear modulus (G_o), net cone resistance (q_n) and the normalized cone resistance (Q_{tn}), since microstructure tends to increase the small-strain shear modulus (G_o) significantly more than it increases the large-strain strength of a soil (reflected in Q_{tn}). Hence, microstructure tends to increase the small-strain shear wave velocity (V_s) more than the larger-strain cone resistance for a soil.

To account for the contribution of microstructure, the methods detailed in Lontzetidis et al (2022) were used to derive the strength gain factor (SGF or K_{DR}) values using Measured to Estimated Velocity Ratio (MEVR) proposed by Andrus et. al (2009) and Measured to Estimated Rigidity Index (MEKG) proposed by Robertson (2015) for this paper. The research presented in Lontzetidis et al (2022) had also identified some improvement in the derived SGF values when filtering the data to only soils considered susceptible to liquefaction based on a Soil Behaviour Type Index, I_c, of less than 2.6 as proposed by Robertson and Wride (1998).

2 DATABASE USED IN THE ANALYSES

Data from 113 SCPTs from twenty different sites across the Waikato region were used for this study, at the locations shown on Figure 1.

The study area is characterised by low rolling hills, flattish alluvial plains, low terraces adjacent to the Waikato River and gullies cutting in to the alluvial plain or the low terraces. The Recent Alluvium and Holocene river deposits are young alluvial deposits typically encountered along the Waikato River and gullies. Taupo Pumice Alluvium (TPA) represents pumiceous deposits that were swept down the Waikato River from a dramatic break-out flood event in about 250 AD. Holocene Swamp Deposits are deposits in the low-lying areas and often contain organic matter. These units can be up to 1,750 years old. Piako Subgroup soils are usually lacustrine or fluvial in origin and ranges from 10,000 to 130,000 year

in age. The Late Pleistocene Hinuera Formation includes volcanogenic alluvial deposits from the ancestral Waipa and Waikato rivers, this unit ranges from 15ka to 65ka years old. Numerous weathered clay-rich tephra layers are usually encountered on the rolling hills, referred to as Hamilton and Kauroa Ashes aged between 0.18Ma to 2.2Ma years old. Soils of the Puketoka Formation are fluvially reworked deposits that are sensitive to disturbance. This age of this unit ranges from 0.8Ma to 1.8Ma years old. The Walton Subgroup comprises sequences of volcanogenic pumiceous sand, gravel, silt and on-welded ignimbrite. This unit is amongst the oldest in the dataset ranging from 2.6 to 3.6Ma.

Table 1 presents a summary of the various geological units that were assessed as a part of this study where a total of 208 sCPTs were available. Across these soil units, a total of 2,173 strength gain factors were calculated from paired SCPT and shear wave velocity data points.

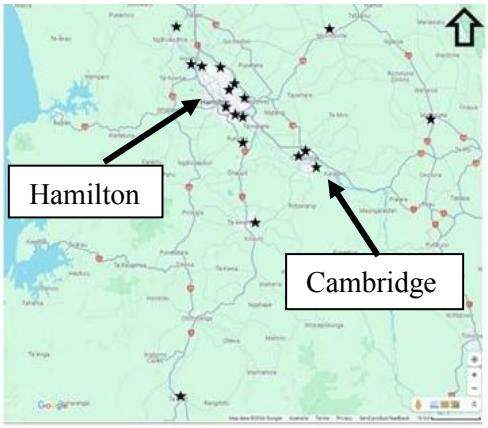

Figure 1: Site Locations Across the Waikato Region

	Taupo Pumice Alluvium + Recent Alluvium + Holocene River Deposits	Holocene Swamp Deposits/Piako Subgroup	Hinuera Formation – Coarse Grained	Hinuera Formation – Fine Grained	Hamilton and Kauroa Ashes	Puketoka Formation	Weathered Walton Subgroup
Sites	8	2	16	13	3	4	10
Relevant seismic CPT's	15	10	66	48	9	17	43
Strength Gain Factors Calculated	98	68	1,131	381	29	89	373

Table 1: Summary of Data

3 RESULTS AND ANALYSIS

RECENT ALLUVIUM, HOLOCENE RIVER DEPOSITS AND TAUPO PUMICE ALLUVIUM (TPA)

Data from Recent Alluvium, Holocene River Deposits and Taupo Pumice Alluvium has been combined based on their similar geological age and a small dataset (we only have 6, 1 and 8 SCPTs for those units respectively). Several data points from this subset of data contained high shear wave velocities (between 210 to 280 m/s), that resulted in higher predicted SGFs for these paired data points, and are shown in red in Figure 2.

SGF plots have been prepared for each soil unit. Two probability distribution plots have been presented: the first plot includes all data and the second plot only includes soils that are prone to liquefaction (i.e. $I_c \leq 2.6$).

As shown in Figure 2, the median SGF values derived using the MEVR and MEKG methods are 0.69 and 0.98 respectively i.e. less than unity, which is considered appropriate for a young soil deposit which is expected to contain very little to no microstructure.

3.2 PIAKO SUBGROUP AND HOLOCENE SWAMP DEPOSITS

Figure 3 shows the median SGF values derived for Piako Subgroup and Holocene Swamp Deposits using the MEVR and MEKG methods are 1.09 and 0.97 respectively. Outliers in calculated SGF values shown in red in Figure 3 have associated shear wave velocities greater than 280 m/s.

As shown in the next few sections, generally the SGF values calculated using the MEVR method have a general trend of increasing with depth whereas SGF values calculated using the MEKG method generally decrease with depth. The exception to this is the Piako Subgroup and Holocene Swamp Deposits, where SGF values calculated using both methods generally increase with depth.

3.3 HINUERA FORMATION

Due to the large dataset available for this subgroup, data points were able to be classified into coarse-grained and fine-grained soils to identify if there is any difference in predicted SGF based on soil grain size. A shown in Figures 4 & 5, the median SGF values derived from the MEVR and MEKG methods for coarse-grained Hinuera Formation soils are 1.14

and 1.11 respectively, whereas the median SGF values for fine-grained Hinuera Formation soils are 1.15 and 1.08 respectively, therefore show very similar results. The median SGF values for the entire dataset (combining coarse and fine-grained soils) are 1.15 and 1.10 for MEVR and MEKG methods respectively.

3.4 HAMILTON AND KAUROA ASHES

As presented in Figure 6, the median SGF values derived from the MEVR and MEKG methods are 0.95 and 1.49 respectively which shows a significant difference between the two methods. This difference may be attributed to the relatively small set of data points for this geological unit where there appears to be large scatter and significant variability in the calculated SGF values. Increasing the dataset for this unit may help to improve the variability in results. Measuring fines content and Atterberg limits or performing paired boreholes and CPTs followed by calculating site-specific I_c cutoff or C_{FC} correction is generally considered to be more appropriate for these units, while assessing liquefaction.

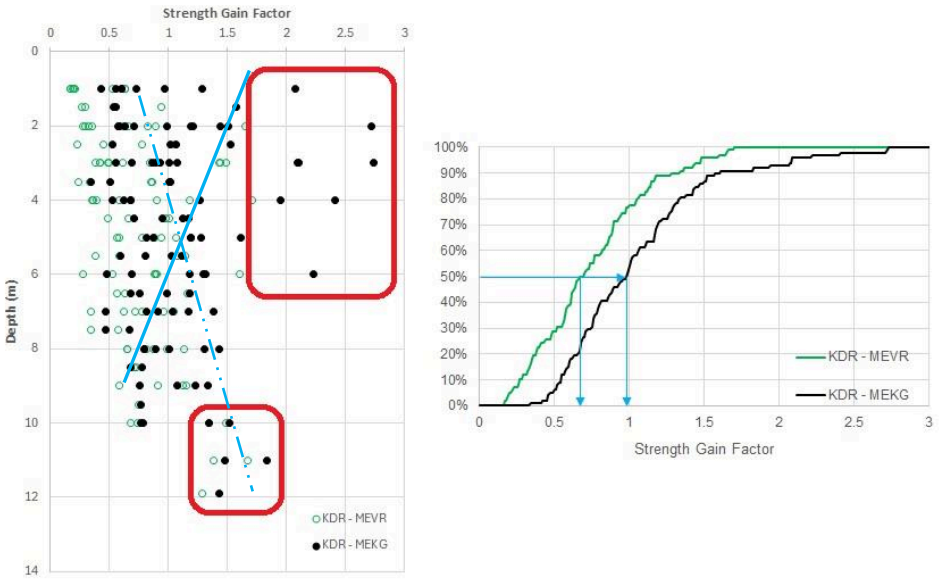

Figure 2: SGF Plots for TPA, Recent Alluvium and Holocene River Deposits

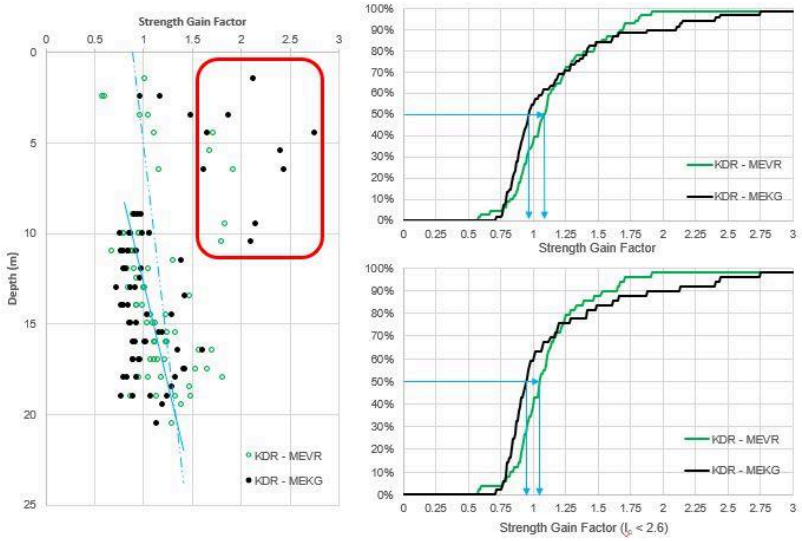

Figure 3: SGF Plots for Piako Subgroup and Holocene Swamp Deposits

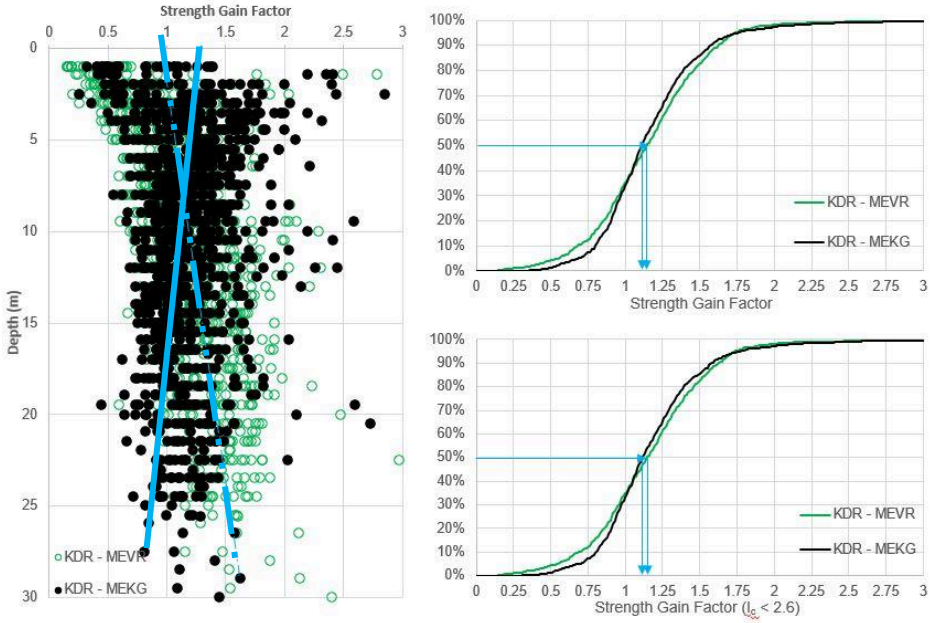

Figure 4: SGF Plots for Hinuera Formation – Coarse Grained

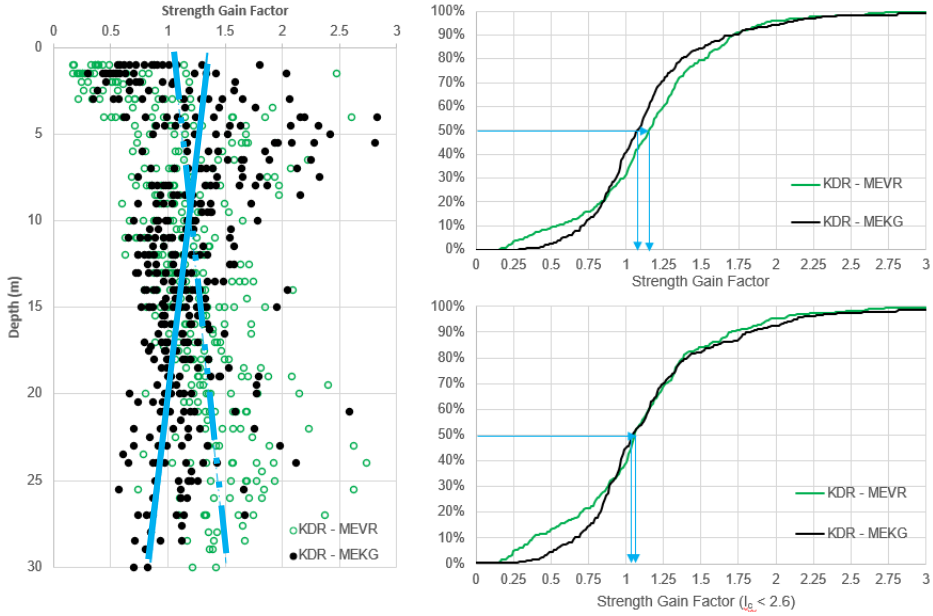

Figure 5: SGF Plots for Hinuera Formation – Fine Grained

3.5 PUKETOKA FORMATION

The median SGF values derived from the MEVR and MEKG methods, as shown in Figure 7, are 1.29 and 1.21 respectively. The higher SGF values for this unit are expected due to the geological age of the unit. Microstructure assessments in this unit should be performed carefully as this unit is sensitivity to disturbance and the measured cone tip resistance values might indicate remoulded and not peak strengths.

Some shallow and deep outliers in calculated SGF values were identified for this dataset, as shown in red in Figure 7. The shallow outliers are all from one site while the deeper outliers are from two SCPTs from the one site. Therefore, these two sites (or similar) may warrant further investigating.

3.6 WEATHERED WALTON SUBGROUP

The median SGF values derived from MEVR and MEKG methods are 1.46 and 1.28 respectively. The SGF values for this subgroup are the highest in this study, which is expected based on the geological age of these deposits. The higher

SGF values for this unit is expected due to the geological age of the unit. The two units are the oldest in the dataset ranging from 0.8Ma to 3.6Ma.

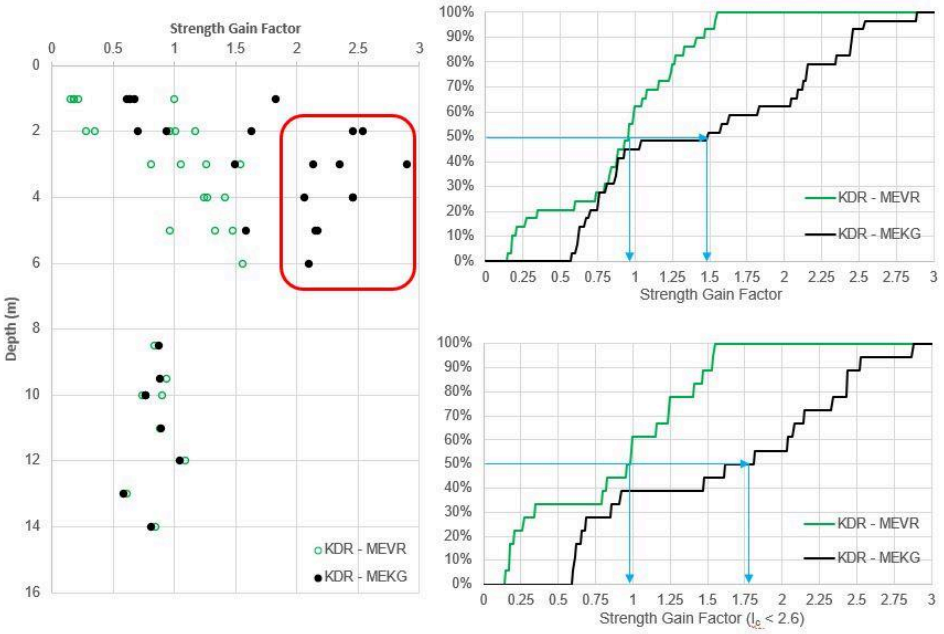

Figure 6: SGF Plots for Hamilton and Kauroa Ashes

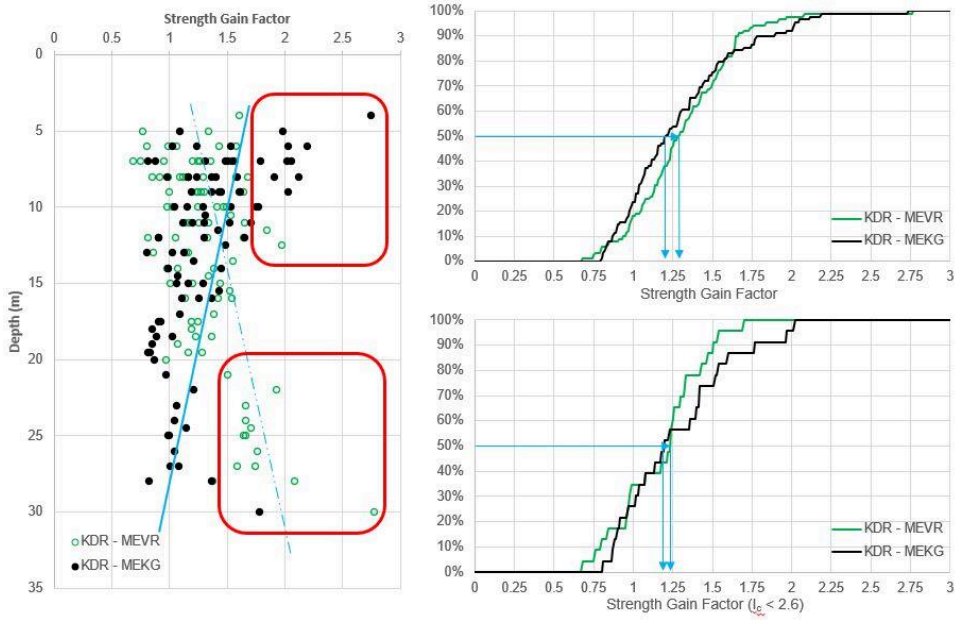

Figure 7: SGF Plots for Puketoka Formation

3.7 SOIL BEHAVIOUR TYPE INDEX

The effect of limiting the paired data points based on the soil behaviour type index (I_c) proposed by Robertson and Wride (1998) is also considered. An I_c value of 2.6 is typically used to differentiate between clay-like and sand-like soils that are considered susceptible to the effects of liquefaction which was applied to the datasets. Where median SGF values are close to and less than 1.0, filtering the dataset has a negligible effect on the median value given that majority of these soils are sand-like. This is applicable for Recent Alluvium, Holocene River Deposits, TPA, Piako Subgroup, Holocene Swamp Deposits, Hamilton and Kauroa Ashes soils. Where median SGF values are between 1.0 and 1.3, filtering the dataset changes the median value by 0.05 to 0.10. This is applicable to Hinuera Formation soils. Where median SGF is greater than 1.3 in Walton Subgroup soils, filtering the dataset appears to increase the median value by 0.10 to 0.15.

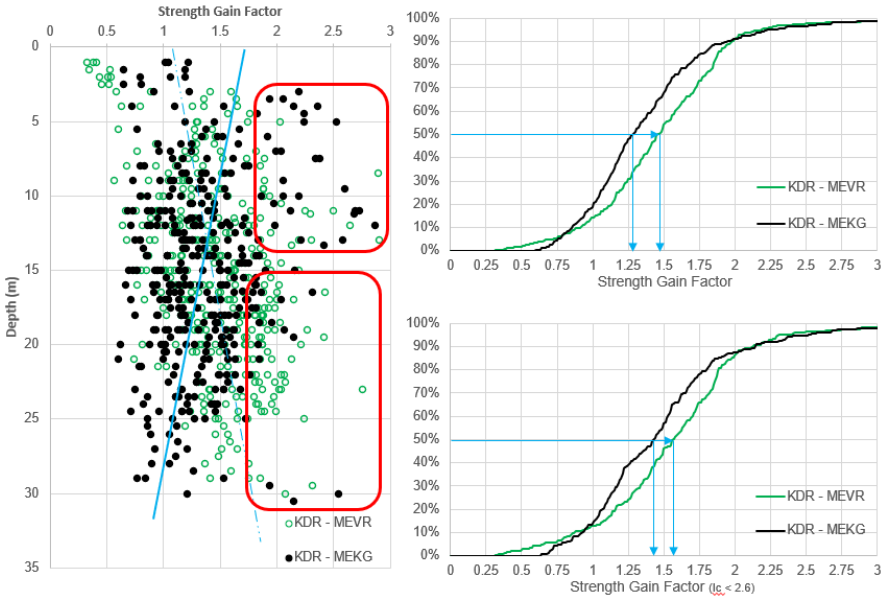

Figure 8: SGF Plots for Weathered Walton Subgroup

4 CONCLUSION

The effects of microstructure can be readily assessed using seismic CPT data. High quality data and high-quality shear wave velocity interpretation are essential to perform microstructure assessments. Geological units at the site, their formation characteristics and age, outliers in interpreted shear wave velocity for the related soil type, variability in calculated strength gain factors should be appropriately considered while performing microstructure assessments. The range of strength gain factors derived for several geological formations has been presented along with an interrogation of some general trends observed based on a dataset of sCPT results from a CMW database. Older units have greater microstructure i.e. higher SGF values than younger deposits in general. The trend for the strength gain factor using the MEVR method is to increase with depth, whereas the trend for the strength gain factor, using the MEKG method, is to decrease with depth. Similar trends were noted in Lontzetidis et al. (2022) and Lontzetidis et al. (2023).

5 REFERENCES

Andrus, R. D., Hayati, H., and Mohanan, N. P. 2009, Correcting liquefaction resistance of aged sands using measured to estimated velocity ratio. *Journal of Geotechnical and Geoenvironmental Engineering* 135(6), 735–744.

Edbrooke, S.W. 2005, *Geology of the Waikato Area. Institute of Geological & Nuclear Sciences, 1:250,000 geological map*.

Eslaamizaad, S., and Robertson, P. K. 1996, Seismic cone penetration test to identify cemented sands, *Proc. 49th Canadian Geotechnical Conf., St John's, Newfoundland, Canadian Geotechnical Society* (CGS), 1, 352–360.

Goto, S., Suzuki, Y., Nishio, S., and Ohoka, H. 1992, Mechanical properties of undisturbed Tone-River gravel obtained by in-situ freezing method. *Soils Found*., 32(3), 15–25.

Hatanaka, M., and Uchida, A. 1995, Effects of test methods on the cyclic deformation characteristics of high quality undisturbed gravel samples. *Proc., ASCE*, 136–151.

Lontzetidis, K., Robertson, P.K. and Morton, D.J. 2022, A simplified method to incorporate the benefits of microstructure for cyclic liquefaction analyses using the sCPT. In: Gottardi, G., Tonni, L. (eds.) *5th International Symposium on Cone Penetration Testing (CPT'22),* Bologna, Italy, pp. 521-527.

Lontzetidis, K., Taylor, R. and Morton, D.J. 2023, Investigating microstructure, a soil characteristic that increases resistance against liquefaction. *14th Australia and New Zealand Conference on Geomechanics (ANZ2023),* Cairns, Australia.

Robertson, P. K. 2015, Comparing CPT and Vs liquefaction triggering methods. Journal of Geotechnical and Geoenvironmental Engineering, 141(9).

Robertson, P.K., and Wride C.E. 1998, Evaluating cyclic liquefaction potential using the CPT. *Canadian Geotechnical Journal,* 35(3), 442- 459.

APPLICATION OF THE FINES CONTENT CORRECTION FACOR (C_{FC}) FOR SOILS SUSCEPTIBLE TO LIQUEFACTION IN THE BAY OF PLENTY

Ella McGurk[1], Harshad Phadnis[2], Robert Taylor[1]
CMW Geosciences Tauranga, New Zealand[1]
CMW Geosciences Hamilton, New Zealand[2]

ABSTRACT

The Cone Penetrometer Test (CPT) has become the most commonly used in-situ test to evaluate simplified triggering methods developed from in-situ and laboratory test data from case histories over the last 50 years.

Engineering properties like the fines content and plasticity index values are shown to have an effect on a soil's susceptibility to liquefaction. However, relationships used to estimate the fines content using CPT data have a high degree of scatter and hence the actual fines content in soils can be estimated incorrectly, thus potentially incorrectly interpreting liquefaction susceptibility.

This paper will discuss how fines content correction factor (C_{FC}) values were determined from paired CPTs and boreholes with laboratory testing, and the effects this has on predicted liquefaction susceptibility for a case study in the Bay of Plenty, New Zealand. A range of C_{FC} values for some soil units were recommended based on the dataset, including recommendations for additional analysis.

1 INTRODUCTION

The Cone Penetrometer Test (CPT) is among the most commonly used in-situ tests to evaluate liquefaction potential of soils. Empirical correlations between fines content (FC) and the soil behaviour type index I_C, have been developed from in-situ and laboratory test data from case histories over the last 50 years (Robertson & Wride 1998, Boulanger & Idriss 2014). However, these correlations have a high degree of scatter and should be verified with drilling and sampling of soils for especially high risk or high consequence projects (MBIE, 2021).

This paper presents site-specific fines content correction factors (C_{FC}) based on paired CPT and laboratory data of various aged soils investigated for a project in the Bay of Plenty, New Zealand.

2 DISCUSSION ON FINES CONTENT AND FINES CONTENT CORRECTION VALUES

Recent studies have shown that liquefaction resistance (CRR) is shown to increase in soils with a higher fines content. However, these studies also show that there is a poor correlation between FC and the CPT derived I_C value from which the FC is estimated for CPT-based liquefaction analyses. Therefore, a fines content correction factor (C_{FC}) can be applied to adjust the estimated FC when paired with laboratory particle size distribution tests.

Due to this poor correlation between FC and I_C, as shown on Figure 1, also recommended that C_{FC} values are varied over a range of -0.29 to +0.29 (approximately equal to a standard deviation of +/- 1).

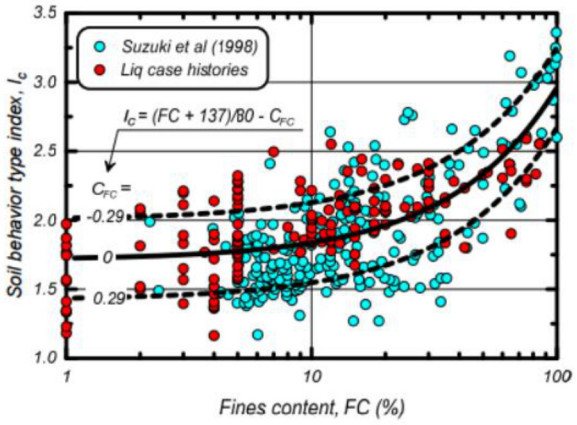

Figure 1: Correlation recommended between Ic and FC (Boulanger and Idriss 2014)

3 DATABASE USED IN THE ANALYSES

Data has been obtained from 58 Cone Penetrometer Tests (CPTs) and 335 particle size distribution (PSD) tests for a project in the Bay of Plenty region of New Zealand. The project site is in a geomorphic region referred to as the Tauranga Basin. This region had been infilled by Pleistocene-aged (0.35 to 2.18Ma) fluvially reworked volcanic deposits known as Matua Subgroup, comprising predominantly Tephra (MST) and Alluvium (MSTA) silt and sand mixtures originating from the Taupo Volcanic Zone as per Briggs et al. 1996. These deposits have been subsequently mantled by several metres of late-Quaternary (<0.35 Ma) volcanic airfall deposits (LQVA) across elevated hills and recent Holocene (<10 ka) alluvial swamp deposits (RA-SD) within low-lying gullies. These deposits are underlain by older ignimbrites.

PSD tests were completed at various depths within the paired machine boreholes (BHs) and/or test pits (TPs) to provide a series of laboratory tested FC values. To obtain FC values from the corresponding CPT data, a representative FC value was determined by averaging the FC values across the same depth range in the CPT. In instances where CPT tests terminated prior to the depth at which PSD sampling occurred, results were omitted.

4 APPLICATION OF THE FINES CONTENT CORRECTION FACTOR

Initially, FC values obtained from particle size distribution laboratory testing were compared against FC values estimated from the CPT data. This was done by plotting both FCs on a scatterplot with a 1:1 line of equality fitted. Data was plotted for each soil unit.

In an attempt to better fit the data to the 1:1 equality line, the following equation by Boulanger and Idriss (2014) was then used to adjust the FC by applying a Fines Content Correction Factor, C_{FC}.

$$FC = 80(I_C + C_{FC}) - 137 \quad (1)$$

A correction factor of 0.05 and 0.1 were chosen for the data sets. The adjusted FC values from CPT data values were also plotted against laboratory FC for comparison with the non-adjusted plots.

5 RESULTS

5.1 OVERALL COMPARISON

Figure 2 presents the overall spread of FC data without a fines content correction factor applied, i.e., C_{FC}=0. The plot illustrates a wide variety of scatter and makes it difficult to identify overall trends, thus each individual soil unit along with the adjusted FC plots are presented in the subsequent sections.

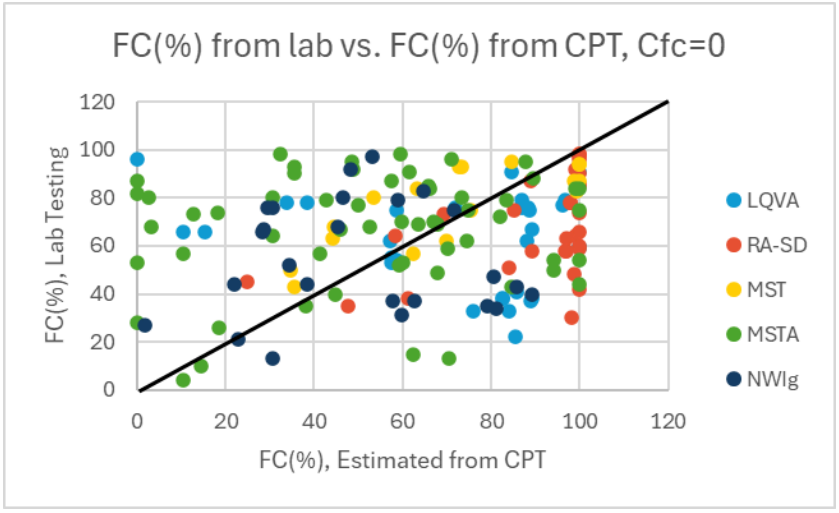

Figure 2: Overall Comparison of FC(%) from Lab vs. FC(%) from CPT, C_{FC}=0

5.2 RECENT (HOLOCENE) ALLUVIAL SWAMP DEPOSITS (RA-SD)

Figure 3 presents the data points for RA-SD with a C_{FC} factor of 0 and -0.10 respectively.

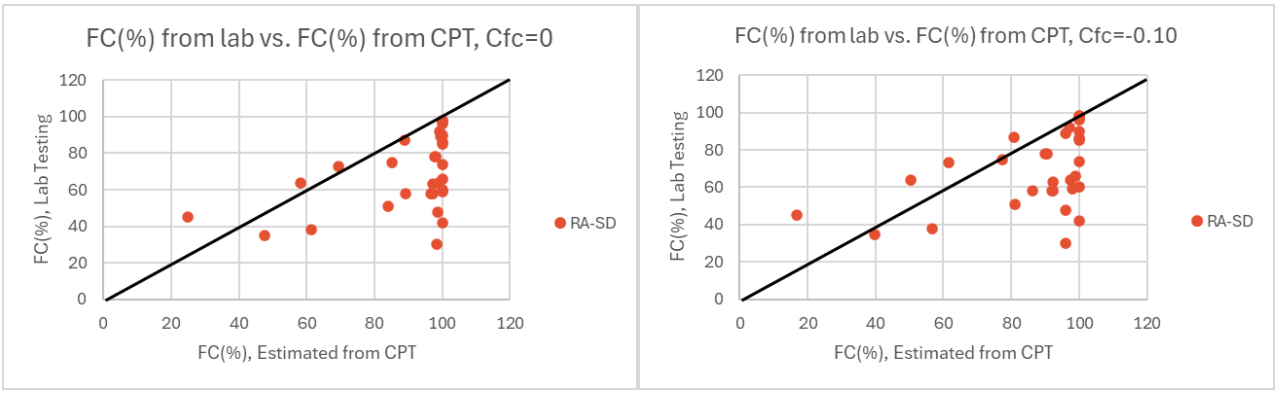

Figure 3: FC Comparison of RA-SD, C_{FC}=0 and C_{FC}=-0.10

5.3 LATE QUATERNARY VOLCANIC ASH (LQVA)

Figure 4 presents the data points for LQVA with a C_{FC} factor of 0 and -0.05 respectively.

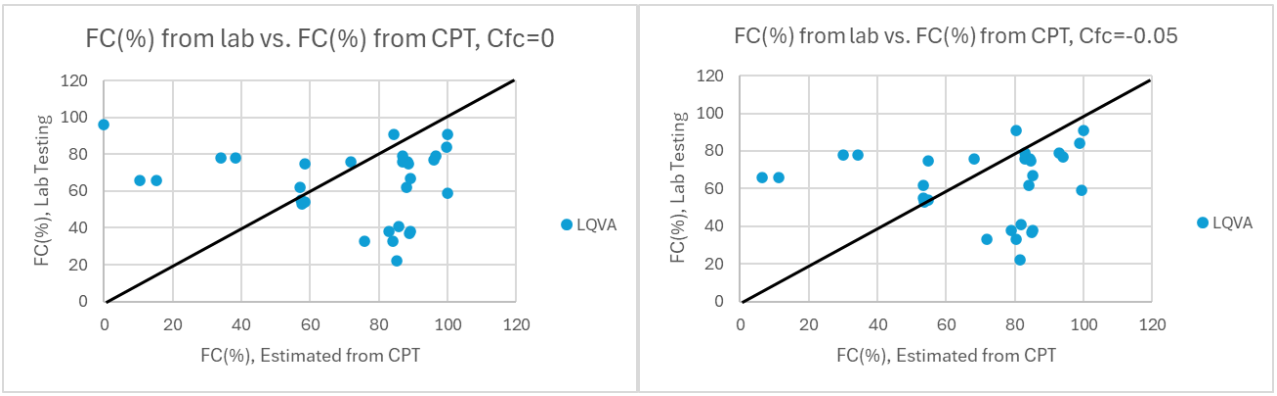

Figure 4: FC Comparison of LQVA, C_{FC}=0 and C_{FC}=-0.05

5.4 MATUA SUBGROUP, TEPHRA AND ALLUVIUM (MST & MSTA)

Figure 5 presents the data points for Matua Subgroup – Tephra (MST) with a C_{FC} factor of 0 and 0.10 respectively.

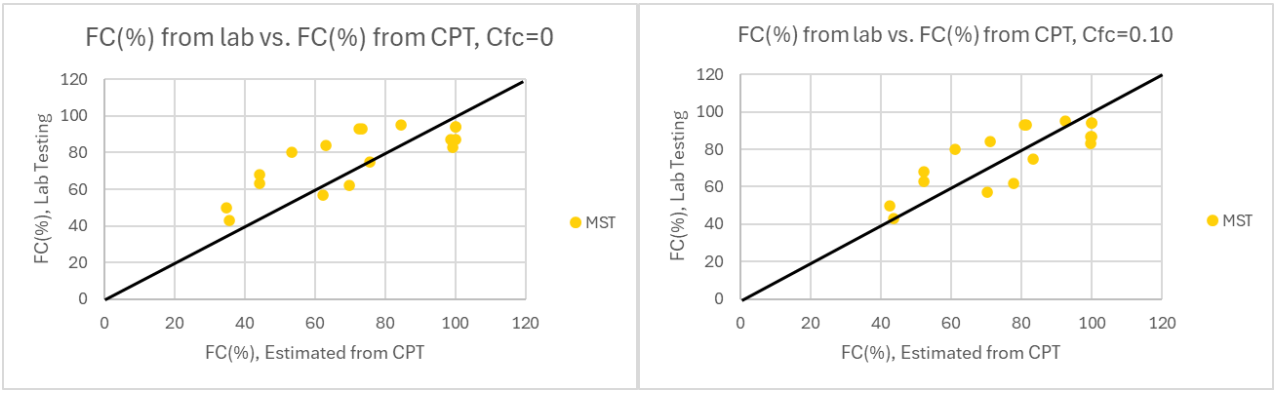

Figure 5: FC Comparison of MST, C_{FC}=0 and C_{FC}=0.10

Figure 6 presents the data points for Matua Subgroup – Tephra and Alluvium (MSTA) with a C_{FC} factor of 0 and 0.05 respectively.

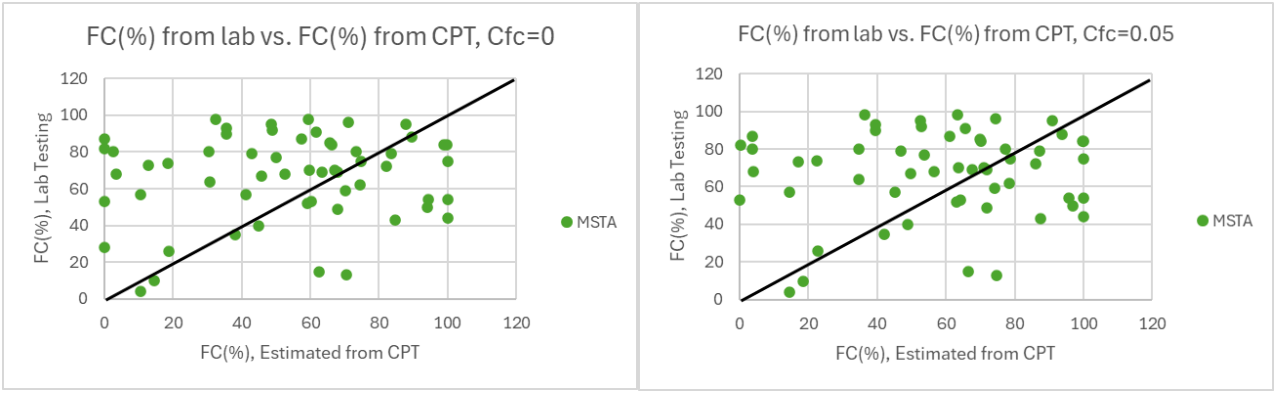

Figure 6: FC Comparison of MSTA, C_{FC}=0 and C_{FC}=0.05

5.5 NON-WELDED IGNIMBRITE (NWIG)

Figure 7 presents the data points for NWIg with a C_{FC} factor of 0 and 0.05 respectively.

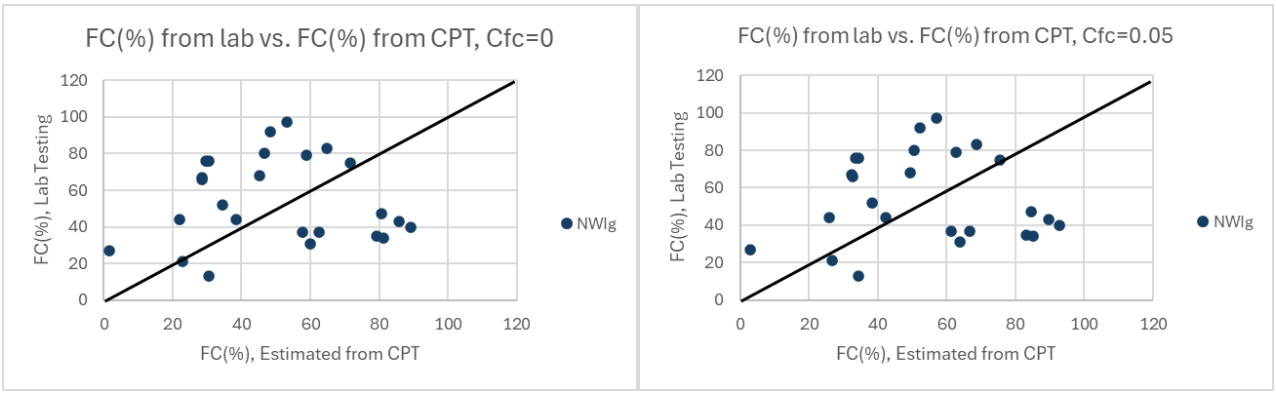

Figure 7: FC Comparison of NWIg, C_{FC}=0 and C_{FC}=0.05

6 DISCUSSION

Despite a large dataset, the data points for most of the soil types was generally found to have a high degree of scatter, particularly for MSTA and NWIg, which made determining an apparent C_{FC} more difficult. It is this author's opinion that the higher degree of MSTA scatter may be due to the highly interbedded nature of this soil unit, and possible vertical and horizontal variability in soil characteristics between the paired CPTs and BH test sites. Additionally, the presence of pumiceous sands, especially within the NWIg unit, may affect CPT-estimated FC's. As discussed in Module 2 of the Earthquake Engineering Guidelines (MBIE, 2021) much of the CPT empirical database is from quartz-derived soils which behave quite differently to pumiceous soils. Additionally, pumice is highly crushable, thus the CPT cone may have broken up the unit and incorrectly estimated the actual portion of fines present. In this case, the results for NWIg may be considered erroneous.

The RA-SD and LQVA plots show a high concentration of data points close to the 100% FC_{CPT} even though the FC_{LAB} varies significantly and even as low as 20% suggesting a poor correlation between the CPT estimated FC and laboratory FC.

7 RECOMMENDATION FOR FURTHER WORK

As identified in Boulanger and Idriss (2014), efforts to obtain site specific correlations for C_{FC} based on small data sets may be less reliable than published generic correlation, which is based on a significant number of data points from various sites and soils. Therefore, it is recommended this study is expanded to include other data sets, ideally within the same soil units, to try and further refine the adopted C_{FC} values.

As discussed, RA-SD and LQVA illustrated a poor correlation between the CPT estimated FC and laboratory FC. These datasets may warrant further interrogation to determine if there is an error in the acquisition of the CPT data or another factor that may explain the poor correlation.

8 CONCLUSION

Data from 58 CPTs and sCPTs and 335 PSDs were paired to help investigate actual vs. empirical fines content values to understand the fines content correct factors for the site.

Generally, it was found that the empirical relationships used to estimate the fines content using CPT data were incorrectly estimating the fines content when determined through laboratory testing, and thus potentially under and over-estimating liquefaction susceptibility. A single fines content correction factor was adopted for each soil unit to adjust the CPT-estimated FC.

Given the high degree of scatter across the data sets for all soil types, determining an apparent C_{FC} for each soil unit was more difficult. It is recommended this study is expanded to include other data sets, ideally within the same soil units, to try and further refine the adopted C_{FC} values

9 ACKNOWLEDGEMENTS

This author acknowledges that this research could not have been carried out without the support from their colleagues at CMW Geosciences.

10 REFERENCES

Briggs, R.M., Hall, G.J., Harmsworth, G.R., Hollis, A.G., Houghton, B.F., Huges, G.R., Morgan, M.D., and Whitbread-Edwards, A.R. (1966). Geology of the Tauranga area. *Department of Earth Sciences Occasional Report No.22*., University of Waikato, Hamilton. Available at: https://www.nzgs.org/libraries/geology-of-the-tauranga-area-text/

Boulanger, R.W., Idriss, I.M. (2014). Soil liquefaction during earthquakes: CPT and SPT based Liquefaction Triggering Procedures. *University of California Davis*, report no. UCD/CGM 14/01 pg. 138. Available at: https://www.ce.memphis.edu/pezeshk/PDFs/Software/Liquefaction/Boulanger_Idriss_CPT_and_SPT_Liq_triggering_CGM-14-01_20141.pdf

MBIE. (2021). Module 2: Geotechnical investigations for earthquake engineering. *Earthquake Geotechnical Engineering Practice*. Available at: https://www.building.govt.nz/assets/Uploads/building-code-compliance/b-stability/b1-structure/geotechnical-guidelines/module-2-geotech-investigations-earthquake-engineering-version-1.pdf

MBIE. (2021). Module 3: Identification, assessment and mitigation of liquefaction hazards. *Earthquake Geotechnical Engineering Practice*. Available at: https://www.building.govt.nz/assets/Uploads/building-code-compliance/b-stability/b1-structure/geotechnical-guidelines/module-3-liquefaction-hazards-version-1.pdf

Phadnis, H., Lonzetidis, K., Taylor, R. (2023). Liquefaction Resistance of Aged Soils in the Upper North Island of New Zealand and Contribution of the Soil Behaviour Type Index. *Proceedings of the 5th International Conference on Transportation Geotechnics (ICTG) 2024, Volume 2,* Australia: Springer Nature.

Robertson, P.K., Wride, C. (1998). Evaluating Cycling Liquefaction Potential Using the Cone Penetration Test. *Canadian Geotechnical Journal*, 35, 442-459. http://dx.doi.org/10.1139/t98-017

RISK AND RELIABILITY ASSESSMENT IN GEOTECHNICAL ENGINEERING

Soumya Sonali

Geotechnical Engineer

Ground and Underground Engineering, Aurecon Australasia Pty Ltd, 25 King Street Bowen Hills 4006, Queensland
Telephone 0452412322, Email: soumya.sonali@aurecongroup.com

ABSTRACT

In geotechnical engineering practice, risk assessments play a crucial role in accounting for uncertainty and facilitating informed decision-making. Traditionally, the method of assessment is very basic, and many important factors are often overlooked in the early design stages leading to time and/or cost overruns during construction.

This technical paper presents an exploration on the importance of geotechnical risk assessments in the early concept design stages of a project and is organised in two parts. The first part compares two distinct methods of risk assessment, namely GIS-supported analysis vs non-GIS analysis. In this part, the details from selected case histories are used to demonstrate the merits and limitations of each method. The second part spotlights a key element of risk assessment which is the reliability assessment of existing geotechnical data and information. A reliability assessment framework is proposed and discussed in relation to factors such as age of information, geological context, horizontal spatial relevance, and relevance of geotechnical design parameters. It compares the materiality of the different factors and discusses the relevance of several other factors including the objectivity and uniformity in applying the framework.

The value of the framework and methodology is demonstrated through a highway upgrade project in Queensland, Australia, involving multiple interchanges and bridges. In conclusion, this paper affirms the essential role of geotechnical risk assessment, particularly in systematically quantifying ground uncertainty and its consequences to improve project outcomes.

1 INTRODUCTION

Variable ground conditions that are not considered in the initial stages of a project can pose significant risks to project performance, leading to cost and/or time overruns. The current industry standard employs a basic risk assessment process that varies in parameters across applicable standards. However, relying solely on measures like a thorough site investigation or a conservative design can substantially increase costs if the risks are not accurately quantified. Hence, it is essential to enhance understanding thus quantifying the geotechnical uncertainty in infrastructure projects of all scales. By doing so, engineers and contractors can make informed decisions regarding risk mitigation strategies, optimize the project's design and construction processes, thus minimizing the potential for unforeseen complications and associated cost and time overruns. This necessitates an effective geotechnical risk assessment approach that goes beyond the rudimentary methods to account for the varied complexities and uncertainties encountered in the subsurface.

2 METHODS OF RISK ASSESSMENT

2.1 GIS SUPPORTED ANALYSIS VS NON-GIS SUPPORTED ANALYSIS

GIS-supported geotechnical risk assessment refers to the use of Geographic Information System (GIS) technology, which integrates various spatial data layers, to evaluate and manage risks associated with geological and geotechnical conditions. It involves the analysis of geotechnical data in a spatial context, visualizing it on maps, and identifying potential areas of risk or hazards. GIS enables professionals to integrate data like geological maps, soil properties, slope stability information, and more, to analyse patterns and relationships, create risk maps and criteria, and make informed decisions regarding geotechnical risks. In comparison, non-GIS-supported geotechnical risk assessment typically involves using traditional methods and techniques to evaluate and manage geotechnical risks. **Table 1** highlights the stages of these risk assessments and frameworks and presents a comparison between the two approaches.

Table 1: A comparison of GIS vs non-GIS based analysis approach in geotechnical risk assessment

Stage	GIS-supported Geotechnical Risk Assessment	Non-GIS-Supported Geotechnical Risk Assessment
Data Acquisition	Gather relevant geotechnical and spatial data, including geological maps, soil and rock properties, topographic data, hydrological information, site investigation reports. Collect data through field surveys, laboratory testing, remote sensing techniques, and other sources.	

Data Integration	Integrate acquired data into a GIS platform for organization, management, and spatial analysis. Visualize various data layers and their spatial relationships for a comprehensive view of the project site.	Analyse collected data using conventional geotechnical engineering techniques. Interpret soil test results, analyse geological formations, and examine historical data.
Geospatial Analysis	Utilize GIS tools for geospatial analysis, modelling geotechnical problems such as slope stability, groundwater flow, soil bearing capacity. Apply GIS- based tools and algorithms to identify patterns, trends, and potential risks.	Apply geotechnical engineering techniques to analyse data and determine geotechnical parameters such as slope stability, groundwater flow, and soil bearing capacity.
Risk Mapping	Generate risk maps through geospatial analysis, visualizing areas of potential geotechnical risks (unstable slopes, landslides, groundwater vulnerability, soil liquefaction). Prioritize resource allocation and plan risk mitigation measures based on identified risks.	Identify and assess potential risks based on collected data. Create maps or reports to highlight areas of concern, such as unstable slopes, landslides, foundation settlement, or hazardous geological features.
Uncertainty Assessment	Evaluate and quantify uncertainties associated with geotechnical parameters. Assess variability in soil properties, reliability of data sources, limitations of modelling techniques. Understand reliability and confidence levels of risk assessments for informed decision-making.	Consider uncertainties but may lack systematic quantification. Assess variability in soil properties, reliability of data sources, limitations of modelling techniques qualitatively.
Risk Communication	Create visually compelling risk maps and presentations using GIS technology, facilitating clear communication of complex geotechnical data and risks to stakeholders, aiding decision-making.	Communicate risks through traditional reports, maps, or presentations. Explain complex geotechnical data and risks to stakeholders using traditional methods.
Mitigation Planning	Analyse and evaluate different risk mitigation measures by overlaying risk maps with spatial information (land-use zoning, infrastructure plans). Identify strategies to minimize or mitigate risks (construction design adjustments, slope stabilization, drainage systems).	Develop strategies and measures to mitigate identified risks. Design appropriate stabilization measures for slopes, modify foundation designs, suggest construction methods to minimize risks.
Monitoring and Updating	Continuously monitor and update risk assessments using real-time monitoring data. Validate and refine risk assessments, assess effectiveness of mitigation measures, adjust strategies as needed.	Conduct ongoing risk monitoring to ensure effectiveness of implemented mitigation measures. Identify any changes or new risks that may arise during construction or operation.

3 ELEMENTS OF RISK ASSESSMENT – RELIABILITY ASSESSMENT

One of the critical parts of a risk assessment that is often overlooked is a geotechnical reliability assessment (GRA) of existing ground information. Geotechnics is not an exact science and predictions of foundation behaviour cannot be made with certainty due to spatial variation of soil and load properties (Lacasse et. al., 1998). Generally, reliability analyses are applied in the design to operational stages of a project to evaluate and quantify the safety and performance of soil and rock-based structures under various conditions of uncertainty.

As a result, GRA can sometimes be underemphasised in the early scoping stages of a project which can cause significant design and cost issues downstream with the progression of the project. This can stem from several factors such as limited initial budgets, focus on other time-critical aspects, or a lack of awareness about the importance of a GRA. Annual publications analysing the root causes of legal claims in the engineering domain indicated "unforeseen ground and geophysical conditions" as the case of two-thirds of a subset of disputes involving geotechnical expertise, surpassing any other source, including installation failure, incomplete design, contract management and/or administration failure and scope changes (Thompson, 2023).

Implementing robust GRA early enhances site selection, design decisions, and risk mitigation. This involves analysing historical data to establish a comprehensive baseline and identify gaps.

Historical data, including reports and logs, offers valuable insights, hence proper assessment is vital. Systematic evaluation helps understand geotechnical conditions, focus investigations, and mitigate risks, optimising design and construction strategies.

As an example of the GIS supported geotechnical risk assessment, this paper discusses a major highway project in Queensland involving multiple new interchanges and bridges ("*Project X*"). This project implemented a web GIS portal to quantify a geotechnical risk assessment to produce a thorough evaluation. A singular site plan was developed that superimposed desk study information such as concept design, historical data, geological and environmental maps and a 3D ground model as data layers into a singular viewable format.

Project X utilized a WebApp to empower users in mapping geohazards and geotechnical risks in the form of polygons. By adhering to a predefined data schema, users were guided through the process of providing relevant risk information. This information encompassed factors such as the likelihood, consequences, potential mitigation strategies, and necessary ground data. The systematic nature of this approach ensured that users undertook a coherent geotechnical risk analysis.

Upon detailing the risk information, the polygons were automatically assigned a unique Risk identifier (ID) for ease of reference. The WebApp provided a seamless experience for the team by facilitating the visualization of ground risks associated with the designs. Key risk information was readily accessible with just a simple click of a button.

In essence, the implementation of these capabilities and novel methods within Project X offered several advantages. It led to cost savings during the desk study and scoping processes and produced a streamlined, detailed risk register applicable from the concept to post-construction stages of the project. Additionally, the team was able to deliver vivid and informative presentations to the client, instilling a deeper appreciation for the geotechnical risk aspects of the project. (**Figure 1**).

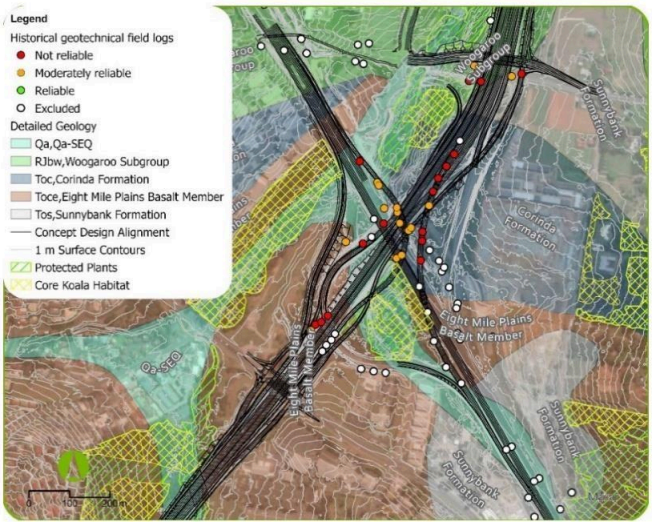

Figure 1: Geological and geotechnical layers superimposed and illustrated for concept design alignment of Project X

3.1 RELIABILITY ASSESSMENT FRAMEWORK AND CRITERIA

In Project X, the client provided historic site investigation reports, which included 1,785 geotechnical PDF logs, to aid in scoping the investigation. These reports were created by various organizations over the past 50 years, resulting in varying spatial information quality. An effort to identify the location of each log was undertaken. The process is illustrated in **Figure 2.**

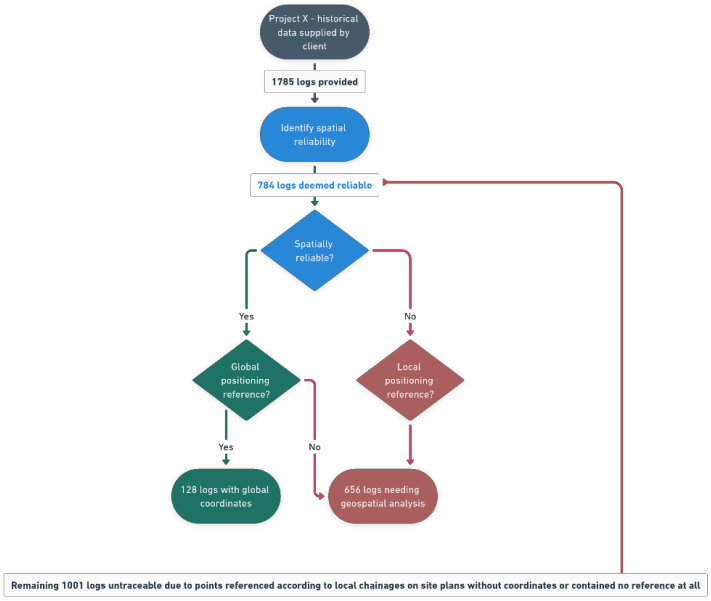

Figure 2: Geological and geotechnical layers superimposed and illustrated for concept design alignment of Project X

Using the 784 spatially reliable logs, a semi-automated reliability assessment of the historical geotechnical data was carried out within the WebGIS. The authors developed an automated capability using a scripted geoprocessing approachto the WebGIS data. GIS tools and Python codes (including Esri Arcpy libraries) were employed to conduct a spatial- based appraisal of each log's data relative to geological maps and geohazards, which were mapped in the WebGIS as polygons. A reliability assessment framework was created by geotechnical engineers and scripted by GIS specialists, allowing computing power to rapidly execute the assessment.

The framework for the automated part of the evaluation included factors, each with predefined criteria:

- **Age of Information**: More recent data, which is likely more representative of in situ conditions and based on refined equipment, was given higher scores, whereas older data received lower scores.
- **Geological Context**: Data from simpler or more homogenous surface geology scored higher, while data from more complex geological areas scored lower.
- **Horizontal Spatial Relevance**: Data closer to geohazards was deemed more reliable and scored higher, whereas data further away scored lower.

For the non-automated assessment, geotechnical engineers evaluated each historic log and its report content in relation to the current designs to determine the Geotechnical Parameter Reliability factor—specifically, the relevance of the depth of ground explored and the geotechnical parameters provided. More relevant data received higher scores. A materiality assessment was conducted to assign weightings to each factor:

- **Geotechnical Parameter Reliability**: Considered the most critical factor governing reliability, as parameters may be reused if relevant, or may indicate estimated values even if moderately relevant - assigned 50% relevancy.
- **Horizontal Spatial Relevance**: Deemed the second most critical factor, as spatial variability of data increases with distance from the design—assigned 30% materiality.
- **Geological Context**: Considered a secondary factor indicating the degree of spatial variability in the area—assigned 10% materiality.
- **Age of Information**: Also considered a secondary factor indicating the quality of the data—assigned 10% materiality.

An in-depth description of the applied framework is presented in **Table 2.**

Table 2: An example of a geotechnical reliability assessment framework applied in Project X

Factors	**Rating**									
	1	**2**	**3**	**4**	**5**	**6**	**7**	**8**	**9**	**10**
General										
Age	Before 1980	1980	1985	1990	1995	2000	2005	2010	2015	After 2020
Geologic context (within 10m)	5 Geologies +	5 Geologies	4 Geologies +	4 Geologies	3 Geologies +	3 Geologies	2 Geologies +	2 Geologies	1 geology +	1 geology
Concept Design										
Spatial (horizontal)	Outside Risk Polygon.50m away from the polygon perimeter	Outside Risk Polygon . 40m away from the polygon perimeter	Outside Risk Polygon . 35m away from the polygon perimeter	Outside Risk Polygon. 30m away from the polygon perimeter	Outside Risk Polygon . 25m away from the polygon perimeter	Outside Risk Polygon . 20m away from the polygon perimeter	Outside Risk Polygon. 15m away from the polygon perimeter	Outside Risk Polygon . 10m away from the polygon perimeter	Outside Risk Polygon . 5m away from the polygon perimeter	Within Risk Polygon
Geotechnical design parameters	No data relevant to the concept design risks	Limited data remotely relevant to the concept design risks	Limited data slightly relevant to the concept design risks	Indirect data moderately relevant to the concept design risks	Indirect data relevant to the concept design risks	Indirect data relevant to the concept design risks	Direct data moderately relevant to the concept design risks	Direct data relevant to the concept design risks	Sufficient data for the reference design	Complete data for the reference design

Notes:
Weighting: Age – 10%. Geologic Context – 10%. Spatial (horizontal) – 30%. Geotechnical data (parameter relevance) – 50%.
+ indicates the presence of an additional nearby but not intersecting lithology.

Reliability Categories

Reliable	Moderately Reliable	Not Reliable
>80	80-50	<50

3.2 OBJECTIVITY OF PARAMETER SELECTION

Geotechnical reliability assessments, particularly those involving non-automated evaluations by engineers, can be subject to a range of subjective influences. Ensuring objectivity in parameter selection is pivotal for maintaining the integrity and accuracy of the assessment process. **Table 3** highlights key factors that can lead to subjectivity in the process described and contribute to variability in the results.

Table 3: Key factors contributing to subjectivity in parameter selection

Key Factor	Description
Human Judgement	Engineers' judgements and interpretations can vary due to individual experiences and biases. Standardised guidelines and protocols can help mitigate discrepancies by providing a structured approach to parameter selection.
Experience and Expertise	Variations in experience and expertise among engineers can affect assessment consistency. Mentorship programmes and peer reviews can provide checks and balances, leveraging collective expertise to improve decision-making.
Data Availability and Quality	The quality and completeness of available data can significantly influence assessments. Proper documentation and transparent reporting of data sources, assumptions, and decision rationales can enhance reliability and reproducibility.
Geological Complexity	Assessing data from geologically complex areas involves interpreting various variables. Collaborative evaluations and the use of advanced analytical tools can improve understanding and reduce subjective influences.
Technological Proficiency	Engineers' proficiency with GIS tools and other analytical software affects assessment outcomes. Regular training and updates on technological advancements can ensure consistent and effective use of these tools.
Stakeholder Influence	External pressures from stakeholders can inadvertently impact judgement. Maintaining professional independence and adhering to stringent ethical standards are crucial for unbiased assessments.

These factors are also illustrated in **Figure 3**, which illustrates their relative impacts on the subjectivity of non-automated geotechnical scoring in reliability assessments.

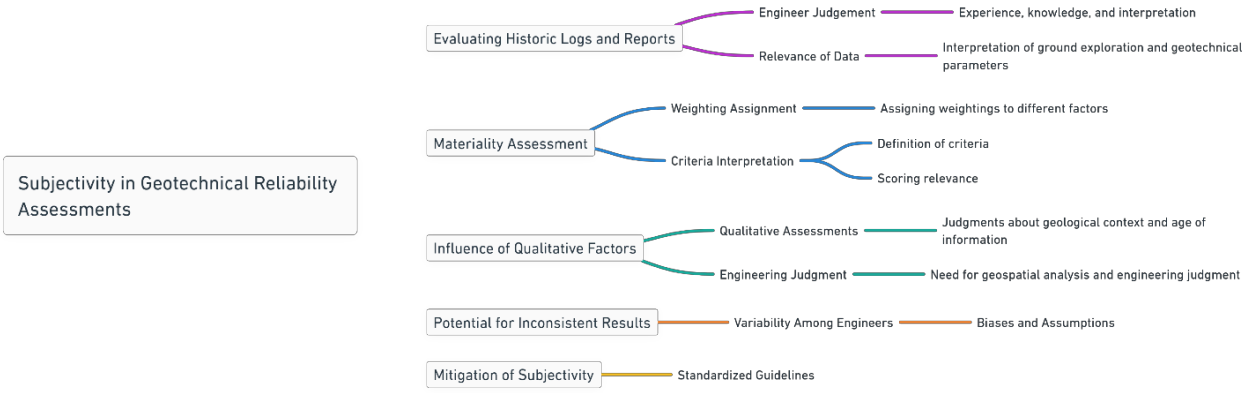

Figure 3: Factors affecting the subjectivity of the non-automated geotechnical scoring in reliability assessments

To mitigate the subjectivity inherent in non-automated processes, several strategies can be adopted:

- **Standardised Guidelines**: Developing and adhering to standardised guidelines for parameter selection ensures consistency across assessments.
- **Peer Reviews**: Implementing peer review mechanisms allows for collaborative evaluation, leveraging diverse perspectives to identify potential biases and gaps.
- **Thorough Documentation**: Detailed documentation of methodologies, assumptions, and decision rationales enhances transparency and allows for reproducibility and validation of assessments.
- **Continual Training**: Regular training programmes on the latest assessment techniques and technologies ensure that engineers stay updated and proficient in their practices.

In summary, while geotechnical reliability assessments inherently involve elements of subjectivity, particularly in non-

automated processes, structured methodologies and collaborative approaches can help manage and reduce the impact of this subjectivity.

4 OPPORTUNITIES

There are numerous opportunities for further research and development in risk and reliability assessment methodologies, especially in the early stages of the geotechnical subset of a project. A general outline of potential areas for advancement is detailed in **Table 4**.

Table 4: Examples for future opportunities in risk and reliability assessment

Section	Focus Area	Description
Advanced Data Integration	Remote Sensing Data	Incorporating high-resolution satellite imagery, LiDAR data, and UAV surveys to enhance spatial data quality.
	Historical Data Digitisation	Digitising and integrating historic geotechnical data to build extensive databases that inform future assessments.
Machine Learning and AI	Pattern Recognition	Identifying complex patterns and relationships in data that may not be evident through traditional analysis.
	Predictive Modelling	Developing predictive models to foresee geotechnical issues and optimise risk mitigation strategies.
Enhanced GIS Capabilities	Real-Time Data Integration	Integrating real-time monitoring data into GIS platforms to facilitate dynamic risk assessments and timely decision-making.
	3D and 4D Modelling	Expanding from 2D to 3D and even 4D (time-based) models to provide a comprehensive understanding of subsurface conditions over time.
Improved Risk Communication Tools	Interactive Visualisation	Utilising interactive GIS dashboards and virtual reality environments to provide stakeholders with an immersive understanding of geotechnical risks.

4 CONCLUSION

Effective risk and reliability assessments are crucial in geotechnical engineering to mitigate uncertainties and improve project outcomes. This paper highlights the advantages of GIS-supported methods over non-GIS-supported ones, showcasing their ability to provide comprehensive, accurate, and visually intuitive analyses for better decision-making and communication.

The Geotechnical Reliability Assessment (GRA) framework proposed here combines automated and non-automated methods to offer a robust understanding of spatial variability, historical data relevance, and parameter reliability. This integrated approach reduces subjectivity and enhances risk assessment precision. While non-automated evaluations can be subjective, strategies such as standardized guidelines, peer reviews, and thorough documentation help mitigate biases and ensure consistent, reliable assessments. Adopting advanced geotechnical risk assessment methodologies, especially those supported by GIS, is essential for minimizing unforeseen issues and achieving cost-effective, timely project completion. The discussed framework and strategies provide a blueprint for improving geotechnical evaluations, leading to more resilient infrastructure. Future work should refine these methods and explore new technologies to enhance geotechnical risk management.

5 REFERENCES

Bridges, C., 2019. Geotechnical risk: It's not only the ground. *Australian Geomechanics,* 54(1). A

Hoek, E. & Palmeiri, A., 1998. *Geotechnical risks on large civil engineering projects.* Vancouver, International Association of Engineering Geologists Congress.

Honzo, Y., Suzuki, M., Hara, T. & Zhang, F., 2009. *Geotechnical Risk and Safety.* 1 ed. s.l.:Taylor & Francis Group.

Lacasse, S. & Nadim, F., 1998. *Risk and Reliability in Geotechnical Engineering.* s.l., International Conference on Case Histories in Geotechnical Engineering.

Thompson, B., 2023. The Benefits of Early Geotech Risk Mitigation. *HKA Global*, 25 October, p. 6

NAVIGATING TEMPORARY WORKS COMPLEXITIES FOR THE BOTHAMLEY PARK TRUNK SEWER UPGRADE

Andrew Hills
Brian Perry Civil Ltd.
andrewhi@fcc.co.nz *+64 27 458 5154*

ABSTRACT

This paper describes the design, construction and monitoring of a temporary bored pile retaining system for the Bothamley Park trunk sewer upgrade in Porirua, New Zealand. The original construction methodology for installation of the sewer at Cannons Creek was to form a 15m high cut slope batter to enable access for a directional drilling rig. Deeper than expected rockhead and excessive seepage from the cut face resulted in earthworks being stopped with a 5m cut remaining to final excavation level and an alternative retaining approach adopted.

The site sits at the interface of an infilled gully feature associated with development of the area in the 1950's and 1960's, resulting in geological complexities including a perched groundwater regime and a variable rockhead depth across the excavation footprint. Other constraints including a sensitive sewer line and temporary mud pond located at the top of the batter restricted traditional methods such as sheet piling or benching the batter.

A bored pile wall and an observational monitoring system including piezometers was adopted and implemented on site successfully during construction using alert and alarm level thresholds, traditional survey, and regular visual observation. This paper highlights not only the technical aspects of the design and construction process but also the importance of adaptive monitoring and intervention strategies in addressing unforeseen challenges during infrastructure projects.

1 INTRODUCTION

The Bothamley Park trunk sewer upgrade is part of a wider scope of works being delivered by the Te Aranga Alliance [TAA] to deliver new housing in eastern Porirua in the Wellington region of New Zealand. The Park is a recreational reserve that follows the Kenepuru Stream through the rugged terrain of eastern Porirua out to the harbour, and so the new sewer is being laid using traditional open cut methods where the terrain permits and through a series of horizontal directional drilling [HDD] tunnelling shots penetrating the bedrock in hilly sections. The rig drills into the rockface directly and as a result, in some areas temporary cut and fill and other retention works are required to remove soil cover and provide access for the rig at the specific elevation of the sewer alignment.

In late June 2023, problems were identified with an earthworks cut being completed to facilitate access for the HDD rig at the 'HDD2' drill shot site location. An approximately ~10m high cut had been made at 1V:1.5H, with a further ~5m near vertical cut into assumed rock required to reach the design level. The face was showing signs of excessive groundwater seepage through the face, concentrated near two thin layers (see right side of Figure 1), and bedrock had not yet been encountered at the expected elevation. As a result, a stop works order was issued on site and a series of meetings set up with the Fletcher Construction site team and project manager, Brian Perry Civil temporary works engineers and TAA permanent works designers to identify a suitable alternative strategy for the works and any further investigations.

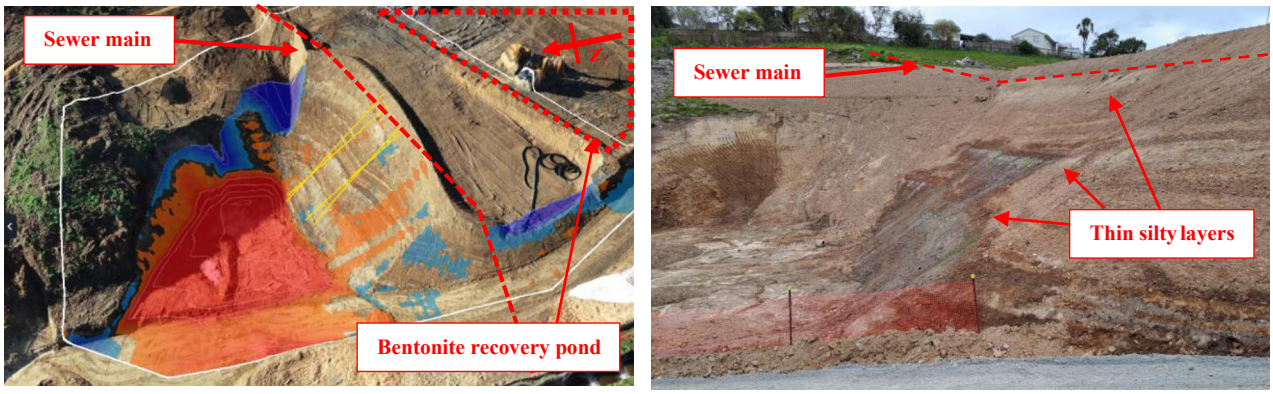

Figure 1: Overview of 1m indicative cut / fill filled contours (red / blue respectively) to achieve design surface levels (left); Photograph of the ~10m high cut slope taken from the haul road facing east (right)

A series of preliminary stability analyses by the Alliance identified that cut slope remedial options were unlikely to be feasible, as these would require either (a) re-aligning and then re-installing a concrete sewer main at the crest of the slope at unacceptable cost and delay to the project; or (b) shifting the HDD rig alignment at the base of the slope, which was not possible. The site is shown in Figure 1, with red contours indicating approximately 5m of near vertical cut remaining at the base of the batter to achieve the design level.

The preliminary remedial design solution selected in agreement with the wider team was to introduce a contiguous bored pile retaining structure offset approximately 1.5m from the base of the slope to facilitate the remaining 5m of vertical cut. The existing slope would first be monitored during the design period to establish realistic existing groundwater levels and stability prior to the piling works commencing, with strict alert and alarm level controls to be agreed based on the analysis, and further measures to encourage further drainage and drawdown in the upper slope implemented if required.

2 GROUND AND GROUNDWATER CONDITIONS

2.1 DESKTOP STUDY & WALKOVER OBSERVATIONS

A review of the historic aerial photography for the site is summarised below. The key change of note occurred in a period of development in the Porirua area in the late 1950's to early 1960's, where material from the peaks of the local hills were cut to form level building platforms and used as fill in the adjoining natural gullies. The former stream was re-aligned into an open channel alongside the current playing fields and a stepped concrete 'cascade' over the steeper end section.

The findings from the aerial imagery review are further supported by a comparison between 2015 LiDAR data and (c.1960) pre-development contours for the area, which show indicative cut and fill depths. This information was used to develop a ground model and coupled with other investigations nearby indicating the depth of alluvium below the stream, gave an estimate for the likely rockhead elevation profile across the toe of the batter.

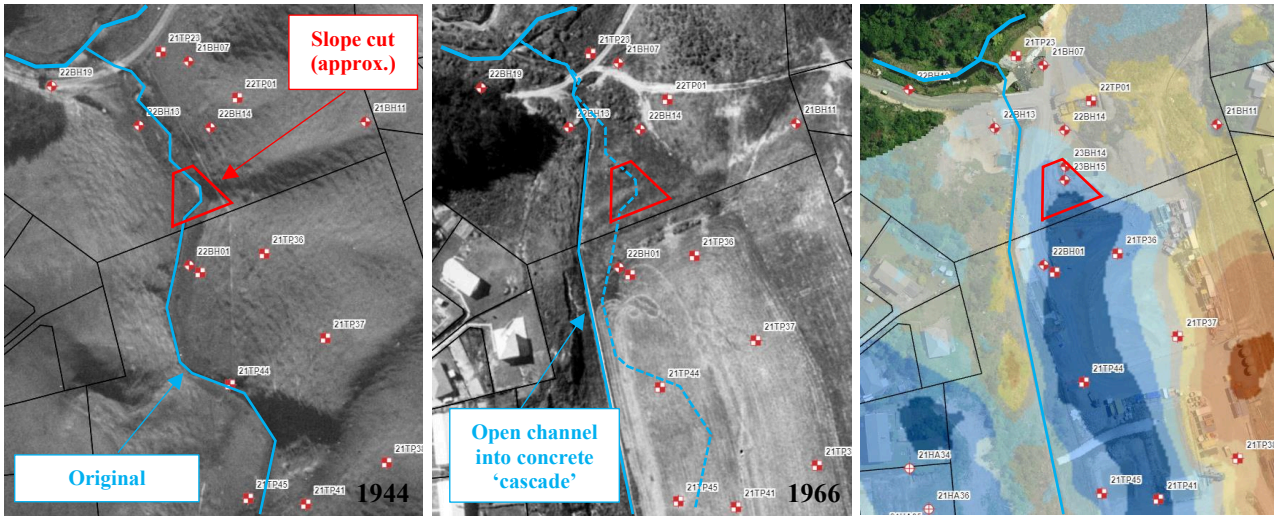

Figure 2: Historic aerial images showing stream re-alignment and gully fill (source: RetroLens); Cut/fill heat map comparison between (c.1960) pre-development contour plans and 2015 LiDAR (right).

The site was surveyed using traditional techniques by taking spot heights at key locations on the slope face, predominantly to identify elevations of the two the clear 'bands' of silt where the seepage was occurring (TAA 2023), and secondly using drone LiDAR. The cloud-based Propeller Aero platform was used to rapidly interrogate the slope geometry and to compare actual vs. design surfaces, as shown in Figure 1.

2.2 INTRUSIVE INVESTIGATIONS

A series of factual geotechnical reports were completed by TAA in 2021 and 2022, and testing generally comprised a series of boreholes and test pits in the area with bulk samples for laboratory testing. The investigations available are shown in Figure 2. Of note are 22TP01 and 22BH14 which were in key locations for the slope design but were unable to be drilled at the time due to access being restricted by soft ground and vegetation.

Particle size distribution (PSD) testing on five bulk samples collected from the borehole and test pit investigations conducted in the playing fields area above the slope site are summarised in Figure 3. The results show a clear distinction between the natural and fill soils that aligned with the known site history and simplified site model. The natural soils were

dominated by fines, being predominantly silts with fractions of clay and fine sand. Comparatively testing showed the fill to comprise well graded soil with similar fractions of gravel, sand, and fines. The 'fill' matched the description of the soils visible over the majority of the slope face, and the low-permeability layers were inferred to be similar to those shown as 'natural' soils. This distinction allowed the perched groundwater scheme to be better understood and indicative permeability ranges to be estimated from the soil fractions (e.g. see Prugh Method, Cashman & Preene (2001)).

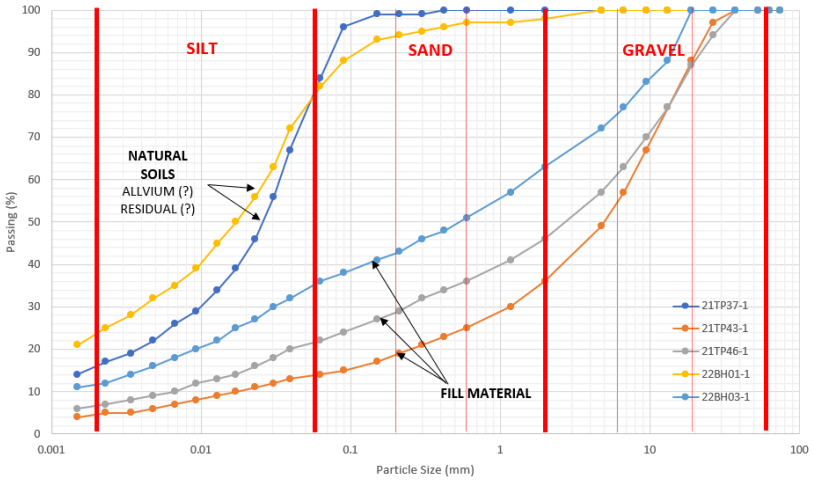

Figure 3: Particle size distributions of soils in Cannons Creek Park used to estimate permeability ranges.

A key consideration for design and options evaluation was establishing a realistic profile for the basement rockhead. A series of additional simple investigations were not limited by drill rig availability were conducted. These included:

- Test pits up to approximately 2m cut at the base of the slope batter, however, were terminated quickly due to rapid groundwater inflow. Two no. dynamic cone penetrometer (DCP) or "scala" did not locate rockhead. No logs were available, photographs only were provided to BPC.
- A steepened cut approximately 55 degrees was dug at the top of the slope to identify soil-rock interface and approximate dip angle on the rockhead, near the eastern end of the slope near the former gully edge.
- Driving a series of 6m length sheet piles to infer rock level across the pile alignment.

2.3 GROUND MODEL

Based on the information described in the previous section the conceptual ground and groundwater model adopted for design is summarised in Figure 4 and Figure 5. Groundwater levels were clearly 'perched' on two low-permeability silty layers within the fill, with recharge likely occurring from the open-channel section of the re-aligned historic stream.

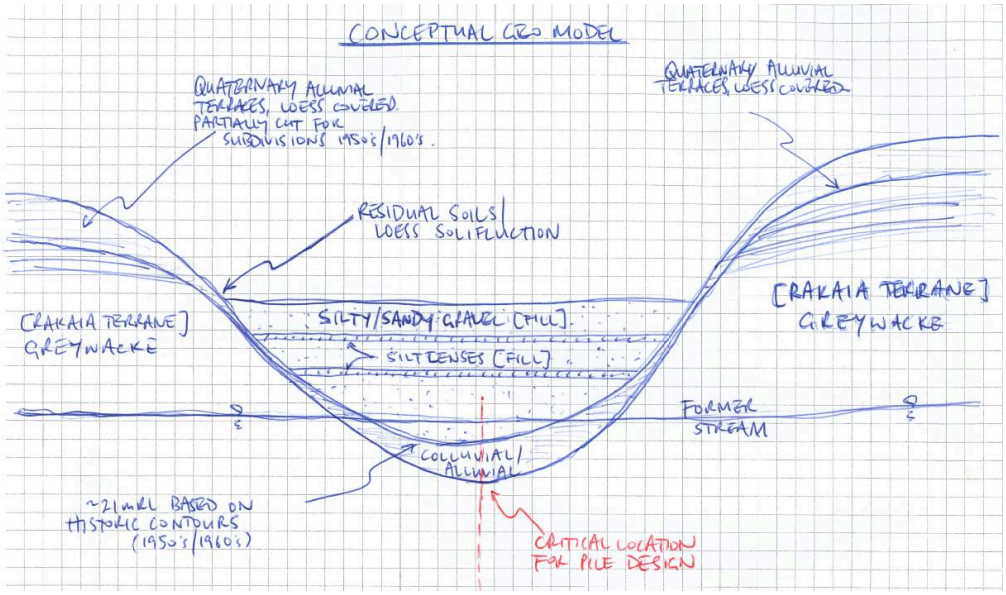

Figure 4. Interpreted ground model for design

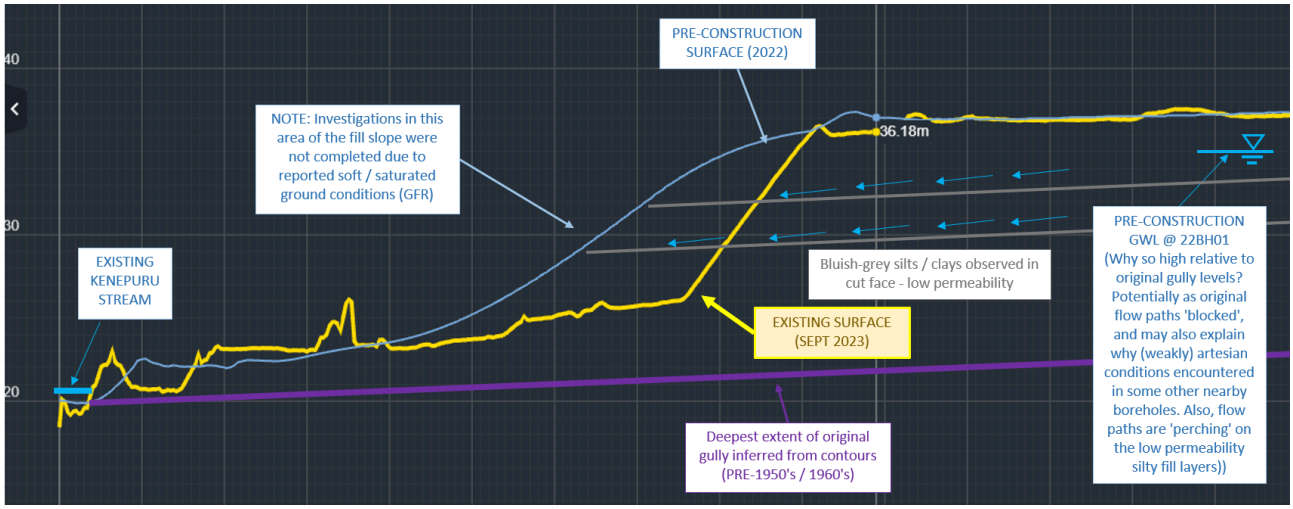

Figure 5. Interpreted geometry and ground/groundwater conditions before and after the earthworks cut

3 TEMPORARY WORKS DESIGN

3.1 DESIGN PHILOSOPHY

Preliminary slope stability modelling by the TAA engineering team (TAA, 2023) using a 'global' groundwater level assumption identified that the existing 10m high cut was only stable under static conditions if groundwater levels remained below a critical level. Further, the overall slope would require battering back significantly and additional groundwater lowering measures implemented to reach the final cut surface level. This was unacceptable as it would require temporarily realigning a sewer main at the top of the slope at excessive cost and delay to the project, the estimated impact being in excess of NZD$1M. Also, the proposed sewer to be installed by the HDD operation at the base of the cut could not be realigned due to other constraints of the permanent design, meaning the batter slope could not be pushed out at the base.

The complete optioneering process is not covered here for brevity but was completed through a series of meetings with the TAA permanent works designers, BPC temporary works designers and the construction team. The process identified that a contiguous bored pile retaining system (i.e. piles with small gaps between) constructed at the base of the cut offered the only realistic and economic design solution given the site constraints. The advantages of the piled option were that a contiguous system would not significantly restrict passive slope drainage; BPC's GEAX EK60 19t rig was well-suited to the drilling conditions and readily available having just completed drilling on a nearby project site; a series of 600mm dia. pile cages of sufficient length were available in BPC's Tawa yard leftover from another project, and provided the depth to rock was not excessive, piles could be socketed into the bedrock and anchoring of the wall would not be required.

The stiff contiguous bored pile wall at the base of the cut would enable the remaining 5m of soil to be retained. There was enough space for a small flat bench around 1.5m wide behind the top of the wall to serve as a toe drain and catch-bench for any sloughing of loose debris from the slope above, and modestly reduce the wall loading from the backslope. An important aspect of the hybrid pile and slope solution was that the slope above could fail along a slip surface independent of the wall itself, and therefore had to be analysed separately. Secondly, a groundwater monitoring scheme needed to be established ahead of construction, since the final solution was not "wished into place" – any construction team working at the base of the cut would be exposed to the existing slope hazard. Lastly, a series of contingency options were considered to lower the groundwater level further if monitoring showed these were being exceeded frequently.

3.2 SLOPE STABILITY AND PILE MODELLING

The existing and proposed slope / pile system were analysed using a finite element model with soil-strength reduction and steady-state groundwater flow in Bentley PLAXIS 2D (see Figure 6). The slope was showing signs of slow but steady drainage since it had been originally cut, and this was expected to continue once the final cut level was reached. Modest improvement in the factors of safety (approximately 10%) were obtained when a perched groundwater hypothesis was tested and back-analysed against the results from the observations at the face of the slope and the water level observed in the standpipe piezometer, compared to a global groundwater level. A second back-analysis was completed against a 55 degree dry test cutting to ensure the adopted strength parameters were robust. The modelling identified that the slope was stable with a factor of safety of approximately 1.3 achieved under normal conditions, and 1.2 with an elevated groundwater condition. The groundwater level for the latter would later serve as an 'alert' level for the ongoing monitoring through construction.

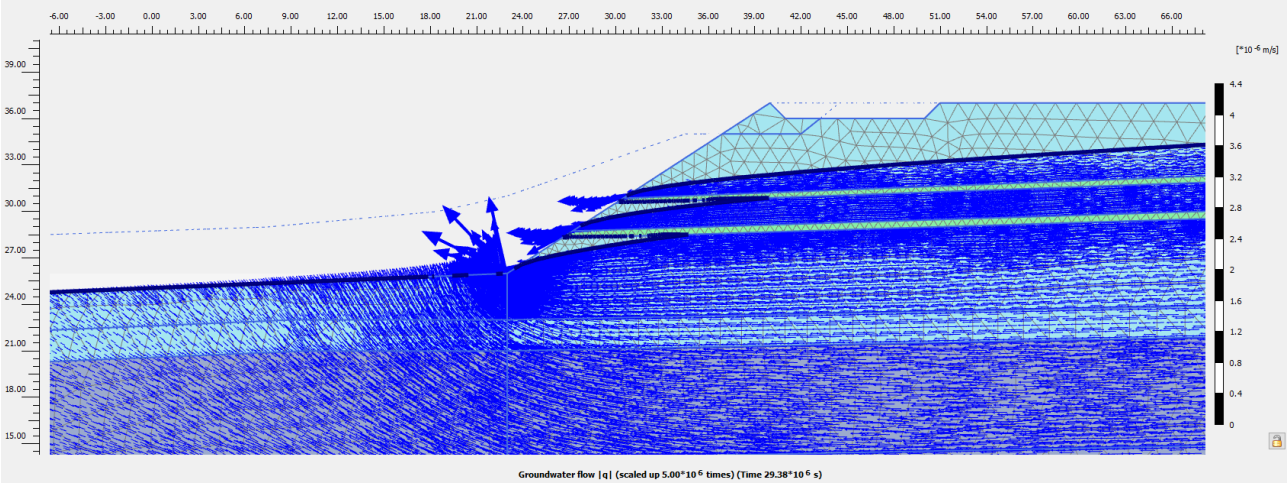

Figure 6: Modelling of perched water conditions in PLAXIS

4 RISKS, CONTINGENCY AND GROUNDWATER MONITORING SCHEME

4.1 GROUNDWATER MONITORING

The critical element for ensuring stability of the slope and wall system was to manage groundwater levels against the design model. Several low-cost dewatering options using both passive and active drainage measures were considered for the detailed design stage, should the monitoring system identify conditions materially worse than those assumed in the preliminary analysis (optioneering) phase. It became clear through interrogation of nearby investigation information at the top of the slope, and ongoing visual monitoring at the exposed face, that the fill layers were oriented favourably for passive drainage and less favourably for sub-horizontal drainage systems. Cashman & Preene (2001) warn against passive slope drainage methods where erosion and subsequent instability can occur particularly in non-plastic silts and fine sands, however the site observations and material gradings indicated this was unlikely to occur and could be dealt with using collector drains at the seepage zones if required. The design team agreed that as a backup redundancy measure, additional measures could be taken to facilitate drainage by either passive or active methods, namely:

- Provision of a gravel collector drain along the slope face above each of the silt layers;
- Drilling a series of holes to ‘punch’ through the low permeability layers and act as passive or pumped active vertical drains, or stone columns;
- Digging vertical cut-off or ‘counterfort’ drains into the slope to intercept groundwater pathways and improve stability, which have shown good results in similar soils (see Price & Fitch (2017)).

The need for these additional measures to be incorporated into the design and construction would be assessed by a preliminary period of monitoring as the design progressed.

4.2 BENTONITE MUD POND

One of the key considerations in the stability analysis was a bentonite mud pond that was being dug at the top of the slope to allow the HDD contractor to recycle the drilling mud used to support the tunnelling bores. The pond was identified as a surcharge load set back from the existing slope crest, but also presented a risk of leakage that could affect fluid levels in the slope face, and therefore stability. Pond lining was discussed as a possible risk-reduction measure, but ultimately agreed as not explicitly required given the chemistry of the material (i.e. typically used to form a filter cake and support borehole drilling, and therefore less likely to ‘leak’ into the slope) and secondly the groundwater monitoring adopted.

As part of the works, two standpipe piezometers were drilled to the level of the upper silt lense to verify the site conditions against the analysis model. The groundwater ‘alert’ level monitoring was exceeded once during the works in early February 2024, as shown on Figure 7. Through subsequent discussions with the site team, it became clear that the pond was being used at that time to store extracted ground and surface water in other parts of the site, on top of its intended primary use for bentonite recovery. Photographs showed that the water in the pond was sitting ‘perched’ on top of the bentonite mud due to its lower density. As a result, the water in the pond was acting as a local groundwater recharge source for seepage into the slope. Construction was allowed to continue under increased monitoring frequency and provided water was immediately pumped out to a second pond dug much further away from the slope. After a few days the water levels at the slope monitoring positions started to fall and returned to acceptable levels.

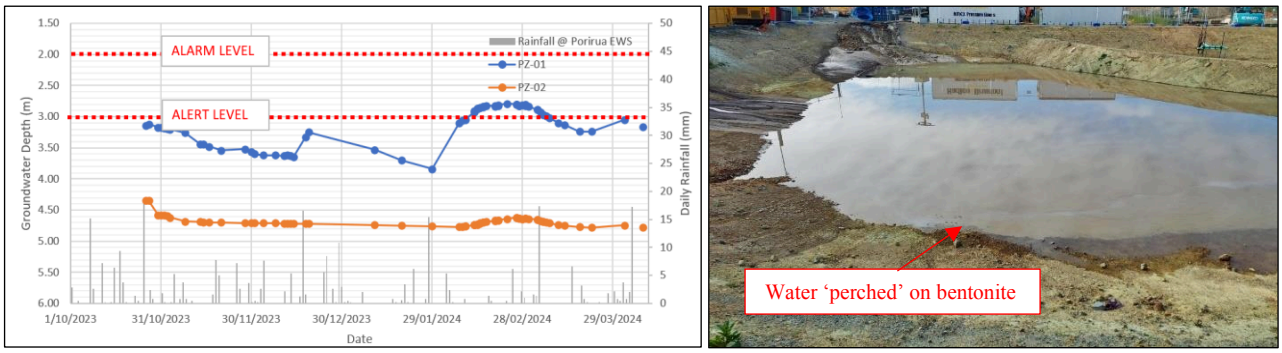

Figure 7. Groundwater 'alert' level was exceeded once at monitoring piezometer PZ-01 as a result of the bentonite pond being used for ground and surface water storage leading to rapid recharge and seepage

5 CONCLUSIONS

The temporary works required for the HDD2 drill shot as part of the Bothamley Park trunk sewer upgrade required navigating several complexities after unforeseen ground conditions were encountered during earthworks. Some of the key project conclusions and learnings are summarised below.

- Temporary works designs that arise from construction issues deviate from traditional design process in that optioneering decisions often need to be made quickly to avoid costly project delays. In this case, the feasibility of the proposed bored pile option relied on establishing a rockhead profile across the alignment to progress to detailed design. This was interpreted using inference from historic contour plans of the area, identifying depth of fill above the gully and former stream, coupled with depth of alluvium in the underlying stream inferred from other investigations nearby, and driving of 6m length sheet piles to refusal to infer rockhead along the alignment.
- Temporary works designs should not rely on "wished into place" solutions. In this case, the piling operation could only proceed safety if designers were confident that the slope above was stable since it required construction teams to work at the base of the slope. Therefore, establishing a groundwater monitoring scheme ahead of the piling was important to ensure the design captured this interim state before the final solution had been constructed.
- Perched water regimes in slopes require alternative analysis approaches to model stability realistically, but also require careful management to ensure face erosion does not occur and result in long-term instability. Assuming a global groundwater table is likely to give overly conservative results.
- Daily (or automated continuous) monitoring provides information that allows designers to better monitor site activities that may not be captured during typical construction monitoring observations without full time supervision. In this case, it became clear quickly that the bentonite pond above the slope was being used to also temporarily store dewatered groundwater which was affecting the slope and resulted in an alert level trigger.

6 ACKNOWLEDGEMENTS

Special thanks to the Fletcher / BPC construction team including Gavin Jones, Charlie Challacombe, Jesse Kirk, Benjamin Eveleigh, Liam Kelly, Greg Cullen, Alastair Dickens, and Beca / TAA design and CPS team Garry Zhang, Christoph Kraus, and Sam Glue.

7 REFERENCES

Begg, J.G. and Johnston, M.R. (2000). *Geology of the Wellington area. Institute of Geological & Nuclear Sciences 1:250,000 geological map 10*. Institute of Geological & Nuclear Sciences, Lower Hutt, New Zealand.

Cashman, P.M. and Preene, M. (2001). *Groundwater lowering in construction – a practical guide to dewatering*, 1st edn, Spon Press, London.

Price, S.L. and Fitch, N.R. (2017). Counterfort drains – design, installation and long-term performance in soils of Greater Auckland. Proc. 20th NZGS Geotechnical Symposium, Napier, New Zealand.

Public Works Department. (1960). *Cadastral Map of the Porirua East Subdivision*. Public Works Department [Housing Division].

Te Aranga Alliance. (2022). *Bothamley Park Trunk Sewer: Geotechnical Factual Report*. Revision 3, dated 11 November 2022. Te Aranga Alliance.

Te Aranga Alliance. (2023). *Bothamley Park HDD2 Cut Slope Stability Assessment*. Revision B, dated 17 August 2023. Te Aranga Alliance.

HIGH-STRAIN DYNAMIC TESTING: AN OPPORTUNITY FOR EFFICIENCY GAINS AND RISK MITIGATION UNDER VARIABLE GROUND CONDITIONS.

Benjamin Fergus
Piletest

ABSTRACT

Risk is ever-present when designing deep foundations for structures and is exacerbated when variable ground conditions are experienced on-site. Throughout a 2400 m^2 Brisbane site, a total of six boreholes, eight Cone Penetration Tests (CPTs) and three test piles (which achieved a practical refusal set) were conducted, which identified expected pile founding depths of between 6.5 m and 27.0 m. The expected pile founding depths were extrapolated between CPT locations using contour plotting software. However, during the installation of the piles, only 42% of piles were pitched at the original design length due to the variability encountered. One third of piles were driven to a practical refusal set (an installation set of less than 2.5 mm per blow) with others achieving an ultimate geotechnical capacity prior.

The as-built pile penetration depths were used to create a second contour plot. This identified a deep trough running diagonally through the site which was not identified in the geotechnical investigation. High-strain dynamic testing using the Pile Driving Analyzer® (PDA) was performed to confirm the bearing capacity even when a refusal set was not achieved. As such, new driving criterion were developed across the site and confidence was given to new pitched pile lengths which relied on the benefits of soil set-up effects rather than solely end bearing capacity. Despite these differences in pile instillation behaviour, this project was completed on-time with an increased testing rate and approximately 200 m more pitched pile length than designed.

INTRODUCTION

Piletest were recently involved in a Brisbane project which encountered a highly variable geotechnical profile across the 2400 m^2 site. The pile design for this industrial structure consisted of 104 No. 275 mm square precast piles which were to be installed with a Banut piling rig operating a 6.0 tonne hydraulic drop hammer. Designed pile lengths varied between 12.1 m to 21.2 m with ultimate geotechnical loads between 429 kN and 877 kN. Site investigation suggested a predominantly clay soil profile with some variability across the site. Most piles were designed to obtain a refusal set (an installation set of less than 2.5 mm per blow), however, upon installation some piles obtained a much larger set. This paper reflects on the differences in pile installation behaviour and the role that high-strain dynamic testing using the Pile Driving Analyzer® (PDA testing) had in risk mitigation and optimisation of the design.

1 SITE INVESTIGATION

Initially, six boreholes and four Cone Penetration Tests (CPTs) were performed at six locations across the 2400 m^2 site. All boreholes were terminated at a depth of 6.0 m and CPTs were terminated at depths between 6.9 m and 15.5 m below surface level. A stiff silty clay was the predominant soil type across all six boreholes with Dynamic Penetrometer Test (DPT) results usually less than 5 blows per 100 mm. CPT results varied, with cone resistances at 7 m depths of approximately 3 MPa, 35 MPa, 8 MPa and 10 MPa. Eurocode 1997-2:2007 (E) *Eurocode 7 - Geotechnical design - Part 2: Ground investigation and testing* (Appendix B) suggests that site investigation should occur in a grid pattern with points at 15 m to 40 m distance for high-rise and industrial structures. As the Brisbane site dimensions were approximately 80 m by 30 m, the Eurocode would suggest six site investigation locations to be appropriate. With consideration given to the pile loads required, the variability of the CPT results and limited deep site investigation, the piling contractor obtained four additional CPTs at new locations around the site. These CPTs were continued until a cone refusal was achieved, at approximate depths of 27.0 m, 28.0 m, 12.0 m and 16.5 m. Australian Standard AS2159-2009 *Piling – Design and installation* (Clause 2.1) states that "… site investigation shall be carried out to provide sufficient information to fulfil the requirements of Clause 2.2 (Information Required)". The piling contractor was able to satisfy this clause with the additional site investigation and relevant experience with similar structures nearby.

For the purposes of comparison, the expected depth of pile refusal was taken where the CPT cone resistance exceeded 20.0 MPa. Six test piles were also installed across the site to further assess the piling conditions. Three of these piles achieved practical refusal; one at 17.8 m and two at 10.7 m below the working platform. Other test piles did not achieve a refusal set and achieved capacity through a combination of shaft and bearing capacity. Using the Surfer plotting software, a contour plot was generated for the expected pile refusal depths (m) across the site. This was done for each stage in the site investigation: initial CPTs (blue circles), additional CPTs (green circles) and test piles (pink squares). The refinement of the expected pile refusal depths can be seen in Figure 1.

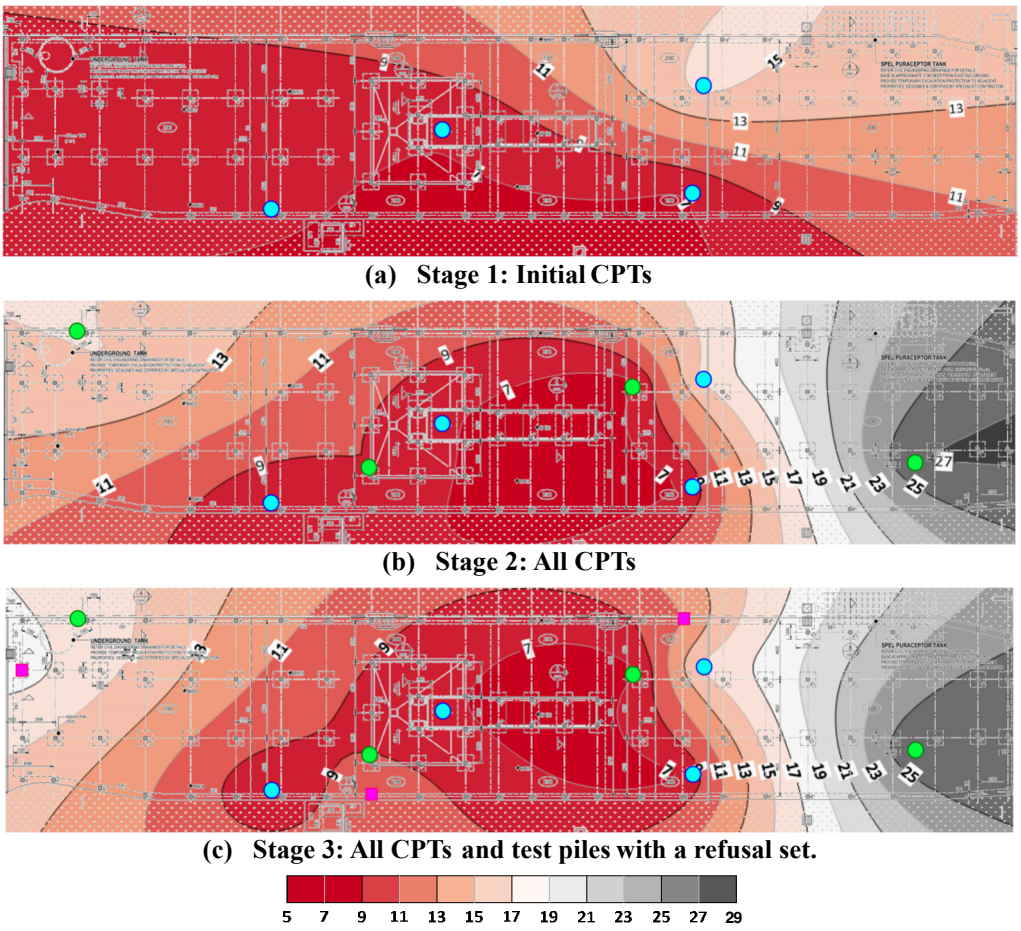

(a) Stage 1: Initial CPTs

(b) Stage 2: All CPTs

(c) Stage 3: All CPTs and test piles with a refusal set.

Figure 1: Expected pile refusal depths [m] based on site investigation.

2 PILE DESIGN AND INSTALLATION

The original design for the industrial structure consisted of 104 No. 275 mm square reinforced concrete precast piles. The original design lengths of these piles were either 15.2 m or 18.2 m and were to be installed using a Banut piling rig operating a six (6.0) tonne hydraulic drop hammer. These lengths were further refined to include 12.1 m, 15.2 m, 18.2 m and 21.2 m piles after the test piles were installed (24 No. piles had not been assigned a new pile length as test piles were not installed in this area at the time of redesign).

Despite the previous site investigations, the pile sets recorded during installation had more variability than what was expected. Of the piles which achieved refusal sets, 15% refused within 1.0 m of the expected depth, 44% refused within 1.0 m to 3.0 m of the expected depth and 41% of piles refused at a depth greater than 3.0 m from the expected depth (Figure 2a). Of the piles installed, 16% were reduced in length from the original design, 41% were increased in length and 42% remained as designed (Figure 2b).

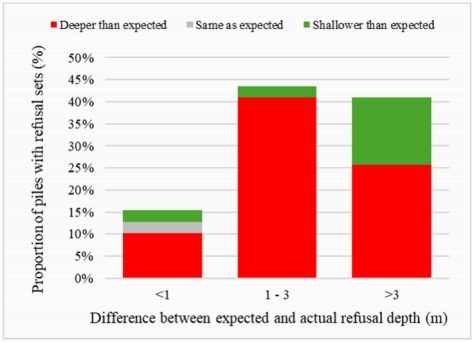

(a) Difference in refusal depths.

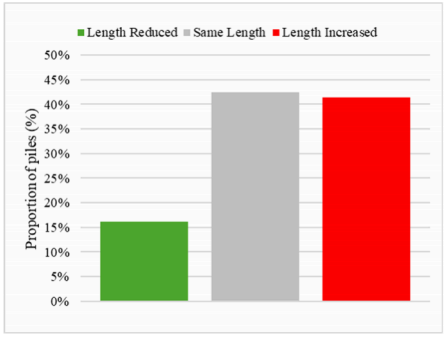

(b) Difference in pitched length.

Figure 2: Differences in pile installation.

The as-build pile penetrations have also been graphed on a contour plot (Figure 3). It should be noted that the as-built pile penetration is only directly comparable to the expected refusal depth for piles that achieved a refusal set (38% of piles). Piles with a refusal set have been highlighted with a black box, while piles with a set greater than 10 mm per blow have been identified with a pink box. Sections without a refusal set (black box) will have a pile refusal depth deeper than the as-built penetration depth. Therefore, for direct comparison with Figure 1, these sections would have a darker grey colour.

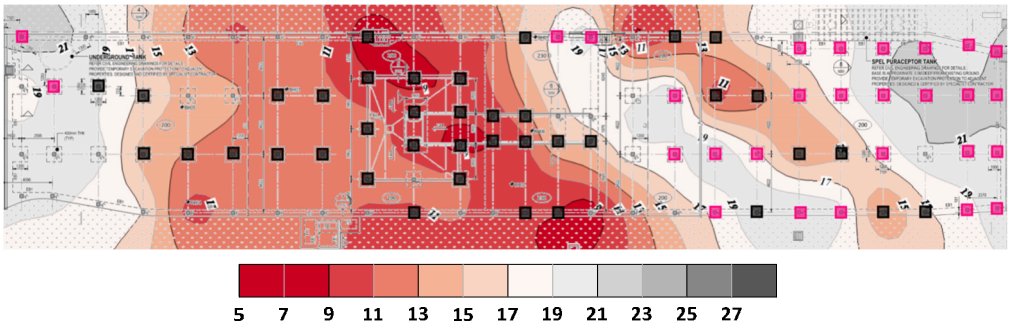

Figure 3: As-built pile penetration depths [m].

There are clear differences between the expected geotechnical profiles (Figure 1) and the as-built pile penetrations (Figure 3). Working from left to right across the site, the differences can be defined as:

1. Deeper than expected pile refusal depth on the left-most section of the site, piles did not achieve a refusal set.
2. As-expected shallow refusal depths through the centre of the site, most piles achieved a refusal set.
3. Unexpected deep trough running diagonally next to the shallow central area, most piles had a set a greater than 10 mm per blow.
4. Unexpected shallow ridge running parallel to the deep trough, all piles achieved a refusal set.
5. As-expected deep section to the right of the site, most piles had an installation set greater than 10 mm per blow.

3 QUALITY ASSURANCE

The as-built foundation design must be sufficient for the structural requirements despite the variable conditions encountered. Pile capacity is achieved through two main components: the end bearing capacity from the toe of the pile and the shaft capacity. Dynamic pile driving formula can be used to estimate pile ultimate capacity in some cases; the Hiley driving formula is commonly recognised. However, Broms in *Precast Piling Practice* (May, 1978) states “Dynamic pile driving formulae should only be used for cohesionless soils and only when the penetration resistance of the pile gradually increases with depth during driving.” These formulae rely on the assumption that the driving resistance is representative of the long-term ultimate bearing capacity of the pile. In cohesive soils, there is the potential for soil set-up to occur, resulting in increased shaft resistance with time. As this site predominantly had a clay profile, the Hiley formula may not be suitable.

Instead, high-strain dynamic testing using the Pile Driving Analyzer® (PDA testing) was conducted. At the time of tendering, a PDA testing program with 5% pile coverage was budgeted. However, due to the variability encountered, an additional 13 piles were tested, increasing the test program coverage to approximately 18%. Piles were tested during four different testing visits with the time between installation and testing varying between piles. Table 1 summarises the driving behaviour and results for the selected test piles.

Table 1: Summary of PDA test results.

Pile ID	Test Day	Days between Install/Re-drive	Installed Length (m)	Pile Penetration (m)	Install Drop Height (mm)	Install Set (mm)	Restrike Drop Height (m)	Restrike Set (mm)	Restrike TC (mm)	PDA Capacity Estimate (RMX) (kN)	$R_{d,ug}$ (kN)
A*	1	2	18.2	17.4	100	42.0	250	38.3	0.0	286	508
B	1	1	18.2	15.6	400	5.5	450	3.3	16.9	1775	458
C	1	1	18.2	17.7	400	8.0	600	4.3	16.6	1599	458
D	1	1	15.2	13.9	400	6.5	500	3.7	16.6	1634	458
E	1	1	15.2	12.9	400	5.5	450	2.0	14.7	1864	458
F	1	1	12.1	11.4	400	8.0	500	3.3	14.7	2003	458
G	2	3	12.1	7.7	400	2.0	500	2.7	11.8	2219	429
H	4	6	12.1	11.4	400	1.7	250	0.0	5.4	1334	436
I	2	4	18.2	17.2	400	16.0	450	8.7	8.3	1163	429
J	3	3	12.1	10.0	400	2.2	450	1.3	14.1	2109	877
K	3	0	15.2	14.7	400	24.0	430	12.7	9.8	1123	877
L	2	4	12.1	10.1	400	5.0	500	2.7	13.4	2201	429
M	2	4	12.1	7.5	400	5.5	400	3.0	16.1	1797	429
N	2	3	21.2	20.8	400	16.0	400	4.0	10.7	1746	429
O	1	1	21.2	12.2	500	3.0	500	2.0	13.2	1880	458
P	2	4	18.2	17.9	400	10.0	500	4.0	13.0	1496	468
Q	4	1	18.2	17.4	400	13.0	400	5.0	6.7	1965	810
R	2	5	18.2	15.6	400	6.0	400	3.3	13.6	2037	429
S	3	6	21.2	20.0	400	15.0	500	7.0	8.8	1642	429

*Note – Pile A was replaced due to having insufficient capacity.

The PDA capacity estimate (RMX) is dependent on an appropriate selection of the case damping factor (J_c). J_c is selected based on the expected soil profile and test type; for this site a J_c value of 0.75 was selected. Piles C, H, I, L, N, P, Q and R were subjected to further analysis using the CAse Pile Wave Analysis Program, CAPWAP®. CAPWAP® combines the measurements of the Case Method with a wave equation type numerical analysis, which provides the testing engineer with the shaft resistance (magnitude and distribution), end bearing, shaft and toe damping, shaft and toe quake and unloading parameters (Pile Dynamics, Inc., 2014). A comparison of CAPWAP® total capacities with the PDA capacity estimate has been provided in Table 2.

Table 2: Comparison of capacity estimates.

Pile ID	PDA Capacity Estimate (RMX)(kN)	CAPWAP® Total Resistance (kN)	$R_{d,ug}$ (kN)
C	1599	1625	458
H	1334	1550	436
I	1163	1325	429
L	2201	2175	429
N	1746	1670	429
P	1496	1600	468
Q	1965	1960	810
R	2037	1980	429

The total resistances determined for these piles average approximately 4% above the PDA field predictions. The damping factor used for the field analysis is, therefore, confirmed. All piles tested, except A, have bearing capacities that exceed the required ultimate geotechnical capacities.

4 DISCUSSION

4.1 PILE DESIGN AND INSTALLATION

The project tender was based on the installation of 275 mm square reinforced concrete precast piles which were to be installed using a 6-tonne hydraulic drop hammer. Based on the expected founding levels from the provided geotechnical investigation, 73% of piles were expected to achieve a refusal set. Piles designed with a length shorter than the founding level were expected to have sufficient shaft resistance to satisfy the load requirements. These piles were located at the left and right edges of the site where a deeper founding level was identified. The pile capacities were to be verified using a high-strain dynamic testing program with 5% pile coverage.

However, at the completion of pile installation, only 38% of piles had achieved a refusal set. Of the piles which did refusal, 77% refused at a depth deeper than expected. This difference in installation behaviour was seen through the comparison of Figure 1 with Figure 3. Piles which did not achieve a refusal set upon installation will have a reduced end bearing capacity than if a refusal set had been achieved. However, these piles still achieved the required capacities through the combination of the shaft and bearing capacity.

4.2 SOIL SET-UP

Sets are typically recorded at the end of driving and throughout restrike testing. All piles tested, except Pile H, were restruck with an equal or greater hammer drop height than installation. Despite transferring no less energy from the pile to the hammer, all pile sets reduced and by an average reduction of 48%. The only pile which did not have a reduction in recorded set was Pile G, which had a set of 2.0 mm per blow at a 400 mm hammer drop on installation and a set of 2.7 mm per blow upon restrike at a larger 500 mm drop. This reduction in pile set from installation to testing is likely caused by soil set-up. During pile installation, excess pore water pressures can be generated and the dissipation of these pressures are time-dependent and site specific. However, Look in *Handbook of Geotechnical Investigation and Design Tables* suggests a soil set-up factor range of 1.2 – 5.5 for clays, indicating the potential for significant capacity improvements with time.

This behaviour is at odds with the assumption made when using the Hiley driving equation; that the driving resistance is representative of the long-term ultimate bearing capacity of the pile. An example of this is with Pile K, which had an installation set of 24.0 mm per blow. If the project team had decided to use the Hiley Formula (despite not being suitable for this geotechnical condition), they would have calculated a pile bearing capacity of 435 kN (see Appendix A). This would suggest that the pile only achieved 49% of the required ultimate geotechnical capacity. However, the actual pile bearing capacity for Pile K was proven to be 1123 kN through the use of high-strain dynamic testing performed on the same day as installation.

4.3 RISK MITIGATION

One of the first opportunities for risk mitigation on a project is through proper site investigation. Initial geotechnical investigation was deemed too shallow to properly define the geotechnical conditions. A further four CPTs were completed by the piling contractor and tests piles were installed. This additional investigation had a significant effect on the expected pile refusal depths, as seen in Figure 1. More piles were expected to refuse at a deeper depth and more variability was identified across the site. This site investigation satisfied the requirements of the Australian Piling Code (AS2159:2009) and exceeded the number of locations recommended in Eurocode 7. While further site investigation could have been used to mitigate risks, there is diminishing effectiveness as seen Figure 1, where stage 2 and 3 appear similar in the trends identified. Economic constraints will always be a limiting factor for additional site investigation.

On this project, PDA testing was used as a risk mitigation method. Due to the variable pile driving behaviour, the PDA testing was increased from 5% to 18%. By performing additional testing, the Testing Engineer was able to confirm bearing capacity on piles which had behaved differently than expected during installation and develop a driving criterion for the

field crew to follow. Testing Engineers performed a total of 20 No. tests during four different site visits totalling 17 hours on-site. While there is a cost associated with performing testing, pile installation was optimised for the site-specific conditions. The original tender offer allowed for 1713 m of total pile length and 1915 m was installed. While this represents a 12% increase in pitched length from the tender, this percentage had the potential to be far more severe without the information obtained from the testing program. Adding an extra 3 m section to all piles which did not achieve a refusal set would have used an additional 195 m of pile length. Based on the average production rate for this project, this would have added an additional two days of rig time. 26% of piles which did achieve a refusal set achieved this more than 3 m deeper than expected; there is no guarantee that this extension would have achieved refusal. From a productivity and sustainability perspective, PDA testing provided a compelling solution.

5 CONCLUSION

Piletest was involved in the testing program of a 104 No. driven precast pile project in Brisbane. Across the 2400 m^2 site, six boreholes and eight Cone Penetration Tests (CPTs) were collected as part of the site investigation and identified a variable ground profile. The expected pile refusal depths (less than 2.5 mm per blow) based on the CPTs and three refusing test piles was used to create a contour plot, interpolating between these locations. During the installation of piles, different driving behaviour was experienced. Plotting the as-built pile penetration depths on a contour plot revealed several significant differences from what was expected. The original design had planned for 73% of piles to achieve a refusal set, however, only 38% did. Despite this, an increased high-strain dynamic testing rate was used to confirm the installed piles were fit for purpose with the benefits of soil set-up. While there was a cost associated with this, the adaptive testing program allowed for driving criteria to be developed in different areas of the site. As such, this project was completed on the expected finish date and used 202 m more pitched pile length than designed. This project is a reminder of the risks in geotechnical design, even with a thorough site investigation, and the unique benefits of dynamic testing in soils with time-dependent capacity improvements.

6 REFERENCES

Broms, B. B. (1978). *Precast Piling Practice.* Stockholm, Sweden.

European Committee for Standardization. (2007). *Eurocode 7 – Geotechnical design – Part 2: Ground investigation and testing.* EN 1997-2:2007.

Look, B. (2007). *Handbook of Geotechnical Investigation and Design Tables.* London, UK. Taylor & Francis Group.

Pile Dynamics, Inc. (2014). *CAPWAP Background Report Version 2014*. Cleveland, USA.

Standards Australia. (2009). *Piling – Design and installation.* AS 2159-2009.

Standards Australia. (2017). *Bridge design. Part 2: Design loads.* AS 5100.2:2017.

APPENDIX A: HILEY EQUATION CALCUALTAION

The Hiley Equation uses pile driving parameters to estimate the overall pile capacity. While multiple modified Hiley Equations exist, Brom's *Precast Piling Practice* suggests:

$$= \frac{h \quad \times 10}{+ 0.5} \times \frac{+}{(\quad + \quad)} \tag{1}$$

Where,

- Mass of hammer (Q_h) = 6 t
- Effective height of fall (h_e) = 0.32 m (assuming 80% efficiency)
- Coefficient of restitution (k) = 0.5 (as suggested)
- Long-term ultimate bearing capacity ($P_{pile\ ult}$) (kN)
- Set per blow (s) = 24 mm
- Total mass of the pile (Q_p) = 6.45 t (assuming 26 kN/m^3 for reinforced concrete, AS 5100.2)
- Elastic compression of the pile/cushion/soil (e) = 5 mm (assumed)

$$= \frac{6 \times 0.32 \times 9.81 \times 10}{24 + 0.5 \times 5} \times \frac{6 + 0.5 \times 6.45}{(6 + 6.45)} = 435 \ !$$

MITIGATING LANDSLIDE RISK TO THE PUKETERAKI EMBANKMENT ON NEW ZEALAND'S MAIN SOUTH LINE

Orion Marshall and Janey Hansen
Beca Limited

ABSTRACT

The Main South Line (MSL) is the only railway line that links Dunedin and Southland to the rest of New Zealand's railway network. The Puketeraki Embankment is between 337.9 km and 338.5 km along the MSL and traverses the Puketeraki Landslide Complex. The Puketeraki Landslide Complex is made up of a series of deep-seated movements and shallower earthflows. Based on the current monitoring data and considering the effects of climate change, the predicted movement of the landslide over the next 50 years is in the order of 7 m horizontally and 2 m vertically along the landslide complex beneath the embankment.

Several historic and recent ground investigations as well as detailed geological mapping throughout the site indicate the embankment is underlain by earthflow materials followed by Otakou and Onekakara Group Sediments. The east-west trending, steeply north-dipping, active Puketeraki Fault is inferred to cross the southern section of the existing rail embankment. Survey monitoring data suggests the average displacement rate of the embankment is 123 mm per year since 1992. Recent inclinometer readings suggest the majority of displacement occurs at approximately 21 m depth, corresponding to the transition from completely weathered to slightly weathered Burnside Mudstone.

Design of measures to arrest the ongoing movement of the landslide is impractical due to its scale, and therefore a practical approach allowing for widening of the existing rail corridor to accommodate the predicted movements coupled with improved site drainage has been adopted. This paper presents a technical overview of the instability mechanisms at the site and conceptual mitigation measures to accommodate the forecasted displacement.

1 INTRODUCTION

Beca Limited (Beca) has been engaged by KiwiRail to undertake assessment and design to minimise the geotechnical risk to the Puketeraki Embankment between 337.9 km and 338.5 km on New Zealand's Main South Line (MSL). The embankment traverses the active Puketeraki Landslide Complex, including deeper-seated movement and earthflows. Historic movement of the landslide has seen the abandonment of a historic rail embankment and railway tunnel, followed by the construction of the new rail embankment and slope cutting in 1936. Surface displacement monitoring shows that on average, the embankment has displaced 2.5 m since 1992. KiwiRail acknowledge from previous studies that design to arrest the movement of the landslide complex is unlikely to be successful, and so remediation measures shall seek to provide the rail network in the area with approximately 50 years of continued, reasonably uninterrupted operation. The objective of this paper is to provide a technical overview of the Puketeraki Embankment project history and the geotechnical mechanisms contributing to its instability, as well as a summary of the proposed remediation measures.

2 SITE OVERVIEW

2.1 SITE DESCRIPTION

The Puketeraki Embankment and adjacent Yellow Cutting are located between approximately 337.9 km and 338.5 km on the MSL, approximately 27 km north of Dunedin. The site is located near the coast, with steep sea cliffs approximately 200 m to the east. The location of the site is presented below in Figure 1.

The Puketeraki Landslide Complex encompasses shallow secondary earthflows, the Crossing and Embankment Earthflows, within a deep-seated landslide. The embankment is situated on the Embankment Earthflow and is affected by both deep and shallow instability, whereas the cutting is situated outside of the earthflows, so is affected by deep instability.

A historic embankment and abandoned tunnel of the MSL are situated immediately upslope of the current embankment and cutting. The historic embankment is mainly composed of sandstone fill from original construction of the Yellow Cutting. The tunnel and original embankment were abandoned in 1936 due to partial tunnel collapse due to slope instability. The Yellow Cutting is approximately 6 m wide at track level and up to 25 m high. The batter slopes are generally steeper at the base and range from 25° to 60°.

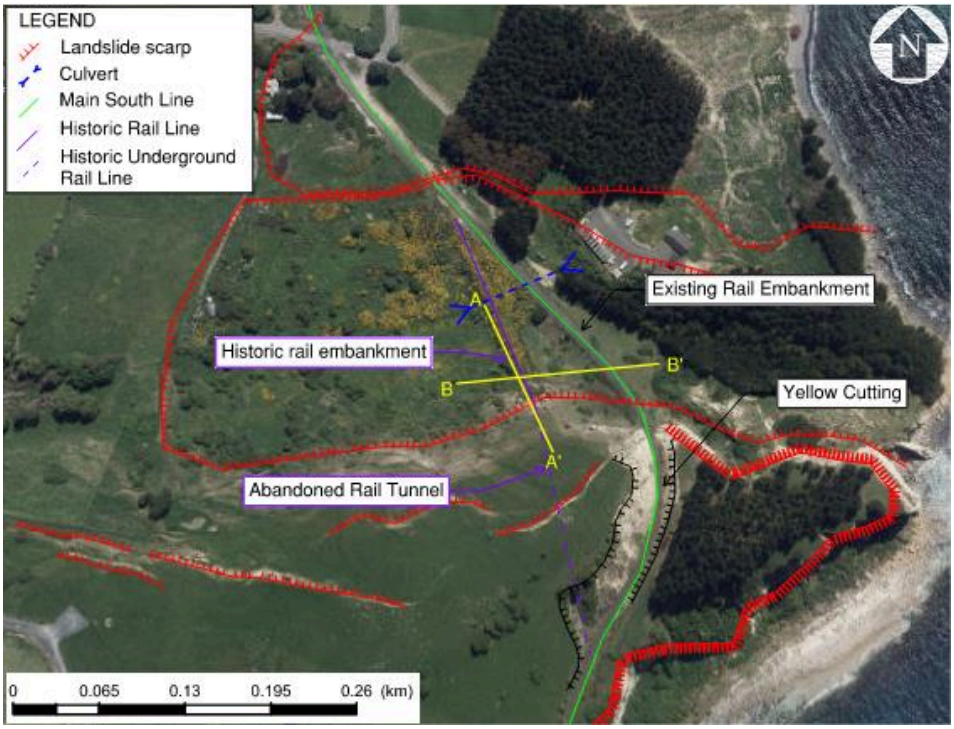

Figure 1: Aerial photo of the site with annotated landslide features.

2.2 PUBLISHED GEOLOGY

According to the Dunedin District Map by Benson (1968), the underlying geology at the Puketeraki Embankment is the Miocene Caversham Sandstone, described as a white or greyish, massive, calcareous, quartz sandstone (Figure 2). To the north of the site, successive stratigraphic units are older than the Caversham Sandstone, including the Concord Greensand, the disconformable Burnside Mudstone and Abbotsford Formation. Outcrops of upper Miocene extrusive volcanics of the second main eruptive phase Volcanic Complex are located near the site and appear to have been offset by the Puketeraki Fault. The inactive normal Puketeraki Fault is mapped to intersect the site. The fault dips steeply to the north and strikes to the east (Sunderland, 1994).

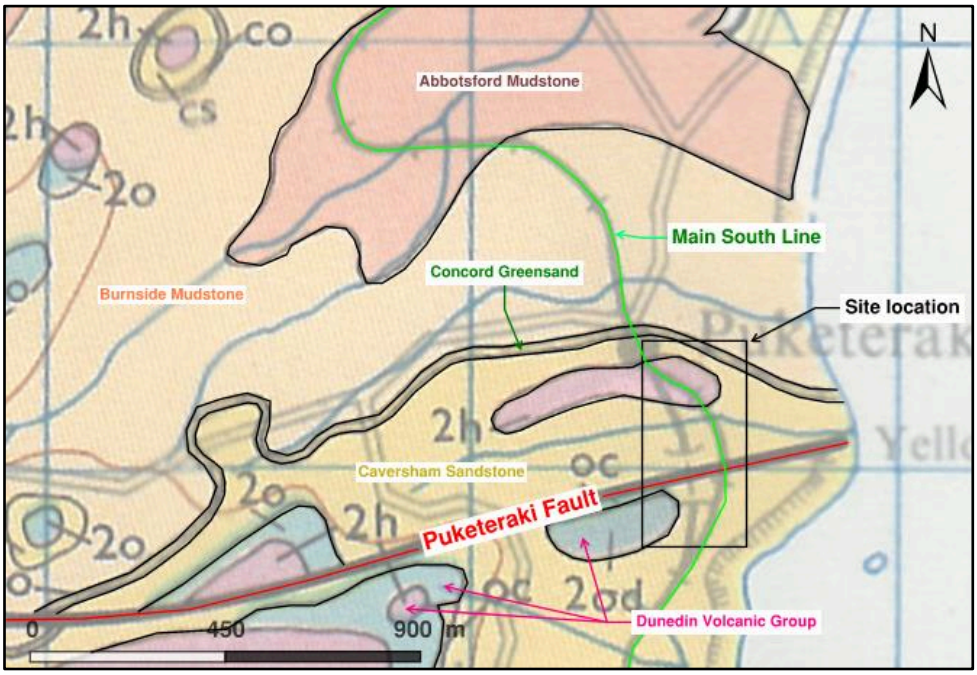

Figure 2: Dunedin District Map (Benson, 1968) excerpt with annotations indicating geology and location of the Puketeraki Embankment site.

3 GEOTECHNICAL INVESTIGATIONS AND GROUND CONDITIONS

3.1 GROUND INVESTIGATIONS

Data from various historic studies throughout the site and recent intrusive ground investigations, drilled in 2024, along the historic rail embankment were utilised to inform the geological and groundwater conditions beneath the site. Investigation data utilised for this project include seven machine boreholes, twelve test pits, seven dynamic heavy penetrometers tests, geological mapping, inclinometer readings on the historic embankment over a six month period (so far), piezometer groundwater monitoring over a six month period as well as capturing drone imagery to inform the ground model and design. Of the seven boreholes drilled around the site, four (two drilled by ENGEO (2015) and two drilled by Beca (2023)) were drilled on either the existing or the historic rail embankment.

3.2 GROUND MODEL

A geological ground model was developed to inform the design of the potential remediation measures. Ground conditions encountered during the investigation were consistent with the mapped geology and the mapped investigations. Cross section of the geology interpreted utilising the borehole investigation data presented in Figure 3. Alignment of each cross section is presented above in Figure 1.

No definitive sheared zones that could represent slip surfaces were observed in the drill core. Observing slip surfaces was challenging due to the presence of drilling fractures, the degree of weathering and bedding laminations within the rock. The contact between the Embankment Earthflow and the Caversham Sandstone is not clear due to lithological and density similarities. The base of the Earthflow has been inferred between 14.4 and 15 m bgl where there is a marked darkening of the colour. Initial inclinometer results suggest the base of the earthflow could be at 12.9 m bgl where approximately 0.2 mm of movement was measured over one month.

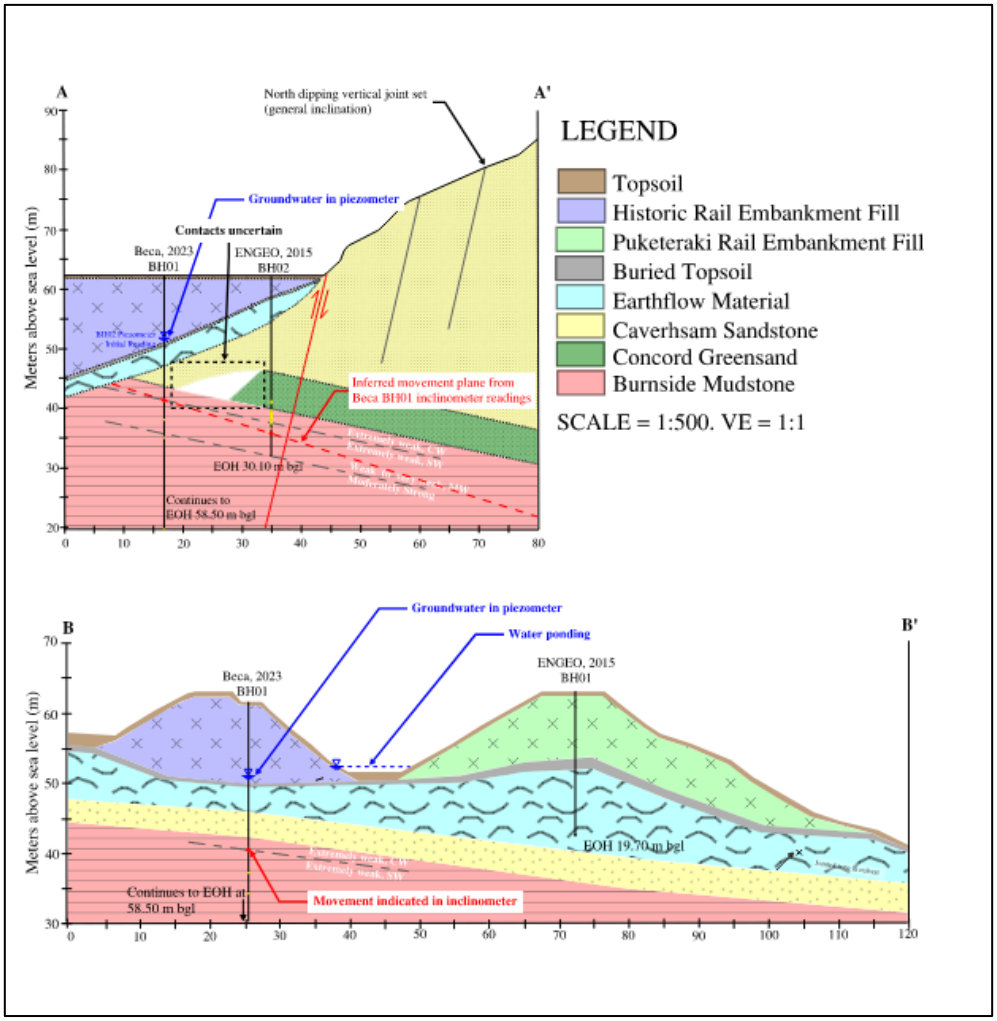

Figure 3: Cross Sections A-A' and B-B'. See Figure 1 for the alignments.

3.3 GROUNDWATER

Telemetered groundwater monitoring was carried out over a six-month period between December 2023 and May 2024. Results from the groundwater monitoring indicate the groundwater has remained relatively consistent over the monitoring period. Monitoring data to date is insufficient to quantify seasonal variations in groundwater levels and its associated relationship (or lack thereof) with landslide movements. Groundwater monitoring is currently being undertaken throughout the wetter months to determine seasonal variation (if any).

4 INSTABILITY MECHANISMS

4.1 SURFACE MONITORING DATA

Surface monitoring ground survey marks have been installed to measure ground deformation on the Puketeraki Landslide Complex since 1992. Findings from the survey show that the Puketeraki Landslide Complex is moving to the northeast at an average bearing of 83 degrees with a slight clockwise (southward) deformation rotation. Over the entire monitoring period, the average rate of total deformation within the Embankment Earthflow ranges from 109 – 130 mm/year absolute average displacement. Based on movements to date, horizontal movements of up to 7 m and vertical movements of up to 2 m may be anticipated over the next 50 years, allowing for a small contingency for climate change effects.

4.2 DEEP SEATED MOVEMENT – PUKETERAKI LANDSLIDE COMPLEX

Inclinometer readings from historic boreholes suggests movement is occurring at 26.5 m bgl within the Burnside Mudstone. Inclinometer readings from Sunderland (1994) suggests movement is occurring at 20.0 – 21.5 m bgl, corresponding with the contact between the Concord Greensand and Burnside Mudstone at 20.3 m bgl. Beca inclinometer readings suggest movement occurring at 21.0 – 22.0 m bgl within the Burnside Mudstone at the change from completely weathered to slightly weathered. Results from the inclinometer monitoring are presented in Figure 4A. The inclinometer data suggests that the movement plane dips to the south. It suggests the movement plane is not strictly at the Concord Greensand contact and instead occurs at a range of depths, generally near the top of Burnside Mudstone unit.

Sunderland (1994) theorises that the displacement of tertiary mudstones and sandstones within the Puketeraki Landslide Complex is due to bedrock wedge sliding between bedding, dipping on average 14° to the southwest and steeply north dipping structures. These structures include the apparent Puketeraki Fault and associated parallel structures observed in the cutting. Sunderland (1994) demonstrates the kinematic feasibility of this theory through stereographic analysis, showing the intersection between the north dipping structures and the bedding. Geometric observations during a site walkover closely match that of Sunderland (1994), as indicated in Figure 4B.

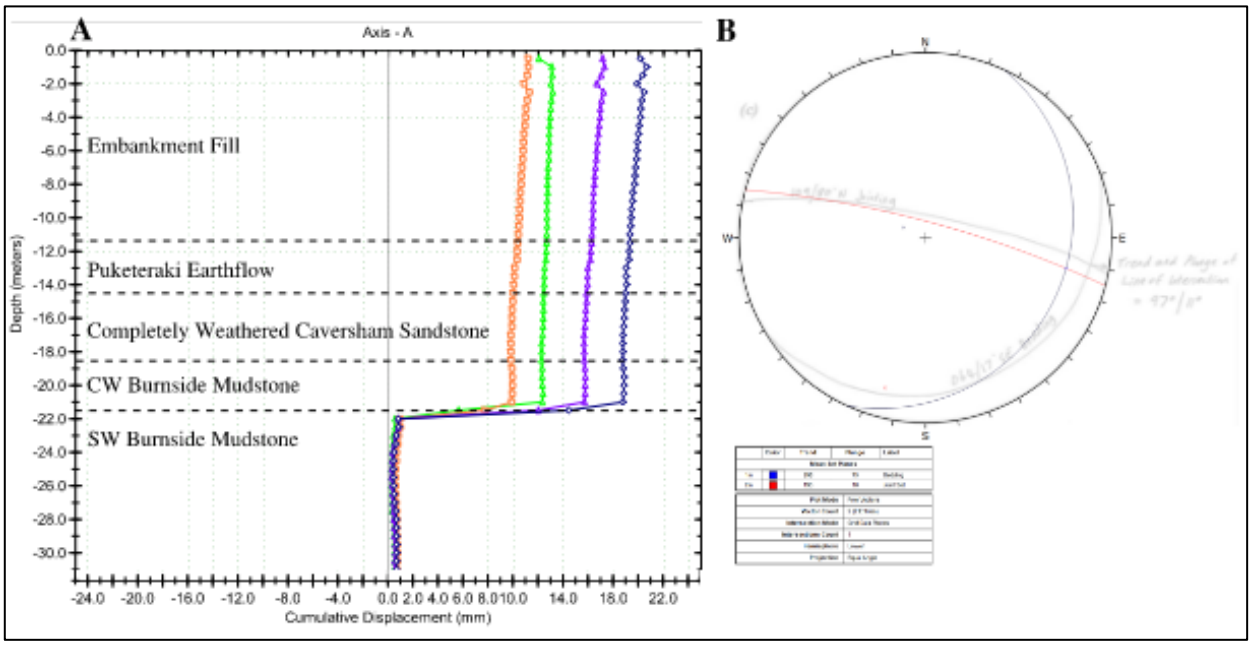

Figure 4: A) Cumulative displacement within Beca BH01 with annotations of basic observed from drill core. B) Stereographic projection of joint set and beddings observations in the Yellow Cutting overlain on Sunderland (1994) hand-drawn observations, showing the intersection between the planes.

4.3 SHALLOW SEATED MOVEMENT – EMBANKMENT EARTHFLOW

Sunderland (1994) describes the lower section of the Embankment Earthflow as an active retrogressive earthflow domain and that the deeper-seated wedge failure could have produced local basins, which trap landslides which then disintegrate as earthflow deposits. Mapping of the geomorphological features at the site suggests that the toe of the landslide is located at or below ocean level and is being eroded by ocean wave action (Sunderland, 1994). Sunderland (1994) infers that the Embankment Earthflow has had internal secondary reactivations and the lateral scarps developed within the earthflow due to the removal of the toe material by coastal erosional processes, both currently and with fluctuations due to glacial periods. Glassey (1993/1994) postulates that the earthflow has higher rates of movements following high rainfall periods.

ENGEO (2015) puts the base of the Embankment Earthflow at 7.6 m bgl in BH02. The base of the earthflow and plane of earthflow movement in Beca BH01 is interpreted to be between 14.4 and 15 m bgl. This suggests that near the Yellow Cutting, the base of the earthflow dips to the north, the opposite dip direction of the deeper-seated movement as picked up in inclinometers (see Figure 3). The Beca BH01 inclinometer results do not pick up obvious earthflow movement at the logged base of the earthflow, however, a small displacement of ~0.2 mm at ~13 m bgl could be attributed to earthflow movement.

5 STABILITY ANALYSIS

5.1 YELLOW CUTTING STABILITY

Based on the geological defect mapping carried out by Sunderland (1994), ENGEO (2015), and Beca (2024), bedding planes within the Caversham Sandstone show no obvious signs of shearing and the risk of sliding along these planes is relatively low. Potential wedge failures daylighting out of the cutting is also unlikely (Sunderland, 1994). Based on the soft-rock nature of the Caversham Sandstone, it is anticipated that “failure” within the cutting, will likely consist of small localised surficial “fretting”.

5.2 GLOBAL STABILITY

Quantitative slope stability analyses under static and seismic conditions were carried out using the GeoStudio Slope/W software. The assessment was carried out considering deep-seated global instability, the existing embankment stability of the eastern slopes, and the embankment stability of the new fill slopes (western side). A back analysis on the existing site geometry has been carried out assuming the existing embankment is marginally stable (factor of safety (FOS) ~1.2) under static conditions. The back analysis assumes the existing embankment is marginally stable (FoS of ~1.2) under the static case. Where seismic design events result in a factor of safety less than 1.0, a Newmark-type sliding block analysis has been undertaken and seismic-induced slope displacements based on the methodologies outlined by Jibson (2007), Ambraseys and Srbulov (1995).

The analyses indicate that shifting and reuse of the material from the historic embankment and placement against the western side of the existing embankment is likely to have a negligible effect on the global stability of the embankment, as there is no net increase in the destabilising loads due to the reuse of existing historic embankment fill. Seismic analysis results indicate Seismic displacements of up to 300 mm may be anticipated for the deep-seated failure mechanism under the ULS (i.e. 1 in 1000 year) shaking event. The ongoing deep seated movements under the static case are considerably higher than the estimated seismic movements. following a rare event.

6 PROPOSED REMEDIATION AND DISCUSSION

Engineering to completely arrest the movement of the deeper-seated Puketeraki Landslide Complex is unlikely to be successful and/or cost effective. Therefore, the proposed design solution aims to widen the rail corridor to accommodate the anticipated 7 m of horizontal and 2 m of vertical movement over the next 50 years. The works includes the widening of an approximately 120 m long section of the existing embankment using the materials removed from the historic embankment and the widening of an approximately 150 m long section of the Yellow Cutting through excavation of the western batter. This provides a sustainable and cost-effective solution by removing the need to import granular fill to site, also resulting in no net increase in de-stabilising forces affecting the large-scale instability. Proposed works also include the installation of two additional machine boreholes with an inclinometer and piezometer, respectively, on the existing embankment to take monitoring measurements during construction of the proposed rail corridor.

6.1 YELLOW CUTTING WIDENING

Design to stop the release of surficial material will likely be ineffective. Proposed works within the cutting include a nominal 2(V):1(H) cut batter along the western face, maintaining the existing slope angle of approximately 63° to horizontal. Surface drainage works should also be carried out along the cutting to properly divert the surficial water from penetrating the soils. Figure 5 presents the conceptual sketch for the proposed remediation measures at the site.

6.2 EXISTING EMBANKMENT WIDENING

The proposed widening is aimed to accommodate the predicted ground movements of up to 7 m horizontally and 2.0 m vertically over the next 50 years. As such, a nominal 11.5 m widening is proposed along the affected section of rail corridor, allowing for 7 m of horizontal movement, 4 m of horizontal movement due to vertical movements and a further 0.5 m contingency. Partial removal of the historic rail embankment will provide a site-won fill source, reducing costs and carbon foot print of the construction works.

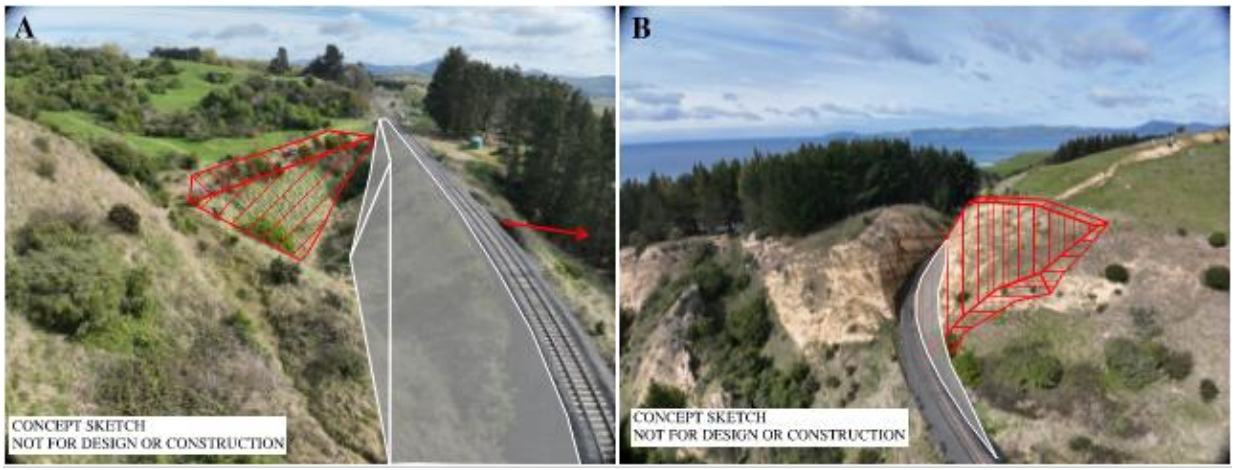

Figure 5: Conceptual overview of the remediation options at A) the Puketeraki Embankment and B) the Yellow Cutting. Hatched area in red indicates areas where material shall be removed. Grey areas indicate widened area of the rail corridor.

7 ACKNOWLEDGEMENTS

The authors would like to thank Paul Horrey and Nima Taghipouran of Beca for their reviews of the paper, Matt Fitzmaurice of Beca for his technical geological guidance throughout the project and KiwiRail for their review and permission to submit this paper.

8 REFERENCES

Ambraseys N and Srbulov M, 1995. Earthquake induced displacements of slopes. Soil Dynamics and Earthquake Engineering volume 14.

Beca Limited (2024). Puketeraki Embankment MSL 337.9 to 338.5 km – Geotechnical Appraisal Report. Report Ref. 3160890-185128443-294

Beca Limited (2024b). Mitigation of Slope Instability, Puketeraki Embankment – MSL 337.9 to 338.5 km – Detailed Design Report. Report Ref. 3160890-185128443-1384

Benson, W. N. (1968). Dunedin District 1:50,000, N.Z. Geological Survey Miscellaneous Series Map 1. Department of Scientific and Industrial Research, Wellington, New Zealand.

ENGEO Limited (2015). Geotechnical Assessment Puketeraki Embankment Main South Line.

GeoSolve. (2020). Geotechnical Report – Puketeraki Embankment and Cutting, MSL 338.100 to 338.500, Puketeraki.

Glassey, P. (1993). *Puketeraki Landslide – Preliminary engineering geology assessment.* Dunedin: Institute of Geological & Nuclear Sciences Limited.

Glassey, P. (1994). *Puketeraki Landslide: Assessment of drilling and monitoring data and recommendations for remedial measures*. Institute of Geological and Nuclear Sciences. Report Ref. 352943.11.

Jibson R.W., 2007. Regression Models for Estimating Co-seismic Landslide Displacement. Engineering Geology, Vol 91, Issues 2-4, pp.209-218.

Sunderland, D. (1994). *Engineering geology assessment of the Puketeraki Landslide Complex, North Otago*. [BSc (Honours) thesis]. University of Canterbury.

UTIKU LANDSLIDE OCCURRENCE ON A MAJOR HIGHWAY – LESSONS LEARNT FROM A COMPLEX GROUNDWATER MODEL

Alexander David Whittaker[1]
Beca Ltd

ABSTRACT

The Utiku Landslide is a large, deep-seated, rock planar landslide ~400 m wide and ~1000 m long near the centre of New Zealand's North Island. Landslide movement has been affecting State Highway 1 and the North Island Main Trunk railway since the 1960s. Sustained periods of high groundwater pressures on the basal clay layer (~60 m below ground level) are the primary cause of movement. Early attempts to dewater the landslide were of limited success in preventing further movement, and with the intensity of rain experienced in 2022-2023, the landslide movement increased, causing large tension cracks and subsidence across the roading pavement. With cracks affecting road users, and further movement likely to occur if no action was taken, the New Zealand Transport Agency (Waka Kotahi) implemented an immediate solution while a design business case for a long-term management approach was progressed. A key component of any solution is the lowering of groundwater levels to reduce pressure on the slip surface. This paper will present the challenges and value of developing a detailed conceptual model of the subsurface and groundwater to help understand the cause of instability, as well as the movement of groundwater and effectiveness of drainage. The paper will also discuss lessons learnt in translating a complex 3D ground model into a 3D finite-difference flow model, and the benefits of collaboration across wider teams and disciplines for project delivery and outcome.

1 INTRODUCTION

The Utiku Landslide is a pre-existing large rock planar landslide that has been extensively investigated and described over the last 60 years (Ker, 1970; Stout, 1977; Massey, 2010; Massey, 2013; Carey et al., 2019). The landslide is ~400 m wide by ~1000 m long and extends beneath State Highway 1 (SH1) and the North Island Main Trunk (NIMT) railway line (Figure 1A & 1B). Intermittent movement of the landslide has been occurring since the 1960s, with attempts at that time to prevent/reduce movement in the landslide being largely unsuccessful, and successive pavement remediation (regrading/resealing) used to maintain safe use of the SH1 road corridor over this slow-moving landslide.

In August 2023, accelerated movement of the landslide resulted in cracking across the landslide scarp that runs along SH1 road corridor. New Zealand Transport Agency - Waka Kotahi (NZTA) engaged Higgins Contractors Ltd and Beca Ltd to undertaken emergency repairs and develop an early design solution to restore safe use of the road as soon as practical, whilst options for a longer-term design solution were investigated by NZTA and Tonkin + Taylor Ltd (T+T).

The aim here is to describe the development of a complex 3D ground model and associated 3D finite-difference groundwater flow model to support design and consenting, including the challenges faced, and lessons learnt throughout the project. Work presented here is the author's understanding and interpretation based on data available during their involvement in the project from November 2023 to July 2024.

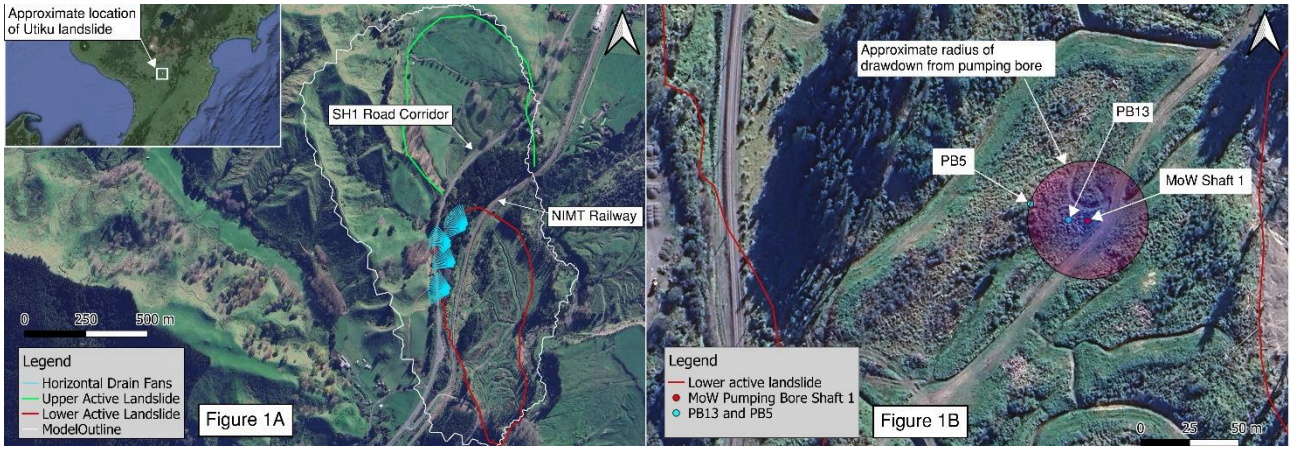

Figure 1A: Location and outline of the landslide, North Island, New Zealand. Figure 1B: Approximate radius of drawdown from a vertical pumping bore in the lower active landslide.

2 BACKGROUND

A basic summary of site conditions and potential design solutions is provided below. Whilst the focus of this paper is on value added and lessons learnt from modelling, modelling decisions should be made with the site context and likely design solution in mind, and so this is important context for model development and the lessons learnt that are presented here.

2.1 GEOLOGICAL SETTING

Landslides in Neogene materials have been damaging infrastructure for decades in the North Island, and also occur in coastal Marlborough, Dunedin and Nelson on the South Island (Prebble and Williams, 2016). It is thought (Ker, 1970) that the Utiku landslide initiated pre-historically (>18,000 years ago), likely caused by erosion and downcutting by the Hautapu River which exposed the weak clay seam at the stratigraphic boundary between the Tarare Sandstone (part of the Utiku Group) and the Taihape Mudstone (Tangahoe Mudstone). The clay seam was identified in historic investigations by others (e.g. Massey, 2010) and recent investigations by Beca at depths ~47 m to ~76 m below ground level (bgl) along SH1. The clay seam is thin with a varied thickness between 5–200 mm, though typically ~20 mm thick. Two key findings from the site investigations are (1) steeply inclined to near vertical fractures occur near surface and allow rainfall to infiltrate the slip, and (2) the clay layer was typically sheared, and with some open sub-horizontal fractures that provide preferential horizontal flow. Between these two features bores encountered relatively low permeability, unfractured Tarare Sandstone and Taihape Mudstone.

2.2 SURFACE WATER FEATURES

Permanent and intermittent/ephemeral water courses were identified and mapped on the site, along with many artificial drainage features. The Hautapu River, three intermittent water courses (Watercourses 1 to 3), and one permanent water course (Watercourse 4) were the most significant surface water features relevant to the water balance of the Utiku landslide. Farming, forestry / planting and previous slip remediation (e.g. digging of drainage channels, bulk earthworks, leaking stormwater networks) have been extensive, and have heavily modified the site and surrounding area. Several wetlands and springs have also developed over time across the landslide.

2.3 LANDSLIDE TRIGGER MECHANISMS

Massey (2010) identified that critical pore pressures prior to the onset of accelerated displacement occurred when groundwater levels (GWLs) were ~3 m higher than the lowest recorded levels. Periods of movement landslide movement follow sustained periods of high GWL, and GWL became raised, lagging long periods of increased precipitation by an estimated 12 to 20 weeks. This was confirmed with movement observed in August 2023, which matches up with a significant “wet” period from late 2022 to March 2023.

Given that the trigger mechanism is water pressure, groundwater lowering is likely to be a part of any short- or long-term solution to improve stability and so requires a groundwater model to assess the likelihood of creating sufficient drawdown to reduce pore pressure on the slip surface.

Works that have been completed in the past (since the 1960s), attempted to lower groundwater by installing horizontal bored drains and vertical pumping wells. Whilst these are understood to have worked in the short term, they were not successful in the longer term, likely due to being too widely spaced.

Based on review of Ministry of Works archive records, ~6.7 m of drawdown was observed in bore PB13 located ~3 m away from shaft 1, but PB5 located ~36.5 m away showed no response to dewatering (Figure 1B). This suggests an effective radius of no more (and potentially much less) than 35 m. Hence, a groundwater model is important for assessing the viability of any groundwater solution moving forward.

3 POTENTIAL DESIGN SOLUTIONS AND IMPLICATONS FOR MODELLING

While design has not been completed, one potential solution is bored inclined drains. This solution has been assessed and is discussed here. It comprises a network of four overlapping splayed fans of drains on the lower active landslide. This will likely consist of up to 21 inclined bored drains at each location (at a 5° incline to encourage self-cleaning and prevent clogging with sediment). The drains would target the vertical fractures which feed surface water into the slope, and so would need to be 100 m long slotted PVC pipes, with each fan radiating out from a single location. To assess this as a potential option, the groundwater model would need to include a 3D distribution of geological units, in particular the more fractured material beneath the road.

Surface water features would likely be affected by any groundwater lowering. Whilst drains could be designed to discharge to the nearest surface water body (to keep flows within the same hydrological catchments to minimise the

potential for adverse effects), it would also be helpful for any model to consider the 3D flow of groundwater and how that is distributed towards surface water bodies This way the model could support both design and consenting.

Based on our understanding of the landslide, the trigger mechanism for movement, the potential design solutions, and likely effects considerations, the need for a 3D ground model and 3D groundwater model was identified.

4 GEOLOGICAL MODEL

4.1 GEOLOGICAL MODEL INPUTS

A three-dimensional (3D) geological model of the site has been developed using LeapFrog v2023.2 (Figure *2*). The model was based on available current and historical geological logs, as well as the geomorphic mapping of Massey (2010) and undertaken as part of the early site response. Surface topography was based on a 1 m DEM for the site which was tied to a local UAV survey. Geological data from the representative bore logs were delineated into the nine (9) key lithological units, with the final geological model shown in Figure 2. The software was used to interpolate the lithological surfaces between the boreholes, and the model surfaces were then edited manually to remove any obvious inconsistencies or modelling artefacts.

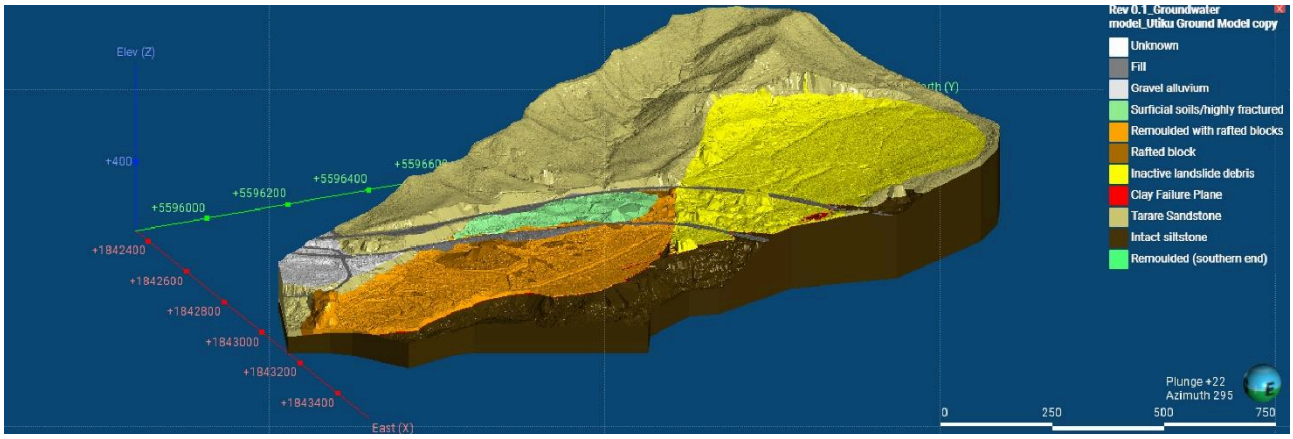

Figure 2: Oblique view of rev0.1 3D geological model, looking from Hautapu River to the north-west across the active landslide, NIMT and SH1. No vertical exaggeration

4.2 GEOLOGICAL MODEL LIMITATIONS

The geological model (Figure *2*) provides a representative interpretation of the subsurface geology based on the reported borehole logs and geomorphic mapping of the area. The model is based on factual data where it is available, but interpolation has been made between these locations to best represent the expected ground conditions. The datasets sourced for the site have been collected over ~60 years by different parties and make consistent interpretation difficult. For example, some bores had been surveyed to old coordinate systems, and the stitching of the DEM that created vertical walls at the surface that had to be removed.

4.3 THE VALUE OF A 3D GEOLOGICAL MODEL

The 3D ground model (Figure *2*) was integral in forming the base of the groundwater model and helped conceptualise the complex geology, allowing delineation of key units for hydrogeological analysis. It also highlighted gaps in data and knowledge of the site (i.e. survey data). Additionally, it can be used for wider stakeholder engagement and communicating the scale of the landslide visually. While not discussed here, the model was also used in slope stability analysis, to calculate the factor of safety before and after drain installation. Factor of Safety would have been significantly more difficult and less reliable to simulate without the 3D geological model to create accurate cross-sections.

5 GROUNDWATER MODEL

5.1 GENERAL OVERVIEW OF GROUNDWATER MODEL

The numerical groundwater model was developed in the 3D finite-difference modelling package Groundwater Vistas (version 8.30 build 169), a software package which uses the MODFLOW-USG (for Unstructured Grid) code.

MODFLOW-USG is one of the major releases of MODFLOW and was developed to support a variety of grid types, which allows flexibility in grid design to accommodate complex geology such as that present at the site. Whilst streams and other surface water bodies are included in the model, it is not a fully coupled surface-water model. The model only considers the exchange between surface water and groundwater, and any in-channel flow or surface water run-off is ignored.

The model area was defined to include the entire active and inactive landslide, as well as the immediate upgradient surface water catchment to include simulation of wetland 12 (located upgradient of the road and landslide). The numerical mesh (Figure 3) was formed from the Leapfrog ground model and has a base cell size of around 80 m but is refined in areas of interest such as surface water features and where bored drains are proposed to be installed.

The model is steady-state only, and so considers the potential long-term impact of drain operation relative to a starting condition that was calibrated to but may not always fully reflect a high groundwater level. As there has been no pumping testing and the available transient data sets are relatively short, or from multiple periods, a transient model has not been developed.

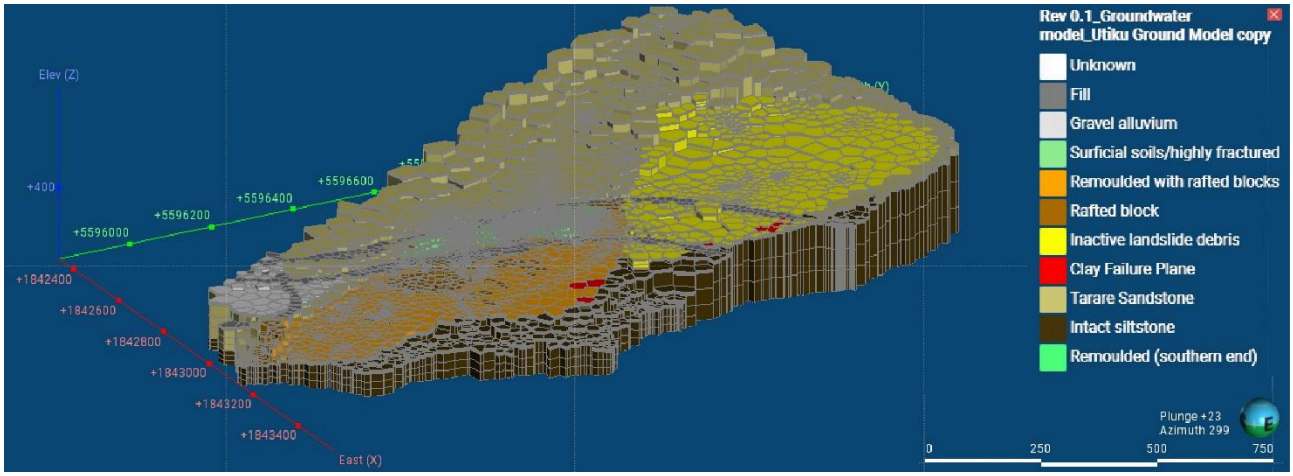

Figure 3: Snip from LeapFrog showing numerical model mesh

5.2 GROUNDWATER MODEL LIMITATIONS

There is known heterogenous flow of groundwater at the site, caused primarily by preferential fracture flow where continuous vertical fractures occurred in the upper units around the scarp head. This was parametrised as a wide zone, utilising anisotropic hydraulic conductivity inputs for hydrogeological units. However, the heterogeneity is more discreet than what can be modelled, and the extent of fractures cannot be known with certainty. This is a limitation of most groundwater models but is particularly important in the context of fractured flow.

Simulations of groundwater levels at 2 of the 27 calibration targets in the model were not able to fully replicate observed high groundwater levels. This infers an unknown variability in the ground conditions affecting groundwater flow in the area, which requires further investigation. Additionally, the use of 'pilot points' in modelling would assist in creating localised variations in hydraulic conductivity to better parametrise local hydrogeological conditions and may be used in further modelling.

Groundwater data was collected through different monitoring periods, and not all the data reflects the actual groundwater range and seasonal highs, and this may be further offset by long-term (non-seasonal) variation in rainfall. Additionally, as the area is part of a landslide, changes in topography have occurred due to movement and reworking of the surface, with additional drainage channels that likely impact the interaction between surface water and groundwater.

Finally, there were several wetlands, springs, ephemeral and permanent streams, rivers, drainage channels, and a flume that had to be input, parametrised and calibrated in the model. Not all features could be accurately modelled, due to limitations with how the groundwater modelling software is able to reflect surface water features. Nevertheless, the effort resulted in a useful model that could be applied to approximate the groundwater dewatering effects on ecologically and culturally significant surface water features.

5.3 THE VALUE OF A 3D GROUNDWATER MODEL

The 3D numerical groundwater modelling indicates that a solution such as bored inclined drains could result in 3 m to 8 m of groundwater lowering in the corridor of SH1, which is likely to improve SH1 resilience in the short to medium term.

Groundwater levels from modelling were able to be extracted and input directly into slope stability models. The 3D groundwater model allowed for assessing different combinations of drain arrangements, identifying which drains offer the best benefit, and whether there was the potential to reduce costs by installing less drains for the same effect. The model can also be used for testing other groundwater solutions.

Several wetlands were identified on and surround the landslide, and the use of a 3D groundwater model was integral in identifying what wetlands would be affected (by drawdown or reduction in flow rate) and to assess the potential magnitude of the effects on each wetland. The groundwater model was also useful in identifying the impact of groundwater drawdown on other important features, such as the Hautapu River. Being able to indicate either no or negligible effect on the river is valuable when discussing effects with the regulator and mana whenua.

6 DISCUSSION OF CHALLENGES AND LESSONS LEARNT

6.1 ONE GROUND MODEL, ONE GROUNDWATER MODEL, FOUR PIECES OF SOFTWARE!

Ideally a model is developed for a single purpose. However, in this case, the Leapfrog 3D geological model was intended to serve multiple purposes, to be used to support groundwater modelling in MODFLOW (finite-difference software), and to support stability modelling in SLOPE/W and SLIDE (limit equilibrium method software). A total of four pieces of software (including Leapfrog) were used by two different design teams and required a collaborative approach to the models undertaken, by communicating between design teams and the Leapfrog modeller. This was useful, as the pooled experience allowed quick solutions to problems encountered, or alternative approaches that could be tested.

The intended purpose of the groundwater model was to estimate the potential drawdown from the long-term operation of bored drains, and to assess the potential for changes in hydrologic function to surface water systems. Ultimately, the model was also used by the DBC team for initial assessment of the longer-term solution also. The model achieved this purpose, but several challenges were posed as a result of early decision-making, and due to the multiple purposes of the ground model, that could have impacted programme and cost on the project if not well managed.

6.2 CHALLENGES

6.2.1 Conversion issues

The conversion of the Leapfrog ground model to a groundwater model was challenging due to utilising a MODFLOW unstructured grid (USG). Whilst this is ideal for the complex topography and geology posed at the Utiku landslide site, multiple issues were encountered during conversion of the geological model to MODFLOW. The USG flow package was unable to utilise ‘refined models’, a type of model in Leapfrog that had been used to initially create the geological model. This was amended by forming a ground model where subunits were included as layers amongst the main units in an appropriate sequence, making the model functional for the purpose. This allowed the project team to retain a level of model complexity that a structured grid would not have allowed for.

A further challenge encountered was the assumed continuous thickness of the clay failure plane, being too thin for the groundwater model to register as a layer. The discussed and agreed solution was to create a copy of the ground model, manually edit the clay failure plane unit to a thickness that would be able to be used for the specific purpose of input into the groundwater model. This resulted in two models being created, one for the slope stability model and one for the groundwater model.

6.2.2 Model errors

The geological model had to be remade without a refined model to allow for use as a groundwater model, which led to further complications. New meshes were reconstructed to shape the various layers, and a Constructive Solid Geometry (CSG) error occurred, indicating that the meshes were preventing a volume from being created in MODFLOW. Additional error messages were also encountered (i.e. “Model used for hydrological properties does not cover active cells”) and help was requested from Seequent to fix. These errors were unforeseen and led to significant delays in modelling, that was largely attributed to the fact that USGs in Leapfrog are a relatively new feature released with Leapfrog version 2022.1. It was tested to see if the same errors occurred with a structured grid, and this identified that these errors only occurred in the USG version i.e. the two model codes are not yet fully compatible.

6.2.3 Equivalent Clay Layer

As noted above, a primary issue encountered was modelling of a thin clay layer in a finite-difference groundwater environment. Where too thin, a layer could affect the stability of calculations used to determine groundwater flow between layers in MODFLOW. To amend this, a second “parallel” ground model had to be created and the clay layer had to be artificially thickened to 0.5 m, ~25× thicker than the typical clay layer thickness. This required hydraulic conductivity calculations to adjust the permeability of the clay unit in the subsequent model. Consequently, the clay layer was given a

higher horizontal and lower vertical hydraulic conductivity to simulate preferential fracture flow along the slip surface similar to what would be expected from a very thin high permeability layer surrounded by lower permeability rock.

6.2.4 Boundary limits

Groundwater models will always require greater extents than geotechnical models. The boundary of the groundwater model was initially defined by the boundary of the geological model it was based on, and availability of data to constrain the geology. Whilst hydraulic boundaries were considered in the initial decision-making, subsequent modelling outputs suggest that the model could have encompassed a larger area to the northeast and west. It could also have been extended to include the whole of the Hautapu River, as the edge of the model where small areas had been clipped off.

6.2.5 Topographic survey artefacts

Additionally, only some areas of the geological model have a high-resolution survey DEM, with the remaining areas of the model filled in by a lower resolution DEM. As described earlier, this led to the topographical features being exaggerated by tree features in some places, which created unrealistically high elevations in some parts that poorly reflect surface and groundwater interactivity and might also have implications for stability modelling. Manual smoothing / filtering of the data was undertaken to remove obvious errors, but some remain and required subsequent model users to apply judgement when examining cross-sections.

6.3 SUMMARY AND LESSONS LEARNT

The 3D groundwater modelling was required to support both the design, effects and stability assessments to help scope potential drainage solutions for a large slow-moving landslide in complex geology. The use of one geological model for three purposes, and one groundwater model for two design teams, was a significant step toward cost reduction, requiring collaborative work across multiple teams using different software to meet a range of project objectives. There were other benefits that are not so easily quantified, such as support for external communications, improved skills in software, consultant (user) feedback to software developers on capability gaps for future updates, and many others.

Groundwater models generally need to be created from a geological model that is specific to the intended use and designed with the required model purposes and outputs in mind. Discussion regarding these purposes and outputs need to occur between the Leapfrog modeller, geotechnical engineer and the hydrogeologist prior to the beginning of modelling, and throughout the modelling process to properly plan and determine what is required for all users.

New developments in the software can improve the function and ability to effectively model groundwater behaviour, but there can be unforeseen teething issues. The issues encountered here could have been circumvented by using a structured grid, but this would have resulted in some reduction in model discretisation and complexity. Instead, a collaborative approach between disciplines, and iterative approach to modelling, allowed for issues to be addressed and overcome.

7 REFERENCES

Carey, J.M., Massey, C.I., Lyndsell, B. and Petley, D.N. (2019) *Displacement mechanisms of slow-moving landslides in response to changes in porewater pressure and dynamic stress*. *Earth Surface Dynamics*, 7(3), pp. 707–722. DOI: https://doi.org/10.5194/esurf-7-707-2019.

Ker, D.S. (1970) *Renewed movement on a slump at Utiku*. *New Zealand Journal of Geology and Geophysics*, 13(4), pp. 996–1017. DOI: https://doi.org/10.1080/00288306.1970.10418214.

Massey, C.I. (2010) *The dynamics of reactivated landslides: Utiku and Taihape, North Island, New Zealand*. PhD Thesis. University of Durham, Department of Geography. Available at http://ethese.dur.ac.uk/587/.

Massey, C.I., Petley, D.N., McSaveney, M.J. (2013) *Patterns of movement in reactivated landslides. Engineering Geology*, 159, pp. 1-19. DOI: https://doi.org/10.1016/j.enggeo.2013.03.011.

Massey, C.I., Abbott, E., McSaveney, M.J., Petley, D.N., & Richards, L. (2016) *Earthquake-induced displacement is insignificant in the reactivated Utiku landslide, New Zealand*. *Landslides and Engineered Slopes. Experience, Theory and Practice*, 1st Edition, pp. 31-52. Available at: https://www.taylorfrancis.com/chapters/edit/10.1201/9781315375007-2/earthquake-induced-displacement-insignificant-reactivated-utiku-landslide-new-zealand-massey-abbott-mcsaveney-petley-richards.

Prebble, W. M., Williams, A. L. (2016) *Block Slides on Extremely Weak Tectonic Clay Seams in Openly Folded Tertiary Mud-Rocks at Auckland and the Rangitikei Valley, North Island, New Zealand. Rock Mechanics and Rock Engineering*, 49, pp. 2217–2234.

Stout, M. L. (1977) *Utiku landslide, North Island, New Zealand. Reviews in Engineering Geology*, 3, pp. 169-184.

COMPARISON OF DESIGN VALUES TO DYNAMIC LOAD TESTING RESULTS FOR BORED PILES IN BRINGELLY SHALE IN WESTERN SYDNEY.

H.Van Den Elsen
Piletest

ABSTRACT

The Sydney Basin is one of the most well-documented geological regions in Australia. Comprising of different rock formations consisting of a geological profile of varying sandstones and shales. These formations vary between classes from I to V based on the overall properties of the rock mass, the compressive strength determined from UCS testing and the overall roughness of the material. These rock properties determine the design parameters for piling applications, namely skin friction and end-bearing stress values. One of the most common formations in the Western Sydney region is Bringelly Shale, most of the correlations used currently are determined from soil sampling and static load testing performed from the 1970's to the late 1990's before the introduction and acceptance of pile dynamic load testing to assess pile capacity.

High Strain Dynamic (PDA) load testing and CAse Pile Wave Analysis Program (CAPWAP) can be used to produce a reliably accurate comparison of pile capacity to an ultimate static load test and so help determine the skin friction and end bearing stress values on a tested pile. This paper aims to compare recent dynamic load test data with CAPWAP analysis to design values based on the geotechnical information provided on-site in the Western Sydney area. From the presented comparisons the potential variance in design values compared to the frictions and base resistance achieved during testing for Bringelly Shale can be demonstrated.

1 INTRODUCTION

The geological region around Western Sydney, New South Wales has historically been a well-documented region for geotechnical engineering purposes. Many studies have addressed the behaviour and the strength characteristics for these formations. Most of the engineering application work for deep foundations has typically used correlations and in-situ testing suggested by the large quantity of technical work produced by Phillip Pells, who has developed many different guidelines and parameters for bored piles. These studies have been paramount to designing in the most common geological formation in this region, known as Bringelly Shale. Bringelly Shale is a siltstone, clay-like sedimentary rock that is predominant in the Western Sydney region. The large amount of research carried out has typically sampled medium to very high strength shale that is moderately weathered to fresh, due to the difficulty sampling and testing lower grade Bringelly Shale (William & Airey, 2004). The typical quality and strength of this material, as seen in this paper, is typically Class V to Class III, with the material either being extremely to highly weathered.

Many correlations, guidelines and ranges for design skin friction and end bearing parameters have been developed from the work done by Pells's. Much of this work was done prior to the acceptance of High Strain Dynamic Testing, where skin friction and end bearing can be determined with reasonable accuracy to verify a bored piles static capacity using CAse Pile Wave Analysis Program (CAPWAP). Using recent test data in the Western Sydney region, this paper will compare the information provided from the Geotechnical reports and consider potential design values for skin friction and end bearing in Low to Medium-strength Bringelly Shale, with reference to results from the testing programs performed on these sites.

2 BACKGROUND INFORMATION

2.1 BRINGELLY SHALE AND PREVIOUS STUDIES

The predominant formation this paper addresses is the Bringelly Shale formation. Bringelly Shale forms part of Wianamatta group, made up of Bringelly Shale, Ashfield Shale and Minchinbury Sandstone (Oo, et al., 2015). This group overlays the Hawkesbury Sandstone formation. The Wianamatta formation is distinct with most rock formations appearing as shales, with some distinct layers of sandstone in certain sections.

The Bringelly Shale, while similar to Ashfield Shale, has the distinction from previous studies as typically having a higher and more reactive clay content (McNally, 2004; Pells, et al., 1998; William & Airey, 2004). Bringelly Shale is also prone to accelerated weathering, especially on exposure to air or water (McNally, 2004).

Previous studies on this material have typically been performed on Bringelly Shale that is encountered beyond depths of common piling applications. Many of the samples tested have unconfined compression strength (UCS) values above 20 MPa, with less degree of weathering than seen in most piled foundation applications (William & Airey, 2004). Previous studies have also determined, from these deeper samples, an Is50 to UCS multiplier for Bringelly Shale is approximately 21 (William & Airey, 2004). However, previous authors have noted this multiplier may reduce in more commonly encountered, highly weathered, very low to medium strength Bringelly Shales. The information gained from these earlier studies has been valuable in forming a baseline application for foundation engineering, but may not be an applicable practice for the more commonly encountered, highly weathered, lower-strength Bringelly Shale often observed in Western Sydney.

2.2 PELLS ROCK DESIGN

Phillip Pells has provided a substantial amount of research and development on the pile design in Sydney rock formations. Across the Sydney region, the typical rock formations encountered can be generalised into sandstones and shales. A common approach from Pells's research is to have the sandstone or shale classified in the range of Class I to V. This classification is based on UCS strength, degree of weathering, defect spacing and a percentage allowance of seams with imperfections of clay, fragmentations, or highly weathered areas of the material (Pells, et al., 1998). The approximate value ranges for shaft resistance and end bearing for cast in-situ piles can be seen in Table 1 below.

Table 1: Phillip Pells Sydney Shale Shaft Friction and End Bearing

Class	Ultimate End Bearing[1] MPA	Serviceability End Bearing[2] MPa	Ultimate Shaft Adhesion[3] kPa
I	> 120	Max 8	1000
II	30 to 120	Max 6, or 0.5 x UCS	600 to 1000
III	6 to 30	Max 3.5, or 0.5 x UCS	350 to 600
IV	> 3	1.0	150
V	> 3	0.7	50 to 100

[1]Ultimate values occur at large settlements (>5 % of minimum footing dimension).

[2]End bearing pressure to cause settlement of <1% of minimum footing dimension.

[3]Clean socket of roughness category R2 or better. Values may have to be reduced because of smear.

2.3 GEOLOGICAL PROFILES FOR COMPARISON

For the comparison of design values to the capacity determined from dynamic testing, Table 2 below provides a summary of the geological profiles at each site location that have the soil profile broken down into the depths each strength class of shale up to Class III was observed. In all site locations, the degree of weathering varied from extremely weathered to highly weathered Bringelly Shale. The soil classification also varies between site locations due to different engineers and consultants logging boreholes and observing pile bores. In most instances, the material in this area is described as Bringelly Shale, but reported as either shale or siltstone. The accuracy and determination of this material is also subject to the interpretation of the professional logging the hole or collecting test samples at the time of the pile construction or borehole drilling.

Table 2: Bringelly Shale geotechnical profile for test site locations

Site Location	Depth range of Bringelly Shale Class (m)		
	V. Low (Class V)	Low (Class IV)	Medium (Class III)
Site 1	1.0 – 4.0	4.0 – 9.0	-
Site 1 TP2 & TP3		1.0-3.0	3.0-5.0
Site 2 TP1 & TP2	-	1.5 – 3.5	3.5-6.0
Site 2 TP3	4.5 - 10.5	10.5 - 12.5	12.5 – 14.0
Site 2 TP4	4.5 – 5.5	5.5 – 7.5	7.5 – 8.5
Site 2 TP3A	-	12.0-14.5	14.5-17.5
Site 2 TP4A	-	6.0 – 9.0	9.0 – 13.5
Site 3	-	-	0.5 – 11.0
Site 4	6.0-14.0	6.0-14.0	-

3 CAPWAP ANALYSIS RESULTS

Dynamic testing and utilising CAse Pile Wave Analysis Program (CAPWAP®) software to analyse the data has become a common practice to determine the shaft friction, end bearing and assess pile integrity of tested piles. During the development of correlations for Sydney Rock from 1970 to 2000, pile capacity verification was typically undertaken using static load testing. While an effective test, non-instrumented static load tests are costly and do not typically provide a detailed analysis of the skin friction of a tested pile or its end bearing as it cannot distinguish between the two in a standard test. Thus, the verification of capacity during this period assumes a total load achieved based on the displacement of the tested pile from the input force.

For site locations 1, 2, 3 and 4, the total number of test piles were 3, 6, 8 and 6 respectively, with a secondary restrike with a larger drop mass on TP3A and TP4A on site 2. A sample of 25 dynamic load tests have been analysed and included for this comparison. The blow selected for analysis in CAPWAP® is one with sound data quality, enough energy to mobilise the pile capacity and to generate a moderate amount of permanent displacement, or pile set. In these instances, it was typically the highest energy blow with the largest in-field capacity determination that was selected.

For a dynamic pile load test on a bored pile, mobilisation of the entire shaft capacity is typically achieved in two to three millimetres of movement (Rausche & Likins, 2000). Full mobilisation of the base capacity in a dynamic load test is typically achieved when the pile has moved in total over the entire test with a total permanent displacement of the diameter divided by 60 (Rausche, et al., 2008). Satisfying both of these criteria ensures the piles have had sufficient movement to show the mobilised shaft and toe capacity. For the piles used for comparison in this paper, all piles have achieved both requirements. For site 3, the piles were constructed with a foam base to produce a “soft toe” pile so the shaft capacity could be better assessed for tension loading by negating any influence on the lowest few metres of the pile from the high-end bearing material encountered at this site. For this particular site, no end bearing comparison has been performed due to the uncertainty of the toe performance having a known soft toe installed.

Table 3 below shows the average friction over the nominated zones from the CAPWAP® analysis, along with the assessed pile end bearing, the transferred energy to the pile, the permanent displacement on the analysed blow (Pile Set) and the total cumulative permanent displacement over the entire test.

Table 3: Test Pile Information and Parameters from CAPWAP®

Pile Name	Pile Size (mm)	Pile Length (m)	Average Skin Friction in Shale (kPa)			End Bearing in Shale (MPa)	Transferred Energy (kN.m)	Pile Set (mm)	Cumulative Set (mm)
			V.Low Class V	Low Class IV	Medium Class III				
S1-TP1	600	5.0	44.0	147.0	-	5.3	26.9	3.0	18.0
S1-TP2	750	5.0	-	162.0	362.0	6.5	40.9	1.3	18.5
S1-TP3	750	8.0	-	222.0	355.0	7.1	34.7	1.3	11.6
S2-TP1	600	5.5	-	228.8	413.5	20.7	147.0	5.0	22.1
S2-TP2	600	6.0	-	88.0	330.3	20.7	154.6	6.0	24.0
S2-TP3	600	14.0	146.6	155.3	187.2	6.2	120.6	13.0	45.0
S2-TP4	600	8.0	246.5	253.2	253.2	6.8	182.8	14.0	55.0
S2-TP3A	600	17.5	-	204	204.0	11.8	149.9	4.0	15.1
S2-TP4A	600	13.5	-	371.7	307.1	12.4	153.1	4.0	14.9
S2-TP3A RS2	600	17.5	-	204.0	204.0	31.3	319.3	6.5	27.0
S2-TP4A RS2	600	13.5	-	371.7	307.1	19.5	207.6	4.0	16.5
S3-TP1	750	11.0	-	-	744.5	-	295.1	3.0	5.0
S3-TP2	750	11.0	-	-	749.7	-	319.7	3.0	5.0
S3-TP3	750	11.0	-	-	615.2	-	208.6	3.0	3.0
S3-TP4	750	11.0	-	-	580.2	-	301.0	6.0	8.0
S3-TP5	750	11.0	-	-	897.0	-	166.3	3.0	3.0
S3-TP6	750	11.0	-	-	643.7	-	233.3	4.5	8.5
S3-TP7	750	11.0	-	-	475.3	-	300.9	8.0	16.0
S3-TP8	750	11.0	-	-	736.3	-	145.2	1.0	4.0
S4-TP1	600	12.6	106.5	106.5	-	2.7	98.2	5.3	46.0
S4-TP2	750	15.1	133.2	133.2	-	3.2	91.5	3.0	21.0
S4-TP3	600	11.6	126.3	126.3	-	7.9	87.3	4.0	39.0

Table 3 continued: Test Pile Information and Parameters from CAPWAP®

Pile Name	Pile Size (mm)	Pile Length (m)	Average Skin Friction in Shale (kPa)			End Bearing in Shale (MPa)	Transferred Energy (kN.m)	Pile Set (mm)	Cumulative Set (mm)
			V.Low Class V	Low Class IV	Medium Class III				
S4-TP4	600	12.5	123.6	123.6	-	9.6	85.5	6.0	35.0
S4-TP5	600	11.8	117.2	117.2	-	7.6	103.0	4.3	38.0
S4-TP6	750	12.4	173.6	173.6	-	12.4	78.1	3.3	32.0

4 DISCUSSION

4.1 SHAFT RESISTANCE

With reference to Table 3 above, the shaft friction has been plotted below in Figure 1. The plot contains additional transparent zones that show the potential shaft friction proposed by Pells for each respective strength class.

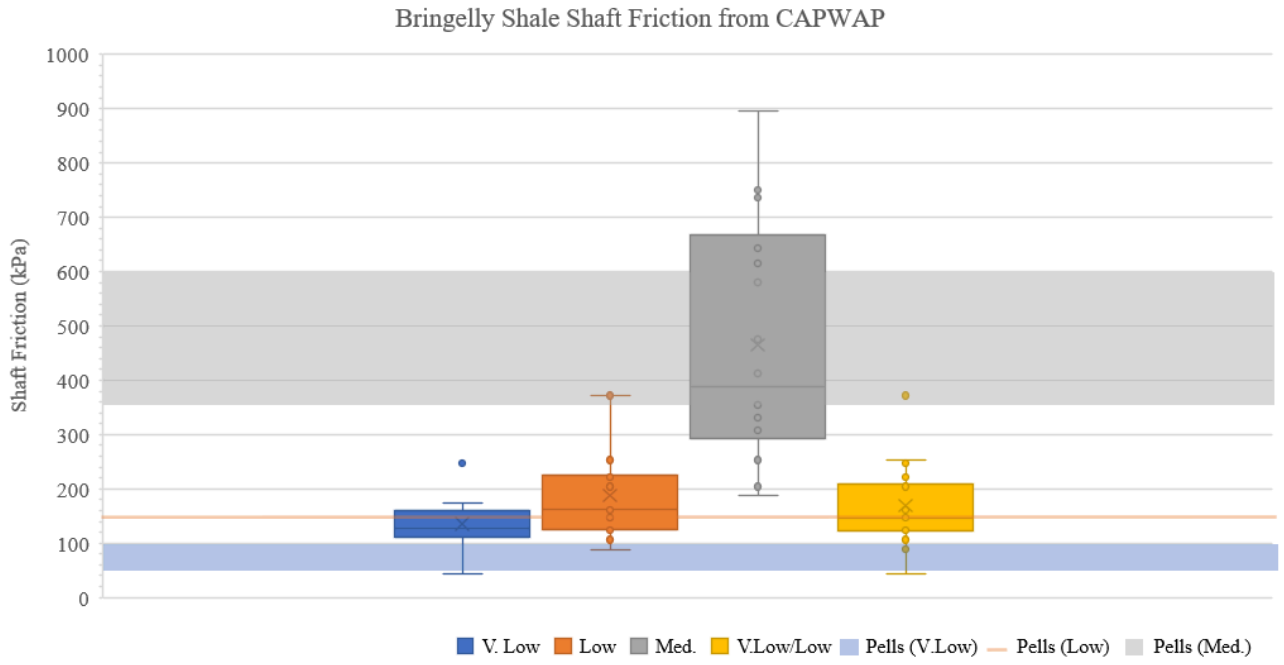

Figure 1: Box and Whisker Plot for Shaft Friction determined in CAPWAP for Bringelly Shale.

For very low to low strength (Class V and IV respectively), the values suggested by Pells are typically conservative compared to those determined during dynamic testing and CAPWAP analysis. The average resistance achieved for these classes is 137 kPa and 187 kPa, respectively. This equates to a 27 % and 20 % increase on the highest resistance in their recommended ranges by Pells (see Table 2).

It should be noted that, with Bringelly Shale in-situ and in laboratory testing it is difficult to correlate strength and/or material properties. This can be seen in the geotechnical profile breakdown in Table 2 for site 4, with the typical shale classification given as V.Low to Low. When combining these classifications and comparing them, the average friction value is 169 kPa, which is a 13 % increase on the maximum value nominated for the range suggested by Pells. The dynamic testing results show that Pells shaft friction guideline is generally conservative, especially for Class V Bringelly Shale.

For the Class III or medium strength, the tested results are typically in agreeance with the range provided by Pells. The average skin friction found from the dynamic testing is approximately 465 kPa compared to the average of Pells range of 475 kPa.

The shaft frictions observed have a broad range from the minimum to maximum values. This variance can be attributed to the variance in weathering of material or "smearing" of the socket or the quality of the construction of the pile, including the roughness of the material. The variance could also be attributed to misclassification of material, as previously discussed with Class V to Class IV material, as well as variance in the assessment of Class III being over or under-predicted by the engineer logging the pile bore.

4.2 END BEARING

Figure 2 below shows the range of end bearing values determined from dynamic testing. In general the V.Low to Low strength shale has an average end bearing of approximately 7.0 MPa and approximately 14.3 MPa for the medium strength. As indicated by the range provided by Pells, more resistance on the base is expected as the pile displacement increases. This trend can be seen in figure 3 below for both strength ranges. The trend for medium strength has a strong correlation if the end bearing results from site 2 for TP3 and TP4 are removed due to their large total sets and low-end bearing. It is considered likely that, for these particular tests, the material was misclassified and is possibly V.Low or Low strength. The low end bearing stresses determined could also be due to the pile bore being left open for an extended duration or not being cleaned properly, which is consistent with observations in relevant literature in the background information. As discussed with the very low to low strength shale, there is less of a correlation between total pile movement and end bearing as the variance in material quality in this range along with the difficulty in classifying it may lead to an increased variability of results.

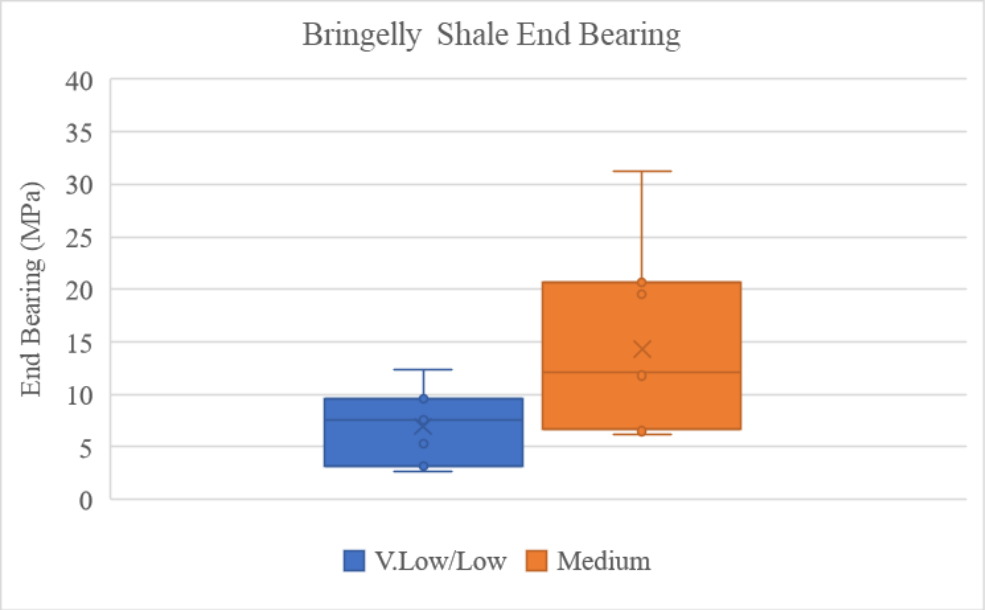

Figure 2: Box and Whisker Plot for End Bearing from CAPWAP for Bringelly Shale

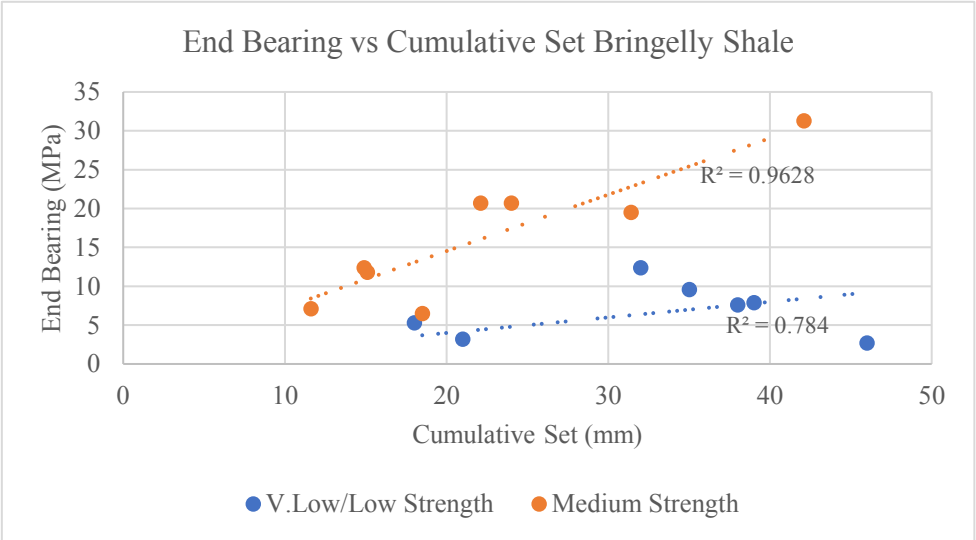

Figure 3: End Bearing vs Cumulative set for Test Piles in different strengths of Bringelly Shale.

While there is a general trend to suggest producing more total displacement results in increased end bearing, caution should be taken when designing for foundations that rely on base resistance to meet their minimum design strength or structures which are sensitive to excessive or differential settlement. The testing across these sites demonstrates that the end bearing was achieved, most test piles had a cumulative set greater than 5 % of the pile's diameter to achieve ultimate end bearing values as seen with Pells which may not be suitable for some design applications.

5 CONCLUSION

Overall, comparing the results obtained from dynamic testing to those proposed by Phillip Pells suggests the potential shaft friction in lower-strength Bringelly Shale provided by Pells may be conservative. As the material progresses towards medium strength, the range provided by Pells correlates well with the PDA and CAPWAP® analysis presented in this paper.

The end bearing ranges proposed by Pells for the lower strength shale appear to be slightly conservative, However, the allowable settlement criteria for structures, with due recognition of the magnitude of pile settlement required to fully mobilise base capacity, should govern how much reliance the foundation design has on-base resistance. To ensure reliable performance, a suitable test program should be adopted on projects where significant risk presents itself, or optimisation of pile length could be achieved.

6 REFERENCES

McNally, G., (2004). Shale, Salinity and Groundwater in Western Sydney. -, *Australian Geomechanics*, 107-122.

Oo, N., Hill, J. & Hsi, J., (2015). Assessment of stability and ground movement associated with tunnelling under a major highway. New Zealand Geotechnical Society, Wellington, 1044-1051.

Pells, P., (1994). A Thumbnail Engineering Geology of the Triassic Rocks of the Sydney Area. s.l., *Australian Geomechanics*, 1-52.

Pells, P., Mostyn, G. & Walker, B., (1998). Foundation on Sandstone and Shale in the Sydney Region. Newcastle, *Australian Geomechanics*, 17-29.

Rausche, F. & Likins, G., (2000). Dynamic Load Testing of Augered Cast-In-Place piles. *Deep Foundations Institute*, St. Louis.

Rausche, F., Likins, G. & Hussein, M., (2008). Analysis of Post-Installation Dynamic Load Test Data for Capacity Evaluation of Deep Foundations. American Society Civil Engineers, Reston, 312-330.

William, E. & Airey, D., (2004). Index properties and the engineering behaviour of Bringelly Shale. s.l., *Australian Geomechanics*, 31-43.

FIELD AND LABORATORY-BASED CHARACTERISATION OF PUMICEOUS SOILS IN THE BAY OF PLENTY

Rhiannon Robinson, Merrick Taylor
Beca Limited

ABSTRACT

The behaviour of pumiceous soil deposits to cyclic loading remains a topic of active research, and methods to evaluate liquefaction hazard in response to earthquake shaking are currently evolving. Recent industry guidelines have highlighted the uncertainty in pumiceous soil response and call for practitioners to adopt a more nuanced approach to assessing liquefaction hazard. This paper presents a recent project where field profiling, advanced sampling, and cyclic laboratory testing methods were employed to characterise the behaviour of pumiceous deposits considered to pose a potentially critical hazard for a site in Bay of Plenty, New Zealand. This paper discusses how the field and laboratory testing provided justification for the use of a less conservative triggering curve for liquefaction assessment, significantly reducing the extent of liquefaction under a design earthquake compared to previous estimates, allowing for significant cost savings for the client and reduced disruption to business. This paper reflects on the benefits which can be provided in the specification of high-quality undisturbed and specialised dynamic laboratory testing of pumiceous soil deposits, and provides recommendations for future application.

1 INTRODUCTION

1.1 BACKGROUND

This paper presents a recent project where an effort was undertaken to better understand the soil liquefaction hazard affecting an existing building in the Bay of Plenty region of New Zealand. Due to the high importance of the building, a detailed seismic assessment (DSA) was undertaken to assess its relative performance against the "new build standard" (NBS) requirements in accordance with the EQ-Assess guidelines (NZSEE et al. 2017). This would inform the Client of the extent of any seismic retrofit work required, or other decisions around the future use of the building.

Having the potential to dominate the seismic rating of the building, was the presence of an 11m high steep slope (~ 1V:1H) situated about 5m from the building, which was underlain by soils susceptible to liquefaction, including the pumiceous Matua Subgroup unit. The DSA showed, using conventional liquefaction triggering assessment methods (e.g. as per the MBIE (2021) Modules), that liquefaction and cyclic strain softening-induced strength loss and instability of the slope was expected following a design earthquake, with shaking hazard significantly lower than NBS. The resulting slope movements and settlement could potentially impact the building foundations, affecting post-quake operational performance and posing a life safety risk. Costly and potentially disruptive ground improvement was identified as a mitigation method to reduce slope displacements to within acceptable limits for the building.

1.2 RECOGNISED LIMITIATIONS OF CONVENTIONAL LIQUEFACTION ASSESSMENT METHODS WITH PUMICEOUS SOILS

The MBIE (2021) Module 3 guideline for liquefaction assessment notes the limitation of conventional empirical methods when applied to sandy soils with a significant pumice content (PC) (hence "pumiceous"). Pumice is a vesicular volcanic glass produced in large volumes by volcanic eruptions. It is found widespread across the North Island, from Auckland to Hawkes Bay, and is particularly prevalent in the Bay of Plenty and Waikato regions. Pumice grains are angular, vesicular, weak, compressible, and prone to crushing under load, including during penetration testing (i.e., CPT, SPT). Orense et al. (2012) note that because of these characteristics, most engineering correlations developed for hard-grained sands are not applicable to pumiceous materials, including the CPT and SPT-based empirical liquefaction triggering evaluation methods such as those of Boulanger & Idriss (2014) [BI14]. The effect of crushing will tend to result in lower SPT N and CPT q_c measurements than for a hard-grained soil of the same density, and consequently the liquefaction resistance will tend to be underestimated if using BI14. The use of shear wave velocity (V_S)-based liquefaction triggering assessment methods is attractive as it avoids the problem of grain crushing, being a 'small strain' measurement. However, recent research by Asadi et al. (2023) found there remained substantial differences in the liquefaction resistance of pumiceous sands compared to the empirical V_S-based triggering method of Kayen et al. (2013) [KEA13], with KEA13 forming a potentially conservative assessment. Based on the results of cyclic triaxial testing, Asadi et al. (2023) found that the liquefaction resistance to be dependent on PC, with the liquefaction resistance of the soil increasing with higher PC. They postulated it was due to the crushing of some pumice grains during cyclic loading, resulting in additional damping of seismic energy giving rise to a higher resistance to liquefaction triggering than for hard-grained soils.

The empirical liquefaction assessment methods developed by KEA13 and BI14 are based on extensive case histories of the observed performance of hard-grained soils following seismic events, while limited information has been collected to date on pumiceous soils. Because of the limitations of empirical correlations, Module 3 recommends engineers consider undertaking high-quality undisturbed samples and cyclic triaxial tests to assess the cyclic resistance of pumiceous soils directly for large or high-consequence projects. For the current project, directly testing the liquefaction resistance of the Matua Subgroup soils in the laboratory was seen as a potential opportunity to reduce the extent of liquefaction triggering and potential need for costly and disruptive ground improvement at the site or derating of the building.

2 FIELD AND LABORATORY TESTING

2.1 ADVANCED PISTON SAMPLING

The key problem with the laboratory testing of soils is that the sampling, transporting and storage of samples may result in disturbance that can significantly affect the test results. This is particularly the case with sands, where loose samples will tend to densify within a sample tube, while dense samples will tend to dilate and become looser. The cyclic test results will therefore tend towards producing the same result, regardless of the in-situ state of the soil (Idriss & Boulanger 2008). Preservation of the in situ 'fabric' (arrangement of particles) and any bonding at grain contacts is also important, as these can significantly affect the cyclic resistance. The so called 'undisturbed sampling' is not possible however, we can attempt to minimise disturbance by using advanced piston sampling methods.

Both Dames & Moore [D&M] and Gel-Push Type S [GP-S] advanced piston samplers were used to obtain undisturbed samples of sands and silts from within the interbedded Matua Subgroup unit. The D&M sampler was developed for fine-grained soils, using sharp-edged, thin-walled brass tubes to minimise disturbance (Stringer et al. 2020). The GP-S sampler was developed for loose to medium dense sands, and uses a gel polymer lubricant to reduce friction between the cut sample and the sample tube (Taylor et al. 2012).

2.2 ADDITIONAL FIELD TESTING

Seismic CPTs were undertaken adjacent to the sampling boreholes. The field measurements of shear wave velocity testing enable the use of V_S -based methods for liquefaction assessment, but also the comparison of field and lab V_S measurements can be used to assess the level of sampling disturbance. Geonor Vane testing was undertaken directly below each of the D&M samples collected to better inform CPT-based correlations to undrained shear strength, used to inform cyclic strain softening assessments in fine-grained soils.

2.3 SAMPLING, TRANSPORT AND STORAGE

Collected sample tubes were securely stored on site in an upright position and allowed to drain for 24+ hours. To minimise disturbance, the sandy (FC<10%) soils samples required freezing prior to transportation to the laboratory (Stringer et al. 2020). The samples were frozen with dry ice from the top down, to allow water to drain and thereby avoid ice-lens formation and disturbance to the sample. Once frozen, the samples were placed in a freezer overnight.

For transport to the laboratory, samples were bubble-wrapped and placed a polystyrene box. A thick piece of foam was laid across the back car seat and the polystyrene box containing the samples was placed on top, before carefully driving to the laboratory in South Auckland for testing.

2.4 LABORATORY TESTING

In addition to cyclic triaxial testing (CTX), consolidation of the sample to its insitu confining stress and bender element testing was undertaken to measure the V_S of each sample prior to testing, the post-cyclic shear strength was also measured by performing an undrained triaxial compression test on the liquefied sample. In accordance with NZS 4402:1986 a suite of soil index tests to further assist with soil characterisation including: solid density, Atterberg Limits, particle size distribution, fines content, pumice content following the method of Stringer (2019), and minimum and maximum dry density were completed. The latter was undertaken in accordance with Japanese testing standards (JIS A1224) which avoid crushing the soil and can be undertaken on a relatively small sample size.

2.4.1 Cyclic Triaxial Testing

During cyclic triaxial testing, the samples were subjected to a sinusoidal load of a particular amplitude and duration (or number of cycles, N_c) with a frequency of 0.1 Hz. The amplitude is set based on the desired Cyclic Stress Ratio (*CSR*) to apply during the test, calculated by:

$$CSR = q/2\sigma'_{\mathrm{G}} \tag{1}$$

where q is the deviator stress and σ'_c is the effective consolidation pressure applied to the sample prior to testing. The N_c required to liquefy each sample was monitored, where 'liquefaction' of a sample was defined as either the N_c resulting in greater than 5% double amplitude (DA) axial strain, a strain-based proxy value approximately co-incident with liquefaction (Ishihara, 1993), or an excess pore pressure ratio, r_u of 1 (liquefaction by definition).

Defining a cyclic strength curve (*CSR* vs N_c plot) for a soil ideally requires three data points minimum, with each point defined by the result of a single cyclic triaxial test performed at a unique *CSR* amplitude and N_c. The three (or more) samples should be from the same soil type and density/condition or as close as practicable (challenging in interbedded deposits). As the curve is unknown prior to testing, a *CSR* must be trialled first, before deciding subsequent values to develop a curve that encompasses a desired wide range of N_c values and allowing interpolation of the *CSR* at 15 cycles, which is the basis for the conventional empirical triggering method (i.e., to allow for direct comparison). Following receipt of the first *CSR*-N_c failure point for the curve, a new *CSR* is chosen for the second test, and the third thereafter, requiring close coordination with the laboratory technician undertaking the tests. Setting a *CSR* too low would mean the cyclic testing could continue to a very large number of cycles (e.g. 100+) potentially without the sample liquefying, or far beyond the range typically imposed by earthquakes, whereas setting the *CSR* too high would result in the sample failing within a single cycle, similar to a monotonic undrained compression test.

2.4.2 Liquefaction Susceptibility

All six cyclically tested samples liquefied during the test (i.e., $r_u = 1$ and 5% DA axial strain). The fines content (FC) of the samples ranged from 35 to 65%, with the Plasticity Index ranging from 3 to 9; hence, the soils are classed as fines dominated (FC>30%) that are 'susceptible' to 'potentially susceptible' to liquefaction in accordance with MBIE (2021) Module 3.

3 ANALYSIS

3.1 CRR CURVES

Prior to plotting and interpretation of the Cyclic Resistance Ratio (*CRR)* for the Matua Subgroup materials, the measured *CSR* values in CTX were corrected for the field stress conditions, and then normalised to a common confining stress (1 atm) for comparison purposes and denoted as *CSR**. CTX testing applies an isotropic confining stress ($\sigma_h = \sigma_v$) prior to shearing, whereas the field conditions are anisotropic ($K_0 \neq 1$), therefore a correction factor, C_r was applied to the test *CSR* values. A K_σ factor was then applied to then normalise to 1 atm. Both corrections (C_r, K_σ) were applied, following the recommendations of Idriss & Boulanger (2008) for hard grained soils which were adopted for pumiceous soils in the absence of soil specific correction factors. For each soil type, fabric, and density we expect a different cyclic strength curve. From a review of the corrected test results, three different *CSR* curves were established. Two curves for sandy silts, with those extracted using GP-S sampling being distinct from those extracted using D&M sampling, and a postulated curve for a clayey sandy silt from one unique sample tested assuming a similar curve as for the fine sandy silt. These are presented in Figure 1. From review of the CTX testing, the Nc resulting in a 5% DA axial strain provided a more reliable and repeatable measure of liquefaction triggering, therefore was used to plot the CSR curves. For comparison with the empirical triggering methods, the CRR^* at 15 loading cycles (CRR^*_{15}) was interpreted through curve fitting and interpolation.

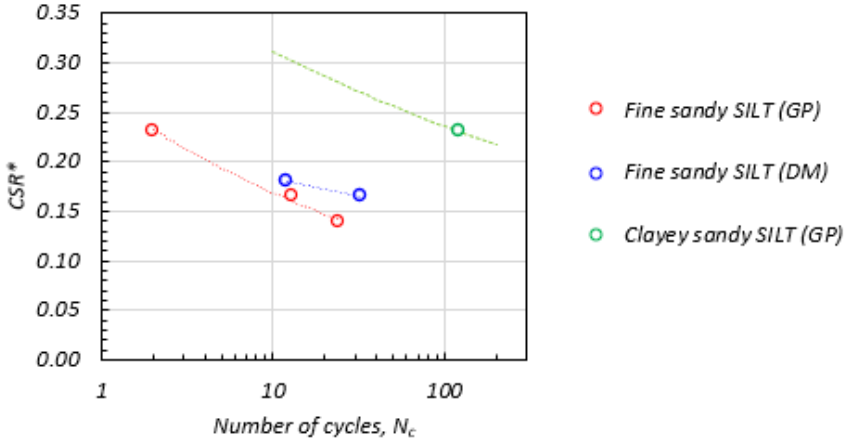

Figure 1. Corrected cyclic strength curves (*CSRvs. N_c to 5% DA ε_a) for samples of differing soil type and sampling method (GP= Gel push S-type, DM= Dames & Moore). Trend lines are inferred.**

As shown in Figure 1, it was apparent that the cyclic strength of the sandy silt varied slightly between the two methods of sampling; the curve for the GP-S samples sits slightly lower than that for the D&M samples, although being broadly similar *CRR** (0.15 – 0.18). The difference could be due to the different sampling methods; the D&M sampling could have densified sandy soils more than the GP-S sampler, due to having greater side-wall friction on the inside of the sample tubes, leading to a slightly higher strength in the test, or differences in properties of the soils themselves. Conversely with fine-grained soils, the thin-walled tube of the D&M may have performed better, inducing less disturbance than the less-sharply angled cutting shoe of the GP-S sampler. It cannot be ascertained from this comparison which of these reflect the in-situ condition best.

As noted previously the V_S of the soils was measured in both the field and the lab, and the velocities once normalised for confining stress ($V_{S,1}$) may be compared, as shown in Figure 2. A lab-to-field $V_{S,1}$ ratio of 1.0 indicates no apparent disturbance. Most of the results had a ratio less than one, meaning the V_S was greater in the field than the lab measurements. The difference in measured V_S may be attributed to loss of 'ageing' effects, or disturbance to fabric and bonding. Despite our best efforts, this may have occurred during the sampling (shearing), removal to the ground surface (reduction in confining stress), freezing, transportation, sample extrusion (shearing), thawing or test preparation. It appears that the temporary loss of confining stress had an impact on the samples, as the shallower samples sit closer to a ratio of one. The sampling type did not appear to make a difference to the ratios, as both GP-S samples and D&M samples appear to follow same trend.

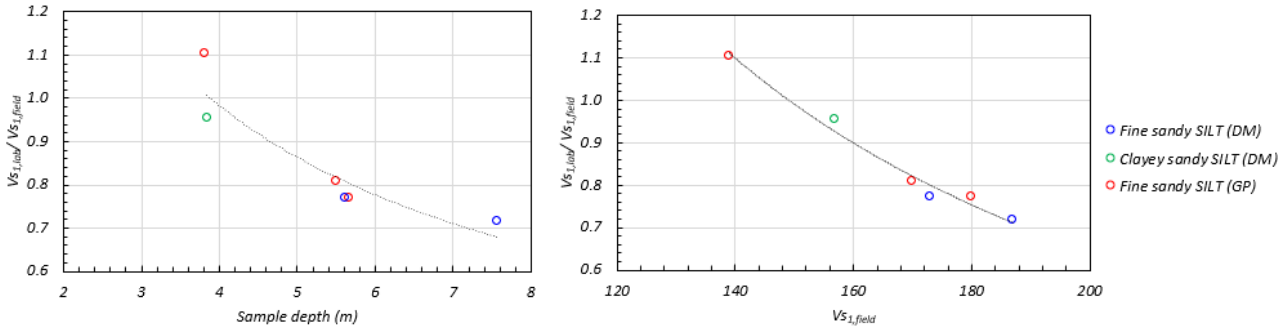

Figure 2. Ratio of lab-to-field measurements of shear wave velocity (stress normalised). Left: Varying with depth; Right: Varying with field measurement.

3.2 COMPARISON TO EMPIRICAL TRIGGERING CURVES

3.2.1 Comparison with BI14 CPT-based Triggering Curve

The CTX results were compared to the empirical liquefaction triggering curve by plotting the CRR^*_{15} values onto the BI14 liquefaction triggering chart. This required assigning a corresponding normalised cone resistance, q_{c1Ncs} value for each CRR^*_{15} value using adjacent CPT q_c values directly. As shown in Figure 3A, the (CRR^*_{15}, $q_{c1N,cs}$) data points plot well above and to the left of the conventional liquefaction CPT-based triggering plot, suggesting that under large strain, the BI14 CPT-based liquefaction triggering method is conservative when used on these soils without soil-specific corrections.

3.2.2 Comparison with KEA13 Shear wave velocity-based Triggering Curve

Figure 3B presents the plots of the lab-based measurement of Vs_1 against the measured CRR^*_{15}. The data points plot very close to the 85th percentile triggering curve or higher (P_L = probability of liquefaction), with the D&M piston samples plotting slightly higher than the 85th percentile curve. This suggests the empirical *Vs*-based triggering method (KEA13) appears to be slightly conservative for these soils. On the basis of these results, we proposed adopting the 50th percentile KEA13 triggering curve for our reassessment of the extent of triggering for the DSA as a moderately conservative assessment of our laboratory testing data.

3.3 PUMICE CONTENT INFLUENCE

In the latter stages of the DSA assessment, Asadi et al. (2023) published their findings and proposed method for assessing liquefaction resistance of sandy soils as a function of V_{S1} and pumice content (PC), which shows promise for future liquefaction assessments of these soils. We compared our results to their more extensive test data and trends, while noting the differences in fines content. Figure 4 presents their plot of CRR^*_{15} vs G_{max} data overlaid with our test data, where G_{max} is the small strain shear modulus ($G_{max} = \rho.V_S^2$). The CRR^*_{15} of pumiceous sands is greater than that for a normal (hard-grained) sand for a given G_{max}. It appears that our lab test results (PC 18-53%) for an interbedded sandy silt plot close to those of Asadi et al. with PC of 35-50%. Figure 5 presents a replot of Figure 3B, overlaying the recommended triggering curves from Asadi et al. (2023) which vary according to pumice content. This indicates that our data points plot close to the samples with a PC of 50 to >70%. The higher liquefaction triggering resistance may be on account of the in-situ fabric

effects of the natural samples, and possibly the high proportion of fines, which may attribute a different triggering resistance compared to the clean pumiceous sands that form the basis of the curves presented by Asadi et al. (2023). The higher fines content may also be expected to reduce the extent of crushing during penetration testing and cyclic loading for a given pumice content, as indicated by testing on a pure pumiceous silt by Chaneva et al. (2023).

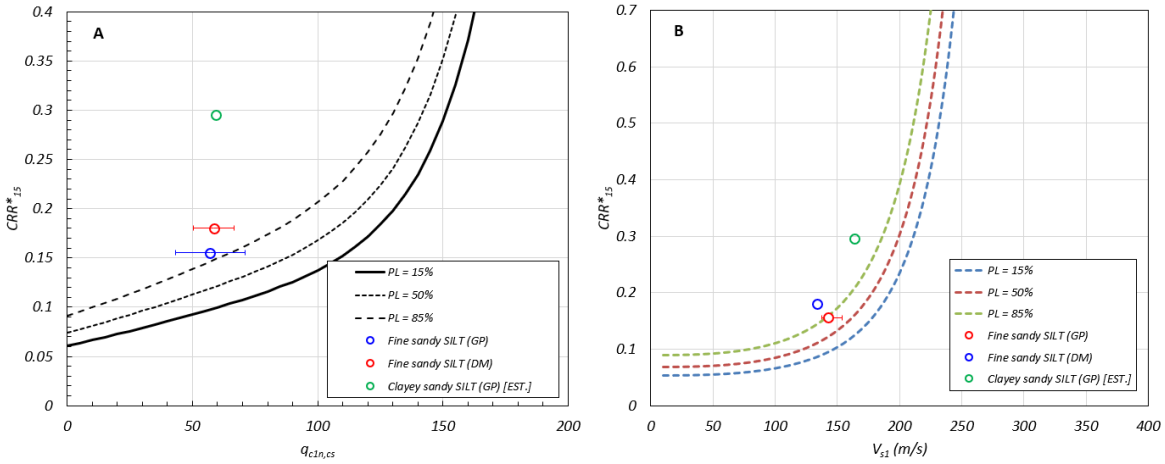

Figure 3A: BI14 CPT-based triggering curve with lab-test CRR^*_{15} and $q_{c1N,cs}$ from adjacent CPT. Figure 3B: KEA13 *Vs*-based triggering curve (FC=40%) with lab-test CRR^*_{15} and lab-tested V_{S1}. NB: The green dot is an estimate only (indicative). P_L = probability of liquefaction, where P_L=15% is the deterministic triggering curve.

The comparison of our results with Asadi et al. (2023) provided further justification for using a KEA13 triggering curve higher than the PL=15% curve recommended by KEA13 for inherent conservatism. In our liquefaction assessment, we therefore applied the PL=50% curve to the Matua Subgroup for the KEA13 method; this value is a moderately conservative, lower bound estimate of the appropriate PL triggering curve relative to the test data and as supported by the results published by Asadi et al. (2023). It is worth noting that this project involved the seismic assessment of an existing building rather than the design of a new building. In accordance with the EQ-Assess guidelines, this requires assessment for what is "probable", not what is "reliable" (i.e., as typically adopted for new build design).

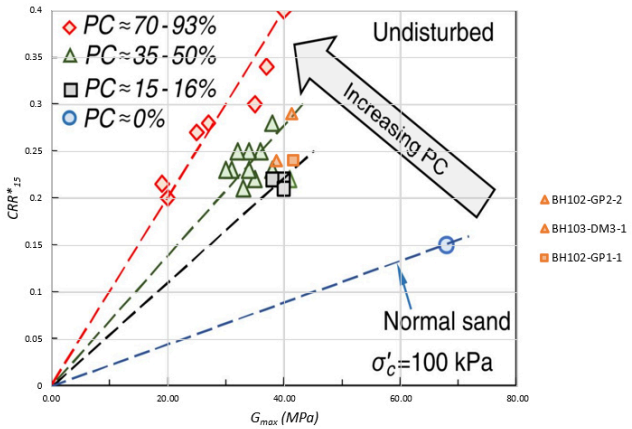

Figure 4. CRR^*_{15} vs. G_{max} plot with our test results (orange data points) overlaid the data and trends presented by Asadi et al. (2023), varying with pumice content (PC).

4 SUMMARY AND CONCLUSIONS

Previous DSAs indicated that, due to the liquefaction of supporting soils, a high-importance building in the Bay of Plenty region would be adversely affected by the performance of an adjacent steep slope at levels of shaking below the 'New Build Standard' as defined in the EQ-Assess guidelines. A suite of further field and laboratory testing, including advanced piston sampling and cyclic triaxial testing, was undertaken to characterise the cyclic resistance of the pumiceous Matua Subgroup deposits at the site and reduce our uncertainty with the use of empirical assessment methods applied to these soils. The CRR^*_{15} values obtained from the cyclic triaxial testing, when compared against the V_S-based empirical liquefaction triggering curve of KEA13, supported by the more extensive testing undertaken by Asadi et al. (2023), justified adopting the PL=50% liquefaction triggering curve as 'moderately conservative' for the liquefaction assessment, rather than the default PL=15% triggering curve as used with hard-grained soils.

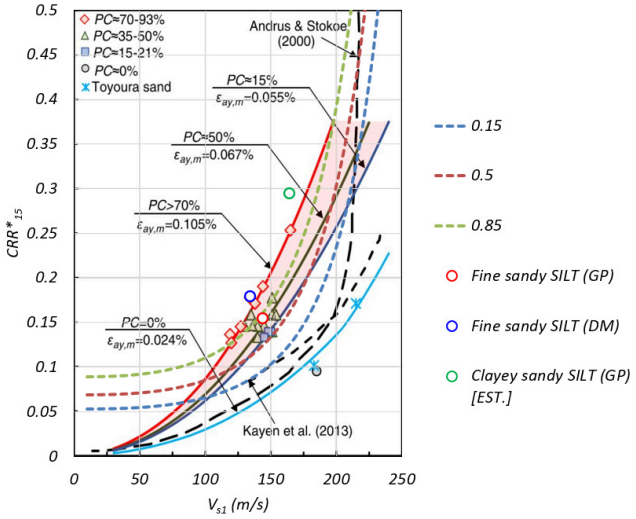

Figure 5. KEA13 *Vs*-based liquefaction triggering plot (FC=40%) and lab-test results (this study) imposed over Figure 15 from Asadi et al. (2023) that presents clean pumiceous sand *Vs*-based triggering curves as a function of pumice content compared to empirical *Vs*-based triggering curves for clean sands.

The adoption of the KEA13 PL=50% triggering curve for the liquefaction assessment significantly reduced the liquefaction extents within the Matua Subgroup unit, resulting in improvements to the slope stability and expected seismic performance. This, in turn, allowed for a significant reduction in ground improvement required to meet the desired %NBS. This provided significant cost savings for the Client as well as minimising disruptions to their business.

It has therefore been observed that, for high-consequence projects, benefits can be provided in the specification of high-quality undisturbed and specialised dynamic laboratory testing of pumiceous soil deposits, as recommended in MBIE Module 3. This comprehensive sampling and testing requires a lot of time and effort (and cost) but can provide an opportunity to go beyond the assumptions made in the simplified liquefaction assessment methods, which are derived from case histories of liquefaction occurrence following major seismic events of largely hard-grained soils. This testing can reduce uncertainty and inherent conservatism when applying these methods to pumiceous soils. New developments also occurred during the analysis process, with the recent publications by Asadi et al. (2023) and Cheneva et al. (2023) providing new insights to the expected response of pumiceous soils. These studies show promise to better inform cases where advanced sampling and testing may yield improvements to assessments in engineering practice and provide comparative data for their interpretation.

5 REFERENCES

Asadi, M.B., Orense, R.P., Asadi, M.S. & Pender, M.J., 2023. Empirical Assessment of Liquefaction Resistance of Crushable Pumiceous Sand Using Shear Wave Velocity. *J. Geotech. Geoenviron*. Eng. pp. 1-14.

Boulanger, R.W. & Idriss, I.M., 2014. CPT and SPT Based Liquefaction Triggering Procedures, California: Dept. of Civil and Environmental Engineering, University of California at Davis.

Chaneva, J., Kluger, M.O., Moon, V.G., et al. 2023. Monotonic and cyclic undrained behaviour and liquefaction resistance of pumiceous, non-plastic sandy silt. *Soil Dynamics and Earthquake Engineering,* 168. 107825.

Idriss, I.M. & Boulanger, R.W., 2008. Soil Liquefaction During Earthquakes, California: Earthquake Engineering Research Institute.

Kayen, R. et al., 2013. Shear-Wave Velocity-Based Probabilistic and Deterministic Assessment of Seismic Soil Liquefaction Potential. *J. Geotech. Geoenviron. Eng*., pp. 407-419.

NZSEE et al. 2017. Seismic Assessment of Existing Buildings – Section C4: Geotechnical Considerations, EQ-Assess.

MBIE/NZGS 2021. Earthquake geotechnical engineering practice. Module 3: Identification, assessment and mitigation of liquefaction hazards, Wellington: New Zealand Geotechnical Society Inc, Ministry of Business, Innovation, & Employment.

Orense, R.P., Pender, M.J. & O'Sullivan, A.S., 2012. Liquefaction Characteristics of Pumice Sands, Auckland: The University of Auckland Faculty of Engineering.

Stringer, M. 2019. Separation of pumice from soil mixtures. *Soils and Foundations*. 59: 1073-1084.

Stringer, M. et al., 2020. Recommendations for High-Quality Field Sampling using the Gel-Push Type S sampler, Christchurch: University of Canterbury.

Taylor, M.L., Cubrinovski, M. & Haycock, I., 2012. Application of new 'Gel-push' sampling procedure to obtain high quality laboratory test data for advanced geotechnical analyses. *Proc. 2012 NZSEE Conference.*

A JOURNEY THROUGH DIGITAL TRANSFORMATION IN MODERN DAY GEOTECHNICS

Chase Benson
Douglas Partners Pty Ltd

ABSTRACT

This paper presents the author's experience in driving the ongoing digital transformation amidst the dynamic landscape of technological evolutions and organisational adaption in modern day geotechnics.

The journey begins with recognition of the challenges of geotechnical logging as a graduate geotechnical engineer in an operating environment which is only beginning to understand the need to change arising from industry demands, spurred by technological advancements. The paper describes the organisational efforts aimed at facilitating digital transformation, and the multifaceted challenges that were encountered, such as transition from legacy systems, cultural shifts, and skill gaps. With hindsight, these obstacles can be appreciated as catalysts for innovation and resilience.

Concurrently, rapidly emerging technologies such as artificial intelligence, cloud computing and data analytics are impacting the digital transformation. Utilisation of these emerging technologies have been seen to improve customer experiences, unlock new avenues for growth but more importantly improve collaboration, knowledge-sharing and foster a culture of continuous improvement propelling the journey forward.

As the journey progresses, it becomes increasingly evident that digital transformation is not a simple "yes or no tick-box" but rather an ongoing pursuit in increasing agility and gaining competitive advantage with the specific needs of our clients and teams in mind.

1 INTRODUCTION

Digital transformation is disrupting geotechnical practice, and it affects all practitioners in various ways. Whether it is how field data is collected and presented, how problems are modelled and analysed, or how advice is delivered to clients, the digital transition the world is moving through has, and continues to, drastically change the way work is conducted (Nguyen, 2022). However, change is not always easy to implement and adopt, nor is it always welcome (Hayat, et al., 2022).

The intent of this paper is to discuss observations and experiences during the implementation of digital tools into geo / environmental engineering workflows and to highlight some key learnings from these undertakings.

Back in 2016 (when the author began his career), most of the steps noted above would have consumed a bunch of paper, and be transported to site in a manilla folder. Technology at the time was limited, with fieldwork supported by under-powered computing, a hand held GPS (accurate to ~ 5 m) and digital cameras.

Since 2016, there have been rapid developments in technology and increasing availability of processing power and data storage, which have in turn altered the way field investigations, analysis and reporting can be undertaken. Enhancements in hardware and communications devices and increased access and affordability of PCs, mobile devices and bespoke tools have seen the geo / environmental engineering landscape change from where it was just a decade ago. More recently the COVID-19 pandemic drove a sudden change to our work life balance by forcing us to consider working remotely away from our traditional office environments requiring the need to access project files and field investigation data remotely.

The author of this paper was fortunate to join the development to lead a process to replace traditional paper-based logging and manually-transcribed presentation of geotechnical data with digital acquisition of field data and software-optimised presentation of geotechnical logs.

2 THE "WHY" OF CHANGE

The drive to deliver digital data was, and continues to be, pushed along by increasing demands for digital engineering to facilitate data interoperability between software and processes at a local level, and engineering disciplines and construction teams holistically. Further, the direction of the digital future has been guided by advice provided by the Australian Government and adoption of digital engineering frameworks by State Governments.

During the mid 2010s, the author's organisation began to see requests from clients specifying "Submission of electronic output (MS Word, PDF and Other)". The "Other" quickly evolved to include the need to supply geotechnical data captured during investigations in the form of AGS 31. RTA 1.1. This data standard, which was released in Australia in 2007, was introduced to allow the transfer of geotechnical investigation data in a structured, low data cost format between the generator and the end client.

During this period, usage of the data in the AGS format after its generation was understood to be limited, and often requested by clients to close contractual requirements. As time went on, clients became increasingly aware of the data standard and began to leverage the data in various ways. However, the data standard required that the data be presented in a strict, structured manner which did not favour the sentence structured data that was typically produced at the time.

The author's organisation identified that the requirement to deliver standardised digital geotechnical data was increasing, often associated with expectations for large scale government projects, and that the available methods to transform the data from sentence structure to the required data standard were tedious, time consuming and costly. With an increase forecasted for spending on government projects at the time, shown in Figure 1 below, the need to develop and enhance the ability to produce structured digital geotechnical data was clear.

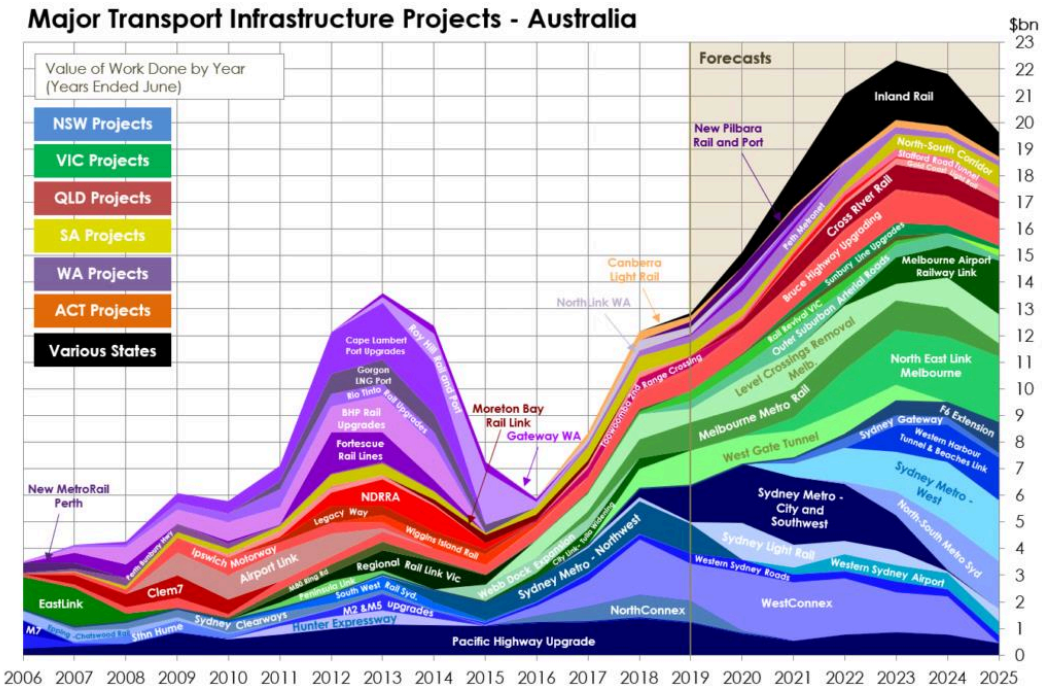

Figure 1: Forecast Spending on Major Transport Infrastructure Projects (Macromonitor, 2019)

3 THE "HOW" OF CHANGE

When the need for change has been identified, going out and purchasing the latest and greatest technological advancement may not always be the best way forward. Having recognised the need for change, the author joined a small innovation team within the organisation to analyse the workflow for the various components in the capture and presentation of geotechnical investigation data. At the time, much of the descriptive information on logs was hand-written in the style of prose. The analysis of this workflow, from field to client, indicated the best way to produce outputs with structured data was to begin the process by acquiring structured data. This paradigm shift began to unlock new ways in which field data could be collected and transferred through the project life cycle to meet client demands.

In order to enable engineers and scientists to collect field data in a structured manner, the innovation team trialled existing and emerging technologies to assess the suitability and operability of these tools against standard practice within the organisation. The assessment of the selected technological opportunities was conducted with a focus on possibility of achieving the following objectives:

- Enable increased ability to produce structured data to AGS standard with the capability to adjust the outputs knowing that changes of the standard were inevitable;
- Enhance quality of the organisation's field data product, being PDF geotechnical logs, by creating a method to systematically handle structured field data;
- Increase data processing efficiency by reducing data entry times; and

- Sustain current data recording/storage redundancy in the system in the event that hardware was damaged, lost or data corrupted.

In order to achieve these objectives, fundamental technical and cultural changes in the way field data was traditionally collected would need to be implemented across the organisation. After researching the different technologies available at the time, it became evident that there were hardware options available which met the above objectives and had been commercially available for several years.

These included using field tablets, digital pens, scannable sheets and direct entry laptops. After assessing these options, the digital pen was chosen, as it offered cost effective solution when attempting to issue to a significant quantity of field staff. It should be noted that none of the available tools assessed met the objectives of the assessment as an "off the shelf" solution.

As this did not constitute a fully-integrated, off-the-shelf system, it was recognised that the hardware which was selected by the team would require extensive computer programming skills and collaboration with its external providers to enable it to be integrated with existing systems. However, in addition to the required integration, the way in which field data would need to be collected would have to fundamentally change, requiring re-training of an extensive field team with various experience levels.

Importantly, it was recognised that consultation with internal stakeholders and the organisation as a whole would also need to be undertaken to ensure that the proposed solution would meet all demands beyond the experiences of those involved in the innovation team.

4 IT'S NOT ALWAYS EASY

Having chosen preferred technologies, the next step was to integrate the new hardware with existing systems, as the new hardware, although capable, was not established with the intention of connecting to geotechnical / geoenvironmental data base software from the field.

When beginning the process of implementing new technology and processes within any working environment, it is important to establish SMART goals (Doran, et al., 1981), that is, goals that are Specific, Measurable, Achievable, Relevant and Timely. From the beginning of implementing the new hardware and processes into the organisation, these SMART goals were quickly challenged, as integration and programming into existing systems was realised to be more difficult that initially anticipated. The interface through which the computer programming had to occur was not overly user-friendly, and the skills to undertake the programming in-house were limited to a very small group of people within the organisation.

In addition to the meeting the challenges of computer programming, as with many projects, management of scope creep also became important. While trying to reconfigure and reprogram existing systems, redevelopment of the interface in which field data was collected was also being undertaken and trailed within a small team of field staff. Following feedback from the field staff group, the interface would undergo various iterations which ultimately affected the way in which the redevelopment of internal systems was being programmed.

The undertaking of the system implementation project was managed in a more traditional, linear fashion as this was the experience of the innovation team to date, learnt through managing geotechnical projects. The problem had been defined and the solution was proposed, however. managing cultural change and keeping track of iterations of programming and design of field capture methods proved difficult.

While the system was being developed by the innovation team, word quickly spread throughout the organisation, of promises to meet objectives, and to exceed expectations pertaining to both the timely implementation of the new system and the significant improvements the new system would offer. A number of presentations were conducted across the wider organisation to introduce the new concepts and technology, with the intent to begin to shift organisational culture and paradigms. In an organisation that had been established at the time for more than 55 years, attempting to try and implement change against the momentum of well-established, ingrained experience proved more difficult than originally anticipated.

5 EXPECATION MANAGEMENT

Following a lengthy inhouse development phase of the project, the new hardware and newly developed digital workflows were ready to be tested. Initially trialled on relatively small projects with targeted variable geological profiles, the testing was to be undertaken by those who were also involved in the development of these new workflows. They were managed out of a single office where the support and resources to facilitate them could be provided. These

initial trials were considered to be relatively successful, in that they met the objectives which had been set out at the inception of the project. Nevertheless, as is found with the implementation of most new technological change, various development and user interface bugs were encountered, which were handled by the development team.

The trails were undertaken in a closed loop manner, with experience and feedback being limited to a single office within the organisation, in which the development team was situated and various learnings and fixes of various bugs were stored in the minds of those involved. Following the success of the field trials, the next step in the process would be to begin implementation of tested workflow into other offices across the organisation.

On the basis of these encouraging results, it was decided to roll the new process out to another, larger office. This was the largest office within the organisation, and the timing coincided with the commencement of a multimillion-dollar geotechnical / geoenvironmental investigation. The process was introduced to the team, with formal training provided to the field team and managers of the field investigation, and with remote support available to the investigation team to coach them through the process, as required. The paradigm shift in how the field team was to collect their investigation results represented a fundamental departure from the traditional methods which had been practiced and taught for generations. The result was that field staff became increasingly frustrated at trying to learn how to use new tools, in new ways, while also under the productivity targets set for the investigation. The learning curve proved steeper than expected, by both the development team and the field staff, suggesting that more training, under more favourable conditions, would have facilitated a smoother technological transition.

In addition to the re-training of engineers and scientists in the field, those processing and presenting the results of the field investigations were also seeing structured data for the first time. In contrast to simply transcribing what the field staff would write, they were now trying to identify which of the more than 70 different tabs the data records had to be stored under. The members of the production team also became increasingly frustrated with the new process. They too were under the productivity demands of the investigation, but encountered difficulty not only trying decipher where various individual records needed to be transcribed, but also identifying bugs in the new workflow which prevented data being pushed through the system.

The development team played a key role during the inaugural large project, attempting to manage expectations of the users whilst assisting the team to resolve issues on various fronts. Though the development team was limited in resources they continued to debug and develop the system, while at the same time assisting the investigation team to master the new process.

At the end of the investigation, the data was successfully supplied to the client in the required AGS format, though the process was not without its challenges, resulting in long working hours and countless outbursts of frustration from various team members. The result of this experience was that the investigation team would no longer support the new process by moving towards a direct entry method against the recommendations of the development team. Unfortunately the experiences from this project spread wide across the organisation leading to increased resistance from other offices/teams to adopt the new process into their project workflows.

Several months later, following further system development and refinement, another office was faced with the challenge of delivering AGS format data for a large scale investigation. The management team of the investigation, having been at the forefront of other emerging technologies in the geotechnical space during their career, understood some of the challenges of implementing change. It was decided that this would provide the next opportunity to utilise the new hardware and changes to traditional workflows to meet the requested delivery investigation results as AGS structured data. The difference was that the expectations for the team involved with this project were lower, and they would anticipate challenges and understand that some manual integration may be required to deliver the project in a timely manner, in the event that new bugs might emerge at critical moments.

The investigation team for this project faced similar challenges to the previous project, as new bugs emerged, and the development team worked to address them. However, as the initial expectations were more realistic, the frustrations were reduced and many of the tricks to making the system work efficiently were worked out “on the fly” by the field team, allowing the project to be delivered successfully.

Following the success of this project, that office continued to utilise the hardware and digital workflows and work with the development team to continue to debug and improve the system. In due course, with the system clearly and reliably meeting the intended objectives, It has been found that when comparing the time required to complete data entry for projects of similar quantities of data, that an increase in efficiency of more than 400% can be achieved, data storage redundancy is in place, and field staff are now being trained in the new methods at the start of their careers.

6 LESSONS LEARNT

When considering the adoption of emerging technologies to improve the organisation's business model, the "why" must be first well understood. The question that must be asked is "should we?" rather than "can we?" as without first understanding the anticipated benefits and risks of implementation, we can find ourselves drifting away from what our business and/or our clients are really needing from our services. In this journey, the why was well understood, as there were emerging trends in large scale, high value government projects, with an increasing demand for structured geotechnical investigation data (AGS 3.1 RTA 1.1) to align with the construction industry's utilisation of Building Information Modelling (BIM) (Morin, 2015).

Determining the "how" in change can be just as challenging. Often the allure of the latest technology can drive the decision to embrace it immediately, but it may not be the right way to solve the problem, or it may only be useful in solving a problem that is not significant for the organisation. Further, adoption of the wrong 'how" can make it difficult to achieve integration of new approaches into existing systems and work flows. For this project, the author believes that the hardware and software "hows" were well chosen, and that the bugs and technological issues that were encountered are an inherent part of first-principles development of a system to transition from manual transcription to digital capture and presentation of data. The how selected in this instance was always going to be challenging to implement, requiring a specific skill set to integrate an understanding of geotechnical / geoenvironmental investigation into the world of computer science. Following from the successful delivery of AGS data for the projects discussed above, the organisation, although having an established IT team, sought to employ a data manager with a focus on computer science. The purpose of the employment was to merge the geotechnical experiences of the development team with resources capable of integrating and managing the data which was now being generated by field teams. Strategically, it would have been beneficial to engage this expertise at the start of the process.

Field staff who had originally been involved in the field investigations eventually became significantly involved in the support of implementation of the new system. In time, some of the original innovation team would leave the organisation after providing a handover of the system to remaining team members. The change of project team lead to a rejuvenation in the project and soon other offices across the organisation were keen to get involved and begin utilising the system for various projects.

With the rejuvenation of the project also came a change in approach to project implementation. As discussed earlier, the project was managed in a more traditional linear fashion. An agile project management approach was adopted with the change which brought tools more tailored to design and implementation of new technology and changes to workflows. Staff have since joined the organisation with skills in this space to provide effective project manage of digital transformation projects of all types throughout the wider organisation. The organisation recognises the importance of change management and continues to focus on improvements in which change is managed across various aspects of operations.

In addition to the various lessons learnt through implementation of change within the organisation, none were more detrimental to the success of the project than the importance of managing of expectations. Early in the phases of the project, it was observed that there may have been little caution in managing expectations which ultimately promoted reluctance to adopt the improved processes across the wider organisation.

The release of AGS 4.1.1 AU 1.2, brought much needed simplification to the data standard, while also adding additional requirements for the supply of geotechnical data across the industry (Wade, et al., 2023). The fundamental way in which the hardware and digital workflow system was developed in this case has enabled the organisation to quickly adapt to and meet the new requirements of the change in standard with relatively minimal changes to systems already in place. This vindicates the "how" adopted in this case.

7 INTO THE IMMEDIATE FUTURE

There are various changes to the geotechnical engineering industry occurring as a result of the disruption that digital transformation is bringing. For example following the COVID-19 pandemic, the increased access to generative artificial intelligence has enabled common geo / environmental practitioners see data in different ways by unlocking the power of computer programming. Prior to the release of generative artificial intelligence in late 2022, programming would be done by members of the team who were recognised as having extensive computer skills, nowadays thanks to platforms such as Chat GPT and Copilot, programming is a skill that most now have access to.

Organisations are beginning to understand the importance of historical data, and there is even a push to establish publicly available centralised data bases to store geotechnical data (Thompson, 2016) (Och, 2021). Recent developments in technology, both hardware and software, are aiding organisations to establish cloud-based internal centralised data bases in the form packages such as OpenGround by Bentley Systems or CoreGS by Geroc. As these data bases grow both with future and historical data, there is an increased application in the space of probabilistic methods to utilise this data and further understand risks associated with various geotechnical problems.

The development of cloud-based computing is enabling mobile device interfaces to connect directly to the cloud, providing the ability to directly enter geotechnical / geoenvironmental data collected in the field to the cloud. Although the hardware and digital workflow which was discussed above continues to be utilised within the organisation, further there is an eagerness to begin using mobile devices to collect field investigation data. Recently recognition of the fact that there may actually be more than one way to collect geotechnical / environmental data has begun to emerge, but the way in which the data is stored and it utilised has become unanimous within the organisation.

8 CONCLUSIONS

There is benefit in having a willingness to leverage the resources we have access to, to make the most of new knowledge and emerging technologies. It is often observed that those team members who are technologically adept are early in their careers as engineers/geologists, while those with significant engineering experience can display increased resistance (decreased aptitude) to change, and to require more assurance when adopting emerging technologies. There has been significant success witnessed when practitioners of all generations combine with one another in teams to enable organisational growth through changes to digital workflows.

Implementing new technological advances into our workflows needs to consider the tools themselves, the implementation process and the psychology of behavioural change. Although the tools and our teams are often considered separately, in order to achieve successful change, both need to be managed simultaneously throughout the process to ensure positive user experiences.

When an organisation is considering the implementation of new technologies or changes to workflows, the need for the change should first be evaluated and understood, and the potential benefits and risks assessed. Even if a new technology is heralded as must-have or game-changing, the first question should really be asked is “how would this improve our current efficiencies?” and not “how quickly can I get one?”.

9 REFERENCES

Hayat, Q., Muir, J. W. & Nelson, H. E., 2022. “Challenges to Digital Transformation in Geotechnical Engineering.” Melbourne, Victoria, *Australian Geomechanics Society Victorian Symposium Digital Geotechnics*, pp. 63-71.

Macromonitor, 2019. Australian Construction Outlook, s.l.: s.n.

Morin, G., 2015. “The Benefits of Geotechnical BIM.” *Engineers Australia,* 87(5), pp. 78-79.

Nguyen, L., 2022. “Digital Optimisation Workflow in Early Project Phases and What it Can Bring When Looking at the Macleamy Curve.” Melbourne, Victoria, *Australian Geomechanics Society Victorian Symposium Digital Geotechnics*, pp. 72-77.

Och, D. J., 2021.0 “A Smart Geotechnical and Geological Approach For Future Building and Transport Infrastrcutre Projects.” Sydey, New South Wales, *Australian Geomechanics Society Sydney Chapter Symposium*, pp. 66-71.

Thompson, T., 2016. “A 2016 Case for Public Geotechnical Databases.*” Geotechnical and Geophysical Site Characterisation 5*, pp. 1045-1050.

Wade, P. et al., 2023. “Development of AGS 4.1 AU Format for Geotechnical Data Transfer in Australia.” Cairns, Queensland, *Proceedings of the 14th Australia New Zealand Conference on Geomechanics*.

REMEDIATION OF CUT AND FILL SLOPE ALONG LINEAR TRANSPORT INFRASTRUCTURE POST-CYCLONE JASPER, QLD

Ali Rukh
WSP Australia Pty Ltd, Brisbane, Australia

ABSTRACT

In response to the significant infrastructural damage inflicted during Tropical Cyclone Jasper (TC Jasper) between 13 and 18 December 2023, this paper presents the adopted approach to the restoration of linear transport infrastructure, particularly focusing on slope remediation at one of the most severely affected site. In collaboration with the Client, WSP carried out a detailed design to address slope instability at this location. An initial aerial inspection identified a compromised fill embankment and an exposed old retaining wall. An ensuing site inspection and slope risk assessment revealed stability risks at the downslope embankment, resulting in the temporary cessation of operations. In consultation with the stakeholders, WSP conducted an options analysis to explore temporary and permanent treatment measures to restore the asset promptly. After options analysis, WSP undertook a detailed design of two preferred treatment measures related to (i) remediation of a 30 m section of the downslope embankment and (ii) construction of temporary deviated alignment by excavating into the upslope batter and widening formation. The excavation of the cutting, measuring 145 m in length and up to 15 m in vertical height, was undertaken in the presence of WSP geotechnical engineers. A combination of passive dowels, reinforced shotcrete, pinned rockfall mesh and subsurface drainage enhancements were proposed for permanent treatment. The design considered local and global slope instability mechanisms, site constraints, and sensitive environmental and cultural heritage settings. Durability requirements were set for a 100-year lifespan for permanent in-ground elements, considering the site's tropical environment and high annual rainfall.

1 BACKGROUND

Over six days between 13 and 18 December 2023, intense rainfall of accumulated total of ~1,891 mm (equivalent to be in the order of a 1 in 50 year to 1 in 100 year average recurrence interval (ARI) storm event) was recorded in the nearby weather station 2 km north of the site associated with TC Jasper (Sugawara et al, 2024). After an initial aerial inspection conducted by the Client and WSP, twenty-six (26) sites were identified as requiring remediation along the transport corridor, including erosion of fill embankments by the elevated river water level and landslide of upslope native batters. The site with the highest priority was selected as the primary example for this paper. The project site is composed of a linear transport corridor constructed adjacent to a major river. It is located within the Djabugay Nation Native Title Claim and the environmentally sensitive Wet Tropics World Heritage Area (WTWHA). The elevated water levels in an adjacent major river resulted in extensive erosion to a section of downslope fill embankment supporting the culturally significant transport corridor in Far North Queensland (FNQ) and exposing an old-buried relic retaining wall. To minimise the economic impact caused by the prolonged suspension of the transport route, a 145 m long section of the alignment was widened by excavating into an adjacent upslope cutting, enabling the alignment to be shifted away from the affected downslope embankment and allowing operations (with restrictions) to resume. Due to the environmental and cultural significance of the site and the proximity to the property boundary, the cutting was steeply profiled with marginal slope stability in the long term.

This paper examines the site inspection, intrusive geotechnical investigation, slope risk assessment, and design approach for the remediation strategy of the affected downslope embankment, which experienced instability within the fill embankment, as well as the design of newly excavated upslope batter in a culturally significant transport corridor.

2 GEOLOGY

2.1 GEOLOGICAL AND GEOMORPHOLOGICAL SETTING

The site is located 8.0 km from the coastline and is composed of the geological unit Hodgkinson Formation – mudstone (Dh/m) as per 1:100k Detailed Surface Geology (DNRME, 2018). The Dh/m is a low-grade metamorphic rock derived from mainly sedimentary rock deposited into a marine basin; the Hodgkinson Basin, between late Silurian (420 Ma) to early Carboniferous (360 Ma) (Willmott & Stephenson, 1989). This basin was about 10 km thick, 160 km wide and stretched 340 km from Cooktown to Tully in FNQ (Martin, 2000). The Dh/m consists of fine-grained, dark grey, thin bedded mudstone (locally phyllitic) with subordinate thin to thick bedded quartzo-feldspathic arenite beds, minor chert, and basalt (Bain & Draper, 1997) that have been metamorphosed to micaceous phyllite. The 1:500k Regional Surface Geology (DNRME, 1997) indicates two prominent structures: (i) sheared zones structures running from north-west to south-east parallel to the river system, potentially resulting in broken rocks as illustrated in Figure 1; (ii) complex gorge system formed through erosion of weaker planes within the Hodgkinson Formation resulting in high defects due to stress relief (Fell et al, 2015). The formation at the site is steeply dipping, highly folded, foliated, and often overturned with prominent cleavage, resulting in high discontinuities (Denaro et al, 2007).

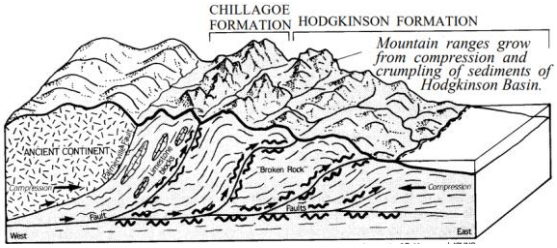

Figure 1: Geological block diagram depicting creation of Hodgkinson Formation (Willmott & Stephenson, 1989)

The outcrops of the unit are generally deeply weathered and consist of varying depths of extremely weathered material, residual soils, and colluvium soils along the mountain slopes. Fresh rock exposure is found mostly in the rejuvenated sections of the river system (Keyser & Lucas, 1968).

3 INVESTIGATIONS

A combination of non-destructive and destructive investigations were conducted throughout the project area to assess subsurface conditions in conjunction with topographic elevation surveys to assist in the development of a geotechnical ground model for use in the detailed design of the permanent works.

3.1 INITIAL AERIAL INSPECTION

An initial geotechnical inspection of the project site was undertaken by helicopter in December 2023, shortly after TC Jasper, to assess damage along the entire infrastructure alignment. Figure 2 provides an aerial overview and closeup of the affected section of the downslope embankment. Elevated river water levels resulted in extensive scouring of the embankment and underlying subsoils and exposure of a relic-buried concrete retaining structure constructed in the 1950s.

Figure 2: Aerial photo of the affected site by TC Jasper (taken from a helicopter).

3.2 INTRUSIVE INVESTIGATION

A targeted intrusive investigation was completed for the subject areas to inform the detailed design. The investigation consisted of three (3) geotechnical boreholes drilled to depths between 3.0 m to 15.0 m below ground level (BGL) and twelve (12) dynamic cone penetration (DCP) tests to depths between 0.5 m to 2.9 m BGL as illustrated in Figure 3. Standard Penetration Test (SPT) was conducted in soil strata at 0.5 m intervals to obtain soil strength parameters of subsoil materials. Table 1 outlines the typical material description based on the sub-surface material units encountered.

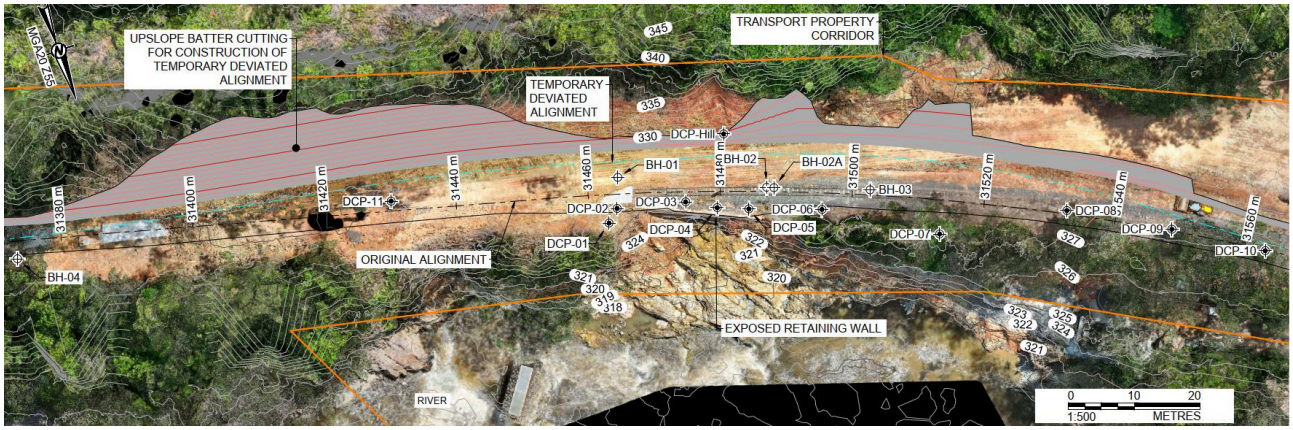

Figure 3: Intrusive site investigation plan for the affected site.

Table 1: Summary of encountered sub-surface material units

Material units	Depth (BGL)	Description
Unit 1 – Fill	0.0 m – 1.0 m	Variable fill materials, typically SAND and GRAVEL.
Unit 2 – Residual Soil	0.5 m – 3.0 m	Low to high plasticity Sandy CLAY, part of residual soils with stiff to very stiff consistency correlated with SPT results.
Unit 3 – XW to HW Phyllite	1.2 m – 9.6 m	Extremely to highly weathered (XW/HW) phyllite, low to medium plasticity Clay to Sandy Gravelly CLAY with a consistency of stiff to hard.
Unit 4 – MW to SW Phyllite	7.0 m – 15.0 m (till termination)	Moderately to slightly weathered (MW/SW) phyllite, medium strength, and indistinctive bedding at a dip of 60 to 80 degrees with chert-enriched localised zones. The defects consisted of sub-horizontal 5^{o} to 30^{o} joints and sub-vertical 60^{o} to 90^{o} joints forming a blocky structure less than ~0.01 m^{3}. The defects were mainly described as cleaned to iron stained, planar to undulating, and rough with spacing within the range of 30 mm to 300 mm. Based on variable joint orientation, the persistence was judged as likely to be limited to a few metres.

The reported Rock Quality Designation (RQD) values for Unit 3 ranged from 0% to 38% and for Unit 4 from 40% to 89%, with the average RQD for moderately or less weathered phyllite being over 60%. The strength of phyllite varied depending upon the weathering condition. Point Load Index (PLI) tests showed high variability in strength, with Unit 3 having axial PLI values of 0.17 MPa and Unit 4 ranging from 0.28 to 1.75 MPa. Diametral PLI results for Unit 3 ranged from 0.06 to 0.99 MPa, and Unit 4 from 0.81 to 4.75 MPa. The ratio of lateral to compressive strength (~3) suggests high horizontal stress near the valley floor (Fell et al, 2015).

4 HAZARD ASSESSMENT

4.1 GEOTECHNICAL DOWNSLOPE RISK ASSESSMENT

The affected section of the embankment was assessed to be ~30 m in length and partly supported by an old concrete retaining wall measuring ~16 m (l) x 3.5 m (h) x 0.4 m (t) and profiled at ~80 degrees. As-constructed details of the wall were unknown; however, a review of available historical imagery indicates the wall was constructed in the 1950s. The wall was observed to be in reasonable condition with no apparent signs of distress except for a local undercut (void). The embankment slope on either side of the retaining wall was 8 m to 11 m high and grades at ~45 to 60 degrees, locally steepening to ~70 to 80 degrees near the crest. The lower riverbank consists of highly undulating and stepped bedrock outcrops. Materials exposed in the upper proportion of the embankment consist of localised wedge fill, underlain by native subsoil units (colluvium and residual soil) and extremely weathered rock (phyllitic), transitioning to low to medium strength or better phyllite. An ground-based field photo of the affected downslope embankment is shown in Figure 4.

Figure 4: Ground-based field photo of the affected section of the downslope embankment.

A slope risk assessment for the affected embankment was carried out in December 2024 in accordance with the TfNSW Geotechnical Risk Assessment and Hazard Management (2019) and modified risk matrix per ongoing Sydney Trains Western Line slope risk assessments (2023 – 2026). The assessment indicated two main hazards: (**Hz1**) quasi rotation-translational slide failure mechanism and (**Hz2**) local failure of the existing retaining wall. The risk rating for Hz1 was assessed to be undesirable high risk (B-, P1), with the risk to loss of life and damage to the transport infrastructure to be Critical. Similarly, Hz2 was assessed to be a tolerable medium risk (C+, P1) with a risk to fatality and damage to transport infrastructure to be Critical. Due to the assessed critical risk level, an early warning system was implemented, including tiltmeters at selected locations on rock face and retaining wall to monitor displacements. Furthermore, the option to widen transport formation for temporary deviated alignment was recommended to minimise risk from slope instability, prevent financial losses from transport disruption and recommence operations.

4.2 GEOTECHNICAL UPSLOPE SLOPE RISK ASSESSMENT

The original transport formation was widened as part of the temporary transport deviation works by excavating into an upslope batter, resulting in an overall transport formation width of ~10 m. This allowed a section of the asset to be subsequently shifted ~5 m away from the crest of the affected downslope embankment and old retaining wall and provide access for downslope embankment remediation. After remedial works, it is intended that the asset will be relocated to its original alignment. A site-specific geotechnical slope risk assessment for the upslope cutting was conducted using a method similar to the downslope embankment. The risk assessment consisted of surface mapping (derived from photogrammetry completed by ADAM Technology using 3DM Analyst software) to characterise the cutting into geological/geotechnical zones, followed by identification of hazards, the associated likelihood and consequence of rockfall or debris flow failure and corresponding risk ranking. The risk ranking was used to develop a catalogue of recommended short-term risk mitigation measures and surveillance requirements to appropriately manage the geotechnical risk to asset users. From a geotechnical stability perspective, the excavated face was characterised by four (4) distinct zones, as shown in Figure 5.

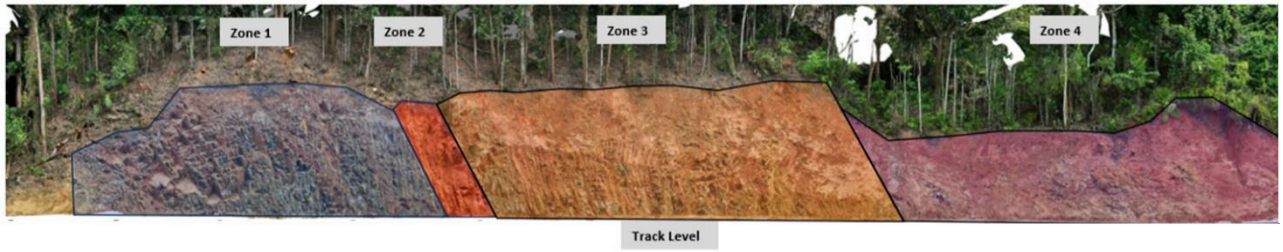

Figure 5: Key zones identified across the excavated upslope cutting.

The results of the slope risk assessment for each zone are outlined in Table 2 and illustrated in Figure 6. Due to the assessed critical risk level, an early warning system was implemented including: (i) crack monitoring gauges; (ii) a camera to record activity on the excavated face; (iii) an automated continuous laser scanner system within Zone 1 and Zone 3 with 30 minutes alert response time; (iv) implementation of existing risk management plan and transport inspection; (v) reduced rainfall trigger level to 50% less than previous trigger level; (vi) implementation of temporary speed restriction upon approach to the site; and (vii) temporary slope stabilisation measures such as reprofiling; till permanent remediation measures are implemented.

Table 2: Summary of slope risk assessment of upslope cutting

No.	Slope description	Failure mechanism	Risk Rating[1]
Zone 1	Fractured-blocky rock mass up to 12 m high with sub-vertical joints, a basal plane dipping ~35 – 40 degrees, and defects filled with soil and roots, indicating groundwater percolation.	"Structurally controlled" large potential "wedge" failure sliding along on a basal plane, ~10 m W, 10 m H, 1 – 5 m D, resulting failure volume of 100 to 150 m^3 with individual block up to 1 m.	(B+) Undesirable (High) **Critical**
Zone 2	Up to ~10 m high, ~80 degree slope of pale brown clayey sand/ sandy clay fill.	Localised surficial instabilities (rill erosion/ soil slumping), Estimated failure volume <10 m^3 mainly soil with isolated blocks up to 0.4 m in size.	(B-, P1) Undesirable (High) **Critical**
Zone 3	Up to 9 m to 12 m high at ~80 degree slope, locally flattening to ~60 degrees at the upper slope, variable weathered rock with closely spaced sub-vertical dipping joints.	Localised rock fragments, small block detachment, and potential surficial instability within the overlying soil mantle.	
Zone 4	Up to 4 m to 7 m high at ~45 degree slope, overlaid by native hillslope at ~35 – 45 degrees, mostly soil slope with weathered rock exposed ~2 m above the track level.	Erosion and potential rotational slides within the range of 20 to 30 $m^{3,}$ possibly extending to the track.	

Note:[1]Risk rating assessment was completed based on TfNSW Geotechnical Risk Assessment and Hazard Management (2019) and the modified risk matrix per ongoing Sydney Trains Western Line Slope Risk Assessments (2023 – 2026).

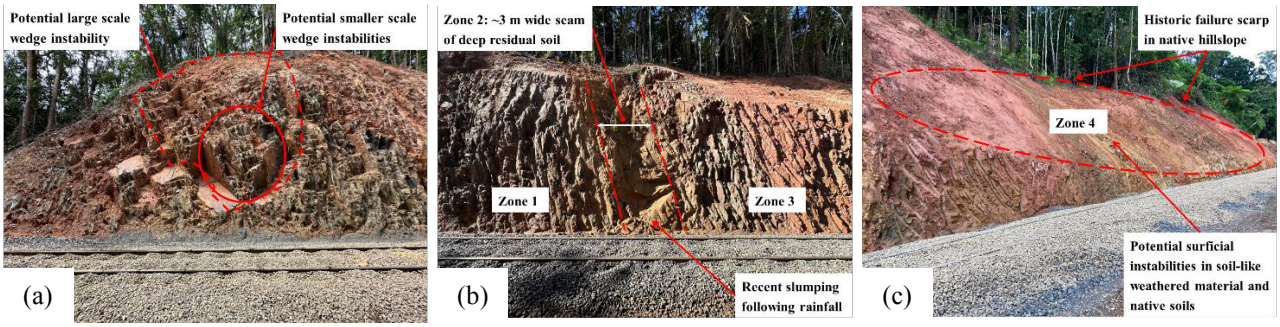

Figure 6: Key zones identified across the excavated upslope cutting: (a) Zone 1 shows potential large-scale wedge instability, (b) Zone 2 shows deep-soil seam, and Zone 3 shows potential isolated block detachment, (c) Zone 4 shows potential surficial instability

5 REMEDIATION DESIGN

5.1 DOWNSLOPE EMBANKMENT

Geotechnical model and design parameters were developed based on a literature review using Burt Look's Handbook of Geotechnical Investigation and Design Tables (2014), intrusive site investigation, surface mapping, site observation, and back analyses of the failure slips. The rock mass Mohr-Coulomb (MC) equivalent strength parameters were estimated using the Rocscience program RocLab based on the Hoek-Brown (HB) failure criterion (Bertuzzi, 2019). The slope stability assessment was carried out using the Geostudio program SlopeW. For back analyses, a factor of safety (FoS) less than or equal to 1 was targeted for wet condition to calibrate and validate the material parameters. The wet condition was simulated using a pore pressure ratio (r_u) available in the program. After validating the geotechnical model, the stability of passive dowels with reinforced shotcrete was analysed in accordance with the Transport and Main Roads Geotechnical Design Standard Minimum Requirement (2020). The bond strength between the ground and the passive dowels was determined from the material strength parameters and experience on similar past projects. The analyses considered instability mechanisms: surficial instabilities within the pre-existing fill and native subsoils and deep-seated quasi-rotational/translational failures extending into the underlying extremely weathered and low-strength phyllite. Moreover, a sensitivity analysis was undertaken, considering an array of credible phreatic surface cases and water levels within the adjacent river system and potential undercutting of the lower riverbank due to erosion over the design life. The design included 8 m and 10 m long passive dowels (28 mm diameter) encased in an HDPE sheath, installed within a 150 mm drill hole at a nominal staggered 1.5 m grid spacings and fitted with terminations consisting of a steel bearing plate and locking nut. The hard facing design consisted of 200 mm thick shotcrete, with 40 MPa concrete, including steel reinforcement consisting of SL81 steel mesh and an additional two N16 bars placed horizontally and vertically at each dowel head. Enhancements to subsurface drainage were incorporated into the design to prevent excess porewater generation behind the hard facing. The subsurface drainage included 10 m long inclined seepage drains at 4 m spacing, 170 mm wide diagonal placed strip drains at 3 m horizontal spacing, and 50 mm diameter weep holes at 3 m grid spacing.

5.2 UPSLOPE CUTTING

Three (3) geotechnical models were developed to represent varying slope geometry, geotechnical conditions and potential instability mechanisms identified along the cutting. The global instability mechanisms were assessed, adopting a similar analysis approach to the downslope embankment design. Additionally, a kinematic stability assessment for potential structurally controlled failure mechanisms within the rock mass (planar, wedge, toppling) was completed using DIPS 8.0 and Unwedge software developed by Rocscience based on the defect orientation data obtained from the photogrammetric mapping. The cutting's overall dip and dip direction was 80/015, consisting of four prominent joint sets (81/243, 82/163, 26/028, and 75/306) intersecting with the slope face. Local stability mechanisms were evaluated using Ruvolum software developed by Geobrugg, the manufacturer of the proposed pinned rockfall mesh system. Analyses considered local instability mechanisms in the form of simple wedge-shaped failures and slumps parallel to the slope face between the individual passive dowels. The Zone 1, 3 and 4 of the upslope area consisted of 6 m long passive dowels (28 mm diameter) at nominal staggered grid spacings between 1.5 m and 2 m and fitted with terminations consisting of a spike plate with domed locking nut, rock mesh (Proprietary Geobrugg TECCO G65/3) and erosion control matting (Proprietary Geobrugg TECMAT). The installation of rock mesh consisted of 14 mm diameter steel perimeter ropes, 4 m long perimeter rope anchors dowels, and 2 m long profiling dowels installed perpendicular to the local slope face. The subsurface drainage was enhanced by adopting inclined seepage drains of 8 m in length and at 4 m staggered spacing. A key selection criterion of the pinned rockfall mesh was the ability of the slope to naturally revegetate in the medium to long term, thereby enhancing visual aesthetics. The Zone 2 of upslope cutting consisted of a hard facing with integrated passive dowels to address the presence of low strength and highly erodible subsoil material exposed in the cut face.

5.3 DESIGN FOR DURABILITY

The in-ground elements of the permanent works were developed based on a 100-year design life in consultation with the Client. Durability requirements for passive dowels were in accordance with TMR specifications, consisting of cement grout annulus around dowels, HDPE sheath, epoxy powder coating, hot-dipped galvanised (HDG) and a sacrificial steel annulus of threadbar. The durability of the exposed elements was less than 100 years and required inspection and maintenance regime over the service life of permanent works.

5.4 CONSTRUCTION QUALITY CONTROL

The permanent design included construction quality control specifications: (i) ultimate load testing on two (2) sacrificial passive dowels installed within target geotechnical units to verify the ultimate bond resistance between grout-to-ground interface and validate design assumptions; (ii) acceptance load testing on min. 10% of the total passive dowels; (iii) compressive strength testing of grout cube and concrete cylinder samples; and (iv) full-time geotechnical site supervision.

6 PROJECT LEARNINGS

- The as-constructed information for the old retaining wall was not available. Orientated borehole drilling through the wall was avoided to prevent triggering further slope instability due to drilling. The boreholes were positioned beyond the influence zone of the retaining wall to manage the risk to the field personnel and plant during the investigation.
- In the absence of site-specific hydrogeological and hydraulic data, a sensitivity analysis was considered with an array of credible phreatic surfaces, elevated water levels within the river system and potential undercutting of the treatment area due to erosion of native materials in the lower riverbank over the design life.
- Due to limited safe access to undertake borehole drilling below the embankment and along the crest of the upslope cutting, the design was developed on the basis that key elements of construction are undertaken under the surveillance of the designer to assess actual conditions encountered during construction and ameliorate the design accordingly to ensure that the as-constructed treatment works satisfy the design intent.

7 ACKNOWLEDGEMENTS

The author wishes to thank WSP for supporting the publication of this paper. The opinions expressed are solely those of the author and do not necessarily reflect those of WSP. The author also extends appreciation to Joseph Parisi and Dr. Pramod Thakur, both of WSP, for their support and guidance.

8 REFERENCES

Bain, J.H.C. and Draper, J.J. (1997). North Queensland Geology. Australian Geological Survey Organisation (AGSO) Bulletin 240, and Queensland Department of Mines and Energy Queensland Geology 9. Australian Geological Survey Qrganisation and Department of Mines and Energy. 225-279.

Bertuzzi, R. (2019). Estimating Rock Mass Properties 1st Edition. Pells Sullivan Meynink (PSM).

Denaro, T., Ramsden, C. and Brown, D. (2007). Queensland Minerals: A summary of major mineral resources, mines and projects 4th edition. Queensland Department of Mines and Energy.

Department of Natural Resources, Mines and Energy (DNRME). (2018). Surface Geology of Cairns 1:100,000 Sheet 8064 Compilation Map. Department of Natural Resources, Mines and Energy. Queensland Government.

Department of Mines and Energy (DME). (1997). Regional Geology of Hodgkinson Province 1:500,000. Australian Geological Survey Organisation. Queensland Government.

Department of Transport and Main Roads (DTMR). (2020). Geotechnical Design Standard – Minimum Requirements. Department of Transport and Main Roads. Queensland Government.

Fell, R., MacGregor, P., Stapledon, D., Bell, G. and Foster, M. (2015). Geotechnical Engineering of Dams 2nd edition. Tayler & Francis. DOI: 10.1201/b17800

Keyser, F.de. and Lucas, K.G. (1968). Geology of the Hodgkinson and Laura Basins, North Queensland. Department of National Development: Bureau of Mineral Resources, Geology and Geophysics. Commonwealth of Australia.

Look, B.G. (2014). Handbook of Geotechnical Investigation and Design Tables 2nd Edition. Taylor & Frances. DOI: 10.1201/b16520

Martin, S. (2000). Wet Tropics Geology. *Tropical Topics*. Environmental Protection Agency (EPA). Cairns, Australia, 63, 1-8.

Sugawara, J., Lester, J. and Sundaram, M. (2024). Reconnaissance Report on Geotechnical Damage Caused By Tropical Cyclone Jasper in December 2023. *Australian Geomechanics*, 59(2), 75-94. DOI: 10.56295/AGJ5923.

Transport for New South Wales (TfNSW). (2014). Geotechnical Risk Assessment and Hazard Management. Transport for New South Wales. NSW Government.

Willmott, W.F. & Stephenson, P.J. (1989). Rocks and landscapes of the Cairns district. Queensland Department of Mines.

ASSESSMENT OF COMPRESSIBLE SOILS AND DIFFERENTIAL SETTLEMENT FOR A PROPOSED COOLING TOWER AT TE MIHI POWER STATION, TAUPO

Jasmine Walden[1], Robert Taylor[2]
[1]*CMW Geosciences, 1422 Hinemoa Street, Rotorua 3010, PH (07) 975 0916; email jasminew@cmwgeo.com*
[2]*CMW Geosciences, 116 Cameron Road, Tauranga , PH (07) 975 0916; email robertt@cmwgeo.com*

ABSTRACT

This paper presents the challenges faced during a geotechnical assessment to support the design of a new Cooling Tower within the Steam Turbine Generator (STG) Platform at Te Mihi Power Sation, Taupo, New Zealand. Along with a variable ground model as a result of extensive historical cuts and fills undertaken within potentially compressible soils across the platform, a previously constructed surcharge in the form of an earthfill embankment also extends across a portion of the future Cooling Tower footprint and has remained in place for the past 12 years. The extents of these soils and historical loading sequence were modelled using Settle3 software to predict potential future total and differential settlement associated with the construction of the proposed Cooling Tower spanning across these various zones.

Analysis showed that total settlements including elastic, primary consolidation and creep for a 50-year period in response to the Cooling Towers' unfactored widespread loads were up to 164mm. Maximum angular distortions of 1:40 were predicted to occur across the transition zone into the previously surcharged area.

An initial option to address the predicted settlements was to extend the existing preload embankment to encompass the remainder of the Cooling Tower footprint that extends over these compressible soils. The intent of this is to over-consolidate the compressible soil in the remainder of the platform to reduce post-construction settlements and differential settlements to within tolerable levels.

Keywords: Consolidation, settlement, preload, compressible soils, Settle 3

1 INTRODUCTION

A geotechnical investigation and assessment was undertaken by CMW Geosciences (CMW) to inform the extent and depths of the compressible soils previously identified within the Steam Turbine Generator (STG) Platform and to undertake an assessment of possible settlements associated with the construction of a new Cooling Tower at Te Mihi Power Station, Taupo.

The proposed Cooling Tower (denoted number 3) is an approximately 236m long, 23m wide structure comprising 13 cells which is used to cool the steam from the turbines and condense it back to water. The tower has an approximate 15kPa load and is to be constructed on a shallow foundation, which given its considerable length, is susceptible to differential settlements.

The location of the proposed tower within the existing Te Mihi Power Station is directly to the south of the existing Cooling Tower 2 where a near level hardstand area is situated at approximately RL 515m. An existing earthfill embankment extending in an east to west direction exists across the western portion of the STG Platform (see Figure 5) and measures approximately 98m by 23m and 3metres in height. The intent of this platform was to over-consolidate previously identified soft soils, however, now only extends over a portion of the propose cooling Tower footprint. Although settlement monitoring pins were positioned within the embankment during construction, no survey information of the settlement monitoring from the 12 years since this embankment was constructed is available.

Based on historic records and recent investigation data, the site has a very variable soil profile. The original topography that spanned across the STG Platform comprised an elevated terrace that extended into a gully system. Extensive cuts and fills of up to 10m and 6m respectively have since occurred to construct the level platform that exists today. The cut fill line runs directly through the Cooling Tower footprint. It is assumed that the preload fill embankment was placed to facilitate both consolidation of the identified compressible soils in the western half of the platform as well as mitigate potential differential settlements associated with the transition from cut to fill across the platform.

Since those prior earthworks and construction of the preload fill embankment, the location of the Cooling Tower footprint has since been moved approximately 9m west and 7m north and therefore extends outside of the preload area. This adds further complexities to the potential for differential settlement and the reason this assessment was facilitated.

2 SITE HISTORY

Initial geotechnical investigation was completed by Maunsell Limited (Maunsell, Aecom. 2007) and Beca (Beca. 2009) between 2007 and 2009 to support the development of the existing Power Station. Earthworks undertaken for the existing Power Station and wider area were completed between 2011 and 2012.

MSP JV (McConnell et al. 2012) completed a series of Cone Penetrometer Tests (CPTs) in 2012 following the completion of earthworks to confirm the adequacy of the fill placed and to observe the nature of the insitu soils beneath the fill. The report indicates that the insitu soils beneath the fill had a similar pattern of variability as encountered at the other two Cooling Tower locations directly to the north. More compressible layers were identified particularly within the western end of the platform and chiefly comprised silt mixtures. In some instances, these soft bands were observed deeper than the previous Cooling Towers at depths of between 12m to 14m below ground level.

A review of historical aerial photographs for the site suggests this preload fill embankment was constructed between 2012 and 2013 following completion of the site earthworks and construction of the current Power Station. The preload spans the fill placed during earthworks and the cut fill interface, as well as the extents of the compressible soils encountered within the MSP JV CPTs.

CMW completed additional investigation in 2023 to support the design of the proposed Cooling Tower and to facilitate laboratory testing required for the detailed design. A series of CPTs and machine boreholes were completed across the STG Platform and the ground profile observed was consistent with that encountered in the MSP JV CPTs. A silt mix layer interpreted as Oruanui Reworked deposits was observed within the investigation data in the western half of the platform and has been inferred as the compressible soils encountered in 2012. One-dimensional consolidation tests were undertaken as part of this investigation to target these soils and provide parameters for the analysis.

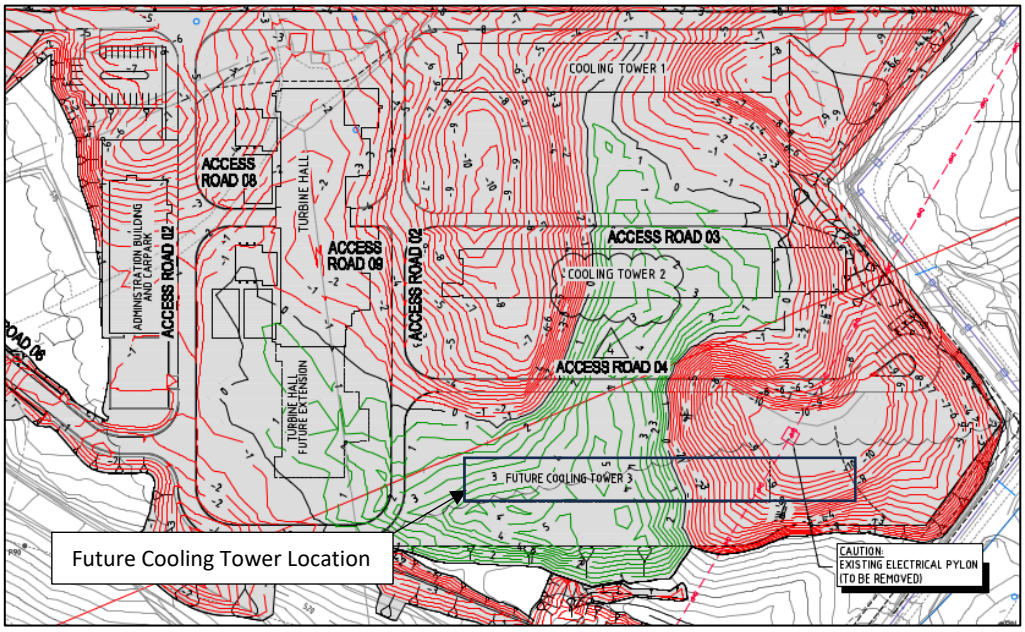

Figure 1: Te Mihi Geothermal Power Project - Cut and Fill Contour Plan (McConnell et al. 2011)

3 GROUND MODEL

The Te Mihi Power Station site is located within the extensive Taupo Volcanic Zone and locally the Wairakei-Tauhara Geothermal Field. The wider site is approximately 7.5km to the north of Lake Taupo which has an eruptive history that spans more than 65,000 years with the largest eruption (Oruanui) occurring 27,000 years ago and depositing a large volume of airfall material (C.J.N. et all. 2004). The most recent eruption occurred approximately 1800 years ago and deposited a large volume of pumice and ash mantling the previous eruptions.

Pumice sands are highly crushable, compressible and lightweight due to the vesicular nature of the particles (Asahi. Et all. 2023). The vesicular nature is due to the violent rhyolite eruption origin when lava with a high content of water and gasses is discharged from a volcano.

The STG Platform sits across an area which originally comprised undulating topography dictated by gully systems which extended throughout the site. The gullies and portions of the elevated slopes in this region are typically mantled by the

recent Holocene-aged Taupo Pumice Formation which comprises rhyolite ignimbrite recovered as loose to medium dense sands and gravels. The thickness of this unit is generally topographically influenced with thinner deposits over elevated sloping ground and thicker in valley floors, and was observed up to 7m thick across the SGT platform.

The Oruanui Formation underlies the Taupo Pumice Formation and the wider area. It is typically up to 200m thick and comprises non-welded rhyolite ignimbrite with pumice clasts in a sandy ash matrix which increases with density with depth (Leonard et al. 2010). The reworked deposit (Oruanui Reworked Formation) comprising firm to stiff silts and loose sand was encountered between the Taupo Pumice and Oruanui units and its origin has been derived from fluvial processes that occurred between the different eruptions.

The 2012 earthworks to form the existing platform resulted in fills between 1m to 5m thick across the western half of the area as illustrated in Cross Section E (Figure 2) which was projected perpendicularly through the platform. The original topography of this section was within a portion of a gully and the fills are underlain with the recent Taupo Pumice as well as the compressible soils of the Reworked Oruanui Formation.

The eastern half of the platform depicted in Figure 3 is the result of extensive cuts which exposes medium dense to dense pumice Ignimbrite from existing ground level.

The groundwater was encountered approximately 15.7m and 32.7m below existing ground level.

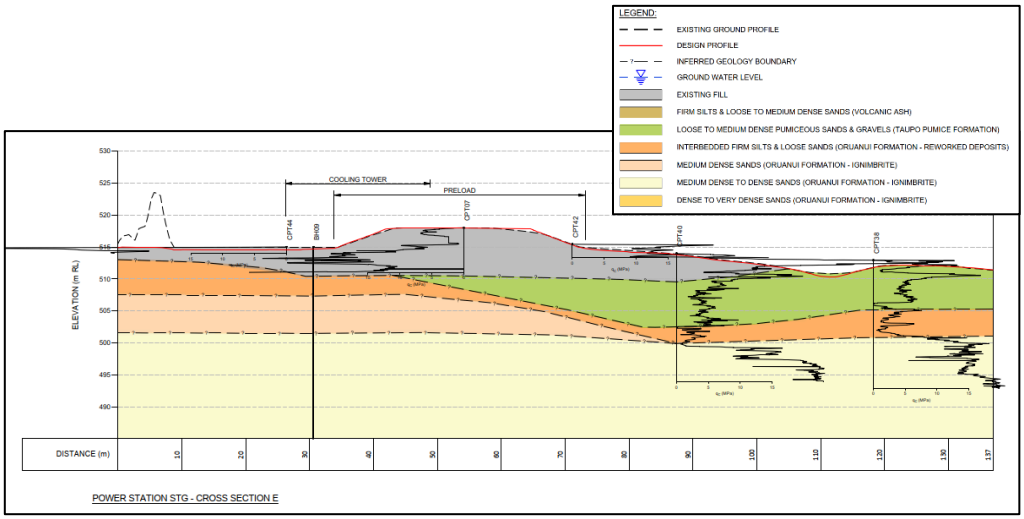

Figure 2: STG Platform – Cross Section E, western half of the platform. (CMW Drawing 17 – Report TGA2023-0083AB Rev 0, dated 8 March 2024)

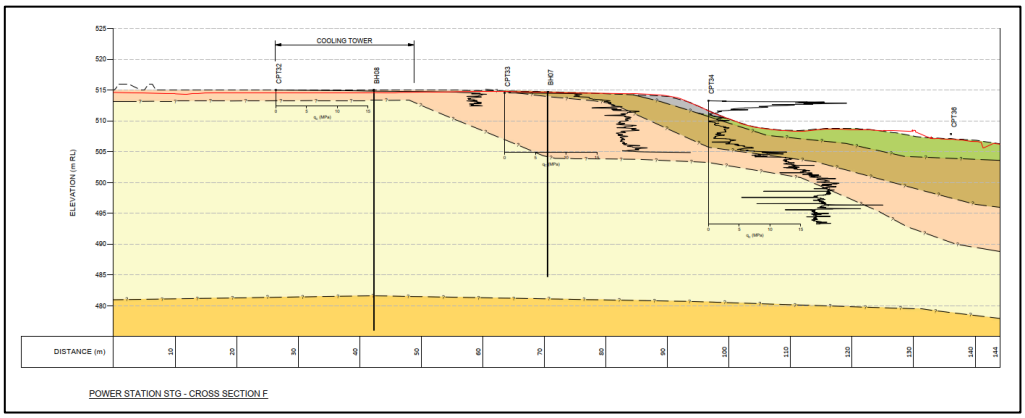

Figure 3: STG Platform – Cross Section F, eastern half of the platform. (CMW Drawing 18 – Report TGA2023-0083AB Rev 0, dated 8 March 2024)

4 SETTLEMENT ANALYSIS

CMW carried out settlement analysis by adopting the updated 2023 ground model that included the recent investigation data and using the proprietary software Settle3 (Rocscience. 2024). The Youngs Modulus and consolidation soil parameters were correlated from the investigation data along with the laboratory testing that had targeted the compressible

soil layer and are presented in Table 1 below. The analysis considered elastic settlement, non-linear primary consolidation and secondary consolidation in accordance with Mesri (Mesri et al. 1996).

Table 1: Soil Parameters

Unit	Unit Weight (kN/m^3)	Youngs Modulus, Es (MPa)	Compression Coefficient, Cc	Recompress, Coefficient, Cr	Coefficient of Consol, Cv (m^2/s)	Void Ratio, e
Existing Fill – silts gravels and sands	15	50	-	-	-	-
Volcanic Ash – firm silts and loose to medium dense sands	17	35	-	-	-	-
Taupo Pumice Formation – loose to medium dense sands and gravels	16	45	-	-	-	-
Oruanui Reworked Deposits – loose sands	16	30	-	-	-	-
Oruanui Reworked Deposits – firm silts	16	10	0.26	0.07	$6.3x10^{-7}$	1.1
Oruanui Formation – Medium Dense Ignimbrite Sands	15	55	-	-	-	-
Oruanui Formation – Medium Dense to Dense Ignimbrite Sands	16	70	-	-	-	-
Oruanui Formation – Medium Dense to Very Dense Ignimbrite Sands	16	125	-	-	-	-

The unit weight for the existing preload was $15kN/m^3$, corresponding to a pressure of 45kPa under the 3m high $2,254m^2$ fill embankment. The design properties of the Cooling Tower were provided by Contact Energy Limited (CEL) and consist of a 236m by 23m rectangular footprint with an estimated structural load of 15kPa.

The settlement analysis included a series of stages to simulate the loading (preloading) sequence as well as applying the proposed Cooling Tower load for the 50-year design life as follows:

- Stage 1 – Simulate construction of the preload embankment (t = 1month).
- Stage 2 – Simulate 12 years since the construction of the preload embankment (t = 144months).
- Stage 3 – Simulate removal of preload prior to construction of the Cooling Tower (t = 150months).
- Stage 4 – Simulate start of Cooling Tower construction (t = 151months).
- Stage 5 – Simulate completion of Cooling Tower construction (t = 152months).
- Stage 6 – Simulate 50-year design life of the Cooling Tower (t = 751months).

The total settlements predicted in response to 12years of preload (Stage 2) and 50years of the Cooling Tower (Stage 6) are illustrated in Figures 4 and 5 below.

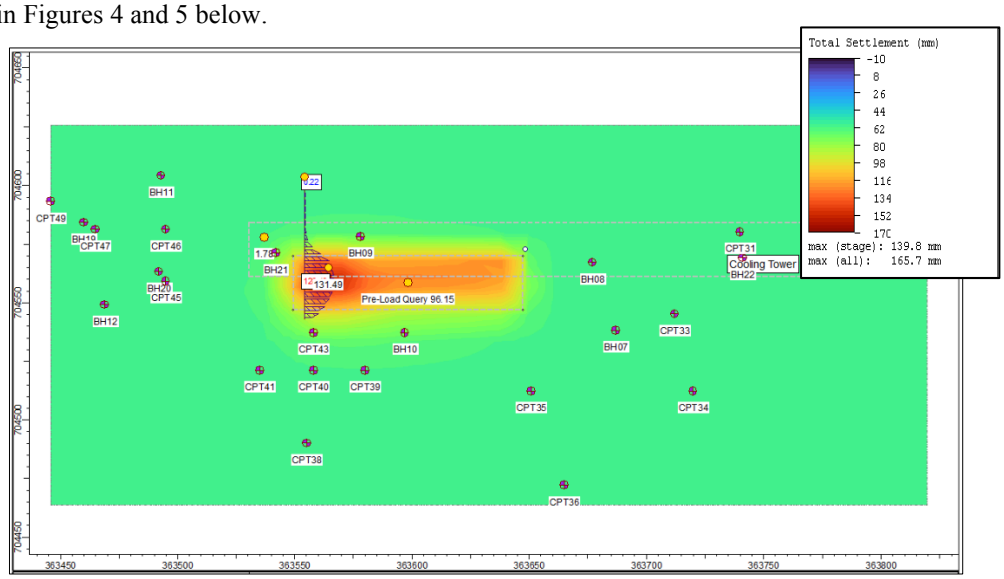

Figure 4: Settle 3 Model – Predicted Total Settlement after 12 years of Preload (Stage 2)

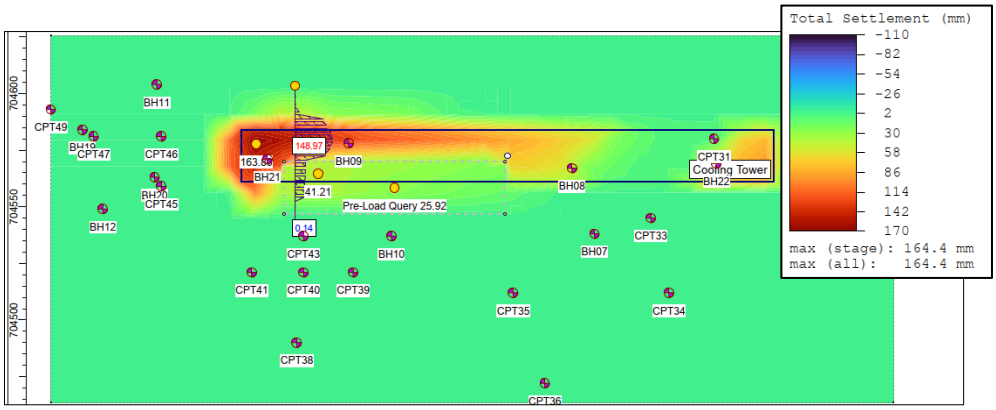

Figure 5: Settle 3 Model – Predicted Total Settlement of Cooling Tower after 50 years (Stage 6)

5 DISCUSSION

Stage 1 of the model simulates the first month following construction of the preload embankment with predicted elastic settlements of 15mm. Following this Stage 2 reflects the 12 years that the preload has been in place and demonstrates predicted settlements of up to 139mm. Stage 5 represents the completion of the construction of the Cooling Tower with up to 75mm of settlement predicted.

Stage 6 simulates the 50-year design life of the Cooling Tower and predicts an additional 89mm of settlement giving a total of 164mm of total predicted settlement across the design life of the structure. This suggests that the majority of the settlement predicted in response to construction of the Cooling Tower will be felt well after construction, attributing to the ongoing consolidation and creep of the Oruanui Reworked deposits. The magnitudes of settlement predicted is not considered to be tolerable for the Cooling Tower.

As detailed in Figure 4 most of the settlement is predicted in the western half of the proposed Cooling Tower footprint with the greater settlements concentrated in the north-western corner of the structure, outside the preload area. Settlements of less than 20mm are proposed across the area that has been historically preloaded. This preload area however creates the potential for sharp differential settlements to occur, with a maximum angular distortion of up to 1:40 (i.e. 80mm over 3m distance) predicted.

The settlement model did not include load compensation effects from the 10m cut that has previously occurred across the eastern half of the site. Relatively small settlements however are predicted in this region due to the dense Ignimbrite sands and the complexity of incorporating this into the model was not considered necessary. This is reiterated by the analysis's outputs showing minimal settlement is proposed across the eastern portion of the Cooling Tower.

The settlement analysis results suggest the existing preload placement and location/extents were chosen to address potential different settlements across the cut fill interface and the compressible soils identified in 2012.

6 REMEDIATION SOLUTION

To address the large magnitude of predicted total and differential settlements within the Cooling Tower footprint, the option of extending the existing preload embankment to encompass the remainder of the Cooling Tower footprint where it extends over the historical fill area has been put forward to the client. The intent of this is to over-consolidate the compressible soils in this area outside of the previously preloaded area and reduce post-construction settlements to within tolerable levels. Given that preload ground improvement typically involves preload durations of 6 to 18months, the design of this additional preload will have to take into consideration the previous preload duration of 12years to reduce the differential settlement between the two areas to reasonable limits.

Based on an unfactored load of 15kPa for the Cooling Tower, and with consideration of the ground model and parameters, a preload embankment height of 3.0m was considered sufficient to reduce post-construction settlements to less than 10mm within approximately 12months. At this magnitude of total settlement, differential settlements are then expected to be within New Zealand Building Code limited of 1:240 (ie 25mm over 6m distance).

To confirm that predicted settlements are occurring as per the preload design, instrumentation in the form of settlement markers will be installed beneath the preload embankment and surveyed frequently to monitor the settlement magnitudes and rates.

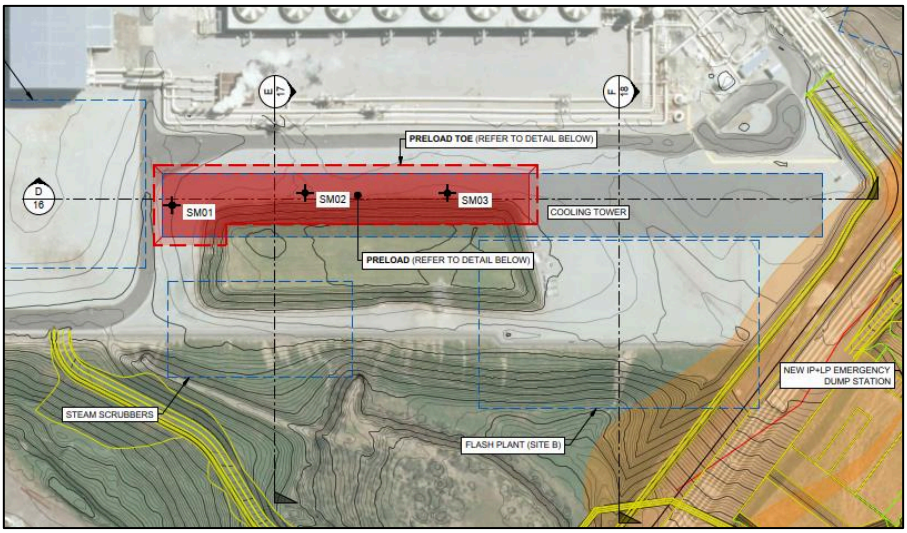

Figure 5: STG Platform – New Preload Location (CMW Drawing 28 – Report TGA2023-0083AB Rev 0, dated 8 March 2024)

7 CONCLUSION

The results of the analysis were generally to be expected given the nature of the subsoils, extensive earthworks history of the site and the extended period of time at which the existing preload embankment has been in place. The significant variation of loading applied across the area, whether from preload or load compensation from deep cut excavations was always likely to create a differential settlement risk for the future structure.

An alternative or additional method to review historic and future settlements is the SatSense (satsense) InSar measurement technique. This is interferometric synthetic aperture radar (InSar) which uses radar imagery to measure ground movement. The radar images are acquired using satellites which emit an electromagnetic beam that is subsequently backscattered from the Earth's surface and received by the sensor on the satellite. By comparing the phase of one radar image with another, whether the ground has moved away from or towards the satellite can be determined. Combining multiple radar images can produce a time history of movements to an accuracy of mm/yr.

8 REFERENCES

Beca Carter Hollings and Ferner Limited., (2009). Te Mihi Geothermal Power Station. *Geotechnical Factual Report, 2920336 – NZ1-137087-7.*

C.J.N Wilson and B.F.Houghton., (2004). Institute of Geological & Nuclear Sciences. *Taupo the Volcano (a single sheet pamphlet).*

Leonard,G.S., Bregg, J.G., Wilson, G.J.N., (2010). Institute of Geological and Nuclear Sciences. *Geological Map 05: Geology of Rotorua Area, 1:250,000.*

Maunsell, Aecom., (2007). Te Mihi Power Station Geotechnical Assessment. *Factual Report on Investigations, 60026836.*

McConnell Dowell, SNC Lavalin and Parsons Brinckerhoff eds., (2011). Te Mihi Geothermal Power Project. *Cut and Fill Contour Plan, THIG-0-UZC-CV-PLN-103.*

McConnell Dowell, SNC Lavalin and Parsons Brinckerhoff JV eds., (2012). Cooling Tower 3: Te Mihi Geothermal Project. *Cone Penetrometer Tests Factual Report, 153936-0-UAD-GT-RPT-003.*

Mesri, G., Kwan Lo, D.O. and Feng., T.W. (1994). *Settlement of embankment on soft clay.* ASCE Geotechnical Special Publications Volume 40, Issue 1, pages 8-56.

Mohannad Bagher Asadi., Rolando P. Orense., Dr. Eng., P.E., M.ASCE., Mohammad Sadeq Asadi., and Nicahael. J. Pender. (2023). *Empirical Assessment of Liquefaction Resistance of Crushable Pumiceous Sand Using Shear Wave Velocity.* Pages 1-14.

Rocscience (2024) *Settle3* (Build 5.023 64bit). Programme.

SatSense, satsense.com. Webpage.

15th Young Geotechnical Professionals Conference

6-9 November 2024
Adelaide, South Australia

PREVIOUS ANZ YOUNG GEOTECHNICAL PROFESSIONALS CONFERENCES

1st ANZ Young Geotechnical Professionals Conference, Sydney, Australia, 1994

2nd ANZ Young Geotechnical Professionals Conference, Auckland, New Zealand, 1995

3rd ANZ Young Geotechnical Professionals Conference, Melbourne, Australia, 1998

4th ANZ Young Geotechnical Professionals Conference, Perth, Australia, 2000

5th ANZ Young Geotechnical Professionals Conference, Rotorua, New Zealand, 2002

6th ANZ Young Geotechnical Professionals Conference, Gold Coast, Australia, 2004

7th ANZ Young Geotechnical Professionals Conference, Adelaide, Australia, 2006

8th ANZ Young Geotechnical Professionals Conference, Wellington, New Zealand, 2008

9th ANZ Young Geotechnical Professionals Conference, Melbourne, Australia, 2012

10th ANZ Young Geotechnical Professionals Conference, Noosa, Australia, 2014

11th ANZ Young Geotechnical Professionals Conference, Queenstown, New Zealand, 2016

12th ANZ Young Geotechnical Professionals Conference, Hobart, Australia, 2018

13th ANZ Young Geotechnical Professionals Conference, Cairns, Australia, 2020 (Cancelled)

14th ANZ Young Geotechnical Professionals Conference, Rotorua, New Zealand, 2022

YGPC 2024

AUSTRALIAN GEOMECHANICS SOCIETY

NEW ZEALAND GEOTECHNICAL SOCIETY INC